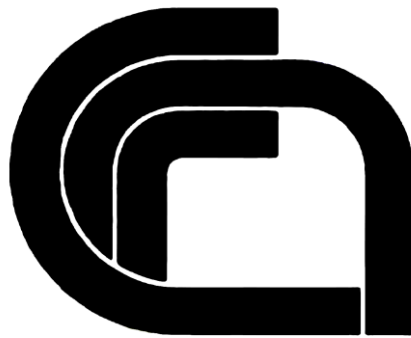


**NATIONAL RESEARCH COUNCIL OF ITALY**

ADVISORY COMMITTEE  
ON TECHNICAL RECOMMENDATIONS FOR CONSTRUCTION

**Guide for the Design, Construction and Control of  
Buildings with Structural Glass Elements**



**CNR-DT 210/2013**

**This document is subject to copyright.**

**No part of this publication may be stored in a retrieval system, or transmitted in any form or by any means – electronic, mechanical, recording, or otherwise – without the prior written permission of the Italian National Research Council.**

**The reproduction of this document is permitted for personal, noncommercial use.**

**CNR-DT 210/2013**

## INDEX

<b>1 INTRODUCTION.....</b>	<b>9</b>
1.1 PREMISE.....	9
1.2 PURPOSE OF THE INSTRUCTIONS.....	9
1.3 OUTLINE OF DOCUMENT.....	11
1.4 STRUCTURAL APPLICATIONS OF GLASS IN CONSTRUCTION WORKS.....	12
1.5 PECULIAR ASPECTS OF GLASS.....	12
1.6 NON-STRUCTURAL ASPECTS INFLUENCING DESIGN.....	14
1.7 DEFINITIONS.....	14
1.7.1 Glass.....	14
1.7.2 Structural glass elements.....	17
1.7.3 Technical glass elements.....	18
1.8 SYMBOLS.....	18
<b>2 MECHANICAL PROPERTIES OF GLASS AND OF MATERIALS COMMONLY USED IN COMBINATION WITH GLASS.....</b>	<b>29</b>
2.1 PROPERTIES OF GLASS.....	29
2.1.1 Physical properties.....	29
2.1.1.1 Mechanisms governing the tensile strength of glass.....	30
2.1.1.2 Definition of the $k_{mod}$ coefficient.....	36
2.1.1.3 Prestressed glass.....	37
2.1.1.3.1 Heat-strengthened and thermally toughened glass.....	38
2.1.1.3.2 Chemically strengthened glass.....	40
2.1.2 Characteristic values of bending strength of glass.....	42
2.1.2.1 General references.....	42
2.1.2.2 Statistical characterisation of the ultimate tensile strength of glass.....	44
2.1.2.2.1 Weibull distribution.....	44
2.1.2.2.2 Influence of speed of application of load.....	46
2.1.2.2.3 Influence of state of stress.....	47
2.1.2.2.4 Influence of the size of the surface under load.....	48
2.1.2.3 Test methods for measuring the tensile strength of glass.....	49
2.1.3 Experimental campaign to determine the influence of the loaded area and of the type of test on the strength of float glass.....	50
2.1.3.1 Experimental results.....	51
2.1.4 Effects of edge finishing: plate edge and holes.....	55
2.1.5 Effects of surface treatments.....	56
2.2 OTHER MATERIALS USED IN COMPOSITION WITH GLASS.....	56
2.2.1 Polymer materials for interlayers.....	57
2.2.1.1 Physical properties.....	57
2.2.1.2 Mechanical properties.....	59
2.2.1.3 Mechanical characterisation of polymer interlayers.....	60
2.2.1.4 Dependence on temperature (master curve).....	61
2.2.1.5 Environmental damage of interlayers in laminated glass.....	62
2.2.2 Adhesives and sealants.....	63
<b>3 GENERAL DESIGN PRINCIPLES.....</b>	<b>65</b>
3.1 HIERARCHY, ROBUSTNESS, REDUNDANCY, FAIL-SAFE DESIGN.....	65
3.1.1 Structural hierarchy.....	65
3.1.2 Structural robustness.....	65
3.1.3 Structural redundancy.....	66

3.1.3.1	Cross-section redundancy .....	66
3.1.3.2	System redundancy .....	66
3.1.4	Post-breakage behaviour.....	68
3.1.5	Durability.....	72
3.2	HIERARCHY AND RELIABILITY OF STRUCTURAL GLASS ELEMENTS .....	73
3.2.1	Classification of structural glass elements .....	73
3.2.2	Design life of the structure .....	76
3.2.3	Expected performance .....	77
<b>4</b>	<b>ACTIONS ON GLASS ELEMENTS .....</b>	<b>78</b>
4.1	GENERAL PRINCIPLES.....	78
4.2	PERMANENT LOADS .....	78
4.3	HUMAN-INDUCED VARIABLE LOADS .....	79
4.3.1	Vertical variable loads .....	79
4.3.2	Horizontal variable loads.....	79
4.3.3	Probabilistic model of human-induced live loads .....	81
4.4	SEISMIC ACTIONS .....	82
4.4.1	Introduction .....	82
4.4.2	Definition of design earthquake .....	82
4.4.2.1	Nominal design life, importance class and reference life.....	82
4.4.2.2	Limit states and corresponding design seismic accelerations .....	83
4.4.2.3	Evaluation of required capacity and performance levels .....	84
4.4.3	Design accelerations on the local element.....	85
4.4.4	Design displacements .....	87
4.4.5	Combination of the seismic action with other actions.....	87
4.5	WIND ACTIONS.....	88
4.5.1	Probabilistic distribution of wind speed .....	88
4.5.2	Wind pressure .....	90
4.6	SNOW LOADS .....	93
4.6.1	Design load.....	93
4.6.2	Probabilistic distribution for snow load .....	93
4.7	THERMAL ACTIONS .....	94
4.7.1	General remarks.....	94
4.7.2	External air temperature .....	95
4.7.3	Internal air temperature .....	95
4.7.4	Maximum solar irradiance.....	96
4.7.5	Temperature gradients in glass .....	101
4.7.5.1	General remarks .....	101
4.7.5.2	Thermal stress .....	101
4.7.5.3	Factors influencing thermal stress.....	102
4.8	WEATHER ACTIONS ON INSULATING GLASS UNITS.....	104
4.8.1	Introduction .....	104
4.8.2	Variations in altitude .....	104
4.8.3	Variations in atmospheric pressure .....	105
4.8.4	Variations in temperature .....	105
4.8.4.1	Simplified method for calculation of internal cavity temperature.....	105
4.8.4.2	Reference values for internal and external air temperature.....	106
4.8.4.3	Reference values for heat transfer coefficients $h_{Ti}$ ed $h_{Te}$ .....	107
4.8.5	Scenarios for calculation of actions.....	107
4.8.6	Correction of cavity temperature .....	108
4.9	EXCEPTIONAL ACTIONS .....	108

4.9.1	Actions due to explosions.....	109
4.9.1.1	Classification of explosions .....	109
4.9.1.2	Characteristic physical variables of a blast wave .....	109
4.9.1.3	Pressure profile of a blast wave.....	111
4.9.1.4	Pressure changes in a blast wave due to obstacles .....	112
4.9.1.5	Mach stem.....	113
4.9.1.6	Actions of structures due to a blast wave .....	114
4.9.2	Actions due to fire .....	116
4.10	DESIGN DURATION OF LOADS .....	117
4.11	ANNEX. SIMPLIFIED METHOD FOR EVALUATING REQUIRED CAPACITY IN TERMS OF DISPLACEMENT.....	118
<b>5</b>	<b>STRENGTH OF GLASS .....</b>	<b>121</b>
5.1	PRELIMINARY CONSIDERATIONS .....	121
5.2	PROBABILISTIC EVALUATION OF STRUCTURAL SAFETY.....	121
5.2.1	Reliability level of structures according to EN1990 .....	121
5.2.2	Reliability methods .....	122
5.2.2.1	Level III methods .....	122
5.2.2.2	Level II methods (first order reliability methods) .....	123
5.2.2.3	Level I methods (or partial factor methods).....	125
5.2.3	Probability of failure and partial factors.....	125
5.2.4	The factor $R_M$ .....	126
5.2.5	Probabilistic function of glass strength .....	127
5.2.5.1	Load duration .....	127
5.2.5.2	Scale effect.....	129
5.3	CALIBRATION OF PARTIAL FACTORS FOR ANNEALED GLASS.....	130
5.3.1	General remarks.....	130
5.3.2	Calibration procedure .....	131
5.3.3	Case studies .....	134
5.3.3.1	Plate subjected to wind action.....	134
5.3.3.2	Roof panel subject to snow loads.....	138
5.3.3.3	Walkable floors .....	140
5.3.3.4	Fin of a façade.....	141
5.3.4	Critical issues in the calibration of partial factors .....	144
5.4	CORRECTION FACTORS .....	148
5.4.1	Influence of load area .....	148
5.4.2	Influence of load duration.....	149
5.4.3	Influence of edge finishing (plate edge and holes).....	149
5.4.4	Influence of surface treatments.....	150
5.5	PRESTRESSED GLASS .....	150
5.5.1	General remarks.....	150
5.5.2	Calibration of partial factors for prestressed glass .....	151
<b>6</b>	<b>CALCULATION MODELS.....</b>	<b>153</b>
6.1	GENERAL REMARKS .....	153
6.2	MODELLING OF MATERIALS .....	155
6.2.1	Glass .....	155
6.2.2	Polymers for interlayers.....	155
6.2.2.1	Level <i>a</i> : effective thickness models (shear transfer coefficient).....	156
6.2.2.2	Level <i>b</i> : linear elastic models.....	157
6.2.2.3	Level <i>c</i> : linear viscoelastic models.....	157

6.2.2.4	Level <i>d</i> : non-linear models.....	161
6.2.3	Other plastic materials used in combination with glass .....	161
6.2.4	Silicone .....	162
6.2.4.1	Level 0: replacement with an equivalent constraint .....	163
6.2.4.2	Level 1: linear elastic model, with constant uncoupled elastic parameters.....	163
6.2.4.3	Level 2: linear elastic model, with constant, continuous elastic parameters.....	164
6.2.4.4	Level 3: non-linear models.....	164
6.2.5	Structural adhesives.....	165
6.2.5.1	General remarks .....	165
6.2.5.2	Mechanical behaviour .....	166
6.2.5.3	Types of joints.....	168
6.2.5.4	Applications and calculations.....	170
6.3	MODELLING OF GLASS ELEMENTS .....	173
6.3.1	General remarks and definitions.....	173
6.3.2	Monolithic glass elements .....	173
6.3.2.1	Preliminary considerations.....	173
6.3.2.2	Modelling of geometry and constraints.....	174
6.3.2.3	Type of structural analysis .....	174
6.3.2.4	Calculation methods.....	175
6.3.3	Laminated glass elements.....	175
6.3.3.1	Level 1: Method of Equivalent Thickness .....	176
6.3.3.1.1	Cahier 3488_V2 (French) .....	178
6.3.3.1.2	TRLV standard (German) .....	178
6.3.3.1.3	European draft standard prEN 16612 (2013) .....	179
6.3.3.1.4	Wölfel-Bennison model .....	179
6.3.3.1.5	Enhanced Effective Thickness (EET) model .....	180
6.3.3.2	Level 2.....	187
6.3.3.3	Level 3.....	188
6.3.4	Insulating glass units .....	188
6.3.4.1	General remarks and definitions.....	188
6.3.4.2	Type of modelling.....	189
6.3.4.3	Type of analysis .....	189
6.3.4.4	Load sharing.....	190
6.3.4.5	Internal loads.....	191
6.4	BUCKLING PHENOMENA .....	192
6.4.1	General remarks and definitions.....	192
6.4.2	Buckling calculation of glass elements under compression .....	193
6.4.2.1	Monolithic glass.....	193
6.4.2.2	Laminated glass.....	194
6.4.2.3	Insulating glass units.....	195
6.4.3	Elements under bending: lateral-torsional buckling verification .....	196
6.4.3.1	Monolithic glass.....	196
6.4.3.2	Laminated glass.....	197
6.4.4	Buckling of glass panels .....	199
6.4.4.1	In-plane compressions.....	199
6.4.4.1.1	Monolithic glass.....	199
6.4.4.1.2	Laminated glass.....	200
6.4.4.1.3	Insulating glass.....	201
6.4.4.2	In-plane shear stress .....	201
6.4.4.2.1	Monolithic glass.....	201
6.4.4.2.2	Laminated glass.....	202
6.4.4.2.3	Insulating glass.....	203
6.5	POST-GLASS-BREAKAGE BEHAVIOUR .....	203
6.5.1	General remarks.....	203

6.5.2 Monolithic glass .....	204
6.5.3 Laminated glass .....	204
6.5.4 Post-breakage assessments .....	207
<b>6.6 ANNEX – TABLES .....</b>	<b>207</b>
6.6.1 Rectangular plates.....	208
6.6.1.1 Rectangular plate simply supported on four edges .....	208
6.6.1.2 Rectangular plate simply supported on three edges .....	211
6.6.1.1 Rectangular plate simply supported on two edges .....	211
6.6.2 Circular plate .....	211
6.6.3 Special cases .....	211
6.6.3.1 Triangular plate simply supported on three edges.....	211
6.6.3.2 Right-trapezoidal plate .....	212
6.6.3.3 Plate with three orthogonal edges and one curved edge.....	212
6.6.3.4 Plate with two parallel and two sloping edges .....	213
<b>7 CALCULATION PRINCIPLES.....</b>	<b>214</b>
7.1 GENERAL REMARKS .....	214
7.2 LIMIT STATES .....	214
7.3 DESIGN ACTIONS .....	216
7.4 DESIGN VALUE OF STRENGTH.....	218
7.5 DESIGN VALUE OF DEFLECTION .....	222
7.6 SEISMIC VERIFICATIONS .....	225
7.6.1 Resistance calculations .....	225
7.6.2 Deflection verifications .....	226
<b>8 CALCULATION EXAMPLES.....</b>	<b>227</b>
8.1 GLASS PLATES SIMPLY SUPPORTED ALONG THE EDGES .....	227
8.1.1 Load analysis .....	228
8.1.2 Design strength .....	228
8.1.3 Monolithic rectangular plate under wind load.....	230
8.1.3.1 Calculation by using formulae and tables .....	230
8.1.3.2 Linear FEM calculation.....	231
8.1.3.3 Non-linear FEM calculation.....	232
8.1.3.4 Comparison of the results obtained with the various methods.....	233
8.1.4 Rectangular laminated glass plate under wind load .....	234
8.1.4.1 Effective thickness model (Wölfel-Bennison) .....	234
8.1.4.2 Model with effective thickness (Enhanced Effective Thickness method) .....	236
8.1.4.3 Finite element linear analysis of the laminated plate .....	237
8.1.4.4 Finite element non-linear analysis of the laminated plate .....	238
8.1.4.5 Comparison of the results obtained with the different models and verifications .....	239
8.1.5 Square laminated glass plate subjected to wind .....	240
8.1.5.1 Model with effective thickness (Wölfel-Bennison) .....	240
8.1.5.2 Model with effective thickness (Enhanced Effective Thickness model) .....	242
8.1.5.3 Linear FEM calculation.....	242
8.1.5.4 Non-linear FEM calculation.....	243
8.1.5.5 Comparison of the results obtained with the various models and verifications .....	244
8.1.6 Verification of the structural silicone joint.....	245
8.1.6.1 Joint thickness calculation.....	246
8.1.6.2 Calculation of the joint under permanent load and wind load.....	247
8.1.7 Post-glass-breakage calculations .....	249
8.2 POINT-WISE SUPPORTED PLATES .....	249
8.2.1 General remarks.....	249

8.2.2	Static scheme .....	252
8.2.3	Calculation example. Laminated glass plate under wind load .....	253
8.2.3.1	Load analysis.....	254
8.2.3.2	Design strength.....	255
8.2.3.3	Calculation of stress and deflection due to the self-weight.....	257
8.2.3.4	Calculation of stress and deflection due to the wind load (3 s).....	257
8.2.3.4.1	Calculation using the “Enhanced Effective Thickness” method .....	257
8.2.3.4.2	3D finite element analysis.....	258
8.2.3.4.3	Comparison of analytical and numerical results .....	260
8.2.3.5	Calculation of stress and deflection due to the wind load (3 s).....	261
8.2.3.5.1	Calculation using the “Enhanced Effective Thickness” method .....	261
8.2.3.5.2	3D finite element analysis.....	261
8.2.3.5.1	Comparison of analytical and numerical results .....	262
8.2.3.6	Evaluation of the stress concentration around the holes .....	263
8.2.3.6.1	Wind load.....	264
8.2.3.6.2	Self-weight action .....	265
8.2.4	Calculation of the plate subjected to different load combinations .....	266
8.2.4.1	Plate subjected to wind load.....	266
8.2.4.2	Local testing of the plate subjected to dead load + wind .....	267
8.2.5	Assessment of the post-breakage behaviour (Collapse Limit State).....	267
8.3	GLASS ROOFS .....	269
8.3.1	Glass roof simply supported on two edges, subjected to snow load and anthropic action (maintenance).....	269
8.3.2	Load analysis .....	270
8.3.3	Design strength.....	270
8.3.3.1	Design strength of the heat strengthened glass ply .....	271
8.3.3.2	Design strength of the thermally toughened (tempered) glass ply .....	272
8.3.4	Calculation of stress and deflection due to the self-weight.....	272
8.3.4.1	Calculation using the “Enhanced Effective Thickness” method.....	273
8.3.4.2	Calculation using tables (with equivalent thicknesses according to the E.E.T. method) ..	274
8.3.4.3	3D finite element calculation .....	274
8.3.4.4	Comparison .....	275
8.3.5	Calculation of stress and deflection due to the snow load.....	276
8.3.5.1	Calculation using the “Enhanced Effective Thickness” method.....	276
8.3.5.2	Calculation using abacuses and tables (with equivalent thicknesses according to the E.E.T. method) .....	277
8.3.5.3	Finite element calculation .....	278
8.3.5.4	Comparison .....	279
8.3.6	Calculation of stress and deflection due to the live anthropic load (maintenance) .....	279
8.3.7	Calculation of the plate subjected to different load combinations .....	281
8.3.7.1	Calculation of the roof subjected to self-weight and snow .....	282
8.3.7.2	Calculation of the roof under self-weight and live load (maintenance) .....	282
8.3.8	Verification of the post-breakage behaviour (Collapse limit state).....	282
8.3.8.1	Calculation for the plate subjected to its own dead load .....	283
8.3.8.2	Calculation of the plate under snow load .....	283
8.4	CALCULATION OF A BUILT-IN PARAPET .....	284
8.4.1	Load analysis .....	285
8.4.2	Design strength.....	286
8.4.3	Hypothesis 1. Parapet with fall protection system .....	287
8.4.4	Hypothesis 2. Parapet without fall prevention system .....	288
8.4.4.1	Solution A. Laminated panel with three glass plies .....	289
8.4.4.2	Solution B. Laminated panel with two glass plies and distributing handrail .....	290
8.4.5	Final considerations.....	292



8.5	GLASS BEAMS AND FLOORS .....	292
8.5.1	Simply supported beam under self-weight, permanent loads and anthropic action .....	294
8.5.1.1	Load analysis.....	294
8.5.1.2	Design strength.....	295
8.5.1.3	Calculation of stress and deflection for a beam subjected to self-weight and dead loads at the CLS .....	296
8.5.1.4	Calculation of stress and deflection for a beam subjected to Cat. B2 action at the CLS ..	296
8.5.1.5	Verification of the beam under different load combinations.....	297
8.5.2	Rectangular floor simply supported on two edges, subjected to self-weight and anthropic action .....	298
8.5.2.1	Load analysis.....	298
8.5.2.2	Design strength.....	299
8.5.2.3	Phase I – pre-breakage behaviour .....	300
8.5.2.3.1	Calculation of stress and deflection for the plate under self-weight .....	300
8.5.2.3.2	Calculation of stress and deflection for the plate subjected to Cat. B2 force .....	303
8.5.2.3.3	Calculation of stress and deflection for the plate subjected to a Cat. B2 concentrated load .....	305
8.5.2.3.4	Verification of the floor subjected to different load combinations.....	306
8.5.2.4	Phase II – Verification of the post-breakage behaviour .....	308
8.5.2.4.1	Calculation of stress and deflection for the plate under self-weight .....	308
8.5.2.4.2	Calculation of the stress and deflection for the plate subjected to a Cat. B2 action (distributed) .....	311
8.5.2.4.3	Verification of the floor under self-weight and distributed live load .....	314
8.6	GLASS FIN THAT SUPPORTS A FAÇADE .....	314
8.6.1	Load analysis .....	316
8.6.2	Design strength.....	316
8.6.3	Phase I – Pre-breakage behaviour .....	318
8.6.3.1	Calculation of stress for the fin subjected to self-weight .....	318
8.6.3.2	Calculation of the stress and deflection for the fin subjected to the wind load.....	318
8.6.3.2.1	Calculation of stress and deflection for the fin subjected to the gust of wind (3 s).....	318
8.6.3.2.2	Calculation of stress and deflection for the fin subjected to 10 minutes averaged wind load .....	319
8.6.3.3	Test on the fin subjected to different load combinations .....	320
8.6.3.3.1	Verification of the fin subjected to self-weight and wind load (3 s) .....	320
8.6.3.3.2	Verification of the fin subjected to self-weight and wind load (10 minutes) .....	320
8.6.3.4	Lateral-torsional buckling verification.....	321
8.6.3.4.1	Lateral-torsional buckling verification for gusts of wind (3 s).....	321
8.6.3.4.2	Lateral-torsional buckling verification for the 10 minutes averaged wind load.....	322
8.6.4	Phase II – Post-breakage behaviour.....	323
8.6.4.1	Calculation of stress for the fin subjected to self-weight .....	324
8.6.4.2	Calculation of stress and deflection for the fin subjected to gusts of wind (3 s).....	324
8.6.4.3	Calculation of stress and deflection for the fin subjected to the 10 minutes averaged wind action .....	324
8.6.4.4	CLS verification of the fin subjected to different load combinations .....	325
8.7	SPECIAL BUCKLING CALCULATIONS .....	325
8.7.1	Design strength.....	325
8.7.2	Compressed beam.....	327
8.7.3	Beam under bending.....	329
8.7.4	Compressed panel.....	330
<b>9</b>	<b>MATERIAL IDENTIFICATION, QUALIFICATION AND ACCEPTANCE PROCEDURES .....</b>	<b>332</b>
9.1	AN OVERVIEW OF NATIONAL (ITALIAN) REGULATIONS .....	332
9.2	AN OVERVIEW OF EUROPEAN LEGISLATIONS .....	333
9.2.1	Specific regulations relative to glass for structural use .....	333
9.2.2	Standards for glass used in construction works.....	333

9.3 MECHANICAL PROPERTIES OF GLASS .....	336
9.4 ADDITIONAL CONTROLS ON GLASS .....	336
9.4.1 Mechanical tests .....	336
9.4.2 Additional tests for thermally or chemically pre-stressed glass .....	337
9.5 MECHANICAL CHARACTERISATION OF THE MATERIALS USED IN COMPOSITION WITH GLASS .....	337
9.5.1 Polymer interlayers .....	337
9.5.1.1 Proposal for a mechanical characterisation of the interlayer .....	338
9.5.1.2 Proposal for mechanical characterisation of the laminate .....	339
9.5.2 Adhesives and sealants .....	339
9.5.2.1 Adhesives for structural use .....	339
9.5.2.2 Structural sealants .....	340
9.5.3 Gasket elements .....	340
9.6 PROPOSAL FOR ADDITIONAL CONTROLS IN THE CONSTRUCTION SITE .....	340
9.7 “STANDARD” MATERIAL IDENTIFICATION DOCUMENT .....	341
9.8 ACCEPTANCE PROCEDURES .....	341
9.8.1 Material choice and tests: duties and responsibilities of the operators .....	341
9.8.2 Transport, storage and movement .....	343
<b>10 BIBLIOGRAPHICAL REFERENCES .....</b>	<b>345</b>
10.1 MONOGRAPHS AND SCIENTIFIC ARTICLES .....	345
10.2 TECHNICAL REGULATIONS AND STANDARDS .....	349

# 1 INTRODUCTION

*... In the openings of my houses, glass occupies the place that precious stone occupies among other materials ... This supermaterial, glass, as we now use it, is a miracle. Air in air, to keep air out or keep it in. Light itself in light, to diffuse or reflect, or refract light itself ... (Frank Lloyd Wright)*

Over the last few decades, technological developments have enabled an astonishing expansion in the variety of applications for glass in the construction sector. Because of its transparency or translucency, the applications of this material, which features prominently in a number of trends in modern architecture, have multiplied, in the form of large panels, roofs, floors, stairs, walls, pillars and railings. Glass elements, which initially had a mere in-fill or decorative function, today constitute structures in themselves, and therefore must undergo the same design, assessment and testing procedures as those used for all other structural materials. The structural function of this ancient material, therefore, is new. However, it demands particular attention to aspects concerning design and use. Building with glass, as opposed to other materials, is neither more difficult nor more complex; however, specific aspects associated with its intrinsic fragility must be taken into account. An informed approach to design may lead to technical solutions that make it possible to achieve levels of reliability and safety comparable to those achievable in construction works employing more traditional structural materials, such as concrete or steel.

## 1.1 Premise

This document supplements the series of National Research Council publications on the use of innovative materials for structural applications.

The document was the subject of a public consultation process between July and December 2012, during which a large number of comments were received. After a detailed analysis of these contributions, modifications and additions were made to the text to correct any printing or typographical errors, to include subjects not dealt with in the original version, and to eliminate others deemed redundant and therefore superfluous.

The updated document was discussed and definitively approved by the National Research Council's Advisory Committee on Technical Recommendations for Construction on December 5<sup>th</sup> 2013 at the Council's Rome headquarters.

The authors would like to thank everybody in the professional, institutional, industrial and academic spheres who actively participated in a process that in a modern, developed nation, is the rightful task of the entire technical and scientific community.

Finally, it should be remembered that the instructions included in this Guide, by their origin and nature, are not legally binding standards, but represent, rather, an aid for technical experts aimed at selecting the vast national and international bibliography which the technical literature places at their disposal, while leaving them with freedom and ultimate responsibility with regard to their choices.

## 1.2 Purpose of the instructions

In applications of a certain importance, with or without specific structural functions, it is already an established design practice to verify and size glass elements according to the principles of structural

---

mechanics, supplemented by practical design rules contained in (mainly foreign) standards or consolidated technical literature. At the international level, the European draft standard prEN 16612-2013<sup>1</sup> “*Glass in building – Determination of the strength of glass panes by calculation and testing*” drawn up by CEN TC 129/WG8, states that glass panes must generally be sized in accordance with the general principles established under Eurocode EN 1990. The essential characteristic of the Eurocodes is their performance-based, non-prescriptive nature: according to the class of consequences arising from failure, buildings are divided into categories and, for each category, a tolerable probability of structural failure is established. Nevertheless, this probabilistic approach to safety, which is broadly accepted at the international level, does not yet seem to have been applied systematically to the specific case of glass by any legislative or regulatory standards, including the aforementioned draft standard.

In the absence of such application, in the design practice load values are frequently taken from the Eurocodes or national technical building standards, while the material strength design values are often taken from other legislative provisions or instructions, usually foreign standards or codes of practice. This may lead to an erroneous evaluation of the safety level of the structure, as the design actions and resistances must be established within a single, organic framework of reference, it being their joint calibration that determines the probability of failure. Using loads and strength values taken from different documents cannot be directly correlated with any quantification of safety, resulting in either undersizing or oversizing, in the latter case compromising the competitiveness of operators in the sector.

In Italy, a note issued by the High Council for Public Works (*Consiglio Superiore dei Lavori Pubblici*) (Prot. no. 0009830-21/20/2011) reiterated the provisions contained in the Ministerial Decree of 14 January 2008 [Technical Construction Standards], i.e. that the use in building works of components, systems and products with an independent static function must be regulated to comply with safety and performance levels established by current technical standards and by the technical references contained in them, in compliance with the basic principles set out in Eurocode EN 1990. The issuance of standardisation documents that are incompatible with these must be avoided in order not to introduce elements of uncertainty among operators in the sector.

The purpose of these instructions is to seek to provide an overview as complete as possible of the various aspects that must be considered in the design, construction and control of glass elements with regard to verifying their mechanical strength and stability. All of the methods proposed below comply with established basic principles and the probabilistic approach to safety, as set out in Eurocode EN 1990. Most of this document is dedicated to deriving – on the basis of experimental results obtained considering a mechanical model – criteria, methods and coefficients that can be used in the design process. It primarily takes into consideration those structural elements that are obtained from industrially manufactured flat glass panels, which may have undergone secondary processes such as toughening or stratification with polymer interlayers. The composition with polymers necessarily entails that the rheological aspects that characterise their mechanical response must also be considered.

Tests must be based on a probabilistic characterisation of strengths and loads, in order to obtain probabilities of failure that are in line with the expected performances, as indicated in Eurocode EN 1990. In addition, the mechanical characterisation of glass must take into account specific phenomena, such as the dependence of the material’s strength on the duration of application of the load (static fatigue). Particular attention is dedicated to all issues associated with the effects of seismic loads, where evaluation of safety must take account of the material’s intrinsic fragility. It also highlights specific aspects of modelling for glass, such as the characterisation of the material starting from fracture mechanics, geometric non-linearities, rheological response of polymeric interlayers and buckling.

---

<sup>1</sup> The prEN 16612-2013 draft standard builds on the work carried out over the previous decade on the prEN 13474 draft standard, which concluded with no definitive approval.

The following information derives from experimental knowledge which represents the state of the art, but which cannot yet be considered complete. This is why, for each subject discussed, the underlying assumptions, the available experimental results, the certainties, the uncertainties and the prospects for future developments, in both the theoretical and experimental fields, are highlighted.

The subjects discussed are specifically associated with the structural use of glass: strength, stability, stiffness, durability, robustness, applicability, sizing, calculation, verification and testing. Processes affecting the mechanical behaviour of glass, such as thermal treatments, lamination, coverings and coatings, are also taken into consideration. Each subject is expounded in light of the most up-to-date scientific and technological progress. Thus the document contains the technical details necessary to apply the process of assessment and verification of constancy of performance by means of experimental tests and structural design based on the principles of structural mechanics.

These recommendations may be used by experts in many specific fields ranging across several areas, such as production processes, materials science and engineering, fracture mechanics, computational analysis, reliability, bonding and anchoring technologies. They therefore emphasise the importance of collaboration and reciprocal interaction between various groups, such as the scientific community, producers, secondary process manufacturers, building firms, installation technicians, designers, project and site managers, inspectors and customers.

### **1.3 Outline of document**

Given its relative novelty, this document aims to be as self-contained as possible. Therefore, in addition to the coefficients and methods necessary for design, it refers to the underlying principles and sets out the various steps which lead to the evaluation of safety, in accordance with the semi-probabilistic limit state method.

Chapter 2 is dedicated to the evaluation and characterisation of the mechanical properties of glass and of other materials used in combination with glass, such as the polymeric interlayers used in lamination. It therefore refers to general notions of fracture mechanics, which constitutes the most consistent approach for evaluating the strength of fragile materials. The characterisation of the viscoelastic behaviour of interlayers and the mechanical properties of adhesives and sealants constitutes the additional knowledge required to evaluate the behaviour of the most commonly used glass elements.

Chapter 3 analyses the basic principles necessary for the design. Given the intrinsic fragility of glass, it is necessary to adopt criteria which allow to achieve a structural ductility compatible with applications in a building. Concepts such as structural hierarchy, robustness, redundancy and fail-safe design represent the principles behind any design process that must necessarily take into account the post-breakage behaviour of glass. Classes of consequences for structural elements are also established, in accordance with the provisions of Eurocode EN 1990.

Chapter 4 considers those aspects of actions on buildings which are of specific interest in the design of glass structures. It focuses particularly on thermal and weather actions, seismic loads and accidental loads such as those resulting from explosions. With regard to wind loads, snow loads and human-induced live loads, reference is made to the probabilistic models which are used for the calculations which follow.

The calibration of the partial factors necessary to use the semi-probabilistic limit state method is carried out in Chapter 5. Given its relative novelty, the calibration process is described in detail, highlighting its underlying principles and illustrating the analytical developments. The chapter also serves as a guide for the design based on the probabilistic method, for construction of particular importance.

Chapter 6 sets out criteria for the correct modelling of a glass structure. In addition to providing the indications required for the numerical approach, it presents simple approximate methods, such as the sizing of laminated glass by establishing the equivalent “effective thickness”. As glass structures are

generally very thin, a part of the chapter is dedicated to evaluating buckling limits under load condition arising in the most common cases of the practice.

Chapter 7 summarises all of the equations necessary for design process, establishing design strengths and structural verifications.

Chapter 8 presents a large number of examples which illustrate the methods developed. The most common cases in the design practice (vertical elements, balaustrades, roofs, beams, floors and fins) are analysed in detail.

Chapter 9 is dedicated to control procedures and provides information relating to identification, qualification and acceptance of the materials that constitute the structural elements to be used in the construction work (glass, polymers for interlayers, structural adhesives, etc.).

Each chapter is, as far as possible, self-contained. Experienced designers only interested in the most practical aspects may refer directly to Chapter 7 and, except for a small number of references, disregard the other chapters on a first reading.

## **1.4 Structural applications of glass in construction works**

In addition to satisfying other kinds of requirements, construction works must be designed and executed so as not to endanger the safety of persons, domestic animals and property. More specifically, they must be designed and built in such a way that the loadings that are liable to act on them during their construction and use will not lead to any of the following:

- a) collapse of the whole or part of the work;
- b) major, deformations to an inadmissible degree;
- c) damage to other parts of the construction works or to fittings or installed equipment, as a result of major deformation of the load-bearing construction;
- d) damage by an event to an extent disproportionate to the original cause.

A “structure” is defined as the organised, permanent association of different parts, designed to withstand environmental and/or man-made and/or accidental loads and to provide appropriate stiffness for its intended use. A structure is formed by parts (essential load-bearing elements) which contribute directly to its strength and/or stiffness to withstand loads acting on it and by (accessory) parts which do not contribute to its strength and/or stiffness and are thus sometimes defined as non-structural elements. The latter may be present in the organisational structure for various reasons, for example for fire protection, for thermal and noise insulation or for aesthetic reasons (e.g. cornices). Accessory elements that form part of a construction are those: 1) whose absence does not significantly alter the strength of the construction in relation to all design loads; 2) whose absence does not significantly alter the stiffness of the construction in relation to all design loads. Elements to which even a single one of these properties does not apply must be considered essential structural elements.

## **1.5 Peculiar aspects of glass**

Glass exhibits substantially a different mechanical response from other construction materials. Compared with the most common metallic alloys, such as steel and aluminium, its behaviour does not have a plastic phase and, unlike the so-called quasi-brittle materials such as concrete, it lacks the capacity to develop the diffused micro-cracks that enable the anelastic mitigation of stress concentrations. Glass is therefore the brittle material *par excellence* and its failure is stochastic in nature. Its lack of plastic adaptation capacity means that local effects cannot be disregarded: for example, stress concentrations around fractures, holes or areas of contact with other materials. The design of glass elements and their connections raises a number of significant specific issues that require great attention in the design of details and construction tolerances.

The strength of glass is determined by its high sensitivity to the presence of surface microdefects, and hence depends upon many factors. Microdefects, which are always present, may in fact increase over time under constant loads, leading to a deterioration in the mechanical performance of glass elements over time (the phenomenon of static fatigue). In addition, surface defects may increase and grow as a result of treatments such as abrasion, screen printing, enamelling, etc. Therefore, in the calibration of partial factors for the structural verification, variations in the intensity and duration of loads, finish conditions and ageing must be taken into account.

Secondary processes may also modify the mechanical and failure properties of glass. Tempering processes,<sup>2</sup> which are performed by means of rapid heat treatments, deliberately induce self-equilibrated stresses characterised by surface compressions, which are beneficial as they cause the micro-cracks from which fractures propagate to close. In annealed glass, by contrast, the random self-equilibrating stresses induced by the production process are virtually cancelled out by a slow cooling process. Tempered glass has a greater strength than annealed glass and shatters into small fragments which are not sharp and present little danger, as the initial failure is followed by the catastrophic release of self-equilibrating stresses. Annealed glass, in contrast, shatters into large fragments, which in safety terms may be dangerous, but enable the pane to remain in place, with a certain amount of residual load-bearing capacity by virtue of other resistance mechanisms coming into play. So-called hardened (or thermally toughened) glass has a lower surface compression state than tempered glass and thus exhibits an intermediate behaviour. A state of surface compression may also be obtained by submersing the glass in a suitable salt bath (chemical tempering).

Two or more plates of glass may also be bonded (laminated) with one or more interlayer sheets, in general polymeric, by a treatment at high temperature and pressure in autoclave. Plies of various thicknesses and types and with different interlayers can be assembled in such a way as to obtain the required mechanical properties, optimising structural solutions in terms of safety. Indeed, laminated glass offers a high degree of reliability in safety terms, as the interlayer retains fragments following breakage of the glass, reducing the risk of injuries and conferring upon the whole a degree of residual post-failure consistency. To improve thermoacoustic performance, two glass panes may also be bonded at their edges, leaving a small cavity (the insulating unit) generally filled with inert gas.

Design procedures for structural glass elements, therefore, are characterised by a number of specific key aspects compared with those commonly used for more traditional materials such as concrete and steel. The verification process is based, in general, on a combination of simplified rules, more accurate analytical methods and experimental testing on prototypes. Approximate methods are useful in the conceptual design phase for evaluating alternative structural layouts or approaches or for carrying out a preliminary cost estimate. More accurate analytical methods need to be adopted in the final detailed design phase. Tests on prototypes are necessary for verifying the design before construction for construction works which feature particularly innovative elements.

Structures must be designed to comply with requirements in relation to various limit states. Glass plates are so thin that they bend, often leading to deflections that are greater than their thickness; this means that the structural design must take into account geometric non-linearities with large-deflection modelling. This aspect can never be overlooked when the panel, in addition to orthogonal loads, is subject to loads parallel to the mid-plane. When the plate is acted upon exclusively by loads that are orthogonal to the mid-plane, failure to take into account geometric non-linearities may lead to evaluations that are detrimental to safety (undersizing) and beneficial to safety (oversizing); the differences

---

<sup>2</sup> English speakers use the term *quenching* to denote the process of rapid cooling which in metals preserves crystalline phases stable only at high temperatures, thereby reducing the mobility of dislocations. The term *tempering*, on the other hand, is used to denote the technique designed to produce a pre-stressed state in the inner part of the material through rapid cooling, without modifying the crystal lattice structure in any way. Specifically, the term *quenched metal* is used to indicate the Italian *metallo temprato* while the term *tempered glass* is used to indicate the Italian *vetro presollecitato* (literally “pre-stressed glass”). In order to preserve the distinction between the terms in the Italian text, we have preferred to adopt the term *vetro temperato* as opposed to *vetro temprato* to indicate glass that has been pre-stressed by means of a rapid cooling process.

between linear and non-linear analysis are much higher in the presence of loads parallel to the middle plane. Problems relating to the buckling of structural elements subject to compression are particularly complex due to the fragile behaviour of the material and, in the case of laminates, due to the viscoelastic behaviour of the interlayer. Particular attention must be dedicated to the design of connections, as they may give rise to high stress concentrations in the surrounding zones.

For glass structures, however, it is necessary above all to consider additional limit states (ultimate limit states) in compliance with the only possible approach given the fragile nature of the material, i.e., the “fail-safe” approach. This is commonly used in aeronautical design, based on the principle that any failure of a component in extreme situations cannot compromise the overall stability of the system, thereby leading to damage that is disproportionate to the event that caused it. From this perspective, it is necessary to take into consideration structural robustness criteria and requirements which control the post-failure structural response of individual elements, ensuring sufficient residual load-bearing capacity to prevent catastrophic failure of the construction work.

## 1.6 Non-structural aspects influencing design

Glass is used above all to create the whole or part of the envelope of the construction, which someone calls the “third skin” (after our body’s skin and our clothing), as it constitutes an optical, acoustic, thermal and hygrometric filter to control environmental comfort.

Therefore, a multiplicity of factors guide the choice of type of glass to use, and cannot be disregarded in the overall design process. These aspects are regulated by a series of harmonised European standards, to which the reader is referred, which govern the preventive evaluation, before they are placed on the market, of construction products which constitute the envelope of a building and which for this purpose alone must bear the CE mark whenever required.

## 1.7 Definitions

### 1.7.1 Glass

- Material: glass.  
Unless otherwise specified, the term refers to flat soda-lime silicate glass.
- Monolithic glass.  
Structural glass element consisting of a single plate of glass.
- Float glass.  
Flat, transparent, clear or tinted soda-lime silicate glass having parallel and polished faces, obtained by continuous casting and floatation on a metal bath, as defined by European Standards EN 572-1, EN 572-2 and EN 572-8. In French *glace* and in German *Floatglas*.
- Drawn sheet glass.  
Flat, transparent, clear or tinted soda-lime silicate glass obtained by continuous drawing, initially vertically, of regular thickness and with the two surfaces fire polished, as defined by European Standards EN 572-1, EN 572-4 and EN 572-8.
- Patterned glass.  
Flat, translucent, clear or tinted soda-lime silicate glass obtained by continuous casting and rolling, as defined by European Standards EN 572-1, EN 572-5 and EN 572-8.



- **Wired patterned glass.**  
Flat, translucent, clear or tinted soda-lime silicate glass obtained by continuous casting and rolling, which has a steel mesh welded at all nodes incorporated in the glass during its manufacturing process. The surfaces may be either patterned or plain, as defined by European Standards EN 572-1, EN 572-6 and EN 572-8.  
In German, wired patterned glass with plain surfaces is called *Drahtglas*.
- **Polished wired glass.**  
Flat, transparent, clear soda-lime silicate glass, having parallel and polished faces, obtained by grinding and polishing the faces of wired patterned glass, as defined by European Standards EN 572-1, EN 572-3 and EN 572-8.
- **Wired or unwired channel-shaped glass.**  
Translucent, clear or tinted soda-lime silicate glass, wired or unwired, obtained by continuous casting and rolling, which is formed into a U shape during the manufacturing process, as defined by European Standards EN 572-1, EN 572-7 and EN 572-8.
- **Decorated glass.**  
Float glass that has undergone surface treatments for aesthetic or decorative purposes (sanding, acid etching, enamelling, etc.). Such treatments generally reduce the strength of the material. Enamelled glass involves the application of a ceramic enamel which, after undergoing a cycle of hardening or thermal tempering, solidifies, becoming an integral part of the glass (European Standards EN 1863-1 and EN 12150-1). Such surface treatments must be duly taken into account as they generally cause surface damage to the extent that they decrease the material's resistance to mechanical stress or temperature changes.
- **Coated glass.**  
Glass products to which a coating has been applied consisting of one or more thin inorganic layers of material applied to the surface using various methods of deposition in order to modify one or more of its properties (European Standard EN 1096-1).
- **Annealed glass.**  
Float glass that has undergone an annealing process. This involves slow, controlled cooling of the glass in order to prevent the formation of tensile stresses in its thickness. Annealing is always performed when the plate is removed from the metal bath in the float process. This reduces risks of failure as the glass undergoes subsequent processes.
- **Prestressed glass.**  
Glass which has undergone a (thermal or chemical) treatment so as to induce a stress field along the thickness of the material (tension in the inner core and compression in the outer surface), making it possible to inhibit the propagation of surface cracks, thus increasing the plate's resistance to mechanical and thermal stresses. Once tempered, the glass plate cannot be cut, drilled or machined along its edges due to the state of tension across its thickness. Tempered glasses can be obtained from float, drawn, moulded and coated glass (toughening and thermal tempering process only) as defined by the respective product standards.
- **Heat-strengthened soda-lime silicate glass.**  
Glass within which a permanent surface compressive stress has been introduced by means of a controlled heating and cooling process in order to impart increased resistance to mechanical and

thermal stress and prescribed fracture patterns. In the case of fracture, heat-strengthened glass shatters in a similar way to annealed glass. The limit (size, fragmentation and mechanical strength) characteristics are defined in product standard EN 1863-1.

- Thermally toughened (or tempered<sup>3</sup>) glass.  
Glass within which a permanent surface compressive stress has been induced by means of a controlled heating and cooling process in order to give it increased resistance to mechanical and thermal stress and prescribed fragmentation properties.  
The limit (size, fragmentation and mechanical strength) characteristics for soda-lime silicate glass to be considered thermally toughened are defined in product standard EN 12150-1.  
The limit (size, fragmentation and mechanical strength) characteristics for borosilicate safety glass to be considered thermally toughened are defined in product standard EN 13024-1.
- Chemically strengthened soda-lime silicate glass.  
Glass manufactured by subjecting soda-lime silicate glass to a process of ion exchange to give it increased resistance to mechanical and thermal stress. Smaller-diameter ions present on the surface and at the edges of the glass are substituted by larger-diameter ions; in this way, the surface and edges of the plates are placed under compressive stress. Chemical strengthening enables greater compressions to be obtained than thermal toughening. However, the depth of the compressed surface layer is a much smaller. In the event of breakage, fragmentation is very similar to that of annealed glass. Chemical strengthening is particularly useful when the geometry of the glass is particularly complex. The limit (size, fragmentation and mechanical strength) characteristics are defined in product standard EN 12337-1.
- Borosilicate glass.  
Silicate glass containing between 7% and 15% boron oxide, as defined by European Standard EN 1748-1-1. Its composition gives it high resistance to thermal shocks and very high chemical (hydrolytic and acid) resistance. Like soda-lime silicate glass, borosilicate glass can be obtained using various production processes (borosilicate float glass, drawn sheet borosilicate glass, rolled borosilicate glass, cast borosilicate glass), it may undergo prestressing processes and machining of the edges and surfaces. It is extremely widely used in precision manufacturing, but rarely used in construction.
- Glass-ceramics.  
Glass consisting of a crystalline and residual glass phase, as defined by European Standard EN 1748-2-1. It is obtained using normal manufacturing methods, such as casting, floating, drawing or rolling, and is subsequently subjected to a heat treatment which transforms, in a controlled manner, part of the glass into a fine-grained crystalline phase. Glass-ceramics have properties which deviate from those of the glass from which they are produced.
- Edge working.  
Any process which removes the sharp edges of surface and/or enables cutting of the plate through smoothing, bevelling, grinding, polishing, etc. Edge working on thermally toughened, tempered and laminated glass must be performed in compliance with the guidelines set out in the relevant product standards.
- Interlayer.  
Layer of material with the function of bonding and separating several plies of glass and/or plastic layers (e.g. polycarbonate or acrylic), as defined by European Standard EN 12543-1 Annex A.

---

<sup>3</sup> See note 2.

Depending on the choice of type of interlayer, it is possible to improve post-fracture behaviour, impact and fire resistance, solar control and acoustic insulation. Its presence has a decisive influence on the behaviour of laminated plates. Types of interlayers and their thicknesses must be duly taken into consideration in the design process.

- **Laminated glass.**  
Assembly consisting of one ply of glass with one or more plies of glass and/or plastic glazing sheet material, joined together with one or more interlayers as defined by European Standard EN 12543-3.
- **Symmetrical laminated glass.**  
Laminated glass in which, starting from both outer surfaces, the sequence of glass panes, plastic glazing sheet material and interlayer(s) by type, thickness, finish and/or general characteristics is the same, as defined by European Standard EN 12543-1.
- **Asymmetrical laminated glass.**  
Laminated glass in which, starting from both outer surfaces, the sequence of glass panes, plastic glazing sheet material and interlayer(s) by type, thickness, finish and/or general characteristics is different, as defined by European Standard EN 12543-1.
- **Laminated safety glass.**  
Laminated glass where, in the event of failure, the interlayer serves to retain the glass fragments, limits the size of the opening, offers residual strength and reduces the risk of cutting or piercing injuries, as defined by European Standard EN 12543-1. On failure it continues to possess residual strength as it keeps glass fragments together, therefore reducing the risk of injury from falling fragments (cutting or piercing injuries). It must comply with the requirements of European Standard EN 12543-2.
- **Folio lamination process.**  
Lamination process where the interlayer is a solid film placed between the plies of glass or plastic glazing sheet material and then subjected to heat and pressure to obtain the final product, as defined by European Standard EN 12543-1. The temperature and pressure levels reached in the autoclave depend on the type of (polymer-based) material used for the interlayer.
- **Cast-in-place lamination process.**  
Lamination process where the interlayer is obtained by pouring a liquid between the plies of glass or plastic glazing sheet material and is then chemically cured to obtain the final product, as defined by European Standard EN 12543-1. The process is called “continuous casting” and takes place from a chamber furnace. During this operation, a pattern or design can be impressed onto the surface.
- **Insulating glass unit.**  
An assembly consisting of at least two panes of glass, separated by one or more spacers, hermetically sealed along the edge, mechanically stable and durable, as defined by European Standard EN 1279-1. The volume bounded by the two plates and frame is filled with air or gas (e.g. argon, krypton, xenon) so as to obtain greater thermal insulation (European Standard EN 1279-5/6).

### **1.7.2 Structural glass elements**

- **Glass beam.**

Element in which one dimension (length) is predominant compared with the other (cross-section diameter), designed to transfer loads that are generally transversal to its own geometric axis to its ledge constraints.

- **Glass plate or panel.**  
Element in which two dimensions are predominant compared with the third (thickness) and whose surface is generally flat (flat plate). Glass plates may exhibit bending behaviour (strain orthogonal to the mid-plane) and membrane behaviour (mid-plane strains).
- **Glass shell.**  
Element in which two dimensions are predominant compared with the third (thickness), with an average surface not generally traceable to a plan, and whose structural behaviour is characterised by the close correlation between membrane stresses and bending stresses.
- **Glass fin.**  
Element projecting from a vertical or sloping surface, usually orthogonal to it, inside or outside, vertical or sloping, with the purpose of strengthening it for actions acting outside the plane of the façade and, sometimes, of bearing the weight of the glass panes themselves. It takes the form of a kind of ribbing on the surface.
- **Joints.**  
Elements which structurally join two or more glass elements and/or glass elements and the load-bearing structure of the construction work.

### **1.7.3 Technical glass elements**

- **Curtain wall.**  
Usually consisting of vertical and horizontal structural elements, connected together and anchored to the load-bearing structure of the building to form a light, continuous envelope which guarantees – in and of itself or jointly with the construction work – all of the normal functions of an external wall, but which does not take on any of the load-bearing characteristics of the building's structure (European Standard EN 13830).
- **Stick system.**  
Light load-bearing framework consisting of components assembled on site to support prefabricated opaque and/or translucent infill panels (European Standard EN 13830).
- **Unitized system construction.**  
Pre-assembled interconnected modules of a height corresponding to one or more floors, complete with infill panels (European Standard EN 13830).
- **Spandrel construction.**  
Pre-assembled interconnected modules of a height corresponding to parts of a floor, complete with infill panels (European Standard EN 13830).

## **1.8 Symbols**

The meanings of the main symbols used in the document are listed below.

---

## General notations

$(.)_{aria}$	value (.) for “air side” of the glass plate;
$(.)_{leff}$	value (.) for effective length;
$(.)_{stagno}$	value (.) for “tin side” of glass plate;
$(.)_{UA}$	value (.) for unit of area;
$(.)_c$	critical or threshold value (.);
$(.)_d$	design value (.);
$(.)_{ed}$	value (.) which considers effect of edge;
$(.)_{eff}$	effective value (.);
$(.)_{est}$	value (.) on outer side;
$(.)_f$	final value (.), sometimes intended as failure value;
$(.)^G$	value (.) for dead load (self-weight);
$(.)_g$	value (.) for glass;
$(.)_i$	initial value (.); $i$ -th value (.);
$(.)_{int}$	value (.) on inner side;
$(.)_k$	characteristic value (.), intended as fractile in statistical distribution;
$(.)_L$	limit value (.);
$(.)_{max}$	maximum value (.);
$(.)_{media}$	mean value (.);
$(.)_{min}$	minimum value (.);
$(.)^P$	value (.) for human load;
$(.)^{P-r}$	value (.) for post-failure phase;
$(.)^Q$	value (.) for Cat. B2 load;
$(.)_R$	value (.) considered as resistance;
$(.)_{ref}$	reference value (.);
$(.)_S$	value (.) considered as stress;
$(.)^S$	value (.) for snow load;
$(.)_{sf}$	value (.) which considers the effect of surface finish;
$(.)_{SLC}$	value (.) for Failure Limit State;
$(.)_{SLE}$	value (.) for Serviceability Limit State;
$(.)_{SLU}$	value (.) for Ultimate Limit State;
$(.)_{test}$	value (.) for experimental tests;
$(.)_{tot}$	total value (.);
$(.)^{w,10min}$	value (.) for wind load (averaged over 10 minutes);
$(.)^{w,3sec}$	value (.) for wind load (3-second gust);
$(.)_x$	value (.) for direction $x$ ;
$(.)_y$	value (.) for direction $y$ ;
$(.)_z$	value (.) for direction $z$ ;
$(.)_\tau$	value (.) for time $\tau$ .

## Upper-case Roman letters

$A$	generic area;
$A^*$	generic area;
$A_0$	generic area of reference;
$A_{eff}$	effective area for statistical characterisation of resistance of glass;
$A_k$	area of influence for gluing, for calculation of equivalent spring value;
$C_l$	coefficient dependent on bending moment distribution;
$C_{10}$	characteristic parameter of material (Neo-Hookean formulation);
$C_D$	aerodynamic drag coefficient;

$C_d$	limit design value for serviceability limit state criterion;
$C_E$	exposure factor for evaluation of snow load;
$C_i$	generic coefficients; characteristic parameter of material (Arruda-Boyce formulation);
$C_p$	specific heat at constant pressure;
$C_r$	coefficient of reflection, obtained from ratio of peak pressure of reflected wave and peak static pressure;
$C_t$	thermal coefficient for evaluation of snow load;
$C_U$	building use coefficient;
$C_v$	specific heat at constant volume;
$D$	bending stiffness of slabs;
$D_{abs}$	bending stiffness of laminated glass plate with independent layer behaviour;
$D_{eq}$	equivalent bending stiffness of laminated glass plate;
$D_{full}$	bending stiffness of laminated glass plate with monolithic behaviour;
$D_p$	interstorey drift;
$E$	effect of stresses;
$E$	Young module: seismic action;
$E_a$	Young module: adhesive;
$E_d$	design value for effects of an action;
$E_p$	Young module: interlayer polymer;
$E_{sil}$	Young module: silicone (structural sealant);
$F_a$	horizontal seismic force;
$F_d$	load acting on element (design action);
$F_D$	result of drag forces on a structure caused by explosion;
$F_{d;i}$	load acting on $i$ -th plate (insulating glass unit);
$F_R$	cumulative distribution function of resistances;
$F_{\sigma,tot,\tau}$	cumulative probability of resistances as a result of action of characteristic duration $\tau$ ;
$F_{\sigma,A,\tau}$	cumulative probability of resistances as a result of action of characteristic duration $\tau$ , for area $A$ ;
$F_{\sigma,pr,\tau}$	cumulative probability of resistances as a result of action of characteristic duration $\tau$ ;
$G$	Performance Function;
$G$	shear modulus of material, dead load;
$G_\infty$	shear modulus, unlimited time;
$G_0$	instantaneous (shear) modulus;
$G_1$	value of actions due to self-weight;
$G_2$	value of actions due to dead loads borne;
$G_a$	shear modulus of adhesive;
$G_{int}$	shear modulus of polymer interlayer in laminated glass;
$G_k$	$k$ -th relaxation (shear) modulus;
$G_{sil}$	shear modulus of silicone (structural sealant);
$G_v$	wind gust coefficient;
$H$	generic height;
$H_0$	horizontal load transmitted by polymer interlayer;
$H_i$	altitude of installation of insulating glass unit;
$H_k$	load distributed on a horizontal line;
$H_p$	altitude of place of manufacture of insulating glass unit;
$H_T$	height of triple point in Mach stem phenomenon;
$I$	solar irradiance;
$I_i$	$i^{\text{th}}$ invariant of left Cauchy-Green strain tensor;
$I_s$	moment of inertia per unit of length, used to calculate effective thicknesses of laminated glass;

---

$I_T$	maximum solar irradiance in relation to a surface with orientation $T$ ;
$I_v$	intensity of turbulence;
$J$	moment of inertia of cross-section;
$J_{abs}$	moment of inertia of laminated glass with independent-layer behaviour;
$J_{eq}$	equivalent moment of inertia of laminated glass;
$J_{full}$	equivalent moment of inertia of laminated glass with monolithic behaviour;
$J_i$	moment of inertia of cross-section of $i^{th}$ plate;
$J_t$	torsional moment of inertia of cross section;
$J_{t,int}$	torsional moment of inertia of interlayer;
$K$	Kelvin volume compression modulus; stress intensity factor;
$K_{\Delta T}$	coefficient for effects of temperature gradient;
$K_{FI}$	multiplier coefficient of actions according to European Standard EN 1990, for modification of probability of failure in shift from verifications to class of different consequences;
$K_i$	generic coefficient;
$K_I$	stress intensity factor (Mode I fractures);
$K_{I0}$	value of stress intensity factor below which crack does not propagate;
$K_{IC}$	critical value of stress intensity factor in Mode I;
$K_{IR}$	value of stress intensity factor in Mode I induced by prestressing/pretensioning;
$K_p$	shape factor for evaluation of coefficient of return period for wind action;
$K_t$	stress concentration factors in proximity to holes;
$L$	distance, generic length;
$L_0$	support span for four-point bending (FPB) test; free bending length;
$L_1, L_2$	load span in four-point bending test (FPB);
$L_{inf}$	bending span;
$L_{min}$	smallest dimension of plate;
$M$	generic moment applied;
$M_{b,Rd}$	critical buckling moment of beam (lateral-torsional stability);
$M_{Ed}$	design acting bending moment (lateral-torsional stability);
$M_R$	elastic moment of resistance of beam (lateral-torsional stability);
$M_{cr}^{(E)}$	Critical Euler moment for lateral-torsional stability;
$N$	generic axial force;
$N_{b,Rd}$	resistant design load for compressed Euler beam;
$N_{Ed}$	Euler axial load design value;
$N_{cr}^{(E)}$	critical load for Euler beam;
$P$	generic load;
$P$	design point;
$P_{ed}$	probability of failure with reference to edge breakage;
$P_{f,\beta}$	probability of failure associated with a given value of $\beta$ ;
$P_f$	probability of breakage;
$P_{f,1y}$	probability of failure of plate in one year of service;
$P_{eqbiax}$	probability of breakage in case of biaxial test;
$P_n$	annual probability of exceedance in a return period of $n$ years;
$P_s$	probability of survival;
$P_v$	wind turbulence intensity reduction factor;
$P_{VR}$	probability of exceedance of reference period $V_R$ ;
$Q$	generic action;
$Q_k$	concentrated live loads;
$Q_{k,1}$	characteristic value of main variable action for a return period of 50 years;
$Q_{k,1,\tau}$	characteristic value of main variable action for a return period of 10 years;
$Q_{k,i}$	characteristic value associated with variable action for a return period of 50 years;

$Q_{k,i,\tau}$	characteristic value associated with variable action for a return period of 10 years;
$R$	domain of resistances;
$R$	radius, or generic distance from a centre taken as a reference point;
$R_0$	radius of support ring in coaxial double ring (CDR) bending test;
$R_1, R_2$	radii of load ring in coaxial double ring (CDR) bending test;
$R_a$	amplification factor of seismic actions
$R_c$	design value of resistance for failure limit state;
$R_d$	design value of resistance;
$R_{d,post}$	additional resistance of glass in addition to decompression;
$R_{d,pre}$	resistance due to precompression induced on surface by tempering process;
$RH$	relative humidity;
$R_M$	multiplier factor for resistances for annealed glass, modifying the probability of failure in going from verifications in class 2 to verifications in class 1;
$R_{M,v}$	multiplier factor for resistances for prestressed glass, modifying the probability of failure in going from verifications in class 2 to verifications in class 1;
$R_s$	surface thermal resistance;
$S$	domain of acting forces;
$S$	coefficient which takes account of ground category and topographical conditions; relationship between load and maximum stress;
$S_a$	maximum non-dimensionalised acceleration due to seismic action;
$S_d$	response spectrum in terms of displacement;
$S_{ij}$	components of deviatoric part of stress tensor;
$T$	temperature;
$T_0$	reference temperature; temperature during installation of silicone;
$T_1$	first fundamental vibration period for building;
$T_a$	fundamental vibration period for non-structural element;
$T_c$	maximum temperature of frame (for calculation of silicone joint);
$T_g$	glass transition temperature (polymer materials);
$T_i$	temperature of place of installation of insulating glass unit;
$T_{int}, T_{ext}$	temperature of gas in cavity of insulating glass unit;
$T_{iVC}$	inside and outside air temperature;
$T_p$	temperature of place of manufacture of insulating glass unit;
$T_R$	return period;
$T_{ref}$	reference temperature;
$T_S$	duration of positive phase of a blast wave;
$T_v$	maximum temperature of glass (for calculation of silicone joint);
$U$	strain energy density;
$UA$	reference unit of area;
$U_{sw}$	speed of advance of wavefront in an explosion;
$V$	coefficient of variation of the series of annual snow load maximums; shear stress;
$V_{b,Rd}$	critical resisting shear stress in stability of panels;
$V_{Ed}$	design shear stress in stability of equilibrium of panels;
$V_N$	nominal design life of structural work;
$V_R$	reference life of structural work;
$V_{cr}^{(E)}$	critical Euler shear stress of a panel;
$W$	elastic resistant modulus of cross-section;
$W_a$	weight of element;
$W_{TNT}$	explosive mass, measured in kg of TNT-equivalent;
$Y$	stress intensity factor modification coefficient which takes into account the shape of the fracture;



$Z$  height of centre of gravity of isolated element measured from ground level; scaled distance.

**Lowercase Roman letters**

$a^*$	characteristic length for response of insulating glass unit;
$a_0$	depth of crack;
$a_g$	peak ground acceleration type A subsoil to consider under the limit state in question;
$a_i$	generic coefficient;
$a_T$	multiplicative factor of scale of frequencies for master curve for a polymer;
$b$	generic width;
$b_i$	generic coefficient;
$c$	characteristic size of crack;
$c_0$	size of crack to which a stress intensity factor equal to the threshold value $K_{I0}$ corresponds
$c_1^0, c_2^0$	Williams, Landel and Ferry equation constants;
$c_c$	size of semi-circular crack at breakage;
$c_{cL}$	limit size of critical crack;
$c_d$	dynamic factor in wind actions;
$c_e$	exposure coefficient in wind actions;
$c_{e1}$	exposure coefficient for mean wind action;
$c_{e2}$	corrective exposure coefficient (in wind actions);
$c_i$	initial size of semi-circular crack;
$c_j$	stiffness of silicone joint in direction $i$ ;
$c_m$	mean wind profile coefficient;
$c_p$	pressure coefficient in wind actions;
$c_r$	return coefficient in wind actions;
$c_t$	friction coefficient in wind actions;
$d$	distance;
$d_0$	distance from ground zero;
$d_{\max}$	maximum displacement;
$d_{\max,G}$	maximum ground displacement;
$d_{\max,MDOF}$	maximum displacement at top of frame;
$e$	thickness of silicone joint;
$e_{ij}$	components of deviatoric part of strain tensor;
$f$	generic displacement;
$f_{b;k}$	characteristic value of tensile strength of prestressed glass;
$f_E$	statistical distribution of effects of actions
$f_g$	tensile strength of glass measured experimentally;
$f_{g;d}$	design strength of glass;
$f_{g;d}^i$	design strength with respect to $i^{\text{th}}$ action;
$f_{g;k}$	characteristic tensile strength or annealed glass;
$f_{g;k;ed}$	characteristic tensile strength or annealed glass, taking account of reduction in strength due to the edge;
$f_{g;k;st}$	characteristic tensile strength of glass to consider in stability verifications;
$f_{g;n}$	nominal tensile strength of annealed glass;
$f_L$	ultimate tensile strength which, applied statistically, would cause failure/breakage in time $\tau_L$ ;
$f_{m;d}$	design strength of materials used in combination with glass;
$f_{m;k}$	characteristic value of strength of materials used in combination with glass;
$f_R$	statistical distribution of resistances;
$f_S$	statistical distribution of stresses;

---

$f_{\sigma,pr,\tau}$	probability density of maximum stress caused by action of characteristic duration $\tau$ ;
$g$	gravitational acceleration;
$g_v$	peak wind speed factor;
$h$	generic thickness;
$h_c$	minimum width of silicone joint;
$h_{ef;w}$	effective thickness for calculation of deformations, according to Wölfel-Bennison model;
$h_i$	thickness of $i^{\text{th}}$ plate in a laminated glass plate;
$h_{i;ef;\sigma}$	effective thickness for calculation of stresses in $i^{\text{th}}$ plate, according to Wölfel-Bennison model;
$h_{int}$	thickness of interlayer;
$\hat{h}_{INTi;\sigma}$	effective thickness for calculation of interface stresses in $i^{\text{th}}$ plate, according to Enhanced Effective Thickness model;
$\hat{h}_{i;\sigma}$	effective thickness for calculation of stresses in $i^{\text{th}}$ plate, according to Enhanced Effective Thickness model;
$h_{Ti}, h_{Te}$	heat exchange transfer coefficient of inner and outer glass (insulating glass);
$h_{Ts}$	heat exchange transfer coefficient of cavity (insulating glass);
$h_v$	length of structural seals;
$\hat{h}_w$	effective thickness for calculation of deformations, according to Enhanced Effective Thickness model;
$i$	specific impulse of blast wave during depression phase;
$i$	centre distance;
$i_p$	centre distance of fins;
$i_{sw}$	specific impulse of blast wave;
$k$	generic constant; multiplicative factor applied to Weibull risk function; shear modulus;
$k_b$	coefficient dependent on stress distribution on edge;
$k_{ed}$	tensile strength reduction factor of annealed glass due to edge effect;
$k_{ed}'$	tensile strength reduction factor of prestressed glass due to edge effect;
$k_i$	stiffness of $i^{\text{th}}$ spring; generic coefficient;
$k_l$	coefficient for calculation of maximum stress;
$k_{mod}$	reduction factor for tensile strength of glass due to duration of loads;
$k_{mod,\tau}$	reduction factor for tensile strength of glass due to load of duration $\tau$ ;
$k_r$	coefficient for description of mean wind profile;
$k_{sf}$	reduction factor for tensile strength of glass due to surface treatments;
$k_v$	reduction factor for increase in tensile strength of glass manufactured by means of prestressing treatment;
$k_\sigma$	stability coefficient (for compressed panels);
$k_\tau$	stability coefficient (for panels subjected to in-plane shear);
$k_\infty$	shear modulus of elastic element (Wiechert model);
$l$	length or span of generic element;
$l^*$	characteristic length of fragments;
$l_b$	length of edge subjected to tensile stress;
$l_p$	length of fin;
$m$	Weibull modulus;
$m^*$	Weibull modulus corresponding to instantaneous breakage (so-called “inert” environment);
$m_{ed}$	Weibull modulus, referring to strength at edge;
$m_L$	reference strength in Weibull statistics for failure under constant load;
$p$	wind pressure; probability;
$p^*$	normalised uniform load;

---

$p_0$	air pressure in environment; parameter governing speed of glass fracture crack propagation; return periods;
$p_{C;0}$	isochoric pressure generated by change in temperature and/or pressure in insulating glass unit;
$p_{H;0}$	isochoric pressure in insulating glass unit;
$p_i$	internal pressure in insulating glass unit;
$p_p$	atmospheric pressure in place of manufacture of insulating glass unit;
$p_r$	peak pressure value of reflected blast wave;
$p_{stag}$	stagnation pressure;
$p_{sw}$	peak static overpressure at wavefront;
$p_w$	wind pressure;
$p_{w,10\ min}$	wind pressure averaged over 10-minute time interval;
$p_{w,10}$	wind pressure referring to return period of 10 years;
$p_{w,3\ sec}$	wind pressure referring to 3-second gust;
$p_{w,50}$	wind pressure referring to return period of 50 years;
$q_a$	structure factor;
$q_k$	uniformly distributed live loads;
$q_s$	snow load value;
$q_{sk}$	characteristic ground snow load reference value (50-year return period);
$q_{sn}$	snow load value for return period of $n$ years;
$q_{sw}$	maximum dynamic pressure of a blast wave;
$q_w$	kinetic pressure of wind;
$q_{w,10\ min}$	kinetic pressure of wind averaged over 10-minute time interval;
$q_{w,3\ sec}$	kinetic pressure of wind referring to 3-second gust;
$q_{w,\tau}$	kinetic pressure of wind averaged over time $\tau$ ;
$r$	ration between principal stress components $\sigma_1$ and $\sigma_2$ ;
$r_a$	thermal resistance of cavity (insulating glass);
$s$	thickness of element;
$s_a$	thickness of adhesive;
$t$	time variable; thickness;
$t^*$	reduced time;
$t_0$	instant at which crack propagation begins;
$t_1, t_2,$	generic instants;
$t_a$	1) instant at which pressure wave caused by blast wave arrives; 2) thickness of adhesive
$t_f$	time in which glass breaks due to growth of crack;
$t_L$	limit time corresponding to failure of glass in the case of constant load;
$v_0$	reference speed of propagation of cracks in glass;
$v_{b50}$	basic reference wind speed, associated with return period of 50 years;
$v_m$	mean wind speed;
$v_p$	peak wind speed;
$v_r$	reference wind speed;
$v_{so}$	speed of sound in air at pressure $p_0$ ;
$w$	deflection;
$w_i$	deflection caused by $i^{\text{th}}$ action at point of verification;
$w_{lim}$	deflection limit value;
$z$	reference coordinate orthogonal to plane of plate; height above ground level;
$z_0$	roughness length.

### Greek capitals

$\Delta$  variation, change, difference;

$\Gamma$	shear transfer coefficient (Wölfel-Bennison model);
$\Gamma_b$	shear transfer coefficient for analysis of buckling;
$\Phi$	parameter for calculation of reduction coefficients in problems of buckling;
$\psi$	angle between the projection of the normal to the crack and the direction of $\sigma_1$ ; dimensional coefficient dependent on load and boundary conditions for calculation of laminated glass with Enhanced Effective Thickness;
$\psi_{0,j}$	load combination coefficients;
$\psi_{2,j}$	coefficients for combination of seismic actions with other actions.

### Lowercase Greek letters

$\alpha$	thermal expansion coefficient; generic angle;
$\alpha^*$	imperfection factor in problems of buckling;
$\alpha_0$	parameter for definition of load which produces buckling;
$\alpha_c$	coefficient of linear thermal expansion of frame;
$\alpha_E, \alpha_R$	coefficients associated with design values to consider in order to obtain a given probability of failure;
$\alpha_i, \alpha_e$	solar energy absorption coefficients for inner and outer glass (insulating glass units);
$\alpha_v$	linear glass thermal expansion coefficient;
$\beta$	reliability index, i.e., parameter measuring distance between safety limit and mean of performance function; generic parameter;
$\beta_1$	reliability index for reference period of 1 year;
$\beta_{50}$	reliability index for reference period of 50 years;
$\gamma$	shear slip; specific weight;
$\gamma_f$	shear stress at end of elastic phase;
$\gamma_F$	generic partial factor for actions;
$\gamma_G$	partial factor for permanent actions;
$\gamma_{G1}$	partial factor for self-weight;
$\gamma_{G2}$	partial factor for dead (permanent) borne loads;
$\gamma_M$	partial factor for strength of annealed glass;
$\gamma_{M,v}$	partial factor for strength of prestressed glass;
$\gamma_{PVB}$	specific weight of PVB;
$\gamma_v$	specific weight of glass;
$\gamma_Q, \gamma_{Q,i}$	partial factor for live (variable) actions;
$\delta_i$	stiffness ratio between plates in insulating glass unit;
$\delta_{ij}$	Kronecker's delta;
$\varepsilon$	deformation;
$\varepsilon_{el}$	elastic deformation;
$\varepsilon_{ij}$	components of strain tensor;
$\varepsilon_{vi}$	deformation due to dashpot in $i^{\text{th}}$ Maxwell element;
$\eta$	generic shear transfer coefficient (Enhanced Effective Thickness model); viscosity;
$\eta_{1D}$	shear transfer coefficient (Enhanced Effective Thickness model) per laminated beam;
$\eta_{1D;2}$	shear transfer coefficient (Enhanced Effective Thickness model) for laminated beam consisting of two layers of glass;
$\eta_{1D;3}$	shear transfer coefficient (Enhanced Effective Thickness model) for laminated beam consisting of three layers of glass;
$\eta_{1D;N}$	shear transfer coefficient (Enhanced Effective Thickness model) for laminated beam consisting of $N$ layers of glass;

$\eta_{2D}$	shear transfer coefficient (Enhanced Effective Thickness model) for laminated plate;
$\eta_i$	viscosity of $i^{\text{th}}$ dashpot;
$\theta$	first invariant of strain tensor;
$\theta_e$	temperature of outer glass (insulating glass unit);
$\theta_i$	temperature of inner glass (insulating glass unit);
$\kappa$	parameter dependent of surface of influence in distribution of human-induced loads;
$\lambda$	thermal conductivity coefficient; shape factor (ratio between dimension in a glass plate);
$\lambda^*$	characteristic length of loss of glass-polymer adhesion;
$\bar{\lambda}$	normalised slenderness of compressed element;
$\bar{\lambda}_{LT}$	normalised slenderness of element under bending
$\lambda_c$	characteristic length of loss of glass-polymer adhesion;
$\lambda_f$	shape factor in plates;
$\lambda_{gA}$	tensile strength reduction factor, which considers the area subjected to maximum stress;
$\lambda_{gA}^{(aria+stagno)/2}$	factor enabling rescaling of the resistance value obtained using methods of testing on an area $A_{eff.test}$ , with respect to the effective area of case under study;
$\lambda_{gl}$	tensile strength reduction factor for stresses on edge;
$\lambda_{g_{ltest} \rightarrow l}$	factor enabling rescaling of the resistance value obtained using methods of testing, with respect to effective length of case under study;
$\lambda_m$	characteristic parameter of material (Arruda-Boyce formulation);
$\lambda_p$	expected value for duration of permanent components of human-induced loads;
$\lambda_q$	expected value for duration of discontinuous component of human-induced loads;
$\mu$	characteristic material parameter (Arruda-Boyce model);
$\mu_E$	mean of effects of actions;
$\mu_G$	mean of performance function;
$\mu_i$	roof shape factor;
$\mu_p$	mean value of dead/permanent component of human-induced loads;
$\mu_q$	mean value of discontinuous component of loads;
$\mu_R$	mean value of resistances;
$\nu$	Poisson's ratio;
$\nu_p$	Poisson's ratio in polymer of laminated glass;
$\rho$	density of glass or generic density;
$\rho_a$	air density;
$\sigma$	stress;
$\sigma_\infty$	admissible tensile stresses for silicone for loads of long duration;
$\sigma_\perp$	mean tensile stress orthogonal to crack;
$\sigma_0$	reference Weibull strength;
$\sigma_{0ed}$	reference Weibull strength, with reference to edge strength;
$\sigma_{0L}$	reference Weibull strength for failure under constant load;
$\sigma_0^*$	reference Weibull strength corresponding to instantaneous breakage (so-called "inert" environment);
$\sigma^i$	stress caused at the verification point by the $i^{\text{th}}$ action;
$\sigma_1, \sigma_2, \sigma_3$	principal components of stress;
$\sigma_{des}$	admissible tensile stress for silicone for loads of short duration;
$\sigma_{eqbiax}$	equibiaxial stress;
$\sigma_E$	mean standard deviation of effects of actions;
$\sigma_f$	increase in surface compression due to prestressing (toughening);
$\sigma_{f0}$	initial mechanical strength;

$\sigma_g$	tensile stress acting along plane of crack
$\sigma_G$	mean standard deviation of performance function;
$\sigma_{Ic}$	critical value of macroscopic stress producing crack opening in Mode I;
$\sigma_{Ic\_eq}$	equivalent value of $\sigma_{Ic}$ ;
$\sigma_L$	limit stress leading to failure/breakage of glass, under constant loading;
$\sigma_{max,INTi}$	in laminated glass, maximum tensile stress acting on the interface between one of the glass plates and the polymeric interlayer;
$\sigma_{max,q}$	maximum tensile stress given by the load $q$ ;
$\sigma_p$	stress due to prestressing (tempering/toughening);
$\sigma_{perm}$	mean standard deviation of the dead (permanent) component of human-induced loads;
$\sigma_q$	mean standard deviation of the variable (live) component of human-induced loads;
$\sigma_R$	mean standard deviation of resistances;
$\sigma_t$	stress caused by temperature difference;
$\sigma_{uniax}$	uniaxial stress;
$\sigma_{U,p}$	standard deviation of distribution of “permanent” human-induced load on the surface;
$\sigma_{U,q}$	standard deviation of distribution of “variable” human-induced load on the surface;
$\sigma_V$	standard deviation of mean intensity of human-induced live loads;
$\tau$	generic interval or moment of time, or generic shear stress;
$\tau_{\infty}$	admissible shear stresses for silicone for loads of long duration;
$\tau_{des}$	admissible shear stress for silicone for loads of short duration;
$\tau_e$	solar energy transmission coefficient;
$\tau_f$	ultimate shear strength; shear strength at beginning of post-elastic phase;
$\tau_{g;d}$	design shear strength of the material;
$\tau_{g;k}$	characteristic shear strength of the material;
$\tau_i$	characteristic relaxation time for $i^{th}$ Maxwell element;
$\tau_k$	$k^{th}$ relaxation time for a viscous material;
$\tau_L$	reference time interval;
$\varphi$	load-sharing factor for actions in insulating glass units; latitude;
$\chi$	curvature; reduction factor for Euler buckling load;
$\chi_{LT}$	reduction factor for flexural-torsional buckling;
$\omega$	frequency;
$\omega_c$	frequency of natural vibrations.

## 2 MECHANICAL PROPERTIES OF GLASS AND OF MATERIALS COMMONLY USED IN COMBINATION WITH GLASS

Characterisation of the mechanical properties of glass presents several peculiarities compared with more traditional construction materials because it is based on the interpretation of experimental results through the use of models based on fracture mechanics. Materials used in combination with glass are essentially polymer-based, for which the viscoplastic component of their deformation predominates over its elastic component. This chapter sets out general aspects for the characterisation of the relevant mechanical variables for glass and materials associated with it, while the reader is referred to Chapter 5 for the nominal and characteristic values to use in structural verifications.

It is pointed out that all materials must in any case conform to their respective European and national product standards. This chapter deals specifically with statistical procedures for evaluating strengths of materials in compliance with the general principles set out in European Standard EN1990, for the correct design and use of structural glass elements in a construction work. These procedures will be used to determine suitable factors and coefficients for structural verifications, calibrated so as to satisfy expected performance goals in terms of safety and reliability as laid down by European and national standards.

### 2.1 Properties of glass

Glass is a mechanically homogeneous, isotropic material, with a linear-elastic behaviour until failure, both under tension and compression. The mechanical strength of glass under compression is generally much greater than its mechanical strength under tension. In soda-lime silicate glass it is of the order of  $1000 \text{ N/mm}^2$ ; this value is an uncertain measurement, as the non-uniform contact between the surfaces of the specimen and loading platens induces stress concentrations, thus producing highly dispersed values for ultimate tensile stresses [CEN/TC129/WG8, 2006]. This chapter deals with the tensile strength of glass, which is generally the decisive property in design. For particular structural applications in which compressive strength must be considered in a specific manner [Royer & Silvestri, 2007], the designer must conduct an appropriate experimental campaign.

The tensile strength of glass is practically independent of its chemical composition. However, it is influenced by atmospheric humidity and also depends on stress amplification factors (microdefects) generally present on the surface as a result of the manufacturing and subsequent processes. Thus, the mechanical strength of glass must be evaluated in accordance with a fracture mechanics model: models of the tensile strength of glass are available in the scientific literature (e.g. Load Duration Theory [Brown, 1972], Crack Growth Model [Evans, 1974], Glass Failure Prediction Model [Beason, 1980]). All of these consider that tensile strength is associated with the propagation of a pre-existing dominant crack, and that its propagation is influenced by the duration of application of the load.

These instructions consider the Crack Growth Model proposed in [Evans, 1974], while modifying it to take into account the fact that a stress intensity factor limit exists in the crack below which it does not increase [Fischer-Cripps & Collins *et al.*, 1995].

#### 2.1.1 Physical properties

Glass *construction products* may differ from each other in composition (soda-lime silicate glass, borosilicate glass, glass-ceramics, etc.), manufacture (float glass, drawn sheet glass, etc.), geometry (flat, curved, etc.), process (annealing, tempering, etc.) and finish (grinding, coating, etc.). Variations in the chemical composition of glass make it possible to obtain a range of products with the most

suitable physical and mechanical properties for a specific application. For comparison purposes, Table 2.1 lists the reference values for the physical properties of soda-lime silicate glasses and of borosilicate glasses used in construction. For a more precise definition of the main characteristics of the various types of glass, the reader is referred to the respective product standards and in any case the manufacturer’s indications.

Table 2.1. Main physical properties of soda-lime silicate and borosilicate glass.

Property	Symbol	Unit of measurement	Value
Density	$\rho$	[kg/m <sup>3</sup> ]	2250 - 2750
Young’s modulus	$E$	[MPa]	63000 - 77000
Poisson’s ratio	$\nu$	[ - ]	0.20 - 024
Thermal expansion coefficient	$\alpha$	[ $\mu\text{m}/(\text{m K})$ ]	3.1 - 6 <sup>(1)</sup> 9 <sup>(2)</sup>
Specific heat capacity	$C_p$	[J/(kg K)]	720 <sup>(1)</sup> 800 <sup>(2)</sup>
Thermal conductivity coefficient	$\lambda$	[W/(m K)]	0.9 - 1
Strength – critical value of stress intensity factor (in Mode I)	$K_{IC}$	[MPa m <sup>1/2</sup> ]	0.75
Transition temperature		[°C]	530
Maximum in-service temperature		[°C]	280
<sup>(1)</sup> borosilicate glass			
<sup>(2)</sup> soda-lime silicate glass			

Unless otherwise specified, in this document the term “glass” refers exclusively to soda-lime silicate float glass manufactured in accordance with EN 572-9.

### 2.1.1.1 Mechanisms governing the tensile strength of glass

The tensile strength of the material is generally measured on annealed glass in order to omit any residual stresses from the calculation. The model used is generally that of classical Linear-Elastic Fracture Mechanics, in which the reference parameter is the stress intensity factor  $K$ . As the size of already existing cracks is generally much smaller than the thickness of the plate, the factor  $K$  can be derived from the elastic problem of an infinite semi-space subject to a biaxial force, with a thumbnail-shaped crack which as initial first-order approximation may be considered semi-elliptical (Figure 2.1).

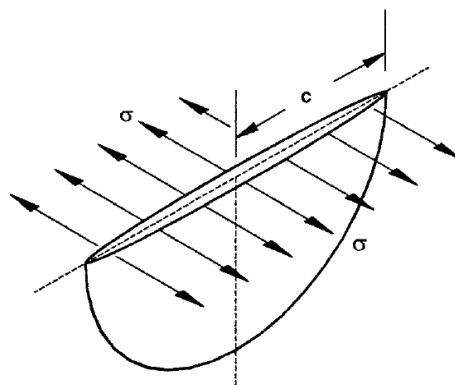


Figure 2.1. Schematic representation of a semi-elliptical thumbnail surface crack



The cause of failure of the glass is almost exclusively the propagation of the fracture in Mode I, as the contributions ascribable to Modes II and III are virtually negligible [Brückner *et al.*, 1996]. For a semi-elliptical surface crack, the factor  $K_I$  of the stress intensity factor is given by

$$K_I = \sigma_g Y \sqrt{\pi c}, \tag{2.1}$$

where  $\sigma_g$  is the tensile stress acting in the normal direction to the plane on which the crack lies,  $c$  is the length of the smallest semi-axis of the ellipse, while  $Y$  is a non-dimensional coefficient which takes account of the geometric shape of the front of the crack as derived from the graph in Figure 2.2 (a) as a function of the ratio between the dimensions of the crack.

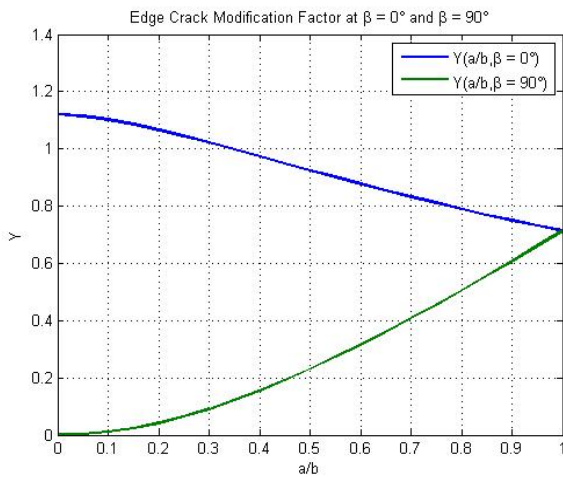


Figure 2.2. (a) Modification factor  $Y$  of a semi-elliptical crack, in the direction of its smallest axis ( $\beta = 0^\circ$ ) and largest axis ( $\beta = 90^\circ$ ), as a function of the ratio  $a/b$  between the dimensions of the crack in the two directions; (b) Fracture mirror of a plate broken by means of a four-point bending test.

Given that the stress amplification factor is greater along the smaller axis than along the larger axis [Lawn & Wilshaw, 1975], it can be shown that initially elliptical cracks tend to develop into circular fractures. As an example, Figure 2.2 (b) shows the characteristic semi-circular shape of a crack in an advanced stage of propagation, caused by a crack that was roughly semi-elliptical in shape. Therefore, in the propagation process it can be assumed that the surface crack is semi-circular and therefore use a modification factor  $Y = 2.24/\pi$  in Eq. (2.1).

It has been shown that cracks can increase in size over time if subjected to a large enough load. The rate of growth is a function of the stress intensity factor  $K_I$  and environmental conditions (Figure 2.3). Two limit values of  $K_I$  have been determined which describe the mode of propagation of the crack: the threshold value,  $K_{I0}$ , which is dependent on environmental conditions and below which no propagation takes place, and the critical value,  $K_{IC}$ , which is characteristic of the material and above which propagation is independent of environmental conditions and occurs at such high speeds as to cause virtually instantaneous failure. The intermediate values of the stress intensity factor define the sub-critical range of fracture propagation, which causes failure to be deferred over time. This phenomenon is termed *static fatigue*.

The critical value  $K_{IC}$  is conventionally defined as the value of  $K_I$  for which the fracture reaches a propagation speed of 1 mm/s. This threshold marks the transition to a stage in which a drastic acceleration takes place, with the propagation speed accelerating rapidly from 1 mm/s up to around 1500 m/s. For soda-lime glass (float glass in accordance with EN 572-2), we can assume  $K_{IC} = 0.75 \text{ MPa m}^{1/2}$ . This value can also be used for borosilicate glass.

Having established the environmental conditions, we can say that the threshold value  $K_{I0}$  is the highest

value of  $K_I$  for which the crack does not propagate. As a rough order of magnitude, for soda-lime silicate glass a value of  $K_{I0} = 0.25 - 0.30 \text{ MPa m}^{1/2}$  may be assumed [Shand, 1961; Wiederhorn & Bolz, 1970; Wan *et al.*, 1961], while  $K_{I0} = 0.32 \text{ MPa m}^{1/2}$  may be assumed for borosilicate glass.

In conclusion, when  $K_I \leq K_{I0}$ , failure does not occur, regardless of the duration of the load; when  $K_{I0} < K_I < K_{IC}$ , failure is deferred over time; when  $K_I \geq K_{IC}$ , failure is instantaneous. The tensile strength of glass is thus defined by  $K_{IC}$ , which depends on the type of glass alone, and the value of  $K_{I0}$ , which depends on the type of glass and specific thermo-hygrometric environmental conditions, while the state of stress in the glass and the initial dimension of the crack determine  $K_I$  according to Eq. (2.1).

The main problem consists in the evaluation of the characteristic dimensions of initial cracks, which are difficult to determine by means of microscopic inspection. An indirect evaluation is generally used, based on a crack growth model calibrated according to macroscopic experimental tests.

Bending tests are conducted in accordance with European Standard EN 1288-1/2001 in conditions of relative humidity of 40-70% and at a temperature of  $23 \pm 5^\circ\text{C}$ , with a rate of increase of load applied so as to increase the stress at a rate of 2 MPa/s. The stress value that characterises failure, represented by  $f_g$ , is the value of the tensile strength of the glass. However, this value cannot be used in structural design, as it depends on the specific testing conditions; it must therefore be appropriately rescaled in accordance with the actual in-service conditions of the construction work, i.e. the duration of application of the load  $t$  and relative humidity conditions.

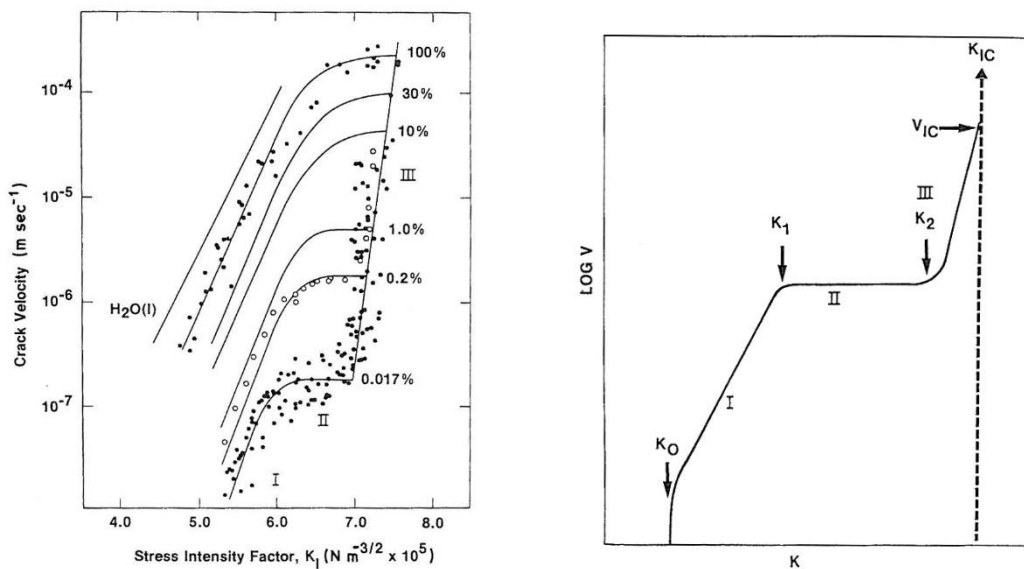


Figure 2.3. Speed of crack growth as a function of stress intensity factor.

The step from laboratory-measured tensile strength to the tensile strength of the element under examination is based on a linear-elastic model of fracture mechanics, defining the relation between the speed of propagation of the crack and the stress intensity factor. With reference to the second graph in Figure 2.3, for the purpose of evaluating safety in construction works the most significant branch is the one labelled I, characterised by a propagation speed of less than  $10^{-4} \text{ m/s}$ .

Wiederhorn proposed an exponential relationship between speed of growth of the fracture and the stress intensity factor  $K_I$  [Wiederhorn, 1969]. Evans [Evans, 1972] subsequently stated that Wiederhorn's experimental data can be correctly interpreted by an equation (currently the most widely used one) of the following type

$$\frac{dc}{dt} = A \cdot K_I^n = v_0 \cdot \left( \frac{K_I}{K_{IC}} \right)^n = v_0 \cdot \left( \frac{\sigma_g \cdot Y \cdot \sqrt{\pi \cdot c}}{K_{IC}} \right)^n, \quad (2.2)$$

where  $c$  is the radius of the crack, which is assumed to be semi-circular, while  $v_0$  and  $n$  are constants which depend on the type of glass and the environmental conditions. It should be noted that  $v_0$  [m/s] is a conventional sub-critical value of fracture propagation, as it represents the speed of growth which the fracture would reach if it were to propagate up to  $K_{IC}$  following the exponential law illustrated in Eq. (2.2).

For soda-lime glass, as a rough estimate, the range is  $n = 12 - 16$ , depending on environmental humidity conditions: for 100% relative humidity we can assume  $n = 16$ , while values are smaller for lower humidity levels. In these instructions, for the sake of safety, we assume that  $n = 16$  regardless of thermal-hygrometric environmental conditions. With regard to the speed  $v_0$ , this may range from 30  $\mu\text{m/s}$  in dry air (0.2% relative humidity) to 0.02 m/s in water. On the safe side, reference is made for the realistically most severe condition by assuming that  $v_0 = 0.0025$  m/s for any condition [Porter & Houlsby, 1999].

In borosilicate glasses, on the other hand, the range is assumed to be  $n = 27 - 40$ . A reasonably conservative value is  $n = 37.2$  [Sglavo *et al.*, 2002b]. Figure 2.4 illustrates experimental graphs for various types of glass.

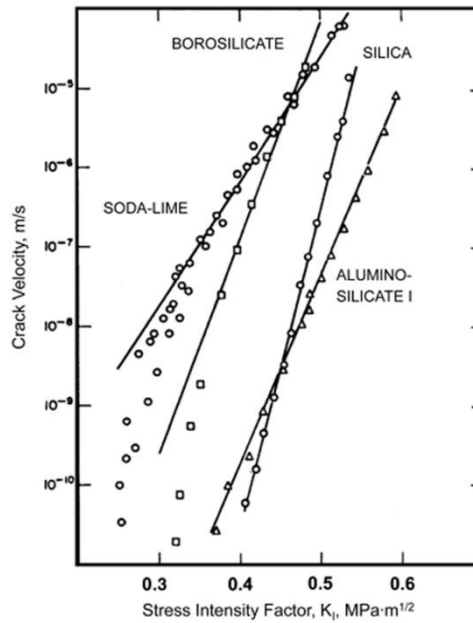


Figure 2.4. Speed of crack growth for various types of glass.

Through the relationship expressed in Eq. (2.2), the standard laboratory test with which  $f_g$  was obtained can be interpreted by returning, *a posteriori*, to the initial size  $c_i$  of the semi-circular crack, i.e., the initial crack which causes the glass to fail at the nominal stress of  $f_g$  with speed  $d\sigma/dt = \dot{\sigma} = 2$  MPa/s (equivalent semi-circular crack).

At the moment of failure, the size of the crack  $c_c$  is the one which corresponds to a stress intensity factor  $K_{IC}$  according to Eq. (2.1), i.e.

$$c_c = \left( \frac{K_{IC}}{Y \cdot f_g \cdot \sqrt{\pi}} \right)^2. \quad (2.3)$$

By integrating Eq. (2.2) for a crack length which ranges from the initial value  $c_i$  to the final value  $c_c$ , it can be observed that glass fails in a time  $t_f$  in which the nominal tensile stress increases in a linear manner from the value 0 to the value  $f_g$ . Hence

$$\int_{c_i}^{c_c} c^{-\frac{n}{2}} \cdot dc = \int_0^{t_f} v_0 \cdot \left( \frac{\sigma(t) \cdot Y \cdot \sqrt{\pi}}{K_{IC}} \right)^n dt = \int_0^{t_f} v_0 \cdot \left( \frac{\dot{\sigma} \cdot t \cdot Y \cdot \sqrt{\pi}}{K_{IC}} \right)^n dt, \quad (2.4)$$

where  $t_f = f_g / \dot{\sigma}$ .

It should be noted that Eq. (2.4) disregards the effect of the static fatigue threshold, i.e., it assumes that also for  $K_I < K_{I0}$  the crack increases. To take account of the fact that for  $K_I < K_{I0}$  the crack does not propagate, the integration should commence from instant  $t_0$  at which the tensile stress reached the level for which, with the initial crack length  $c_i$ ,  $K_I = K_{I0}$ . Taking this effect into consideration, the integration of Eq. (2.4) could not be carried out in a closed form as  $t_0$  is not explicitly known. However, the error committed is marginal and in any case represents a positive safety margin. In what follows, therefore, this approximation will be made. However, whenever greater precision is required, we can take account of the  $K_{I0}$  limit with an iterative procedure. In this circumstance, with a first-attempt estimate of  $c_i$ , the time  $t_0$  necessary to reach a combination of length of crack and acting tensile stress for which  $K_I = K_{I0}$  is obtained: this value is added to Eq. (2.4) as the first instant of integration, thus finding a second value of  $c_i$ ; the procedure is repeated until the value of  $c_i$  converges with a set tolerance. Naturally Eq. (2.4) also disregards the dynamic effects of the loading. However, this effect is difficult to evaluate and generally non-significant.

Assuming the parameters  $v_0$  and  $n$  to be constant, Eq. (2.4) can be integrated in closed form, obtaining

$$\frac{2}{n-2} \cdot \left( c_i^{\frac{2-n}{2}} - c_c^{\frac{2-n}{2}} \right) = \frac{v_0}{n+1} \cdot \left( \frac{Y \cdot \sqrt{\pi}}{K_{IC}} \right)^n \cdot f_g^n \cdot t_f = \frac{v_0}{n+1} \cdot \left( \frac{Y \cdot \sqrt{\pi}}{K_{IC}} \right)^n \cdot \frac{f_g^{n+1}}{\dot{\sigma}}. \quad (2.5)$$

Given that the exponent  $n$  is rather high (16 for soda-lime silicate glasses and even larger for borosilicate glasses), if  $c_i/c_c < 0.5$  the term containing  $c_c$  in the first member of Eq. (2.5) can be ignored in respect of the corresponding member with  $c_i$  (error  $< 1\%$  for  $n = 16$  e  $c_i/c_c = 0.5$ ). This approximation is generally legitimate in this phase as, given the low speed of application of the load in the standard test, the critical (final) size of the crack  $c_c$  is significantly greater than the initial size of the crack  $c_i$  (the crack is given time to grow); in any case there are cases in which the  $c_i/c_c$  ratio tends towards 1 and as a result the aforementioned approximation is no longer acceptable. In these instructions, in contrast with common practice, this approximation is not assumed.

In the standard test, relative humidity is between 40 and 70 %, corresponding to values of  $v_0 = 0.0013$  m/s and  $n = 16$ . From Eq. (2.5) the value  $c_i$  is thus immediately obtained in the form

$$c_i = \left[ \frac{n-2}{2} \cdot \frac{v_0}{n+1} \cdot \left( \frac{Y \cdot \sqrt{\pi}}{K_{IC}} \right)^n \cdot \frac{f_g^{n+1}}{\dot{\sigma}} + \left( \frac{Y \cdot f_g \cdot \sqrt{\pi}}{K_{IC}} \right)^{n-2} \right]^{\frac{2}{2-n}}. \quad (2.6)$$

Once  $c_i$  has been derived using the model just described, the ultimate tensile strength can be obtained for load histories and conditions different from those from the standard test. Indeed, if  $c_i$  is known

and the load history established, given  $n$  and  $v_0$  according to the type of glass and conditions of humidity, by resolving the differential equation (2.2) we derive the curve representing the growth of the crack over time and the moment of failure when  $K_I$  reaches the critical value  $K_{IC}$ .

A case that is certainly of interest is that of constant load, for which a limit time  $t_L$  corresponding to failure of the glass can be determined. Ignoring any dynamic effects and temporary arrangements, assuming that conditions of humidity do not change over time  $t_L$  so that  $v_0$  and  $n$  also remain constant, the model makes it possible to derive the limit stress  $\sigma_L$  which, applied constantly for duration  $t_L$  in the conditions of humidity considered, causes the glass in question to fail. From Eq. (2.4) we derive – once again ignoring temporary effects – the integral equation

$$\int_{c_i}^{c_{cL}} c^{-\frac{n}{2}} \cdot dc = \int_0^{t_L} v_0 \cdot \left( \frac{Y \cdot \sigma_L \cdot \sqrt{\pi}}{K_{IC}} \right)^n dt, \quad (2.7)$$

where the critical limit dimension of the crack  $c_{cL}$  is defined by an analogous equation to Eq. (2.3), where  $f_g$  is substituted by  $\sigma_L$ . By integrating, we obtain

$$\frac{2}{n-2} \cdot \left( c_i^{\frac{2-n}{2}} - c_{cL}^{\frac{2-n}{2}} \right) = v_0 \cdot \left( \frac{Y \cdot \sqrt{\pi}}{K_{IC}} \right)^n \cdot \sigma_L^n \cdot t_L. \quad (2.8)$$

Given the high value of the exponent  $n$ , this equation shows that the duration of application of the load plays a primary role in the strength of the material. Expanding, we obtain:

$$\sigma_L^n \cdot t_L = \frac{\frac{2}{n-2} \cdot \left( c_i^{\frac{2-n}{2}} - c_{cL}^{\frac{2-n}{2}} \right)}{v_0 \cdot \left( \frac{Y \cdot \sqrt{\pi}}{K_{IC}} \right)^n} = \frac{\frac{2}{n-2} \cdot c_i^{\frac{2-n}{2}} \cdot \left[ 1 - \left( \frac{c_i}{c_{cL}} \right)^{\frac{n-2}{2}} \right]}{v_0 \cdot \left( \frac{Y \cdot \sqrt{\pi}}{K_{IC}} \right)^n}, \quad (2.9)$$

which provides the final domain of interaction of the stress applied and the time of application. This equation is obviously valid only when  $\sigma_L$  lies within the range

$$K_{I0} / (Y \sqrt{\pi \cdot c_i}) < \sigma_L < K_{IC} / (Y \sqrt{\pi \cdot c_i}). \quad (2.10)$$

In conclusion, having established the constant acting stress  $\sigma_L$ , equation (2.9) directly gives us the time  $t_L$  necessary to induce failure. Contrariwise, having established the duration of the load  $t_L$ ,  $\sigma_L$  can be found using a simple iterative process, given that  $c_{cL}$  also depends on the unknown  $\sigma_L$ .

The model expounded thus makes it possible to go from tensile strength  $f_g$  measured in the laboratory to the value corresponding to the duration of the load and the environmental conditions of the situation under consideration. Naturally, this assumes that the glass in service exhibits the same defectiveness as the glass tested in the laboratory. Unfortunately, as stated above, glass undergoes significant processes prior to installation, and these processes generally increase its defectiveness, which must be taken into account with appropriate coefficients.

For extremely short load durations (measured in thousandths of seconds), the growth of the crack under load is imperceptible and the static fatigue may be ignored. In this case  $\sigma_L$  can be derived directly from Eq. (2.1) in the form

$$\sigma_L = \frac{K_{IC}}{Y \cdot \sqrt{\pi \cdot c_i}}. \quad (2.11)$$

If  $t_L > 0.01$  s, since  $c_{cL}$  is significantly greater than  $c_i$ , the term  $c_i/c_{cL}$  in (2.9) may be ignored, obtaining

$$\sigma_L^n \cdot t_L = \frac{\frac{2}{n-2} \cdot c_i^{\frac{2-n}{2}} \cdot \left[ 1 - \left( \frac{c_i}{c_{cL}} \right)^{\frac{n-2}{2}} \right]}{v_0 \cdot \left( \frac{Y \cdot \sqrt{\pi}}{K_{IC}} \right)^n} \cong \frac{\frac{2}{n-2} \cdot c_i^{\frac{2-n}{2}}}{v_0 \cdot \left( \frac{Y \cdot \sqrt{\pi}}{K_{IC}} \right)^n} \Rightarrow \sigma_L \cong \frac{K_{IC}}{Y \cdot \sqrt{\pi}} \left[ \frac{2}{n-2} \frac{c_i^{\frac{2-n}{2}}}{v_0} \right]^{\frac{1}{n}} t_L^{-\frac{1}{n}}. \quad (2.12)$$

For  $t_L = 0.01$  s, using Eq. (2.12) in place of Eq. (2.9) gives an error of approximately 3.1%; for load application durations in the order of around one second, the error can be completely disregarded.

If the action is variable over time, in order to derive its effects it is necessary to integrate equation (2.2). It is nevertheless common practice in the design process to replace the action actually applied with an equivalent constant static action of an appropriate duration. Eqs. (2.9) or (2.12) thus make it possible to derive the accumulation of damage over time.

Given the stress  $\sigma_g$  applied to the glass, Eq. (2.1) directly furnishes the size of the crack corresponding to a stress intensity factor equal to the threshold value  $K_{I0}$  in the form

$$c_0 = \left( \frac{K_{I0}}{\sigma_g \cdot Y \cdot \sqrt{\pi}} \right)^2. \quad (2.13)$$

If  $c_i < c_0$ ,  $\sigma_g$  does not in any case bring about the sub-critical growth of the crack and no static fatigue is produced. Current design practice usually leaves out the threshold value  $K_{I0}$ . However, this decision, which is always conservative, in the most common relevant cases does not lead to significant differences.

### 2.1.1.2 Definition of the $k_{mod}$ coefficient

Many standards (AS 1288-2066, ASTM E1300-09, prEN 16612-2013) introduce a coefficient  $k_{mod}$ , which appropriately reduces the tensile strength of glass in order to take account of the phenomenon of static fatigue in a practical manner. Given the tensile strength,  $f_g$ , of glass, calculated in accordance with the relevant standard, and the characteristic duration,  $t_L$ , of the action which causes the stress  $\sigma_L$  (assumed to be constant), the  $k_{mod}$  factor is defined by the condition

$$\sigma_L = k_{mod} f_g \Leftrightarrow c = c_L \text{ for } t = t_L. \quad (2.14)$$

In other words, a load which acts for a duration  $t_L$  and which causes a lower stress value than  $k_{mod} f_g$ , does not cause the material to fail.

Using the value  $f_g = 45$  MPa, i.e., the minimum prescribed value in the product standards for annealed soda-lime silicate float glass, Table 2.2 illustrates the values of the  $k_{mod}$  coefficient as a function of a few load durations  $t_L$ , as are characteristic of typical actions on constructions.

The values for  $k_{mod}$  derived from the Linear-Elastic Fracture Mechanics (LEFM) model described above are compared in the same table with the corresponding values proposed by the European draft standard prEN 16612 (2012 edition). This comparison is also represented by the graphs in Figure 2.5. It is pointed out that, in general, the values set out here are slightly more conservative. In practice, prEN 16612 assumes the value  $k_{mod} = 1$  for actions of shorter duration (e.g. gusts of wind), while the LEFM model assumes that  $k_{mod} = 1$  for instantaneous actions.

Table 2.2.  $k_{mod}$  factor derived from the LEFM theory for  $f_g = 45$  MPa,  $v_0 = 0.0025$  m/s and  $n = 16$ , for various load application times  $t_L$ . Comparison with values provided in prEN16612-2013.

Duration $t_L$	$k_{mod}$ LEFM	$k_{mod}$ prEN16612	Example
3-5 seconds	0.91 - 0.88	1.00	wind (gust)
30 seconds	0.78	0.89	temporary transit
10-15 minutes	0.65 - 0.64	0.74 - 0.72	wind (cumulative)
11 hours	0.50	0.57	daily temperature variations
1 week	0.42	0.48	snow (1 week)
3 months	0.36	0.41	snow (3 months)
6 months	0.35	0.39	seasonal temperature variations
50 years	0.26	0.29	self-weight

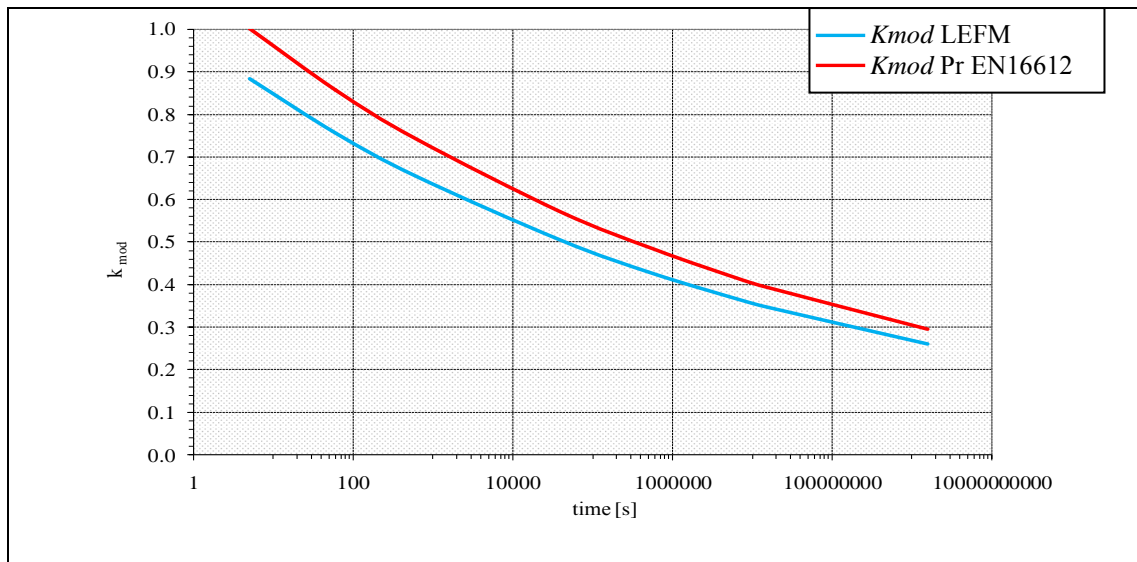


Figure 2.5. Graphical comparison between values of  $k_{mod}$ , derived with the LEFM model ( $f_g = 45$  MPa,  $v_0 = 0.0025$  m/s,  $n = 16$ ), with the values provided in prEN 16612 (2013 edition).

By applying least squares regression to the data in Table 2.2, for the  $k_{mod}$  factor we derive the equation

$$k_{mod} = 0.585 \cdot t_L^{-1/16}, \tag{2.15}$$

where  $t_L$  represents the duration of the load expressed in hours.

Different values of  $k_{mod}$  can be obtained by considering environmental conditions to which a different  $v_0$  corresponds. For environmental conditions for which  $v_0 = 0.0013$  m/s, we obtain slightly higher values of  $k_{mod}$ , although they are approximately 8% lower than those indicated in prEN 16612 (2013 edition).

### 2.1.1.3 Prestressed glass

In prestressed glass, the stress intensity factor is not directly proportional to the stress  $\sigma_g$  acting upon it, (nominal stress), but depends on the algebraic sum of  $\sigma_g$  and the residual stresses caused by the tempering process conducted on the glass plate.

In terms of stress intensity factor, the contribution of the prestressing process (which induces compressions on the surface of the plate) can be taken into account by means of an additional, negative term  $K_{IR}$ . In this way, the stress intensity factor  $K_I$ , due to the external applied stress  $\sigma_g$ , assumed to be virtually constant along the length of the characteristic crack  $c$ , and the residual stresses resulting from the prestressing process, may be written in the form

$$K_I = Y \cdot \sigma_g \cdot \sqrt{\pi \cdot c} + K_{IR} . \quad (2.16)$$

In (2.16) the only difficulty consists in the evaluation of the factor  $K_{IR}$ .

### 2.1.1.3.1 Heat-strengthened and thermally toughened glass

Residual stresses imparted through the thermal tempering process are usually assumed to follow a parabolic curve across the thickness  $s$ , i.e. in the form

$$\sigma_R(z) = \sigma_p \cdot \left[ 1 - 6 \cdot \frac{z}{s} + 6 \cdot \left( \frac{z}{s} \right)^2 \right], \quad (2.17)$$

where  $z$  is the reference coordinate orthogonal to the plane of the plate, while  $\sigma_p (< 0)$  represents the residual surface compression stress (on the faces  $z = 0$  and  $z = s$ ). From (2.17) it transpires that the plate is under compressive stress on both of the faces down to a depth of approximately 20% of the thickness, while the central part (i.e. about 60% of the thickness) is under tensile stress. The thickness under compressive stress due to the tempering process is much greater than the depth of the cracks normally present on the surface of the plate.

Assuming the case of a semi-circular surface crack with a radius  $c$ , the stress intensity factor for the residual stresses  $K_{IR}$  can be derived from the equation [Aben & Guillemet, 1993; Le Bourhis, 2008]

$$K_{IR} = Y \cdot \sqrt{\pi \cdot c} \cdot \frac{2}{\pi} \int_0^c \frac{\sigma_R(z)}{\sqrt{c^2 - z^2}} dz , \quad (2.18)$$

which, considering Eq. (2.17), gives us

$$K_{IR} = Y \cdot \sqrt{\pi \cdot c} \cdot \sigma_p \cdot \left[ 1 - \frac{12}{\pi} \cdot \frac{c}{s} + 3 \cdot \left( \frac{c}{s} \right)^2 \right]. \quad (2.19)$$

In the case of a plate subjected to bending, the stress varies in a linear fashion in relation to the thickness; by denoting the maximum tensile stress in proximity to the surface as  $\sigma_{g\text{-max}}$ , the stress curve in relation to thickness can be written as

$$\sigma_g(z) = \sigma_{g\text{-max}} \cdot \left( 1 - 2 \cdot \frac{z}{s} \right), \quad (2.20)$$



hence (2.16) assumes the form

$$K_I = Y \cdot \sqrt{\pi \cdot c} \cdot \left\{ \sigma_{g\text{-max}} \cdot \left( 1 - \frac{4}{\pi} \cdot \frac{c}{s} \right) + \sigma_p \cdot \left[ 1 - \frac{12}{\pi} \cdot \frac{c}{s} + 3 \cdot \left( \frac{c}{s} \right)^2 \right] \right\}. \quad (2.21)$$

In general, disregarding the variation in  $\sigma_g$  in relation to the depth of the crack acts as a positive safety margin, given that  $c/s \ll 1$ . Hence the following equation is preferred here:

$$K_I = Y \cdot \sqrt{\pi \cdot c} \cdot \left\{ \sigma_{g\text{-max}} + \sigma_p \cdot \left[ 1 - \frac{12}{\pi} \cdot \frac{c}{s} + 3 \cdot \left( \frac{c}{s} \right)^2 \right] \right\}. \quad (2.22)$$

As  $\sigma_p < 0$ , for the purpose of determining mechanical strength, we are only interested in the values of  $\sigma_{g\text{-max}}$  for which  $K_I > 0$ . When  $\sigma_{g\text{-max}}$  determines that  $K_I = K_{IC}$ , the glass fails immediately; when  $\sigma_{g\text{-max}}$  determines that  $K_{I0} < K_I < K_{IC}$ , the glass is subjected to static fatigue. In tempered glass, nevertheless, the sub-critical propagations of the crack is much faster than in annealed glass: indeed, the further the apex of the crack propagates inwards, the greater the tensile stresses it encounters, as precompression decreases.

Assuming approximate precompression values of  $\sigma_p = -90$  MPa for tempered glass and  $\sigma_p = -45$  MPa for thermally toughened glass, the mechanical strength which would be obtained by assuming  $K_I = K_{IC}$  in (2.22) are shown in Figure 2.6 for various thicknesses as a function of the depth of the crack  $c$ . The graph generally illustrates the considerable beneficial effect produced by precompression.

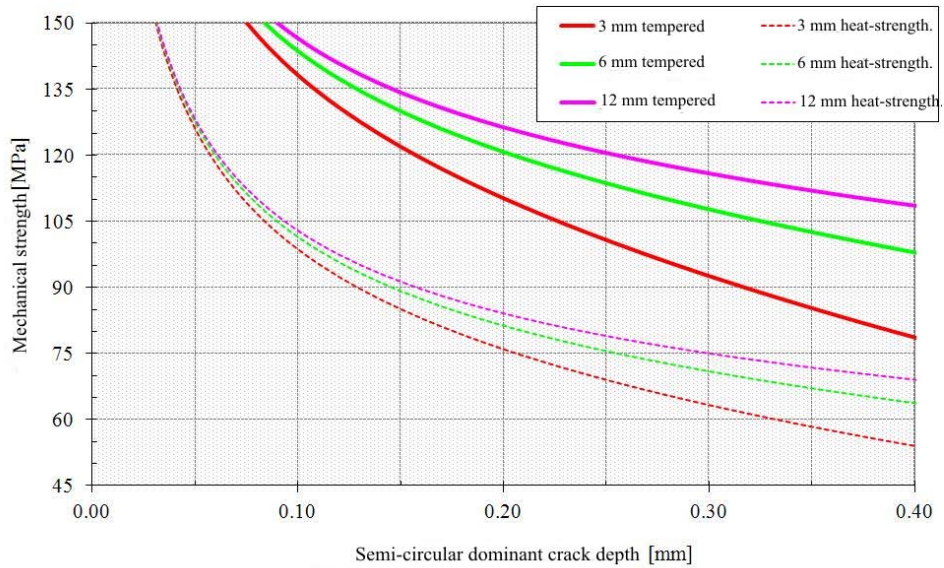


Figure 2.6. Mechanical strength under bending as a function of the dominant crack depth (assuming semi-circular cracks) for different thicknesses of tempered glass ( $\sigma_p = -90$  MPa) and thermally toughened glass ( $\sigma_p = -45$  MPa).

The macroscopic stress value corresponding to the activation of the sub-critical growth of the crack is obtained by assuming  $K_I = K_{I0}$  in (2.22). The corresponding graph is shown in Figure 2.7, where it can be noted that the phenomenon occurs for much higher stress values than in annealed glass.

The apparent reduction in mechanical strength as a result of the duration of the application of the load, calculated from (2.22) and the fracture mechanics model proposed, is illustrated in Figure 2.8

for  $v_0 = 0.0025$  m/s and  $n = 16$ . For comparison purposes, the data for annealed glass and from draft standard PrEn16612-2013 are also provided.

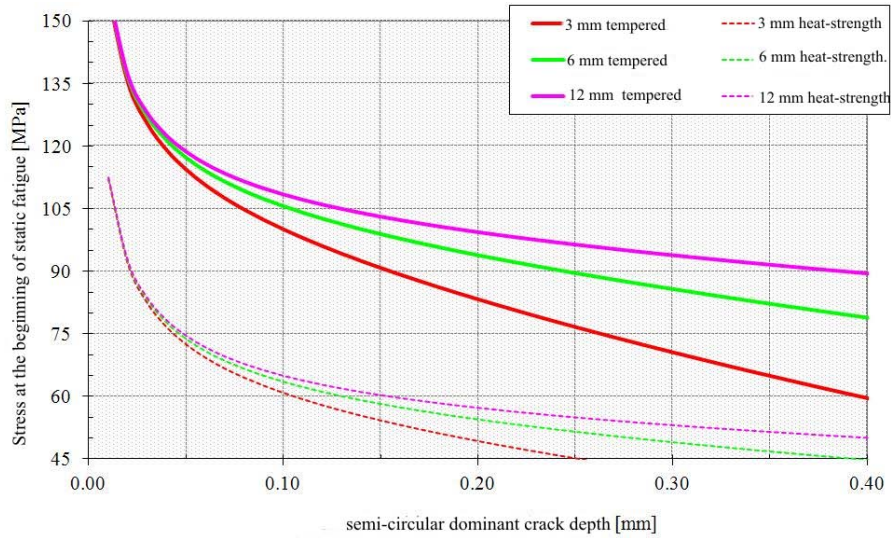


Figure 2.7. Macroscopic stress in the bending test corresponding to the beginning of static fatigue as a function of the dominant crack depth for different thickness of tempered glass ( $\sigma_p = -90$  MPa) and thermally toughened glass ( $\sigma_p = -45$  MPa).

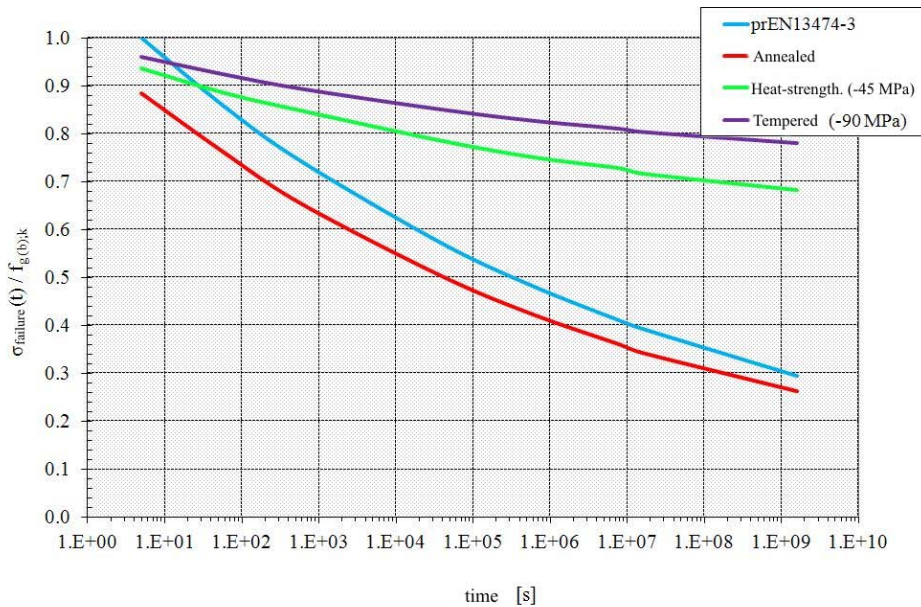


Figure 2.8. Apparent reduction in mechanical strength as a result of the duration of application of load in tempered glass ( $\sigma_p = -90$  MPa) and thermally toughened glass ( $\sigma_p = -45$  MPa) for  $v_0 = 0.0025$  m/s and  $n = 16$ . Comparison with data from draft standard prEN16612 (2013 edition).

### 2.1.1.3.2 Chemically strengthened glass

Chemically strengthened glass, sometimes called chemically tempered glass, requires a different equation from Eq. (2.16) as its residual stress profile is drastically different from that of thermally toughened glass. More specifically, the compressive stresses induced by the process affect a smaller thickness (approximately 0.04 mm) than in thermally toughened glass, and generally smaller than the depth of the crack (0.1 mm).

For chemically strengthened glass, therefore, a model [Green, 1984] can be used in which the crack is assumed to be only partially closed as a result of surface compression (Figure 2.9a). When the

depth of the crack exceeds the thickness  $t$  of the layer under compression, the strengthening due to the increase in surface compression  $\sigma_p$  is subject to saturation: the lower the ratio  $t/a_0$ , i.e. of the thickness of the layer under compression  $t$  to the size of the crack  $a_0$ , the less the strengthening that can be obtained, irrespective of the surface compression introduced (Figure 2.9b).

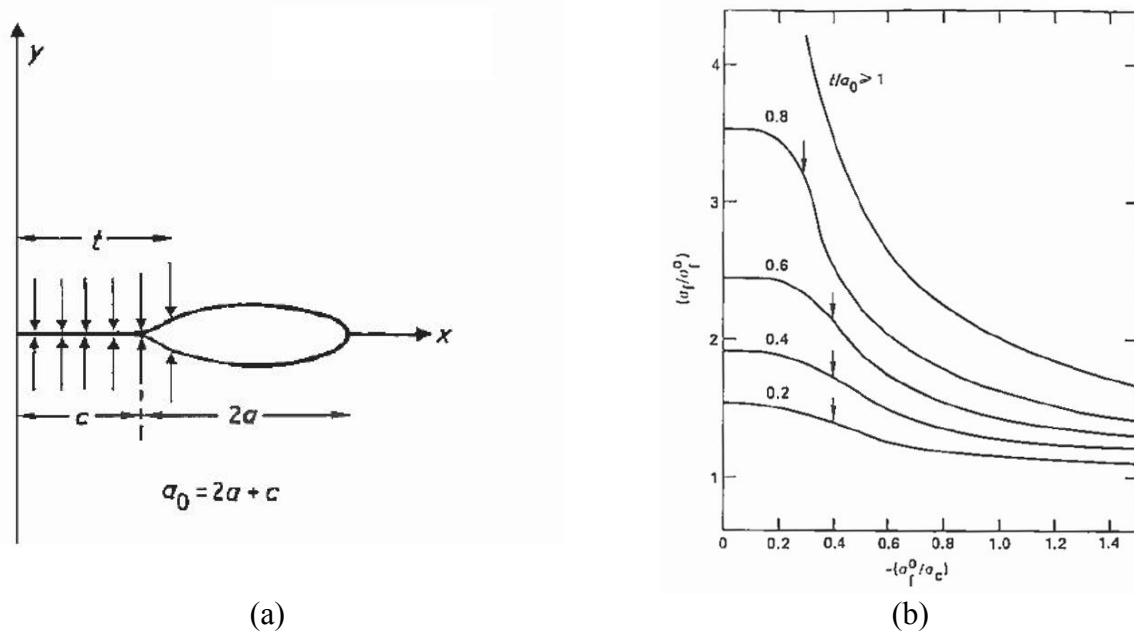


Figure 2.9. (a) Surface crack partially closed by the compressive tension introduced by chemical strengthening. (b) Strengthening due to chemical strengthening ( $\sigma_f/\sigma_{f0}$ ) as a function of initial mechanical strength ( $\sigma_{f0}$ ) and of surface compression ( $\sigma_c$ ) with the change in the ratio of thickness layer under compression and size of crack  $t/a_0$ .

Tensile strength is thus strongly influenced by all events following the production phase (handling, transport, installation and service) which cause particularly deep cracks to be present. The phenomenon of saturation accounts for the limit of 150 MPa recommended by product standard UNI EN 12337-1 for the characteristic strength of chemically strengthened float glass, although the surface compression attainable may be much higher than the compression introduced by the process of thermal toughening. In order to achieve a greater degree of strengthening, it would be necessary to increase the depth of the layer under compression; however, increasing the thickness of the compressed zone leads to a considerable increase in the length of time necessary for the chemical strengthening process – which is already particularly lengthy compared with the process of thermal toughening – and as a result, an increase in manufacturing costs.

Tensile strengths above the limit of 150 MPa are accepted only if it is possible to adequately demonstrate both the level of surface compression and the depth of the compressed surface layer (case depth) [ASTM C1422-99] or if the glass element has been protected against potential damage by post-manufacturing processes (e.g. protection of the glass plate, or chemically strengthened glass plates as part of laminates).

By way of example, ASTM C1422-99 defines various classes of chemically strengthened glass depending on the surface compression value  $\sigma_p$  (levels 1-5) as well as the tempering depth (levels A-E). These values are set out in Table 2.3.

Table 2.3. Classification of types of chemically tempered glass according to ASTM C1422-99.

Surface compression	$\sigma_p^*$ [MPa]	Tempering depth	$t$ [ $\mu\text{m}$ ]
Level 1	$7 < \sigma_p \leq 172$	Level A	$t \leq 50$
Level 2	$172 < \sigma_p \leq 345$	Level B	$50 < t \leq 150$
Level 3	$345 < \sigma_p \leq 517$	Level C	$150 < t \leq 250$
Level 4	$517 < \sigma_p \leq 690$	Level D	$250 < t \leq 350$
Level 5	$\sigma_p > 690$	Level E	$350 < t \leq 500$

\*Value for specific measurement method

### 2.1.2 Characteristic values of bending strength of glass

The tensile strength of glass can be defined by means of the stress intensity factor, which depends on nominal tensile strength and the length of the crack. Nevertheless, in structural design it is standard practice to conduct tests in terms of stress. Recourse to the model which uses the stress intensity factor therefore serves to define a nominal tensile strength, which is dependent on the duration of the load, and can be used directly in structural tests. These values will be used to calculate the design strengths in Chapter 5 below.

#### 2.1.2.1 General references

Minimum values for characteristic tensile bending strength are indicated in specific product standards. Table 2.4 shows the characteristic values ( $f_{g;k}$ ) (for annealed glass) and  $f_{b;k}$  (for prestressed glass) as set out in European Standards EN 1863, EN 12150 and EN 12337.

Table 2.4. Minimum values of characteristic tensile bending strength for anneal glass plates ( $f_{g;k}$ ) and prestressed glass plates ( $f_{b;k}$ ) prescribed by product standards.

Product	An-nealed	Heat-strength-ened	Thermally toughened	Chemically strength-ened
Float glass plates	45 MPa	70 MPa	120 MPa	150 MPa
Patterned glass plates	-	55 MPa	90 MPa	150 MPa
Enamelled glass plates	-	45 MPa	75 MPa	-

In order to determine the characteristic strength of annealed float glass, the CEN/TC129-WG8 working group conducted a study in which 30 samples underwent testing, each consisting of an average of 25 specimens with sides of 1000 mm and a nominal thickness of 6 mm, supplied by different companies or by the same company but manufactured at different times. The samples were broken in accordance with EN 1288-2 (double ring on large surface).

The results for each production batch each yielded their own average, which was different from the others. In addition, it was noted that a single sample consisting of 25 test pieces (from a single production run) could not be representative of glass strength. Specifically, the analysis of a single sample is not sufficient to provide reliable values with regard to the lower values of probability of fracture. Indeed, it will be noted from Figure 2.10 that the data are highly dispersed, particularly for fracture probabilities lower than 10%.

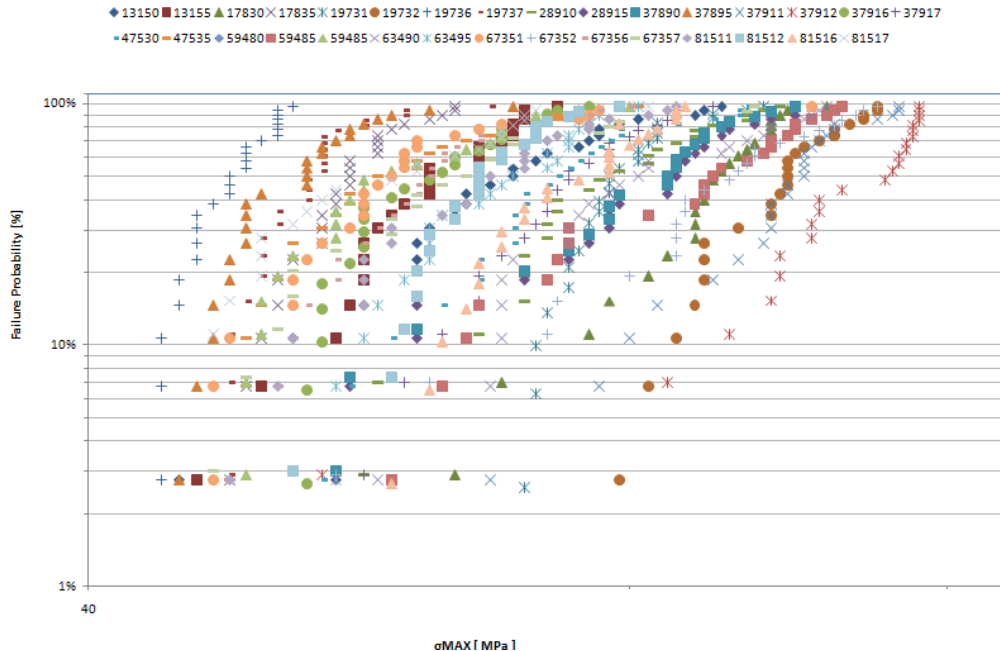


Figure 2.10. Probabilities of fracture derived from CEN experimental data on float glass plates with a thickness of 6 mm.

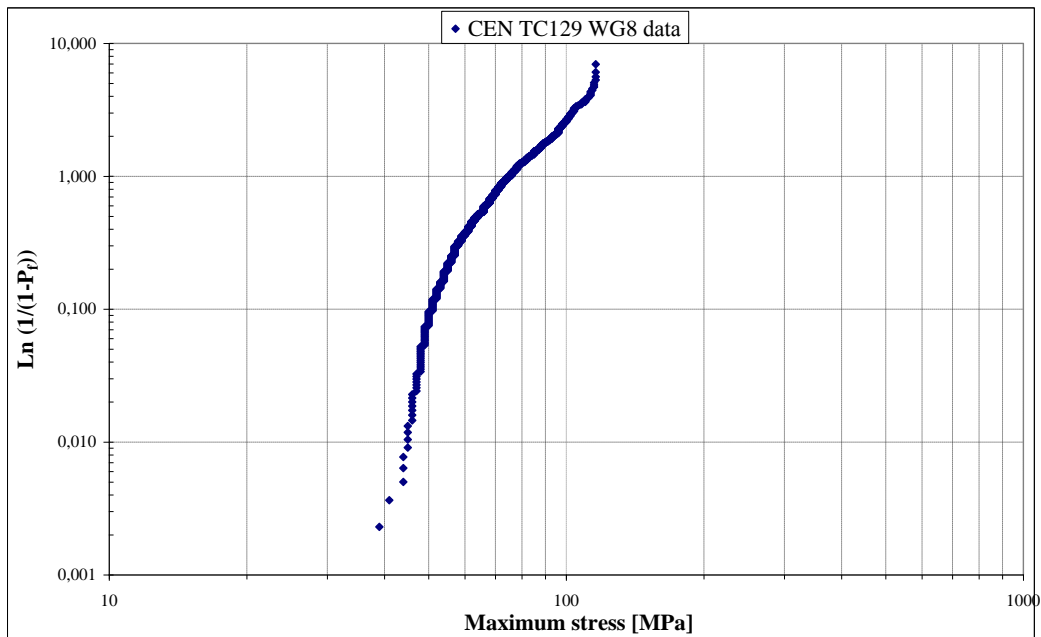


Figure 2.11. Weibull diagram of probability of failure as a function of the maximum stress grouping the CEN experimental data from tests performed on samples with a thickness of 6 mm.

The total number of test pieces (740 altogether) makes it possible to estimate the probability distribution shape for fracture as a function of stress. By indicating the probability of failure with  $P_f$ , the graph in Figure 2.11 gives the value of  $\text{Ln}[\text{Ln}(1/(1-P_f))]$  as a function of the logarithm of the ultimate tensile strength. If the Weibull distribution were perfectly applicable, the graph would show a straight line. It can thus be noted that the experimental data are not clearly interpretable using this statistical procedure and that, what is more, not even conventional statistics (two-parameter Weibull, Gaussian and log-normal distribution) are applicable. Nevertheless, the Weibull distribution is traditionally considered the most suitable, as it is the one which is traditionally applied to the case of fragile materials.

Fitting the best Weibull curve to the experimental data in Figure 2.11, it may be observed that the lower 5% fractile associated with the statistical distribution parameters is 45 MPa, while direct elaboration of the experimental data would yield a value of 48 MPa. Moving to even smaller lower fractiles (e.g. 1/10000) would in contrast lead to an underestimation of the ultimate stress compared with the values encountered in current practice.

It should also be pointed out that surface damage to the pane in use generally lowers the mean mechanical strength but also reduces dispersion of data. As a result, the value of the lower fractile is higher than that of a fractile relating to a distribution with the same average value but more widely dispersed data. The partial material safety factor must therefore take this effect into account in order to evaluate the design strength.

Finally, it is important to point out that the characteristic values of strength for heat-strengthened and thermally toughened glass and for chemically strengthened glass set out in the respective product standards are minimum acceptable values and are not derived from experiments comparable to the one carried out on annealed float glass by CEN. In the relevant product standards, compliance with this minimum value refers to four-point bending tests (EN 1288-3), i.e. for a state of uniaxial stress. The potential influence of the biaxial nature of any load is therefore not considered.

## 2.1.2.2 Statistical characterisation of the ultimate tensile strength of glass

### 2.1.2.2.1 Weibull distribution

As the mechanical strength of glass essentially depends on the presence of surface cracks of random sizes and orientations, experimental data are generally highly dispersed and require a statistical basis in order to be interpreted. In the area of fragile materials, the most widely used statistical formulation is the Weibull distribution.

For a two-dimensional solid (such as a plate), if  $A$  is the area of its middle surface, we may consider it to be divided into a large number of elements with an area  $dA$ , each with its own tensile strength. Fractures arising from the application of an external stress occur when any element of area  $dA$  fails (the “weakest link in the chain” model). The probability of failure of an element is therefore connected to the probability that said element is able to contain a critical defect.

Taking existing surface defects to be cracks which are orthogonal to the surface, it is convenient to define the tensile strength of glass not by reference to the stress intensity factor, but rather to the mean stress calculable in the element assumed to be free of defects. It can thus be said that the fracture propagates when the stress component in the direction of the normal to the crack plane exceeds the critical value  $\sigma_{Ic}$ , which represents the maximum mean uniaxial force in an element with the dominant crack aligned orthogonally to the axis of action of the stress (Mode I) in the absence of static fatigue. In general, the size, density and orientation of cracks on the surface of the solid can be interpreted using statistical distribution. According to the Weibull framework, the mean number of cracks *in the unit of area* with mechanical strength lower than  $\sigma_{Ic}$  can be expressed as follows [Evans, 1978; Batdorf & Heinisch, 1978; Chao & Shetty, 1990]

$$N(\sigma_{Ic}) = \left( \frac{\sigma_{Ic}}{\sigma_0^*} \right)^{m^*} . \quad (2.23)$$

The parameters  $m^*$  (modulus) and  $\sigma_0^*$  (reference strength) depend on the fracture toughness of the material and on the statistical distribution of the dimensions of the cracks on the surface. A high value of  $m^*$  indicates a low degree of dispersion of mechanical resistances, corresponding to evenly distributed defectiveness in the test sample. For  $m^* \rightarrow \infty$  the range of mechanical resistances tends towards 0, and all of the elements have the same mechanical strength.

Assuming that all portions of the surface  $A$  have the same probability of containing cracks and that

for these surface cracks all orientations contained within the angle  $\pi$  have the same probability of being present (homogeneous and isotropic defectiveness), the probability of fracture is given by [Munz & Fett, 1999]

$$P = 1 - \exp \left\{ - \int_A \left[ \frac{1}{\pi} \int_0^\pi N(\sigma_\perp) d\psi \right] dA \right\}, \quad (2.24)$$

where  $A$  is the surface area under tensile stress and  $\sigma_\perp$  the mean tensile stress orthogonal to the crack. For a state of in-plane tensile stress, if  $\sigma_1$  and  $\sigma_2$  are the principal stresses and  $\psi$  represents the angle between the projection of the normal to the crack on the plane  $\sigma_1$ - $\sigma_2$  and the direction  $\sigma_1$ , if  $r = \sigma_2/\sigma_1$ , the tensile stress  $\sigma_\perp$  is

$$\sigma_\perp = [\sigma_1 \cdot \cos^2(\psi) + \sigma_2 \cdot \sin^2(\psi)] = \sigma_1 \cdot [\cos^2(\psi) + r \cdot \sin^2(\psi)], \quad (2.25)$$

so that Eq. (2.24) can be written thus:

$$\begin{aligned} P &= 1 - \exp \left\{ - \int_A \left[ \frac{1}{\pi} \int_\psi \left( \frac{\sigma_\perp}{\sigma_0^*} \right)^{m^*} d\psi \right] dA \right\} \\ &= 1 - \exp \left\{ - \int_A \left[ \left( \frac{\sigma_1}{\sigma_0^*} \right)^{m^*} \frac{1}{\pi} \int_\psi (\cos^2 \psi + r \sin^2 \psi)^{m^*} d\psi \right] dA \right\}. \end{aligned} \quad (2.26)$$

More generally, when the state of stress is not in-plane or the normal to the crack forms an angle  $\psi \neq \pi/2$  with the normal to the plane  $\sigma_1$ - $\sigma_2$ , the main stresses may be reduced to an equivalent in-plane stress. However, we do not consider this possibility here.

Following [Beason & Morgan, 1984], it is therefore possible to introduce a correction factor  $C$  for the state of biaxial stress in the form

$$C = \left[ \frac{2}{\pi} \int_0^\alpha (\cos^2 \psi + r \cdot \sin^2 \psi)^{m^*} d\psi \right]^{1/m^*}, \quad (2.27)$$

where  $\alpha = \pi/2$  if  $\sigma_2 \geq 0$  or  $\alpha = \arctan \sqrt{|1/r|}$  if  $\sigma_2 < 0$ . Equation (2.24) thus becomes

$$P = 1 - \exp \left[ - \int_A \left( \frac{C \cdot \sigma_1}{\sigma_0^*} \right)^{m^*} dA \right]. \quad (2.28)$$

In this equation,  $C$  is non-dimensional,  $\sigma_1$  has the dimensions of a stress, while  $\sigma_0^*$  encompasses the dimensions of the area on which the integration is performed. For example, if the area is expressed in  $\text{mm}^2$  and the stresses in MPa, then  $\sigma_0^*$  is measured in  $\text{MPa} \cdot \text{mm}^{2/m^*}$ .

Although the Weibull statistical distribution model applied to the fracture of fragile solids refers to instantaneous failure, the effects of the sub-critical growth of the fracture may in any case be considered in order to predict the lifetime of the solid subjected to tensile stress.

### 2.1.2.2.2 Influence of speed of application of load

Suppose that we wish to provide a statistical interpretation of mechanical strength values obtained experimentally in standardised environmental and testing conditions, in which the phenomenon of static fatigue plays a non-negligible role. The Weibull parameters  $m$  and  $\sigma_0$  provide the best interpretation of the experimental data according to an analogous equation to Eq. (2.23), henceforth expressed without asterisks in order to distinguish them from  $m^*$  and  $\sigma_0^*$ , which correspond to the ultimate (i.e. failure) tensile strengths (in a so-called “inert” testing environment).

Let  $f_g$  be the orthogonal stress to the plane of the crack that in the experimental and standardised testing conditions causes failure of the test piece; in accordance with the model illustrated above, this corresponds to an initial crack length  $c_i$  derived from Eq. (2.6). With such an initial defect, the test piece would fail instantaneously at an equivalent inert stress of  $\sigma_g = \sigma_{Ic\_eq}$  which is obtained from (2.1) by assuming  $K_I = K_{IC}$  and  $c = c_i$ . By substituting the corresponding equations, we obtain

$$\sigma_{Ic\_eq} = \left[ \frac{n-2}{2} \frac{v_0}{n+1} \left( \frac{Y\sqrt{\pi}}{K_{IC}} \right)^2 \frac{1}{\dot{\sigma}} + \frac{1}{f_g^3} \right]^{\frac{1}{n-2}} \cdot f_g^{\frac{n+1}{n-2}} \cong \left[ \frac{n-2}{2} \frac{v_0}{n+1} \left( \frac{Y\sqrt{\pi}}{K_{IC}} \right)^2 \frac{1}{\dot{\sigma}} \right]^{\frac{1}{n-2}} \cdot f_g^{\frac{n+1}{n-2}}. \quad (2.29)$$

Obviously, the probability of obtaining failure at the stress value  $f_g$ , under standardised testing conditions, and at the stress value  $\sigma_{Ic\_eq}$ , in neutral instantaneous conditions, must be equal to one another. Using Eq. (2.23) we obtain the condition

$$\left( \frac{f_g}{\sigma_0} \right)^m = \left( \frac{\sigma_{Ic\_eq}}{\sigma_0^*} \right)^{m^*}, \quad (2.30)$$

from which we derive

$$m = \frac{n+1}{n-2} \cdot m^*, \quad \sigma_0 = \left[ \frac{\sigma_0^{*n-2}}{\frac{n-2}{2} \frac{v_0}{n+1} \left( \frac{Y\sqrt{\pi}}{K_{IC}} \right)^2 \frac{1}{\dot{\sigma}}} \right]^{\frac{1}{n+1}}. \quad (2.31)$$

In conclusion, the step from a statistics based on instantaneous values obtained in a neutral environment and statistics obtained in testing conditions that take into consideration the phenomenon of static fatigue can be made without any particular difficulties by means of Eq. (2.31).

Under testing conditions, the probability of failure is therefore analogous to (2.28), i.e.

$$P = 1 - \exp \left[ - \int_A \left( \frac{C \cdot \sigma_1}{\sigma_0} \right)^m dA \right], \quad (2.32)$$

where

$$C = \left[ \frac{2}{\pi} \int_0^\alpha (\cos^2 \psi + r \cdot \sin^2 \psi)^m d\psi \right]^{\frac{1}{m}}. \quad (2.33)$$

Once the parameters  $m$  and  $\sigma_0$  have been determined, they can be used to predict the probability of failure of other test pieces under a different stress distribution.



**2.1.2.2.3 Influence of state of stress**

It should be stressed that the results of uniaxial tests are not directly comparable with those of equibiaxial tests (tests according to European Standards EN 1288-2 or EN 1288-5 are not truly equibiaxial). A test piece subjected to a uniaxial stress in fact has a lower probability of failure compared with that for the same piece subjected to a biaxial stress; in the second case a greater number of cracks will be orthogonal to the principal direction of the stress applied. Thus a criterion which allows the results to be made consistent is required.

In the case of an ideally equibiaxial test ( $\sigma_2 = \sigma_1 = \sigma$ ),  $C = 1$ , Eq. (2.32) reduces to

$$P_{eqbiax} = 1 - \exp \left[ - \int_A \left( \frac{\sigma}{\sigma_0} \right)^m dA \right]. \tag{2.34}$$

Assuming uniform stress and with the area under stress being equal, having established the probability of fracture, the correspondence between the uniaxial stress  $\sigma_{uniax}$  and the equibiaxial stress  $\sigma_{eqbiax}$  is given by

$$\sigma_{uniax} = \frac{\sigma_{eqbiax}}{\left[ \frac{2}{\pi} \int_0^{\pi/2} \cos^{2m}(\psi) d\psi \right]^{1/m}}. \tag{2.35}$$

The change in the ratio of the uniaxial stress  $\sigma_{uniax}$  to the equibiaxial stress  $\sigma_{eqbiax}$  as a function of the Weibull modulus  $m$  is illustrated in Figure 2.12.

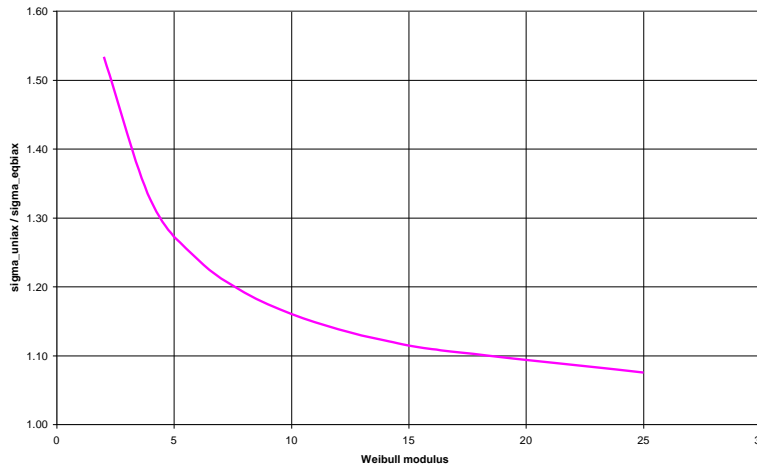


Figure 2.12. Change in the ratio of the uniaxial stress  $\sigma_{uniax}$  to the equibiaxial stress  $\sigma_{eqbiax}$  as a function of the Weibull modulus  $m$ .

When the true stress field is neither uniaxial nor equibiaxial, the effect of the state of stress and of the area  $A$  under stress on the probability of fracture can be condensed down to a multiplicative factor  $k$  to apply to the Weibull risk function, thus obtaining

$$P(\sigma_{max}, A) = 1 - \exp \left[ -k \cdot A \cdot \left( \frac{\sigma_{max}}{\sigma_0} \right)^m \right], \tag{2.36}$$

where  $\sigma_{\max}$  is the maximum principal stress on area  $A$ , while the product  $kA$  is indicated as the effective area  $A_{\text{eff}}$  for the stress  $\sigma_{\max}$ . In this case too it is assumed that the dimensions of the area  $A$  are encompassed in the parameter  $\sigma_0$ , whose dimensions are therefore those of a stress for an area elevated to  $1/m$ .

#### 2.1.2.2.4 Influence of the size of the surface under load

Having defined the characteristic tensile strength of glass  $f_{g,k}$  as the stress associated with a probability of failure  $P = 5\%$ , from Eq. (2.36) it can be deduced that this value must refer to the testing method used (stress field and area under stress), as it is highly dependent on the effective area  $A_{\text{eff}}$ , as illustrated in Figure 2.13 [Wereszczak *et al.*, 2010].

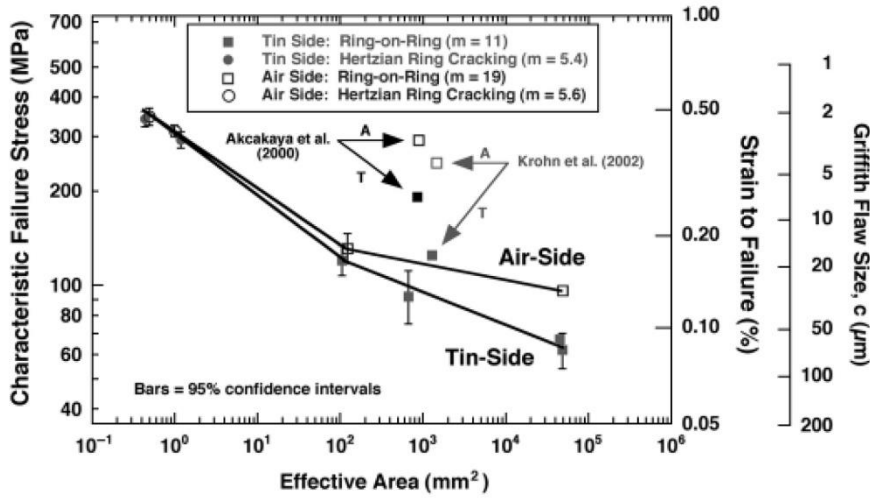


Figure 2.13. Scale effect of tin-side and air-side failures for float glass. Griffith flaw size ( $c = K_{IC}^2 / Y^2 \sigma^2$ ) calculated using the failure stress  $\sigma$  and assuming  $K_{IC} = 0.76 \text{ MPa}\sqrt{\text{m}}$  and  $Y=1.5$  [Wereszczak *et al.*, 2010]

Given a population of experimental results, the data can be rescaled appropriately so as to obtain a second (virtual) population that would correspond to various testing conditions. Therefore, if we interpret the experimental data by means of probability distribution (Eq. (2.36)) for another series of statistically identical samples subjected to an equibiaxial test which applies uniform stress to the unit of area  $UA = 1 \text{ m}^2$ , from Eq. (2.34) the following distribution is obtained:

$$P_{\text{eqbiax}} = 1 - \exp \left[ -UA \cdot \left( \frac{\sigma_{\max, \text{eqbiax}, UA}}{\sigma_0} \right)^m \right]. \quad (2.37)$$

The statistical distributions Eqs. (2.36) and (2.37) are identical, on condition that

$$UA \cdot \left( \sigma_{\max, \text{eqbiax}, UA} \right)^m = kA \left( \sigma_{\max, A_{\text{eff}}} \right)^m \Rightarrow \sigma_{\max, \text{eqbiax}, UA} = \sigma_{\max, A_{\text{eff}}} \left( \frac{kA}{UA} \right)^{1/m}, \quad (2.38)$$

where, for the purpose of distinguishing it, the value of  $\sigma_{\max}$  that appears in Eq. (2.36) is represented as  $\sigma_{\max, A_{\text{eff}}}$ . The relationship in Eq. (2.38) makes it possible to compare experimental results obtained using different test methods by relating the population of mechanical strengths to the conventional situation of unit of area under stress ( $UA = 1 \text{ m}^2$ ) subjected to an equibiaxial stress field. Specifically, with regard to the characteristic mechanical strength values for glass,  $f_{g,k}$ , we obtain

$$f_{g;k-UA} = f_{g;k-A_{eff}} \left( \frac{kA}{UA} \right)^{1/m} . \quad (2.39)$$

The effect of the different stress field and the different size of the surface under stress diminishes as the value of the Weibull modulus increases, as in the case of glass abraded artificially using sanding or similar treatments ( $m \geq 25$ ). However, it cannot generally be disregarded for float glass plates ( $m \sim 5$  air-side,  $m \sim 7$  tin-side).

If the stress is variable, the surface under load must be divided into a sufficiently large number of portions so that it can be considered effectively uniform in each one of them. Using Eq. (2.33), the probability of failure is then calculated by approximating the integral in Eq. (2.32) with the Riemann sums. From the comparison of the value of  $P_f$  thus obtained from Eq. (2.36), the effective area  $A_{eff} = kA$  can then be calculated.

### 2.1.2.3 Test methods for measuring the tensile strength of glass

The tensile strength of glass must be estimated on the basis of an experimental test which determines  $f_{g;k}$  under established, repeatable conditions. Essentially, two types of test are used for this purpose: Four-Point-Bending (FPB) and Coaxial-Double-Ring (CDR). In the former, the stress field generated is primarily uniaxial, while in the second it is biaxial. The two methods, described in European Standard EN 1288 (Parts 1, 2, 3 and 5), share the common goal of subjecting the test pieces to a uniform stress field within the load area.

It should in any case be noted that EN 1288 prescribes subjecting the weakest surface of the glass plate to tensile stress. This refers generally to the pre-treatment and surface condition of the test piece subjected to testing, but not explicitly to surface damage caused indirectly by treatments such as the influence of the tin side for float glass, or the surface passed over the furnace rollers for horizontally tempered glass plates.

Similarly, EN 1288 also highlights the possibility that tensile strength values may differ as a result of the load areas used and the stress states generated under testing, yet without going into further detail. As the results depend heavily on the surface conditions of the plate and on environmental conditions, during the tests it is essential to:

- separate surfaces with different intrinsic flaws (e.g. tin/air side for float glass, roller side for thermally tempered glass plates);
- maintain a constant rate of increase of stress ( $2 \pm 0.4$  MPa/s);
- monitor environmental conditions ( $T = 23 \pm 5^\circ\text{C}$ ; relative humidity = 40 – 70%).

Given the high dispersion of values for the mechanical strength of glass, EN 1288 prescribes the use of a high – yet unspecified – number of tests in order to determine the characteristic bending strength of glass plates. In order to perform a statistical evaluation of the results, the minimum representative sample of a batch is considered to be at least formed by 30 specimens.

EN 1288-2 and EN 1288-5 describe the double-ring bending test, with and without overpressure.

For tests conducted without overpressure, EN 1288-5 makes provision for different geometries (bearing and loading ring radii), chosen to limit geometric non-linearity, with the aim of rendering the radial and shear stresses within the loading ring as similar and uniform as possible (equibiaxiality) so that analytical relationships can be used to obtain the values of the resisting stresses starting from the failure loads.

The use of small stress areas is reflected in a greater dispersion of the results obtained and usually leads to an overestimation of the mechanical strength of the glass; this makes it necessary to increase the number of test pieces in order to obtain a correct estimation of the characteristic strength.

Given the large sizes of the panes, EN 1288 recommends the double-ring test with overpressure (EN 1288-2) to estimate the mechanical strength to be used in design, while it recommends the usual

double-ring tests without overpressure (EN 1288-5) as a method for comparative evaluation of the bending resistance of glass. In fact, in bending tests with a simple double ring, geometric non-linearity generally causes a peak in radial stresses below the loading ring, while the double-ring test method described in EN 1288-2 makes it possible to maintain biaxiality in the stress field in the central zone, although the presence of overpressure in the case of high loads causes a significant amount of variation in shear stresses and therefore the loss of equibiaxial behaviour.

Considering the size of the plates, the double-ring test with overpressure requires a purpose-designed device and a delicate simultaneous force and pressure control-management and application system. The complexity of this test can lead to low repeatability and greater dispersion of the experimental results obtainable from different laboratories; this circumstance increases the already considerable uncertainties regarding the mechanical strength of glass.

The four-point bending test (EN 1288-3) is much more widespread compared with the double-ring test. However, it is more strongly affected by machining of the plate edge and the effective state of stress on the bent surface.

The analysis of experimental data in accordance with the physical interpretation of the probability of fracture, however, makes it possible to correctly derive the statistical parameters which describe the mechanical strength of tests with similar stress states conducted with different areas of stress [Krohn *et al.*, 2002], provided that the effective Weibull area is not less than 100 mm<sup>2</sup> [Wereszczak *et al.*, 2010].

With regard to four-point bending tests, it should be pointed out that as a result of the size of the test pieces used (1100 × 360 mm<sup>2</sup>), the state of stress between the loading rollers is neither perfectly uniaxial nor constant along a cross-section. The maximum longitudinal stresses are concentrated along the edges, where the flaws are greatest; this variation in the stress field must not be disregarded when failures from the edge are also considered in evaluating the mechanical resistance of flat glass. Given the high probability of edge fracture of test pieces (especially in the case of annealed glass), the data obtained from in accordance with EN 1288-3 are also not representative of the mechanical strength of the surface of glass.

In conclusion, given the imperfect uniaxiality/equibiaxiality and uniformity of stress field produced in test conditions, the mechanical strength data to use in the design phase cannot be derived from a simple regression of the experimental values of ultimate failure stress. It is necessary to associate each ultimate failure value with the corresponding effective Weibull area and ultimately determine the parameters modulus  $m$  and reference strength  $\sigma_0$ , with a dependence only on the material tested and not on the test configuration.

### **2.1.3 Experimental campaign to determine the influence of the loaded area and of the type of test on the strength of float glass**

A campaign of experimental tests was conducted by the Stazione Sperimentale del Vetro on 400 annealed float glass plates of 6 mm in thickness. The samples used were provided by a single manufacturer, who cut and submitted the plates. All of the test pieces were square plates, 400 × 400 mm<sup>2</sup>, with unground edges, in order to have similar surface damage for the various families of samples. The dimensions of the test pieces (< 500mm) were chosen in order to be able to perform a coaxial double ring (CDR) test while taking account of the usual configuration of the test machines so as to make it easily repeatable.

The 400 test pieces were stressed to failure: 200 of them by subjecting the tin-side surface to tensile stress, and 200 the air-side surface. Of the 200 test pieces for each type of surface, 100 were broken using the coaxial double ring test without overpressure (approximately biaxial stress field) while 100 were subjected to the four-point bending test (primarily uniaxial stress field). For both CDR and FPB tests, two different load areas were used (50 test pieces for each area).

The side under tensile stress was always the one opposite to the surface where the incision had been

---

made to cut the test piece, so as to reduce edge failures during four-point bending tests. This made it possible to minimise the influence of edge breakages on the determination of the bending strength of the surface.

In the tests, which were conducted in strain driven conditions using a Tiratest 2750 testing machine, the stroke speed was controlled so as to maintain an increase in stress of  $2 \pm 0.4$  MPa/s, as specified in UNI EN 1288-1.

The CDR test uses a bearing ring with a radius of  $R_0 = 150$  mm and two loading rings with respective radii of  $R_1 = 75$  mm (A1) and  $R_2 = 53$  mm (A2), in order to highlight the effect of the area under load. The dimensions of the rings were chosen in order to attain the maximum load area, minimum geometric non-linearity and negligible edge failures. The stress field produced was analysed using the finite element method (FEM).

The FPB test, conducted for comparison purposes, differs from EN 1288-3 only for the geometric aspects (support/bearing and load beams, dimensions of test pieces). By maintaining a support beam  $L_0 = 360$  mm, two test areas were chosen, one with a load beam  $L_1 = 200$  mm (A1) and the other with a load beam  $L_2 = 120$  mm (A2). The stress field was analysed using FEM analysis, in order to estimate the tensile stress on the edge of the plate.

### 2.1.3.1 Experimental results

The experimental results summarised in Table 2.5 [Dall'igna *et al.*, 2010] confirm the need to maintain a distinction between the specimens subjected to tensile stress on the tin side or the air side. In general, plates which fail on the air side display considerably higher ultimate tensile strengths than those which fail on the tin side, but with more highly dispersed results. This difference is particularly marked because the test pieces, which were submitted for testing directly by the manufacturer after cutting, had not undergone any additional processes of transformation and hence any further damage. It is pointed out, in fact, that while surface damage on the one hand reduces average strength, on the other hand reduces dispersion considerably.

For FPB tests, the difference between the tin-side/air-side ultimate tensile strength is greater than the difference recorded with CDR tests, as many failures start from the edge of the plate where such diversification is less important.

It should be noted that for an identical type of test, the ultimate tensile strength increases as area decreases, as the probability of finding critical defects diminishes. The influence of area is of particular importance in evaluating experimental results and assumes fundamental importance when it is necessary to compare results obtained from tests with different geometries. Tests with the same load area but different stress fields (uniaxial/biaxial) still give different strength values. Specifically, greater strengths are observed for uniaxial stress fields (FPB tests). To sum up, lower strength values are observed for test pieces undergoing testing on the tin side, with biaxial stress fields, and for load areas with greater sizes.

It is clearly important that, when referring to strength values for glass, it is clearly mentioned which test has been used, which is the effective test area and what are the surface conditions.

The stress values corresponding to ultimate failure loads were calculated using three-dimensional numerical FEM simulations, with geometric non-linearity. The principal stresses acting on the surface under bending were processed by implementing an algorithm in MATLAB for determining the Weibull parameters ( $m$ ,  $\sigma_0$ ) for each sample, taking into consideration both the effect of the area and the effect of biaxiality. The respective results are reported in Figure 2.14 and Table 2.6, which refer to the case in which, in (2.36), the areas are measured in  $\text{mm}^2$  and the stresses in MPa. As a result, the parameter  $\sigma_0$  is expressed in  $\text{MPa mm}^{2/m}$ .

The numerous edge failures in FPB tests were interpreted as upper bounds in relation to the mechanical strength of the surface; this enabled a better statistical analysis of the experiments by making it possible to consider the presence of both families of defects (surface and edge) in evaluating the probability of fracture.

Once the parameters of the surface were known, it was possible to rescale the experimental data using Eq. (2.38) to the unit of area under equibiaxial stress. These data were then interpolated again with a Weibull statistic, obtaining the result in Figure 2.15 and the Weibull parameters in Table 2.7, where  $\sigma_0$  is again measured in  $\text{MPa mm}^{2/m}$ . The Weibull parameters obtained refer exclusively to the samples tested. Finally, Table 2.8 illustrates the strengths for a unit of area ( $UA = 1 \text{ m}^2$ ) and biaxial stress corresponding to a probability of fracture  $P = 5\%$ .

Although the double-ring without-pressure test is not currently regulated by a standard, the testing conducted indicates that this method is optimal for the determination of the characteristic strength of flat glass. Therefore we shall refer below to this type of test, the main virtues of which are its simplicity, the biaxial stress field produced and the absence of edge failures. The imperfect equibiaxiality induced by the geometrically non-linear behaviour of the plates subjected to bending was overcome by means of FEM analysis, calculating the effective stress distribution and introducing an appropriate effective area in the processing of the data, as described in Section 2.1.2.2.4. The values obtained for any given area can be converted in order to obtain the values for different reference areas.

The Weibull distribution interprets the experimental values in an optimal manner, which seems to confirm the validity of Weibull statistics to describe the phenomenon of breakage for glass.

Indeed, 50 test pieces are an adequate sample to obtain representative results for each single family of plates, making it possible to obtain a sound interpretation of the experimental data through the Weibull distribution.

The well-known difference in mechanical strength observable on the two surfaces of float glass (tin side and air side) has also been confirmed; this circumstance must be given due consideration in order to determine the characteristic mechanical strength of glass.

The different strength distributions within the same defectiveness family make clear their high degree of dependence on variations in the type of test (uniaxial and biaxial) and the size of the area under load.

Table 2.5. Number of specimens tested ( $n_{\text{tot}}$ ), ratio of the number of failures starting from the edge ( $n_e$ ) to failures starting from the surface ( $n_s$ ), external action (load) causing failure: maximum ( $F_{\text{max}}$ ), minimum ( $F_{\text{min}}$ ), mean ( $F_{\text{media}}$ ), standard deviation. Thickness of plates 6mm. Rate of stress increase 2 MPa/s.

Test method	Surface under bending	$n_{\text{tot}}$	$n_e/n_s$	$F_{\text{max}}$ [N]	$F_{\text{min}}$ [N]	$F_{\text{media}}$ [N]	Standard deviation [N]
FPB – A1	tin side	50	33/17	7763	2670	5355	1118
	air side	50	26/24	9726	3008	6474	1620
FPB – A2	tin side	50	38/12	5230	2367	3894	612
	air side	50	23/27	7207	1688	4509	1284
CDR – A1	tin side	51	51/0	10649	4493	7557	1271
	air side	50	50/0	20179	5047	13663	3441
CDR – A2	tin side	49	49/0	7689	3255	5486	1056
	air side	50	50/0	18292	4879	10485	3001

Table 2.6. Weibull parameters for float glass, annealed 6-mm plates. Rate of stress increase 2 MPa/s.

Test method	Surface under bending	$m$	$\sigma_0$ [MPa mm <sup>2/m</sup> ]
FPB – A1	tin side	7.4	403
	air side	5.9	750
FPB – A2	tin side	9.0	317
	air side	4.9	1118
CDR – A1	tin side	7.7	363
	air side	6.4	763
CDR – A2	tin side	7.0	419
	air side	5.1	1205

Table 2.7. Weibull parameters for surface of 6-mm annealed float glass plates obtained from mechanical strength data for unit of surface area (UA = 1 m<sup>2</sup>).

Test method	Surface under bending	$m$	$\sigma_0$ [MPa mm <sup>2/m</sup> ]
CDR – UA	tin side	7.3	406
	air side	5.4	1096

Table 2.8. Stress with probability of fracture 5% with reference to unit of surface area (UA = 1 m<sup>2</sup>), obtained for 6-mm annealed float glass plates.

Test method	Surface under bending	$\sigma_{5\%\_UA}$ [MPa]
CDR-UA	tin side	40.7
	air side	48.9
FPB-UA	tin side	54.4
	air side	56.5

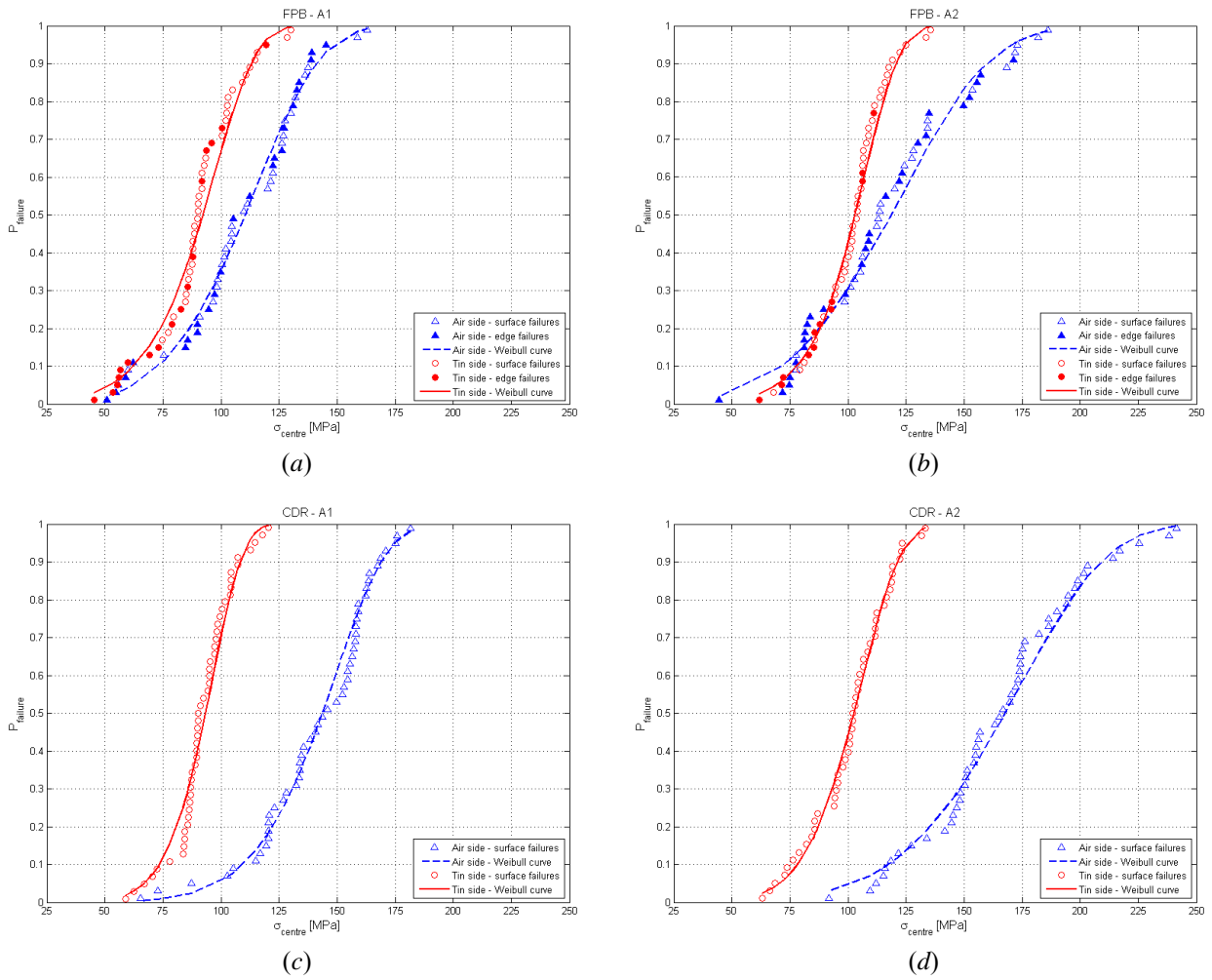


Figure 2.14. Cumulative probability of fracture as a function of failure stress (at the centre):  
 a) FPB with area  $A_1 = L_0 \cdot L_1$ ; b) FPB with area  $A_2 = L_0 \cdot L_2$ ; c) CDR with area  $A_1 = \pi R_1^2$ ; d) CDR with area  $A_2 = \pi R_2^2$ .

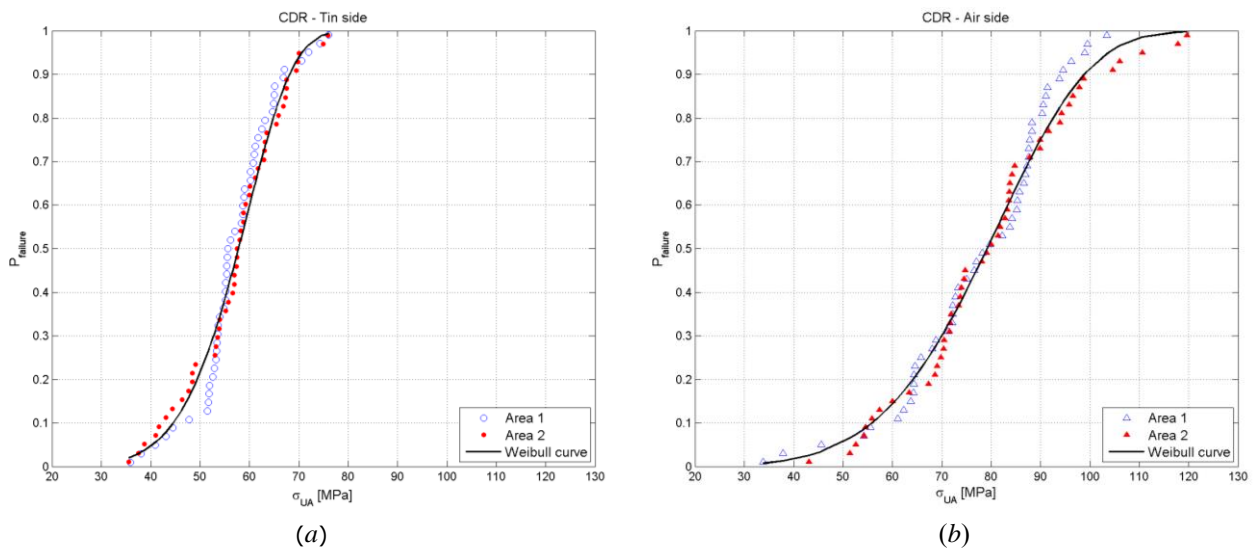


Figure 2.15. Cumulative probability of fracture as a function of effective stress (on unit of area) obtained from CDR test: a) tin side; b) air side.



### 2.1.4 Effects of edge finishing: plate edge and holes

Plates may be cut using various systems. The most common involves scoring the surface to facilitate and guide failure under bending, so as to obtain the desired dimensions. This operation, however, may produce cracks along the edge of the plate, with a consequent reduction in mechanical strength. The process of edge seaming (from a rough to a smooth edge) has the purpose of limiting the effects of this deterioration. Currently no systematic tests exist which indicate with any certainty the extent of the reduction in the value of the mechanical strength of the edge of the plate compared with that of its surface. The same considerations hold for deterioration in proximity to the surfaces of holes.

Discordant values are found in the literature. In the ASTM E1300-12a Standard, the deterioration due to cutting operations and grinding processes can be derived by comparing admissible stresses on the edge with those on the surface for annealed, heat-strengthened or thermally toughened glass; the reduction reaches a maximum of approximately 30% for the edge of unground annealed glass plates (Table 2.9). The [AS 1288-2006] and [prEN13474/3]<sup>4</sup> (2005 edition)] standards, in contrast, estimate a reduction of 20% in mechanical strength in proximity to the edge. Guideline values for the reduction factor  $k_{ed}$  for the mechanical resistance of the edge compared with those for the inner surface, derived from European draft standard prEN13474/3 (2005 edition) are given in Table 2.10.

However, in European draft standard prEN 16612-2013, as in other standards (e.g. VORSCHLAG ÖNORM B 3716-1:2006, DIN 18008), which primarily regards plates under bending, no reduction in edge mechanical strength is proposed. Therefore it is considered that such a reduction can be ignored for plates under bending, while it is recommended, as a precautionary measure, that it be taken into account for elements whose entire edge is subject to maximum tensile stress conditions, as may occur with glass beams or fins.

Table 2.9. Admissible stress on the surface and edge of annealed, heat-strengthened and thermally toughened plates for different edge machining processes ( $P_f < 0.008$ , load maintained for 3 s) [ASTM E1300-09a].

		Surface	edge		
			clean cut	seamed	Polished
annealed	$\sigma_{0.8\%; 3s}$ [MPa]	23.3	16.6	18.3	20
heat-strengthened	$\sigma_{0.8\%; 3s}$ [MPa]	46.6	-	36.5	
thermally toughened	$\sigma_{0.8\%; 3s}$ [MPa]	93.1	-	73.0	

Table 2.10. Mechanical resistance reduction factor  $k_{ed}$  for annealed glass plates according to European draft standard prEN13474/3 (2005).

Products	$k_{ed}$		
	clean cut	seamed	polished
Float glass plates	0.8	0.9	1.0
Patterned glass plates	0.8	0.8	0.8

<sup>4</sup> Until 2009 the European draft standard prEN 13474 was divided into three parts (prEN 13474/1, prEN 13474/2 and prEN 13474/3). Since 2010 this distinction has been omitted.

### 2.1.5 Effects of surface treatments

Surface treatments such as acid etching, sand-blasting, decoration with inorganic frit, etc. all lead to a reduction in mechanical strength, as they introduce surface defects. This reduction in mechanical strength in relation to the characteristic strength can be expressed by means of a reduction factor to account for surface treatment,  $k_{sf}$ .

In the literature, an approximate quantification of deterioration owing to sand-blasting or etching is 60% [AS 1288-2006].

Experimental data obtained using mechanical strength tests performed by the working group CEN-TC129/WG19 on float glass discs with a diameter of 100mm and a thickness of 6mm, tested according to EN 1288-5, indicate that the process of sand-blasting causes a greater reduction in strength compared with that of acid etching. In the case of thermally toughened glass, the reduction in mechanical strength is of a lower percentage and of a different degree if the operation is performed before or after the thermal treatment.

Guideline values for the strength reduction factor due to surface treatment are provided in Table 2.11.

Table 2.11. Strength reduction factors  $k_{sf}$  due to surface sanding or acid etching treatment [AS 1288-2006, CEN-TC129/WG19]

	Surface treatment	CEN TC129/WG19	AS 1288-2006
annealed	sandblasted	0.52	0.4
	acid etched	0.94	
thermally toughened	toughened – sandblasted	0.82	-
	sandblasted – toughened	0.98	

For chemically strengthened glass, the processes of sand-blasting or etching cannot be performed. Enamelling, too, causes a reduction in mechanical strength depending on various factors (e.g. thermal dilatation coefficient, disperse crystalline phase particle size, thickness, etc.).

Product standards for heat-strengthened or thermally toughened glasses provide the minimum accepted value for 4-point bending resistance tests (EN 1288-3) on enamelled glass, from which we can derive a strength resistance factor due to enamelling of ~ 63% (thermally toughened glass) and ~ 64% (heat-strengthened glass).

## 2.2 Other materials used in composition with glass

Glass is also commonly used in combination with sheets of interlaid plastic materials, called interlayers, which make it possible to couple two or more plies, producing what can be defined as composite or laminated glass. The main purpose of creating a composition with plastic sheets is to retain falling fragments of glass in the event of failure of the glass, in order to prevent damage to things or injury to people.

The manufacture and marketing of laminated (safety) glass are subject to compulsory CE marking; the applicable harmonised product standard is EN 14449.

Generally, laminated glass plates are used to create elements whose behaviour from the mechanical point of view is that of mainly bent plates. Many of the plastic materials used as interlayers are capable of achieving a certain degree of coupling between the glass plates, i.e. of transferring shear stresses, which is sufficient to produce a resistant bending moment on the part of the composite element which is greater than the sum of the resistant bending moments of the individual plates. This capacity of the plies to collaborate under bending stress may be taken into account during the design phase, provided

that the mechanical properties of the interlayer are known, both as a function of the in-service temperature and of load time. In other words, the shear secant modulus of elasticity must be known according to temperature and duration of load.

Other materials are used to finish glass products, particularly the so-called “structural” façades and roofs, in order to re-establish the continuity between glass elements in the absence of adjacent parts in metal and of seals. In particular sealants, generally silicone-based, create a barrier between indoor and outdoor environments. However, these sealants may also perform a mechanical retention role. Other types of adhesive may also be used for connecting glass elements.

### 2.2.1 Polymer materials for interlayers

By extension, the term “polymer” defines a material consisting of polymer molecules of large size, i.e., natural or synthetic molecules made up of a sequence of units forming a chain with one another, generally through covalent bonds. Polymer chains, normally formed from a sequence of carbon atoms, may be linear, branched or crosslinked. These extremely long chains (Figure 2.16) are arranged in the form of “statistical clusters” (Figure 2.17), sometimes creating a series of crosslinks which increase the stiffness of the polymer. The lateral branches, on the other hand, reduce the degree of “wrapping”, encouraging a random arrangement and weakening the secondary links and thereby tensile strength. Some non-crosslinked polymers tend locally to take on an ordered arrangement (crystallites). The degree of crystallinity or amorphism therefore determines the polymer’s performance.

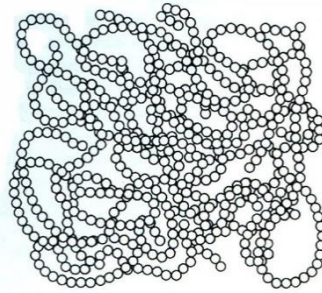


Figure 2.16. Schematic representation of a polymer chain [Moffatt *et al.*, 1965].

#### 2.2.1.1 Physical properties

The glass transition temperature  $T_g$  represents the temperature below which an amorphous material behaves as a vitreous solid. The glass transition temperature is determined experimentally by cooling molten polymer and recording the specific-volume vs. temperature curve (Figure 2.18). The glass transition temperature is signalled in an amorphous material by a change in the specific volume gradient; the presence of a crystalline phase, in contrast, produces a sharp change in specific volume values; the greater the degree of crystallinity, the more marked this sharp change is. In amorphous polymers, the exceeding of  $T_g$  is accompanied by a progressive transition from a behaviour similar to that of glass to a “rubber-like” behaviour and then to a fluid state. In the transition from solid to fluid, viscous behaviour gradually takes over from elastic behaviour.

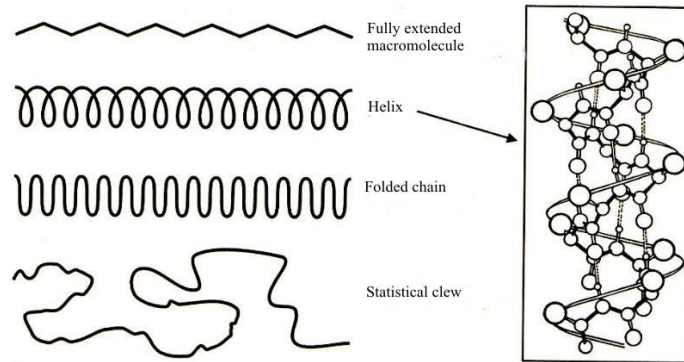


Figure 2.17. Possible arrangements of macromolecules; the box illustrates the helical model of  $\alpha$ -keratin. [Bertolini *et al.*, 2001]

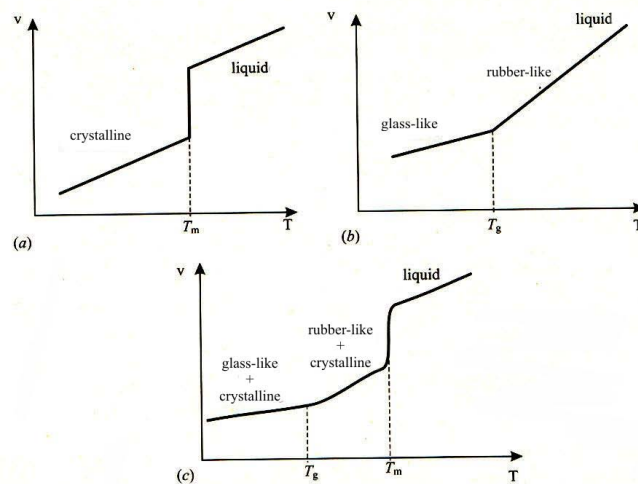


Figure 2.18. Diagram of specific-volume vs. temperature curves for polymers: a) perfectly crystalline (ideal situation); b) amorphous; c) semicrystalline [Bertolini *et al.*, 2001].  $T_g$  glass transition temperature;  $T_m$  melting temperature.

In polymer materials, the structure at the microscopic scale is directly responsible for macroscopic behaviour. However, the use of micromechanical models is difficult to achieve, insofar as the material is almost always mixed with other substances, which correct a number of its defects mainly relating to its sensitivity to chemical deterioration as a result of environmental factors and the difficulty of applying extrusion processes to it. After polymerisation, therefore, a premix is created, or in some cases the premix may undergo an initial melting process, after which it is reduced to granules (compound). This stage of the production process, known as finishing, may be performed by the original manufacturer or by the user. Hence, it is practically impossible to ascertain the properties of a polymer starting from its chemical structure, except in an extremely approximate manner. An industrial product manufactured with a known polymer may exhibit significantly different properties as a result of the processes which it undergoes during production. These considerations give rise to the need to provide accurate procedures to qualify the materials, providing the necessary information for the design process.

The main purpose of the interlayer is to retain fragments in the event of the glass failing. It is possible to achieve this goal if the fracture of a plate does not propagate into the plastic material, but deviates to the interface instead, thus initiating delamination. This effect is obtained, for example, with thermoplastic polymers which at room temperature exhibit a much lower modulus of elasticity than that

of glass. Polyvinyl butyral (PVB) is the material most commonly used for this purpose. A vinyl, amorphous polymer, it is characterised by long, branched, geometrically disordered polymer chains. PVB exhibits a glass transition temperature which is close to normal in-service temperatures and is therefore capable of exhibiting a rubber-like behaviour. Adhesion to the glass is generally performed in an autoclave at a high temperature and is due to the chemical bonds which are established between the interfaces: the hydroxyl groups along the polymer chains bond with the silane groups present on the surface of the glass.

Another commonly used material in the manufacture of laminated glass is the copolymer ethylene-vinyl acetate (EVA). Other interlayers are available on the market, such as polyurethane and the so-called “ionoplastic” layers. Recently polycarbonate (PC) has also been used, as it offers the advantage of a high glass transition temperature (approximately 150° C), but is assembled with adhesive sheets of materials. Nevertheless, other products may also potentially enter the laminated glass market which have unknown mechanical performance levels and sometimes originate from sectors other than the construction sector.

Generally, materials used as interlayers are highly sensitive to temperature variations. Due to their low glass transition temperature, at room temperature they exhibit a behaviour generally described as rubber-like, with ultimate strain values that can be as high as 200-300%, which generally arise when they are subjected to prolonged loads. Under this type of action the spherical part of the deformation (change in volume) remains negligible compared with the deviatoric part (change in shape).

### **2.2.1.2 Mechanical properties**

The most commonly used plastic materials in the manufacture of interlayers, i.e. PVB, EVA and ionoplastic polymers, may be considered isotropic, at least in the initial phase of the load history. When glass plates are sound, the interlayer is constrained by a material which has greater stiffness and hence it exhibits relatively small deformations. In this phase, therefore, it is sufficient to use a constitutive description of the linear viscoelastic kind. As viscosity is exhibited primarily in the deviatoric part of the strain, in order to simulate the viscous behaviour it is sufficient to provide a description of the dependency of the shear modulus of elasticity on time using a generalised Maxwell model. For an accurate description of the behaviour of the material, 5 suitably calibrated Maxwell elements assembled in parallel (Prony series) may be sufficient.

The high degree of dependency of the properties of plastic materials on temperature means that it is necessary to evaluate such properties under in-service temperature conditions.

Currently no certain experimental data are available that would allow an evaluation of the effect of ageing on materials used as interlayers. Nevertheless, it is well known that these plastic materials are extremely sensitive to the effects of humidity, which means that caution is recommended regarding their use in wet or humid environments. In addition, processes of deterioration have been observed, particularly in the adhesion between glass and interlayers, where the edge of the laminated layer is not adequately aerated or protected, such deterioration being mainly attributable to humidity stagnation.

After the failure of all of the glass plates that constitute laminated glass, the behaviour of the element is entrusted to the capacity of the interlayer to remain fixed to the restraints. If we wish to analyse this behaviour, it is necessary to describe the constitutive relationships of the sheet of plastic material. For this purpose it is necessary to use constitutive models for large deformations that are capable of reproducing the process of equilibrium of rubber-like materials, for example the typical uniaxial test diagram which evidences an inflection point. The parameters for hyperelastic models must be appropriately calibrated by means of experimental tests which also include pluriaxial tests. Post-critical analyses in general aim at evaluating the robustness of the constraints. Failure of the interlayer may in any case be taken into consideration during this phase.

### 2.2.1.3 Mechanical characterisation of polymer interlayers

Apparently identical plastic materials may be manufactured and marketed with different molecular weights and charges which modify their specific properties, particularly their glass transition temperature and thus their capacity to exhibit viscous deformations (creep), the amount of which increases rapidly with temperature. For this reason, if a little known material is used or in any case whenever it is desired to take into account the capacity for shear coupling produced by the interlayer on the constituent plies, it is recommended that all the documentation relating to the mechanical behaviour of the plastic material be requested with regard to temperature levels and load duration, i.e., the values of the shear modulus of elasticity as a function of temperature and load duration.

It should be emphasised that the process of adhesion between glass and interlayer involves a bond of the chemical type; because of the alterations that this can introduce into the behaviour of materials in contact with each other, this fact requires mechanical tests to be performed on laminated specimens, in order to correctly evaluate the overall behaviour. As currently there are no standard guidelines in this regard, it is possible to ignore the local stiffening effect associated with the chemical lattice that forms between glass and polymer, and conduct mechanical tests only on the plastic material, obviously considering that the stiffness is being underestimated and the deformability of the composite plates overestimated.

Generally, time-dependent mechanical behaviours are analysed using test methods which apply load cycles chosen to highlight the phenomenon as clearly as possible, also in relation to stress values in use and service. The load gradients taken into consideration in structural engineering range from  $10^{-9}$  Hz to 1 Hz, although higher frequencies are useful in studying problems of impact and explosion. The most common methods of testing to highlight the rheological properties of plastic materials are outlined below.

With regard to the state of stress and strain to be produced in the specimens, test methods which return the shear modulus of elasticity directly are particularly recommended, as this modulus is directly involved in load transfer capacity between the plates of laminated glass.

#### *Creep/relaxation tests*

Rheological tests can be carried out by imposing a load relatively rapidly and recording the resulting deformation during the subsequent time period (creep tests), or by imposing a displacement and recording the resulting change in the system of forces (relaxation tests).

#### *Forced oscillations*

If strain (or stress) changes periodically, at full performance after a number of cycles, within the limits of the Boltzman principle, the stress (or strain) will also change with the same law and same frequency, but will be out of phase in relation to the strain (or stress). For example, if an isotropic viscoelastic material is subjected to creep in the form  $\gamma = \gamma_0 \sin \omega t$ , it can easily be shown that the shear stress can be represented in the form  $\sigma = \gamma_0 (G'(\omega) \sin \omega t + G''(\omega) \cos \omega t)$ , where  $G'(\omega)$  and  $G''(\omega)$  are a function of the frequencies and represent the storage modulus of elasticity and the loss modulus of elasticity.  $G'(\omega)$ , in fact, is the ratio between stress in phase with the strain and the strain itself and is proportional to the energy accumulated in a cycle, while  $G''(\omega)$  is the ratio between the stress which is out of phase by  $\pi/2$  in relation to the strain and the strain itself and is proportional to the energy dissipated in a cycle.

The direct measurement of stresses and strains during forced vibrations is carried out for frequencies of between 0.001 Hz and 100 Hz.

#### *Free oscillations*

Free oscillation of a test piece is characterised by a constant frequency  $\omega_c$  and by a gradually decreasing value. Viscoelastic properties can be calculated starting from these two measurements. Free oscillation tests cover a range of frequencies from 0.01 Hz to 25 Hz.

#### *Wave resonance and propagation methods*

For frequencies higher than 100 Hz, the wavelength of the displacement becomes too small in relation to the size of the test piece. In this case, the speed of propagation of the wave trains and its attenuation can be recorded, furnishing the components of the overall modulus. Longitudinal and bending waves passing through thin strips of material can cover a range of frequencies between 100 Hz and  $10^7$  Hz.

#### **2.2.1.4 Dependence on temperature (master curve)**

Given a certain frequency  $\omega$ , the viscoelastic variables obtained from mechanical tests depend on testing temperatures. Many viscoelastic materials exhibit the peculiarity that, representing on a logarithmic scale the function  $G(\omega)$ , i.e. the shear modulus  $G$  as a function of the angular velocity  $\omega$  of the applied force, the experimental points obtained at a given temperature can be translated until they overlap the points obtained at a different temperature. The effects of a change in temperature from  $T$  to  $T_0$  are produced by multiplying the frequency scale by a given constant  $a_T$  and the scale of  $G$  by  $T_0\rho_0/T\rho$ , where  $\rho$  and  $\rho_0$  represent the density of the polymer at temperatures  $T$  and  $T_0$ , respectively. As it is generally possible for all viscoelastic variables to determine a translation value  $\log a_T$  which is dependent only on the temperature difference, it is possible to obtain a single composite curve which represents the dependence of a viscoelastic property on frequency. This curve is called the master curve.

A generally accepted form in the analysis of polymers for the representation of the dependence of  $a_T$  on  $(T-T_0)$  is the one proposed by William, Landel and Ferry (WLF equation) in the form

$$\log a_T = \frac{-c_1^0 (T - T_0)}{c_2^0 + T - T_0}. \quad (2.40)$$

Having determined the constants  $c_1^0$  and  $c_2^0$ , which allow the experimental points obtained at the various temperatures to be compared, it is possible to construct the master curve at a reference temperature  $T_0$  for all viscoelastic variables.

Caution however should be exercised in using this tool for the representation of properties in relation to times or frequencies which are various orders of magnitude away from the domains of the experimental measurements. The accumulation of experimental errors and chemical modifications that are produced in the long term (environmental deterioration) may make the aforementioned values unreliable.

When the “master curve” and the coefficients of the WLF equation are known, we can calculate the secant modulus of elasticity for any temperature value and load duration (Figure 2.20).

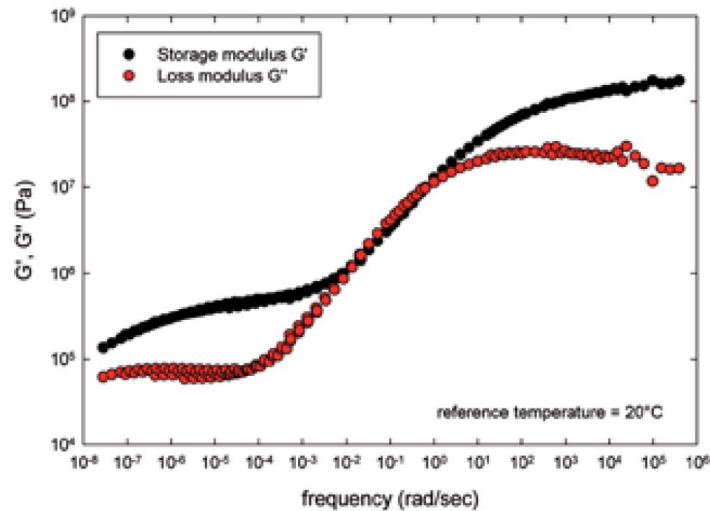


Figure 2.19. Master curve obtained using PVB test pieces for the shear modulus of elasticity at reference temperature of 20°C. Loss modulus and storage modulus. From [D'Haene & Savineau, 2007].

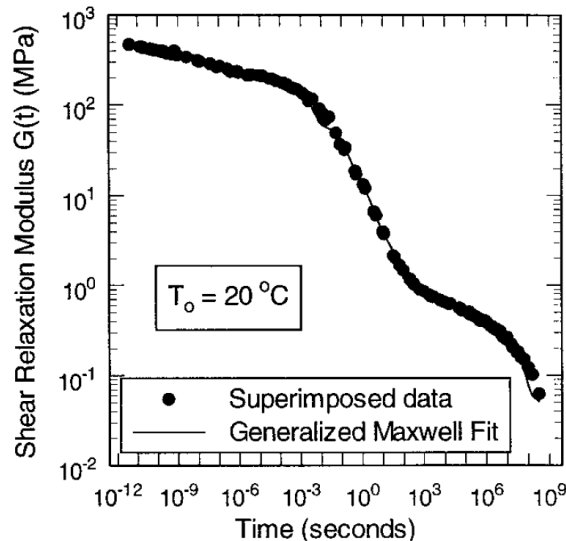


Figure 2.20. Relaxation curve for shear modulus of elasticity obtained with Butacite® Dupont (PVB) specimens at reference temperature of 20°C. The interpolation is obtained using a Generalised Maxwell model Fit (Prony series) [Van Duser *et al.*, 1999].

### 2.2.1.5 Environmental damage of interlayers in laminated glass

Plastic materials used in combination with glass for the production of laminated glass are generally subject to effects of environmental deterioration over the lifetime of the construction work. In the absence of certain data on the effects of such degradation, particular care should be taken in the case of environments with high levels of humidity. Laminated glass elements that have been installed for several years often show signs of delamination, starting from the edges, while the presence of humidity is evidenced by a gradual opacification of the interlayer, once again starting from the edges. The effects of deterioration show up initially in visible defects which are already evident under observation (bubbles, delamination, opacity), and it is reasonable to believe that these defects reflect alterations in the mechanical behaviour of the element. In the absence of information about alterations in mechanical behaviour, a number of important precautions in designing glass elements are recommended, particularly if the elements in question are for structural use.



- Laminated glass elements for structural use must be inspectable, with a regular inspection and maintenance schedule.
- Laminated glass elements for structural use must be replaceable and the procedure of replacement provided for, as the lifetime of glass elements, including laminated elements, is generally shorter than the lifetime of the (construction) work.

Test methods for determining durability are regulated by European Standard EN ISO 12543-4 “Glass in building – Laminated glass and laminated safety glass – Test methods for durability”. It should however be pointed out that this standard only considers defects that are detectable by means of a visual inspection and that have extended in the material to a distance of 15 mm from an original edge and 25 mm from a cut edge, but does not take into account any kind of deterioration of mechanical characteristics.

### **2.2.2 Adhesives and sealants**

The sealant generally used to re-establish continuity between glass elements in the absence of adjacent metal parts and seals is silicone. Silicone may be entrusted solely with the function of sealant but may also play a structural role.

Silicone is obtained by substituting the carbon of polymer molecular chains with siloxane groups; silicones are generally catalogued together with rubbers, with which they share the capacity to exhibit large deformations.

These instructions do not deal with the performance of silicone in cases where it is used only to seal glass panes to prevent fluids from penetrating, to which other specific standards apply. Nevertheless, the stiffness and deformation capacity of the sealant must be taken into account whenever – for example under seismic loads – the frame is subjected to considerable displacements. Indeed, although glass planes are normally disregarded in calculating the load-bearing capacity of the building, they may make a significant contribution in terms of overall stiffness: in this structural collaboration, silicone joints, despite not having a structural function, may play a decisive role.

Silicones with a structural function (structural silicones) may be used to obtain a seal between adjacent glass members and at the same time create a restraint between the plates, or contribute to the action of other restraints. In this case, it is necessary to evaluate the state of stress of the joint in order to ensure that it does not exceed its ultimate tensile strength or loss of adhesion, and choose the appropriate thickness so that its elastic strain is compatible with the displacements required.

With regard to the constitutive behaviour of silicone, which is commonly catalogued together with synthetic rubbers, what has already been said above of polymer interlayers also applies to this material, in the sense that it exhibits a highly non-linear, time-dependent behaviour. Therefore, what is required is adequate experimental analysis by means of transient or dynamic tests and accurate modelling by means of time-dependent hyperelastic models. On the instructions of the European Commission, the EOTA has laid down guidelines for drawing up a European Technical Assessment, ETAG, now AED, 002 – Edition November 1999, *Guideline for European Technical Approval (now Assessment) for Structural Sealant Glazing Systems (SSGS)*, amended October 2001. The document, which consists of three parts (Part 1: Supported and Unsupported Systems; Part 2: Coated Aluminium Systems; Part 3: Systems incorporating profiles with thermal barrier), sets out tests on stresses and methods for analysing the thickness of silicone joints using specific modulus of elasticity, shear modulus of elasticity and shear stress design values.

The modulus of elasticity is measured by the manufacturer in accordance with European Standard EN ISO 527 at a given loading speed (5 mm/min). Both the tangent modulus at the origin and the secant modulus in proximity to marked pairs of points of the stress-strain curve can be determined. However, which of these values is to be used in tests is not specified. The shear stress design value under dynamic load is determined by means of a test described in ETAG 002, while the constant load design value is provided by the manufacturer without any reference to usable test procedures. ETAG

002 also makes reference to EN ISO 8339 for the determination of material tensile properties and partly follows EN 15434, Glass in building – Product standard for structural and/or ultra-violet resistant sealant (for use with structural glazing and/or insulating glass units with exposed seals).

Lastly, it should be noted that silicone materials exhibit a different behaviour under compression and under tensile stress and are subject to problems of elastic instability when subject to compressive loading. For the determination of behaviour under compressive loading, reference is made to EN ISO 604, Plastics – Determination of compressive properties.

## 3 GENERAL DESIGN PRINCIPLES

Construction design must ensure that strength, operation, and durability requirements are satisfied. Glass, however, presents a large number of peculiar aspects which distinguish its design process from the approach traditionally used for more traditional building materials.

### 3.1 Hierarchy, robustness, redundancy, fail-safe design

For the purposes of structural behaviour, the brittle behaviour of glass, together with the dispersion of values of its strength and resistance characteristics, has led to the introduction of general design principles that are based on the concepts of *hierarchy*, *robustness* and *redundancy*. Hierarchy assigns indicators of importance to the various structural elements, while robustness and redundancy guarantee adequate safety even in the event of accidental breakage of a glass component.

Such a perspective is typical in aircraft design, where it is accepted that certain components may fail in extreme situations without compromising the overall stability of the structural system. This type of performance is indicated by “fail safe” Glass structures can be considered fail-safe if the failure of one or several of their components does not compromise the safety of the whole structure to safeguard human lives. The application of concepts of hierarchy, robustness and redundancy allows to obtain at the structural level the ductility that is lacking within the material and the individual structural elements.

Thus, in designing glass structures, it is of fundamental importance to check that the structure is capable of redistributing the loads by providing alternative paths for stresses and accepting spontaneous and/or accidental breakage of a number of elements or part of them.

#### 3.1.1 Structural hierarchy

Structural elements are classified according to the potential consequences of their collapsing, in terms of both material and human loss. In this specific case it is necessary to consider the possibility of failure of glass, also as a consequence of unforeseeable events such as accidental impacts, acts of vandalism or the presence of microdefects. With regard to the latter aspect, a particularly hazardous case is the presence of inclusions of nickel sulphide which may cause spontaneous failure of tempered glass even significant time after the installation.

In accordance with European Standard EN 1990, and as explained more in detail in Section 3.2, glass structures are classified according to the class of consequences for their eventual crisis. On this basis, they will be classified into first, second and class 3 elements.

#### 3.1.2 Structural robustness

Structural robustness is the capacity of an element or a structural part to prevent disproportionate damage as a consequence of a cause that should have led to a limited damage. For example, robustness refers to the capacity to prevent structural collapse in the event of local failures due to accidental or unforeseen actions (e.g. impacts or acts of vandalism) or spontaneous failure events (defects in the material, such as inclusions of nickel sulphide, or thermal gradients). Satisfying this requirement allows to obtain structures that are capable of putting all of their reserves of strength into action until they fail by activating multiple alternative load transfer paths. At the same time the risk of a global failure following localised failures in the structure is reduced (progressive collapse).

Structural robustness can also be achieved by adopting appropriate design choices and adequate structural measures. For example:

- avoiding, eliminating, or reducing any risks to which the structure may be subject.
- adopting a structural solution characterised by low sensitivity to the considered risks.
- designing a structural system capable of safely withstanding:
  - accidental failure of a structural element (e.g. a fin in a façade or a load-bearing beam in a deck) or localised damage in the element itself (e.g. failure of a glass plate in a laminated element);
  - accidental failure of a small portion of the structure.

### **3.1.3 Structural redundancy**

Structural redundancy is the capacity of a structure to redistribute *within itself* a state of stress in such a way that the failure of one of its parts does not cause the failure of the entire structure. Such a requirement thus constitutes a means of designing robust structures, as indicated in point 3.1.2. In a redundant structure, loads may be withstood:

- by the initial load resistance mechanism itself, which however offers lower resistance as a result of the damage caused to it (for example in cases in which the cross-section is reduced);
- by alternative load resistance mechanisms (for example, when a fin in a continuous pane fails).

In the case of glass structures, the requirement of redundancy is extremely important, given the brittle nature of glass and the potential risk of spontaneous failure events. Specifically, structural redundancy can be defined at various levels, such as *i*) redundancy for a cross-section; *ii*) redundancy for the whole structural system.

#### **3.1.3.1 Cross-section redundancy**

Cross-section redundancy is the capacity of a section of a structural element to maintain residual strength following the failure of one of its parts or, in an equivalent manner, the property due to which the failure of a part of the section does not lead to failure of the whole.

It is important to observe that in glass structures, in contrast to reinforced concrete or steel sections, a low rate of work on the part of the material does not confer redundancy on the cross-section. This is because the material is characterised by a low degree of toughness; as a result, cracks, once triggered, propagate almost instantaneously, and also because failures may be triggered spontaneously even under low stress levels (for example as a result of the presence of microdefects) or may be the result of unforeseeable events (for example accidental impacts or acts of vandalism).

As a result, a monolithic glass element in which the thickness is increased in comparison with the minimum design thickness cannot be considered structurally redundant. On the contrary, a typical example of cross-section redundancy can be found in laminated glass, where additional plates can be added to those strictly necessary to withstand design actions. In the event of accidental breakage of a plate, the surviving plates may wholly or partially bear design loads.

In the case of elements exposed to impacts, such as floors, external plates are generally redundant and are often termed “sacrificial”. They protect the lower layers, which are demanded to satisfy load-bearing capacity requirements.

#### **3.1.3.2 System redundancy**

System redundancy is the capacity of a structure to transfer loads after the failure of an element or a part thereof, by means of alternative mechanisms with respect to the design ones.

A classic example of system redundancy is represented by the façades of the *Grandes Serres* in the *Parc de la Villette* in Paris, which are formed by toughened, non-laminated glass modules, hanging from each other. Failure of one of the modules could cause immediate changes in the system of suspension, since if the uppermost module of a group fails, the remaining ones lower down are no longer supported. However, the designer made provision for a special system of connections capable of transferring stresses to the adjacent modules *via* horizontal connecting elements, as indicated in the original sketches shown in Figure 3.1.

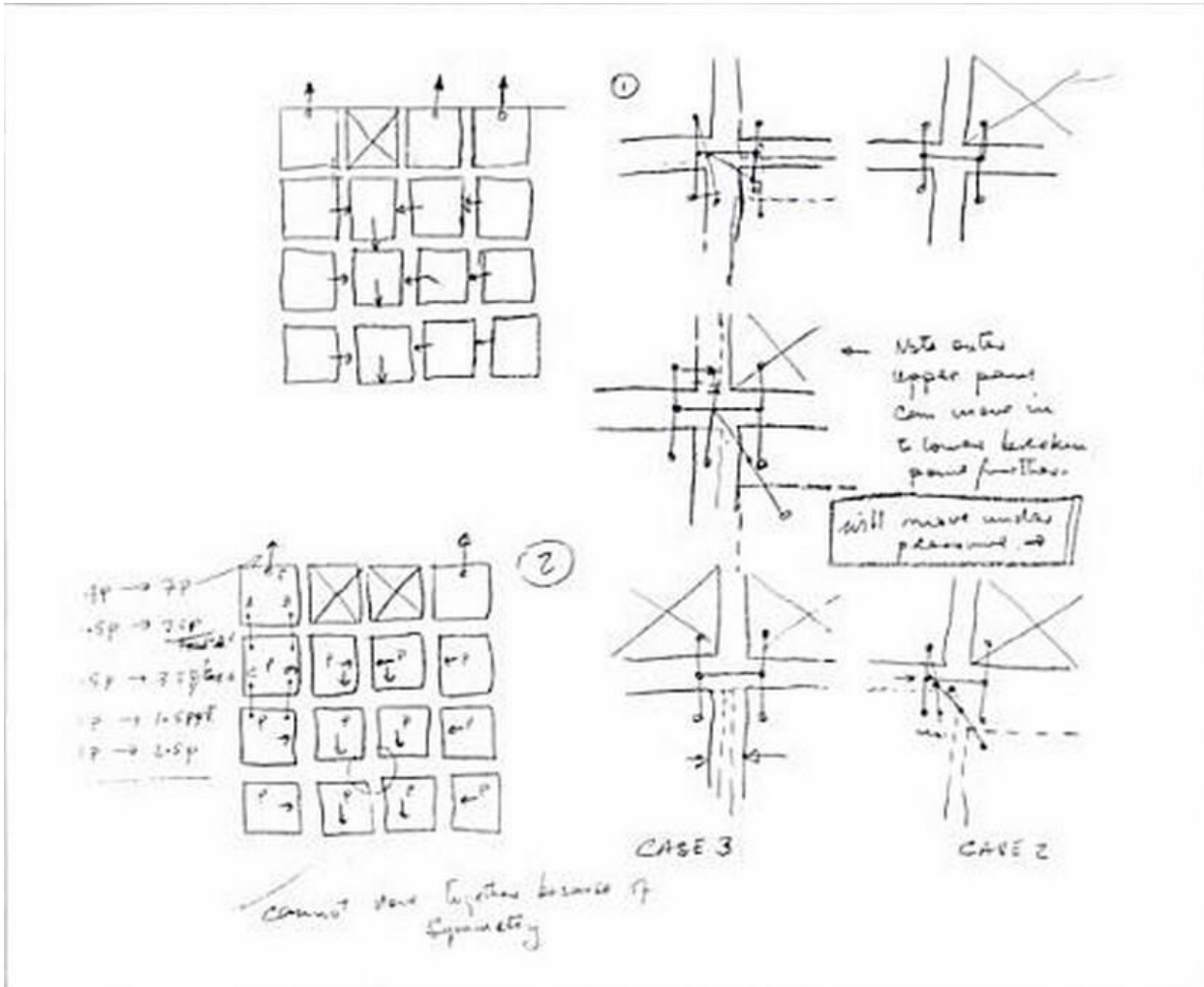


Figure 3.1 Peter Rice, study sketches for the glass façades of the *Grandes Serres* in *Parc de la Villette*, Paris.

The choice of the level of redundancy must be made in relation to the events against which protection is desired. A possible classification in this regard is provided in Table 3.1.

Table 3.1. Possible classification of the redundancy level required.

Structural redundancy	
Event	Possible solutions
Spontaneous/accidental breakage of glass	<i>Cross-section redundancy:</i> use of laminated glass or elements of protection against fragments falling from above.
Act of vandalism involving a structural element	<i>System redundancy:</i> provides alternative structural paths for load in the event of failure of a structural element.

### 3.1.4 Post-breakage behaviour

The “post-breakage” behaviour of glass depends mainly on the type of glass used (for example float, heat strengthened or tempered glass or a combination thereof), on the boundary conditions and on any association with other materials (for example interlayers for laminates, reinforcements or tie-beams). In general, it is important to evaluate the time necessary for a partially or wholly damaged glass element subject to normal operating loads to fail permanently.

In addition to the serviceability design, a glass structural element must be designed for the post-critical phase; this implies that the choice of the type of glass to use is of fundamental importance.

Naturally, compared to monolithic glass, laminated glass has better post-breakage behaviour, due to the presence of the interlayer, which retains shards, reduces the size of major cracks, provides residual load-bearing capacity and reduces the risk of sharp injuries for users. Post-failure performance is influenced by the size and shape of the shards. The type of fragmentation depends on the type of glass: in this regard, annealed glass is better than toughened glass, as the larger size of the fragments guarantees greater adhesion to the interlayer. Other important factors include type of load (impulsive or quasi-static), accumulated elastic strain energy, type of fixing, type of interlayer and properties of adhesion between glass and interlayer.

A qualitative indication of the post-failure load-bearing capacity of laminated glass according to type of glass is provided in Table 3.2.

Post-breakage behaviour of laminated glass depends, in addition to its composition, on the type of restraint. With regard to glass plates with support on two sides, the aspect ratio also is important, as important is if the restraints are located along the vertical or the horizontal sides in the case of vertical application. If point glazing systems with countersunk holes are used, the difference in behaviour also stems from the type of point fittings used, for example whether they have a single fixing ring or a double one which enables the inner plate to be secured separately from the outer one. The hole in this case is conic-cylindric and the inner plate of the laminate is offset in relation to the outer one. Ultimately, all considerations should be made on a case-by-case basis: a purely qualitative classification is provided in Table 3.3.

Naturally the choice of the type of glass to use depends to a large extent on the type of coupling. Panes which use point fittings with *through-holes* may be single, laminated or insulated. There must always be at least one pane that has been tempered with a consequent HST treatment (*Heat Soaked Thermally toughened safety glass*). Indeed, since the panes have holes, they must be able to withstand the high stress concentrations that arise around the holes housing the point fittings. These indications are summarised in Table 3.4.

Panes for point fittings with *non-through holes* may be single, laminated or insulated. Each of the preceding compositions may be implemented with panes that have undergone the following heat treatments. Single (monolithic) glass panes must be tempered using HST treatment, but cannot be used for railings (or when there is a risk of falling); the use of annealed monolithic panes is to be avoided. Laminated glass at an angle from the vertical between 0° and 5° must have holes also in the outer pane: the external plate will be toughened to increase its resistance to local stresses; the inner plate must not be toughened in order to obtain a process of fragmentation which permits a degree of

residual post-failure cohesion. Insulated glass must have structural bonding of the edges. The types of glass recommended are listed in Table 3.5.

Panes for point fittings *without holes* (Table 3.6) may be single, laminated or insulated. Each of the previous compositions may be implemented with panes that have undergone heat toughening or tempering processes followed by HST treatment.

In the case of elements that are susceptible to specific human-induced actions such as railings and barriers, it must be remembered that guidelines regarding their safety in use are also contained in specific product standards, including European Standards EN 12600, UNI 10805, UNI 10806, UNI 10809, EN 14019 and EN 12150. Generally, post-failure performance can be assessed using direct tests, the most common of which is impact tests with a tilting impacting body released from a fixed fall height. For this type of test, the reader is referred to current standards. An indication regarding the type of glass to use for the purpose of post-breakage behaviour is provided in Table 3.7. Impact performance classes for various construction applications of flat glass are provided in EN 12600.

Table 3.2. Qualitative indications regarding the post-failure load-bearing capacity of laminated glass according to glass type.

Type of laminated glass	
Annealed + Annealed	Generally good performance, mainly due to the large fragment sizes which maintain good adhesion, although it should be kept in mind that the cutting edges of the fractures can sometimes damage the interlayer.
Heat-strengthened + Heat-strengthened	Comparable performance to “Annealed + Annealed”.
Heat toughened + Heat toughened	Poor performance with deformable interlayers (e.g. PVB). Performance improves with increased stiffness of the interlayer (e.g. ionoplastic polymers). Small, non-sharp fragments do not damage the interlayer but are more prone to detach.
Heat toughened + Heat-strengthened	Intermediate performance. In general a good compromise between post-failure load-bearing capacity and risks associated with fragmentation.
Heat toughened + Chemically strengthened	Good performance as the fragments are large in size. This combination should however be considered with great caution, as breakage is extremely fragile and the sudden release of energy may cause failure.

Table 3.3. Qualitative indications concerning post-failure load-bearing capacity of laminated glass according to type of restraint.

Type of restraint	
Continuous support on perimeter	Generally good performance, which improves with increasing depth of support.
Panes with edges bonded to a frame	Generally good performance, as the adhesive bonding of the edge of the pane, if correctly sized, ensures that the glass plate is retained in the event of failure.
Support on two sides	To consider with caution. The depth of the support must be carefully sized due to the risk of falls in the case of severe deflections such as those which occur during the post-failure phase.
Point fixing with pass-through devices, fixing caps and cylindrical holes	Good performance, as the cap prevents the broken glass from coming loose. Performance improves with increasing strength of the interlayer.
Point fixing with pass-through devices and countersunk holes	To consider with caution, as in the event of localised failure at the fixing point, the fixing method used does not stop it from coming loose. Its application is not recommended in the case of suspended plates (attachment at the top part of the plate).
Point fixing with “clamp”	To consider with caution. The clamping must be evaluated carefully in order to minimise the risk of detachment in the event of severe deflections.
Point fixing with pass-through hole on only one layer	To consider with caution because of the danger associated with the loosening of the plate in the event of localised glass failure.

Table 3.4. Type of glass for structural glass elements sustained by points with through-holes.

Glass plates with through-holes				
Type of glass	Nature of components		Vertical wall	Horizontal wall <sup>1</sup>
Monolithic	Heat toughened		YES <sup>2</sup>	NO
	Heat-strengthened		YES <sup>2</sup>	NO
	Annealed		NO	NO
Laminated	Annealed/Annealed Annealed/Heat-strengthened Annealed/Heat toughened		NO	NO
	Heat-strengthened/Heat-strengthened		YES <sup>3</sup>	YES
	Heat-strengthened/Heat toughened		YES <sup>3</sup>	YES
	Heat toughened/Heat toughened		YES <sup>3</sup>	YES <sup>4</sup>
Insulating	<b>element A</b>	<b>element B</b>		
	Heat-strengthened	Heat-strengthened	YES	YES
	Heat-strengthened	Heat toughened	YES	YES
	Heat toughened	Heat toughened	YES	YES

(1) Walls inclined by over 15° from the vertical which overlook an occupied area.  
 (2) With the exception of railings, as Standard UNI 7697 for the safety of glass elements requires the use of certified class 1(B)1 impact-resistant laminated glass in accordance with EN 12600.  
 (3) For protection against falls, the glass pane must be certified class 1(B)1 impact-resistant laminated glass as required by Standard UNI 7697.  
 (4) The “Heat toughened + Heat toughened” laminate is most suitable for vertical walls; for roofs a toughened/strengthened composition is recommended.



Table 3.5. Type of glass for structural glass elements sustained by points with non-through-holes.

<b>Glass plates <u>with non-through-holes</u></b>				
<b>Type of glass</b>	<b>Nature of components</b>		<b>Vertical wall</b>	<b>Horizontal wall<sup>1</sup></b>
Monolithic	Heat toughened		YES <sup>2</sup>	NO
	Heat-strengthened		YES <sup>2</sup>	NO
	Annealed		NO	NO
Laminated	Annealed/Annealed Annealed/Heat-strengthened Annealed/Heat toughened		NO	NO
	Heat-strengthened/Heat-strengthened		YES <sup>3</sup>	SI
	Heat-strengthened/Heat toughened		YES <sup>3</sup> , with hole in at least the strengthened layer <sup>4</sup>	
	Heat toughened/Heat toughened		NO	NO
Insulating glass <sup>5</sup>	<b>element A</b>	<b>element B</b>		
	Heat-strengthened	Heat-strengthened	YES	YES
	Heat-strengthened	Heat toughened	YES	YES
	Heat toughened	Heat toughened	YES	YES

(1) Walls inclined by over 15° from the vertical which overlook an occupied area.  
 (2) With the exception of railings, as Standard UNI 7697 for the safety of glass elements requires the use of certified class 1(B)1 impact-resistant laminated glass in accordance with EN 12600.  
 (3) For protection against falls, the glass pane must be certified class 1(B)1 impact-resistant laminated glass as required by Standard EN 12600 UNI 7697.  
 (4) The hole must be made at least in the strengthened layer, as heat toughened glass is subject to shattering into small fragments, and thus there is no guarantee that the fixing point remains attached to the glass if the panel breaks. The failure of heat-strengthened glass in larger elements allows the laminated glass to remain in one piece and attached to the fixing point.  
 (5) Insulating glass must have structural bonding along the edges.

Table 3.6. Type of glass for structural elements with coupling, without holes in the glass.

<b>Glass <u>without holes</u></b>				
<b>Type of glass</b>	<b>Nature of components</b>		<b>Vertical wall</b>	<b>Horizontal wall<sup>1</sup></b>
Monolithic	Heat toughened		YES <sup>2</sup>	NO
	Heat-strengthened		YES <sup>2</sup>	NO
	Annealed		NO	NO
Laminated	Annealed/Annealed <sup>4</sup>		YES <sup>3</sup>	YES
	Annealed/Heat-strengthened Annealed/Heat toughened Heat-strengthened/Heat-strengthened Heat-strengthened/Heat toughened		YES <sup>3</sup>	
	Heat toughened/Heat toughened		NO	
	Insulating	<b>element A</b>	<b>element B</b>	
Heat-strengthened		Heat-strengthened	YES	YES
Heat-strengthened		Heat toughened	YES	YES
Heat toughened		Heat toughened	YES	YES

(1) Walls inclined by over 15° from the vertical which overlook an occupied area.  
 (2) With the exception of railings, as Standard UNI 7697 for the safety of glass elements requires the use of certified class 1(B)1 impact-resistant laminated glass in accordance with EN 12600.  
 (3) For protection against falls, the glass pane must be certified class 1(B)1 impact-resistant laminated glass as required by Standard EN 12600 [UNI 7697].  
 (4) Class 1(B)1 glass is difficult to obtain with the “Annealed + Annealed” composition.

Table 3.7. Type of glass for railings and barriers.

Type of glass	Nature of components	Vertical wall	Minimum impact resistance performance class as provided for by UNI 12660 in accordance with UNI 7697
Monolithic	Heat toughened	YES (if failure of the component does not entail the risk of falls)	According to application, as provided for by the UNI 7697 standard. (Example: class 1(B)1 in the case of risk of falls)
Laminated	Heat toughened/Heat toughened	YES	
	Heat toughened/Heat-strengthened Heat toughened/Annealed	For railings with point fixed glass, see Tables 3.5, 3.6 and 3.7 according to the type of hole used in the fixing	
	Heat-strengthened/Heat-strengthened Heat-strengthened/Annealed Annealed/Annealed		
Note: The UNI 7697 standard recommends the use of laminated glass in cases where falls may occur.			

With regard to structural elements with the function of floors, monolithic glass must not be considered admissible. Generally, for this category of structure the type of glass to be used must be indicated. Minimum safety requirements in use are also set out in technical product standards, including UNI 7697.

Table 3.8. Type of glass for floors.

Type of glass	Nature of components	Horizontal element
Laminated (at least three layers-breakage of at least one element must be foreseen)	Heat toughened/Heat toughened/Heat toughened	YES (with perimetrical fixing system)
	Heat toughened/Heat-strengthened/Heat toughened Heat-strengthened/Heat toughened/Heat-strengthened <sup>(1)</sup> Heat-strengthened/Heat-strengthened/Heat-strengthened	YES
	Annealed/Annealed/Annealed <sup>(2)</sup>	NO
<sup>(1)</sup> Although this is a possible combination, it is less suitable than the preceding “Toughened/Strengthened/Toughened” combination, as it is generally more appropriate to keep the most abrasion-resistant material, as well as the material that is most resistant to bending stresses (i.e. heat toughened glass), on the surface; the least resistant material, which in any case remains most compact after failure as it shatters into larger fragments (i.e. heat-strengthened glass), should be kept close to the neutral axis. <sup>(2)</sup> This combination is not recommended, as annealed glass is characterised by poor resistance to surface abrasion.		

For particularly large structures, fracture tests should also be performed on full-scale elements *in situ* or by reproducing the same conditions of use (walking surfaces open to the public, roofs in environments open to the public, etc.). These tests must comply with the “design by testing” requirements of the Eurocodes.

### 3.1.5 Durability

With regard to durability, it is necessary to distinguish between the behaviour of glass, which in general boasts excellent performance, and the behaviour of materials used in combination with glass, which are generally polymer-based and highly sensitive to temperature, humidity and ageing. From tests carried out, it is clear that both increase and decrease in temperature have a negative effect on post-breakage behaviour. Nevertheless, for temperatures between -20°C and +60°C, i.e., within the typical range for construction works, there is no significant change in load-bearing capacity and failure modes. Specific analyses, on the other hand, must be carried out for cases of high temperatures caused, for example, by fire.

Thermal cycles also do not significantly modify the post-breakage behaviour of glass. However, it should be kept in mind that the effects of hot-cold thermal cycles become increasingly important as the size of the elements increase, due to the different deformations of glass and interlayer.

The effects of humidity on glass are still not completely clear. For ordinary humidity levels, no appreciable changes in mechanical performance are observed. However, particular caution is required when glass is used in environments with a particularly high level of humidity (for example certain geographical areas, swimming pools, gyms, etc.).

Particular attention, on the other hand, should be given to polymeric interlayers. In particular, for most of them the glass transition temperature is approximately 20°C, and their stiffness is significantly reduced beyond this limit. Adhesion between interlayer and glass may fail, especially at low temperatures. Another factor to take into account is the fact that polymer-based interlayers are extremely sensitive to conditions of humidity. It is therefore necessary to prevent water or humidity from accumulating on the edges of laminated glass plates exposed to a potentially humid environment. Lastly, another certainly non-negligible factor concerns the effects of ageing, which is due both to exposure to ultraviolet radiation and direct contact with the atmosphere (in this case, as in the other cases already mentioned, it is recommended that adequate ventilation of the edges of laminated glass plates may always be permitted, so to enable the humidity to evaporate and dry out rapidly where the edge of the interlayer is in direct contact with the atmosphere). All of these effects cause the stiffness and load-bearing capacity of interlayers to deteriorate, which must be taken into account during the design phase, in accordance with the parameters highlighted below.

The issue also certainly concerns adhesive bonding processes, where the main problem is a lack of information regarding their durability, due primarily to a lack of long-term testing. The best bonding agents are the inorganic silicone-based ones, as they offer greater resistance to ultraviolet rays, heat and humidity. They also maintain an unchanged modulus of elasticity with temperature changes within the range of -20°C and +60°C. This property makes them particularly suitable for the use in residential buildings.

In order to evaluate performance in terms of durability, reference may be made to theoretical models, experimental research, deductions from applications already implemented, or adequately documented test campaigns.

In order to ensure durability, due consideration must be given to the following aspects:

- the intended use;
- the expected environmental conditions;
- the composition, properties and performance of products used over time and in the various expected environmental conditions;
- the choice of type of connections;
- the quality and level of monitoring of execution;
- the specific protective measures, for example with regard to fire and impacts;
- the intended maintenance during the design working life.

## **3.2 Hierarchy and reliability of structural glass elements**

### **3.2.1 Classification of structural glass elements**

On the basis of the potential consequences of the failure of structural elements in economic, social and environmental terms as well as loss of human life, Annex B1 in the UNI EN1990 standard defines three classes of consequences, CC1, CC2 and CC3. They are in general associated with various categories of construction works based on their importance (e.g. agricultural buildings, residential buildings and public buildings designed for large crowds).

---

In general, glass structural works are installed in prestigious buildings. However, it would not be correct to apply high classes of consequence to all of the various glass elements that constitute the building. Glass elements, in fact, generally constitute localised parts of the building (beams, railings, floors, staircases, etc.), the failure of which can have more or less serious consequences and is hardly ever associated with the failure of the entire building.

In the case of structural glass elements, the most correct classification is therefore one which is made according to elementary principles, that is to say, on the severity of the potential consequences of local or total failure of the elements. Here, therefore, we provide a definition of the various classes of consequences, CC1, CC2 and CC3, which follows the same guidelines as the ones set out in European Standard EN1990, while for the sake of completeness class CC0 is added, which includes all specifically non-structural glass construction products. The following classes of consequences are defined:

**CC0:** specifically non-structural construction products. Their failure has extremely limited consequences in economic, social and environmental terms and in terms of loss of human life.

**CC1:** structural elements. Their failure has limited consequences in terms of loss of human life and small or negligible consequences in economic, social or environmental terms. This category includes structures in buildings where people are present only occasionally and, by extension, those glass elements whose structural failure has limited consequences.

**CC2:** structural elements. Their failure has medium consequences in terms of loss of human life and considerable consequences in economic, social or environmental terms. Examples of structures that belong to this class are residential or office buildings. By extension, the class includes all structural elements whose failure leads to consequences of a medium level of severity.

**CC3:** structural elements. Their failure has high consequences in terms of loss of human life and very great consequences in economic, social and economic terms. Structures which belong to this class are public buildings, stages and covered grandstands, where the consequences of failure are high (for example concert halls, shopping malls susceptible to overcrowding, etc.). By extension, the class includes all structural glass elements whose failure has severe consequences.

Glass elements used in construction works can be distinguished into the following classes; *class zero*, *class 1*, *class 2* or *class 3* depending on their importance, in accordance with the definitions that follow.

**Class zero:**

Construction products without a structural function, with consequences class CC0.

**Class 1:**

Structural elements with consequences class CC1.

**class 2:**

Structural elements with consequences class CC2.

**class 3:**

Structural elements with consequences class CC3.

The probability of failure accepted for such elements decreases with each class, from class zero to class 3, as they correspond to different classes of consequences.

These instructions deal solely with structural elements belonging to the first, second and third class. Each class of structural element is associated with a given probability of failure, which is in line with the values prescribed by European Standard EN1990 for the first, second and third class. With regard to class zero, reference should be made to other specific indications.

This document regards performance and not prescriptions, and therefore sets out design and assessment methods to obtain performance compatible with the probability of failure corresponding to each class. This is a particularly delicate aspect, as it is generally impossible to associate each structural category (e.g. beams, floors or roofs) unambiguously with a specific consequences class. For instance, if the failure of a glass railing does not lead to any risks of falling (because it is located at a height almost close to zero, or because it is protected by an adequate metal containing structure), it may be considered class 0; a geometrically similar railing located at a great height without any additional fall protection installed must be considered class 1 or class 2, depending on its intended use and the potential consequences of failure.

Nevertheless, a distinction should be made with regard to pre-failure and post-failure assessments of glass. In pre-glass-failure assessments, the characteristic return period of actions regards the design life of the structure, while post-failure assessments must take into account that the damaged element remains in use for a short period of time, i.e., the time required to arrange for its replacement: therefore the return period of actions should be reduced accordingly. Additionally, it is assumed that the failure of a structural element entails immediate countermeasures, such as propping or isolating the area interested by damage. Therefore, the same structural elements may be downgraded (for example from class 2 to class 1) when passing from pre-failure to post-failure assessments.

Table 3.9 illustrates a proposal for classification based on the most common conditions of use. These indications are intended to constitute a simple rule of thumb which, in the absence of precise reference standards, may aid the designer in establishing the class of the element on which to base assessments. When several choices are indicated within the same category, the designer will choose the most or least demanding class for pre- and post-glass-failure assessments according to the importance of the work, the degree of danger in the event of failure, and whether safety countermeasures can be immediately implemented in order to reduce the consequences of failure (e.g. propping, protection measures, fences, etc.).

Table 3.9. Classification of structural glass elements according to conditions of use. By definition, non-structural construction products fall under class 0.

Type	Class for pre-glass-failure assessment*	Class for post-glass failure assessment
Vertical elements** with continuous edge restraint	1	1/NA***
Vertical elements** with fixing points	2/1	1/NA***
Horizontal roofs**	2	2/1
Railings with danger of fall	2	2/1
Reinforcement fins	2	2/1
Floors, load-bearing beams	2	2
Pillars	3 (specific analyses with Level II or Level III methods)	2 (with pre-failure actions)

Notes:

(\*) Within the same category, the choice of the most or least restrictive class of assessment depends on the importance of the work, the degree of danger arising in the event of failure of the glass, and whether safety countermeasures can be immediately implemented in order to reduce the consequences of failure (e.g. propping, protection measures, fences, etc.).

(\*\*) An element is considered vertical if the angle of its plane from the vertical is less than 15°. An element which does not fall under this definition is considered horizontal.

(\*\*\*) NA stands for “No Assessment”. When failure of the glass produces negligible risks in terms of damage or human life, post-failure assessment may be omitted.

The most severe case (due to the obvious consequences in the event of collapse) is that in which the structural glass element is called upon to support horizontal structures (glass pillars). In this case, for the purpose of pre-glass-failure assessment it is necessary to conduct specific analyses with Level II or Level III methods so as to ensure failure probabilities that are comparable with those required for the third consequences class (see Section 5.2). Nevertheless, structures of this type must be appropriately designed in order to satisfy the robustness, redundancy and fail-safe criteria set out in Section 3.1. In post-glass-failure assessments the same events used for pre-failure assessments, without reducing the return period.

By definition, non-structural construction products belonging to class zero are not subject to these instructions. Nonetheless, all components, systems and products that perform an autonomous static function must be used in conformity with adequate safety and performance levels.<sup>5</sup>

Particular attention must be given to potential interactions on the part of glass elements on the overall stiffness, and therefore on the dynamic behaviour, of the building.

### **3.2.2 Design life of the structure**

Eurocode EN 1990 establishes that the level of structural reliability of construction works – that is, their probability of failure – is in proportion to the design life of the structure, the importance of the work, and the severity of any potential consequences (loss of human life and damage to property).

The nominal or design life of a structure or structural element is defined as the period during which it is assumed that the structure is to be used for its intended purposes, with scheduled maintenance but without any major repair work being necessary. The reference values for the design life of various types of construction work are shown in Table 3.10.

In most cases, structural glass elements are positioned inside category 4 construction works, i.e., with a design life of 50 years. In the case of monumental buildings, buildings of strategic importance, bridges or particular types of construction, the category of design life is raised to level 5, with specific analyses being carried out for the case in question.

These instructions assume that for pre-failure assessments the nominal design life is 50 years for both second-class and first-class elements. For construction works in category 5, the designer must increase design loads in accordance with the provisions of technical standard EN 1991. For third-class elements, specific analyses must be conducted.

---

<sup>5</sup> The *Norme Tecniche per le Costruzioni* (Technical Standards for Construction) provided for by the Ministerial Decree of 14/01/2008, state as follows: “Construction and plant components, systems and products which do not form part of the overall structure but which perform an autonomous static function must be designed and installed in accordance with the safety and performance levels described below”. Manufacturers must also comply with the provision of Legislative Decrees 115/1995 and 172/2004 concerning “general safety of products”, that is, they can market only “... safe products such that their operation, installation and maintenance do not cause any risk or present minimal risks compatible with the use of the product and considered acceptable in accordance with a high level of human health protection and safety ...”.

Table 3.10. Design life categories (EN1990)

Design life category	Design life (years)	Examples
1	10	Temporary structures <sup>(1)</sup>
2	10 – 25	Replaceable structural parts (bearings, supports)
3	15 – 30	Agricultural or similar structures
4	50	Buildings and other common structures
5	100	Monumental buildings, bridges, other civil engineering structures
<sup>(1)</sup> Structures or parts of structures that can be dismantled with a view to being reused, must not be considered as temporary.		

For post-failure assessments, the nominal design life conventionally assumed is:

- 10 years for second-class elements;
- 10 years for first-class elements.
- based on specific analyses for third-class elements.

### 3.2.3 Expected performance

Each class is associated with a precise probability of failure which, for the first, second and third classes corresponds to the values indicated in EN1990 (Annex B2). The values indicated are the following.

**class zero:**

Not dealt with by these instructions.

**class 1:**

In accordance with EN 1990: probability of failure  $4.83 \cdot 10^{-4}$  in 50 years; probability of failure  $1.335 \cdot 10^{-5}$  in 1 year.

**class 2:**

In accordance with EN 1990: probability of failure  $7.235 \cdot 10^{-5}$  in 50 years; probability of failure  $1.30 \cdot 10^{-6}$  in 1 year.

**class 3:**

In accordance with EN 1990: probability of failure  $8.54 \cdot 10^{-6}$  in 50 years; probability of failure  $9.96 \cdot 10^{-8}$  in 1 year.

The probabilities indicated refer to the pre-failure phase. Post-failure assessment is conducted by suitably rescaling the design load as indicated in Section 3.2.2.

Definition of the value of the failure probability for elements belonging to class zero is beyond the scope of this document. Once this value has been established, it is possible to calibrate the partial factors for the materials using the same procedure described in Chapter 5, thus harmonising the design approach.

## 4 ACTIONS ON GLASS ELEMENTS

### 4.1 General principles

In the area of structural design, an “action” (A) is defined as any cause which is capable of modifying the mechanical, physical or chemical state of an element. Such modifications take the name of “effects” (E). Specifically, actions capable of inducing limit states in a given element are relevant to safety assessments.

As described in Chapter 2 above, glass displays mechanical, physical and chemical characteristics which render it particularly sensitive to a wide range of actions and their variability over space and time, which can produce significantly different effects, depending on the specific case in question. Materials commonly used in composition with glass, both in the manufacture of laminated glass (polymers for interlayers, resins, etc.) or insulated glass units (seals, sealants, etc.) and in the manufacture of bonds and supports (anchors, gaskets, etc.) are also extremely sensitive to the nature, intensity and duration of actions. In particular, for these materials, thermal actions or any actions which can lead to deterioration must not be disregarded.

The characteristic values of actions, in addition to design combinations, must be determined in accordance with the provisions of EN1991 or current national standards. Unless otherwise specified, the reference values will always be those of the characteristic values of the 5% upper fractile for a reference period of 50 years. Where the provisions of the aforementioned standards are insufficient, reference may usefully be made to foreign standards of proven validity, on condition that they are compatible with the principles underlying this document. The following sections describe in detail only those aspects of actions which demand – specifically in relation to glass structures – a more detailed discussion than the one that is generally found in technical standards concerning constructions.

### 4.2 Permanent loads

In order to evaluate actions caused by permanent fixed loads (self-weight of structural materials) and no-fixed permanent loads (non-structural loads), reference will be made to current national standards and to Eurocode 1 (EN 1991).

For the specific weight of glass, in the absence of more accurate data the value of 25 kN/m<sup>3</sup> can conventionally be assumed. This value can be accepted for the purpose of safety assessments on condition that the density of the glass in question is within the range illustrated in Table 2.1.

The influence of polymer interlayers on the specific weight of laminated glass plates can usually be disregarded. In cases where it is not negligible, in the absence of data provided by the manufacturer, reference may be made to Table 4.1.

Table 4.1. Specific weight of a number of materials used as interlayers.

Material	Specific weight kN/m <sup>3</sup>
PVB	10.5 - 10.7
Ionoplastics	9.5 - 10.0
Urethanes	11.5
EVA	9.4 - 9.7
Polycarbonate	12



### 4.3 Human-induced variable loads

The values of live variable loads of human origin are determined in accordance with the provisions of current national standards and with Eurocode 1 (EN 1991) with regard to parts not covered by current national standards.

#### 4.3.1 Vertical variable loads

Reference is made to the provisions of current national standards and Eurocode 1 (EN 1991) for each specific structural category.

Variable loads must provide for uniformly distributed vertical loads  $q_k$  and concentrated vertical loads  $Q_k$ . The loads  $Q_k$  assume particular importance, especially in the case of glass floors, given the fragile nature of the material; they should be understood to be conventional actions for the calculation of local stresses and must not be added to the distributed vertical loads, which instead should be used for the calculation of overall stresses.

In the absence of specific indications, concentrated loads are considered to be applied on a footprint of 50×50 mm.

The characteristic values of variable vertical loads for the various categories of buildings are the ones set out in current applicable standards.

#### 4.3.2 Horizontal variable loads

The design of glass railings, walls or facades which also have the function of protecting users from falls must take into consideration horizontal crowd actions. It is not necessary to take these actions into account only in cases in which railings or fences are structurally independent from the glass panes and sized in accordance with applicable current standards and which prevent contact – including accidental contact – with the glass.

The designer must always ensure that the construction work is sized in accordance with the design horizontal actions established under applicable current standards. It is worth remembering that [BSI 6399-1] and the guidelines provided by the British *Centre for Window and Cladding Technology* include a more detailed description of horizontal loads, which is summarised in Table 4.2 according to the intended use of the structure. Three types of action are considered: actions distributed evenly over the area of the element, actions distributed evenly along a horizontal line 1.20 m above the walking surface or over the handrail or upper edge of the railing, and actions concentrated on a 100×100 mm area located in the most unfavourable position. The foregoing references require these actions to be considered as conventional, *not acting simultaneously* on the element under consideration.

Table 4.2. Minimum horizontal load values to apply non-simultaneously on horizontal elements, in accordance with [BSI 6399-1] and the guidelines of the *Centre for Window and Cladding Technology*.

Cat.	Intended use	Example of specific use	Uniformly distributed load (kN/m <sup>2</sup> )	Load distributed on horizontal line (kN/m)	Concentrated load (kN)
A	Buildings for residential use	Private dwellings, including stairs and landings, but excluding all external railings and roofs	0.50	1.00	0.25
		Other residential applications (hotels etc.) excluding common areas where overcrowding is possible	1.00	1.00	0.50

B1/B2	Offices and work areas unless otherwise specified, including warehouses	Light access stairs and gangways less than 600mm in width	Not applicable	1.00	Not applicable
		Light traffic gangways in factories, depots and warehouses, except designated escape routes	0.50	1.00	0.25
		Areas not susceptible to overcrowding in private and public offices and industrial enterprises, except for cases stated above	1.00	1.00	0.50
C1	Hospitals, restaurants, cafés, banks and schools	Areas with fixed seating less than 530mm from barrier, balustrade or parapet	1.50	1.50	1.50
C2	Balconies and external accessways, conference rooms, cinemas, theatres, churches, stands with fixed seating		1.50	2.00	1.50
C3	Areas without obstacles to people moving, such as museums, exhibition halls, railway stations, dance halls, gymnasiums, stands without fixed seating, buildings for public events, concert halls, sports arenas and stands	Stairs, landings, corridors and ramps	1.00	3.00	0.50
		Terrace and roof railings. Footways and pavements, in courtyards, near basements and areas below the water level of swimming pools or aquariums	1.00	3.00	0.30
		Pedestrian walkways and pavements less than 3m in width near areas below the water level of swimming pools or aquariums	1.50	3.00	1.50
		Theatres, cinemas, discothèques, bars, auditoriums, shopping malls, meeting rooms, recording studios. Footways and pavements more than 3m in width near areas below the water level of swimming pools or aquariums	1.50	3.00	1.50
		Grandstands and stadiums	According to specific standards or requests of competent authorities. In any case load distributed along a line not less than 3.00 kN/m		
D	Buildings for commercial use	Shops, shopping centres, department stores, bookshops	1.50	2.00	1.50
E	Libraries, archives, warehouses and buildings for industrial use	Libraries, archives, warehouses, depots, manufacturing workshops	1.50	1.00	0.25
		Buildings for industrial use	To be evaluated on a case-by-case basis		
F/G	Zones subject to vehicular traffic	Pedestrian areas in car parks: stairs, landings, ramps, terrace railings and edges of roofs	1.50	1.50	1.50
		Horizontal loads imposed by vehicles	To be evaluated on a case-by-case basis		
H1/H2	Roofs and lofts	Roofs and lofts accessible for maintenance only	Not applicable	1.00	.25
		Accessible roofs	According to category		

### 4.3.3 Probabilistic model of human-induced live loads

The actions referred to in Sections 4.3.1 and 4.3.2 are generally represented by characteristic values for a return period of 50 years. In order to calibrate the partial factors on a statistical basis, which is done in Chapter 5 below, it is necessary to have a probabilistic model for human-induced live loads. Variable loads on floors are induced by the weight of furniture, equipment, archived items and people, without including in this category structural and non-structural permanent loads. They are distinguished according to the intended use of the building.

Variable loads exhibit the property of randomly varying over both time and space: change over space is assumed to be homogeneous, while change over time is divided into two components: “permanent” and “discontinuous”. The former takes into account furniture and heavy equipment: the small fluctuations in this load are included in the uncertainties. The discontinuous component represents all types of variable loads not covered by the “permanent” component, such as gatherings of people, crowded halls during special events or stacked objects during rebuilding/renovation work. Both components are modelled as stochastic processes.

The stochastic field representing the load intensity is defined by means of two independent variables,  $V$  and  $U$ . The former is associated with variation in the average load intensity on the surface, while the latter represents the random spatial distribution of the load on the surface itself.

The “permanent” component is modelled as an equivalent uniformly distributed load, which can be represented with a Poisson process in which the time between one load event and the next is distributed exponentially with an expected value of  $\lambda_p$ . The intensity of the permanent load is assumed to have a gamma distribution with an expected value of  $\mu_p$  and a standard deviation  $\sigma_{perm}$  of

$$\sigma_{perm} = \sqrt{\sigma_V^2 + \sigma_{U,p}^2 \cdot \kappa \frac{A_0}{A}}, \quad (4.1)$$

where  $\sigma_V$  is the standard deviation of the random variable  $V$ , while  $\sigma_{U,p}$  represents the standard deviation of the variable  $U$ . Additionally, in this equation,  $\kappa$  is a parameter that depends on the influence surface (which for plates is assumed to be equal to 2),  $A_0$  is a reference area which depends on the intended use, while  $A$  is the total surface area subjected to the load, with the convention that when  $A_0/A > 1$ , it is assumed that  $A_0/A = 1$ . The parameters which describe the distribution depend on the intended use and are found in [PMC Part 2, 2001]. The data used below are found in Table 5.6.

The “discontinuous” component is also modelled as a Poisson process. The time between one event and the next is distributed according to an exponential distribution with an expected value of  $\lambda_q$ . The intensity of the “discontinuous” component is assumed to be interpretable with a Gamma distribution with an expected value of  $\mu_q$  and a standard deviation

$$\sigma_q = \sqrt{\sigma_{U,q}^2 \cdot \kappa \frac{A_0}{A}}, \quad (4.2)$$

where  $\sigma_{U,q}$  is the standard deviation of the stochastic field which describes the variability of the distribution of the load on the surface. These parameters, together with the reference interval  $D_q$  of the discontinuous load, are given in [PMC Part 2, 2001].

The maximum load is therefore obtained through a combination of the “permanent” component and the “discontinuous” component by assuming the stochastic independence between the two load. Lastly, the maximum load during a reference period  $T$  is obtained using the theory of extreme values.

## 4.4 Seismic actions

### 4.4.1 Introduction

From a seismic perspective, except in specific cases, structural glass elements can be considered “secondary” elements,<sup>6</sup> that is, both the stiffness and strength of such elements does not significantly influence the overall response of the construction work. Glass elements, in fact, are either designed with adequate gaps in the connections to “isolate” them from the behaviour of the main structure, as they are able to withstand its deformations without stress, or, given the fragility of the material, they are assumed to shatter under seismic actions.

In cases where glass elements cannot be considered secondary because they provide the construction work with stiffness/strength during seismic actions, specific studies are required – including experimental tests – to demonstrate their suitability for use. These types of structure must in any case be considered class 3 structures, as specified in Section 3.2.1.

If the glass element is required not to suffer damage under seismic actions, it must be suitably *protected* by isolating it seismically from the structure to which it is connected. The support system must therefore ensure that the glass panels can move rigidly in-plane or out-of-plane: in international technical terms, this capacity is termed *clearance*.

### 4.4.2 Definition of design earthquake

The design earthquake is defined in accordance with the building importance class, its reference life and the limit states that need to be taken into consideration.

#### 4.4.2.1 Nominal design life, importance class and reference life

The nominal design life of a structure ( $V_N$ ) is the number of years for which the structure can be used for the purpose for which it is designed, on condition that it is subject to maintenance. For glass construction works subject to seismic actions, in the absence of additional prescriptions, it can be assumed that  $V_N = 50$  years.

With reference to the consequences of an interruption of service or ultimate failure, constructions are divided into importance classes thus defined:

*Class I:* constructions with only occasional presence of people, agricultural buildings.

*Class II:* constructions designed for normal crowd levels, without essential public and social functions. Factories.

*Class III:* constructions designed for significant crowd levels.

*Class IV:* constructions with important public or strategic functions, including those with relevance in disaster management.

Seismic actions are evaluated in relation to a reference period  $V_R$  (reference life) which is derived by multiplying the nominal design life  $V_N$  by the use factor  $C_U$  by means of the equation

$$V_R = V_N \times C_U \quad (4.3)$$

where the value  $C_U$  is a function of the importance class as shown in Table 4.3. Assuming that  $V_N = 50$  years, the values for the reference period illustrated in Table 4.4 follow:

<sup>6</sup> Cf. 7.2.3, [NTC 2008]

Table 4.3. Values of use factor  $C_U$  and corresponding reference period  $V_R$ .

IMPORTANCE CLASS	I	II	III	IV
$C_U$	0.7	1.0	1.5	2.0

Table 4.4. Values of reference period  $V_R$  for  $V_N = 50$  years.

IMPORTANCE CLASS	I	II	III	IV
$V_R$	35	50	75	100

#### 4.4.2.2 Limit states and corresponding design seismic accelerations

Seismic acceleration is calculated in accordance with methods established under national standards, with reference to the following limit states:

- **Operability limit state** (SLO - “*Stato Limite di Operatività*”): as a result of an earthquake, the construction as a whole, including structural elements, non-structural elements and any equipment relevant to its functionality, must not suffer significant damage or interruptions in use.

- **Damage limit state** (SLD – “*Stato Limite di Danno*”): as a result of an earthquake, the construction as a whole, including structural elements, non-structural elements and any equipment relevant to its functionality, suffers damage which does not put users at risk and does not significantly compromise strength and stiffness against vertical and horizontal actions, remaining immediately usable even in the case of interruption of use of part of the equipment.

- **Limit state for the safeguard of human life** (SLV – “*Stato Limite di salvaguardia della Vita*”): as a result of an earthquake, the construction suffers failures and collapses of non-structural and system components and significant damage to structural components, which is associated with a significant loss of stiffness against horizontal actions; the construction however retains a part of its strength and stiffness to withstand vertical actions and a safety margin in relation to failure due to horizontal seismic actions.

- **Collapse prevention limit state** (SLC – “*Stato Limite di prevenzione del Collasso*”): as a result of an earthquake, the construction suffers severe failures and collapses of non-structural and system components and extremely serious damage to structural components; the construction however still retains a margin of safety for vertical actions and a slight margin of safety in relation to failure due to horizontal actions.

The probabilities of exceedance ( $P_{V_R}$ ), in the reference period  $V_R$ , which is to be referred to in order to identify the acting seismic action in each of the limit states under consideration, are illustrated in Table 4.5.

Table 4.5. Probability of exceedance  $P_{V_R}$  for the different limit states under consideration

IMPORTANCE CLASS	SLO	SLD	SLV	SLC
$P_{V_R}$	81%	63%	10%	5%

For each limit state, a return period ( $T_R$ ) for the seismic action is determined according to the reference life ( $V_R$ ) of the construction and therefore its importance class. Table 4.6 shows the values obtainable from the following equation:

$$T_R = -\frac{V_R}{\ln(1 - P_{V_R})} . \quad (4.4)$$

Table 4.6. Return period  $T_R$  (years) as a function of limit state and importance class.

IMPORTANCE CLASS	I	II	III	IV
<i>SLO</i>	21	30	45	60
<i>SLD</i>	35	50	75	100
<i>SLV</i>	333	475	713	950
<i>SLC</i>	683	975	1463	1950

The return period corresponding to the limit state under consideration for the various importance classes of the structure defines the design accelerogram of the seismic action, obviously according to the construction site and geomorphological characteristics of the supporting ground. This characterisation is usually carried out according to national standards.

#### 4.4.2.3 Evaluation of required capacity and performance levels

In order to limit the risks deriving from damage to and/or failure of structural glass elements, the system, i.e. the set of glass and connecting elements, must be designed and constructed in such a way as to guarantee adequate stability. The required performance levels are identified starting from four levels, as defined in Table 4.7, which can be correlated to the same number of limit states. The partial or total control of the previous levels depend on the importance class of the structure and the desired guaranteed limit state for the structure itself.

The performance requirements are shown in Table 4.8, which presents the required performance level according to the importance class of the structure (Section 4.4.2.1) for each one of the four limit states defined (see Section 4.4.2.2). The performance level is identified by the denomination indicated in Table 4.7, where the subscript identifies the return period ( $T_R$ , see Table 4.6) of the reference seismic action. This return-period value uniquely defines the design accelerogram.

Table 4.7. Performance levels required against seismic actions.

Name	Description
ND – No damage	It is assumed that the system is free of any damage that requires the glass panes to be replaced for the functionality of the building. Specifically, façade and roof elements must maintain their requirements of impermeability to wind and to rain.
SD – Slight damage	It is assumed that the system may suffer loss of functionality of some elements, the rapid replacement of which does not involve particular technical details, with the building remaining usable overall. There is no risk for users connected with partial failures.
HD – Heavy damage	The system suffers heavy damage, with a high degree of loss of functionality, with high costs in terms of re-establishing functionality, but without risks of falls of material which could potentially lead to high risk situations.
F – Failure	The system suffers severe damage and exhibits extended evidence of failure. Any falling material would cause risks comparable to those caused by other elements such as cornices and external cladding.

Table 4.8. Performance levels for the “glass” system

Level	Importance class			
	I	II	III	IV
<i>SLO</i>	-	-	ND <sub>45</sub>	ND <sub>60</sub>
<i>SLD</i>	SD <sub>35</sub>	SD <sub>50</sub>	SD <sub>75</sub>	SD <sub>100</sub>
<i>SLV</i>	HD <sub>333</sub>	HD <sub>475</sub>	HD <sub>713</sub>	HD <sub>950</sub>
<i>SLC</i>	-	-	F <sub>1463</sub>	F <sub>1950</sub>

#### 4.4.3 Design accelerations on the local element

In the absence of more specific analyses, the horizontal force  $F_a$ , to be used for out-of-plane assessments can be defined by the equation

$$F_a = \frac{S_a W_a}{q_a}, \tag{4.5}$$

where

- $F_a$  is the horizontal seismic force acting in the centre of mass of the element; if the assessment regards individual glass plates, the action  $F_a$  can be considered a distributed load;
- $W_a$  is the weight of the element;

- $q_a$  the behaviour factor;
- $S_a$  is peak acceleration, which is normalised with respect to the acceleration of gravity, to which the element is subject during the seismic event. It must be evaluated based on the provisions of national standards, according to a) the limit state under consideration and b) the geomorphological characteristics of the ground.

In the absence of a more accurate evaluation, the acceleration  $S_a$  can be determined as

$$S_a = a_g / g \cdot S \cdot R_a , \tag{4.6}$$

with the magnification factor  $R_a$  defined as

$$R_a = \max \left\{ \begin{array}{l} \frac{3(1+Z/H)}{1+(1-T_a/T_1)^2} - 0,5, \\ 1, \end{array} \right. \tag{4.7}$$

where:

- $a_g/g$  is the ratio between the peak ground acceleration on type A ground to be considered in the limit state in question and the acceleration of gravity;
- $S$  is the factor which takes account of the soil category and topographical conditions, as specified in national standards;
- $Z$  is the height of the centre of gravity of the non-structural element measured from the foundation level;
- $H$  is the height of the construction measured from the foundation level. For buildings isolated at the base it is assumed that  $H = 0$ ;
- $T_a$  is the fundamental vibration period of the non-structural element;
- $T_1$  is the is the fundamental vibration period of the construction in the direction considered;

The graph of magnification factor  $R_a$  as a function of  $T_a/T_1$  for various values of the ratio  $Z/H$  is shown in Figure 4.1.

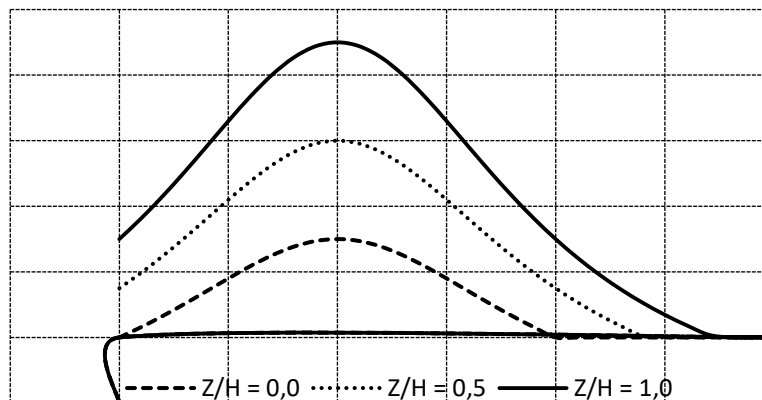


Figure 4.1. Magnification factor  $R_a$  as a function of  $T_a/T_1$  for various values of  $Z/H$ .

It is to be remarked, however, that in general local actions due to the seismic acceleration are usually smaller than actions caused, for example, by wind. As a result, verification against local actions is insignificant.



#### 4.4.4 Design displacements

Displacements of the building and in particular interstorey drift caused by seismic actions are the essential parameters for the design of glass panes. In general, these derive from the structural analysis of the building for the various limit states and performance levels required. The glass structure designer must consult these data in order to size the joints and connection systems of the glass elements with respect to the characteristics of the rest of the structure.

For pre-sizing or preliminary evaluation purposes only, the designer can conduct simplified statistical analyses of the kind illustrated in Annex 4.11.

#### 4.4.5 Combination of the seismic action with other actions

In order to determine the combination of actions, reference may be made to national technical regulations in force [NTC 2008]. For each limit state, evaluations must be carried out by combining the seismic action ( $E$ ) with the action resulting from dead ( $G$ ) and characteristic variable loads ( $Q_{kj}$ ), in accordance with the following combination rule, which refers to the combination coefficients ( $\psi_{2j}$ ) in Table 4.9.

$$G + E + \sum_j \psi_{2j} Q_{kj} \cdot \tag{4.8}$$

Table 4.9. Value of combination coefficients

Category Variable action	$\Psi_{2j}$
<i>Category A: Buildings for residential use</i>	0.3
<i>Category B: Offices</i>	0.3
<i>Category C: Buildings susceptible to crowding</i>	0.6
<i>Category D: Buildings for commercial use</i>	0.6
<i>Category E: Libraries, archives, warehouse and buildings for industrial use</i>	0.8
<i>Category F: Garages and parking areas (for vehicles <math>\leq 30</math> kN)</i>	0.6
<i>Category G: Garages and parking areas (for vehicles <math>&gt; 30</math> kN)</i>	0.3
<i>Category H: Roofs</i>	0.0
<i>Wind</i>	0.0
<i>Snow (<math>\leq 1000</math> m a.s.l.)</i>	0.0
<i>Snow (<math>&gt; 1000</math> m a.s.l.)</i>	0.2
<i>Temperature changes</i>	0.0

Effects of seismic actions are evaluated taking into account the masses associated with the gravitational loads

$$G + \sum_j \psi_{2j} Q_{kj} \cdot \tag{4.9}$$

The actions indicated above will be used to evaluate the displacements of the connection points of the glass elements, by conducting structural calculations in accordance with the procedures illustrated in Section 7.6.2.

## 4.5 Wind actions

### 4.5.1 Probabilistic distribution of wind speed

With regard to wind action, reference is mainly made to the model implemented in the instructions CNR-DT207/2008. This action is evaluated from the *reference velocity*  $v_r$ , which characterises the windiness of the zone in which the building is located. This is conventionally defined as the mean wind speed during a time interval  $T = 10$  minutes, at a height of 10 m above ground level, on a flat and homogeneous terrain with a roughness length  $z_0 = 0.05$  m (exposure category II, Section 3.2.3 [CNR-DT207/2008]), with reference to a design return period  $T_R$ .

In the absence of specific, adequate statistical surveys,  $v_r$  can be expressed by the relationship

$$v_r = v_{b50} \cdot c_r, \quad (4.10)$$

where:

$v_{b50}$  is the reference basic wind speed associated with a return period  $T_R = 50$  years;

$c_r$  is the return period factor furnished by Eq. (4.11) and illustrated in the graph in Figure 4.2:

$$c_r = \begin{cases} 0.75, & \text{for } T_R = 1 \text{ year,} \\ 0.75 + 0.0652 \ln(T_R), & \text{for } 1 \text{ yr} < T_R \leq 5 \text{ yrs,} \\ 0.75 \sqrt{1 - 0.2 \ln \left[ -\ln \left( 1 - \frac{1}{T_R} \right) \right]}, & \text{for } 5 \text{ yrs} < T_R \leq 50 \text{ yrs,} \\ 0.65 \left\{ 1 - 0.138 \ln \left[ -\ln \left( 1 - \frac{1}{T_R} \right) \right] \right\}, & \text{for } T_R > 50 \text{ yrs.} \end{cases} \quad (4.11)$$

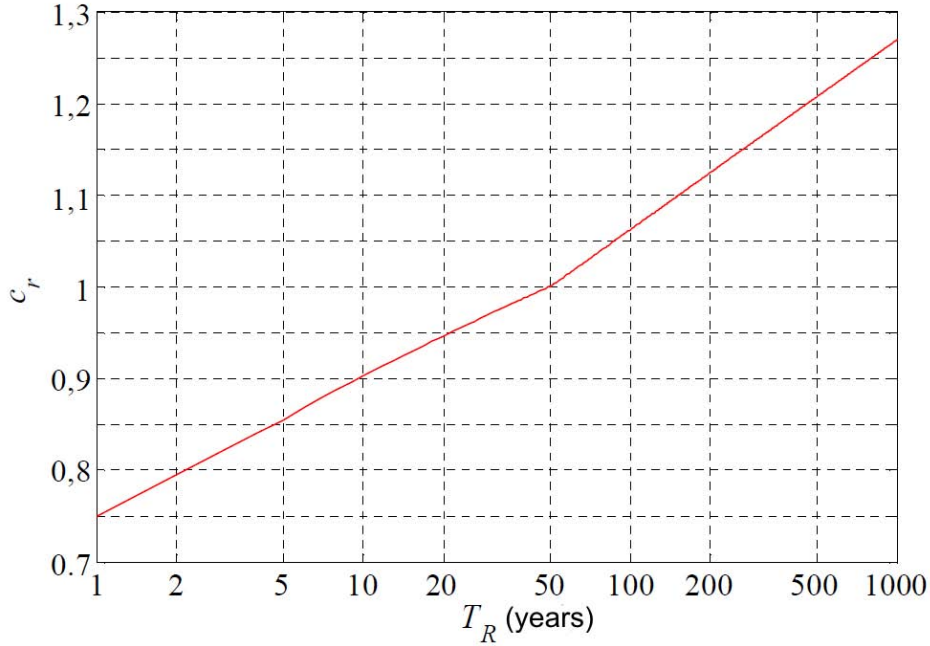


Figure 4.2. Diagram of return period factor  $c_r$  as a function of the return period  $T_R$ .

[CNR-DT207/2008] - Annex A, contains a number of recommendations concerning choice of design return period according to the construction properties, while Annex B provides a number of guidelines for evaluating the reference design speed  $v_r$  on the basis of adequately corroborated methods and data.

The reciprocal of the return period  $1/T_R$  expresses the probability  $p$  that the peak annual wind velocity exceeds the value  $v_r$  ( $p = 1/T_R$ ). The cumulative distribution function  $F(v_r)$ , which represents the probability that  $v_r$  is not exceeded in 1 year, is therefore given by

$$F(v_r) = 1 - p = 1 - \frac{1}{T_R} = \begin{cases} 0, & \text{for } v_r \leq 0.75v_{b50}, \\ 1 - \exp\left(\frac{0.75v_{b50} - v_r}{0.0652v_{b50}}\right), & \text{for } 0.75v_{b50} < v_r \leq 0.85v_{b50}, \\ \exp\left[-\exp\left(\frac{1}{0.2} - \frac{v_r^2}{0.2 \cdot 0.75^2 v_{b50}^2}\right)\right], & \text{for } 0.85v_{b50} < v_r \leq v_{b50}, \\ \exp\left\{-\exp\left[\frac{1}{0.138} \left(1 - \frac{v_r}{0.65 v_{b50}}\right)\right]\right\}, & \text{for } v_r > v_{b50}. \end{cases} \quad (4.12)$$

It should perhaps be pointed out that the model considered here is more complex than the one set out in the *Circolare Esplicativa alle Norme Tecniche per le Costruzioni* (Explanatory Circular Concerning Technical Standards for Constructions) [NTC 2009], which considers only the third branch of Eq. (4.11), independently of the duration of the return period. Equally, the model set out under point 4.2 (2)P of European Standard EN 1991-1-4, states that the coefficient  $c_{prob}$ , which multiplied by the reference velocity  $v_{b50}$  gives the value of the wind velocity having a probability for annual exceedance equal to  $p$ , can be calculated by means of the equation

$$c_{prob} = \left( \frac{1 - K \cdot \ln(-\ln(1 - p))}{1 - K \cdot \ln(-\ln(0.98))} \right)^n, \quad (4.13)$$

where  $K$  is the shape parameter depending on the coefficient of variation of the extreme-value distribution. By assigning to  $K$  and  $n$  respectively the values recommended by the Eurocode, 0.2 and 0.5, and substituting the probability  $p$  with the reciprocal of the return period ( $p = 1/T_R$ ), Eq. (4.11c) is obtained for the coefficient  $c_r$ .

#### 4.5.2 Wind pressure

The reference kinetic wind pressure, indicated by  $q_w$ , is given by the equation

$$q_w = \frac{1}{2} \rho_a v_r^2, \quad (4.14)$$

where  $v_r$  represents the reference design wind velocity and  $\rho_a$  indicates air density, assumed to be  $1.25 \text{ kg/m}^3$ .

As glass is subject to the phenomenon of static fatigue (Section 2.1.1.1), it is important to define not only the peak value of the action but also its characteristic duration, as relative weak actions but with long durations can cause greater damage than peak actions. This is why, this section shows the method which allows peak wind velocity (averaged over 3 seconds) and mean wind velocity over 10 minutes to be determined.

The mean wind velocity  $v_m$  over a reference time interval  $T = 10$  minutes depends, in general, on the height from the ground  $z$ , on the windiness of the zone in question, on the design return period and on the local characteristics of the site on which the construction stands. Except in specific cases, its direction is assumed to be generally horizontal.

In the absence of specific analyses which take into account wind direction and the effective roughness and orography of the terrain surrounding the construction, for above-ground heights not exceeding  $z = 200$  m, the mean wind velocity is given by the equation

$$v_m(z) = v_r \cdot c_m(z), \quad (4.15)$$

where  $v_r$  is the reference design wind velocity, while  $c_m(z)$  is the wind mean profile coefficient furnished by the equation

$$c_m(z) = \ln\left(\frac{z}{z_0}\right) \cdot k_r \cdot c_t, \quad \text{with } z = z_{\min} \text{ for } z \leq z_{\min}, \quad (4.16)$$

where  $k_r$  is the terrain factor,  $z_0$  the roughness length and  $z_{\min}$  the minimum height, which all depend on the exposure category of where the construction is located, while  $c_t$  is the topography coefficient. The values of these coefficients are provided in Section 3.2.5 of CNR-DT207/2008. The reference kinetic pressure averaged over an interval of 10 minutes is therefore given by the equation

$$q_{w,10\min}(z) = \frac{1}{2} \rho_a \cdot v_m^2(z) = \frac{1}{2} \rho_a \cdot v_r^2 \cdot c_m^2(z). \quad (4.17)$$

For convenience, the equation

$$q_{w,10\min}(z) = \frac{1}{2} \cdot \rho_a \cdot v_r^2 \cdot c_{el}(z), \quad (4.18)$$

can be introduced, where  $c_{e1}$  is the *exposure coefficient for mean wind action* which, for Eqs. (4.16) and (4.17), takes the following form:

$$c_{e1}(z) = \left( \ln \left( \frac{z}{z_0} \right) \right)^2 \cdot k_r^2 \cdot c_t^2, \text{ with } z = z_{\min} \text{ for } z \leq z_{\min}. \quad (4.19)$$

Peak wind velocity  $v_p$  is defined as the expected maximum wind speed value over the course of a time interval  $T = 10$  minutes, averaged over a time interval  $t$  which is much shorter than  $T$ . It depends on the height from the ground  $z$ , the windiness of the zone in question, the design return period and the local characteristics of the site on which the construction stands.

In the absence of specific analyses which take into account wind direction and the effective roughness and orography of the terrain surrounding the construction, for above-ground heights of not more than  $z = 200$  m, the peak wind speed can be evaluated through the following equation [CNR-DT207/2008, Annex F]

$$v_p(z) = v_m(z) \cdot G_v(z), \quad (4.20)$$

where  $v_m$  is once again the mean wind velocity at height  $z$  and  $G_v$  is the gust factor expressed by the formula

$$G_v(z) = 1 + g_v(z) \cdot I_v(z) \cdot P_v(z), \quad (4.21)$$

where  $g_v$  is the peak wind velocity factor,  $I_v$  turbulence intensity and  $P_v$  a coefficient which takes account of the reduction in the intensity of turbulence due to the time period  $\tau$  over which the peak speed is averaged.

By making a number of reasonable approximations and safe-side assumptions (see equation (F.7), Annex F, CNR-DT207/2008), the following equation can be derived for the kinetic peak wind pressure (excluding dynamic and pressure coefficients) over a reference period  $t = 3$  sec:

$$q_{w,3\text{sec}}(z) = \frac{1}{2} \cdot \rho_a \cdot v_m^2 \cdot [1 + 7 \cdot I_v(z)], \quad (4.22)$$

where the turbulence intensity  $I_v$  is defined as (point 3.2.6 [CNR-DT 207/2008])

$$I_v(z) = \frac{1}{\ln \left( \frac{z}{z_0} \right) \cdot c_t}, \text{ with } z = z_{\min} \text{ for } z \leq z_{\min}. \quad (4.23)$$

Equation(4.22) may also be expressed in the form

$$q_{w,3\text{sec}}(z) = \frac{1}{2} \cdot \rho_a \cdot v_r^2 \cdot c_e(z), \quad (4.24)$$

where the *exposure coefficient*  $c_e(z)$  is

$$c_e(z) = k_r^2 \cdot \ln \left( \frac{z}{z_0} \right) \cdot c_t(z) \cdot \left[ \ln \left( \frac{z}{z_0} \right) \cdot c_t(z) + 7 \right], \text{ with } z = z_{\min} \text{ for } z \leq z_{\min}. \quad (4.25)$$

Peak kinetic pressure  $q_{w,3\text{sec}}$  and mean pressure over 10 minutes  $q_{w,10\text{min}}$  can be compared by introducing an exposure correction coefficient  $c_{e2}$  according to the expression

$$q_{w,3\text{sec}}(z) = \frac{1}{2} \cdot \rho_a \cdot v_m^2 \cdot c_{e2}(z) = q_{w,10\text{min}}(z) \cdot c_{e2}(z), \quad (4.26)$$

where

$$c_{e2}(z) = \frac{c_e}{c_{e1}} = 1 + \frac{7}{\ln\left(\frac{z}{z_0}\right) \cdot c_t}. \quad (4.27)$$

Wind pressure on the structure (averaged over 10 minutes or peak pressure) is obtained by multiplying the kinetic pressure for the relative pressure coefficient  $c_p$  and the dynamic factor+  $c_d$ , whose values are provided by technical recommendations.

Finally, kinetic pressure averaged over 10 minutes becomes

$$p_{w,10\text{min}}(z) = \frac{1}{2} \cdot \rho_a \cdot v_r^2 \cdot c_{e1}(z) \cdot c_p \cdot c_d, \quad (4.28)$$

while 3-second peak kinetic pressure can be assumed to be

$$p_{w,3\text{sec}}(z) = \frac{1}{2} \cdot \rho_a \cdot v_r^2 \cdot c_e(z) \cdot c_p \cdot c_d. \quad (4.29)$$

The cumulative distribution function  $F(v_r)$ , which expresses the probability that the reference wind velocity value  $v_r$  is not exceeded in one year, is provided by Eq. (4.12).

Similarly, the cumulative distribution function for wind pressure  $p_{w,\tau}$  averaged over time  $\tau$  ( $\tau = 3\text{sec}$  or  $\tau = 10\text{min}$ ) is obtained by substituting  $v_r$  from Eqs. (4.28) and (4.29) into Eq. (4.12), obtaining

$$F(p_{w,\tau}) = \begin{cases} 0, & \text{for } \frac{p_{w,\tau}}{\frac{1}{2} \rho_a c_{e,\tau} c_p c_d} \leq (0.75 v_{b50})^2, \\ 1 - \exp\left[ \frac{1}{0.0652 v_{b50}} \left( 0.75 v_{b50} - \sqrt{\frac{2 p_{w,\tau}}{\rho_a c_{e,\tau} c_p c_d}} \right) \right], & \text{for } (0.75 v_{b50})^2 < \frac{p_{w,\tau}}{\frac{1}{2} \rho_a c_{e,\tau} c_p c_d} \leq (0.85 v_{b50})^2, \\ \exp\left[ -\exp\left( \frac{1}{0.2} - \frac{2 p_{w,\tau}}{0.2 \cdot 0.75^2 \rho_a v_{b50}^2 c_{e,\tau} c_p c_d} \right) \right], & \text{for } (0.85 v_{b50})^2 < \frac{p_{w,\tau}}{\frac{1}{2} \rho_a c_{e,\tau} c_p c_d} \leq v_{b50}^2, \\ \exp\left\{ -\exp\left[ \frac{1}{0.138} \left( 1 - \frac{1}{0.65} \sqrt{\frac{2 p_{w,\tau}}{\rho_a v_{b50}^2 c_{e,\tau} c_p c_d}} \right) \right] \right\}, & \text{for } \frac{p_{w,\tau}}{\frac{1}{2} \rho_a c_{e,\tau} c_p c_d} > v_{b50}^2, \end{cases} \quad (4.30)$$

where

$$c_{e,\tau} = \begin{cases} c_e & \text{for } \tau = 3\text{sec}, \\ c_{e1} & \text{for } \tau = 10\text{min}, \end{cases} \quad (4.31)$$

$c_{e1}$  and  $c_e$  being defined by Eqs. (4.19) and (4.25), respectively.

## 4.6 Snow loads

### 4.6.1 Design load

The load  $q_s$  caused by snow on roofs is calculated by means of an equation of the following type:

$$q_s = \mu_i q_{sk} C_E C_t, \quad (4.32)$$

where:

$\mu_i$  is the roof shape coefficient;

$q_{sk}$  is the characteristic reference value for the ground snow load for a return period of 50 years;

$C_E$  is the exposure coefficient which is a function of the specific orographic characteristics of the area in which the construction stands;

$C_t$  is the thermal coefficient which takes into account the reduction in the snow load due to loss of heat of the construction.

The values of the coefficients referred to above can be found in national technical standards and in [UNI EN 1991].

### 4.6.2 Probabilistic distribution for snow load

The snow load probabilistic model, used in the procedure proposed for calculating the partial factors for glass structures, has been derived starting from formula (D.1) used to adjust the ground snow load according to changes in the return period as illustrated in Annex D of [EN 1991, 1-3]. This equation applies to cases in which the distribution of annual maximum snow loads can follow the Gumbel probability distribution function. The equation takes the form

$$q_{sn} = q_{sk} \left\{ \frac{1 - V \frac{\sqrt{6}}{\pi} [\ln(-\ln(1 - P_n)) + 0.57722]}{(1 + 2.5923V)} \right\}, \quad (4.33)$$

where:

$q_{sk}$  is the characteristic value of the ground snow load (with a return period of 50 years);

$q_{sn}$  is the snow load for a return period of  $n$  years (thus for an annual exceedance probability  $P_n$ );

$P_n$  is the annual probability of exceedance (approximately equal to  $1/n$ , where  $n$  is the corresponding return period (years));

$V$  is the coefficient of variation of annual maximum snow load.

As  $P_n$  is the annual exceedance probability, it follows that  $1 - P_n$  is the annual non-exceedance probability and therefore the ordinate of the cumulative distribution function for the ground snow load with a reference period of 1 year. Thus, calculating  $1 - P_n = F(q_{sn})$  from Eq. (4.33) the abovementioned cumulative distribution function is obtained in the following form:

$$F_{q_{sn}}(x) = \exp \left[ -\exp \left[ \left[ 1 - \frac{x}{q_{sk}} (1 + 2.5923V) \right] \cdot \frac{\pi}{V \cdot \sqrt{6}} - 0.57722 \right] \right]. \quad (4.34)$$

This function depends on the parameters  $q_{sk}$  and  $V$ . The value of  $q_{sk}$  is provided by the standard and is a function of climate zone and altitude. The value of the coefficient of variation should be provided by the competent national authority; however, to date in the Italian national annexes a precise value has not been specified. [EN 1991 1-3] provides a graph in which the coefficient of variation is assumed to be in a variable range from 0.2 to 0.6. In the probabilistic analysis conducted in Section 5.3.3.2 below, two extreme values are assumed and the results obtained are compared.

Once the ground snow load has been established, it is possible to derive the snow load on roofs,  $q_s$ , from Eq. (4.32). By substituting Eq. (4.32) into Eq. (4.34), we obtain the following equation for snow load distribution on roofs:

$$F_{q_s}(x) = \exp \left[ -\exp \left[ \left[ \left[ 1 - \frac{x}{q_{sk} \mu_i \cdot C_E \cdot C_t} (1 + 2.5923V) \right] \cdot \frac{\pi}{V \cdot \sqrt{6}} - 0.57722 \right] \right] \right]. \quad (4.35)$$

This equation is used in Section 5.3 to calibrate the partial factors in the various case studies conducted.

## 4.7 Thermal actions

Because of its intrinsic brittleness, glass is extremely sensitive to actions caused by temperature changes. Hence we consider it helpful to provide an adequate treatment of the subject, which deserves more details than those usually found in technical standards for traditional construction materials.

### 4.7.1 General remarks

Thermal actions are of interest in cases where they may generate stress states in the glass element. Such stresses may be caused by two mechanisms:

- impeded dilations in the glass structure or in its supports;
- temperature gradients in the same glass plate.

In both cases, it is necessary to determine the temperature of the glass element, which may be obtained by means of a number of rather complex calculations, which are influenced by numerous factors, such as:

- conduction of the materials comprising the glass structure;
- surface, natural or forced convection (e.g. through ventilators in double-skin facades) and ventilation conditions;
- solar irradiance;
- absorption and reflection of solar energy on the part of the glass plates in question;
- emissivity of the glass plates in question;
- external air temperature;
- internal air temperature;
- temperature of gas inside the insulating glass unit.

The severity of thermal actions is generally also influenced by other factors such as local climate conditions, exposure, overall mass of the structure and the presence of any insulating elements.



With regard to procedures for calculating temperatures of glass elements, the reader is referred to specialist references. The characteristic values of thermal conduction and expansion for glass and the materials most commonly used in association with it are illustrated in Table 4.10 and Table 4.11.

Table 4.10. Indicative values of thermal conductivity coefficients

Material	Thermal conductivity coefficient $\lambda$ [ $\text{W m}^{-1} \text{K}^{-1}$ ]
Glass	1
Aluminium	236
Carbon steel	36 - 54
Silicone	0.25
Concrete (dry)	0.70

Table 4.11. Indicative values of thermal expansion coefficients

Material	Thermal expansion coefficient $\alpha$ [ $\text{K}^{-1}$ ]
Glass	$9 \cdot 10^{-6}$
Aluminium	$23 \cdot 10^{-6}$
Carbon steel	$12 \cdot 10^{-6}$
PVB	$80 \cdot 10^{-6}$
Concrete	$12 \cdot 10^{-6}$

The absorption, reflection and emissivity coefficients of a glass plate are influenced by the colour of the glass and surface treatments (i.e. coatings) and are typical of each product; the relevant values are commonly provided by the manufacturer of the glass itself (e.g. solar factor, transmission, reflection and absorption indicators, etc.).

The heat transmitted by convection and the consequent influence on the temperatures of the components can be calculated according to classical thermodynamics, for which the reader is referred to specialist references. Solar irradiance, external temperature and internal temperature are dealt with in the following sections.

#### 4.7.2 External air temperature

External air temperature,  $T_{est}$ , can assume the values  $T_{max}$  or  $T_{min}$ , defined respectively as maximum summer and minimum winter air temperature in the location of the construction, based on a return period of 50 years. An initial evaluation may assume a temperature variation between the extreme values  $\Delta T = \pm 30^\circ\text{C}$ . For more accurate evaluations reference may be made to current legislation.<sup>7</sup>

#### 4.7.3 Internal air temperature

In the absence of specific data for the building under consideration, the conventional internal temperatures illustrated in Table 4.12 and expressed in degrees Celsius [UNI 5364:1976], may be assumed.

<sup>7</sup> Tables of "day degrees" for Italian municipalities grouped by region and province can be found in Ministerial Decree 06/08/1991 (published in Official Gazette no. 197, 24/08/1994 and republished with corrections in Official Gazette no. 203 of 31/08/1994), Ministerial Decree 16/05/1995 (Official Gazette no. 119, 24/05/1995), which also repeals Ministerial Decree 06/08/1991, and Ministerial Decree 06/10/1997 (Official Gazette no. 242, 16/10/1997).

Table 4.12 Values of conventional internal temperatures expressed in degrees Celsius [UNI 5364:1976].

Housing and offices, intended to daytime living of people who are at rest, or occupied in reading, writing, conversation	18-21
- Housing for the night rest	17-19
- Hotel rooms, hospitals, intended to stay day and night	18-20
- Rooms of shops, warehouses, etc., where customers do not take their coat off and staff holds a moderate activity, standing up	14-16
- Churches, museums, where people do not take off their coat	12-14
- Public places, like cinemas, theatres, restaurants, where people take off their coat	16-18
- Public places, like opera houses and luxury restaurants, where people wear evening gowns	18-20
- Communities (schools, barracks) where numerous people stay overnight (dormitories)	15-17
- Public rooms, hosting several people at rest, occupied in reading, writing, conversation (reading and meeting rooms, classrooms)	17-19
- Canteens, locker rooms, or similar places for short stay	16-18
- Public passing places: stairs, corridors	12-14
- Short standing time rooms, for people who perform light work or custodial duties (warehouses, archives)	14-16
- Showers, swimming pools, bathrooms, rooms for medical visits, where may people take off their clothes	22-24
- Surgery rooms, with special requirements	24-30
- Gyms, halls for heavy games, dance halls	12-14
- Industries: temperature depends upon the specific activity, compatibly with technological requirements.	

#### 4.7.4 Maximum solar irradiance

Irradiance is defined as the ratio of the radiating energy per unit of time on a surface and the area of the surface.

In the absence of specific data for the site in question, the maximum summer incident solar irradiance values on a vertical surface illustrated in Table 4.13 and expressed in  $W/m^2$  for various latitudes may be used as reference [UNI 10349:1994].

Table 4.13 Maximum summer solar irradiance [UNI 10349:1994].

**Prospetto XVII — Maximum summer solar irradiance on vertical surfaces (W/m<sup>2</sup>)**

Time	South	S-E	East	N-E	North	N-W	West	S-W	Diffused	Horizontal
<b>Latitude 46° N</b>										
5	11	58	137	143	71	11	11	11	11	30
6	50	312	562	511	192	50	50	50	50	198
7	86	509	750	595	147	79	79	79	79	381
8	177	631	764	536	109	102	102	102	102	552
9	321	679	713	402	120	120	120	120	120	698
10	439	655	568	234	133	133	133	140	133	810
11	515	567	374	148	141	141	141	250	141	881
12	541	427	156	144	144	144	156	427	144	909
13	515	250	141	141	141	146	374	567	141	881
14	439	140	133	133	133	234	568	655	133	810
15	321	120	120	120	120	402	713	679	120	698
16	177	102	102	102	109	536	764	631	102	552
17	86	79	79	79	147	595	750	509	79	381
18	50	50	50	50	192	511	562	312	50	198
19	11	11	11	11	71	143	137	56	11	30
<b>Latitude 44° N</b>										
5	7	38	92	96	48	7	7	7	7	19
6	46	300	546	500	191	48	48	48	48	188
7	85	499	747	601	157	79	79	79	79	377
8	161	620	766	549	110	103	103	103	103	554
9	300	665	716	420	124	121	121	121	121	706
10	414	639	571	254	134	134	134	140	134	822
11	488	549	377	150	143	143	143	232	143	895
12	514	408	157	145	145	145	157	408	157	920
13	488	232	143	143	143	150	377	549	143	895
14	414	140	134	134	134	254	571	639	134	822
15	300	121	121	121	124	420	716	665	121	706
16	161	103	103	103	110	549	766	620	103	554
17	85	79	79	79	157	601	747	499	79	377
18	46	48	48	48	191	500	546	300	48	188
19	7	7	7	7	48	96	92	38	7	19
<b>Latitude 42° N</b>										
5	4	21	52	54	27	4	4	4	4	10
6	47	267	529	487	189	47	47	47	47	178
7	83	489	744	606	166	78	78	78	78	374
8	145	606	767	562	112	103	103	103	103	556
9	279	651	718	438	126	122	122	122	122	713
10	390	622	573	274	136	136	136	141	136	833
11	461	531	379	153	144	144	144	213	144	908
12	486	369	159	147	147	147	159	389	159	934
13	461	213	144	144	144	153	379	531	144	908
14	390	141	136	136	136	274	573	622	136	833
15	279	122	122	122	126	438	718	651	122	713
16	145	103	103	103	112	562	767	606	103	556
17	83	78	78	78	166	606	744	489	78	374
18	47	47	47	47	189	487	529	267	47	178
19	4	4	4	4	27	54	52	21	4	10

*(segue prospetto)*

(seguito del prospetto XVII)

Time	South	S-E	East	N-E	North	N-W	West	S-W	Diffused	Horizontal
Latitude 40° N										
5	2	8	20	21	11	2	2	2	2	4
6	45	274	511	473	166	45	45	45	45	168
7	82	479	740	610	176	76	78	78	78	369
8	126	596	787	575	113	103	103	103	103	557
9	256	636	720	455	127	122	122	122	122	719
10	384	605	576	295	137	137	137	141	137	842
11	433	512	381	155	145	145	145	194	145	920
12	457	369	160	148	148	148	160	369	160	948
13	433	194	145	145	145	155	361	512	145	920
14	384	141	137	137	137	295	576	605	137	842
15	256	122	122	122	127	455	720	636	122	719
16	126	103	103	103	113	575	787	596	103	557
17	82	76	76	76	176	610	740	479	78	369
18	45	45	45	45	166	475	511	274	45	168
19	2	2	2	2	11	21	20	8	2	4
Latitude 38° N										
5	0	2	4	4	2	0	0	0	0	1
6	42	260	491	457	182	42	42	42	42	157
7	81	466	736	614	165	77	77	77	77	364
8	115	584	787	567	116	103	103	103	103	558
9	238	621	722	473	129	123	123	123	123	723
10	338	587	578	316	138	138	138	141	138	651
11	404	492	382	158	147	147	147	174	147	931
12	428	349	162	150	150	150	162	349	162	958
13	404	174	147	147	147	158	382	492	147	931
14	338	141	138	138	138	316	576	587	138	651
15	236	123	123	123	129	473	722	621	123	723
16	113	103	103	103	116	576	787	584	103	558
17	81	77	77	77	165	614	736	466	77	364
18	42	42	42	42	182	457	491	260	42	157

To calculate maximum incident summer solar irradiance on a vertical surface at a specific time of the day, the latitude of the location in question must be known (provided in [UNI 10349:1994]) in order to interpolate linearly, between the values relating to latitudes in the table, according to the following equation:

$$I_T(\varphi) = I_T(\varphi_{r1}) + \frac{I_T(\varphi_{r2}) - I_T(\varphi_{r1})}{\varphi_{r2} - \varphi_{r1}} (\varphi - \varphi_{r1}), \tag{4.36}$$

where:

- $I_T$  maximum solar irradiance for a surface with orientation  $T$ ;
- $\varphi$  latitude of the location in question;
- $\varphi_{r1}$  latitude provided by Table XVII of [UNI 10349:1994] immediately greater than that of the location in question;
- $I_T(\varphi_{r1})$  maximum solar irradiance for the surface with orientation  $T$  taken from Table XVII of [UNI 10349:1994] for latitude  $\varphi_{r1}$ .
- $\varphi_{r2}$  latitude provided by Table XVII of [UNI 10349:1994] immediately lower than that of the location in question;
- $I_T(\varphi_{r2})$  maximum solar irradiance for the surface with orientation  $T$  taken from Table XVII of [UNI 10349:1994] for latitude  $\varphi_{r2}$ .

It may be interesting to observe the diagrams contained in the following figures, which provide the radiance values on vertical surfaces for various exposure (north, east, south or west), as well as on a horizontal surface. Data refer to a northern Italian city.

From these figures it can be observed that maximum solar irradiance, for a south-facing vertical surface, does not occur in the summer but in the autumn and winter. This is due to the position of the sun in different seasons and at different times of the day. Indeed, as the sun is lower on the horizon during the autumn and winter, the angle of incidence of the sun's rays is closer to perpendicular with the surface than it is during the summer.

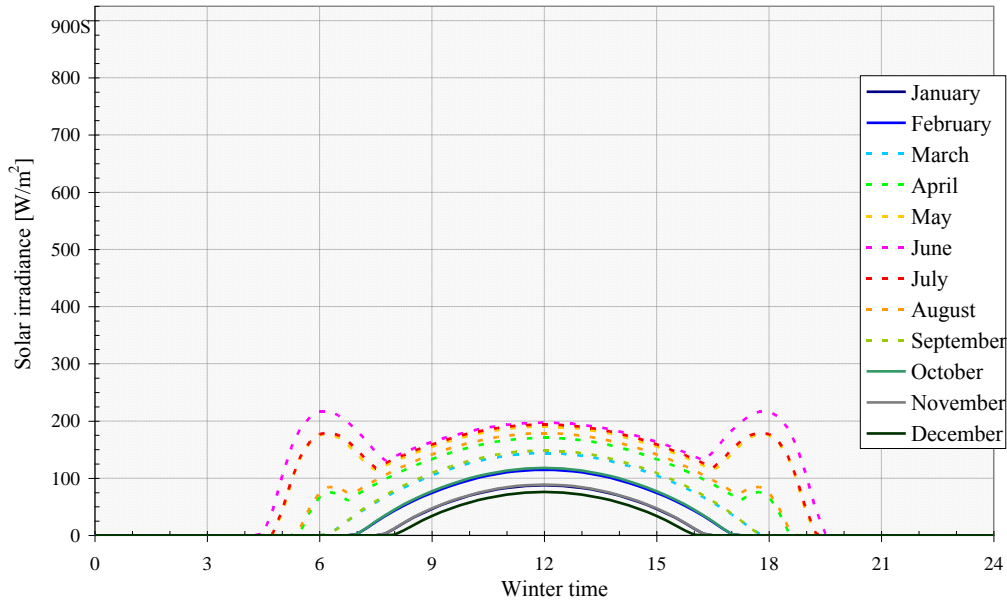


Figure 4.3 Lat.: 45° 25' N. Solar irradiance on north-facing vertical surface.

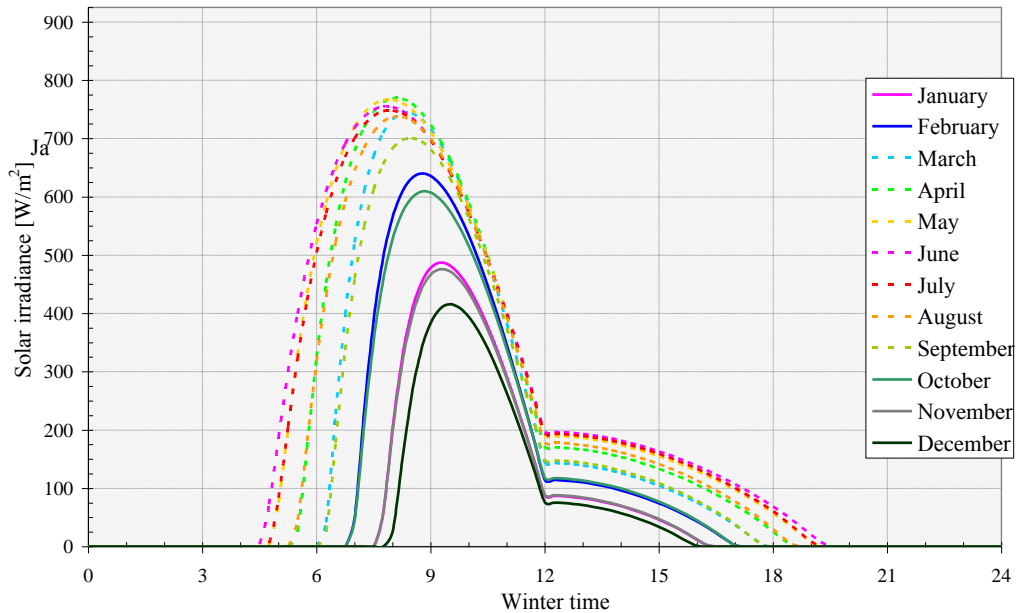


Figure 4.4 Lat.: 45° 25' N. Solar irradiance on east-facing vertical surface.

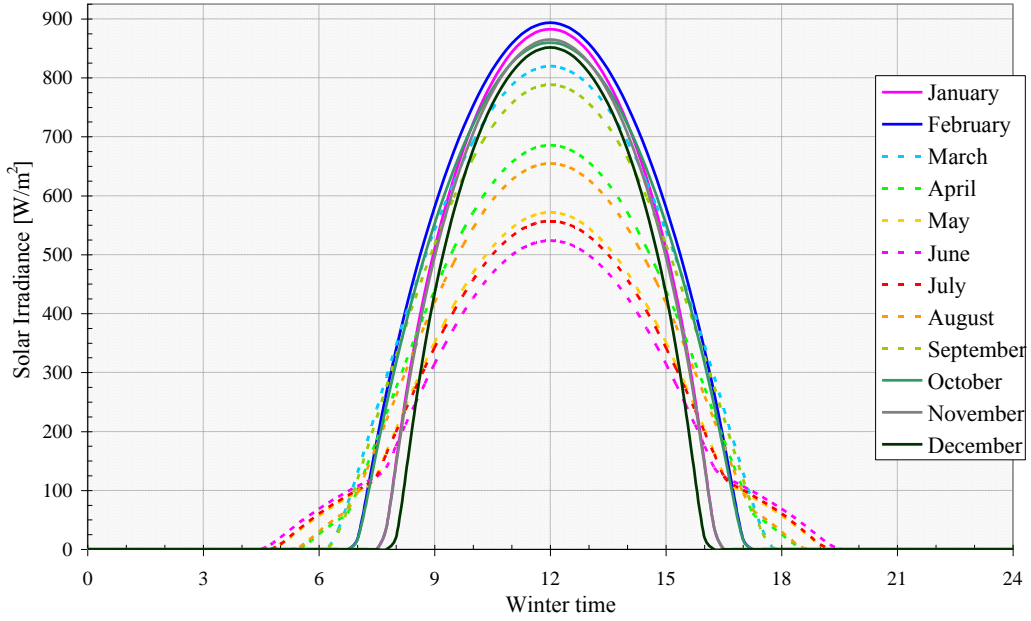


Figure 4.5 Lat.: 45° 25' N. Solar irradiance on south-facing vertical surface.

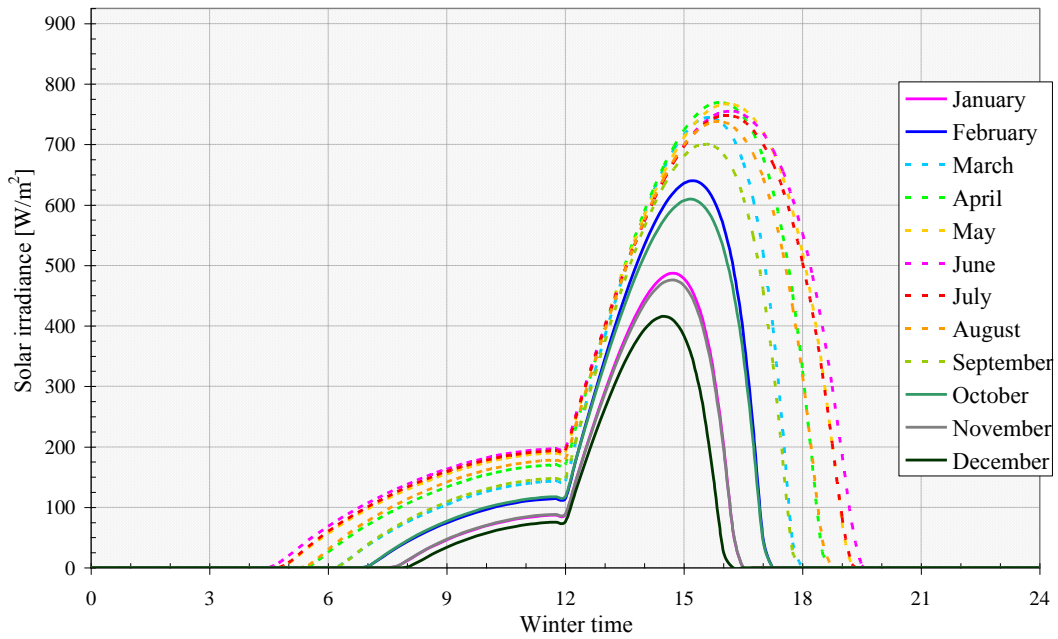


Figure 4.6 Lat.: 45° 25' N. Solar irradiance of west-facing vertical surface.

## 4.7.5 Temperature gradients in glass

### 4.7.5.1 General remarks

Exposed glass panes on building facades may be the site of temperature gradients. A large number of factors can influence the value of the temperature gradient. These include:

- solar exposure and intensity of incident solar radiation;
- direct solar energy absorption by the glass;
- coatings, enamelling, printing;
- daily variation in external temperature;
- localised heating (radiators, high-temperature radiant-tube heaters, etc.);
- daily variation in internal temperature (fan-coils or localised overheating);
- thermal inertia of the type of frame;
- surface heat transfer coefficients;
- objects or structures which trap or reflect heat in the glass (curtains, blinds, obstacles behind glass, etc.);
- shadows on glass (sunbreakers, fins, parts of buildings, etc.);
- pane dimensions;
- glass thickness.

Temperature gradients cause stress that can cause glass to fail.

### 4.7.5.2 Thermal stress

The intensity of thermal stress in a glass pane depends on the temperature difference between the hottest part (the central part which receives solar radiation) and the coolest part (near the edges of the frame). The part receiving solar radiation absorbs heat and dilates, causing tensile stress on the edge of the glass which can cause a crack to propagate, leading to fracture of the glass itself. Such fractures are generally easily recognisable as they mainly originate from the edge of the glass, while their direction is orthogonal along the glass thickness (Figure 4.7). The presence of defects at the edge of glass plates, and consequently the grade of finish of the edge itself, therefore have clear implications with regard to strength.

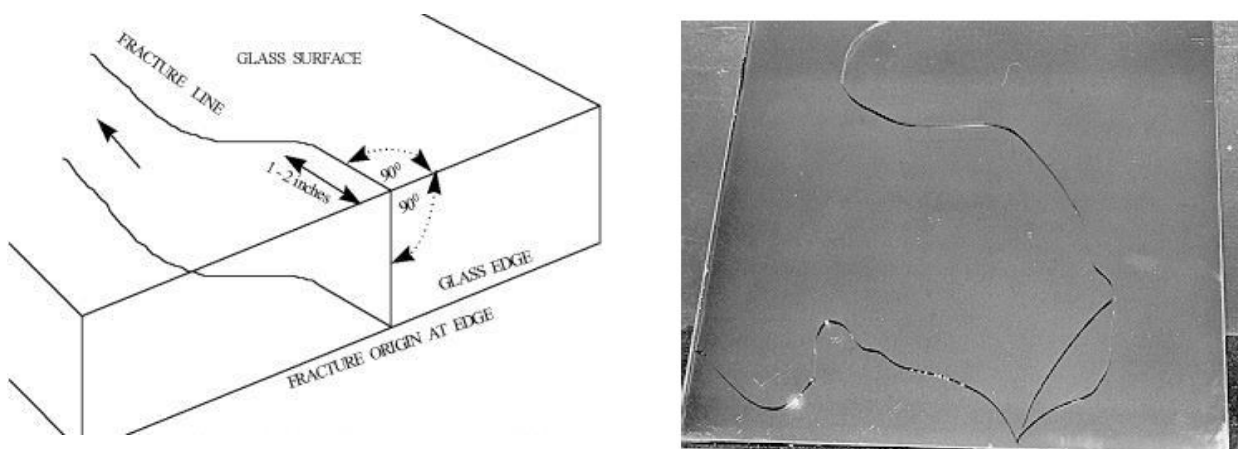


Figure 4.7. Example of thermal fracture in an annealed glass pane.

Stress caused by temperature differences can be expressed in the following form:

$$\sigma_t = \Delta T E \alpha K_{\Delta T} , \tag{4.37}$$

where  $\Delta T$  is the maximum temperature gradient in the glass,  $E$  is the elastic modulus of the glass ( $\cong 70000$  MPa),  $\alpha$  is the thermal expansion coefficient ( $\cong 9 \cdot 10^{-6} \text{ K}^{-1}$ ), while  $K_{\Delta T}$  is a coefficient which takes account of the effects that can influence the value of the temperature gradient (shape of areas of shadow, frame characteristics, etc.); values of this coefficient can be found in European Standard prEN THSTR-2007. The stress calculated by means of Eq. (4.37) must be compared with admissible thermal stress as defined by prEN THSTR-2007.

Given the direct connection between temperature difference and stress induced, the admissible values for the resistance of glass to the effects of a temperature gradient can be directly expressed in terms of temperature gradient  $\Delta T$ . By way of example, Table 4.14, taken from European Standard prEN THSTR-2004,<sup>8</sup> shows the typical temperature difference values ( $\Delta T$  in K) that various types of glass are able to withstand, including the influence of grade of edge finish.

Table 4.14. Typical tolerable temperature difference values ( $\Delta T$  in K) for various types of glass

Type of glass	State of edge		
	Arrised	Ground	Polished
annealed float glass, thickness $\leq 12$ mm	35	40	45
annealed float glass, thickness 15 mm o 19 mm	30	35	40
annealed float glass, thickness 25 mm	26	30	35
patterned glass	26	26	26
wired patterned glass or wired polished glass	22	22	22
heat-strengthened glass (all types)	100	100	100
thermally toughened glass (all types)	200	200	200
laminated glass	minimum value for component plates		

The equations which relate force to temperature distribution, even if a generalized plane state of stress is assumed, are extremely complex and can only be solved numerically and, therefore, they generally require specialist analyses.

#### 4.7.5.3 Factors influencing thermal stress

Some of the factors which influence the generation of thermal stress in glass and must therefore be given due consideration in the analysis are described below.

- *Solar radiation*

The higher the solar radiation, the greater the stress intensity in the glass. The intensity of solar radiation is derived according to the geographical disposition of the building (latitude, altitude, urban zone or otherwise, etc.), the orientation of the facade (north, south, east or west), season and time of day, as well as other factors such as cloud cover, air pollution and reflection from the ground or other adjacent structures.

Maximum solar irradiance occurs when solar radiation reaches the element at a quasi-normal incidence for most of the time of exposure.

- *Presences of internal walls, objects and blinds*

<sup>8</sup> European draft standard for assessment of risk of failure due to thermal stresses, document drafted by WG8 of CEN Technical Committee TC129. More detailed values and an evaluation method are also provided by a French document, DTU 39 P 3 “Travaux de bâtiment - Travaux de vitrerie-miroiterie - Partie 3 : Mémento calculs des contraintes thermiques”, October 2006.



Internal walls and blinds interfere with the natural movement of air in contact with glass and reflect, absorb and re-radiate incident solar radiation, contributing to an increase in the temperature on the glass and therefore also in thermal stresses.

A typical case is that of the “shadow-box”<sup>9</sup> and venetian blinds positioned on the inside. Heat sources (e.g. radiators) may also have an effect by increasing temperature on glass.

- *Type of glass and edge finishing*

The speed at which temperature increases in a glass element depends on its thickness and its capacity to absorb radiation. Low-emissivity glass absorbs much more heat than clear float glass. The temperature in the former is greater and so are internal stresses.

Thermally hardened or toughened glass is able to withstand higher temperature gradients than annealed glass.

For annealed glass, the edge finishing conditions play a major role (it will be recalled that stresses leading to failure originate from the edges): grinding, for example, increases the resistance factor with regard to thermal shock.

- *Frame type*

The shape and thermal characteristics of the frame influence the temperature of the edge of the glass and can generate high temperature gradients. For example, a frame with high thermal inertia generates lower temperatures at the glass edge.

The effect of the frame type is not completely separable from the effect of any shadows cast on the glass itself.

- *Shadows cast on glass*

Shadows cast on glass can cause large temperature differences, which vary according to the shape and size of the zone in shadow. Peak stress levels occur when less than 25% of the surface is in shadow and when the shadow includes over 25% of the perimeter. Generally horizontal, vertical or diagonal shadows are not as critical as combinations of them (e.g. “V-shaped” shadows, see Figure 4.8).

Cornices, terraces, sunbreakers and fins, as well as surrounding buildings and trees, may cast shadows on glass surfaces.

Figure 4.8 shows a purely indicative classification of various type of shadows, from the least dangerous to the most dangerous. Whenever there is a risk of failure due to thermal shock, the use of hardened or thermally toughened glass is recommended. The choice must in any case be made according to the type of glass and type of construction.

- *Other factors*

It must be stressed that critical thermal stresses are more likely to arise in the case of insulating glass units and become more significant as the number of panes and cavities increases (e.g. triple or quadruple glazing, etc.).

In the case of openable or sliding elements it should also be noted that when they are kept open they overlap with fixed panes, thus reducing heat dissipation and increasing the risk of failure due to temperature difference.

---

<sup>9</sup> A “shadow box” is a construction method used to create an impression of depth and light penetration in “storey-marker” zones (spandrels) on glass facades, column coverings and other “opaque” zones where an effect of visual depth from the outside is desired, while the true view of the internal zone through the glass is not desired or is not necessary.

---

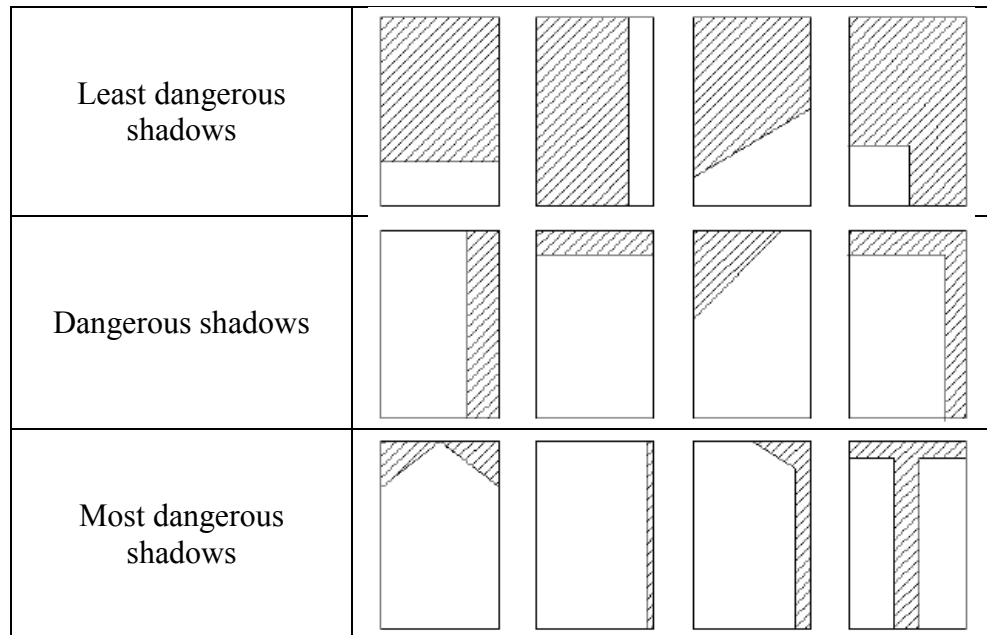


Figure 4.8. Examples of shadows cast on glass.

## 4.8 Weather actions on insulating glass units

### 4.8.1 Introduction

The gas enclosed inside the cavities of insulating glass units may exert non-negligible pressure on the inner surfaces of glass panes as weather conditions change inside and outside of the cavity. Insulating glass units, in fact, are usually sealed in the factory and then transported to the place of installation where environmental conditions may be different. Changes in barometric pressure (due both to changes in the weather and altitude) are particularly important. When they are sealed, glass insulating units are in a state of equilibrium, as internal and external pressure and temperature are the same; contrariwise, once installed, external conditions are no longer the same as internal conditions and, as a result, overpressure or depressions may arise inside the cavity. The following sections provide the various parameters used to calculate these changes in pressure, according to the procedures in Section 6.3.4.

It should be remembered that glass insulating units with non-sealed cavities can be manufactured (i.e. in communication with the external environment). For these types of glass, weather conditions differences do not cause changes in internal pressure. If the panes are to be transported to very high altitudes, they may also be sealed on site in order to prevent any effects arising from the change in altitude and those arising from temperature variations.

It is recommended to request that the manufacturer provides meteorological data (temperature and barometric pressure) at the time of sealing of the cavity, if this information is available. We indicate altitude, temperature and barometric pressure in the place of manufacture at the time of sealing with  $H_p$ ,  $T_p$ , and  $p_p$ , respectively.

### 4.8.2 Variations in altitude

Atmospheric pressure decreases as altitude increases. Usually both the place of manufacture and installation of the plates are known. If, during the initial sizing phase, the place of manufacture is not known, it is recommended that an altitude of  $H_p = 0$  m or 600 m (above sea level) be used, choosing the most severe condition according to combinations with other parameters.

### 4.8.3 Variations in atmospheric pressure

Atmospheric pressure changes during the year. In the absence of specific analyses, the minimum and maximum reference values for pressure  $p_p$  may be assumed to be 990 hPa and 1030 hPa [VORSCHLAG ÖNORM B 3716-1:2006], choosing the most severe condition according to combinations with other parameters. Possible situations at the time of sealing and on site should be taken into account in order to obtain the most severe situation.

### 4.8.4 Variations in temperature

Heating or cooling of the gas inside the cavity causes it to expand or contract, resulting in changes in pressure on the surface of the glass. At the time of sealing, in the absence of more accurate data, an initial approximation can be made, with temperature in the place of manufacture (and therefore of the gas in the cavity  $T_p$ ) assumed to be between 15 °C and 30 °C (as recommended by [VORSCHLAG ÖNORM B 3716-1:2006] and [CSTB Cahier 3488-V2, 2011]), choosing the most severe condition according to combinations with other parameters.

Once installed, the insulating glass unit separates the external from the internal environment and the temperature of the cavity depends on several factors, such as:

- internal air temperature of the building;
- external air temperature;
- heat transfer coefficients of the glass surfaces;
- thermodynamic behaviour of the gas;
- overall thermal transmittance of the glass pane;
- solar irradiance;
- spectrometric characteristics of the glass;
- the presence of low-emissivity or reflective deposits on the glass;
- the presence of curtains or sunscreens in front of or behind the glass panes;
- the presence of heating or cooling elements in proximity to the glass.

In order to take these factors into account, dedicated thermal engineering software may be used to make the necessary calculations. Alternatively, the simplified method described below may be used. Parameters relating to the thermodynamic characteristics of the glass and the gas inside the cavity as well as internal and external heat transfer coefficients can be found in [EN 673:2011].

#### 4.8.4.1 Simplified method for calculation of internal cavity temperature

The method described below is taken from the [CSTB Cahier 3488-V2, 2011]. In approximate terms, the temperature of the gas inside the cavity may be considered to be the average of the temperatures of the panes, i.e.

$$T_{iVC} = \frac{\theta_e + \theta_i}{2}, \quad (4.38)$$

where  $\theta_e$  and  $\theta_i$  are the temperature of the outer and inner panes.

The temperatures of the panes can be determined as follows:

$$\theta_e = \frac{\frac{\alpha_i \tau_e I + T_{int} h_{Ti}}{r_a} + (\alpha_e I + T_{ext} h_{Te}) \left( h_{Ti} + \frac{1}{r_a} \right)}{h_{Te} h_{Ti} + \frac{1}{r_a} (h_{Te} + h_{Ti})}, \quad \theta_i = \frac{\frac{\alpha_e I + T_{ext} h_{Te}}{r_a} + (\alpha_i \tau_e I + T_{int} h_{Ti}) \left( h_{Te} + \frac{1}{r_a} \right)}{h_{Te} h_{Ti} + \frac{1}{r_a} (h_{Te} + h_{Ti})} \quad (4.39)$$

where:

- $\alpha_i$  and  $\alpha_e$  are solar energy absorption coefficients for the inner and outer panes, inside the insulating unit, which take into account the effect of multiple internal reflections,<sup>10</sup> illustrated in Figure 4.9.
- $\tau_e$  is the solar energy transmission coefficient of the outer glass pane, which can be derived from the technical specifications provided by glass manufacturers;
- $I$  is the solar irradiance, the values of which are provided in Section 4.7.4 [UNI 10349:1994];
- $T_{ext}$  and  $T_{int}$  are the external and internal air temperatures, approximate values for which are provided below;
- $r_a$  is the thermal resistance of the cavity, the value of which can be estimated as indicated in [UNI EN 673:2011] by assuming  $r_a = 1/h_{Ts}$ , where  $h_{Ts}$  is the heat transfer coefficient of the cavity;
- $h_{Te}$  and  $h_{Ti}$  are the heat transfer coefficients of the outer and inner panes, which are determined as indicated in Section 4.8.4.3.

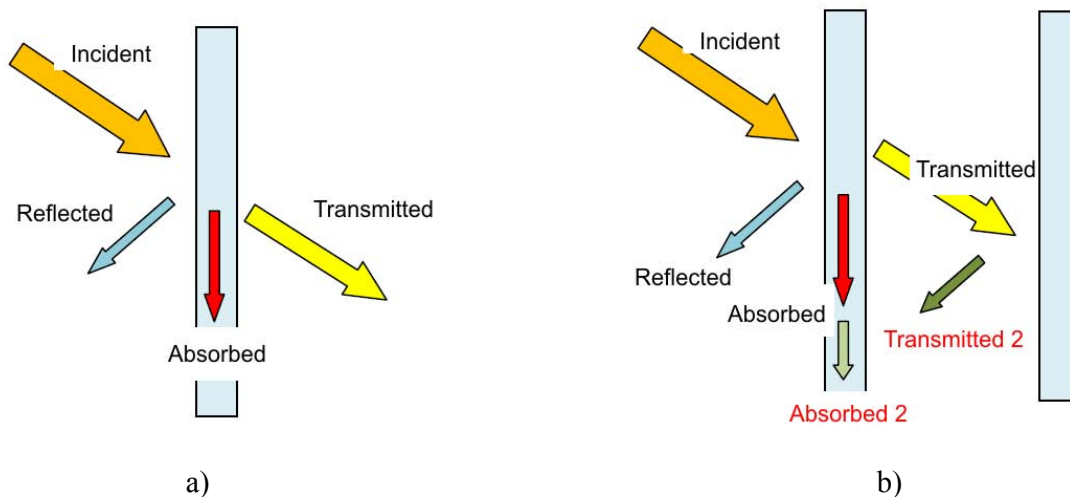


Figure 4.9 Reflected, transmitted and absorbed energy in the case of: a) a single plate; b) additional insulating glass plate.

Equations (4.39) must be determined on the basis of the least favourable irradiance conditions (including zero nighttime irradiance) and temperature conditions. For multiple glazing, appropriate thermodynamic scenarios must be used.

#### 4.8.4.2 Reference values for internal and external air temperature

Reference values for internal and external air temperature can be taken from legislation (see Sections 4.7.2 and 4.7.3). Nevertheless, it should be remembered that the internal air temperature in the immediate vicinity of the glass may be significantly different from the mean room temperature. For insulating glass units it may also be important to evaluate eventual transient situations during both transport and installation (for example, lack of heating or cooling in the building, storage in particularly hot or cold environments, etc.). The following table illustrates the temperatures recommended by [CSTB Cahier 3488-V2, 2011].

<sup>10</sup> These coefficients can be calculated in accordance with European Standard EN410.

Table 4.15. Maximum and minimum external and internal temperature (see [CSTB Cahier 3488-V2, 2011]).

Application	$T_{ext,min}$	$T_{ext,max}$	$T_{int,min}$	$T_{int,max}$
Glass plates with angle of inclination < 30° from horizontal	See	See	See	40 °C
Other cases	Section 4.7.2	Section 4.7.2	Section 4.7.3	25 °C

#### 4.8.4.3 Reference values for heat transfer coefficients $h_{Ti}$ ed $h_{Te}$

To determine such coefficients, reference may be made to the standards [ISO 10077-1:2006] and other documents of proven validity ([UNI EN 673:2011]).

In general, these coefficients are defined as the reciprocal of the thermal resistance coefficients, that is

$$h_{Ti} = \frac{1}{R_{s,int}}, \quad h_{Te} = \frac{1}{R_{s,est}} \quad (4.40)$$

For the sake of completeness, the surface thermal resistances  $R_{s,int}$  and  $R_{s,est}$  according to [ISO 10077-1:2006] are provided below. It may be useful to observe in this case that the limit angle of inclination from the horizontal of 60° is different from the limit angle of inclination of 75° shown in Table 3.4 and the following tables: in that case the distinction was made in relation to the consequences of mechanical failure, while in this case the difference regards thermal conduction.

Table 4.16. External and internal surface thermal resistance coefficients [ISO 10077-1:2006]

Position of glass	$R_{s,est}$ [m <sup>2</sup> K/W]	$R_{s,int}$ [m <sup>2</sup> K/W]
Uncoated glass with angle of inclination from horizontal $\geq 60^\circ$	0.04	0.13
Glass with angle of inclination from horizontal < 60°	0.04	0.10

#### 4.8.5 Scenarios for calculation of actions

Insulating glass during its lifetime may undergo changing weather conditions: stresses caused by changes in pressure increase as in-service conditions diverge from the weather conditions at the time of cavity sealing. For the purpose of verifications and for the application of Eqs. (4.38) and (4.39), two reference scenarios may be considered, as identified by [VORSCHLAG ÖNORM B 3716-1:2006], which represent the limit conditions for insulating glass. It is pointed out that insulating glass can be subjected to particular stresses during transportation, storage and installation; where necessary, these situations must also be taken into account.

##### Summer scenario (cavity sealed in winter)

- Maximum solar irradiance (based on orientation and angle of inclination of the glass, see Section 4.7.4).

- External and internal air temperature equal to the maximum in Table 4.15.
- Heat transfer coefficients determined with reference to Table 4.16.
- Atmospheric pressure 1010 hPa.
- Temperature of gas at the time of sealing (as an initial approximation the value  $T_p = 15\text{ °C}$  can be assumed, subject to verifications carried out after manufacture).
- Atmospheric pressure at the time of sealing  $p_p = 1030\text{ hPa}$  (insulating glass containing gases other than air may have internal pressures that are different from atmospheric pressure; additional details must be provided by the manufacturer).
- Altitude at site of manufacture  $H_p = 0\text{ m}$  (unless otherwise indicated by the manufacturer).

**Winter scenario (cavity sealed in summer)**

- Solar irradiance absent.
- External and internal air temperature equal to the minimum in Table 4.15.
- Heat transfer coefficients determined with reference to Table 4.16.
- Atmospheric pressure 1030 hPa.
- Temperature of gas at the time of sealing (as an initial approximation the value  $T_p = 30\text{ °C}$  can be assumed, subject to verifications carried out after manufacture).
- Atmospheric pressure at the time of sealing  $p_p = 990\text{ hPa}$  (insulating glass containing gases other than air may have internal pressures that are different from atmospheric pressure; additional details must be provided by the manufacturer).
- Altitude at site of manufacture  $H_p = 600\text{ m}$  (unless otherwise indicated by the manufacturer).

**4.8.6 Correction of cavity temperature**

As mentioned above, the temperature of the gas enclosed in the cavity depends on several factors. Specifically, the calculation method set out in Section 4.8.4.1 is only applicable to glazing that is sufficiently far from walls, curtains, venetian blinds, etc. Table 4.17 illustrates the corrective values to add to the gas temperature in the cavity, and the corresponding increase in pressure [VORSCHLAG ÖNORM B 3716-1:2006].

Table 4.17. Values to be added to the increase in temperature  $\Delta T$  and pressure  $\Delta p$  of the gas in the cavity, under specific installation conditions.

	Cause of increase in temperature difference	$\Delta T$ (K)	$\Delta p$ (kN/m <sup>2</sup> )
Summer	Absorption between 30% and 50%	+9	+3
	Internal (ventilated) solar protection	+9	+3
	Absorption over 50%	+18	+6
	Internal (non-ventilated) solar protection	+18	+6
	Thermal insulation on rear of panel	+35	+12
Winter	Unheated building	-12	-4

**4.9 Exceptional actions**

In order to determine loads caused by exceptional actions such as fire, impacts and explosions, reference may be made to the indications contained in national technical standards and in Eurocode [UNI EN 1991]. In this section, only actions caused by explosions are considered: a particularly relevant

issue in terms of protecting against terrorist attacks, but one which has not yet been dealt with in a systematic fashion in the various technical standards.

#### **4.9.1 Actions due to explosions**

The design of a structure subject to the risk of explosive loads is required in essentially two cases: structures for the storage of explosive materials (explosives proper or particularly flammable materials) and for structures subject to the risk of bombings or terrorist attacks. In both situations, the sizing of the various components must be preceded by an estimate of the maximum forces acting on the building, the value of which depends essentially on the explosion load involved.

While for storage structures this load may be determined simply by evaluating the quantity of explosives that can be stored in the building, for structures at risk of terrorist attacks there are no methods for calculating this value with any certainty, as it may depend on a large number of factors, such as accessibility of the building, for example, or the degree of security desired by the client.

Therefore one of the most problematic aspects of the design of glass facades to withstand explosions is the choice of the design explosion load. Generally the value of such a load will be defined in the design specifications, and therefore assumed to be known; in addition, this analysis is restricted to the case of an explosion occurring outside the building. This is both because the aim of this document is to provide design criteria for glass elements whose purpose is to protect the occupants of the building, and because the size, composition and distribution of the interior spaces create a multitude of different conditions in the case of an explosion inside a building, making a general discussion of the problem impossible.

Therefore, what follows is a discussion on the determination and quantification of the parameters that describe the blast wave generated by the detonation of an explosive load outside a building.

##### **4.9.1.1 Classification of explosions**

Explosions can have various causes. Depending on the means by which the energy released by them builds up, they can be divided into three types: physical, chemical and nuclear. In the first group, energy may build up in the form of high pressures (for example a pressurised tank). In the second group, it takes the form of a chemical reaction. Finally, in the third type energy is released by nuclear fission or fusion processes.

This section will deal solely with explosions that are chemical in origin and in particular will refer exclusively to high or “condensed” explosives, whose compound also contains the oxygen necessary for the reaction.

In general mixes of high explosives are in solid or liquid form and when triggered react violently, producing heat and releasing gas, which expands, causing pressure waves in solid materials, or blast waves if the expansion occurs in air.

We speak of deflagration when the reaction speed of an explosive mix is much lower than the propagation speed of the sound within the mix itself; deflagration is propagated as a result of the heat released by the reaction.

Contrariwise, we speak of detonation when the reaction speed, termed detonation speed, exceeds the speed of sound, ranging from 1500 to 9000 m/s; detonation generates a shock wave which is always extremely intense.

##### **4.9.1.2 Characteristic physical variables of a blast wave**

When a high explosive is triggered, at the first stage the reaction develops extremely hot gases, which can reach pressures of 100-300 kbar and temperatures in the order of 3000-4000 °C. These gases

expand violently, pushing the air that they encounter on their path. This process causes a highly compressed layer, called a *blast wave*, which encapsulates most of the energy released by the explosion. As the gas expands, its pressure and therefore the pressure on the front of the blast wave decreases. At the same time, as a result of the inertia possessed by its particles, the gas continues to expand and therefore cools down. This causes a further reduction in its pressure which, falling at a certain point below the atmospheric pressure, generates an inversion of the motion of the air and gas molecules which return toward the origin of the explosion. This motion ceases when atmospheric pressure is re-established.

Having defined the progress of the blast wave generated by an explosion in qualitative terms, there now follows a series of extremely important parameters for defining its characteristics in quantitative terms.

An analytical solution for the parameters of the progress of the wavefront of a shock wave was calculated for the first time by Rankine and Hugoniot [Rankine, 1870; Hugoniot, 1887], with reference to ideal gases and to an expansion in air away from obstacles. The equations that describe the rate of advance of the wavefront  $U_{sw}$  and the maximum dynamic pressure  $q_{sw}$  of a shock wave are [Rankine, 1870]

$$U_{sw} = \sqrt{\frac{6p_{sw} + 7p_0}{7p_0}} \cdot v_{so}, \quad q_{sw} = \frac{5p_{sw}^2}{2(p_{sw} + 7p_0)}, \quad (4.41)$$

where  $p_{sw}$  is peak static overpressure at the wavefront,  $p_0$  is air pressure in the environment and  $v_{so}$  is the speed of sound in air at pressure  $p_0$ .

According to Brode [Brode, 1955], the value of peak static overpressure for a spherical wave is equal to

$$\begin{cases} p_{sw} = \frac{6.7}{Z^3} + 1 \text{ bar}, & \text{per } p_{sw} > 10 \text{ bar}, \\ p_{sw} = \frac{0.975}{Z} + \frac{1.455}{Z^2} + \frac{5.85}{Z^3} - 0.019 \text{ bar}, & \text{per } 0.1 < p_{sw} < 10 \text{ bar}, \end{cases} \quad (4.42)$$

where  $Z$ , termed scaled distance, equals

$$Z = \frac{R}{\sqrt[3]{W_{TNT}}}. \quad (4.43)$$

In the expression of  $Z$ ,  $R$  represents the distance in metres of the point at which  $p_s$  is calculated from the centre of the explosion load, while  $W_{TNT}$  is the explosive mass, measured in kilograms of TNT (trinitrotoluene). The parameter  $Z$  expresses a distance of equivalence in the effects of charges of different sizes.

TNT is universally used as a reference explosive, as it is easily accessible for experimental tests, and it has the major advantage of being formed of a single component and thus has a more regular, constant behaviour than many other explosives. At the moment of evaluation of the effects of the explosion, therefore, it is necessary to convert the mass of the explosive in question into a ‘‘TNT-equivalent’’ mass.

Guidelines concerning how to proceed in this conversion can be found in Standard ISO 16933:2007 *Glass in building – Explosion resistant security glazing – Test and classification for arena air-blast loading*, Annex B, §B.2 [ISO 16933: 2007] which also provides many other useful recommendations regarding how to conduct a test of this type and how to classify the results.



Other important parameters concerning blast waves are the duration of the positive phase  $T_s$ , during which the pressure is higher than the ambient pressure, and the specific impulse of the wave  $i_{sw}$ , equal to the area under the pressure-time curve between the instant,  $t_a$ , at which the pressure wave arrives and the instant at which the positive phase finishes [Mays & Smith, 1995]:

$$i_{sw} = \int_{t_a}^{t_a+T_s} p_{sw}(t) dt . \tag{4.44}$$

Figure 4.10 shows a typical pressure-time profile of a blast wave [De Bortoli, 2003].

It may be observed that the overpressure phase is followed by a depression phase which reaches the minimum value

$$\Delta p_{\min} = \frac{-0.35}{Z} \quad (Z > 1.6) . \tag{4.45}$$

This second phase is associated with a specific impulse  $i^-$  given by

$$i^- = i_{sw} \left[ 1 - \frac{1}{2Z} \right] . \tag{4.46}$$

It is important to observe that the calculations described thus far, hold for a detonation far from any surface that may reflect the blast wave. When an explosion occurs in contact with the ground, a number of corrections must be made to the explosive mass to add to the formulas given previously. In general, a good fit is obtained with experimental data if the explosive mass is multiplied by a factor of 1.8.

In the case of an ideal flat reflecting surface, this factor would be equal to 2.

#### 4.9.1.3 Pressure profile of a blast wave

The pressure-time curve of a blast wave, illustrated qualitatively in Figure 4.10, is well described by exponential functions such as the Friedlander equation [De Bortoli, 2003]

$$p(t) = p_{sw} \left[ 1 - \frac{t}{T_s} \right] e^{-\frac{bt}{T_s}} , \tag{4.47}$$

in which  $b$  is the waveform parameter, which describes the rate of decay of overpressure. Sometimes, however, and especially in calculations, it is preferred to approximate Eq. (4.47) by means of linear functions. For this purpose, various approaches may be adopted: for example, working to higher safety standards, a linear profile can be traced which joins the initial pressure peak to the point at which the real pressure-time curve intersects the x-axis, thus conserving the peak pressure value and the duration of the positive phase  $T_s$  of the real wave, overestimating the specific impulse  $i_{sw}$ ; alternatively, by maintaining the initial peak pressure, a conventional value for the duration of the positive phase  $T_s$  can be determined, making it possible to keep the value of the specific impulse  $i_{sw}$  unchanged. We may observe that in Figure 4.10, atmospheric pressure  $p_0$  has been added to the  $p(t)$  curve so that the beginning of the negative phase corresponds to the instant at which absolute pressure falls below atmospheric pressure.

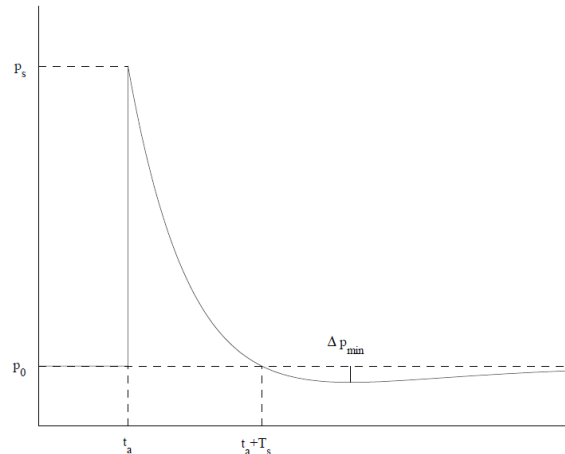


Figure 4.10. Pressure-time curve of a blast wave [De Bortoli, 2003].

#### 4.9.1.4 Pressure changes in a blast wave due to obstacles

When a blast wave encounters a solid body, or a denser-than-air medium, it is reflected and, depending on the size and the geometry of the body, diffracted around it. In the simplest case of a blast wave which hits an infinite flat plane with zero angle, the wavefront is seen to come to a stop before being compressed and then reflected, generating a wave in which the overpressure is greater than that of the incident wave.

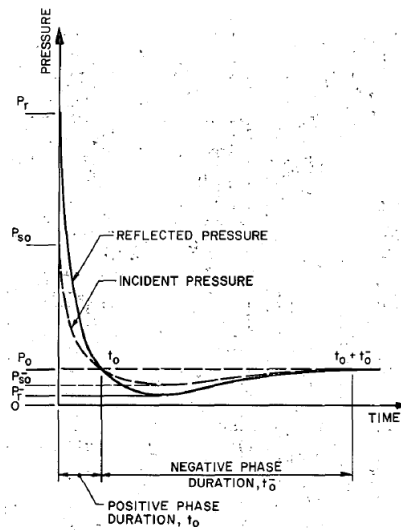


Figure 4.11. Incident pressure and reflected pressure [TM 5-1300, 1990].

The peak pressure value  $p_r$  of the reflected wave has been calculated by Rankine and Hugoniot, in the case of a real gas, as a function of dynamic pressure  $q_{sw}$ , peak static pressure  $p_{sw}$  and the ratio between the specific heat at constant pressure,  $C_p$ , and the specific heat at constant volume,  $C_v$ . Specifically the following equation is obtained [Mays & Smith, 1995]:

$$p_r = 2p_{sw} + \left(1 + \frac{C_p}{C_v}\right) q_{sw} \quad (4.48)$$

By substituting Eq. (4.41b) for  $q_{sw}$  into Eq. (4.48) we thus obtain

$$p_r = 2p_{sw} \frac{7p_0 + 4p_{sw}}{7p_0 + p_{sw}}, \quad (4.49)$$

having assumed for air  $C_p/C_v = 1.4$ .

If we now define the *reflection coefficient*,  $C_r$ , as the ratio of peak pressure of the reflected wave and peak static pressure

$$C_r = \frac{p_r}{p_{sw}} = 2 + 6 \frac{p_{sw}}{7p_0 + p_{sw}}, \quad (4.50)$$

it can be shown from Eq. (4.50) that it varies between 2, for low values of  $p_{sw}/p_0$ , and 8 for high values of  $p_{sw}/p_0$ . In practice, for explosions very close to the reflecting surface, increments in  $C_r$  of up to 20 are observed, due to the dissociation of the gas molecules which causes an increase in reflected pressure.

#### 4.9.1.5 Mach stem

The phenomenon of reflection just described is called *regular reflection* and occurs in the case of waves that meet a surface at an angle of incidence of between  $0^\circ$  and  $40^\circ$ . For an angle of  $90^\circ$  there is no reflection and the pressure induced on the surface is equal to static peak overpressure.

However, when the angle of incidence exceeds  $40^\circ$ , a phenomenon called *Mach reflection* is observed, in which the incident wave “slides” over the reflecting surface as opposed to bouncing off of it. The result of this process leads to the reflected wave merging with the incident wave at a point above the surface; this produces a third wavefront, called “Mach front”, or more commonly “Mach stem”. The point at which the incident wave, the reflected wave and the Mach stem is called the *triple point* and its distance from the reflecting surface is called the *height* of the Mach stem.

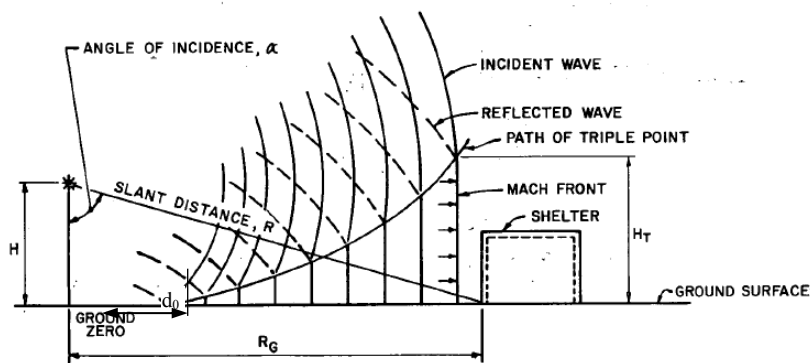


Figure 4.12. Diagrammatic representation of the Mach stem phenomenon [TM 5-1300, 1990].

The change in pressure beyond the height of the Mach stem is negligible. The region below this height is called the Mach reflection region while the region above it is called the regular reflection region. In the Mach reflection region the direction of the wave is horizontal while its front is cylindrical (the axis of the cylinder is normal to the reflecting surface passing through the point of origin of the explosion); in addition, inside the cylinder it can be observed that, although the pressure is constant, the gas particles vary in density and speed.

With reference to Figure 4.13, it can be said that the Mach stem begins to form when the angle of incidence of the blast wave exceeds  $40^\circ$ .

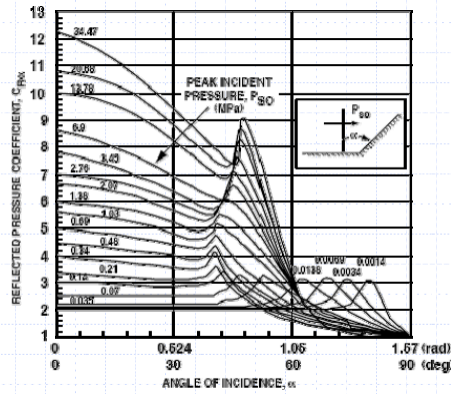


Figure 4.13. Reflection coefficient as a function of angle of incidence [Heffernan, 2006].

Therefore, according to the height  $H$  at which the explosive is positioned and the angle of incidence  $\alpha$ , a distance  $d_0$  from ground zero (Figure 4.12) can be determined, in other words the distance from the point on the ground which is on the same vertical axis as that of the explosive load, within which the Mach reflection does not arise. Beyond this distance, the height of the triple point,  $H_T$ , can be expressed by the following experimentally verified equation

$$H_T = 0.07H \left( \frac{d}{d_0} - 1 \right)^2. \quad (4.51)$$

In Eq. (4.51), the parameter  $d$  represents the distance from ground zero of the point at which we wish to measure  $H_T$ . Determining  $H_T$  is especially important, as the pressures that are present on the Mach front are greater than the pressures that are present in the regular reflection region. It is therefore opportune to estimate their exact size.

#### 4.9.1.6 Actions of structures due to a blast wave

The pressure wave generated by an explosion induces a multiplicity of actions on a structure. These actions depend not only on the quantity of explosive and the distance of the explosion from the structure but also on the characteristics of the structure itself, including dimensions and shape. Without taking into account the effects of interaction of the dynamic kind, we can distinguish three distinct cases [Heffernan, 2006].

When a blast wave of large proportions encounters a building – and therefore a system of equally large dimensions – the latter is struck and surrounded by the wave which, in addition to pressure loads, generates a drag force. This type of load is called diffraction loading.

In contrast, when a blast wave of large proportions encounters a structure of small proportions, such as a vehicle, in addition to the effects described above, there is a brief period of time in which the whole structure is surrounded by an overpressure which tends to compress it. Although in this case the drag force acts for a shorter period of time than the previous condition, it may have sufficient energy to move the structure, in this case causing most of the damage.

Finally, we have the case of a blast wave produced by a relatively small explosive charge that interacts with a structure of large dimensions. While in the situations considered previously it can be assumed that the structure is struck at every point by the same load, in this case the response must be analysed by applying to each elements of the system a loading value that depends both on time and the distance from the point of origin of the explosion, as it is no longer possible to assume that the pressure wave strikes all of the sub-components of the system simultaneously.

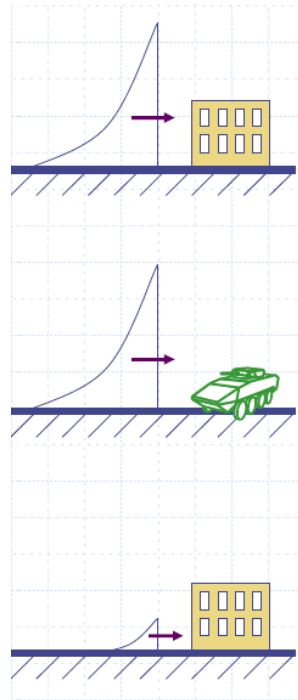


Figure 4.14. Relationship between incident blast wave and dimensions of the structure [Heffernan, 2006].

Changes over time in the pressure and drag forces acting on a structure struck by a blast wave for the first two cases mentioned above can be described [Heffernan, 2006].

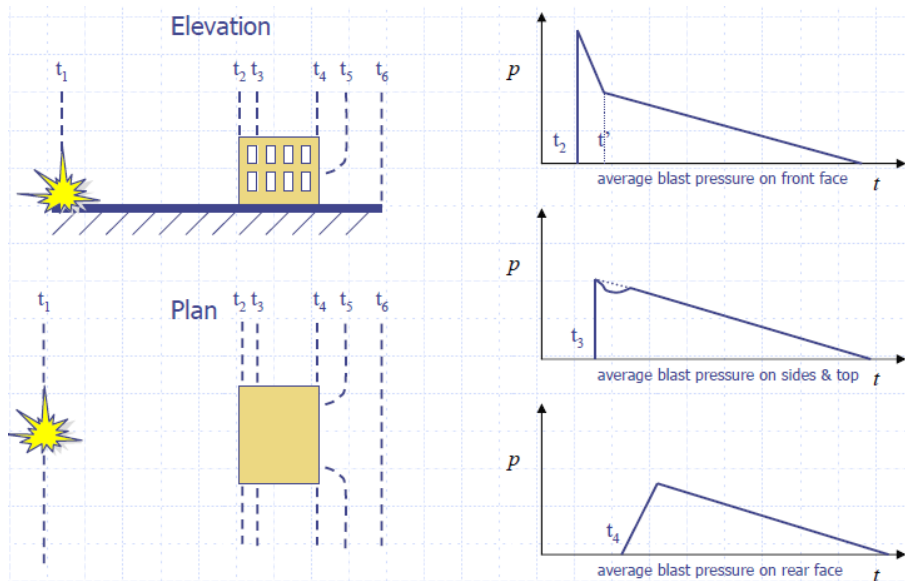


Figure 4.15. Transition phases of a blast wave striking a building [Heffernan, 2006]

By adding together the effects of the various actions, it may be observed that the structure is subjected to a load in the direction of the wave at the moment that one of its sides is struck by overpressure, followed by a slightly smaller load in the opposite direction as soon as the diffraction is completed. The drag force causes a load in the direction of the wave movement on the side where the building is struck, following by a depression on its opposite side; these loads are due to the *blast wind*, i.e. not due to pressure, but to the displacement of air particles dragged by the blast wave.

The peak overpressure to which the face struck at time  $t_2$  is subjected is equal to the peak reflected wave value  $p_r$ ; this overpressure then falls during the time interval  $t' - t_2$  to the stagnation pressure value  $p_{stag}(t)$ , given by the sum of static and dynamic pressure. Time  $t'$  is approximately

$$t' = 3 \frac{\min(B/2, H_B)}{U_{sw}}, \quad (4.52)$$

where  $B$  is the width of the front part of the structure,  $H_B$  is its height and  $U_{sw}$  is the speed of propagation of the wavefront as defined by Eq. (4.41a).

With regard to the result of the drag forces, we may write

$$F_D = C_D A q_{sw}(t), \quad (4.53)$$

where  $A$  is the area of the normal section of the structure perpendicular to the direction of the blast wave and  $C_D$  is the aerodynamic resistance coefficient of the structure.

For small structures the time interval  $t_2 - t_4$  is very short, and so the force which produces the greatest effects is the drag force.

## 4.9.2 Actions due to fire

Fire is an exceptional condition which may affect the whole or individual components of a building. With regard to structures, the action of fire involves a rapid increase in temperature with potential overpressures. For safety purposes, it is necessary to distinguish between the need to maintain the load-bearing capacity of structural elements (mechanical stability) and separation capacity in order to prevent fire from spreading from one environment to another (fire isolation and resistance capacity).

Safety performance requirements in the event of fire are regulated by specific product standards and national fire prevention legislation. The fire resistance of a structural or construction element is defined as its capacity to maintain its load-bearing capacity, smoke protection and thermal insulation for a given time under the action of a conventional fire. Standards and regulations refer to nominal fire curves for product classification and standard tests. The use of advanced models representing effective expected fire conditions (natural fire) is admissible.

Glass elements capable of withstanding the action of fire and ensuring separation between compartments (fire-resistant glass) are obtained either through the lamination of float glass with intumescent gel interlayers or with special additives added to the glass paste. In the first case, in the event of exposure to fire, the intumescent gel reacts by expanding, becomes opaque and creates an insulating foam with progressive failure of the float glass layers; in the second case, the glass plate softens gradually until it breaks, without the opacification of the glass.

Glass panes of this type guarantee mechanical strength (R) and smoke protection (E). However, they are not suitable to guarantee insulation capacity (I). Unlike, laminated glass with intumescent gel can guarantee a high level of fire insulation performance as there is no limit to the number of layers; on the other hand the weight of the glass increases considerably. A convenient solution is to use EW glass, which guarantees protection against hot fumes and limit the flow of heat transmitted from the non-exposed surface. Taking into account the fact that in general combustible material is not present near glass elements, in most cases EI glass and EW glass are replaceable.

Fire-resistant glass may be used to create separation barriers without a structural function or for façade cladding. In this case the glass breaking may allow fire to propagate outside the building and cause damage due to falling fragments. Technical guides and support documents are available for the design of such elements.

In contrast, glass elements may not be used for load-bearing structures such as beams and pillars. In order to obtain fire-resistant elements it would be necessary to use protections, thereby altering the distinctive features of the elements. Glass floors may be installed and their load-bearing and compartmentalisation capacity guaranteed. Generally a load-bearing glass plate is coupled to a fire-resistant glass, with an air cavity between them if necessary.

When on the other hand specific fire resistance performance levels are not required, the following considerations can be made regarding the vulnerability of glass elements. In the preceding sections we have described the effects of temperature on the mechanical behaviour of glass and shown how failures are primarily caused by temperature gradients. In the event of fire the temperature excursion is of the non-stationary type, resulting in continuous variation in the temperature gradients of the elements through both the thickness and plane of the plates. Tempered glass can withstand higher temperatures and temperature gradients than float glass. However, it is completely incompatible with expected temperatures in the event of a fully developed fire (800°-1000° C). HST treatment further reduces the vulnerability of glass plates to rapid temperature changes. An additional consideration regards the presence of a plastic layer as an interlayer in laminated glass. This layer participates in the combustion process and renders laminated glass combustible and capable of propagating fire. Specific fire reaction tests enable products to be classified into reaction-to-fire classes.

For safety purposes, it is important to evaluate the potential consequences of failure and falling fragments in the event of fire. Failure of float glass may cause it to fragment into shards of considerable size, while there is no guarantee that these fragments will remain in place, being retained by a plastic layer. The combustibility and softening of the layer means that non-detachment of the fragments is not guaranteed. In the case of toughened glass designed to fragment into granular chunks, the entire plate may detach from its supports, as the mechanical strength of the fixing points is no longer guaranteed.

Particular caution must be considered with regard to the use of insulating glass units in roofs, as generally no fire resistance is guaranteed for the inner layer which may fall even in the event of moderate temperature increases.

#### 4.10 Design duration of loads

In order to evaluate the strength of glass, it is essential to know the duration of loads acting upon it. In the absence of specific data, reference may be made to Table 4.18, which shows the nominal duration value corresponding to a time  $t$  equivalent to the integral of the load spectrum, i.e. the time  $t$  for which the action, which is assumed to be constant, produces the same effects as the variable action during the lifetime of the structure, which is assumed to be 50 years.

Table 4.18. Nominal value of load duration.

Action	Load spectrum		Time $t$ equivalent to integral of spectrum
	Characteristic reference value	Type	
Wind	Averaged over 3 seconds	Maximum pressure peak	5 sec
	Averaged over 10 minutes	Repeated pressure peaks	15 minutes
Snow	Annual maximum		3 months
Live operating load (maintenance)	Brief	Single load peak	30 seconds
Crowd-induced load	Brief	Single load peak	30 seconds
Daily temperature variation	Maximum daily difference	Duration of maximum peak	11 hours
<b>Permanent actions</b>			
Self-weight and other dead loads	Permanent	Invariable load over time	Nominal lifetime

For example, the values corresponding to the maximum wind pressure peak are those which correspond to the characteristic value for a return period of 50 years of the population of wind values

averaged over 3 seconds; for this action, the time  $t$ , that is equivalent to the integral of the load spectrum, is assumed to equal 5 seconds.

The corresponding glass strength reduction factors  $k_{mod}$  are shown in Table 2.2.

The reference values of the actions (variable operating load, snow load and daily temperature variations) are the ones that correspond to the characteristic values (upper 5% fractile) that can be derived from national or international regulations.

#### 4.11 Annex. Simplified method for evaluating required capacity in terms of displacement

During bidding by glass manufacturing firms, data regarding the displacements of the fixing points of glass elements under design seismic actions may not be available. It may therefore be useful to provide a simplified method to carry out an approximate pre-sizing of the various glass elements. A method suitable only for cases of highly ductile multistorey-frame buildings is outlined below. It is recommended in any case that the displacements of load-bearing structures calculated by the designer be used in the design of glass elements, as the method proposed should preliminarily be considered only an initial approximation.

Having established the site and geomorphological category of the terrain and the importance class of the construction, according to the return period taken from Table 4.6 the response spectra in terms of pseudo-acceleration are calculated in relation to each of the limit states (SLO, SLD, SLV and SLC). From the spectra in terms of pseudo-acceleration  $S_a(T)$  it is possible to derive spectra in terms of displacement  $S_d(T)$  with an equation of the following type:

$$S_d(T) = S_a(T) \left( \frac{T}{2\pi} \right)^2 . \tag{4.54}$$

The typical  $S_d(T)$  curve is shown in Figure 4.16, where it will be observed that for higher periods a horizontal plateau occurs, corresponding to the maximum displacement of a single-degree-of-freedom oscillator under design seismic action.

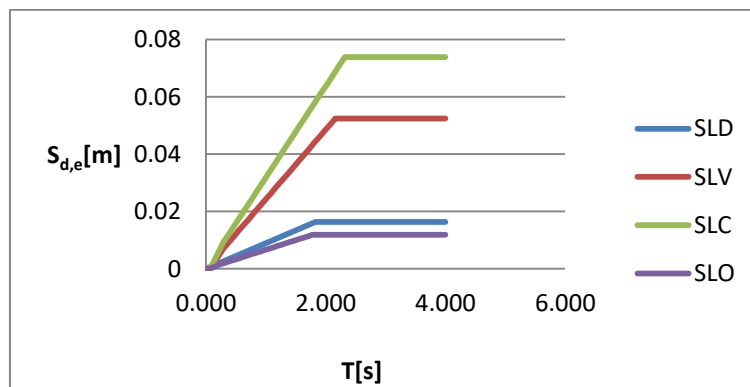


Figure 4.16. Graph of response spectrum in terms of displacement  $S_d(T)$  for SLO, SLD, SLV and SLC limit states.

The value  $d_{max,SLC}$  of the maximum displacement for SLC may be taken as a reference value. Figure 4.17 shows the graph of the ratio  $S_d(T)/d_{max,SLC}$  for SLO, SLD and SLV limit states. From this graph it may be observed that, in general, taking the threshold corresponding to the horizontal plateau for each of the limit states (SLO, SLD, SLV and SLC) as the design ground displacement provides a positive margin of safety.



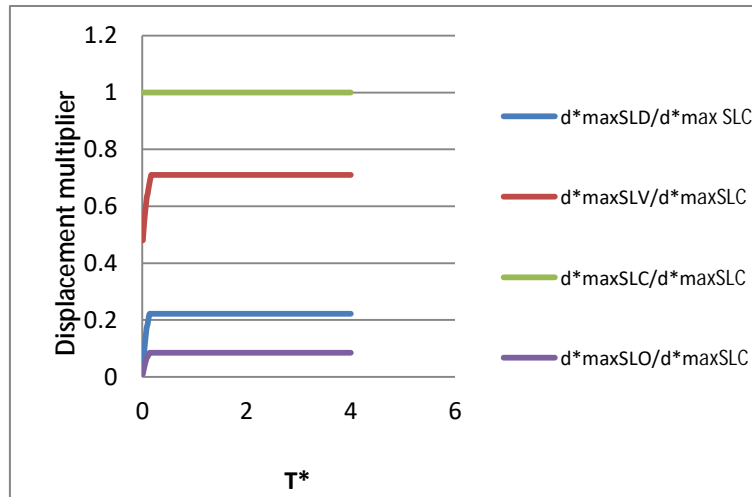


Figure 4.17. Graph of response spectrum in terms of displacement  $S_d(T)$  for SLO, SLD, SLV and SLC limit states.

Using the data set out in the current national seismic legislation (Ministerial Decree for Infrastructure, 14/01/2008), it can be seen that the ratios between the values corresponding to the horizontal thresholds remain virtually constant, as indicated in the second column of Table 4.19. It will be noted that these values coincide almost exactly, and are in any case more conservative, than those recommended by the United States Federal Emergency Management Agency [FEMA 273] provided in the same table for comparison purposes.

Table 4.19. Ratio between maximum ground displacement corresponding to various limit states. Comparison with FEMA recommendations.

Limit state	Maximum ground displacement, simplified method	Maximum ground displacement, FEMA recommendations
SLO	0.085	0.08
SLD	0.22	0.20
SLV	0.71	0.60
SLC	1	1

The simplified method consists in taking the maximum displacement at the base to be the corresponding value at the SLC,  $d_{max,SLC}$ , and assuming for the other limit states SLV, SLD and SLO an appropriately rescaled value according to the coefficients in Table 4.19.

With simple models it is possible to estimate, at least as an initial approximation, the coefficient  $\Gamma$  which correlates the maximum displacement of a multi-degree-of-freedom structure with the maximum displacement at the base.

Purely by way of example, by approximating the first deformation mode of a multi-storey frame with a triangular shape as described in Figure 4.18, it can be deduced that the maximum displacement at the top of the frame  $d_{max,MDOF}$  is correlated to the maximum ground displacement  $d_{max,G}$  by means of an equation of the following type:

$$d_{max,MDOF} = \Gamma d_{max,G}, \quad \Gamma = \frac{3n}{(2n+1)}, \quad (4.55)$$

where  $n$  represents the number of storeys. Interstorey drift  $D_p$  can therefore be estimated as  $D_p = d_{max,MDOF} / n$ .

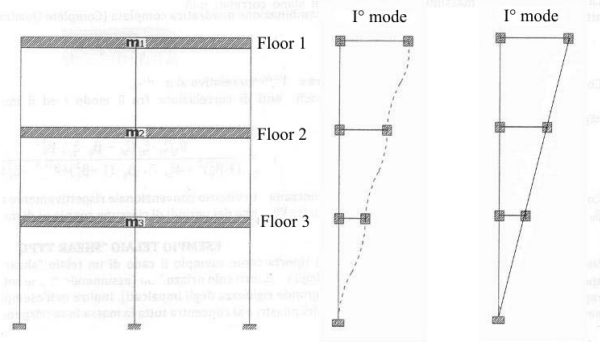


Figure 4.18. First deformation mode for a multi-storey frame and approximation thereof with a triangular deformation.

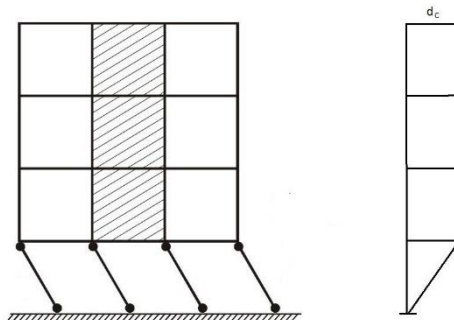


Figure 4.19. Approximation of first deformation mode for a frame with soft storeys.

Equally simple considerations may be made for the case of a frame with soft storeys. In this case, by approximating the deformation mode as illustrated in Figure 4.19, we obtain  $\Gamma = 1$  and  $D_p = d_{\max,G}$ . More generally, interstorey drift may be estimated using simplified models, rescaling the data appropriately according to the limit state under consideration using the coefficients in Table 4.19.

## 5 STRENGTH OF GLASS

### 5.1 Preliminary considerations

In order to evaluate the safety level, the semi-probabilistic limit state method, classified as a Level I method [EN 1990] is used. The method applies partial amplification factors to actions and reduction factors to resistances in order to guide safety evaluation with a direct comparison between weighted values of stresses and resistances. These partial factors must be calibrated in such a way that, from a probabilistic safety perspective, this comparison is indicative of the performance level required to the construction in terms of probability of failure. These performance levels are prescribed by the Eurocode [EN 1990] according to the design life and importance of the construction as well as the potential consequences of failure.

Structural elements have already been divided into classes in Section 3.2.1, according to the importance of the construction. In accordance with the provisions of EN 1990, Section 5.2.3 sets out required performance levels in terms of probability of failure for each class.

This chapter considers partial factors for glass. They are calibrated with reference to paradigmatic cases. For each of these elements, sizing is carried out on the basis of Level III probabilistic verification methods; the partial factors for the material are thus calibrated by choosing values which lead to the same structural sizing and consequently the same probability of failure.

It should be remembered that, in general, the probabilistic distributions for actions differ from the Weibull distribution which, as shown in Section 2.1, is the one that interprets the strength of glass. Section 2.1 also amply demonstrates how glass is subject to the phenomenon of static fatigue, i.e., to failure under the prolonged action of a load. The statistical distributions for mechanical resistances, derived from standard tests, must therefore be appropriately rescaled in order to interpret the strength distribution in the prescribed environment and under design loads. This rescaling is performed according to the fracture mechanics model illustrated in Section 2.1.1.1, which constitutes the key to interpreting the response of the material.

### 5.2 Probabilistic evaluation of structural safety

#### 5.2.1 Reliability level of structures according to EN1990

As established under EN1990, the level of structural reliability of construction works, i.e. the probability of failure, must be commensurate with the design life of the structure, the importance of the construction work and the seriousness of potential failure (loss of life and damage to property).

The meaning of “design life” has already been introduced in Section 3.2.2. Evaluation of the risk level deemed to be acceptable is carried out on the basis of the classes of consequences (CC1, CC2, CC3) described in Section 3.2.1. However, since the use of glass structures is generally limited to local portions of the structure, at least in the most common applications it is sufficient to consider classes CC2 and CC1.

In particularly demanding construction works, in which the glass structure is the only load-bearing structure (e.g. load-bearing frames in glass), class CC3 must be considered, for which the partial factors are not calibrated here. In such cases, the designer shall verify the required level of safety using Level II or Level III methods, as described in Section 5.2.2.

## 5.2.2 Reliability methods

### 5.2.2.1 Level III methods

Level III methods are the most complete, as they assume that the probability of failure is evaluated directly based on the statistical distributions of loads acting on the construction and the mechanical strengths of the various materials.

If  $\mathbf{S}$  summararily represents the domain of actions,  $f_S(s)$  indicates the statistical distribution of the values  $s \in \mathbf{S}$ ; similarly, if  $\mathbf{R}$  represents the domain of resistances,  $f_R(r)$  indicates the statistical distribution for  $r \in \mathbf{R}$ . The probability of failure can be characterised through the Performance Function  $G(\mathbf{R}, \mathbf{S})$  which identifies the safe zone of the plane  $(\mathbf{R}, \mathbf{S})$  as  $G > 0$ , and the zone corresponding to failure as  $G < 0$ . The probability of failure  $P_f$  can therefore be identified, based on the probability distribution laws of  $r \in \mathbf{R}$  and  $s \in \mathbf{S}$ , as the probability of occurrence of the condition  $G(\mathbf{R}, \mathbf{S}) \leq 0$ . Summarising, we have

$$P_f = P[G(\mathbf{R}, \mathbf{S}) \leq 0]. \quad (5.1)$$

A diagrammatic representation of the plane  $(\mathbf{R}, \mathbf{S})$  and the performance function  $G(\mathbf{R}, \mathbf{S})$  is provided in Figure 5.1.

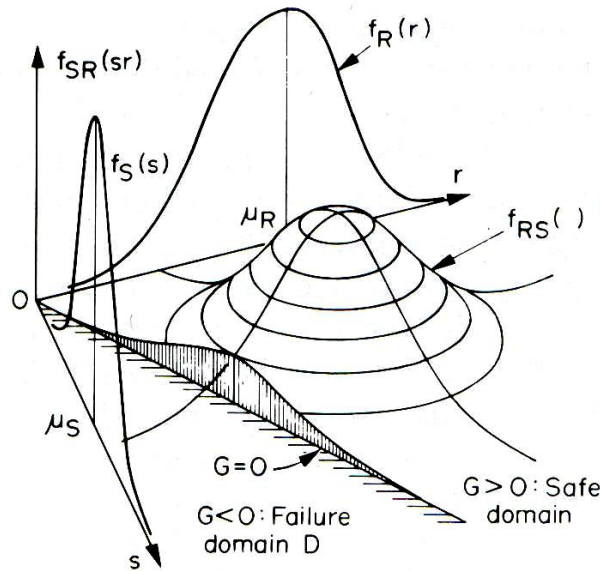


Figure 5.1. Statistical distribution of resistances and stresses and performance function  $G$ .

If  $\mathbf{R}$  and  $\mathbf{S}$  are uncorrelated (independent variables), we obtain, more simply

$$P_f = P[\mathbf{R} - \mathbf{S} \leq 0] = \int_{-\infty}^{+\infty} \int_{-\infty}^{s \geq r} f_R(r) \cdot f_S(s) dr ds, \quad (5.2)$$

whereas if the domain of resistances and stresses are made to coincide (stress or section-level verifications), then  $r \equiv s \equiv x$ ,  $x \in \mathbf{X}$ , and we obtain

$$P_f = P[\mathbf{R} - \mathbf{S} \leq 0] = \int_{-\infty}^{+\infty} F_R(x) f_S(x) dx, \quad (5.3)$$

where  $F_R(x)$  represents the cumulative distribution function of resistances, or the probability in  $X$  of obtaining any value lower than  $x$ . Eq. (5.3) can be expressed graphically, as in Figure 5.2.

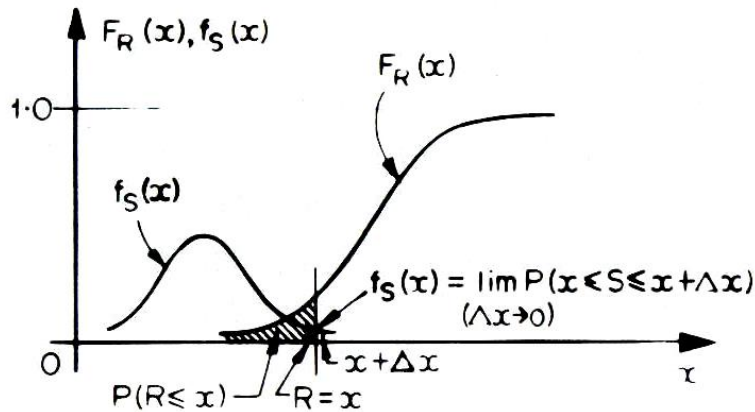


Figure 5.2. Evaluation of failure probability in the case of independent stresses and resistances.

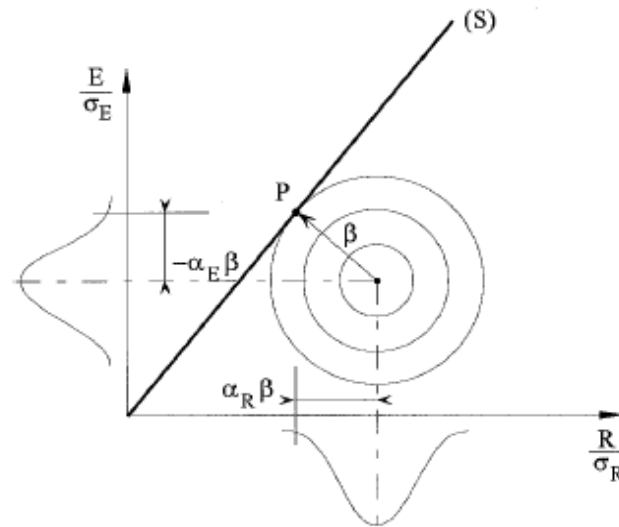
### 5.2.2.2 Level II methods (first order reliability methods)

In this method, a number of simplifying assumptions allow to evaluate the failure probability directly. Specifically, it is assumed that the variables  $R$  and  $S$  are independent and that the effect  $E$  of the stresses  $S$  is being evaluated, for example, by calculating the state of stress induced using a model (e.g. elastic, plastic, linear, non-linear, etc.) in such a way that both  $R$  and  $E$  are defined on the same domain. It is assumed that the probability distributions  $f_R(r)$  and  $f_E(e)$  are normal Gaussian distributions, and that  $\mu_R$ ,  $\mu_E$  and  $\sigma_R$ ,  $\sigma_E$  are the mean and standard deviation of  $R$  and  $E$ , respectively. With regard to the assumption of independence of stresses and actions, the performance function takes the form  $G = R - E$ , and consequently  $\mu_G = \mu_R - \mu_E$ ,  $\sigma_G = \sigma_R - \sigma_E$ .

The reliability index  $\beta$  is defined by the following equation:

$$\beta = \frac{\mu_G}{\sigma_G} \Rightarrow \mu_G - \beta \sigma_G = 0. \tag{5.4}$$

This coefficient has a simple geometric interpretation in the plane  $(R, E)$  in Figure 5.3 as the distance from the line  $(S)$  defined by the equation  $G = R - E = 0$ , which represents the failure boundary, from the point representing the mean  $\mu_G$ .



(S) failure boundary  $g = R - E = 0$   
 P design point

Figure 5.3. Design point P, failure boundary (S) and geometric interpretation of  $\beta$ .

From the assumption of normal probability distribution, we can conclude that a relationship exists between the value of  $\beta$  and the value of the probability of failure  $P_{f;\beta}$  associated with it, i.e.

$$\mu_G - \beta\sigma_G \leq 0 \Leftrightarrow P[R - E \leq 0] = P_{f;\beta} \tag{5.5}$$

The values of  $P_{f;\beta}$  are provided in Table 5.1 as a function of  $\beta$ . The design point P in Figure 5.3 also defines the factors  $\alpha_R$  and  $\alpha_E$ , shown in the same figure, which are associated with the design values  $e_d \in E$  and  $r_d \in R$ , which have to be considered to obtain the probability of failure associated with  $\beta$ . More specifically, we obtain  $e_d = \mu_E + \beta \cdot \alpha_E \cdot \sigma_E$  and  $r_d = \mu_R - \beta \cdot \alpha_R \cdot \sigma_R$ .

The values of  $\alpha_R$  and  $\alpha_E$  depend in general on the distributions of stresses and resistances. However, if  $0.16 < \sigma_E/\sigma_R < 7.6$ , it can be assumed – at least as an initial approximation – that  $\alpha_R = 0.8$  and  $\alpha_E = 0.7$ .

Table 5.1. Relationship between the failure probability and the factor  $\beta$

$P_{f;\beta}$	$10^{-1}$	$10^{-2}$	$10^{-3}$	$10^{-4}$	$10^{-5}$	$10^{-6}$	$10^{-7}$
$\beta$	1.28	2.32	3.09	3.72	4.27	4.75	5.20

By dividing the design values  $e_d$  and  $r_d$  by the respective nominal characteristics, we obtain the partial factors for actions and resistances to consider in verifications.

Eurocode [EN 1990] establishes for each of the classes of consequence the corresponding value of  $\beta$  set out in Table 5.2.

Table 5.2. Consequences class and minimum values for  $\beta$  (EN 1990)

Consequences class	Minimum values for $\beta$	
	1 year reference period	50 years reference period
CC3	5.2	4.3
CC2	4.7	3.8
CC1	4.2	3.3

If the probability distributions for actions or resistances are not normal Gaussian distributions, the level II method cannot be applied directly. However, transfer functions exist [Madsen *et al.*, 1985] which allow equivalent Gaussian distributions to be defined, at least as an initial approximation, starting from other types of statistical distribution (e.g. log-normal, Weibull, etc.). Therefore, in the case of glass, before applying level II methods, it is necessary to transform the (Weibull) statistical distribution of resistances into an equivalent Gaussian distribution. This solution, however, is complex; hence it is preferable to apply the level III method directly, as illustrated in the following sections.

### 5.2.2.3 Level I methods (or partial factor methods)

Because of their simplicity, Level I methods are the most commonly used in design practice. According to this approach, starting from the nominal values of the base variables (i.e. actions, resistances and geometric properties) through the use of partial factors for the material and actions, design values are obtained with which the structures can be verified in order to ensure that no relevant limit state is exceeded.

### 5.2.3 Probability of failure and partial factors

In accordance with EN1990, structural elements are divided into classes, and a precise probability of failure is associated with each one. As also outlined in Section 3.2.1, the following probability characterisation applied.

#### class zero.

Beyond the scope of these instructions.

#### class 1: elements in CC1.

Reliability index  $\beta_{50} = 3.3$  for a reference period of 50 years (as in Table B2, EN1990), corresponding to a probability of failure of  $4.83 \cdot 10^{-4}$  in 50 years; reliability index  $\beta_1 = 4.20$  for a reference period of 1 year, corresponding to a probability of failure of  $1.335 \cdot 10^{-5}$  in 1 year.

#### class 2: elements in CC2.

Reliability index  $\beta_{50} = 3.8$  for a reference period of 50 years (as in Table B2, EN1990), corresponding to a probability of failure of  $7.235 \cdot 10^{-5}$  in 50 years; reliability index  $\beta_1 = 4.7$  for a reference period of 1 year, corresponding to a probability of failure of  $1.30 \cdot 10^{-6}$  in 1 year.

#### class 3: elements in CC3.

Reliability index  $\beta_{50} = 4.3$  for a reference period of 50 years (as in Table B2, EN1990), corresponding to a probability of failure of  $8.54 \cdot 10^{-6}$  in 50 years; reliability index  $\beta_1 = 5.2$  for a reference period of 1 year, corresponding to a probability of failure of  $9.96 \cdot 10^{-8}$  in 1 year.

The partial factors for resistances ( $\gamma_M$ ) and actions ( $\gamma_Q$ ) provided in the technical standards generally correspond to a structure with a reliability index  $\beta$  greater than 3.8 for a reference period of 50 years,

i.e., to the CC2 consequences class, to which second-class elements belong (Table B2, EN1990). These factors are calibrated assuming Gaussian or log-normal distributions of resistances. As glass follows a Weibull distribution (Section 2.1.3) instead, the partial factors  $\gamma_M$  of materials resistances must be specifically calibrated in such a way as to obtain the abovementioned probability of failure. In these recommendations, the partial factors  $\gamma_Q$  for the actions are assumed to be the same as those set out in the Eurocodes and in national standards and legislation. The partial factors  $\gamma_M$  for materials are specifically calibrated according to Weibull statistics for paradigmatic design practice cases, so that the abovementioned probabilities of failure are obtained.

#### 5.2.4 The factor $R_M$

To go from second-class verifications (consequences class CC2) to first-class verifications (CC1), Eurocode EN 1990 (point B3.3) prescribes reducing partial factors for actions by means of a multiplication factor  $K_{FI} < 1$ . Specifically, point B3.3 of EN 1990 recommends the value  $K_{FI} = 0.9$ , calibrated assuming Gaussian statistical distributions of material resistances (different from the Weibull distribution usable for glass). Calibrating  $K_{FI}$  for glass would give values much lower than 0.9 as recommended in the Eurocodes, as the statistical dispersion of resistances for this material is much higher than for other, more traditional materials. As a result, even a small increase in the failure probability would lead to a sharp decrease in the factor  $K_{FI}$ , which would be in the order of  $K_{FI} = 0.7$ . In these instructions, the shift from verifications in class CC2 to CC1 is accounted for by appropriately reducing the partial factor for the material as opposed to the factor for actions.

For linear problems, there is no significant difference between choosing the procedure of decreasing the factors for actions or the factors for materials, as it is their product which determines the safety threshold. However, in problems involving marked geometric non-linearities, such as for thin glass structures, a significant reduction in design actions would lead to a reduced evaluation of second-order effects. Given the specific nature of glass and since the decisive factor in calculating the probability of failure lies not so much in the probabilistic distribution of actions as in the (Weibull) probabilistic distribution of resistances, we have chosen to modify the partial factor for resistances rather than consider the multiplication factor for actions  $K_{FI}$ , as recommended in EN 1990.

Specifically, and as described in more detail below, for second-class verifications a factor  $\gamma_M$  is used, while for first-class verifications a reduced factor,  $\gamma_M^* = R_M \gamma_M$ , is used, where  $R_M < 1$  is calibrated with probabilistic methods in order to obtain the required degree of reliability. For post-glass-failure assessment, a greater probability of failure can be tolerated as the damaged element will soon be replaced. Therefore, the same partial factors are conventionally assumed for materials strength for verifications in class 1 or in class 2, but the actions are conventionally reduced, by considering them in relation to a return period of 10 years for calculations in class 2 and of 10 years for calculations in class 1.

In conclusion, the safety verification using level I methods takes the following form:

$$S(\gamma_Q Q) \leq \frac{f_g}{R_M \gamma_M}, \quad (5.6)$$

where  $S(\gamma_Q Q)$  represents the stress due to the action  $Q$  (multiplied by the partial factor  $\gamma_Q$ ), while  $f_g$  generically represents the strength of glass,  $\gamma_M$  is the partial factor for the material and  $R_M$  is the multiplication factor that takes into account, in probabilistic terms, the transition from verifications in class 2 ( $R_M = 1$ ) to verifications in class 1 ( $R_M < 1$ ).

It should be remarked that this aspect of the calculation is different from the classical approach in Eurocode EN1990. Here  $\gamma_Q$ , the partial factor for actions, is not reduced, while the partial factor  $\gamma_M$  for the resistance of glass is reduced.



## 5.2.5 Probabilistic function of glass strength

As set out in Section 2.1, the tensile strength of glass is the macroscopic manifestation of the growth of surface cracks, which may advance over time under constant load. It is pointed out that the nominal strength of glass  $f_g$  is defined on the basis of a standardised test [UNI EN 1288], under precise thermo-hygrometric conditions [ $T=23^\circ\text{C}$ ,  $RH=55\%$ ] and at a constant stress rate [ $\dot{\sigma} = 2\text{MPa} / \text{s}$ ] as indicated in Section 2.1.1.1. The distribution of the values  $f_g$  thus obtained can be interpreted by means of a Weibull statistical distribution (Section 2.1.3). The experimental results obtained in the campaign of tests are briefly summarised in Table 2.5, while the corresponding Weibull parameters are illustrated in Table 2.6.

In order to obtain mechanical resistance values that are applicable in any condition, without the need for over-elaborate differentiations for design, in the following steps reference is made to coaxial double ring (CDR) bending tests without overpressure, the results of which are less dependent on edge defects with respect to the four-point bending (FPB) tests. Although the CDR test is not standardised, it is considered the most appropriate test for determining the strength characteristics of glass (for more details, see Section 2.1.3.1).

As the state of stress in CDR tests is approximately equibiaxial, the results obtained are the least favourable ones in terms of the effects of the form of the stress state in relation to failure. Nevertheless, the data regarding biaxial stress states can be rescaled in order to interpret the experimental results if the same samples had been hypothetically subjected to a uniaxial state of stress, by using Eq. (2.35) (see also Figure 2.12).

With regard to the influence of the loaded area, the failure values obtained experimentally have been rescaled to refer to a conventional area of  $1\text{ m}^2$ , using the model described in Section 2.1.2.2.4 and in particular Eqs. (2.36) and (2.39). Thus the data for the series of samples A1 and A2 in Table 2.6, which differ from each other solely with regard to the loaded area, may be compared by referring to the conventional unit area (UA). The final result is the one summarised in Table 2.7, to which reference is made for the calibration of the factors.

Specifically, as the surface under load (tin or air side) is always random, the probability that the surface under the greatest stress is the tin side or air side surface is considered to be equal. In conclusion, the Weibull parameters used for the statistical evaluation of safety are the ones relating to the CDR-UA case (double ring with reference to the unit area) provided in Table 2.7.

It should perhaps be pointed out that, although the mean and characteristic (fractile) values of ultimate strength at failure are lower for the tin side than the air side (Table 2.8), it is not necessarily the case that the stress on the tin side is worse in probabilistic terms. As a matter of fact, the statistical distribution for the air side is characterised by much greater dispersion, with a significantly lengthened lower tail in which the distribution function is higher compared with the tin side. Therefore, as is shown below in the evaluation of safety in accordance with level III methods, the two surfaces are comparable from the statistical point of view.

### 5.2.5.1 Load duration

The parameters in Table 2.7 interpret the experimental results obtained using the standardised test method, at a well defined stress rate. In safety verifications, by contrast, it is assumed that the load acts constantly for a precise characteristic time, as illustrated in Section 4.10. Given the phenomenon of static fatigue, the same test piece would fail at different stress levels as the stress rate changes. In order to be able to calibrate the partial factors for strengths, therefore, we must have their statistical distribution under constant load. More specifically, as the characteristic load application time is assumed to be known, it is necessary to know the statistical distribution of those loads which, acting for the same assigned period of time, cause the glass to break and fail. This distribution can be obtained

analytically, using the damage model described in Section 2.1.1.1 to rescale the Weibull parameters of the statistical distribution of failures obtained in standard testing conditions.

Let  $m$  and  $\sigma_0$  therefore be the parameters relating to the Weibull distribution which best fit the  $f_g$  data, i.e. the strengths at failure derived from the standardised test,  $t_L$  a reference time interval and  $f_L$  the failure stress which, applied statistically, would cause failure (as a result of static fatigue) in time  $t_L$ . Following the notation used in Section 2.1.1.1, it follows from Eq. (2.12) that

$$f_L^n \cdot t_L = \frac{\frac{2}{n-2} \cdot c_i^{\frac{2-n}{2}} \cdot \left[ 1 - \left( \frac{c_i}{c_{cL}} \right)^{\frac{n-2}{2}} \right]}{v_0 \cdot \left( \frac{Y \cdot \sqrt{\pi}}{K_{IC}} \right)^n} \cong \frac{\frac{2}{n-2} \cdot c_i^{\frac{2-n}{2}}}{v_0 \cdot \left( \frac{Y \cdot \sqrt{\pi}}{K_{IC}} \right)^n}, \quad (5.7)$$

where the term in  $(c_i/c_{cL})$  is ignored as  $n$  is high ( $n = 16$  can be assumed) and, as can be verified *a posteriori* for relevant characteristic periods  $t_L$ , the final critical crack  $c_{cL}$  is much larger than the initial crack  $c_i$ .

With regard to the dimensions  $c_i$  of the initial crack, Eq. (2.6) can be used. It can be approximated in the form

$$c_i = \left[ \frac{n-2}{2} \cdot \frac{v_0}{n+1} \cdot \left( \frac{Y \cdot \sqrt{\pi}}{K_{IC}} \right)^n \cdot \frac{f_g^{n+1}}{\dot{\sigma}} + \left( \frac{Y \cdot f_g \cdot \sqrt{\pi}}{K_{IC}} \right)^{n-2} \right]^{\frac{2}{2-n}} \cong \left[ \frac{n-2}{2} \cdot \frac{v_0}{n+1} \cdot \left( \frac{Y \cdot \sqrt{\pi}}{K_{IC}} \right)^n \cdot \frac{f_g^{n+1}}{\dot{\sigma}} \right]^{\frac{2}{2-n}}, \quad (5.8)$$

because, as it can be verified *a posteriori*, the second term is negligible compared with the first for the corresponding data.

The  $c_i$  equation above must be substituted into Eq. (5.7). However, it must be noted that while Eq. (5.8) is derived from the data of the standardised test, in very precise thermo-hygrometric conditions, Eq. (5.7) interprets obtainable results in real conditions, which may be more aggressive compared with laboratory conditions (particularly higher humidity conditions). In all cases  $K_{IC} = 0.75 \text{ MPa m}^{1/2}$ ,  $\dot{\sigma} = 2 \text{ MPa/s}$ , and  $Y = 2.24/\pi$ . However with regard to the parameters governing static fatigue, in Eq. (5.8) the values obtained in lab conditions are considered, i.e.  $n = 16$ ,  $v_0 = 0.0013 \text{ m/s}$ , while in Eq. (5.7) parameters for a different environment are considered. Reasonably conservative values for Eq. (5.7) are  $n = 16$  and  $v_0 = v_0^* = 0.0025 \text{ m/s}$ . By substituting Eq. (5.8) into Eq. (5.7) we obtain

$$f_L^n \cdot t_L \cong \frac{1}{n+1} \frac{v_0}{v_0^*} \frac{f_g^{n+1}}{\dot{\sigma}}, \quad (5.9)$$

which enabled the data to be rescaled.

Now, given the equivalence just discussed between test under standardised conditions and the situation under constant load, the probability of failure in the two conditions must be the same taking account of equation (5.9). Referring to Eq. (2.23) we thus have

$$\left( \frac{f_g}{\sigma_0} \right)^m = \left( \frac{f_L}{\sigma_{0L}} \right)^{m_L}, \quad (5.10)$$

where  $m$  and  $\sigma_0$  are Weibull parameters for the standardised laboratory test, while  $m_L$  and  $\sigma_{0L}$  are the Weibull parameters for failure under constant load. By substituting Eq. (5.9) into Eq. (5.10) we obtain

$$\left(\frac{f_g}{\sigma_0}\right)^m = f_g^{\frac{m_L(n+1)}{n}} \frac{1}{\sigma_{0L}^{m_L}} \left(\frac{1}{(n+1)\dot{\sigma} t_L} \frac{v_0}{v_0^*}\right)^{\frac{m_L}{n}}, \quad (5.11)$$

from which it follows that

$$\frac{m_L(n+1)}{n} = m, \quad \frac{1}{\sigma_0^m} = \frac{1}{\sigma_{0L}^{m_L}} \left(\frac{1}{(n+1)\dot{\sigma} t_L} \frac{v_0}{v_0^*}\right)^{\frac{m_L}{n}}. \quad (5.12)$$

Hence we derive

$$m_L = \frac{n}{n+1} m, \quad \sigma_{0L} = \sigma_0^{\frac{m}{m_L}} \left(\frac{1}{(n+1)\dot{\sigma} t_L} \frac{v_0}{v_0^*}\right)^{\frac{1}{n}} = \sigma_0^{\frac{n+1}{n}} \left(\frac{1}{(n+1)\dot{\sigma} t_L} \frac{v_0}{v_0^*}\right)^{\frac{1}{n}}, \quad (5.13)$$

which facilitates the transition between the statistical distributions of the standardised test and the statistical distributions for a constantly applied load for a fixed period of time.

### 5.2.5.2 Scale effect

According to Eq. (2.38), the effects of the maximum stress  $\sigma_{\max, A_{eff}}$  applied on an effective area  $A_{eff}$  are equivalent, in probabilistic terms, to the effects of the equibiaxial stress  $\sigma_{\max, eqbiax, UA}$  acting on an element with a unit area  $UA$ . Considering two geometrically similar elements, under the same constraint and loading conditions, but with effective areas  $A_{1eff} = k_1 A_1$  e  $A_{2eff} = k_2 A_2$ , from Eq. (2.38) we obtain

$$\sigma_{\max, eqbiax, UA} = \sigma_{\max, A_{1eff}} \left(\frac{k_1 A_1}{UA}\right)^{1/m}, \quad \sigma_{\max, eqbiax, UA} = \sigma_{\max, A_{2eff}} \left(\frac{k_2 A_2}{UA}\right)^{1/m}, \quad (5.14)$$

which provides the scale effect

$$\sigma_{\max, A_{2eff}} = \sigma_{\max, A_{1eff}} \left(\frac{k_1 A_1}{k_2 A_2}\right)^{1/m}. \quad (5.15)$$

The meaning of Eq. (5.15) is that the stresses  $\sigma_{\max, A_{1eff}}$  and  $\sigma_{\max, A_{2eff}}$  produce the same effects, for probabilistic purposes, when they act on the effective areas  $A_{1eff}$  and  $A_{2eff}$ . It is thus confirmed that surfaces with a larger area are more prone to failure. The factors  $k = k_1$  and  $k = k_2$  can be calculated by determining the value of  $C$  defined by Eq. (2.27) at every point, calculating the probability of failure provided by Eq. (2.28) and comparing this expression with Eq. (2.36).

Using the results of the experimental test illustrated in Section 2.1.3.1, we obtain for  $m$  the values summarised in Table 2.7, which are distinguished according to whether the tin side or the air side of the glass is subjected to tension. In the scaling transition, the effects due to the geometric non-linearity of the problem are important, as a consequence of which the factor  $k$  depends on the size of the load applied.

## 5.3 Calibration of partial factors for annealed glass

### 5.3.1 General remarks

As a rule, the numerical values for partial factors for material verifications may be determined by means of one of the following two methods:

- by carrying out a calibration based on experience and building traditions (as is the case for most of the partial factors currently recommended in the Eurocodes);
- based on statistical evaluation of experimental data and field observations. This approach must be considered within the framework of a probabilistic reliability theory.

If method b) is used, on its own or in combinations with method a), the partial factors for the various materials and actions must be calibrated such that the reliability levels for representative structures are as close as possible to the target reliability index.

Figure 5.4 presents a diagrammatic overview of the various methods available for calibration of partial factors.

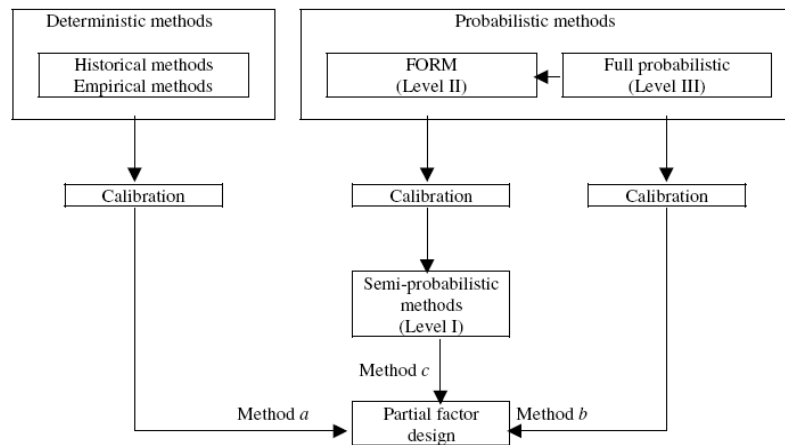


Figure 5.4. Outline diagram of partial factor calibration methods.

The probabilistic calibration procedures for partial factors can be divided into two main categories: *i*) full probabilistic methods or Level III methods (Section 5.2.2.1); *ii*) First Order Reliability Methods (FORM) or Level II methods (Section 5.2.2.2). For the sake of completeness, it is pointed out that Level II methods also include Second Order Reliability Methods (SORM), which, however, are generally not used at the legislation level.

Full probabilistic methods (Level III) give in principle correct answers to the reliability problem, but they are difficult to apply. Level II methods make use of certain well defined approximations and lead to results which for most structural applications of traditional construction materials (for example steel, concrete and wood) can be considered sufficiently accurate.

In both methods (Level II and III), the measure of reliability must be identified with the survival probability  $P_s = (1 - P_f)$ , where  $P_f$  is the failure probability for the considered failure mode or limit state, calculated for a given reference period. If the calculated failure probability is higher than a pre-set target value, then the structure must be considered to be unsafe.

For the calibration of partial factors for glass, the full probabilistic method (Level III) has been chosen, since, for the reasons set out above, the material is considered innovative from the structural perspective (in particular as it can be interpreted by a Weibull distribution). As Level II methods are calibrated according to statistical distributions for traditional materials, their direct application to glass would give unreliable results.

Here, therefore, the factors are calibrated by considering a number of “paradigmatic” examples (case studies), designed using Level III methods: the partial factors for the material are calibrated in such a way as to lead to the same sizing.

### 5.3.2 Calibration procedure

Given the statistical distribution of actions, it is possible to find, through calculation, the cumulative probability of maximum stress in the plate. The equation

$$F_{\sigma,pr,\tau}(x), \quad (5.16)$$

thus indicates the probability that the maximum stress in the plate as a result of the action, of characteristic duration  $\tau$ , is lower than the value  $x$  over the reference time, here assumed to be one year. The probability density function for the stresses  $f_{\sigma,pr,\tau}$  is naturally obtained by deriving Eq. (5.16) with respect to  $x$ , i.e.

$$f_{\sigma,pr,\tau}(x) = \frac{d}{dx} F_{\sigma,pr,\tau}(x). \quad (5.17)$$

With regard to the strength of glass, in order to determine the parameter  $k$  in Eq. (2.36) which rescales the area  $A$  of the plate in question in order to define the effective area  $A_{eff} = k A$ , the representative domain of the glass surface subject to tensile stresses is hypothetically divided into  $N$  elementary areas and for the  $i$ -th element the mean value of the principal stress components  $\sigma_{1,i}$  and  $\sigma_{2,i}$  and the ratio  $r_i = \sigma_{2,i}/\sigma_{1,i}$  are considered. The factor  $C = C_i$  defined by the integral equation (2.27) is then calculated, assuming  $r = r_i$ . Taking  $\Delta A_i$  as the area of  $i$ -th element of division, for Eq. (2.28) the probability of obtaining failure of the plate for the given loading condition can be approximated by the expression

$$P = 1 - \exp \left[ - \sum_{i=1}^N \left( \frac{C_i \sigma_{1,i}}{\sigma_{0L}} \right)^{m_L} \Delta A_i \right]. \quad (5.18)$$

From the comparison with Eq. (2.36) the following equation is obtained:

$$k = \frac{\sum_{i=1}^N (C_i \sigma_{1,i})^{m_L} \Delta A_i}{A (\sigma_{\max})^{m_L}}. \quad (5.19)$$

The value of  $k$  thus depends in general on the factor  $m_L$  but not on  $\sigma_{0L}$ .

As the glass arrangement is completely random, being difficult or impossible to differentiate between air and tin side on site, there is an equal probability that the face subjected to maximum tensile stresses is the tin side or the air side face. To account for the equal probability of these two *incompatible* events, the probability function considered is the arithmetic average of the probability functions, Eq. (2.36), calculated for the two surfaces. The parameters  $\sigma_{0L}$  and  $m$  correspond to these probabilistic functions and, starting from the data provided in Table 2.7, are calculated by supposing in Eq. (5.13)  $t_L = \tau$ , i.e. the characteristic duration time of the action. Thus

$$F_{\sigma,A,\tau}^{(air+tin)/2}(x) = 1 - \frac{1}{2} \left\{ \exp \left[ -k_{air} A \left( \frac{x}{\sigma_{0L,air}} \right)^{m_{L,air}} \right] + \exp \left[ -k_{tin} A \left( \frac{x}{\sigma_{0L,tin}} \right)^{m_{L,tin}} \right] \right\}, \quad (5.20)$$

represents the cumulative probability of obtaining failure for lower maximum stresses in the plate than the value  $x$  over the reference period, here assumed to be one year. The probability of plate collapse in one year of life is obtained through the convolution integral

$$P_{f,1y} = \int_{-\infty}^{+\infty} F_{\sigma,A,\tau}^{(air+tin)/2}(x) \cdot f_{\sigma,pr,\tau}(x) \cdot dx . \quad (5.21)$$

To obtain in this equation the target value defined in Section 5.2.3 for elements in the first or second class of consequences, the characteristic parameters that define the action (for example the characteristic value of wind pressure) are made to vary until the desired value is obtained.

At this point, we move onto plate design using Level I methods. The characteristic values of the action that produce the target failure probability, multiplied by suitable partial factors  $\gamma_Q$ , are used as deterministic values in order to calculate the maximum stress  $\sigma_{\max,d,\tau}$  in the glass.

With regard to the characteristic strength of glass, the comparison value is provided by  $f_{g,k}$ , the characteristic strength with reference to the *equibiaxial* test conducted on a coaxial double ring with overpressure in accordance with EN 1288-2 (see Section 2.1.2.3) for which  $A_{eff,test} = k_{test} A_{test} = A_{test} = 0.24\text{m}^2$ , since  $k_{test} = 1$ .

As indicated in Section 5.2.3, for elements falling under the class 2 it is assumed that  $R_M = 1$  and the factor  $\gamma_M$  for the material is calculated so that equality is satisfied in the inequality

$$\sigma_{\max,d,\tau} \leq \frac{k_{\text{mod},\tau} \lambda_{gA_{test} \rightarrow kA}^{(air+tin)/2} f_{g,k}}{R_M \gamma_M}, \quad (5.22)$$

where  $k_{\text{mod},\tau}$ , with reference to time  $\tau$ , is defined in Table 2.2 (“LEFM” column, values derived using the Linear-Elastic Fracture Mechanics model), while the characteristic strength value of the glass,  $f_{g,k}$ , is conventionally assumed to be equal to the nominal value 45 MPa, as illustrated in Table 2.4.

The factor  $\lambda_{gA_{test} \rightarrow kA}^{(air+tin)/2}$  makes it possible to rescale the characteristic strength value, which is obtained by means of testing on an area  $A_{eff,test} = k_{test} A_{test} = A_{test} = 0.24\text{m}^2$ , with respect to the effective area  $A_{eff}$  of the case study. With regard to the effective area for the maximum stress (the area which, if subjected to an equibiaxial stress equal to the maximum area, would have the same probability of fracture as would be determined by the effective stress field acting upon the physical area), different stress fields may be compared, by reference to a conventional area – for the sake of convenience, the effective area of the tests used to determine the mechanical strength of glass  $A_{test}$  – and deriving the value of the equibiaxial stress which would give the same probability of fracture. If the two stress fields act upon different areas but have the same probability of fracture, the scale effect for the stress expressed by Eqs. (5.14) and (5.15) is obtained.

Assuming Eq. (5.20), the equal probability of fracture on different stress fields that act, respectively, on the area of the case study and the area of the test (under equibiaxial conditions), provides the following equation:

$$\begin{aligned} & \exp \left[ -k_{air} A \left( \frac{\sigma_{\max,A}}{\sigma_{0L,air}} \right)^{m_{L,air}} \right] + \exp \left[ -k_{tin} A \left( \frac{\sigma_{\max,A}}{\sigma_{0L,tin}} \right)^{m_{L,tin}} \right] \\ & = \exp \left[ -1 A_{test} \left( \frac{\sigma_{\max,test}}{\sigma_{0L,air}} \right)^{m_{L,air}} \right] + \exp \left[ -1 A_{test} \left( \frac{\sigma_{\max,test}}{\sigma_{0L,tin}} \right)^{m_{L,tin}} \right]. \end{aligned} \quad (5.23)$$

The factor  $\lambda_{gA_{test} \rightarrow kA}^{(air+tin)/2}$  is obtained from the preceding equation, assuming that  $\sigma_{max.test} = f_{g,k}$  and assuming that  $\lambda_{gA_{test} \rightarrow kA}^{(air+tin)/2} f_{g,k} = \sigma_{max.A}$ . However, as the argument of the exponentials is small, passing to the series expansion  $e^x = 1 + x + o(x)$ , and neglecting higher than first-order terms, the expression is reduced to

$$k_{air} A \left( \frac{\lambda_{gA_{test} \rightarrow kA}^{(air+tin)/2} f_{g,k}}{\sigma_{0L.air}} \right)^{m_{L.air}} + k_{tin} A \left( \frac{\lambda_{gA_{test} \rightarrow kA}^{(air+tin)/2} f_{g,k}}{\sigma_{0L.tin}} \right)^{m_{L.tin}} = A_{test} \left[ \left( \frac{f_{g,k}}{\sigma_{0L.air}} \right)^{m_{L.air}} + \left( \frac{f_{g,k}}{\sigma_{0L.tin}} \right)^{m_{L.tin}} \right] \quad (5.24)$$

This equation, although rigorous, is of little utility as it is not analytically invertible. An approximate expression can be obtained by evaluating the failure probability of the air and tin side surfaces separately and evaluating the scale effects on the arithmetic average of the rescaled stresses. If the exposed surface subjected to tension is the air side surface or the tin side surface, Eq. (5.15) gives, respectively

$$\begin{aligned} \sigma_{max.A}^{air} &= \sigma_{max.test} \left( \frac{A_{test}}{k_{air} A} \right)^{1/m_{L.air}} \Rightarrow \lambda_{gA_{test} \rightarrow kA}^{air} f_{g,k} = f_{g,k} \left( \frac{A_{test}}{k_{air} A} \right)^{1/m_{L.air}}, \\ \sigma_{max.A}^{tin} &= \sigma_{max.test} \left( \frac{A_{test}}{k_{tin} A} \right)^{1/m_{L.tin}} \Rightarrow \lambda_{gA_{test} \rightarrow kA}^{tin} f_{g,k} = f_{g,k} \left( \frac{A_{test}}{k_{tin} A} \right)^{1/m_{L.tin}}. \end{aligned} \quad (5.25)$$

Therefore, assuming

$$\sigma_{max.A}^{(air+tin)/2} := \frac{1}{2} (\sigma_{max.A}^{air} + \sigma_{max.A}^{tin}) =: \lambda_{gA_{test} \rightarrow kA}^{(air+tin)/2} f_{g,k}, \quad (5.26)$$

finally we obtain

$$\lambda_{gA_{test} \rightarrow kA}^{(air+tin)/2} = \frac{1}{2} \left[ \left( \frac{A_{test}}{k_{air} A} \right)^{1/m_{L.air}} + \left( \frac{A_{test}}{k_{tin} A} \right)^{1/m_{L.tin}} \right]. \quad (5.27)$$

In general, given the high value of the exponents  $m_{L.air}$  and  $m_{L.tin}$ , Eqs. (5.24) and (5.27) generally lead to expressions that differ very little from one another. It can be verified directly, in the case studies analysed below, that the difference between the values obtained from the two expressions is less than one percentage point.

Finally, it should be noted that in strictly probabilistic terms, the value of  $f_{g,k}$  to consider in Eq. (5.22) for the calibration of the partial factor  $\gamma_M$  should be the characteristic value of resistances associated with the distribution in Eq. (5.20). However, as the nominal value in Table 2.4 is always used in the design process, we have chosen to use this value.

Once the factor  $\gamma_M$  has been determined, the case of elements in the class 1 can be analysed. Now, in Eq. (5.22) the factor  $R_M$  is the one which, in accordance with the analysis set out in Section 5.2.3, appropriately remodulates the resistance values so that they correspond to different failure probabilities. By using the previously determined value of  $\gamma_M$ , we can determine the factor  $R_M$  which enables the equality in Eq. (5.22), corresponding to the target failure probability for elements in the class 1, to be found.

### 5.3.3 Case studies

#### 5.3.3.1 Plate subjected to wind action

The case considered is that of a monolithic  $1000 \times 1000 \times 6 \text{ mm}^3$  glass plate simply supported at the edges, subjected to the wind pressure  $p_w$ . In relation to this action, two calculations are conducted for peak wind pressures with different characteristic times, i.e. 3 seconds and 10 minutes.

The stresses that develop at all points in the plate are determined with a numerical code both for a linear-elastic regime and while preserving constitutive linearity but considering geometric non-linearity. The results obtained are illustrated in Figure 5.5 for maximum stresses at the centre of the plate: it is clear that neglecting the non-linear aspects may lead to errors for the higher values of  $p_w$ . For the case under consideration, interpolating the results with a second-order polynomial, we find that the stress  $\sigma_{\max}$  [MPa] can be approximated as a function of  $p_w$  [daN/m<sup>2</sup>] in the following form:

$$\sigma_{\max} = -6 \cdot 10^{-5} p_w^2 + 0.0836 p_w =: S(p_w). \quad (5.28)$$

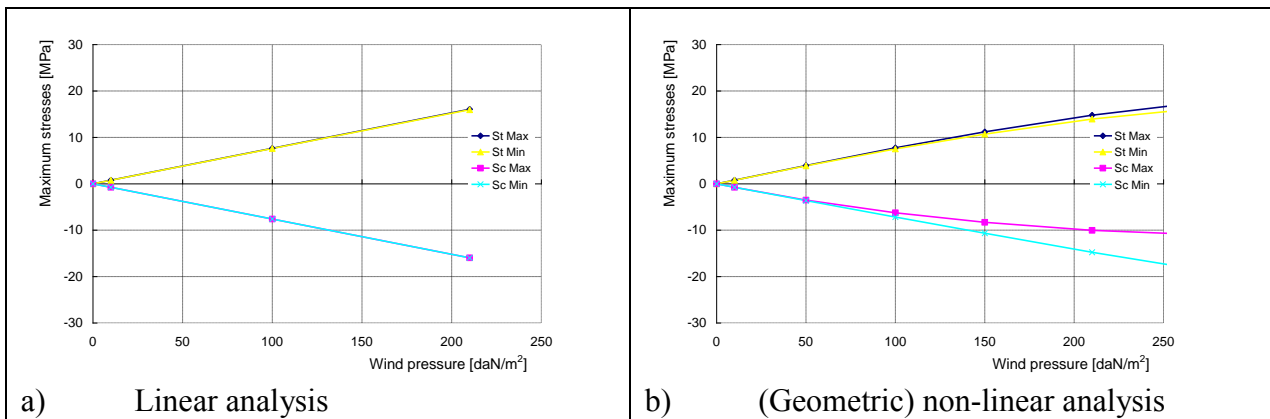


Figure 5.5. Maximum stress at the centre of the plate as a function of wind pressure: a) linear-elastic analysis; b) elastic analysis with geometric non-linearity.

For significant values of  $p_w$ , Eq. (5.28) can be easily inverted to obtain the wind pressure that causes a given maximum stress, a relationship that is indicated as  $p_w = S^{-1}(\sigma_{\max})$ . Substituting into Eq. (4.30), we obtain the cumulative probability of maximum stress in the plate arising from the maximum annual wind pressure calculated as an average over the characteristic time interval  $\tau$ . This takes the following form:



$$F_{\sigma,pr,\tau}(x) = \begin{cases} 0, & \text{for } \frac{S^{-1}(x)}{\frac{1}{2}\rho_a c_{e,\tau} c_p c_d} \leq (0.75v_{b50})^2, \\ 1 - \exp\left[\frac{1}{0.0652v_{b50}} \left(0.75v_{b50} - \sqrt{\frac{2S^{-1}(x)}{\rho_a c_{e,\tau} c_p c_d}}\right)\right], & \text{for } (0.75v_{b50})^2 < \frac{S^{-1}(x)}{\frac{1}{2}\rho_a c_{e,\tau} c_p c_d} \leq (0.85v_{b50})^2, \\ \exp\left[-\exp\left(\frac{1}{0.2} - \frac{2S^{-1}(x)}{0.2 \cdot 0.75^2 \rho_a v_{b50}^2 c_{e,\tau} c_p c_d}\right)\right], & \text{for } (0.85v_{b50})^2 < \frac{S^{-1}(x)}{\frac{1}{2}\rho_a c_{e,\tau} c_p c_d} \leq v_{b50}^2, \\ \exp\left\{-\exp\left[\frac{1}{0.138} \left(1 - \frac{1}{0.65} \sqrt{\frac{2S^{-1}(x)}{\rho_a v_{b50}^2 c_{e,\tau} c_p c_d}}\right)\right]\right\}, & \text{for } \frac{S^{-1}(x)}{\frac{1}{2}\rho_a c_{e,\tau} c_p c_d} > v_{b50}^2, \end{cases} \quad (5.29)$$

where  $x$  (in MPa) represents the current value of maximum stress, while  $S^{-1}(x)$  is the function introduced above, which provides the wind pressure (in daN/m<sup>2</sup>) that generates the maximum stress  $x$  in MPa. The probability function for the stresses  $f_{\sigma,pr,\tau}$  is naturally obtained by deriving Eq. (5.29) in respect of  $x$ , i.e.

$$f_{\sigma,pr,\tau}(x) = \frac{d}{dx} F_{\sigma,pr,\tau}(x), \quad (5.30)$$

which exhibits discontinuities, as the function represented by Eq. (5.29) is not smooth. The graph for  $f_{\sigma,pr,\tau}$ , which shows the 4 branches that comprise Eq. (5.29), is of the type illustrated in Figure 5.6.

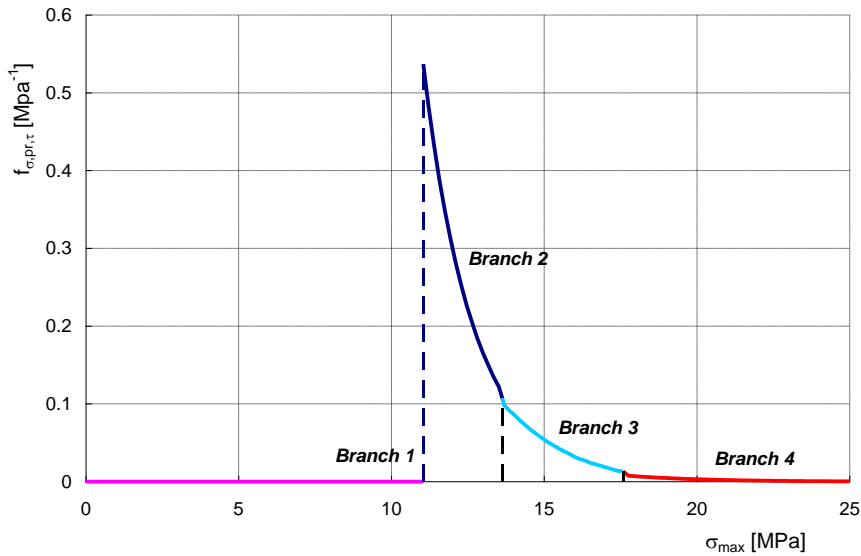


Figure 5.6. Typical graph for  $f_{\sigma,pr,\tau}$ . case  $\tau = 3$ sec,  $v_{b50} = 30$  m/s,  $c_e = 3.822$ ,  $c_p = 1.2$ ,  $c_d = 1$ .

With regard to the Weibull distribution of resistances, reference is made to Eq. (2.36), in which the Weibull parameters to consider are  $m_L$  and  $\sigma_{0L}$  which define the failure probability occurring in a characteristic time  $t_L$ . These parameters can be derived from Eq. (5.13) as a function of the Weibull parameters  $m$  and  $\sigma_0$  derived directly from the results obtained by means of the test procedure. Considering the data for the double ring test at a constant load rate on the reference unit area provided in Table 2.7, through Eq. (5.13) the values shown in Table 5.3 are obtained.

Table 5.3. Weibull parameters for test conditions and for failure in characteristic times  $t_L$ , for the reference unit area.

Weibull parameters		$m_L$	$\sigma_{0L}$ [MPa mm <sup>2/<math>m_L</math>]</sup>
Test CDR-UA	Tin	7.3	406
	Air	5.4	1096
$t_L = 3$ sec CDR-UA	Tin	6.9	425
	Air	5.1	1220
$t_L = 10$ min CDR-UA	Tin	6.9	305
	Air	5.1	876

To determine the parameter  $k$  in Eq. (2.36) which rescales the area  $A$  of the plate in order to define the effective area, the square domain representing the glass is hypothetically divided into  $N = 400$  squares of  $50 \times 50$  mm, and for the  $i$ -th square the mean value of the principal components of stress  $\sigma_{1,i}$  and  $\sigma_{2,i}$  and the ratio  $r_i = \sigma_{2,i}/\sigma_{1,i}$  are considered. The factor  $C = C_i$  defined by the integral equation Eq. (2.27) is then calculated, assuming that  $r = r_i$ . Taking  $\Delta Ai$  as the area of the  $i$ -th square of division, the factor  $k$  is derived using Eq. (5.19). For the case in question we obtain  $k_{air} = 0.1764$  and  $k_{tin} = 0.138$ . In order to take into account the equal probability that the surface most subjected to stress is the air side or the tin side, the probability function considered is the arithmetic mean of the probability functions as described by (5.20). The failure probability of the plate in one year of service is provided by (5.21).

It should be observed that, in the case under consideration, the largest contributions to the convolution integral, Eq. (5.21), come from the tail of the cumulative distribution function for resistances  $F_{\sigma_A, \tau}$ , where the probability density function for the effects of actions  $f_{\sigma, pr, \tau}$  is significantly non-zero (Figure 5.7a). This portion is enlarged in Figure 5.7b, where the cumulative distribution function for strengths corresponding to the mean (air + tin/2) is juxtaposed to the parts corresponding to the air side and to the tin side only. It will be noted that in the significant interval, the tin side function is generally greater than the air side function: this means that the probability of obtaining very small strength values is higher on the air side than on the tin side. This confirms that although the air side is, in the average, stronger than the tin side, the opposite occurs in statistical terms in proximity to the distribution tails, for small values of strength. As a result, in terms of the probabilistic evaluation of strengths for low failure probabilities, the tin side is better than the air side, as on the former we are less likely to find very low strengths than on the latter.

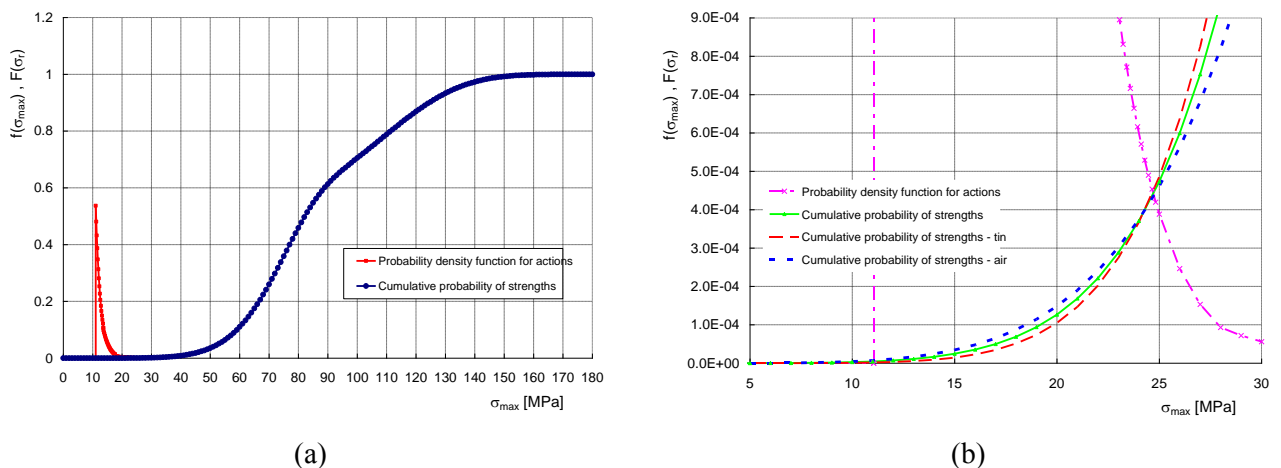


Figure 5.7. a) Probability density function for actions and cumulative probability of strengths. b) Enlargement of the significant portion, with indication of the cumulative probability function of strengths distinguished into air side (*air*) and tin side (*tin*) components.

In Eqs. (5.29) and (5.30), without loss of generality, let  $v_{b50} = 30$  m/s,  $c_d = 1$  and  $c_p = 1.2$ . The height  $z$  of the construction is chosen so that, through Eqs. (4.19) and (4.25), we obtain the values of the factors  $c_{e1}$  and  $c_e$  for which the integral function represented by Eq. (5.21) gives the probability  $P_{f,1y}$  which is equal to the target values established in Section 5.2.3, i.e.  $P_{f,1y} = 1.335 \cdot 10^{-5}$  for elements in class 1 and  $P_{f,1y} = 1.301 \cdot 10^{-6}$  for elements in class 2. Using these values for the factors, the design of the plate under consideration is optimised.

At this point we can move on to the design of plates using Level I methods. The design wind pressure  $p_{w,d,\tau}$  is obtained from Eq. (4.28) for  $\tau = 10$  min, or from Eq. (4.29) for  $\tau = 3$  sec. It follows from the above that the factors  $c_{e1}$ ,  $c_e$ ,  $c_p$  and  $c_d$  are known, as are the other parameters (height of the construction, etc.) which play a role in the definition of the parameters.

The maximum stress value in the plate is obtained by placing the design wind pressure in Eq. (5.28). For elements in class II, the design pressure is obtained by multiplying  $p_{w,d,\tau}$  by the partial factor for actions  $\gamma_Q$ , hence  $\sigma_{\max,d,\tau} = S(\gamma_Q p_{w,d,\tau})$ . Assuming  $R_M = 1$  for second-class verifications, the factor  $\gamma_M$  for the material is calculated so that equality is satisfied in the inequality

$$\sigma_{\max,d,\tau} = S(\gamma_Q p_{w,d,\tau}) \leq \frac{k_{\text{mod},\tau} \lambda_{gA_{\text{test}} \rightarrow A}^{(air+tin)/2} f_{g,k}}{R_M \gamma_M}, \tag{5.31}$$

where  $\gamma_Q = 1.5$ , the factor  $k_{\text{mod},\tau}$  is defined in Table 2.2 (LEFM column) and the function of the nominal time of load application  $\tau$  established in Table 4.18. The characteristic strength value of the glass,  $f_{g,k}$ , is assumed to be 45 MPa, in accordance with the product standards set out in Table 2.4. With regard to the factor  $\lambda_{gA_{\text{test}} \rightarrow kA}^{(air+tin)/2}$ , by using the values in Table 5.3, from Eq. (5.27) we obtain the following value for the case in question:

$$\lambda_{gA_{\text{test}} \rightarrow kA}^{(air+tin)/2} = \frac{1}{2} \left[ \left( \frac{0.24 \text{ m}^2}{0.176 \cdot 1 \text{ m}^2} \right)^{1/m_{L,air}} + \left( \frac{0.24 \text{ m}^2}{0.138 \cdot 1 \text{ m}^2} \right)^{1/m_{L,tin}} \right] = 1.07, \tag{5.32}$$

This value holds for both  $t_L = 3$  sec and  $t_L = 10$  min.

For elements in class 1, the same equation is used. However, now, in accordance with Section 5.2.3,  $R_M$  is the factor which, by taking into account the statistical distribution of actions and resistances, suitably remodulates the value of the resistances so that it corresponds to different failure probabilities. The value of the factor  $R_M$  is calibrated in such a way as to obtain in Eq. (5.31) a value  $\gamma_M$  that is equal to the value obtained for second-class verifications. The values obtained for the case under consideration are summarised in Table 5.4.

Table 5.4. Verifications and partial coefficients for a plate subjected to wind action.

no	Class	Design wind pressure	Verification formula	Probabilistic performance function	$P_{f,1y}$	$T_R$	$R_M$	$\gamma_M$
1	2	$Q_{w,\max}$ ( $c_e$ )	$\sigma_{\max,d,3\text{sec}} \leq \frac{f_{g,k} \lambda_{gA_{\text{test}} \rightarrow kA}^{(air+tin)/2} (k_{\text{mod}} = 0.90)}{R_M \gamma_M}$	$f_{g(CDA;A_{\text{eff}};3\text{sec})}^{(air+tin)/2}$	$1.3 \times 10^{-6}$	50	1	2.52
2	2	$Q_{w,\text{av}}$ ( $c_{e1}$ )	$\sigma_{\max,d,10\text{min}} \leq \frac{f_{g,k} \lambda_{gA_{\text{test}} \rightarrow kA}^{(air+tin)/2} (k_{\text{mod}} = 0.65)}{R_M \gamma_M}$	$f_{g(CDA;A_{\text{eff}};10\text{min})}^{(air+tin)/2}$	$1.3 \times 10^{-6}$	50	1	2.46

3	1	$Q_{w,max}$ ( $c_e$ )	$\sigma_{max,d,3sec} \leq \frac{f_{g,k} \lambda_{gAtest \rightarrow kA}^{(air+tin)/2} (k_{mod} = 0.90)}{R_M \gamma_M}$	$f_{g(CDA;Aeff;3sec)}^{(air+tin)/2}$	$1.3 \times 10^{-5}$	50	0.696	2.52
4	1	$Q_{w,av}$ ( $c_{e1}$ )	$\sigma_{max,d,10min} \leq \frac{f_{g,k} \lambda_{gAtest \rightarrow kA}^{(air+tin)/2} (k_{mod} = 0.65)}{R_M \gamma_M}$	$f_{g(CDA;Aeff;10min)}^{(air+tin)/2}$	$1.3 \times 10^{-5}$	50	0.675	2.46

It should be observed, first of all that, the value of  $R_M$  thus obtained is in the order of 0.7. As has already been extensively illustrated, it is perhaps useful to point out at this point that in order to modify the failure probability, point B3.3 in EN 1990 prescribes the use of a multiplication factor  $K_{FI}$  of 0.9. This difference in values is due to the fact that the value recommended by EN 1990 has been essentially calibrated on Gaussian distributions for strength, while the distribution of strengths for glass is a Weibull distribution, with extremely dispersed data. As a result, even a small increase in the tolerated probability of failure may be associated with a significant decrease in design actions.

It should also be noted that the old 2009 edition of European draft standard PrEN 13474/3,<sup>11</sup> for structures which it improperly defined as secondary, and which here are deemed to be equivalent to structures in the class 1, recommends the value  $\gamma_M = 1.8$  and the value  $\gamma_Q = 1.5$ . These data are only apparently different from the data provided in Table 5.4. Indeed, ignoring geometric non-linearities, one has that  $S(\gamma_Q p_{w,d,\tau}) \cong \gamma_Q S(p_{w,d,\tau})$ . It is therefore clear from Eq. (5.31) that,  $f_{g,k}$  and  $k_{mod,\tau}$  remaining equal, what influences the design is the product  $a = \gamma_Q R_M \gamma_M$ . In PrEN 13474/3,  $a = 1.5 \times 1 \times 1.8 = 2.70$ , while for the data in Table 5.4,  $a = 0.696 \times 1.5 \times 2.52 = 2.63$  is obtained for case 3 (pressure peak), while  $a = 0.675 \times 1.5 \times 2.46 = 2.49$  for case 4 (average wind). In the case of linear-elastic behaviour, design using the old PrEN 13474/3 or the factors in Table 5.4 would not lead to any significant difference for elements in the class 1.

It is important to remark that the discussion here is based on probabilistic distributions obtained experimentally and on a damage model. The result for elements in the class 1 is in perfect agreement with the recommendations of prEN 13474/3 (2009), which was mainly based on experience and building traditions. More substantial differences are obtained, in contrast, in the design of elements in the second class, since for these structures factors of  $\gamma_M \cong 2.50$ , as against the value of  $\gamma_M = 1.8$  recommended by prEN13474/3 (2009), should be considered.

Finally, it must be remembered that prEn13474/3 (2009) does not take the scale effect into account, whereas the verification represented by Eq. (5.31) includes the factor  $\lambda_{gAtest \rightarrow kA}^{(air+tin)/2}$ , which for this case is greater than one.

### 5.3.3.2 Roof panel subject to snow loads

The procedure is analogous to the one illustrated in Section 5.3.3.1. From the relationship derived from the finite element model between the uniformly distributed load and the maximum tensile stress [ $\sigma_{max,q} = f(q) \Rightarrow q = g(\sigma_{max,q})$ ], it is possible to determine the statistical distribution of maximum stress on a plate subjected to snow loads. From the convolution integral between the probability density function of the maximum tensile stress in the plate subjected to snow loads and the cumulative distribution function for the glass fracture strength, it is possible to determine the failure probability of the plate subjected to snow loads. In the present case, an equivalent characteristic duration of the load is conventionally assumed to be 1 month.

Let us consider a monolithic 1000×1000×6 mm plate falling under the class 2 of reliability (CC2), corresponding to a target failure probability of  $1.301 \times 10^{-6}$ . The probabilistic model for the snow load is the one described in Section 4.6.2. In a first analysis, we set the snow load variation factor defined

<sup>11</sup> Until 2009 the draft standard prEN 13474 was divided into three parts (prEN 13474/1, prEN 13474/2 e prEN 13474/3). Since 2010 this distinction has been omitted.

in Eq. (4.33) at  $V = 0.2$ . Thus, altitude is varied until the value of  $P_f$  obtained with the convolution integral equals the target  $P_f$  value. Keeping height unchanged, the deterministic design procedure is carried out by varying the material safety factor until the maximum value admitted by the resistance verification is reached, which takes the following form:

$$\sigma_{\max,d,\tau} (\gamma_Q q_{s,d,\tau}) \leq \frac{k_{\text{mod},\tau} \cdot \lambda_{gA_{\text{test}} \rightarrow kA}^{(air+tin)/2} f_{g,k}}{R_M \gamma_M}, \quad (5.33)$$

where

- $q_{s,d,\tau}$  is the design snow load;
- $R_M = 1$  for second-class verifications
- $k_{\text{mod},\tau} = 0.388$  relative to a load application duration  $\tau = 1$  month.

In this case, as in Eq. (5.32), a value for the factor  $\lambda_{gA_{\text{test}} \rightarrow kA}^{(air+tin)/2}$  of the order of 1.07 is obtained.

The procedure has been repeated for the reliability class CC1, thus setting a target failure probability of  $1.335 \times 10^{-5}$ . The altitude above sea level is varied again until the value of  $P_f$  obtained is the same as the target  $P_f$  value. Keeping altitude unchanged, the deterministic design process is carried out by keeping the safety factor constant at the value derived for CC2, and thus deriving the maximum value for  $R_M$ , admitted by the resistance verification represented by Eq. (5.33).

The calculations were repeated in a similar way also for a variation factor of  $V=0.6$ . The results obtained are provided in Table 5.5.

Table 5.5. Verifications and partial factors for a plate subjected to snow loads. Results for a  $1000 \times 1000 \times 6$  mm plate.

No.	Class	V	Verification formula	Probabilistic performance function	$P_{f,1y}$	$T_R$	$R_M$	$\gamma_M$
1	2	0.2	$\sigma_{\max,d,1\text{month}} < \frac{f_{g,k} \cdot \lambda_{gA_{\text{test}} \rightarrow kA}^{(air+tin)/2} (k_{\text{mod}} = 0.388)}{R_M \gamma_M}$	$f_{g(CDA;Aeff;1\text{month})}^{(air+tin)/2}$	$1.3 \times 10^{-6}$	50	1	2.50
2	2	0.6	$\sigma_{\max,d,1\text{month}} < \frac{f_{g,k} \cdot \lambda_{gA_{\text{test}} \rightarrow kA}^{(air+tin)/2} (k_{\text{mod}} = 0.388)}{R_M \gamma_M}$	$f_{g(CDA;Aeff;1\text{month})}^{(air+tin)/2}$	$1.3 \times 10^{-6}$	50	1	2.30
3	1	0.2	$\sigma_{\max,d,1\text{month}} < \frac{f_{g,k} \cdot \lambda_{gA_{\text{test}} \rightarrow kA}^{(air+tin)/2} (k_{\text{mod}} = 0.388)}{R_M \gamma_M}$	$f_{g(CDA;Aeff;1\text{month})}^{(air+tin)/2}$	$1.3 \times 10^{-5}$	30	0.668	2.50
4	1	0.6	$\sigma_{\max,d,1\text{month}} < \frac{f_{g,k} \cdot \lambda_{gA_{\text{test}} \rightarrow kA}^{(air+tin)/2} (k_{\text{mod}} = 0.388)}{R_M \gamma_M}$	$f_{g(CDA;Aeff;1\text{month})}^{(air+tin)/2}$	$1.3 \times 10^{-5}$	30	0.674	2.30

It will be observed therefore that the condition  $V = 0.2$  is generally more conservative than the condition  $V = 0.6$ . The values of the factors thus obtained are comparable to those for wind actions, although they are slightly less restrictive. For elements in the class 1, in fact, we have  $a = \gamma_Q R_M \gamma_M = 0.668 \times 1.5 \times 2.50 = 2.505$  for  $V = 0.2$  (case 3) and  $a = 0.674 \times 1.5 \times 2.30 = 2.325$  for  $V = 0.6$ . The coefficients for wind action are therefore more conservative.

### 5.3.3.3 Walkable floors

The case study of a walkable glass floor finds typical applications in shopping malls and buildings open to the public in general, i.e. where people can gather. It is however unlikely to be suitable to bear the “permanent” variable load component as defined in Section 4.3.3. Indeed, glass floors are rarely used to bear the loads imposed by furniture or other furnishings which would diminish the value of their transparency. On the other hand, it is possible that a large number of people gather on the structure.

Therefore, with regard to the probabilistic model (Section 4.3.3), only the “discontinuous” component relating to the typical load of a shopping mall has been taken into account, assuming as a distributed load of 5 kN/m<sup>2</sup> for deterministic design.

From the relation derived from the finite element model for the plate between the uniformly distributed load and the maximum tensile stress [ $\sigma_{\max,q} = f(q) \Rightarrow q = g(\sigma_{\max,q})$ ], it is possible to derive the distribution of the maximum stress in the plate subjected to the variable load. From the convolution integral represented by Eq. (5.21) between the probability density function for maximum tensile stress in the plate subjected to the live load and the cumulative probability function for the ultimate tensile strength of the glass, the failure probability of the plate subjected to the live load can be found.

The methods by which the distribution function for the ultimate tensile strength of the glass is obtained are analogous to the ones relating the glass plate subjected to wind loads described in Section 5.3.3.1. In the case under consideration here, the load duration is assumed to be 12 hours.

In analysing this case study, as the load is fixed and no parameter is available to vary the design load (such as altitude in the case of snow), the geometry was changed until a design that led to a probability of failure, obtained with the convolution integral, close to the target value was achieved. Hence, by conducting the deterministic design on the plate, it was possible to vary the material partial safety factor until the limit value admitted by the resistance verification was reached.

Table 5.6 provides the parameters assumed for the probabilistic load model defined by Eq. (4.2) in Section 4.3.3, in accordance with [PMC Part 2, 2001]. The dimensions of the plate that achieves optimal design under design loads are 940 × 940 × 14mm. According to Eq. (5.27), such dimensions correspond to a value of the coefficient  $\lambda_{gA_{\text{test}} \rightarrow kA}^{(air+tin)/2}$  once again equal to approximately 1.07.

Table 5.6. Parameters which define the “discontinuous” component of live loads, as defined by [PMC Part 2, 2001].

Intended use	$A_0$ [m <sup>2</sup> ]	$\mu_q$ [kN/m <sup>2</sup> ]	$\sigma_{U,q}$ [kN/m <sup>2</sup> ]	$\lambda_q$ [years]	$D_q$ [days]
Shopping malls and markets susceptible to overcrowding	100	0.4	1.1	1.0	5

The verification is performed only for elements in the second class, because, as indicated in Table 3.9, the classification in the class 1 of elements whose failure may cause people to fall is not recommended. The values obtained from the case study are provided in Table 5.7. It should be noted that the order of magnitude of the factor  $\gamma_M$  thus obtained coincides in practice with the factors for wind action illustrated in Table 5.4, and snow loads as indicated in Table 5.5.

Table 5.7. Verifications and partial factors for a glass plate subjected to the action of human-induced live loads. Results for a 940 × 940 × 14 mm plate.

No.	Class	Verification formula	Probabilistic performance function	$P_{f,ly}$	$T_R$	$R_M$	$\gamma_M$

1	2	$\sigma_{\max, d, 12h} < \frac{f_{g,k} \cdot \lambda_{g/Atest \rightarrow k}^{(air+tin)/2} (k_{mod} = 0.501)}{R_M \gamma_M}$	$f_{g(CDA: Aeff; 12h)}^{(air+tin)/2}$	$1.3 \times 10^{-6}$	50	1	2.52
---	---	------------------------------------------------------------------------------------------------------------------------------	---------------------------------------	----------------------	----	---	------

In this case, too, the values are compatible with those found previously.

### 5.3.3.4 Fin of a façade

The case described here differs significantly from the other as it is a glass element in which the maximum tensile stresses are produced in proximity to the edge. Unfortunately, no experimental data for the specific strength of the edge are currently available, and even less is known about the corresponding fracture probability distribution curve. In fact, the mechanical strength of the edge of the plate (disregarding any chipping during handling or installation) is a consequence of edge finishing operations (cutting, grinding, etc.) and it is therefore wholly independent of defects on the surfaces of the plate. In general, any mechanical processes carried out on the surface produce homogeneous “damage” that tends to lower mean mechanical strength (low  $\sigma_0$ ) and reduce its dispersion (high Weibull coefficient  $m$ ).

In the absence of experimental data, the scope of this section is limited to indicating the procedure that should be followed for the calibration of the partial factors, once the statistical distribution of the resistances at the edge is known.

In the study case under consideration, a 450mm × 7000mm × 30mm fin consisting of 5 plates with a thickness of 6mm, simply supported at their extremities, forming part of a façade in which the fins, arranged at a centre-to-centre distance from each other of  $i_p = 1500$ mm, have the purpose of taking up the horizontal action caused by wind pressure  $p_w$ . In relation to this action, as was done with plates, it is necessary to conduct two verifications for peak winds with different characteristic times, i.e. 3 seconds and 10 minutes.

The maximum stresses that develop at the edge of the fin at midspan can be evaluated with the linear relationship between the bending moment and the maximum stress for a rectangular cross-section

$$\sigma_{\max} = \frac{M_{\max}}{W_x} = \frac{p_w \cdot i_p \cdot l^2}{8 \cdot W_x}, \tag{5.34}$$

where, with obvious meaning of the symbols,  $W_x$  represents the section modulus.

The probabilistic representation of the wind action is expressed by the same formulas described previously. The probabilistic representation of the *effect* of the action is given by the cumulative distributions function, the expression of which is obtained from Eq. (5.29), with

$$S^{-1}(x) = \frac{x \cdot W_x \cdot 8}{i_p \cdot l_p^2}. \tag{5.35}$$

Its derivative with respect to  $x$  furnishes the probability density function for the stresses  $f_{\sigma, pr. \tau}$ .

For a simply supported static scheme and given the load condition, in each ply that forms the fin the regions subject to tensile stress are one of the edges and the contiguous half of the two lateral faces. In the probabilistic analysis, the probability that failure occurs in this region was considered. It should nevertheless be noted that of the two faces of the plate, one is certainly the “tin side”, while the other is the “air side”, each one thus having a different statistical distribution of resistances.

With regard to edge strength, following [Sedlacek *et al.*, 1999], as also described in [Haldimann, 2006], this depends on the length of the edge itself, rather than on the area of the edge, as the critical point is the angle between the face and the edge. It is thus deemed that the cumulative probability of failure can be interpreted, in a similar way to Eq. (2.34), by a Weibull distribution of the form

$$P_{ed} = 1 - \exp \left[ - \int_l \left( \frac{\sigma(s)}{\sigma_{0,ed}} \right)^{m_{ed}} ds \right], \quad (5.36)$$

where  $m_{ed}$  and  $\sigma_{0,ed}$  represent the Weibull distribution parameters, while the integral is assumed to extend to the whole length of the tensile edge. Since the stress state on the edge is uniaxial, in this expression  $\sigma(s)$  represents the stress at the edge point with coordinate  $s$ , whose form is known from the boundary and load condition. Calibration of the distribution parameters must be based on a standardised test, about which, however, there is no unanimous agreement. [Sedlacek *et al.*, 1999] refers to a three-point bending test on beams of length  $l_{test} = 0.46$  m. Thus, assuming that stress is linear along the edge, Eq. (5.36) may be expressed in the following form, equivalent to Eq. (2.36):

$$P_{ed} = 1 - \exp \left[ - l_{eff.test} \left( \frac{\sigma_{max}}{\sigma_{0,ed}} \right)^{m_{ed}} \right], \quad l_{eff.test} = k_{l.test} l_{test}, \quad (5.37)$$

where  $l_{test}$  is the length of the edge for the reference test specimen ( $l_{test} = 0.46$  m), while  $l_{eff.test} = k_{l.test} l_{test}$  is its effective length. In this equation  $\sigma_{0,ed}$  is a parameter with the dimensions of a stress for a length raised to the power of the exponent  $1/m_{ed}$ .

With regard to the lateral surfaces, in the calculation procedure the effective area  $kA$  can be estimated for both “tin” and “air” side with the aid of finite element (shells) modelling of the fin; for each finite element the main surface stresses are calculated and, by applying the same procedure as the one described in Section 5.3.2, the factor  $k$ , which defines the effective area according to Eq. (5.19), is determined.

With regard to the edge, by substituting into Eq. (5.36) the expression for stresses in a beam layout with simple supports under uniform load, we obtain

$$P_{ed} = 1 - \exp \left[ - l_{eff.bp} \left( \frac{\sigma_{max}}{\sigma_{0,ed}} \right)^{m_{ed}} \right], \quad k_b = \frac{n \cdot \int_0^{l_p} \left[ \frac{P_w \cdot i_p \cdot s}{W_x} \frac{s}{2} (l_p - s) \right]^{m_{ed}} ds}{(\sigma_{max})^{m_{ed}} l_p}, \quad l_{eff.bp} = k_b l_p, \quad (5.38)$$

where:

$l_p$	fin span
$l_{eff.bp} = k_b l_p$	effective length of the fin edge
$s$	longitudinal coordinate of the fin
$n$	number of layers of glass forming the fin.

The following values were obtained from the calculation.

Effective area of “tin” side surfaces:

$$k_{tin} = 0.004793;$$

$$A_{eff.tin} = 5 l_p h_p k_{tin} = 0.075 \text{ m}^2;$$

Effective area of “air” side surfaces:



$$k_{\text{air}} = 0.007523;$$

$$A_{\text{eff.air}} = 5 l_p h_p k_{\text{air}} = 0.118 \text{ m}^2.$$

Obviously it is not possible to derive the effective length of the fin edge , as the factor  $m_{ed}$  is not known.

Once the effective areas are known, it is possible to derive the cumulative distribution function of resistances of the surfaces and the edge. For the two cases of lateral surface and the edge, the cumulative probability with regard to resistances can be expressed as follows:

$$F_{A_{\text{eff.tin}}}(x) = 1 - \exp \left[ -A_{\text{eff.tin}} \left( \frac{x}{\sigma_{0L.tin}} \right)^{m_{L.tin}} \right]; \quad (5.39)$$

$$F_{A_{\text{eff.air}}}(x) = 1 - \exp \left[ -A_{\text{eff.air}} \left( \frac{x}{\sigma_{0L.air}} \right)^{m_{L.air}} \right]; \quad (5.40)$$

$$F_{l_{\text{eff.bp}}}(x) = 1 - \exp \left[ -l_{\text{eff.bp}} \left( \frac{x}{\sigma_{0L.ed}} \right)^{m_{L.ed}} \right]. \quad (5.41)$$

In these equations, the values of  $\sigma_{0L.air}$ ,  $\sigma_{0L.tin}$ ,  $\sigma_{0L.ed}$  and of  $m_{L.air}$ ,  $m_{L.tin}$ ,  $m_{L.ed}$ , are the ones that are obtained by rescaling the values in Table 5.3 to take account of the duration of application of the load (in the case at hand, peak wind over 3 seconds or wind averaged over 10 minutes) through Eq. (5.13). As failure can occur in general due to the growth of a crack present on the lateral “tin” side surfaces, on the lateral “air” side surfaces or on the surface of the edge, in order to obtain the overall strength of the fin it is necessary to calculate the total probability function for the combination of the three functions (lateral air side surface, lateral tin side surface and edge), considered independent but *compatible*. Established theorems in probability theory thus give us

$$\begin{aligned} F_{\sigma_{tot,\tau}}(x) &= F_{A_{\text{eff.tin}}}(x) + F_{A_{\text{eff.air}}}(x) + F_{l_{\text{eff.bp}}}(x) \\ &- F_{A_{\text{eff.tin}}}(x) \cdot F_{A_{\text{eff.air}}}(x) - F_{A_{\text{eff.tin}}}(x) \cdot F_{l_{\text{eff.bp}}}(x) - F_{A_{\text{eff.air}}}(x) \cdot F_{l_{\text{eff.bp}}}(x) \\ &+ F_{A_{\text{eff.tin}}}(x) \cdot F_{A_{\text{eff.air}}}(x) \cdot F_{l_{\text{eff.bp}}}(x). \end{aligned} \quad (5.42)$$

Substituting Eqs. (5.39), (5.40) and (5.41) into (5.42) we obtain

$$F_{\sigma_{tot,\tau}}(x) = 1 - \exp \left[ -A_{\text{eff.tin}} \left( \frac{x}{\sigma_{0L.tin}} \right)^{m_{L.tin}} - A_{\text{eff.air}} \left( \frac{x}{\sigma_{0L.air}} \right)^{m_{L.air}} - l_{\text{eff.bp}} \left( \frac{x}{\sigma_{0L.ed}} \right)^{m_{L.ed}} \right]. \quad (5.43)$$

However, given that the critical element of a fin under bending is always the edge, the dominant term in this expression is probably the last term of the exponential relating to the edge itself. This affirmation must be confirmed by a careful experimental investigation. However, as implicitly suggested also in [Sedlacek *et al.*, 1999], Eq. (5.43) may be approximated with an expression such as

$$F_{\sigma_{tot},\tau}(x) \cong 1 - \exp \left[ -l_{eff.bp} \left( \frac{x}{\sigma_{0L.ed}} \right)^{m_{L.ed}} \right], \quad (5.44)$$

which significantly facilitates the analysis.

At this stage, operating as in the cases described previously, from the convolution integral of Eq. (5.21) between the probability density function for the stresses  $f_{\sigma,pr,\tau}$  and the cumulative distribution of the resistances  $F_{\sigma_{tot},\tau}$ , we obtain the failure probability of the glass fin subjected to wind action. As in the case described in Section 5.3.3.1, by placing in Eq. (5.29), with the position indicated in Eq. (5.35),  $v_{b50} = 30$  m/s,  $c_d = 1$  and  $c_p = 1.2$ , the altitude of the construction  $z$  is chosen so that, via Eqs. (4.19) and (4.25), we obtain values of the factors  $c_{e1}$  and  $c_e$  for which the integral (5.21) furnishes the probability  $P_{f,1y}$  that is equal to the target value  $P_{f,1y} = 1.301 \cdot 10^{-6}$  for elements in class 2. In fact, as a glass fin is generally placed in the class 2 (Table 3.9), the verifications are limited to this case.

Moving on to level I verifications, the design pressure  $p_{w,d,\tau}$  associated with  $P_{f,1y} = 1.301 \cdot 10^{-6}$  for  $\tau = 10$  min or for  $\tau = 3$  sec is used to derive the maximum stress  $\sigma_{max,d,\tau} = S(\gamma_Q p_{w,d,\tau})$ , with the partial factor for the actions  $\gamma = 1.5$ .

If  $R_M = 1$  (second-class verifications), the material factor  $\gamma_M$  is calculated so that equality is satisfied in the following inequality:

$$\sigma_{max,d,\tau} = S(\gamma_Q p_{w,d,\tau}) \leq \frac{k_{mod,\tau} \lambda_{gltest \rightarrow l} k_{ed} f_{g,k}}{R_M \gamma_M}. \quad (5.45)$$

In this expression,  $k_{mod,\tau}$  and  $f_{g,k}$  are defined in the same way as before. With regard to the scaling factor  $\lambda_{gltest \rightarrow l}$ , in the same way as in Section 5.2.5.2, it can be expressed by comparing Eq. (5.37) with Eq. (5.38), giving us

$$\lambda_{gltest \rightarrow l} = \left( \frac{l_{eff.test}}{l_{eff.bp}} \right)^{1/m_{ed}}. \quad (5.46)$$

The factor  $k_{ed}$  is the one that allows to go from the characteristic value  $f_{g,k}$ , obtained by means of a coaxial double ring bending test, to the characteristic edge strength value  $f_{g,k,ed}$ , obtained using the experimental test which generate the distribution represented by Eq. (5.37), so that

$$f_{g,k,ed} = k_{ed} f_{g,k}. \quad (5.47)$$

Two verifications must therefore be conducted: the first for peak gusts over  $\tau = 3$  sec, the second for wind averaged over  $\tau = 10$  min. We are still waiting for the experimental data that will allow these factors to be calibrated.

### 5.3.4 Critical issues in the calibration of partial factors

The lack of experimental data for characterising the strength of plate edges has already been highlighted with regard to the case study illustrated in Section 5.3.3.4. Here we shall refer to more general issues connected with the calibration of the partial factors as performed in Sections 5.3.3.1, 5.3.3.2, and 5.3.3.3.

First of all, it should be remembered that the statistical function for resistances used here has been calibrated on the basis of a relatively small number of tests. A more extensive campaign of experiments, including products from various manufacturers and countries, is necessary to achieve greater precision in the calibration of the material partial factors. From these data a “universal” probabilistic function will need to be found for both the tin side and the air side, to be used in the necessary analytical steps. Once this function is known, the characteristic value  $f_{g,k}$  of the statistic considered shall be added to the verification formula (5.22): this may be different from the nominal value currently established under product standards (see Table 2.4).

In the absence of these data, the values of the partial factors obtained from the case studies illustrated in Section 5.3.3 cannot be considered final, although they are indicative of the procedure to follow. In any case, it is pointed out that for structures in class 1, these factors are perfectly in line with those recommended in the 2009 version of the draft standard PrEN13474/3, based on experience and established practice.

Another uncertainty exists, however, related to the fact that the failure probabilities accepted in accordance with EN 1990 are very low (in the order of  $10^{-5}$  -  $10^{-6}$  in 50 years). The calibration of the material Weibull statistic is made on the basis of a number of experimental data that is much lower than would be necessary to estimate with precision the left-hand-side tail of the distribution. Since in convolution integrals such as Eq. (5.21) the largest contributions are found in proximity to the extreme tail of the cumulative function for resistances (Figure 5.7), the statistical model must be extrapolated on strength values that are usually much lower than the values measured experimentally. To verify the reliability of the cumulative function for strengths a campaign of experimental tests with tens of thousands tests would be required.

The partial factor calibration procedure carried out in Section 5.3.3 is expected in any case to be on the safe side. To illustrate this aspect, we refer to the experiments described in [Durchholtz *et al.*, 1995] on pristine glass plates and artificially damaged plates from various manufacturers. The campaign of experiments showed that the damaged plates, with extremely low mechanical strength, may be interpretable using less penalising Weibull statistics than those applied to pristine materials.

Each sample was tested in accordance with EN1288 with stress considered to be equibiaxial on an effective area  $A_{\text{test}} = 0.24 \text{ m}^2$ , or on an effective area  $A_{\text{test}} = 2.54 \text{ cm}^2$ . The experimental data were represented with a Weibull statistic in the following form:

$$P = 1 - \exp \left[ - \left( \frac{x}{\Theta} \right)^m \right], \quad (5.48)$$

where  $\Theta$  is derived experimentally (the values are provided in Table 5.8). The normalised parameters referred to the unit surface area are obtained by observing that the equibiaxial test gives  $A_{\text{eff}} = k A_{\text{test}} = A_{\text{test}}$  in Eq. (2.36), since  $k = 1$ . Equalising the probability functions

$$P = 1 - \exp \left[ - \left( \frac{x}{\Theta} \right)^m \right] = P = 1 - \exp \left[ - A_{\text{test}} \left( \frac{x}{\sigma_0} \right)^m \right], \quad (5.49)$$

we thus obtain the following correspondence:

$$\sigma_0 = (A_{\text{test}})^{1/m} \Theta. \quad (5.50)$$

Table 5.8 provides the Weibull parameters as defined above, in relation to several samples, each one consisting of around 30 test specimens, obtained from three different manufactures, both pristine (series LN1, LN2 and LN3) and with uniform, artificially impressed surface damage (series LN1d, LN2d and LN3d).

The same table provides the material partial factors  $\gamma_M$  and the reduction factors  $R_M$ , calculated using the same procedure as the one described in Section 5.3.3.1, in relation to peak wind pressure with a duration of 3 seconds. These factors are calculated in accordance with Eqs. (5.31) and (5.32).

Table 5.8. Weibull parameters for experiments by [Durchholtz *et al.*, 1995]. Factors  $R_M$  and  $\gamma_M$  calculated for the same case as Section 5.3.3.1 under peak wind pressure with a duration of 3 seconds.

Sample	$m$	$\Theta$	$A_{\text{test}}$	$\sigma_0$	$R_M$	$\gamma_M$
LN1	4	149 MPa	2.54 cm <sup>2</sup>	594.8 Mpa mm <sup>2/4</sup>	0.68	22.01
LN1d	23	47 MPa	2.54 cm <sup>2</sup>	59.8 Mpa mm <sup>2/23</sup>	0.90	1.685
LN2	4	133 MPa	2.54 cm <sup>2</sup>	530.9 Mpa mm <sup>2/4</sup>	0.70	23.18
LN2d	19	47 MPa	2.54 cm <sup>2</sup>	62.9 Mpa mm <sup>2/19</sup>	0.88	1.93
LN3	3	154 MPa	2.54 cm <sup>2</sup>	975.2 Mpa mm <sup>2/3</sup>	0.81	35.76
LN3d	22	47 MPa	2.54 cm <sup>2</sup>	60.5 Mpa mm <sup>2/22</sup>	0.89	1.73

To interpret these data, it should be noted that in the Weibull distribution the parameter  $m$  depends on the dispersion of the results: the higher the value of  $m$ , the less dispersed the results and vice versa. However, the factor  $\sigma_0$  is correlated with mean resistance values: the higher the value of  $\sigma_0$ , the higher the strength of the material “on average”. It can thus be seen from Table 5.8 that the damaged glass plates always exhibit much lower “average” resistances compared with pristine plates, but that the corresponding dispersion is far lower.

The data for the pristine materials however are *exceptionally* dispersed: indeed, for ordinary float glass, values for  $m$  in the order of 5-7 are commonly accepted in practice. These values are confirmed by the experimental results illustrated in Section 2.1.3. This anomalous dispersion value is probably due to the fact that these data are the result of tests conducted on small pieces (cut from a plate) and modest sample sizes (around 30 test pieces per sample): in this case the dispersion of the results may be due to having “hit upon” different types of defect which, belonging to a single plate, would have given a single result if it had been tested in its entirety. The assumption of applicability of Weibull statistics (including the scale effect) requires uniform defectiveness. However, on test areas that are too small, this assumption is not verifiable. Standard EN 1288 states that tests with a small double ring (EN1288-5, such as the one used by the authors of the article mentioned above) are to be used for comparative tests, but are not suitable for determining the strength of glass. Nevertheless, in purposely damaged glass plates, defectiveness may be assumed to be uniform even on small test areas. Therefore the data in Table 5.8 should only be considered in qualitative terms; they clearly indicate that damaged specimens can have much smaller dispersions than pristine specimens.

Thus, although the results shown in Table 5.8 cannot be considered fully representative, they may nevertheless suggest a number of observations at the qualitative level which will need to be examined more closely in future studies.

First of all, it will be observed that by using the data for the damaged samples, the partial factors are much lower than those for the undamaged samples. This would seem counterintuitive, as we would expect damage to have a detrimental effect. However, the following considerations should be made. The abrasion procedure used in [Durchholtz *et al.*, 1995] may have a beneficial effect, as it may “smooth” the surface, increasing the number of small defects, but reducing the characteristic size of the predominant defects.

In any case, it is clear from the analytical perspective that the partial factors so far calculated depend primarily on the parameter  $m$ . The values corresponding to  $m = 3$  or  $m = 4$  are much higher than the ones obtained in the case studies illustrated in Section 5.3.4, while those corresponding to  $m \cong 20$  are lower. This result is due to the convolution integral (5.21), which for low failure probabilities, such

as the ones sought, makes only the extreme tail of the cumulative distribution of resistances significant (Figure 5.7). In this region, what counts is the asymptotic nature of the distribution, i.e. the factor  $m$ . As this parameter interprets the dispersion of the results, it may be concluded that the extrapolation towards very low probabilities of failure is determined, first and foremost, by the dispersion of the results: the more dispersed the results, the higher the failure probability, leaving the other parameters unchanged. The Weibull coefficient  $\sigma_0$  is correlated with mean resistance values. However, this value is decisive in Eq. (5.21) only when relatively high failure probabilities are considered. With regard to low probabilities, for practical purposes only the parameter  $m$  counts.

Therefore, the factors  $\gamma_M$  so calculated penalise high dispersions in a decisive manner. It should be noted that if the target failure probability is increased – i.e. going from second-class to first-class verifications, the factor  $R_M$  is lower in pristine materials than in damaged materials. This is due to the fact that as the probability of failure increases, the parameter  $\sigma_0$  becomes increasingly important compared with  $m$ , because in the integral equation (5.21) the contributions of the central points in the cumulative distribution of resistances tend to assume greater importance.

The following issue thus remains unresolved. To what extent is it possible to extrapolate data relating to a theoretical Weibull distribution, calibrated on the basis of a limited number of experimental points? Specifically, by damaging the surface of a small number of elements, would it be possible to estimate the behaviour of the weakest elements in a much larger population?

At the present time it is not possible to provide an answer to these questions, nor can we estimate the number of damaged samples to be considered representative. From a purely heuristic perspective, in order to take this effect into account, a cumulative distributions of resistances might be considered in the integral equation (5.21) with the following form:

$$F_{\sigma,A,\tau}(x) = \begin{cases} F_{\sigma,A,\tau}^{damaged}(x), & \text{per } 0 < x \leq x_0, \\ F_{\sigma,A,\tau}^{(air+tin)/2}(x), & \text{per } x > x_0, \end{cases} \quad (5.51)$$

where  $F_{\sigma,A,\tau}^{damaged}(x)$  represents the cumulative function of strengths for damaged samples. The link variable  $x_0$  could be identified through the condition  $F_{\sigma,A,\tau}^{damaged}(x_0) = F_{\sigma,A,\tau}^{(air+tin)/2}(x_0)$ . At the current time, however, no certain data for damaged samples are available. Secondly, the plates should be damaged according to a standardised procedure which has not been defined yet. Thirdly, the effectiveness of Eq. (5.51) should be verified by drawing up data for a very large population sample, which is considered significant for the purpose of estimating very low failure probabilities.

In any case, the introduction of a second branch for the probabilistic distribution of strength for stresses lower than a value  $x_0$  may be a way of introducing a lower bound for short loading times on float glass. The low degree of dispersion of measured data for purposely damaged glass plates is not illustrative of the damage naturally caused to installed plates, where defectiveness is highly variable (glass plates with the same “life” generally exhibit quite different types and extents of damage). It is, however, indicative of the fact that mechanical strength does not appear to fall below a lower bound, which is significantly higher than would be expected from extrapolating the experimental data from pristine glass plates. This possibility needs to be verified by further studies. Nevertheless, the results obtained by extrapolating the data from the pristine test pieces, as in Section 5.3.3, would appear to be conservative. In fact, data from the literature on damaged specimens seem to confirm, albeit at a qualitative level, that an increase in surface defects reduces dispersion of the results.

Finally, it should be pointed out that glass develops surface damage over time, especially if exposed to atmospheric agents. For the reasons set out above, such damage does not appear to influence the

probability of failure as long as this is assumed to be extremely low, as the limits indicated in EN 1990. However, by increasing the target failure probabilities to levels of the order of  $10^{-3}$ , it will be necessary to take into account surface “ageing” of the glass, as at this level the average values in the population are significant compared with the extreme values. This consideration may be helpful in the calibration of partial factors for elements in class zero, as defined in Section 3.2.1, for which, as indicated in Section 3.2.3, a lower probability of failure than the limits established by EN 1990 is tolerated.

## 5.4 Correction factors

### 5.4.1 Influence of load area

Referring to Section 5.3.2, from the verification formula (5.22), considering the case of a plate with a generic area  $A$ , we obtain

$$\sigma_{\max,d,\tau} \leq \frac{k_{\text{mod},\tau} \lambda_{gA_{\text{test}} \rightarrow kA}^{(\text{air}+\text{tin})/2} f_{g,k}}{R_M \gamma_M}, \quad (5.52)$$

where

$$\lambda_{gA_{\text{test}} \rightarrow kA}^{(\text{air}+\text{tin})/2} = \frac{1}{2} \left[ \left( \frac{A_{\text{test}}}{k_{\text{air}} A} \right)^{1/m_{L,\text{air}}} + \left( \frac{A_{\text{test}}}{k_{\text{tin}} A} \right)^{1/m_{L,\text{tin}}} \right]. \quad (5.53)$$

The latter equation can be used to take account of the scale effect if an accurate evaluation is desired, after determining the effective areas  $k_{\text{air}} A$  and  $k_{\text{tin}} A$  for the case at hand. The factors  $k_{\text{air}}$  and  $k_{\text{tin}}$  can be calculated through Eq. (5.19).

It should be pointed out, however, that in practice, although the air side exhibits greater dispersion than the tin side ( $m_{L,\text{air}} < m_{L,\text{tin}}$ ), generally this effect is offset by the fact that the characteristic ultimate tensile strength for the air side is greater than for the tin side (see Table 2.8). In addition, for the effective areas encountered in the most pertinent practical cases, the factors  $m_{L,\text{air}}$  and  $m_{L,\text{tin}}$  are very close to each other and generally so high as to render the distinction made in Eq. (5.53) of relative importance. For the purpose of simplification, and in accordance with the indications provided by other technical standards (e.g. ASTM E1300-09a), as an initial approximation it is recommended that the value  $m_{L,\text{air}} \cong m_{L,\text{tin}} \cong 7$  be assumed in Eq. (5.53). We thus obtain

$$\lambda_{gA_{\text{test}} \rightarrow kA}^{(\text{air}+\text{tin})/2} \cong \left( \frac{A_{\text{test}}}{k A} \right)^{1/7} = \left( \frac{0.24 \text{ m}^2}{k A} \right)^{1/7}, \quad (5.54)$$

where the factor  $k$  is determined by considering  $m_L = 7$  in Eq. (5.19). Now, given the geometric non-linearity of the problem,  $k$  depends on the size of the plate and the extent of the loads as well as on the boundary conditions. In the paradigmatic case of a plate supported on 4 sides, as discussed in Section 5.3.3, a parametric analysis shows that the factor  $k$  decreases with increasingly slender plates as a result of second-order effects. In most cases, the upper limits of the value of  $k$  are obtained by disregarding the geometric non-linearity, that is, by conducting a linear-elastic analysis on the plate. Therefore, for the most common cases in the design practice relating to plates under bending, the factor  $k$  can be directly obtained from Table 7.5.

### 5.4.2 Influence of load duration

In order to take into account the phenomenon of static fatigue, the factor  $k_{\text{mod}}$  as defined in Section 2.1.1.2 is introduced. Its expression is given by Eq. (2.16). The values of  $k_{\text{mod}}$  for the most representative load durations are shown in the third column of Table 2.2.

### 5.4.3 Influence of edge finishing (plate edge and holes)

The effects of the edge finish on the mechanical strength of glass plates have already been discussed in Section 2.1.4. Naturally, this aspect is even more important when fractures propagate from the edge.

This effect can be taken into account by defining the reduction factor  $k_{ed}$  for the characteristic tensile stress when the maximum stress occurs on the edge, in agreement with Eq. (5.47).

To date, no systematic experimental test campaigns have been conducted to evaluate the factor  $k_{ed}$ . The values recommended by the ASTM standard are provided in Table 2.9, while other standards recommend a flat reduction in resistance of 20% (Table 2.10), as illustrated in Section 2.1.4.

The influence of the scale effect is defined by the factor  $\lambda_{g/\text{test} \rightarrow l}$  which, in accordance with Eq. (5.45), is more generally defined by an equation of the following type:

$$\lambda_{g/\text{test} \rightarrow l} = \left( \frac{l_{\text{eff},\text{test}}}{l_{\text{eff},b}} \right)^{1/m_{ed}} = \left( \frac{k_{l,\text{test}} l_{\text{test}}}{k_b l_b} \right)^{1/m_{ed}}, \quad (5.55)$$

where  $l_{\text{eff},b} = k_b l_b$  represents the effective length of the edge of the considered element.

With regard to the recommendations made in [Sedlacek *et al.*, 1999], the value  $m_{ed} = 5$  is suggested for polished edges, while  $m_{ed} = 12.5$  is suggested for ground edges. Using the expression (5.38)<sub>2</sub>, for  $m_{ed} = 12.5$ , we obtain values for  $k_b$  equal to 1 for the uniform stress distribution,  $k_b = 0.2434$  for parabolic distribution (symmetrical in relation to the centre line and zero at the extremities) and  $k_b = 0.0741$  for triangular distribution (symmetrical in relation to the centre line and zero at the extremities). For  $m_{ed} = 5$  we find  $k_b$  which is always equal to 1 for uniform stress distribution,  $k_b = 0.3694$  for parabolic distribution and  $k_b = 0.1667$  for triangular distribution. Therefore, with reference to the experiments of [Sedlacek *et al.*, 1999] in which the distribution of stresses in the test is triangular and  $l_{\text{test}} = 0.46$  m, we obtain

$$\text{polished edges:} \quad \lambda_{g/\text{test} \rightarrow l} = \left( \frac{0.1667 \cdot 0.45 \text{ m}}{k_b l_b} \right)^{1/5}, \quad (5.56)$$

$$\text{ground edges:} \quad \lambda_{g/\text{test} \rightarrow l} = \left( \frac{0.0741 \cdot 0.45 \text{ m}}{k_b l_b} \right)^{1/12.5}. \quad (5.57)$$

The values of  $k_b$  to consider are, respectively, those associated with  $m_{ed} = 5$  and  $m_{ed} = 12.5$ , while  $l_b$  represents the total length of the edge of the element under tensile stress. For elements such as beams or fins, the use of arrised edges is not recommended.

As already mentioned in Section 2.1.4, systematic experimental data and consistent guidelines are not currently available in the literature. In any case, it is recommended that a reduction in edge strength be taken into account, in accordance with the considerations contained in this section, for elements subjected to maximum tensile stress on the whole border, as may be the case in glass beams

or fines, while the scale effect defined by the factor  $\lambda_{gltest \rightarrow l}$  becomes of less importance for plates under bending.

#### 5.4.4 Influence of surface treatments

As described in Section 2.1.5, surface treatments applied to glass, such as sanding or acid etching, may decrease its mechanical strength. For statistical purposes, this effect may be taken into account by introducing the mechanical strength reduction factor  $k_{sf}$ , according to the definition which follows: in terms of probabilistic resistance, the effects of the stress  $\sigma_{max}$  in a pristine plate and the effects of the stress in the same plate with surface treatment

$$\sigma_{max,sf} = k_{sf} \sigma_{max} , \tag{5.58}$$

are equivalent.

Naturally the value of  $k_{sf}$  depends on the type of surface treatment, the level of edge finishing and any prestressing processes (thermal toughening or chemical strengthening). However, scarce experimental data concerning this aspect is currently available. For sanding or acid etching treatments, indicative values for the factor  $k_{sf}$  as deduced from the tests conducted by CEN-TC129/WG19 on 100 mm diameter float glass discs (Section 2.1.5) are provided in Table 2.11. Values derived from standard design practice for enamelled or patterned glass are provided in Chapter 7, Table 7.4.

### 5.5 Prestressed glass

#### 5.5.1 General remarks

As discussed in Section 2.1.1.3, in the case of prestressed glass the stress intensity factor at the apex of the cracks is not directly proportional to the acting stress  $\sigma_g$ , but also depends on the algebraic sum of  $\sigma_g$  and the self-equilibrating stresses induced by the tempering process. Sections 2.1.1.3.1 and 2.1.1.3.2 describe, respectively, the profile of the state of pre-compression induced in glass by thermal or chemical treatments: this verification could therefore be conducted at the micromechanical level, using the crack growth model described in Section 2.1.1.1.

In structural verifications, however, it is preferred to refer always to the macroscopic values of the stresses applied, which can be calculated through elastic modelling of the body. In Level III methods, taking  $Q_{d,\tau}$  to be the value of the generic action applied for the characteristic duration  $\tau$  and  $\sigma_{max,d,\tau} = S(\gamma_Q Q_{d,\tau})$  to be its effect in terms of maximum stress, the verification concludes with an inequality:

$$\sigma_{max,d,\tau} = S(\gamma_Q Q_{d,\tau}) \leq R_{d,pre} + R_{d,post} , \tag{5.59}$$

where  $R_{d,pre}$  is resistance due to the precompression induced on the surface by tempering, while  $R_{d,post}$  represents the additional resistance of the glass beyond decompression. The meaning of Eq. (5.59) is in agreement with the conclusions of Section 2.1.1.3: the failure mechanism of glass as a result of propagation of the dominant fracture is triggered only after the crack lips have been decompressed: the total resistance is given by the sum of the two effects.

Furthermore, from this perspective, the post-decompression resistance  $R_{d,post}$  is the same as the resistance measured for annealed glass in the absence of prestressing: its characterisation in probabilistic terms is thus the same as in Section 5.3.



The contribution of  $R_{d,pre}$  on the other hand is consequent upon a (thermal or chemical) tempering treatment induced by means of controlled procedures and in general associated with a different statistic in respect of the one used for annealed glass. In this regard it must be borne in mind that:

- the precompression state in the glass is generally uniform;
- the precompression value is not influenced by the type of face, i.e. whether tin or air side;
- no significant losses in precompression are observed over time (this is due to the very high relaxation time at temperatures below 300 °C);
- no effects which are dependent on the effective loaded area are observed;
- the state of precompression may be different in proximity to edges or holes.

In conclusion, for  $R_{d,pre}$  and  $R_{d,post}$  equations of the following type may be assumed:

$$R_{d,post} = \frac{k_{mod,\tau} f_{g,k}}{R_M \gamma_M}, \quad R_{d,pre} = \frac{(f_{b,k} - f_{g,k})}{R_{M;v} \gamma_{M;v}}, \quad (5.60)$$

where the meaning of the symbols with regard to  $R_{d,post}$  is the same as in Eq. (5.31), while in  $R_{d,pre}$ ,  $f_{b,k}$  indicates the characteristic ultimate tensile strength of prestressed glass, with  $\gamma_{M;v}$  being the value of the partial factor regarding precompression and  $R_{M;v}$  the correction factor for the step from second-class to first-class verifications.

It is pointed out that in the equation for  $R_{d,pre}$  the factor  $k_{mod}$  does not appear, since the state of prestressing is generally independent of the load application time. The self-equilibrating stresses however are significantly different in proximity to the edges (which does not necessarily correspond to a reduction): this effect must be taken into account with a correction factor analogous to  $k_{ed}$  in Section 5.4.3. Thus the factors  $k_{ed}$  and  $k'_{ed}$  can only be defined by means of a probabilistic calibration procedure analogous to the one adopted for the other factors.

## 5.5.2 Calibration of partial factors for prestressed glass

The factors  $\gamma_v$  and  $R_v$  in Eq. (5.60) for  $R_{d,pre}$  can be calibrated by evaluating, as in Section 5.3, the probability of failure with Level I methods for a number of paradigmatic cases. Specifically, the probability of failure in one year of service is derived by means of an equation analogous to Eq. (5.21), i.e.

$$P_{f,1y} = \int_{-\infty}^{+\infty} F_{\sigma,A,\tau}(x) \cdot f_{\sigma,pr,\tau}(x) \cdot dx, \quad (5.61)$$

where  $f_{\sigma,pr,\tau}$  represents the probability density of the effects of the actions while  $F_{\sigma,A,\tau}$  is the cumulative probability of obtaining failures for maximum stresses in the plate below the value  $x$ .

Having determined an optimal design which achieves the target failure probability for second-class verifications, the factor  $\gamma_{M;v}$  is calibrated so that equality is satisfied in the inequality, analogous to (5.31):

$$\sigma_{max,d,\tau} = S(\gamma_Q Q_{d,\tau}) \leq \frac{k_{mod,\tau} f_{g,k}}{R_M \gamma_M} + \frac{f_{b,k} - f_{g,k}}{R_{M;v} \gamma_{M;v}}, \quad (5.62)$$

where the values of  $k_{mod,\tau}$ ,  $f_{g,k}$ ,  $R_M$  and  $\gamma_M$  are the ones for float glass,  $\gamma_Q = 1.5$  and  $R_{M;v} = 1$  for second-class verifications. With regard to the characteristic ultimate tensile strength value of prestressed glass,  $f_{b,k}$ , the nominal values are provided in Table 2.4 for various treatments (heat-strengthened,

thermally toughened and chemically strengthened glass).

Subsequently, an optimal design in the class 1 which achieves the target failure probability is considered, and the value of  $R_{M,v}$  is determined which enables equality to be satisfied in the inequality in (5.31), considering the value of  $\gamma_{M,v}$  previously found.

Unfortunately, no systematic tests analogous to those conducted for annealed glass currently exist which allow an accurate statistical evaluation of the failure probability of prestressed glass. Pending further specific studies, calibration is performed on the basis of experience and established building traditions, with reference to current standards, in particular the recommendations of CEN-TC129/WG8.

Table 2 of the European draft standard prEN 16612 (2013) recommends for structures equivalent to first-class structures the value  $R_{M,v} \cdot \gamma_{M,v} = 1.2$ . As already noted at the end of Section 5.3.3.1, if geometric non-linearities are disregarded, the role of the factor  $R_M$  in structural verifications is analogous to that of the multiplication factor for actions introduced by EN1990 (point B3.3). In accordance with the value  $K_{FI} = 0.9$  recommended in EN1990, the value  $R_{M,v} = 0.9$  is therefore suggested for first-class verifications; the value  $\gamma_{M,v} = 1.2/0.9 = 1.33$  follows.

Rounding the aforementioned values, it is suggested that the factors  $\gamma_{M,v} = 1.35$  and  $R_{M,v} = 0.9$  be used for first-class verifications, assuming as usual  $R_{M,v} = 1$  for second-class verifications.

## 6 CALCULATION MODELS

### 6.1 General remarks

In general, the analysis of a structural problem by means of a calculation model requires the definition of the geometry, the constitutive model and the model for the structural analysis. Different degrees of accuracy may be chosen for each of these models.

The level of accuracy of the modelling process should be commensurate with the importance of the building, determined by various factors such as the economic cost of the construction and the structural use of the element, connected with the danger related to its failure.

The economic cost is differentiated according to whether replacement of the element does not create particular difficulties (because of the simplicity of the structure or because appropriate systems for replacement are incorporated since the design phase) or is particularly costly because of the geometry of the building (e.g. glazing installed at a great height or complexity of the fixing system).

The structural demands grow with the construction type of the element. The following is an illustrative list, in increasing order of importance:

- vertical and horizontal panels restrained on more than one side, with mechanical constraints;
- vertical and horizontal panels restrained on more than one side, with silicone joints;
- vertical and horizontal point-fixed glazing;
- vertical fins;
- horizontal beams;
- specific structures (e.g. glass-only frames, large-span structures, structures with complex joints, pillars, etc.).

The importance of the construction work is classified according to its importance class, as in Section 4.4.2.1, i.e. *Class I*: buildings with only occasional presence of people; *Class II*: buildings designed for normal crowd levels; *Class III*: buildings designed for significant crowd levels; *Class IV*: strategic buildings.

The level of risk in the event of failure depends on the performance and safety levels that the structure is able to guarantee following its collapse. Various levels of danger are recognised, depending on whether in the event of collapse:

- there are no significant consequences in terms of both serviceability and safeguarding of human life;
- serviceability is compromised;
- there is any risk of loss of human life.

If the potential collapse of the building entails serious risks to human life, post-glass-breakage performance shall be considered as in Section 3.1.4, with particular regard to seismic actions.

The minimum required procedures for modelling are defined in accordance with the structural demands of the construction work.

- For vertical and horizontal panels mechanically restrained on more than one side, the following procedures are required:
  - a) linear elastic analysis;
  - b) one- or two-dimensional structural analysis, depending on the type of constraints, with the Effective Thickness method, if the panel is made of laminated glass and if the constraint conditions allow to use this method (see Section 6.3.3);
  - c) non-linear geometric analysis, if the deflection is more than one half the total thickness of the plate.

- In the case of floors where failure may pose a threat to the physical safety of the occupants, unless experimental tests have been provided for, the post-glass-breakage behaviour of the glass must be analysed.
  - For vertical and horizontal panels restrained on more than one side with silicone joints, the following procedures are required:
    - a) linear-elastic analysis;
    - b) one- or two-dimensional analysis, depending on the type of constraints, with the Effective Thickness method, if the panel is made of laminated glass and if the constraint conditions allow to use this method (see Section 6.3.3);
    - c) non-linear geometric analysis, if the deflection is less than one half the total thickness of the plate.
    - d) For the modelling of the adhesive joint, associated with the specific characteristics of silicone, see Section 6.2.4.
  - For point-fixed vertical glazing, the following procedures are required:
    - a) for calculation of the stress at points distant from the restraints, an analysis with linear-elastic models, or, eventually, with geometric non-linearities and with the Effective Thickness method if the panel is made of laminated glass (see Section 6.3) and point-fixed, with plate/shell modelling;
    - b) evaluation of the stress concentrations in proximity to the constraints, in the absence of specific manufacturer certification of the point-fixing system, using a three-dimensional model with linear-elastic behavior of the components and with elastic parameters calibrated according to the service temperature and load duration. An alternative is two-dimensional modelling, by using a dedicated multilayered element (Section 6.3.3.2).
  - For horizontal point-fixed glass plates, in addition to the procedures for vertical glass panes, if danger for people is present and no post-breakage experiments have been performed, the behaviour of the glass plate after partial or total breakage must be modelled.
  - For vertical fins, the following procedures are required:
    - a) Two-dimensional elastic modelling, accounting for the geometric non-linearities, with particular attention to the problems of shell instability;
    - b) evaluation of stress concentrations around holes or intermediate joints, in the absence of specific manufacturer certification of the fixing system, using a three-dimensional model with linear-elastic modelling of the component and with elastic parameters calibrated according to the service temperature and duration of loads. An alternative to three-dimensional modelling is two-dimensional modelling using a dedicated multilayered element (Section 6.3.3.2).
  - For horizontal beams, the following procedures are required:
    - a) one- or two-dimensional non-linear geometrical elastic modelling, with particular attention to instability phenomena;
    - b) evaluation of stress concentrations around holes or intermediate joints, in the absence of specific manufacturer certification of the fixing system, using a three-dimensional model with linear-elastic modelling of the components and with elastic parameters calibrated according to the service temperature and duration of loads. An alternative to three-dimensional modelling is two-dimensional modelling using a dedicated multilayered element (Section 6.3.3.2).
-

In the absence of specific post-glass-breakage tests, the behaviour after partial or total glass breakage must be modelled.

- For specific structures (e.g. glass-only frames, large-span structures, structures with complex joints, pillars, etc.), suitably reliable models should be considered on a case-by-case basis.

## 6.2 Modelling of materials

### 6.2.1 Glass

Float glass, for temperatures below 300-400°C, can be modelled as a linear-elastic material. The values of the mechanical characteristics that define its behaviour, product by product, and their variability owing to factors connected with the manufacturing process, can be obtained from the following product standards (see Chapter 2): UNI EN 572-1, UNI EN 1748-1-1, UNI EN 1748-2-1, UNI EN 1863-1, UNI EN 12150-1, UNI EN 12337-1, UNI EN ISO 12543-1, UNI EN 13024-1, UNI EN 14178-1, UNI EN 14179-1, UNI EN 14321-1.

The mechanical characteristics of the material can vary, according to Table 2.1. However, when the modelling process does not require absolute precision, the following values can be assumed:

- |                                             |                                            |
|---------------------------------------------|--------------------------------------------|
| • modulus of elasticity (Young's modulus)   | $E = 70000 \text{ MPa}$                    |
| • Poisson's ratio                           | $\nu = 0.22$                               |
| • density                                   | $\rho = 2500 \text{ kg/m}^3$               |
| • thermal expansion coefficient at 20-300°C | $\alpha = 9 \times 10^{-6} \text{ K}^{-1}$ |

Linear elasticity for glass can be assumed for any “level of accuracy” chosen for the analysis of the considered structure.

### 6.2.2 Polymers for interlayers

In the case of laminated glass elements, the plates are connected by a polymeric interlayer. For architectural applications, the most commonly used materials are:

- Polyvinyl butyral (PVB);
- ionoplastics (e.g. SG®);
- ethylene-vinyl acetate (EVA);
- polyurethane (PU).

Unlike glass, the constitutive response of these interlayer materials is generally not linear and is heavily influenced by factors such as service temperature and conditions (duration) of load (see Section 2.2.1), as the graphs in Figure 6.1 make clear.

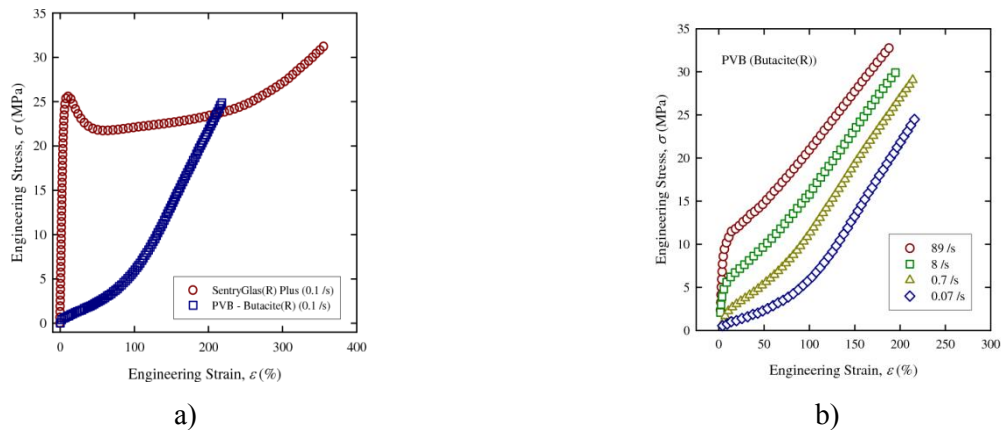


Figure 6.1. Stress-strain diagrams: a) SG<sup>®</sup>-PVB comparison at  $T=20^{\circ}\text{C}$ ; b) comparison between tests conducted on PVB at the same temperature and at different loading speeds

For this reason, modelling of the mechanical properties of the interlayer may be performed according to different levels:

- level *a*: model with effective thickness;
- level *b*: linear-elastic model, with constant elastic parameters;
- level *c*: linear viscoelastic model;
- level *d*: non-linear models.

Tests for determination of the mechanical properties of polymeric interlayer and the experimental data interpretation must be performed in accordance with product standards EN ISO 6721-1, ISO 6721-4 and ISO CD 6721-11, as already defined in Section 2.2.1.3.

### 6.2.2.1 Level *a*: effective thickness models (shear transfer coefficient)

Level *a* models may be used only in the case of flat plates under bending, with load applied orthogonally to the mid-plane, under continuous constraint conditions (plate without holes and not point-fixed).

These methods provide, in general, for the definition of the *effective thicknesses for the calculation of stresses and deflections*, i.e., the thickness of the monolithic beam which exhibits the same behaviour in terms of stress and deflection respectively, of the laminated beam under examination, thus incorporating within it the effect of the shear coupling offered by the interlayer.

The effective thickness may be determined using a *shear transfer coefficient*, which guarantees an adequate estimate of the actual transfer of the shear actions between the plates on the part of the interlayer. In defining it, therefore, we must take into account aspects strictly linked to the mechanical characteristics of the polymeric interlayer, the geometry (thicknesses, size, restraints, etc.) of the problem under consideration, and the type of load applied (distributed or concentrated loads, of long or short duration, etc.). With changes in polymeric material, loads, geometry and composition of the laminated package, the shear transfer coefficient may assume a value of between 1, indicating perfect shear transfer and overall behaviour of the laminate comparable to that of a monolithic glass plate of equivalent thickness (monolithic limit), and 0, indicating that the polymer does not transfer any shear actions (layered limit).

Once the equivalent thicknesses have been defined, design and verification of laminated glass plates is performed by means of two-dimensional analyses, by considering an equivalent monolithic glass plate.

In this simplified model, the viscoelastic polymeric interlayer is modelled as a linear-elastic material. Specifically, the shear modulus  $G$ , which generally varies according to the service temperature, the

duration of application of loads and ageing of the polymer, is assumed to be constant and equal to the secant modulus for the characteristic duration of the applied loads.

#### **6.2.2.2 Level *b*: linear elastic models**

In this model, the elastic parameters of the material are assumed to be constant during the analysis. The choice of the Young's modulus and of Poisson's ratio (and, consequently, of the shear modulus) for the interlayer must in any case depend upon the service temperature and the duration of application of design loads.

For the mechanical characteristics of polymers, reference must be made to the experimental data provided by manufacturers or by consolidated technical literature. The experimental tests and interpretation of the results must in any case follow the instructions provided in Section 2.2.1.

The choice of the parameters characterising the mechanical behaviour of the material must take into consideration not only the most unfavourable service conditions (temperature and duration of loads) but also the phenomenon of ageing, which may be caused by water absorption (humidity, solvents and cleaning agents) and exposure to ultra-violet rays.

Any concomitant loads of different duration, acting on the same plate, must be duly taken into account.

#### **6.2.2.3 Level *c*: linear viscoelastic models**

The service temperature and the duration of design loads play a fundamental role both in the global behaviour of plates under bending and in the local behaviour, with regard to the fixing system. In the case of moderate strains ( $\varepsilon < 1\%$ ) the behaviour of polymeric materials may be schematised with the classical linear viscoelastic model. This assumption may be considered valid for all standard architectural applications. Nevertheless, particular attention must be given to the modelling of material and to verifying that the assumption of small deformations is respected also in zones of high stress concentrations, which may be caused by abrupt changes in geometry, concentrated loads and the presence of "point-localised" restraints. This type of modelling is useful if thermoviscoelastic analysis is conducted, i.e., if the variability of the mechanical characteristics of materials with changes in temperature and load durations is taken into account.

In the case of linear viscoelasticity, the different material constitutive laws may be obtained by using simplified models consisting of ideal springs and dashpots combined in series (Maxwell model) or in parallel (Kelvin-Voigt model). Depending of the number and ways in which these elements are placed in correlation, the various aspects of the mechanical response of the material (e.g. viscosity and relaxation) can be adequately represented.

A particularly suitable model for describing the behaviour of a polymer is the Wiechert model, which consists of  $n$  Maxwell elements (spring and dashpot in series) connected in parallel with an elastic spring. The model, illustrated in Figure 6.2, consists of an elastic element (characterised by a shear modulus  $k_\infty$ , correspondent to the rubber state) placed in parallel with a series of Maxwell elements, each consisting of an elastic element (of modulus  $k_i$ ) and a dashpot (with viscosity  $\eta_i$ ).

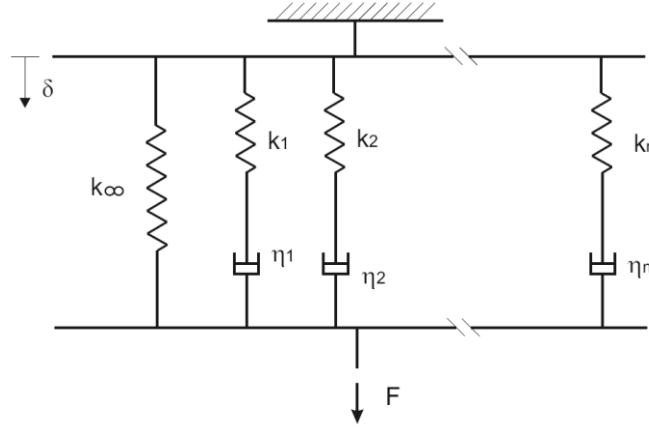


Figure 6.2. Schematic diagram of the Wiechert model.

The resulting constitutive equations are differential equations of the type

$$\eta_i \dot{\varepsilon}_{vi} = k_i (\varepsilon - \varepsilon_{vi}) \Rightarrow \dot{\varepsilon}_{vi} + \frac{1}{\tau_i} \varepsilon_{vi} = \frac{1}{\tau_i} \varepsilon, \quad \tau_i = \frac{\eta_i}{k_i}, \quad i = 1, 2, \dots, n, \quad (6.1)$$

where  $\varepsilon$  is the total strain,  $n$  is the number of Maxwell elements connected in parallel,  $\varepsilon_{vi}$  is the strain due to the dashpot in the  $i^{\text{th}}$  Maxwell element,  $\tau_i = \eta_i/k_i$ . The physical meaning of the characteristic relaxation time  $\tau_i$  becomes clear when the behaviour of the material is modelled by using a single Maxwell element, consisting of a spring (with stiffness  $k$ ) and a dashpot (with viscosity  $\eta$ ) in series; in this case  $\tau = \eta/k$  and can be defined as the time necessary for the stress to diminish during a stress relaxation test until it reaches a value which is  $1/e$  times its initial value, where  $e$  is Napier's constant. The viscoelastic modulus of the material  $k(t)$ , defined as the ratio between the applied total force and the displacement of the entire element, can therefore be expressed as a function of time as

$$k(t) = k_\infty + \sum_{i=1}^n k_i e^{-t/\tau_i}. \quad (6.2)$$

Generally it is assumed that the viscous response of the polymer is linear, i.e., that the Boltzmann superposition principle is valid. According to this principle, the response of the material at time  $t$  can be obtained through the integral equation

$$\sigma_{ij}(t) = \int_0^t 2G(t-\xi) \frac{d(\varepsilon_{ij}(\xi) - \frac{1}{3} \delta_{ij} \theta(\xi))}{d\xi} d\xi + \int_0^t K(t-\xi) \delta_{ij} \frac{d\theta(\xi)}{d\xi} d\xi, \quad (6.3)$$

where  $\sigma_{ij}$  are the components of the Cauchy stress tensor,  $\varepsilon_{ij}$  the components of the infinitesimal strain tensor,  $\theta = \varepsilon_{11} + \varepsilon_{22} + \varepsilon_{33}$  is the first invariant of the strain tensor and  $\delta_{ij}$  is the Kronecker delta. The functions  $G(\tau)$  and  $K(\tau)$  represent the shear relaxation modulus and the bulk relaxation modulus of the material. Generally, the bulk modulus is higher and exhibits a much lower dependence on time than the shear relaxation modulus. In practice, the contribution of the strain components connected with change in volume (incompressibility of material) can be neglected, or, at least,  $K(\tau)$  can be assumed to be constant, thus significantly simplifying the analysis. In this case, the stress component variable over time due to the viscosity, which can be expressed by means of a Prony series as shown in Eq. (6.2), is only the deviatoric component.



The shear relaxation modulus may therefore be represented as a function of time  $\tau$  in the form of a Prony series

$$G(\tau) = G_{\infty} + \sum_{i=1}^n G_i e^{-\tau/\tau_i}, \quad (6.4)$$

where  $\tau_i = \eta_i/G_i$  represents the characteristic time of the  $i^{\text{th}}$  Maxwell element.

For the sake of illustration, Table 6.1 provides the values of  $G_i$  and  $\tau_i$  at  $T=20^{\circ}$  for standard PVB supplied by two of the largest manufacturers on the market. From the table it is clear that the data proposed may be given with various orders of approximation, and that materials in the same category may exhibit significantly different viscoelastic behaviours. Moreover, viscoelastic behaviour may also depend on lamination parameters, such as autoclave temperature and pressure.

Table 6.1. Terms of Prony series at  $T = 20^{\circ}\text{C}$ , for two different commercially available PVB types.

Term no.	PVB type A		PVB type B	
	$G_i/G_{\infty}$ ( $G_{\infty} = 471 \text{ MPa}$ )	$\tau_i$	$G_i/G_{\infty}$ ( $G_{\infty} = 146.12 \text{ MPa}$ )	$\tau_i$
1	0.160600	$3.2557 \cdot 10^{-11}$	0.01550	$1.0 \cdot 10^{-5}$
2	0.0787770	$4.9491 \cdot 10^{-9}$	0.1727	$1.0 \cdot 10^{-4}$
3	0.2912000	$7.2427 \cdot 10^{-8}$	0.2111	$1.0 \cdot 10^{-3}$
4	0.0711550	$9.8635 \cdot 10^{-6}$	0.2684	$1.0 \cdot 10^{-2}$
5	0.2688000	$2.8059 \cdot 10^{-3}$	0.1988	$1.0 \cdot 10^{-1}$
6	0.0895860	$1.6441 \cdot 10^{-1}$	0.0974	$1.0 \cdot 10^0$
7	0.0301830	$2.2648 \cdot 10^0$	0.0254	$1.0 \cdot 10^1$
8	0.0076056	$3.5364 \cdot 10^1$	0.00508	$1.0 \cdot 10^2$
9	0.0009634	$9.3675 \cdot 10^3$	0.00114	$1.0 \cdot 10^3$
10	0.0004059	$6.4141 \cdot 10^5$	0.000485	$1.0 \cdot 10^4$
11	0.0006143	$4.1347 \cdot 10^7$	0.000554	$1.0 \cdot 10^5$
12			0.000752	$1.0 \cdot 10^6$
13			0.00070	$1.0 \cdot 10^7$
14			0.000985	$1.0 \cdot 10^8$

In general the function  $G(\tau)$  is highly dependent on temperature. Therefore, for each material, the relaxation function  $G(T_{ref}, \tau)$  must be known at the reference temperature  $T_{ref}$ . The graph representing  $G(T_{ref}, \tau)$  as a function of  $\log(\tau)$  is usually denoted to as *master curve* (Section 2.2.1.4). This may be defined by the manufacturer of the polymer, providing the values of the coefficients  $G_i(T_{ref})$  and  $\tau_i(T_{ref})$ , which represent the shear modulus and the characteristic time of the  $i^{\text{th}}$  Maxwell element in the Wiechert model at the reference temperature. Alternatively, the master curve must be determined experimentally.

The behaviour of the material at different temperatures  $T$  may be derived by appropriately translating the master curve relating to the reference temperature ( $T_{ref}$ ) by means of an appropriate shift function,  $a_T$ , through an equation of the following type:

$$G(T, e^{\log(\tau)}) = G(T_{ref}, e^{\log(\tau) - \log(a_T)}) \Rightarrow G(T, \tau) = G(T_{ref}, \tau / a_T) \quad (6.5)$$

which allows to derive the relaxation modulus  $G(T, \tau)$  at temperature  $T$  starting from the known master curve  $G(T_{ref}, \tau)$ . Relationship (6.5) shows that the relaxation modulus at the generic temperature  $T$  can be inferred from the master curve for the reference temperature  $T_{ref}$  by considering, instead of

the actual time  $\tau$ , the reduced time  $\tau^* = \tau/a_T$ . If the temperature is variable, i.e.  $a_T = a_T(T(\tau))$ , the reduced time  $\tau^*$  and the current time  $\tau$  are related one to each other by the shift factor through the equation

$$\tau^* = \int_0^\tau \frac{dt}{a_T(T(t))}. \quad (6.6)$$

For “thermorheologically simple” polymer materials, an assumption that can generally be made for currently commercially-available interlayers, it is standard practice to use the Williams-Landel-Ferry (WLF) equation to define  $a_T$ . This provides a good correspondence for the shift function  $a_T$  within a temperature range between the reference temperature  $T_{ref}$  and  $T_{ref} + 200$  °K, through the equation

$$\log(a_T) = -\frac{C_1 \cdot (T - T_{ref})}{C_2 + T - T_{ref}}, \quad (6.7)$$

where  $T \neq T_{ref}$  [°C] is the considered temperature, and  $C_1$  and  $C_2$  are constants dependent on the material (as defined by the manufacturer or obtained experimentally). If the reference temperature is chosen to be equal to the glass transition temperature  $T_g$  of the interlayer, the two constants assume absolute values, independent of the material and applicable to a vast range of polymers, i.e.

$$\log a_T = \frac{-17.44(T - T_g)}{51.6 + (T - T_g)}, \quad (6.8)$$

where temperature  $T$  must be expressed in degrees Celsius. In applying this equation, it should be noticed that a singularity exists for values of  $T = T_g - 51.6$ °C.

It may be remarked from Eqs. (6.7) and (6.8) that  $a_T$  decreases as  $T$  increases. From Eq. (6.5) it can thus be observed that as  $T$  increases, the times required to obtain the same decline of the elastic modulus become shorter, i.e. the viscous effect increases.

Thus, having defined the master curve for a polymer by means of a Prony series, the Boltzmann integral equation, which defines the components of the deviatoric part of stress  $S_{ij}$  as functions of the components of the deviatoric strain  $e_{ij}$  (it is possible to operate on the bulk part in a similar way), from Eq. (6.3) can be written in the following form:

$$S_{ij}(t) = \int_0^t 2 \left( G_\infty + \sum_{k=1}^n G_k e^{-\frac{t-\xi}{a_T \tau_k}} \right) \frac{de_{ij}(\xi)}{d\xi} d\xi. \quad (6.9)$$

By introducing the reduced time  $t^* = t/a_T$ ,  $\xi^* = \xi/a_T$ , it is possible to obtain the general equation

$$S_{ij}(t^*) = \int_0^{t^*} 2 \left( G_\infty + \sum_{k=1}^n G_k e^{-\frac{t^*-\xi^*}{\tau_k}} \right) \frac{de_{ij}(\xi^*)}{d\xi^*} d\xi^* = 2G_0 \left( e_{ij}(t^*) - \sum_{k=1}^n \alpha_k \varepsilon_{ij}^k(t^*) \right), \quad (6.10)$$

where

$G_0 = G_\infty + \sum_{k=1}^n G_k$  is the instantaneous shear modulus

$\alpha_k = G_k/G_0$ ,

$\varepsilon_{ij}^k(t^*) = \int_0^{t^*} \left( 1 - e^{-\frac{(t^*-\xi)}{\tau_k}} \right) \frac{d e_{ij}(\xi)}{d\xi} d\xi$  represents the viscous component of the strains present in each term

of the series.

In order to numerically integrate this equation in a finite time interval, it may be assumed that the strain linearly varies with  $t^*$ , enabling  $d e_{ij}/d\xi^*$  to be substituted with  $\Delta e_{ij}/\Delta \xi^*$ . Thus, it is possible to obtain a finite-difference equation which provides the variation of the viscous deformation in the  $i^{\text{th}}$  Maxwell element  $\Delta \varepsilon_i$  during the  $i^{\text{th}}$  time interval and, therefore, the increase in stresses in the form

$$\Delta S_{ij} = 2G_0 \left( \Delta e_{ij} - \sum_{k=1}^n \alpha_k \Delta \varepsilon_{ij}^k \right). \tag{6.11}$$

It is thus possible to explicit the value of the reduced time as a function of the actual time using the shift factor  $a_T(T)$ , calculated by means of the WLF equation. In the general case in which temperature also varies with time, at each integration step the log function  $a_T(T)$  can be approximated by a linear function of temperature along the time interval obtaining:

$$\log a_T^{(h+1)} - \log a_T^{(h)} = \frac{1}{a_T^{(h)}} (T^{(h+1)} - T^{(h)}) . \tag{6.12}$$

In this case,  $a_T$  is a function of time and, therefore, the integration must be performed directly on Eq. (6.9).

#### 6.2.2.4 Level d: non-linear models

These models may be used in the case of finite strains. Generally these conditions arise in the case of post-failure analyses when the loads are sustained by the interlayer only, stiffened by fragments of broken glass.

Any non-linear formulation (Mooney-Rivlin [Mooney, 1940; Rivlin, 1948], Neo-Hookean [Ciarlet, 1988], Arruda-Boyce [Arruda & Boyce, 1993]) used in calculation for modelling the polymeric interlayers must be justified and validated by appropriate experimental tests, given the lack of an adequate established literature on the subject. For these models, the reader is referred to Section 6.2.4.4.

### 6.2.3 Other plastic materials used in combination with glass

In certain specific applications, laminated glass elements consisting of both glass plates and plates of plastic material connected by resins or polymeric interlayers are used. The most commonly used materials for plastic plates are polycarbonate, acrylic and, recently, transparent silicones.

The modelling of laminated glass with interlayers obtained from these materials is carried out in an analogous manner to the procedure described in Section 6.2.2 for polymer interlayers. The manufacturer must provide the necessary coefficients for the constitutive modelling of the interlayer or, if they are not available, they shall obtain them experimentally.

### 6.2.4 Silicone

Silicone can have two functions:

- sealant, as in the example illustrated in Figure 6.3;
- structural (Figure 6.4).

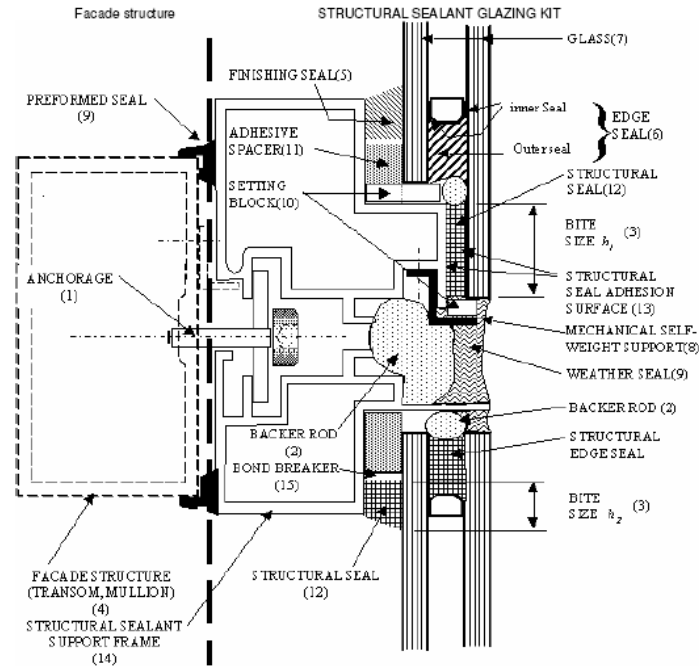


Figure 6.3. Example of silicone joints [ETAG 002 - Part 1].

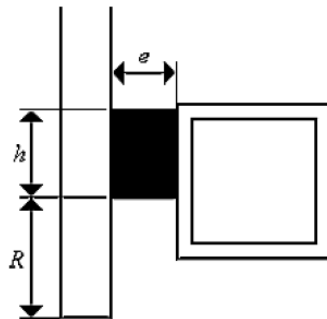


Figure 6.4. Reference dimensions for a structural silicone joint [EN 13022-2:2006, Part 2].

The *structural* function of silicone allows to obtain the connection between the glass and the support element. For glass panels, the resulting constraint condition must be appropriately defined on a case-by-case basis.

In order to simulate the constraint given by the silicone, different levels of modelling are admitted:

- level 0: replacement with an equivalent restraint;
- level 1: linear elastic model, with constant, separate elastic parameters;
- level 2: linear elastic model, with constant, continuous elastic parameters;
- level 3: non-linear models.

### 6.2.4.1 Level 0: replacement with an equivalent constraint

The presence of the silicone itself – as a material with its own mechanical properties – is neglected, and only its function as a constraint for the glass is considered. This constraint is assumed to be fixed, and modelled in most cases as an ideal hinge.

### 6.2.4.2 Level 1: linear elastic model, with constant uncoupled elastic parameters

In this case, in order to respect the validity of the linear model itself, *a posteriori* verification of the strains is required. The strain limit must comply with the specifications declared by the manufacturer. In the absence of precise data, a conventional elastic deformation limit of approximately  $\varepsilon_{el} = 12.5\%$  can be assumed for most of the structural silicones.

By representing the joint with equivalent springs, it is necessary to discretise the continuous elastic element of the joint into an adequate number of elementary springs, each one corresponding to a portion  $A_k$  of the bond area:

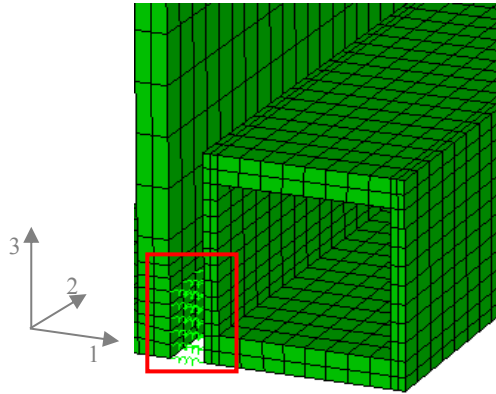


Figure 6.5. Example of modelling of a silicone joint by means of equivalent springs.

The response in the various directions is supposed to be uncoupled, so that each spring must be schematised with three stiffness parameters  $k$ :

- $k_1$  tensile;
- $k_2$  shear, longitudinal to joint;
- $k_3$  shear, transversal to joint.

As an initial approximation, the spring stiffness parameters may be calculated as

$$k_j = c_j \frac{A_k}{s} \quad , \quad (6.13)$$

where:

- $c_j$  stiffness of silicone in the considered direction  $j$ , in accordance with the manufacturer's specifications [ $\text{N}/\text{mm}^2$ ];
- $A_k$  area of influence for a spring [ $\text{mm}^2$ ];
- $s$  thickness of the joint [ $\text{mm}$ ].

### 6.2.4.3 Level 2: linear elastic model, with constant, continuous elastic parameters

In this case, too, *a posteriori* verification of strains is required, as already indicated for “level 1” models. At this level, three-dimensional finite element analysis may be performed, simply by using the elastic constants of the silicone as material parameters for the numeric model.

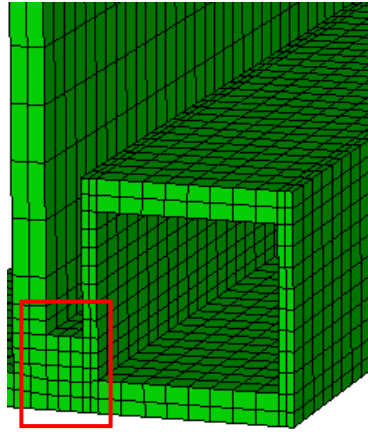


Figure 6.6. Example of modelling of a silicone joint by means of solid elements.

It is important to discretize the silicone joint by using more than one layer of finite elements, since a single layer would generally lead to overestimation of the stiffness of the joint itself.

For what concerns the linear modelling, the values of Young’s modulus and Poisson’s ratio provided by the manufacturer may simply be used. In the absence of precise data, the values of  $E = 1.5$  MPa and  $\nu = 0.499$  may be assumed, and it is required *a posteriori* verification that the elastic limit is satisfied, as described above.

In each of the two cases (discretisation with spring elements and with solid elements), given the typical width of a silicone seal and the dimensions of the glass bonded by it, the modelling is rather computationally burdensome, involving an extremely fine mesh of the glass itself, particularly along all the bonded edges of the glass pane. The total number of required elements increases still further if solid elements are used, as the thickness of the joint comes into play, for the reasons illustrated above.

The correct proportion of the elements to be used and their number must be the subject of careful evaluation.

### 6.2.4.4 Level 3: non-linear models

In general, this approach is necessary for sophisticated analyses, for example in order to deal with large deformations that, usually, are outside the scope of ordinary building practice.

With regard to the implementation of constitutive laws of the non-linear kind, it may be observed that the simple “Neo-Hookean” [Treloar, 1948], or “Arruda-Boyce” [Arruda & Boyce, 1993] formulations have proven to closely match experimental data across a very broad range of deformations. Nevertheless, other formulations – for example those proposed by Ogden, Marlow or Mooney-Rivlin – are possible and valid in the range of deformations in which silicone is commonly used. However, they have proven to match experimental data less closely than those previously mentioned in the case of very high levels of deformation [Jousset, 2007].

Under static conditions, silicone may reasonably be considered an *incompressible* material and, therefore, the strain energy density functions, by indicating with  $I_1$  and  $I_3$  the first and third invariant of the left Cauchy-Green strain tensor<sup>12</sup> assume the following forms:<sup>13</sup>

- Neo-Hookean formulation:

$$U = C_{10}(I_1 - 3), \quad I_3 = 1, \quad (6.14)$$

where  $C_{10}$  is a material constants;

- Arruda-Boyce formulation [Arruda & Boyce, 1993]:

$$U = \mu \sum_{i=1}^5 \frac{C_i}{\lambda_m^{2i-2}} (I_1^i - 3^i), \quad I_3 = 1, \quad i = 1, \dots, 5, \quad (6.15)$$

where  $\mu$ ,  $\lambda_m$  and  $C_i$  (for  $i = 1, \dots, 5$ ) are material constants.

These parameters must be furnished by the manufacturer on the basis of experimental tests. These models, that have proven their ability to provide stable solutions in the considered field of application, are based only on the first invariant and require a limited number of parameters. In general, the use of models with a larger number of parameters (e.g. higher-order polynomial models) is difficult, due to the necessity of correct calibration of the parameters.

Nevertheless, it should be taken into account that the mechanical characteristics of silicone are strongly influenced by the shape of the seal (width and thickness), by temperature and by the duration of the load – as many other elastomers – while the nominal values available are derived from test pieces of standard size and subjected to testing in standard conditions, as regulated by the relevant standards for the industry (see also Section 2.2.2). Therefore, for more complex cases, specific tests are recommended.

## 6.2.5 Structural adhesives

### 6.2.5.1 General remarks

A structural adhesive is generally a polymer-based material which, when applied to surfaces, can join them and resist against detachment with an adequate degree of safety. It must always be considered that:

- a substance defined as an adhesive does not perform its function independently of the specific application;
- no adhesive exists which can make any material adhere to any other material.

The following are the most frequent terms used in relation to adhesives:

- adherend: one of the two or more parts that must be joined;
- primer: the material applied to the surface of the adherend in order to enhance its chemical and physical properties and, thus, to improve the performance of the adhesive;
- adhesive: the substance capable of holding together the faces of the adherends;

<sup>12</sup> Indicating with  $\Omega$  the reference configuration of the body and with  $\mathbf{y}$ :  $\Omega \rightarrow \Omega'$  the deformation,  $\mathbf{F} = \nabla \mathbf{y}$  indicates the deformation gradient. The left Cauchy-Green tensor is therefore  $\mathbf{B} = \mathbf{F}\mathbf{F}^T$ , while  $I_1 = \text{tr}(\mathbf{B})$  and  $I_3 = \det(\mathbf{B})$ . The condition of incompressible material is therefore  $I_3 = 1$ .

<sup>13</sup> In general, under dynamic conditions, it is no longer possible to ignore the compressibility of the material, as this would give the result of infinite velocity of propagation of longitudinal elastic deformations waves.

- adhesion: the property of a set of various materials, connected by means of an adhesive, of remaining joined together.

Structural adhesives can be classified according to the following categories: hybrid adhesives (e.g. epoxy resins hardened by means of rubbers, silicones, polymers resistant to high temperatures, etc.), thermosetting polymers (e.g. epoxy, phenolic and acrylic resins), thermosetting rubbers (e.g. polyurethanes and polyether) and elastomers (e.g. neoprene and styrene).

### 6.2.5.2 Mechanical behaviour

The constitutive uniaxial tensile law governing the response of the materials used as structural adhesives (and thus also the peeling response) is generally of the linear elastic type with fragile behaviour, as illustrated in Figure 6.7a. In order to characterise such behaviour, the values of the elastic modulus  $E$  and ultimate tensile strength  $\sigma_{\max}$  are sufficient.

In the absence of specific data obtained from experimental tests or supplied by the manufacturer, it is possible to assume that  $E_a = 3.5$  GPa and  $\sigma_{a,\max} = 70$  MPa for fast loads and/or low temperatures ( $T < 20^\circ\text{C}$ ),  $E_a=2.0$  GPa and  $\sigma_{a,\max}=50$  MPa for slow loads and/or high temperatures ( $T > 35^\circ\text{C}$ ). The mechanical properties of adhesives, in fact, vary significantly with changes in time and temperature, as illustrated, by way of example, in Table 6.2.

Table 6.2. Elastic modulus  $E_a$  of different adhesives, for different values of temperature.

Type	$E_a$ (GPa) T = $-70^\circ\text{C}$	$E_a$ (GPa) T = $50^\circ\text{C}$
Epoxy	4.1	2.8
Epoxy+rubber	3.3	2.2
Epoxy+vitrous	4.3	3.1
Hybrid(with silanes)	4.3	2.5

For what concerns the Poisson's ratio, values between 0.41 and 0.49 may be considered.

Under shear actions, three different types of behaviour are observed. Each can be approximated with bilinear functions which differ only in the post-elastic phase behaviour.

- Linear elastic - perfectly plastic bonds (Figure 6.7). This behaviour is determined uniquely by the shear elastic modulus  $G$ , by the stress at the end of elastic branch  $\tau_s$  and by the ultimate shear strain  $\gamma_f$ . Materials which behave in this manner are adhesives with low yield stress (for example, non-thermosetting neoprene elastomers).



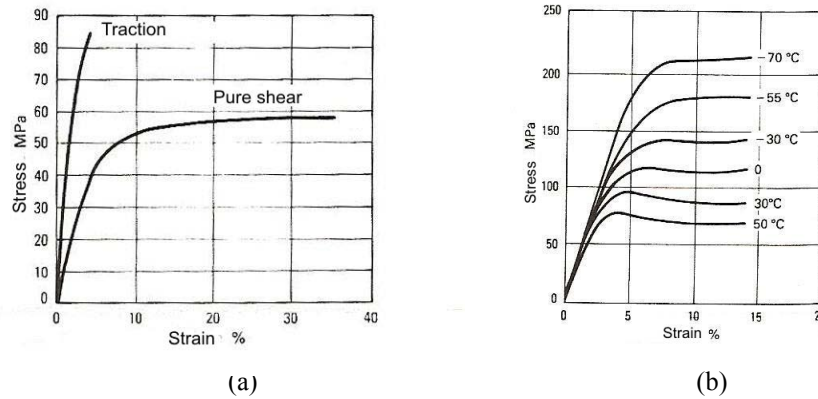


Figure 6.7. (a) Constitutive law with plastic plateau for shear. (b) Constitutive law with plastic plateau for shear as a function of temperature [Various authors, 1990]

b) Linear elastic bond with descending post-elastic branch (Figure 6.8). In addition to  $G$ ,  $\tau_s$  and  $\gamma_f$ , to characterise this material it is necessary to know the slope  $G_p$  (which is negative) of the descending branch, or the ultimate tensile strength  $\tau_f$  (lower than  $\tau_s$ ). Most adhesives behave in this way, in particular epoxy resins and thermosetting rubbers.

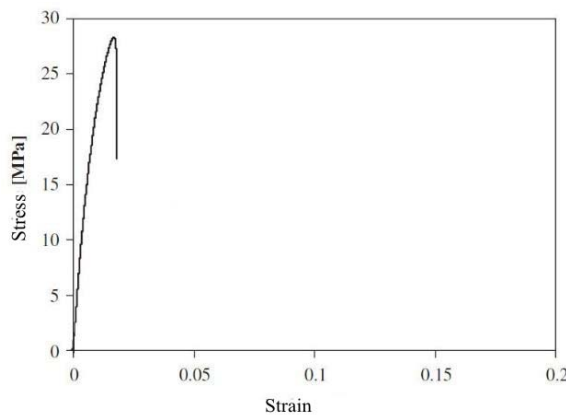


Figure 6.8. Bilinear constitutive law with descending branch [Borsellino *et al.*, 2007].

c) Linear elastic law with ascending post-elastic branch (Figure 6.9). In this case, too, knowledge of  $G$ ,  $\tau_s$ ,  $\gamma_f$  and  $G_p$  (now positive) – or  $\tau_f$  (now higher than  $\tau_s$ ) – uniquely characterise the material. Resins hardened with rubber belong to this third type.

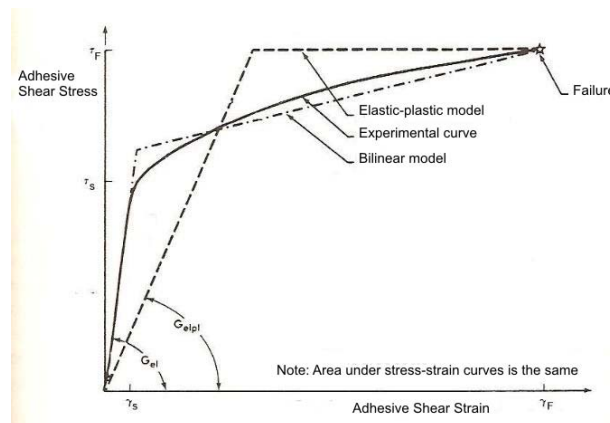


Figure 6.9. Constitutive law with ascending branch [Adams & Wake, 1984]

The mechanical shear properties of adhesives are also highly dependent on time and temperature, as illustrated in Figure 6.7(b).

The stress value at the end of elastic behaviour (or yield stress)  $\tau_s$  and the ultimate strength  $\tau_f$  of an adhesive are influenced by the mechanical properties of the materials that comprise the joint, the characteristics of the contact surfaces, the presence (or absence) of internal stresses, the geometry of the node and the design details of the load mechanism. Therefore, it is particularly important to have certified tests on the material to be used in order to have statistically valid values to compare with the design values. In the absence of such certified tests, it is in any case necessary to have certifications provided by the manufacturers.

For all of the models illustrated, as an initial approximation and in the absence of certified experimental data – the importance of which is underlined once again – for preliminary evaluations it is suggested to use for  $G$  values between 0.60 and 1.10 N/mm<sup>2</sup>, for  $\gamma_f$  values between 20% and 40%, for  $\tau_s$  values between 12.0 and 16.0 MPa and for  $\tau_f$  values between 18.0 e 24.0 MPa. These values are valid for loads of medium duration and in ordinary temperature conditions (around 25°C). With regard to epoxy resin adhesives, the upper limits of the ranges can be used. For non-thermosetting elastomer-based adhesives the lower limits are appropriate, while for mainly rubber-based adhesives the intermediate values can be used.

In order to identify the parameters of the model chosen from the experimental tests, it is appropriate to choose the theoretical curves so that the area below the real curve is the same as the area below the theoretical curve, in order to have a model that correctly captures the energy necessary to break the adhesive. For example, both of the bilinear curves illustrated in Figure 6.9 satisfy this requirement.

As shown in Figure 6.8, some adhesives exhibit a behaviour very similar to the models used to evaluate delamination phenomena. The possibility of delamination between glass and adhesive must be avoided by applying an adequate safety coefficient to the ultimate relative displacement between the two faces. Nevertheless, to evaluate delamination – which is, in any case, useful to assess the real resistance of the joint – bilinear models such as the one illustrated in Figure 6.10 can be used, including the ultimate horizontal branch which corresponds to the detachment of the adherends.

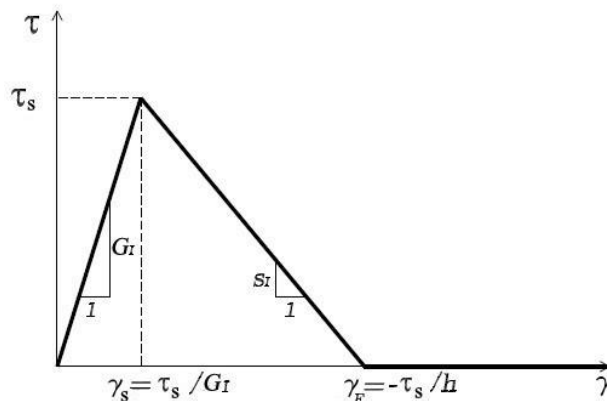


Figure 6.10. Bilinear law [Cottone *et al.*, 2010]

### 6.2.5.3 Types of joints

Figure 6.11 shows a series of adhesive joints. Each of these joints is designed for a specific construction application. All of these configurations induce a shear mechanism, both in single-lap and double-lap joints, and thus improve load transfer between surfaces, although particularly dangerous spurious normal tensile stresses may be present (the so-called “peeling” phenomenon).

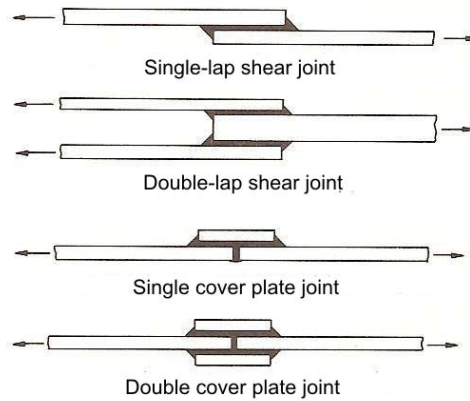


Figure 6.11. Typical joints created with adhesives [Adams & Wake, 1984].

With regard to stress analysis, considering the common single-lap joint (Figure 6.11a), as a first approximation the average shear stress can be used (Figure 6.12a)

$$\tau = \frac{P}{bl}, \tag{6.16}$$

where  $b$  is the width of the joint of length  $l$  and  $P$  is the load. This is correct even if a non-linear behaviour develops in the adhesive, although only in cases where the adherends can be considered rigid.

If, on the contrary, the adherends cannot be considered rigid, the shear stress undergoes a redistribution, as illustrated diagrammatically in in Figure 6.12b, with maximum points in proximity to the extremities. If the joint is also sufficiently long, the stress decreases to nil at a certain point along the adhesion surface.

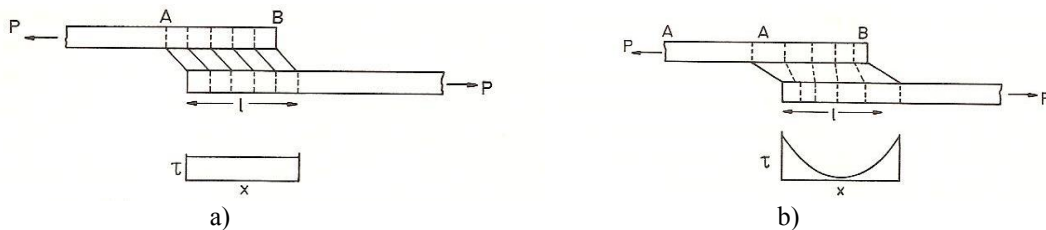


Figure 6.12. Curve of shear stress in the adhesive [Adams & Wake, 1984].

The following formulas, based on fracture mechanics, provide the maximum shear stress *per* unit of width of the bonded joint,  $\tau_{max}$ , and the distance  $L$  beyond which this stress becomes nil (Figure 6.13)

$$\tau_{max} = \frac{kP}{\sqrt{\frac{t \cdot t_a E}{G_a}}}, \quad L = k \sqrt{\frac{t \cdot t_a E}{G_a}}, \tag{6.17}$$

where  $t$  is the thickness of the adherend,  $t_a$  the thickness of the adhesive,  $E$  the elastic modulus of the adherend,  $G_a$  the elastic shear modulus of the adhesive,  $P$  the load applied and  $k$  the limit value of the stress intensity factor. This depends on the ratio between the thickness of the adhesive and the thickness of the adherends (e.g., if  $t = t_{ad}$  then  $k = 0.5$ , if  $t = 4t_{ad}$  then  $k = 0.25$ , if  $t \gg t_{ad}$  then  $k = 1$ ).

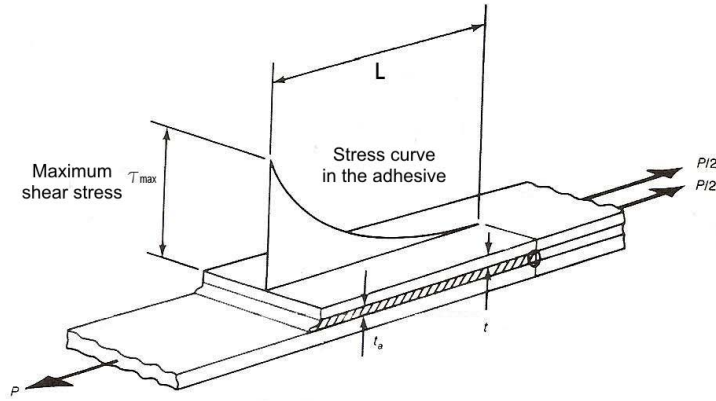


Figure 6.13. Stress curve and maximum stress value in a joint with adhesive [Various authors, 1990].

If the shear modulus  $G$  decreases, the maximum stress decreases too, while the effective adhesion length increases, even if the load does not change. The value of  $G$  thus assumes a critical role in the modelling process, and, hence, particular care must be taken in choosing it and considering its change with temperature, humidity and loading speed, with reference to certified tests and/or manufacturer certifications. Nonetheless, in the absence of specific values, and in particular during the approximate pre-sizing phase, values of  $G$  between  $0.60$  and  $1.10 \text{ N/mm}^2$  may be used.

If finite element models are used, it is preferable – given the simplicity of implementation – to consider shear and normal stress simultaneously, reaching a more detailed level of analysis.

The possibility that normal stresses develop in the joint (peeling) must be avoided in glass structures, given the considerable difference in stiffness of the materials.

#### 6.2.5.4 Applications and calculations

When it is necessary to determine both shear and normal stresses transmitted by the joint, and to consider at the same time a joint subjected not only to axial but also to shear and bending actions, an elastic simplified model may be used. From the model described in [Bigwood & Crocombe, 1989] and illustrated in Figure 6.14, cases of pure peeling stress and pure shear stress can be derived, thus obtaining the following formulas:

- peeling stress due to shear  $V$ :

$$\sigma_y(V) = \frac{-\sqrt{2} b_1 V}{(b_1 + b_2)^{0.75}}, \quad (6.18)$$

- peeling stress due to bending moment  $M$ :

$$\sigma_y(M) = \frac{-b_1 M}{\sqrt{b_1 + b_2}}; \quad (6.19)$$

- shear stresses due to normal stress  $N$ :

$$\tau_{xy}(N) = \frac{-a_1 N}{2\sqrt{a_1 + a_2}}; \quad (6.20)$$

- shear stresses due to shear:

$$\tau_{xy}(V) = \frac{3V}{4h_1}; \tag{6.21}$$

- shear stresses due to bending moment:

$$\tau_{xy}(M) = \frac{3a_1 M}{h_1 \sqrt{a_1 + a_2}}. \tag{6.22}$$

The coefficients  $a_i$  and  $b_i$  can be derived from the following equations

$$b_i = \frac{12E_a(1-\nu_i^2)}{E_i h_i^3 t_a}, \quad a_i = \frac{G_a(1-\nu_i^2)}{E_i h_i t_a}, \quad i = 1, 2. \tag{6.23}$$

where  $E_a$  and  $G_a$  are the elastic moduli of the adhesive,  $t_a$  is the thickness of the adhesive,  $h_i$  are the thicknesses of the adherends,  $E_i$  are the elastic moduli of the adherends and  $\nu_i$  are the Poisson's ratios for the adherends.

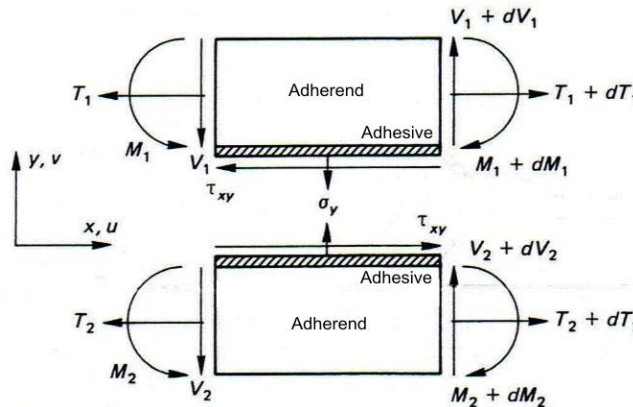


Figure 6.14. Reference model for compound stresses [Bigwood & Crocombe, 1989]

Once determined the maximum stresses acting on the adhesive, it is necessary to compare them with the maximum admissible stresses that are able to be carried by the adhesive. The classical failure criteria used in Solid Mechanics, such as Tresca or Von Mises, cannot be applied, as they ignore the spherical component of the stress tensor, the role of which is not negligible.

A more general criterion that may be used is the Mohr criterion (intrinsic curve criterion), as it can be reconstructed starting from the results of the three basic experimental tests (uniaxial tensile test, uniaxial compressive test and pure shear test), which are generally supplied by manufacturers in the technical specifications of the adhesive.

**Annex**

The differential equations that describe the behaviour of the model under consideration (Figure 6.14) are

$$\frac{d^3\tau_{xy}}{dx^3} - K_1 \frac{d\tau_{xy}}{dx} = -K_2\sigma_y, \quad \frac{d^4\sigma_y}{dx^4} + K_3\sigma_y = K_4 \frac{d\tau_{xy}}{dx}, \quad (6.24)$$

where the coefficients  $K_1$ ,  $K_2$ ,  $K_3$  and  $K_4$ , which depend on the elastic moduli and thicknesses of adhesives and adherents in the form

$$K_1 = \frac{4G_a}{t_a} \left( \frac{(1-\nu_1^2)}{E_1 h_1} + \frac{(1-\nu_2^2)}{E_2 h_2} \right), \quad K_2 = \frac{6G_a}{t_a} \left( \frac{(1-\nu_1^2)}{E_1 h_1} - \frac{(1-\nu_2^2)}{E_2 h_2} \right),$$

$$K_3 = \frac{E_a}{t_a} \left( \frac{1}{C_1} + \frac{1}{C_2} \right), \quad K_4 = \frac{E_a}{2t} \left( \frac{h_1}{R_1} - \frac{h_2}{R_2} \right). \quad (6.25)$$

In these equations,  $E_a$  and  $G_a$  are the elastic moduli of the adhesive,  $t_a$  is the thickness of the adhesive,  $h_{1,2}$  are the thicknesses of the adherents,  $E_{1,2}$  are the elastic moduli of the adherents and  $\nu_{1,2}$  are the Poisson's ratios. The constants  $C_{1,2}$  are given by

$$C_i = \frac{E_i h_i^3}{12(1-\nu_i^2)}, \quad i = 1, 2. \quad (6.26)$$

The system (6.24) may alternatively be written as a single equation in terms of  $\tau_{xy}$ , or in terms of  $\sigma_y$ , in the form

$$\frac{d^7\tau_{xy}}{dx^7} - K_1 \frac{d^5\tau_{xy}}{dx^5} + K_3 \frac{d^3\tau_{xy}}{dx^3} - K_5 \frac{d\tau_{xy}}{dx} = 0, \quad (6.27)$$

$$\frac{d^6\sigma_y}{dx^6} - K_1 \frac{d^4\sigma_y}{dx^4} + K_3 \frac{d^2\sigma_y}{dx^2} - K_5\sigma_y = 0, \quad (6.28)$$

with  $K_5 = (K_1 K_3 - K_2 K_4)$ .

The solutions of the preceding equations are

$$\tau_{xy} = C_1 \cosh(k_3 x) + C_2 \sinh(k_3 x) + C_3 \cosh(k_1 x) \cos(k_2 x) +$$

$$+ C_4 \cosh(k_1 x) \sin(k_2 x) + C_5 \sinh(k_1 x) \cos(k_2 x) + C_6 \sinh(k_1 x) \sin(k_2 x) + C_7, \quad (6.29)$$

$$\sigma_y = D_1 \cosh(k_3 x) + D_2 \sinh(k_3 x) + D_3 \cosh(k_1 x) \cos(k_2 x) +$$

$$+ D_4 \cosh(k_1 x) \sin(k_2 x) + D_5 \sinh(k_1 x) \cos(k_2 x) + D_6 \sinh(k_1 x) \sin(k_2 x) + D_7, \quad (6.30)$$

where the coefficients  $k_1$ ,  $k_2$  and  $k_3$  are given by

$$k_1 = (x^2 + y^2)^{0.25} \cos \left[ 2 \cos \left( \frac{x}{x^2 + y^2} \right) \right]^{-1}, \quad k_2 = (x^2 + y^2)^{0.25} \sin \left[ 2 \cos \left( \frac{x}{x^2 + y^2} \right) \right]^{-1}, \quad k_3 = \sqrt{G_1}, \quad (6.31)$$

being  $x$  and  $y$  the coefficients respectively of the real part and the imaginary part of the roots of the characteristic equations associated with the differential equations (6.27) and (6.28).

## 6.3 Modelling of glass elements

### 6.3.1 General remarks and definitions

Glass elements generally have a very small thickness in relation to the other two dimensions. This aspect enables their behaviour to be described using simplified models, of which it is possible to determine a solution which, although approximate, may be considered adequate for design purposes.

Glass elements can be characterised by a behaviour that is predominantly:

- flexural;
- membrane;
- membrane and flexural.

Structural analysis must be based on appropriate calculation models. The chosen assumptions and the calculation model used, in particular, must be capable of reproducing the global behaviour of the structure and the local behaviour of its sections, structural elements, connections and restraints. As glass is an elastic brittle material, in modelling a glass panel it is important to direct attention towards all of the points in the structure in which stress concentrations may arise. The ultimate failure load for a glass panel is strongly influenced, for example, by the distance of any holes from the border of the plate.

Modelling of the constraint, which may be continuous or localised, is of fundamental importance. In both cases, the constraint may be assumed to be fixed or compliant. In any case the constraint model used must accurately reproduce the real kinematic conditions.

When there are redundant constraints, attention must be paid to possible states of coaction. In some cases, redundant restraints may be arranged deliberately to induce coactive stress states in the glass, in order to slightly alter the shape of the glass element (cold forming). In general, modelling must be as simple as the case in question allows.

In the following sections, the levels of structural and geometric modelling for the cases of monolithic, laminated and insulating glass are examined.

### 6.3.2 Monolithic glass elements

#### 6.3.2.1 Preliminary considerations

Glass used in construction works may be annealed, heat-strengthened and thermally toughened (tempered). However, from the point of view of the modelling, they are identical, although the three types present different design strength (see Section 7.4).

Given their slenderness, the static or dynamic response of monolithic glass panels may be significantly influenced by phenomena of geometric non-linearity. In addition, the usual constraint conditions generally requires at least a two-dimensional (plate) model. Simpler (e.g. linear or one-dimensional) modelling may be used only when the geometric and mechanical characteristics of the element allow it, and in any case it must be verified that the results obtained are compatible with the adopted simplified assumptions.

Two- or three-dimensional finite element models may be used effectively for specific geometries (with reference to the actual constraint) or as solutions for the purpose of comparison and verification. In this case, it is necessary to carefully validate the type of discretisation used, making sure that locking phenomena do not occur, as they are particularly insidious in the case of slender elements primarily subject to flexural deformations.

Irrespective of the complexity of the model adopted, particular care must be taken in modelling the constraints and in the description of:

- design details (e.g. system for fixing the panel to the load-bearing structure, load transferring from the glass to the structure, etc.);
- holes for anchoring elements (size, distance from edges, etc.);
- joints (type of connection, stiffness of join, dissipative capacities, etc.).

### 6.3.2.2 Modelling of geometry and constraints

Ideally, a two-dimensional plate or isotropic-shell model will be used for both continuous and concentrated constraints. For pointwise supports, two-dimensional models yield reliable results far from the supports; however, in proximity to them, any flaws, as well as the actual force-transmitting mechanism of the constraints, must be taken into account.

One-dimensional models (according to the beam model, under the hypotheses that plane sections remain plane and that the shear strains are negligible) are admitted only when the deformed shape of the monolithic glass element is cylindrical (that is for slender flat beams and slender panels restrained on two opposite sides). In this case, naturally, the constraint conditions must be compatible with the cylindrical deflection. If the width of the element subjected to bending is comparable with its length, the displacements obtained with this model must take into account the Poisson's effect.

Three-dimensional continuous models are generally necessary only for complex geometries.

Restraints may be modelled as continuous (supports on edges) or pointwise. The presence of deformable material between the constraint and the plate may also be modelled by means of systems with concentrated elasticity (springs), or detailed geometrical models based on numerical analyses.

In each type of modelling approach it is in any case important to take account of any eccentricities of the constraint with respect to the mid-plane of the plate. In the case of linear analysis, restraints may be applied to the midplane of the plate, by accounting for the actions arising from such eccentricity as appropriately introduced external loads. Any design eccentricities of the restraints with respect to the mid-plane of the plate must be explicitly taken into account if a non-linear analysis is performed.

### 6.3.2.3 Type of structural analysis

In any case, a linear elastic analysis is recommended, if only for comparison purposes with the results obtained by means of more sophisticated analyses.

Because of their high flexibility, structural glass elements generally exhibit non-linear behaviour, caused by the occurrence of large displacements or rotations. In such cases a coupling between the membrane and flexural response arises.

In order to evaluate the effects of deformations on the stress level, on instability phenomena or on other structural response parameters, it is recommended to evaluate stresses and strains by means of second-order analyses, i.e. by imposing equilibrium requirements on the deformed configuration of the element. Any geometrical or structural flaws (e.g. lack of straightness or verticality, eccentricity of connections, etc.) must be considered in the modelling and verification of the individual plate.

Linear or non-linear geometrical analyses may be conducted. In the former, the structural reference model is the Kirchhoff-Love theory of thin isotropic shells (or, when possible, simplified beam models). In the latter case, Von Karmán's non-linear model, or other more complex shell models, may be adopted.

It is generally sufficient to conduct only a *geometrically linear* analysis when:

$$f_{\max} < \frac{s}{2} \quad \text{for panels,}$$

$$f_{\max} < \frac{L}{300} \quad \text{for fins and beams,}$$



where

- $f_{\max}$  maximum deflection of the element [mm];
- $s$  thickness of the element [mm];
- $L$  beam span (or effective length  $L_0$ ; for example,  $L_0 = 2L$  is the effective length for cantilever beams) [mm].

In other cases, *non-linear analysis* is recommended.

Furthermore, *Non-linear analysis* is expressly required in cases when a significant axial load is combined with bending.

#### 6.3.2.4 Calculation methods

Calculation may be performed either by means of analytical exact solutions (when available) or the use of numerical codes, in particular when a non-linear analysis is required. The annex to Chapter 6 provides a series of tables that may be of help to the designer.

Three-dimensional continuous models are not recommended for the structural analysis of monolithic glass plates, given their extreme slenderness, which would demand an extremely fine discretisation. They are however particularly suitable for the study of local effects.

Three-dimensional continuous linear models, which are recommended for the analysis of local stress and strain states, may also be used as a sub-model for the evaluation of stress concentrations, which must always be taken into consideration. As a first approximation, these may be estimated as mean stresses over a significant volume of characteristic size not greater than one half of the thickness of the plate. Nevertheless, it is always recommended to refine the model for the zone of interest.

In any case, verification of the results obtained with simpler two-dimensional or one-dimensional models is always recommended.

In general, the mesh must be sufficiently fine and particular attention must be directed towards modelling of the contact zones. In order to prevent *locking* phenomena, the use of a mixed formulation (*incompatible modes*) is suggested, which guarantees greater accuracy in the evaluation of the flexural behaviour.

The dimensions of the mesh must satisfy the following criteria:

- maximum element dimension in the thickness of the plate:  $\frac{s}{2}$ ,
- ratio of maximum and minimum dimensions of the element:  $\frac{\max}{\min} \leq 6$ ,

where

- $s$  thickness of the element of monolithic glass [mm];
- $\max$  maximum dimension of mesh [mm];
- $\min$  minimum dimension of mesh [mm].

In zones with stress concentrations, a ratio between maximum and minimum dimensions of the elements close to 1 should be assumed.

### 6.3.3 Laminated glass elements

Laminated glass consists of two or more glass plates bonded together, by means of pressing and heating, with a layer of material between them (the *interlayer*), adhering to the whole surface of the plates. The glass panels may be annealed, heat-strengthened and heat-toughened (tempered) glass, or any combination of these types.

The interlayer consists of a sheet of elastomeric material which must have good adhesion to the glass and high stretching capacity before tearing. The mechanical characteristics of the elastomer are highly dependent on time and temperature; in any case the stiffness of the elastomers is much lower than

that of glass, which means that even when adhesion is effective, the polymer is subject to a large degree of shear slip.

For what concerns the modelling of geometry and constraints, the reader is referred to Section 6.3.2.2 (monolithic glass elements). The focus is made here on specific aspects of structural modelling. In particular, in the following sections different level of methods will be discussed:

- *Level 1*: the laminated glass element (beam or plate) is modelled as a monolithic glass element which exhibits the same flexural behaviour;
- *Level 2*: the laminated glass element is modelled as an element consisting of glass plates connected by shear-deformable equivalent springs;
- *Level 3*: the laminated glass plate is three-dimensional modelled using a finite-element-based code.

### 6.3.3.1 Level 1: Method of Equivalent Thickness

The behaviour of a laminated glass element formed by  $n$  glass plies, depending on the degree of shear coupling offered by the interlayer, is somehow intermediate between that of a layered element, with glass plies with no shear interaction, and of a monolithic element.

The limit cases are therefore:

- layered behaviour: free-sliding glass plies, without shear connection between them. In this case the curvature  $\chi$  assumed by the laminated package, consisting of  $n$  layers, due the bending moment  $M$  is given by

$$\chi = \frac{M}{EJ_{abs}} \tag{6.32}$$

where

$$J_{abs} = \sum_{i=1}^n J_i \tag{6.33}$$

with

$J_i$  = moment of inertia of a single ply [ $\text{mm}^4$ ].

In this case, no shear force is transmitted at the interface between the plies..

- monolithic behaviour: the interlayer assure perfect bonding between glass plies; by neglecting the flexural stiffness of the interlayer, we thus have

$$\chi = \frac{M}{E J_{full}}, \tag{6.34}$$

where

$$J_{full} = \sum_{i=1}^n (J_i + A_i d_i^2) = J_{abs} + \sum_{i=1}^n A_i d_i^2, \tag{6.35}$$

where

$d_i$  = distance of the centre of gravity of the  $i^{\text{th}}$  plate from the geometric centre of gravity of the cross-section of the laminated package, as illustrated in Figure 6.15 [mm];  
 $A_i$  = area of the cross-section of the  $i^{\text{th}}$  plate [mm<sup>2</sup>].

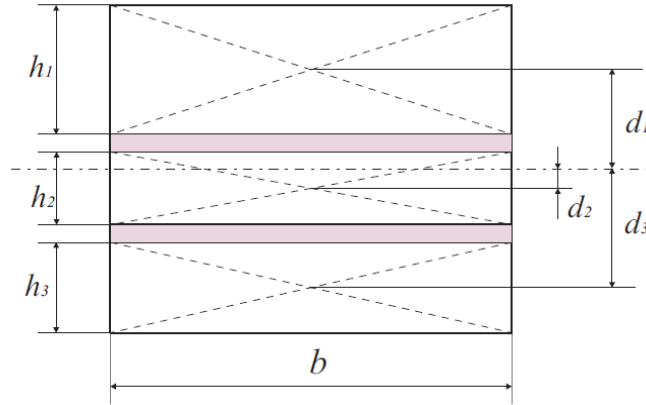


Figure 6.15. Geometry of a laminated glass element.

In the case of two layers only, the flexural stiffness becomes

$$EJ_{full} = EJ_{abs} + EA^*d^2, \quad (6.36)$$

where

$$A^* = \frac{A_1 A_2}{A_1 + A_2}, \quad d = d_1 + d_2 = \frac{h_1 + h_2}{2} + h_{int}. \quad (6.37)$$

For the case of two glass plies,  $d_1 = \frac{d h_2}{h_1 + h_2}$ ,  $d_2 = \frac{d h_1}{h_1 + h_2}$ .

A horizontal shear force,  $H_0$ , per unit of width is transmitted to the interface between the plates. It is given by

$$H_0 = \tau_i b, \quad (6.38)$$

where  $\tau_i$  is the value of the shear stress at the interface.

In the intermediate cases, the presence of the interlayer produces a limited degree of slip between the plates, hence the horizontal force per unit of length transmitted to the interface between the plates is equal to a fraction of  $H_0$ . At accuracy level 1, a shear transfer coefficient is defined according to the properties of the interlayer, of the glass and of the geometry of the laminate. This allows to establish the flexural behaviour of the composite element, the curvature of which is given by

$$\chi = \frac{M}{EJ_{eq}}, \quad (6.39)$$

where  $J_{eq}$  is the equivalent moment of inertia of the laminated package, which assumes an intermediate value between the values of the moments of inertia  $J_{abs}$  and  $J_{full}$ .

Once the equivalent moment of inertia has been evaluated, the *effective thicknesses* can be defined, i.e. the thicknesses of monolithic elements which, under the same boundary and loading conditions,

presents the same flexural behaviour in terms of stiffness and strength of the element under consideration.

The following values can therefore be defined:

- *deflection-effective thickness*: thickness of the monolithic beam that exhibits the same maximum deflection of the laminated glass beam under consideration.
- *Stress-effective thickness*: thickness of the monolithic beam that exhibits the same maximum stress occurring in one of the plies of the laminated glass beam under consideration. Generally it is possible to define a stress-effective thickness for each glass ply composing the laminated element.

The literature and the standards on this subject contain several models for calculating the equivalent moment of inertia in relation to the shear deformability of the interlayer, to the geometry and to the boundary conditions of the element. The main references are listed below, along with their strengths and weaknesses.

#### **6.3.3.1.1 Cahier 3488\_V2 (French)**

The French instructions [CSTB Cahier 3488-V2, 2011] propose a simplified method for the calculation of effective thicknesses based on two factors  $\alpha$  and  $\beta$ , which depend on the aspect ratio of the laminated glass plate and on the type of load, and are provided by the standard itself exclusively for the case of a rectangular plate with continuous support on four sides. The model is extremely approximate, as the effective thicknesses are independent of the shear resistance of the interlayer. The model enables effective thicknesses to be calculated only for laminated packages consisting of two glass plates.

#### **6.3.3.1.2 TRLV standard (German)**

German TRLV technical rules (*Technische Regeln für die Verwendung von Linienförmig gelagerten Verglasungen*) [TRLV] take into account the interaction between the various plies of the laminate only when the glass is annealed. No equivalent thickness is explicitly proposed, because the rules do not officially acknowledge the existence of an interaction mechanism between the glass and the interlayer, on the contrary stating that the plates should be treated as there were no interaction. However, an increase in admissible stress is proposed when the glass is laminated: this increase is equivalent to indirectly assuming that interaction exists between the layers, due to the coupling effect of the interlayer. Specifically, the following indications are offered.

- For long duration loads: compared with an admissible stress of 12 MPa for a simple annealed glass plate, a limit of 15 MPa is suggested as the maximum admissible stress for a laminated annealed glass plate. For glass roof plates, these limits apply always and in any case, regardless of the load duration.
- For short duration loads: compared with an admissible stress intensity of 18 MPa for a simple annealed glass plate, a limit of 22.5 MPa is suggested as the maximum admissible stress for a laminated annealed glass plate.

If these increased strength are considered, the TRLV rules require to verify also the total coupling condition of the plates (monolithic limit), by ensuring that the corresponding stresses not exceed the ordinary strength values (12 MPa for long duration loads and 18 MPa for short duration loads).

The TRLV rules were recently replaced by the DIN 18008 standard.

### 6.3.3.1.3 European draft standard prEN 16612 (2013)

The Project of European Norm prEN 16612 (2013) proposes a simplified method for calculating the effective thicknesses to be used for evaluating stress and deflection, for laminated packages consisting of two or more glass plates. These effective thicknesses depend on a coupling parameter,  $\varpi$ , the values of which are tabulated in [prEN 16612] according to the “interlayer stiffness family” of the polymer used for the interlayer and to the type of load (that is related to the load duration and temperature). The various stiffness families are defined in the Project of European Norm prEN 16613 (2013).

Although the model proposed by prEN 16612 is extremely simple and easy to apply, it ignores the influence on the degree of coupling provided by interlayers of important factors such as load type and geometry (such as beam or plate dimensions or composition of the laminated package). In general, the approach set out by prEN 16612 is not recommended, as it is inaccurate in most cases [Galuppi, Royer-Carfagni 2013b].

### 6.3.3.1.4 Wölfel-Bennison model

This method [Wölfel, 1987; Bennison, 2009] has been adopted by ASTM E1300-09a (Appendix XII). The formulation, based on work originally developed by Wölfel [Wölfel, 1987] concerning steel composite beams, was subsequently applied by Bennison to the case of laminated glass. It prescribes for the flexural stiffness of the laminated element, a value intermediate between the stiffness of a monolithic element and that of an element with independent layers, determined by means of a linear interpolation through a shear transfer coefficient  $\Gamma$ , varying between  $\Gamma=0$  (for layered behaviour) and  $\Gamma=1$  (for monolithic behaviour).

The model allows to calculate the effective thicknesses only for laminated packages consisting of two glass plates. In this case, the equivalent moment of inertia of the monolithic beam is given by the weighted mean of the moments of inertia related to the layered limit ( $J_{abs}$ ) and the monolithic limit ( $J_{full}$ ), i.e.,

$$J_{eq} = \Gamma J_{full} + (1 - \Gamma) J_{abs} = J_1 + J_2 + \Gamma A^* d^2, \quad (6.40)$$

where  $A^*$  and  $d$  are defined by Eq. (6.37).

Introducing the quantity:

$$I_s = \frac{d^2 A^*}{b} = \frac{h_1 + h_2}{h_1 h_2} d^2 = h_1 d_1^2 + h_2 d_2^2, \quad (6.41)$$

according to Wölfel’s original model, the shear transfer coefficient  $\Gamma$  is given by

$$\Gamma = \frac{1}{1 + 9.6 \frac{h_{int} E I_s}{G_{int} l^2 d^2}} = \frac{1}{1 + 9.6 \frac{h_{int} E A^*}{G_{int} l^2 b}}, \quad (6.42)$$

where:

- $h_{int}$  thickness of the polymeric interlayer;
- $b$  width of the beam;
- $l$  length of the beam;
- $E$  Young’s modulus of the glass;

$G_{\text{int}}$  shear modulus of the interlayer;  
 $A^*$  is given by Eq. (6.37).

The deflection-effective thickness is:

$$h_{ef:w} = \sqrt[3]{h_1^3 + h_2^3 + 12\Gamma I_s}, \quad (6.43)$$

while the stress-effective thicknesses, for each of the glass plies, are

$$h_{1,ef;\sigma} = \sqrt{\frac{h_{ef:w}^3}{h_1 + 2\Gamma d_1}}, \quad h_{2,ef;\sigma} = \sqrt{\frac{h_{ef:w}^3}{h_2 + 2\Gamma d_2}}. \quad (6.44)$$

The validity of this model is limited, as it has been devised for statically determinate beams, in which the thickness of the outer layers is negligible compared with that of the interlayer; it may be applied, with good results, only to cases in which the geometry is of the “beam” type and in cases where deflection is cylindrical, with maximum deflection at the centre. It is therefore not recommended for plates, except in the case of rectangular plates with simple support on two opposite sides and subjected to uniformly distributed loads acting orthogonally to the plane.

### 6.3.3.1.5 Enhanced Effective Thickness (EET) model

This model, proposed in [Galuppi, Royer-Carfagni, 2012a], [Galuppi, Royer-Carfagni, 2012b] and [Galuppi *et al.*, 2013a], is a simple model, suitable for the evaluation of the effective thicknesses for both “beam” and “plate” geometries.

For a laminated glass beam (case 1D), the method defines the equivalent moment of inertia as the harmonic mean of the moment of inertia of the cross-section at the monolithic limit and that of the cross-sections not connected by an interlayer (layered limit), weighted using a coefficient,  $\eta$ , which takes account of the “degree of coupling” between glass plies due to the presence of the interlayer. We therefore have

$$\frac{1}{J_{eq}} = \frac{\eta_{1D}}{J_{full}} + \frac{1 - \eta_{1D}}{J_{abs}}, \quad (6.45)$$

where  $\eta_{1D}$  is a non-dimensional coefficient which depends on the geometry of the beam, on the loading and boundary conditions and on the mechanical characteristic of glass and interlayer. The value of this coefficient ranges from 0 (corresponding to the layered limit) and 1 (corresponding to the monolithic limit).

The deflection-effective thickness, being the deflection proportional to the moment of inertia and, therefore, to the cube of the thickness of the equivalent monolithic beam, is equal to:

$$\hat{h}_w = \sqrt[3]{\frac{1}{\frac{\eta}{\sum_{i=1}^N h_i^3 + 12\sum_{i=1}^N (h_i d_i^2)} + \frac{(1-\eta)}{\sum_{i=1}^N h_i^3}}} \quad (6.46)$$

In formula (6.46) the generic coefficient  $\eta$  appears, because the formula is valid for both the one-dimensional (beam) and two-dimensional (plate) cases. For what concerns the calculation of the maximum stresses, the effective thickness is obtained by positing

$$\sigma_{i,max} = \max_x \frac{6 |M(x)|}{b \hat{h}_{i;\sigma}^2} = \max_x \left| \frac{N_i(x)}{A_i} \pm \frac{M_i(x)}{I_i} \frac{h_i}{2} \right| \quad (6.47)$$

It can be shown (see [Galuppi & Royer-Carfagni, 2012a; Galuppi & Royer-Carfagni, 2012b]) that the stress-effective thickness in the  $i^{\text{th}}$  plate is given by

$$\hat{h}_{i;\sigma} = \sqrt{\frac{1}{\frac{2\eta |d_i|}{\sum_{i=1}^N h_i^3 + 12 \sum_{i=1}^N (h_i d_i^2)} + \frac{h_i}{\hat{h}_w^3}}} \quad (6.48)$$

In formula (6.48), the generic coefficient  $\eta$  appears, because the formula is valid for both the one-dimensional (beam) and two-dimensional (plate) cases.

For the case of a beam consisting of only two glass plates, the coefficient  $\eta_{1D}$  is given by:

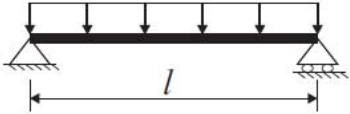
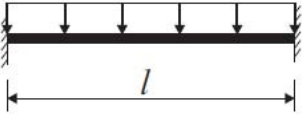
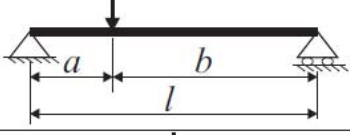
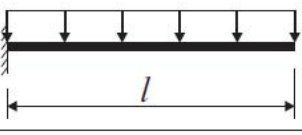
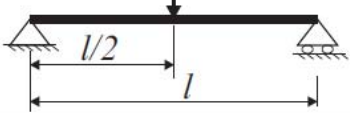
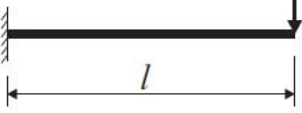
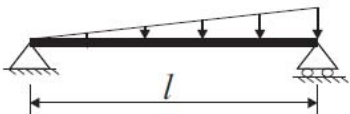
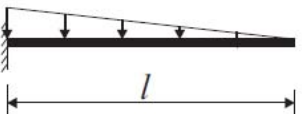
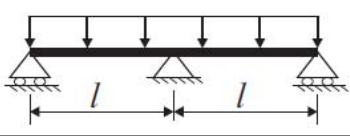
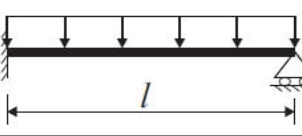
$$\eta_{1D;2} = \frac{1}{1 + \frac{E h_{int} J_{abs}}{G_{int} b J_{full}} A^* \Psi} \quad (6.49)$$

where:

- $h_{int}$  thickness of the polymeric interlayer;
- $b$  width of the beam;
- $l$  length of the beam;
- $E$  Young's modulus of the glass;
- $G_{int}$  shear modulus of the interlayer;
- $A^*$  area defined by Eq. (6.37);
- $J_{abs}$  moment of inertia at the layered limit, defined by Eq. (6.33);
- $J_{full}$  moment of inertia at the monolithic limit, defined by Eq. (6.35);
- $\Psi$  dimensional coefficient, dependent on loading and boundary conditions.

Table 6.3 provides the values of the coefficient  $\Psi$  for the most common cases in design practice.

Table 6.3 Laminated glass beams: values of coefficient  $\Psi$  for different loading and boundary conditions.

Boundary and load conditions	$\Psi$	Boundary and load conditions	$\Psi$
	$\frac{168}{17 l^2}$		$\frac{42}{l^2}$
	$\frac{15}{l^2+2ab}$		$\frac{14}{5l^2}$
	$\frac{10}{l^2}$		$\frac{5}{2l^2}$
	$\frac{10}{l^2}$		$\frac{45}{14l^2}$
	$\frac{21}{l^2}$		$\frac{21}{l^2}$

**EET method for multi-laminates**

The method can also be extended to the case of multi-laminates (see [Galuppi, Royer-Carfagni, 2013c]). The formulas below allow to calculate the shear transfer coefficient  $\eta_{1D}$  for:

- Laminated glass beams consisting of three glass plies of arbitrary thicknesses, bonded by polymeric interlayer of arbitrary thickness ( $h_{int,1}$  and  $h_{int,2}$ ):

$$\eta_{1D,3} = \frac{1}{1 + \frac{E\Psi}{G_{int} \left( \sum_{i=1}^3 h_i^3 + 12 \sum_{i=1}^3 h_i d_i^2 \right) \left( \frac{(d_1 + d_2)^2}{h_{int,1}} + \frac{(d_2 + d_3)^2}{h_{int,2}} \right) \sum_{i=1}^3 h_i^3 \sum_{i=1}^3 h_i d_i^2}} \quad (6.50)$$

- Laminated glass beams consisting of a generic number  $N$  of glass plates of the same thickness  $h$ , bonded by interlayers all of thickness  $h_{int}$  :

$$J_{full} = \frac{Nb}{12} [h^3 + h(h + h_{int})^2 (N - 1)(N + 1)]$$

e

$$\eta_{1D,N} = \frac{1}{1 + \frac{Eh_{int}}{12G_{int}} \frac{Nh^3 (N + 1)}{h^2 + (h + h_{int})^2 (N^2 - 1)} \Psi}$$

(6.51)



The coefficient  $\Psi$  is independent of the number of layers, and its values are tabulated in Table 6.3. Once the coefficient  $\eta_{1D}$  has been determined, the effective thicknesses must be calculated using Eqs. (6.46) and (6.48).

**EET method for plates**

The EET can also be extended to two-dimensional cases (i.e. plate behaviour) [Galuppi, Royer-Carfagni, 2012b]. In the most common case of the design practice, consisting of two glass plates bonded by an interlayer, the flexural stiffness in the case of layered behaviour is given by

$$D_{abs} = \sum_{i=1}^2 D_i = \sum_{i=1}^2 \frac{E h_i^3}{12(1-\nu^2)}, \tag{6.52}$$

where  $\nu$  is Poisson’s ratio of glass. In the limit case of monolithic behaviour, the flexural stiffness is given by

$$D_{full} = D_{abs} + \frac{E}{(1-\nu^2)} \frac{h_1 h_2}{h_1 + h_2} d^2. \tag{6.53}$$

By analogy to Eq. (6.45), the flexural stiffness in the intermediate case may be expressed in the following form:

$$\frac{1}{D_{eq}} = \frac{\eta_{2D}}{D_{full}} + \frac{1-\eta_{2D}}{D_{abs}}, \tag{6.54}$$

where  $\eta_{2D}$  is, once again, a non-dimensional coefficient which depends on the geometry of the plate, the loading and boundary conditions and the mechanical characteristics of the glass and interlayer. In the case of two plates of laminated glass, this coefficient is given by

$$\eta_{2D} = \frac{1}{1 + \frac{h_{int} E}{G_{int} (1-\nu^2)} \frac{D_{abs}}{D_{full}} \frac{h_1 h_2}{h_1 + h_2} \Psi} \tag{6.55}$$

where:

- $h_{int}$  thickness of the polymer interlayer;
- $h_i$  thickness of the  $i^{th}$  layer of glass,  $i = 1, 2$ ;
- $D_{abs}$  flexural stiffness at the layered limit, defined by Eq. (6.52);
- $D_{full}$  flexural stiffness at the monolithic limit, defined by Eq. (6.53);
- $E$  Young’s modulus of the glass;
- $G_{int}$  shear modulus of the interlayer;
- $\nu$  Poisson’s ratio of the glass;
- $\Psi$  dimensional coefficient dependent on loading and boundary conditions.

The values of the coefficient  $\Psi$  [ $\text{mm}^{-2}$ ] $\cdot 10^{-6}$  are provided in Table 6.4 for rectangular plates of dimensions  $a \times b$ , subjected to various loading and boundary conditions, as a function of the length of

the plate  $a$  and the aspect ratio  $\lambda = b/a$ . Other loading and boundary conditions can be considered using the expressions provided in [Galuppi et al., 2013a].

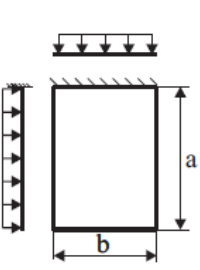
It is important to note that:

- for plates subjected to loading and boundary conditions which are equal in the two directions (for example, plates supported on four sides),  $a$  is the length of the longest side (it will be noted that Table 6.4 provides, for these cases,  $\lambda = b/a < 1$ );
- for plates subjected to loading and boundary conditions which are different in the two directions (for example plates supported on two opposite sides), Table 6.4 provides the necessary information for determining which side corresponds to length  $a$ ; in these cases we have both cases  $\lambda < 1$  and  $\lambda > 1$ .

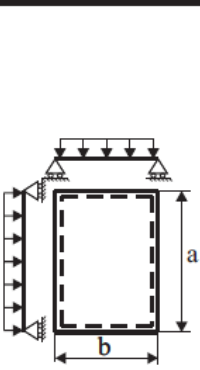
For example, the value of the coefficient  $\Psi$  for a 3000 mm x 1800 mm plate, supported on the 1800 mm length sides, corresponds, in Table 6.4 to  $a = 3000$  mm,  $\lambda=0.6$ .

For plates with dimensions of intermediate values between the one shown in the table, the value of the coefficient  $\Psi$  can be derived by means of linear interpolation.





Table 6.4 Laminated glass plates: values of the coefficient  $\Psi$  [ $\text{mm}^{-2}$ ]\* $10^{-6}$  for different loading and boundary conditions.

	$\lambda=b/a$	every value									
	a(mm)	0.1	0.2	0.3	0.4	0.5	0.6	0.7	0.8	0.9	1
	500	4018.00	1042.79	486.328	290.422	199.746	150.612	121.070	101.947	88.8653	79.5280
	600	2790.28	724.160	337.728	201.682	138.713	104.592	84.0766	70.7962	61.7120	55.2278
	800	1569.53	407.340	189.972	113.446	78.0259	58.8328	47.2931	39.8229	34.7130	31.0656
	1000	1004.50	260.698	121.582	72.6055	49.9366	37.6530	30.2676	25.4866	22.2163	19.8820
	1500	446.445	115.866	54.0364	32.2691	22.1940	16.7347	13.4523	11.3274	9.87392	8.83644
	2000	251.125	65.1744	30.3955	18.1514	12.4841	9.41325	7.56690	6.37166	5.55408	4.97050
	2500	160.720	41.7116	19.4531	11.6169	7.98985	6.02448	4.84281	4.07786	3.55461	3.18112
	3000	111.611	28.9664	13.5091	8.06728	5.54851	4.18367	3.36307	2.83185	2.46848	2.20911
	3500	82.0001	21.2814	9.92506	5.92698	4.07645	3.07372	2.47082	2.08054	1.81358	1.62302
	4000	62.7813	16.2936	7.59887	4.53785	3.12104	2.35331	1.89172	1.59291	1.38852	1.24262
	4500	49.6050	12.8740	6.00405	3.58546	2.46600	1.85941	1.49470	1.25860	1.09710	0.98183
	5000	40.1800	10.4279	4.86328	2.90422	1.99746	1.50612	1.21070	1.01947	0.88865	0.79528
	5500	33.2066	8.61810	4.01924	2.40018	1.65080	1.24473	1.00058	0.84253	0.73442	0.65726
	6000	27.9028	7.24160	3.37728	2.01682	1.38713	1.04592	0.84077	0.70796	0.61712	0.55228

	$\lambda=b/a$	every value									
	a(mm)	0.1	0.2	0.3	0.4	0.5	0.6	0.7	0.8	0.9	1
	500	4018.00	1042.79	486.328	290.422	199.746	150.612	121.070	101.947	88.8653	79.5280
	600	2790.28	724.160	337.728	201.682	138.713	104.592	84.0766	70.7962	61.7120	55.2278
	800	1569.53	407.340	189.972	113.446	78.0259	58.8328	47.2931	39.8229	34.7130	31.0656
	1000	1004.50	260.698	121.582	72.6055	49.9366	37.6530	30.2676	25.4866	22.2163	19.8820
	1500	446.445	115.866	54.0364	32.2691	22.1940	16.7347	13.4523	11.3274	9.87392	8.83644
	2000	251.125	65.1744	30.3955	18.1514	12.4841	9.41325	7.56690	6.37166	5.55408	4.97050
	2500	160.720	41.7116	19.4531	11.6169	7.98985	6.02448	4.84281	4.07786	3.55461	3.18112
	3000	111.611	28.9664	13.5091	8.06728	5.54851	4.18367	3.36307	2.83185	2.46848	2.20911
	3500	82.0001	21.2814	9.92506	5.92698	4.07645	3.07372	2.47082	2.08054	1.81358	1.62302
	4000	62.7813	16.2936	7.59887	4.53785	3.12104	2.35331	1.89172	1.59291	1.38852	1.24262
	4500	49.6050	12.8740	6.00405	3.58546	2.46600	1.85941	1.49470	1.25860	1.09710	0.98183
	5000	40.1800	10.4279	4.86328	2.90422	1.99746	1.50612	1.21070	1.01947	0.88865	0.79528
	5500	33.2066	8.61810	4.01924	2.40018	1.65080	1.24473	1.00058	0.84253	0.73442	0.65726
	6000	27.9028	7.24160	3.37728	2.01682	1.38713	1.04592	0.84077	0.70796	0.61712	0.55228

Legend:	
	Free edge
	Clamped edge
	Simply supported edge
	Supported corner

	$\lambda=b/a$	<b>0.1</b>	<b>0.2</b>	<b>0.3</b>	<b>0.4</b>	<b>0.5</b>	<b>0.6</b>	<b>0.7</b>	<b>0.8</b>	<b>0.9</b>	<b>1</b>	
	a[mm]	<b>500</b>	4918.34	1232.69	567.067	334.994	230.168	177.772	153.440	148.958	162.509	193.633
		<b>600</b>	3370.58	856.090	393.202	232.176	160.114	125.082	110.414	110.681	124.492	150.377
		<b>800</b>	1887.99	481.156	220.499	130.284	90.4864	71.9804	65.5937	68.3750	79.1656	96.0054
		<b>1000</b>	1208.10	307.557	140.793	83.2878	58.1740	46.8728	43.5895	46.4238	54.3862	65.7299
		<b>1500</b>	536.820	136.349	62.3643	36.9883	26.0733	21.4107	20.4625	22.3430	26.4174	31.6262
		<b>2000</b>	301.823	76.5778	35.0205	20.8068	14.7442	12.2309	11.8469	13.0732	15.4890	18.4274
		<b>2500</b>	193.088	48.9613	22.3909	13.3188	9.46975	7.90479	7.71696	8.56	10.1521	12.0289
		<b>3000</b>	134.046	33.9778	15.5392	9.25103	6.59278	5.52651	5.42301	6.03981	7.15987	8.45939
		<b>3500</b>	98.4581	24.9511	11.4114	6.79789	4.85275	4.08025	4.01837	4.48608	5.31751	6.26962
		<b>4000</b>	75.3670	19.0961	8.73398	5.20544	3.72076	3.13561	3.09636	3.46268	4.10387	4.83105
		<b>4500</b>	59.5398	15.0839	6.89918	4.11349	2.94324	2.48479	2.45877	2.75320	3.26254	3.83589
		<b>5000</b>	48.2209	12.2151	5.58722	3.33231	2.38625	2.01744	1.99960	2.24129	2.65555	3.11911
		<b>5500</b>	39.8477	10.0932	4.61679	2.75425	1.97363	1.67055	1.65799	1.85989	2.20335	2.58587
	<b>6000</b>	33.4800	8.47979	3.87887	2.31454	1.65948	1.40601	1.39699	1.56813	1.85750	2.17847	
	$\lambda=b/a$	<b>0.2</b>	<b>0.4</b>	<b>0.6</b>	<b>0.8</b>	<b>1</b>	<b>1.25</b>	<b>1.667</b>	<b>2.5</b>	<b>5</b>		
	a[mm]	<b>500</b>	1242.09	355.153	234.435	274.020	354.166	402.080	404.202	387.899	371.011	
		<b>600</b>	864.232	251.531	177.918	213.601	261.980	283.978	281.063	269.376	257.647	
		<b>800</b>	487.212	145.743	111.758	134.304	155.248	161.826	158.254	151.525	144.926	
		<b>1000</b>	312.029	95.1575	76.0756	90.4562	101.516	104.100	101.321	96.9761	92.7528	
		<b>1500</b>	138.661	43.5030	36.3993	42.3936	46.0711	46.4920	45.0480	43.1006	41.2235	
		<b>2000</b>	77.9587	24.8262	21.1563	24.3577	26.1226	26.1994	25.3430	24.2441	23.1882	
		<b>2500</b>	49.8734	16.0270	13.7900	15.7659	16.7882	16.7835	16.2206	15.5162	14.8405	
		<b>3000</b>	34.6237	11.1941	9.68840	11.0252	11.6882	11.6619	11.2648	10.7752	10.3059	
		<b>3500</b>	25.4319	8.25803	7.17541	8.13863	8.60194	8.57122	8.27642	7.91645	7.57166	
		<b>4000</b>	19.4678	6.34195	5.52605	6.25249	6.59398	6.56416	6.33676	6.06103	5.79705	
		<b>4500</b>	15.3798	5.02283	4.38588	4.95302	5.21489	5.18757	5.00690	4.78896	4.58039	
		<b>5000</b>	12.4562	4.07621	3.56513	4.02007	4.22712	4.20262	4.05564	3.87906	3.71011	
		<b>5500</b>	10.2934	3.37398	2.95481	3.32777	3.49551	3.47369	3.35180	3.20583	3.06621	
	<b>6000</b>	8.64860	2.83873	2.48871	2.79998	2.93860	2.91917	2.81646	2.69379	2.57647		
	$\lambda=b/a$	<b>0.2</b>	<b>0.4</b>	<b>0.6</b>	<b>0.8</b>	<b>1</b>	<b>1.25</b>	<b>1.667</b>	<b>2.5</b>	<b>5</b>		
	a[mm]	<b>500</b>	59.8176	55.7770	51.6762	48.5518	46.3972	44.6462	42.9996	41.5644	41.6559	
		<b>600</b>	41.5400	38.7340	35.8862	33.7165	32.2203	31.0043	29.8609	28.8641	28.5614	
		<b>800</b>	23.3663	21.7879	20.1860	18.9655	18.1239	17.4399	16.7967	16.2361	15.6021	
		<b>1000</b>	14.9544	13.9442	12.9190	12.1379	11.5993	11.1615	10.7499	10.3911	10.4140	
		<b>1500</b>	6.64640	6.19744	5.74180	5.39464	5.15525	4.96069	4.77774	4.61826	4.41235	
		<b>2000</b>	3.73860	3.48606	3.22976	3.03449	2.89983	2.79039	2.68748	2.59777	2.60350	
		<b>2500</b>	2.39270	2.23108	2.06705	1.94207	1.85589	1.78585	1.71999	1.66257	1.70853	
		<b>3000</b>	1.66160	1.54936	1.43545	1.34866	1.28881	1.24017	1.19443	1.15457	1.10309	
		<b>3500</b>	1.22077	1.13831	1.05462	0.99085	0.94688	0.91115	0.87754	0.84825	0.83878	
		<b>4000</b>	0.93465	0.87152	0.80744	0.75862	0.72496	0.69760	0.67187	0.64944	0.65087	
		<b>4500</b>	0.73849	0.68860	0.63798	0.59940	0.57281	0.55119	0.53086	0.51314	0.47613	
		<b>5000</b>	0.59818	0.55777	0.51676	0.48552	0.46397	0.44646	0.43000	0.41564	0.42713	
		<b>5500</b>	0.49436	0.46097	0.42708	0.40125	0.38345	0.36898	0.35537	0.34351	0.33329	
	<b>6000</b>	0.41540	0.38734	0.35886	0.33717	0.32220	0.31004	0.29861	0.28864	0.27577		

	$\lambda=b/a$	<b>0.2</b>	<b>0.4</b>	<b>0.6</b>	<b>0.8</b>	<b>1</b>	<b>1.25</b>	<b>1.667</b>	<b>2.5</b>	<b>5</b>		
	a[mm]	500	37.6068	37.7268	37.9083	38.1086	38.2943	38.4868	38.7153	38.9639	39.2186	
		600	26.1158	26.1992	26.3252	26.4643	26.5933	26.7270	26.8856	27.0583	27.2351	
		800	14.6902	14.7370	14.8079	14.8862	14.9587	15.0339	15.1231	15.2203	15.3197	
		1000	9.40170	9.43169	9.47707	9.52714	9.57357	9.62171	9.67881	9.74099	9.80464	
		1500	4.17853	4.19186	4.21203	4.23429	4.25492	4.27632	4.30169	4.32933	4.35762	
		2000	2.35043	2.35792	2.36927	2.38179	2.39339	2.40543	2.41970	2.43525	2.45116	
		2500	1.50427	1.50907	1.51633	1.52434	1.53177	1.53947	1.54861	1.55856	1.56874	
		3000	1.04463	1.04797	1.05301	1.05857	1.06373	1.06908	1.07542	1.08233	1.08940	
		3500	0.76749	0.76993	0.77364	0.77773	0.78152	0.78545	0.79011	0.79518	0.80038	
		4000	0.58761	0.58948	0.59232	0.59545	0.59835	0.60136	0.60493	0.60881	0.61279	
		4500	0.46428	0.46576	0.46800	0.47048	0.47277	0.47515	0.47797	0.48104	0.48418	
		5000	0.37607	0.37727	0.37908	0.38109	0.38294	0.38487	0.38715	0.38964	0.39219	
	5500	0.31080	0.31179	0.31329	0.31495	0.31648	0.31807	0.31996	0.32202	0.32412		
	6000	0.26116	0.26199	0.26325	0.26464	0.26593	0.26727	0.26886	0.27058	0.27235		
	$\lambda=b/a$	<b>0.1</b>	<b>0.2</b>	<b>0.3</b>	<b>0.4</b>	<b>0.5</b>	<b>0.6</b>	<b>0.7</b>	<b>0.8</b>	<b>0.9</b>	<b>1</b>	
	a[mm]	500	30.2878	30.4745	31.0830	32.3923	34.6861	38.1471	42.5340	46.6298	48.1868	45.6010
		600	21.0332	21.1628	21.5854	22.4946	24.0875	26.4911	29.5375	32.3818	33.4631	31.6674
		800	11.8312	11.9041	12.1418	12.6532	13.5492	14.9012	16.6148	18.2148	18.8230	17.8129
		1000	7.57194	7.61861	7.77075	8.09807	8.67152	9.53678	10.63349	11.6575	12.0467	11.4003
		1500	3.36531	3.38605	3.45367	3.59914	3.85401	4.23857	4.72600	5.18109	5.35409	5.06678
		2000	1.89298	1.90465	1.94269	2.02452	2.16788	2.38420	2.65837	2.91436	3.01168	2.85006
		2500	1.21151	1.21898	1.24332	1.29569	1.38744	1.52588	1.70136	1.86519	1.92747	1.82404
		3000	0.841326	0.846513	0.863417	0.899785	0.963502	1.05964	1.18150	1.29527	1.33852	1.26670
		3500	0.618117	0.621928	0.634347	0.661067	0.707879	0.778513	0.868040	0.951629	0.983404	0.930633
		4000	0.473246	0.476163	0.485672	0.506129	0.541970	0.596049	0.664593	0.728591	0.752919	0.712516
		4500	0.373923	0.376228	0.383741	0.399904	0.428223	0.470952	0.525111	0.575677	0.594899	0.562976
		5000	0.302878	0.304745	0.310830	0.323923	0.346861	0.381471	0.425340	0.466298	0.481868	0.456010
	5500	0.250312	0.251855	0.256884	0.267705	0.286662	0.315265	0.351520	0.385371	0.398238	0.376868	
	6000	0.210332	0.211628	0.215854	0.224946	0.240875	0.264911	0.295375	0.323818	0.334631	0.316674	
	$\lambda=b/a$	<b>0.2</b>	<b>0.4</b>	<b>0.6</b>	<b>0.8</b>	<b>1</b>	<b>1.25</b>	<b>1.667</b>	<b>2.5</b>	<b>5</b>		
	a[mm]	500	325.393	114.750	74.9377	60.4550	53.5051	48.9526	45.3585	42.6990	37.9068	
		600	225.968	79.6875	52.0400	41.9827	37.1563	33.9949	31.4989	29.6521	32.7445	
		800	127.107	44.8242	29.2725	23.6153	20.9004	19.1221	17.7182	16.6793	19.9520	
		1000	81.3484	28.6875	18.7344	15.1138	13.3763	12.2382	11.3396	10.6747	9.47670	
		1500	36.1548	12.7500	8.32641	6.71723	5.94501	5.43918	5.03983	4.74433	4.02073	
		2000	20.3371	7.17187	4.68360	3.77844	3.34407	3.05954	2.83490	2.66869	2.36918	
		2500	13.0157	4.59000	2.99751	2.41820	2.14020	1.95811	1.81434	1.70796	1.90781	
		3000	9.03871	3.18750	2.08160	1.67931	1.48625	1.35980	1.25996	1.18608	1.00518	
		3500	6.64068	2.34184	1.52934	1.23378	1.09194	0.99903	0.92568	0.87141	0.63410	
		4000	5.08427	1.79297	1.17090	0.94461	0.83602	0.76489	0.70873	0.66717	0.59229	
		4500	4.01720	1.41667	0.92516	0.74636	0.66056	0.60435	0.55998	0.52715	0.44643	
		5000	3.25393	1.14750	0.74938	0.60455	0.53505	0.48953	0.45358	0.42699	0.47695	
	5500	2.68920	0.94835	0.61932	0.49963	0.44219	0.40457	0.37486	0.35288	0.27907		
	6000	2.25968	0.79687	0.52040	0.41983	0.37156	0.33995	0.31499	0.29652	0.25130		

The effective thicknesses can be calculated by means of Eqs. (6.46) and (6.48), which are valid for both the one-dimensional (beam) and two-dimensional (plate) case.

In certain specific cases, it may be necessary to calculate the stresses at the interface between one of the glass plates and the polymer interlayer. This may occur, for example, in cases where the glass layers have different mechanical strengths and it is thus necessary to verify the resistance of both plates to the maximum *tensile* strength acting on each one. Indeed, when the plates are not perfectly

coupled, the stress diagram is of the type illustrated in Figure 6.16, and, hence, stresses at the interface  $|\sigma|_{\max INT_i}$  may become significant.

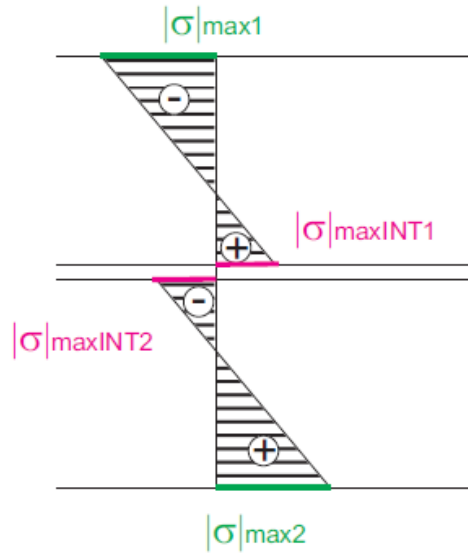


Figure 6.16. Typical stress diagram for a laminated glass plate.

The maximum stresses at the interface on the  $i^{\text{th}}$  layer are given by

$$\sigma_{i,\max} = \max_x \frac{|M(x)|}{b \hat{h}_{INT1;\sigma}^2} = \max_x \left| \frac{N_i(x)}{A_i} \mp \frac{M_i(x)}{I_i} \frac{h_i}{2} \right|. \quad (6.56)$$

It can therefore be shown that the effective thicknesses for calculating the maximum stresses at the interface in plate 1 and in plate 2 take the following form:

$$\hat{h}_{INT1;\sigma} = \sqrt{\frac{1}{\left| \frac{2\eta h_{s;2}}{h_1^3 + h_2^3 + 12I_s} - \frac{h_1}{\hat{h}_w^3} \right|}}, \quad \hat{h}_{INT2;\sigma} = \sqrt{\frac{1}{\left| \frac{2\eta h_{s;1}}{h_1^3 + h_2^3 + 12I_s} - \frac{h_2}{\hat{h}_w^3} \right|}}. \quad (6.57)$$

It must be pointed out that the use of these approximate models must always (and without exceptions) be restricted to the calculation of the maximum stress at the centre of the plate and to the estimation of maximum bending. Specifically, it is critically important to avoid the practice – sometimes carelessly adopted in design – of using effective thickness methods for the calculation of local effects, such as stress concentrations in proximity to holes or cut-outs.

### 6.3.3.2 Level 2

At this level, a simplified multilayer model is used, in which the deformation of the glass plates is considered to be due to bending only, and the interlayer is modelled by means of a layer of equivalent shear-deformable springs. The model is derived from the one introduced by Newmark [Newmark *et al.*, 1951], for composite steel/concrete beams with shear connectors. According to the actual boundary conditions, glass elements can be modelled as beams or elastic shells. Various authors have used this approach for both beam and plate elements, using linear constitutive laws for springs. The shear-deformable springs which simulate the interlayer may also be modelled as viscoelastic elements. In

the case of beam elements, it is possible to obtain solutions in closed form also for glass elements with several layers and for moderate geometric non-linearities.

In more geometrically complex cases it is possible to use two-dimensional numerical models of multilayer glass plates, wherever it is possible to introduce the layer of shear-deformable springs without imposing the rigid rotation of the director. Two-dimensional shell elements may be used when it is shown that they are capable of give accurate results in large displacements non-linear analyses. The considered elements must adequately take into account the shear deformability of the individual layer, because the transversal deformability of the interlayer may influence the overall response of the plate.

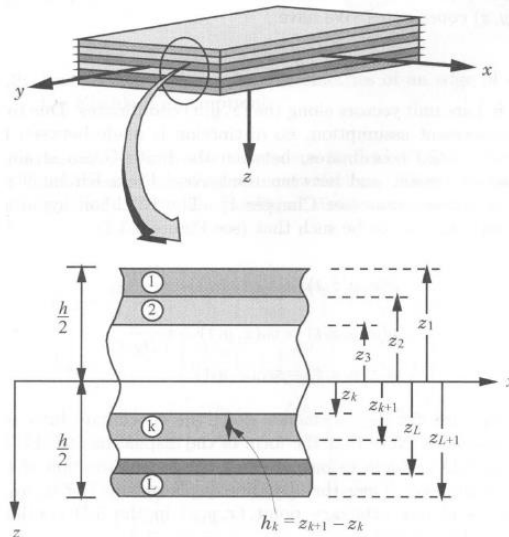


Figure 6.17. Modelling of a laminated panel.

### 6.3.3.3 Level 3

In the case of three-dimensional modelling, the domain of the laminated plate may be discretised by means of solid elements with 8 - 20 nodes. The mesh must be defined in such a way as to satisfy the requirements laid down for monolithic glass (see Section 6.3.2.3).

For glass plates, it is recommended to use solid elements with incompatible modes, a formulation which improves the accuracy in the calculation of flexural behaviour, while the interlayer can be modelled by using incompatible mode elements in a hybrid formulation. For the interlayer, the choice of the hybrid formulation depends on the characteristics of the material, as the polymers are virtually incompressible (high Poisson's ratio). The connection between the glass plates and the interlayer can be modelled by means of a kinematic constraint preventing the displacements with respect to the interface between the various layers or by means of a suitable interface element which allows to simulate delamination. In order to allow shear slip in the interlayer, 3-4 elements must be arranged across its thickness, according to the type of element adopted. This constitutes a great challenge, because it usually implies a large number of nodes.

With respect to geometric non-linearities, the indications for monolithic glass (see Section 6.3.2.2) also apply here.

## 6.3.4 Insulating glass units

### 6.3.4.1 General remarks and definitions

Insulating glass consists of an assemblage of two or more panels, separated from each other around their edges by a spacer (usually an extruded aluminium profile) containing salts (molecular sieves) to dry the air, specifically designed to obtain a dehumidified air cavity between the panes (product standards UNI EN 1279). Various procedures for sealing the edges in polymer material (for example hot extruded butyl, mixtures of polysulphides, polyurethanes or silicones) impede air exchange with the external environment.

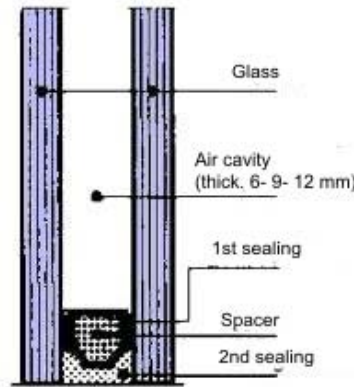


Figure 6.18. Cross-section of an insulating glass unit (detail).

The plates may be made of:

- monolithic glass (annealed, hardened or toughened);
- laminated glass;
- a combination of monolithic and laminated glass.

This type of panel provides various levels of thermal and acoustic insulation with energy and light performance in relation to the types of glass used, that are far superior to those of a single pane of glass. In particular, if the insulating glass unit consists of a laminated glass plate, it ensures particularly good sound insulation. To achieve higher thermal insulation values, inert gases (such as Argon, Krypton or Xenon) may be injected into the cavity.

#### 6.3.4.2 Type of modelling

Glass plates can be modelled as described in previous sections according to the type of glass (i.e. monolithic or laminated). The cavity can be modelled as a perfect gas or, in any case, as an elastic medium so that the interaction and transfer of loads between the panes can be taken into consideration.

#### 6.3.4.3 Type of analysis

With regard to the glass plates, the type of analysis is analogous to the one described in Sections 6.3.2 and 6.3.3. In the case of insulating glass units, stresses must be calculated in each plate. Nevertheless, insulating glass units exhibit a number of peculiarities compared with the cases considered above. Specifically, the effects of the presence of the hermetic seal and the quantity of gas in the cavity need to be considered by taking into account the following aspects:

- the presence of the fixed quantity of gas causing actions which are applied to only one pane to develop effects in the other panes in the insulating glass unit (a phenomenon also known as *load sharing*);
- changes in ambient barometric pressure conditions relative to the barometric pressure at the time of sealing the insulating glass unit, causing actions (internal actions) which develop effects in all the panes ;

- changes in the temperature of the gas in the cavity causing actions (internal actions) which develop effects in all the panes.

### 6.3.4.4 Load sharing

Let us consider the insulating glass unit illustrated in Figure 6.19, consisting of two plates of thickness  $h_1$  (outer pane) and  $h_2$  (inner pane) and with a cavity of thickness  $s$ , subjected to a uniformly distributed static load  $F_d$  (self-weight, wind, snow, etc.). The sharing of the load between the two panes essentially depends on the relationship between their stiffnesses partition,  $\delta_1$  and  $\delta_2$ . Assuming a beam behaviour, at least as an initial approximation, we have:

$$\delta_1 = \frac{h_1^3}{h_1^3 + h_2^3}, \quad \delta_2 = \frac{h_2^3}{h_1^3 + h_2^3} = 1 - \delta_1, \tag{6.58}$$

and the insulating unit factor  $\varphi$  in the following form:

$$\varphi = \frac{1}{1 + \left(\frac{a}{a^*}\right)^4} \tag{6.59}$$

In this equation  $a$  is the actual dimension of the element, which for rectangular elements supported on all sides is equal to the length of the shortest side, while  $a^*$  is the characteristic length of the element, dependent on the thicknesses of the glass plates  $h_1$  and  $h_2$ , on the gas space  $s$  and on the shape of the unit, according to an equation of the following type:

$$a^* = 28.9 \cdot \left( \frac{s \cdot h_1^3 \cdot h_2^3}{(h_1^3 + h_2^3) \cdot k_5} \right)^{0.25} \tag{6.60}$$

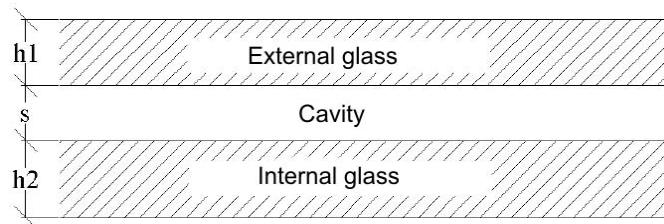


Figure 6.19. Cross-section of an insulating glass unit.

Through the pressure of the cavity, the load  $F_d$  is distributed on both of the plates according to the contributions  $F_{d;1}$  and  $F_{d;2}$ , that may be evaluated according to the load application, the insulating unit factor  $\varphi$  and the stiffnesses partition, as indicated in Table 6.5.

Table 6.5. Load sharing for insulated glazed units.

Load	Plate under load	Load shared by plate 1	Load shared by plate 2
$F_d$	1 (outer)	$F_{d;1} = (\delta_1 + \varphi \cdot \delta_2) \cdot F_d$	$F_{d;2} = (1 - \varphi) \cdot \delta_2 \cdot F_d$
	2 (inner)	$F_{d;1} = (1 - \varphi) \cdot \delta_1 \cdot F_d$	$F_{d;2} = (\varphi \cdot \delta_1 + \delta_2) \cdot F_d$



The coefficient of volume  $k_5$  appearing in Eq. (6.60) is evaluated exclusively as a function of the aspect ratio  $\lambda$ , which in the case of a rectangular plate is equal to the ratio between the lengths of the two sides and assumes the values shown in Table 6.6 and graphically represented in Figure 6.20. Specific analyses must be performed for plates with non-rectangular shapes.

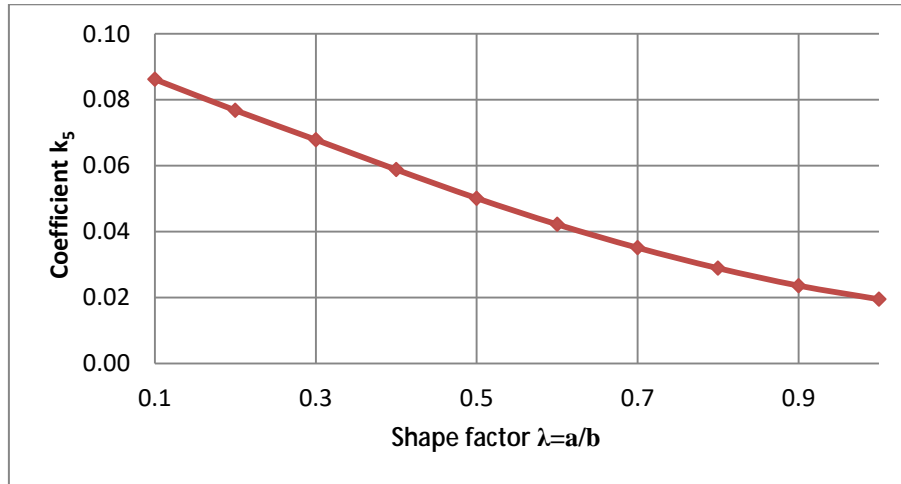


Figure 6.20. Values of the dimensionless coefficient  $k_5$ , as a function of the shape factor  $\lambda$ .

Table 6.6. Values of the coefficient  $k_5$  for the calculation of change in volume of the gas.

$\lambda = a/b$	1.0	0.9	0.8	0.7	0.6	0.5	0.4	0.3	0.2	0.1
$k_5$	0.01947	0.02362	0.02891	0.03511	0.04220	0.05014	0.05883	0.06789	0.07681	0.08621
where:	$k_5 = \left[ \frac{z_1}{16\lambda^2} \right] \cdot \left[ 0.4198 + 0.22 \cdot \exp(-6.8 \cdot (\lambda)^{1.33}) \right],$ $z_1 = 192(1 - \nu^2) \lambda^2 \left[ 0.00406 + 0.00896 \left( 1 - \exp\left( -1.123 \left( \frac{1}{\lambda} - 1 \right)^{1.097} \right) \right) \right].$									

The values of the coefficient  $k_5$  provided in Table 6.6 are valid for Poisson’s ratio  $\nu$  between 0.20 and 0.24. If necessary, these values can be interpolated linearly. For other boundary conditions and for non-rectangular elements, specific analyses are necessary.

### 6.3.4.5 Internal loads

In insulating glass units, the presence of gas in the cavity causes internal actions which have effects in all of the plates. In an insulating glass unit consisting of two plates with thicknesses  $h_1$  (outer pane) and  $h_2$  (inner pane), with  $s$  the thickness of the cavity (Figure 6.19), the internal actions caused by the isochoric pressure  $p_i$  on each plate can be calculated as a function of their flexibility, thickness and shape by multiplying the pressure  $p_i$  by the insulating glass unit factor  $\varphi$  (Table 6.7).

Table 6.7. Internal loads due to internal pressure  $p_0$ .

Isochoric pressure	Load shared by plate 1	Load shared by plate 2
$p_i$	$-\varphi \cdot p_i$	$\varphi \cdot p_i$

The factor  $\varphi$  is calculated as illustrated in Section 6.3.4.4.

The isochoric pressure  $p_i$  generated by a change in weather conditions can be evaluated with the expression

$$p_i = p_{H;0} + p_{C;0}, \quad (6.61)$$

where  $p_{H;0}$  represents the isochoric pressure generated by a change in altitude (between the place of manufacture and the place of installation of the insulating glass unit), which can be calculated by means of the following equation

$$p_{H;0} = c_H \cdot (H - H_p), \quad (6.62)$$

where:

$H_p$  altitude of production of the insulating glass unit [m];

$H$  altitude of installation of the insulating glass unit [m];

$c_H = 0.012$  kPa/m.

In Eq. (6.61),  $p_{C;0}$  represents the isochoric pressure generated by a change in temperature and/or pressure, which can be expressed in the form

$$p_{C;0} = c_T \cdot (T_i - T_p) - (p - p_p), \quad (6.63)$$

where:

$T_p$  temperature in the place of production of the insulating glass unit [K];

$p_p$  pressure in the place of production of the insulating glass unit [kPa];

$T_i$  temperature in the place of installation of the insulating glass unit [K];

$p$  pressure in the place of installation of the insulating glass unit [kPa];

$c_T = 0.34$  kPa/K.

In the absence of precise indications, conservative values of  $p_p$  and  $p$  shall be used.

## 6.4 Buckling phenomena

### 6.4.1 General remarks and definitions

Given their high degree of slenderness, glass elements subject to compressive or bending loads must be verified with regard to potential failure as a result of buckling.

Buckling phenomena of structural glass elements are strongly influenced by:

- boundary conditions (fixing mechanism);
- manufacturing tolerances (thickness of glass, flatness, etc.) and installation tolerances;
- eccentricity of loads;
- initial flaws;
- material used for the interlayer (in the case of laminated glass);
- the viscoelastic behaviour of polymer interlayers (in the case of laminated glass).

Because of the intrinsic fragility of glass, this type of collapse can lead to catastrophic failure of the plates.

## 6.4.2 Buckling calculation of glass elements under compression

This section provides equations for the calculation of the critical buckling load and maximum stress and deflection in monolithic or laminated glass elements under compression. These equations may be applied only in well-defined cases from a structural point of view, that can be schematically represented with a beam-based model.

### 6.4.2.1 Monolithic glass

A beam subjected to axial loading, as illustrated in Figure 6.21, is considered. The stability of the compressed beam must be verified according to the following equation:

$$N_{Ed} \leq N_{b,Rd} \quad , \quad (6.64)$$

where

$N_{Ed}$  design compressive axial load;  
 $N_{b,Rd}$  compressed laminated glass beam buckling resistance, defined by

$$N_{b,Rd} = \chi A f_{g;d} \quad , \quad (6.65)$$

where

$\chi$  reduction factor;  
 $A$  cross-sectional area of the element;  
 $f_{g;d}$  design tensile strength of the material, to be evaluated as in Eq. (7.5).

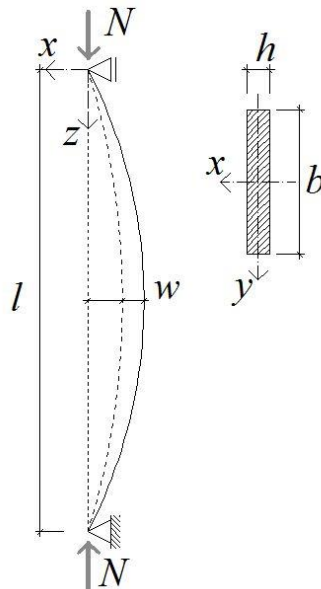


Figure 6.21. End-loaded glass beam.

For the buckling verification of compressed monolithic glass beams, the value of the reduction factor has the form

$$\chi = \frac{1}{\Phi + \sqrt{\Phi^2 - \bar{\lambda}^2}}, \text{ con } \chi \leq 1 \quad (6.66)$$

where

$$\Phi = 0.5 \left[ 1 + \alpha^* (\bar{\lambda} - \alpha_0) + \bar{\lambda}^2 \right], \quad (6.67)$$

with

$\alpha^* = 0.71$ : imperfection factor,

$\alpha_0 = 0.60$ : coefficient delimiting the curve branch in which  $\chi = 1$ ,

having defined the following quantities:

normalised slenderness of the element 
$$\bar{\lambda} = \sqrt{\frac{A f_{g;k;st}}{N_{cr}^{(E)}}}; \quad (6.68)$$

Euler critical load of the element 
$$N_{cr}^{(E)} = \frac{\pi^2 EJ}{l^2}; \quad (6.69)$$

$f_{g;k;st}$  characteristic tensile strength of glass, to be considered in buckling verifications, calculated as

$$f_{g;k;st} = k_{mod} k_{ed} k_{sf} \lambda_{gA} \lambda_{gl} f_{g;k} + k'_{ed} k_v (f_{b;k} - f_{g;k}), \quad (6.70)$$

where

$f_{g;k}$  characteristic value of tensile bending strength of annealed glass (in common cases, UNI EN 572-1 may be applied);

$f_{b;k}$  characteristic value of tensile bending strength of glass due strengthening treatment (Table 7.7);

$k_{mod}$  strength reduction factor, dependent on the load duration and environmental conditions, as defined in Sections 2.1.1.2 and 5.4.2; the values of  $k_{mod}$  for certain load durations (actions constant in time) are shown in Table 2.2.

The coefficients  $k_{ed}$ ,  $k_{sf}$ ,  $\lambda_{gA}$ ,  $\lambda_{gl}$ ,  $k'_{ed}$ ,  $k_v$ , are defined in Section 7.4.

$E$  Young's modulus of glass;

$J = \frac{bh^3}{12}$  moment of inertia of the cross-section with respect to the plane in which bending occurs.

#### 6.4.2.2 Laminated glass

For the analysis of laminated glass elements subjected to compressive axial loads, it is useful to introduce the notion of equivalent thickness, i.e. the thickness of monolithic glass with equivalent flexural properties to the laminated glass.

Consider a laminated glass element of width  $b$  and effective buckling length  $l$ . Assuming that the laminated glass consists of two glass plates of thicknesses  $h_1$  and  $h_2$ , bonded by an interlayer of thickness  $h_{int}$ , verification of the stability of the compressed laminated glass beam is performed on the basis of Eq. (6.64). In this case, the Euler critical load of the element is defined as

$$N_{cr}^{(E)} = \frac{\pi^2 EJ_{eq}}{l^2}, \quad (6.71)$$

where

$$J_{eq} = bh_{ef;w}^3/12, \quad (6.72)$$

where the deflection-effective thickness, according to the Wölfel-Bennison model illustrated in Section 6.3.3.1, is given by

$$h_{ef;w} = \sqrt[3]{h_1^3 + h_2^3 + 12\Gamma_b I_s}, \quad (6.73)$$

and the shear transfer coefficient for buckling verification is given by:

$$\Gamma_b = \frac{1}{1 + \pi^2 \beta \frac{h_{int} EI_s}{G_{int} \xi^2 d^2}}, \quad (6.74)$$

where

$$\beta = 1, \xi = l, \quad (6.75)$$

while  $I_s$  and  $d$  are given, respectively, by Eqs. (6.41) and (6.37).

In these expressions,  $G_{int}$  represents the shear elastic modulus of the interlayer, dependent on load duration and temperature.

In this case, the design compressive axial load of the compressed beam  $N_{b,Rd}$ , defined by (6.65), must be calculated as a function of the total area  $A$ , which is representative of the sum of the cross-sectional areas of the glass plated only. The same area  $A$  must also be taken into consideration in calculating the normalised slenderness of the laminated element, as suggested by Eq. (6.68).

### 6.4.2.3 Insulating glass units

The behaviour of an insulating glass unit consisting of two monolithic glass plates and subjected to end-loading can be analysed as illustrated in Section 6.3.4 above. A fraction  $N_i$  of the total compressive load  $N$  is carried by each plate, where  $N_i$  is given by

$$N_i = N \frac{A_i}{A_{tot}}, \quad (6.76)$$

where  $A_i$  is the area of the cross-section of the  $i^{\text{th}}$  plate, and  $A_{tot}$  the total area of the plates. Buckling verification of an insulating glass unit under compressive loads can be partitioned into verifications of the individual plates, each one subject to a compression  $N_{Ed} = N_i$ .

Verification is considered to be satisfied if, for the glass plate placed under the higher fraction of axial load, the condition stated in Eq. (6.64) is satisfied. If one or both of the glass plates are laminated, the factors described in Section 6.4.2.2 are taken into account.

### 6.4.3 Elements under bending: lateral-torsional buckling verification

A beam under bending moment may exhibit a lateral-torsional instability. The typical deformed configuration is characterised by lateral bending and torsional rotation (Figure 6.22). For glass elements, lateral-torsional instability constitutes the typical instability mode for beams and fins.

The sections that follow contain simplified formulas for the evaluation of the critical moment for lateral-torsional buckling of rectangular sections of monolithic or laminated glass, as well as a number of useful recommendations for finite element modelling and numerical analysis.

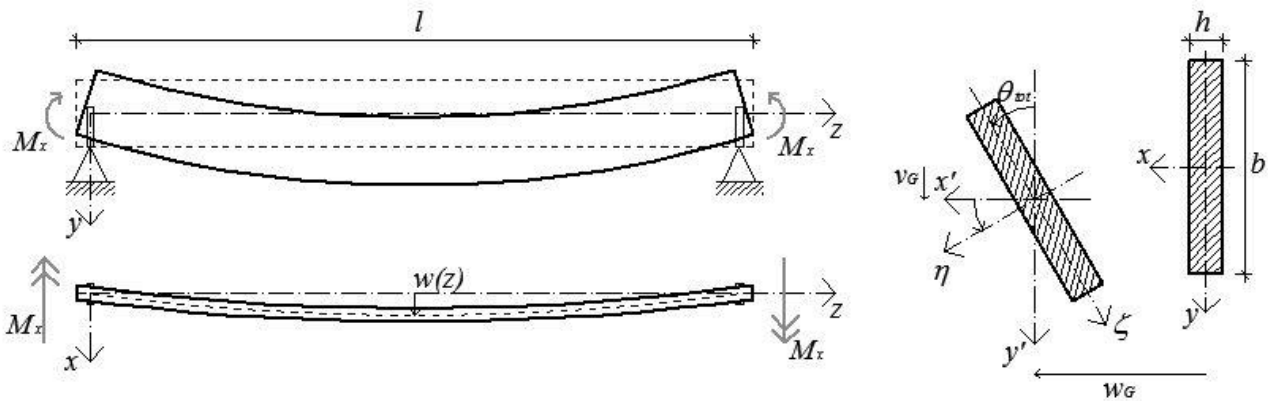


Figure 6.22. Flexural-torsional deformation of a beam element.

#### 6.4.3.1 Monolithic glass

The lateral-torsional stability of a beam must be verified according to the equation

$$M_{Ed} \leq M_{b,Rd} \tag{6.77}$$

where

$M_{Ed}$  constant design bending moment due to the external load;  
 $M_{b,Rd}$  beam buckling strength (bending moment causing buckling), to be calculated as

$$M_{b,Rd} = \chi_{LT} M_R \tag{6.78}$$

with

$\chi_{LT}$  reduction factor for lateral-torsional stability;  
 $M_R = W_x f_{g;d}$  elastic resisting bending moment;  
 $W_x = b^2 h / 6$  section (elastic) modulus;  
 $f_{g;d}$  tensile strength of the material, as defined in Eq. (7.5).

For the lateral-torsional buckling verification of monolithic glass beams under bending, the value of the coefficient  $\chi_{LT}$  must be calculated with an equation analogous to Eq. (6.66), where  $\Phi$  is similarly defined by Eq. (6.67), with

$\alpha^* = 0.26$ , imperfection factor;

$\alpha_0 = 0.20$ , coefficient delimiting the curve branch in which  $\chi_{LT} = \chi = 1$ .

The normalised slenderness of the element, in this case, is given by

$$\bar{\lambda} = \bar{\lambda}_{LT} = \sqrt{\frac{W_x f_{g;k;st}}{M_{cr}^{(E)}}}, \tag{6.79}$$

$$M_{cr}^{(E)} = C_1 \frac{\pi}{l} \sqrt{EJ_y GJ_t}, \tag{6.80}$$

with

$f_{g;k;st}$  characteristic tensile strength, to be considered in buckling verifications, as defined in Section 6.4.2.1, Eq. (6.70);

$J_y$  moment of inertia with respect to the y axis in Figure 6.22;

$GJ_t = Gbh^3/3$  torsional stiffness;

$G$  shear elastic modulus of the glass;

$C_1$  coefficient dependent on the distribution of the bending moment, according to Table 6.8.

Table 6.8. Factor  $C_1$  as a function of distribution of the bending moment.

<i>Distribution of the bending moment</i>	$C_1$
Constant	1.00
Bilinear (zero at beam mid point)	2.70
Parabolic (zero at both ends and maximum at the centre)	1.13
Triangular (zero at both ends and maximum at the centre)	1.36

### 6.4.3.2 Laminated glass

The critical bending moment characterising the lateral-torsional buckling in a laminated glass beam (or fin) can be calculated, as in the case of compressed elements, with reference to the effective thickness model, by using Eq. (6.73). In this context, in order to adequately take into account the connection offered by the interlayer, its torsional stiffness may be appropriately evaluated by means of an equivalent torsional stiffness  $G J_{t,int}$ , derived from the theory of sandwich panels.

Lateral-torsional buckling verification of a laminated element of dimensions  $b \times l$ , consisting of two glass plates (of thicknesses  $h_1$  and  $h_2$ ) and an interlayer (of thickness  $h_{int}$ ) requires that the condition in Eq. (6.77) be satisfied.

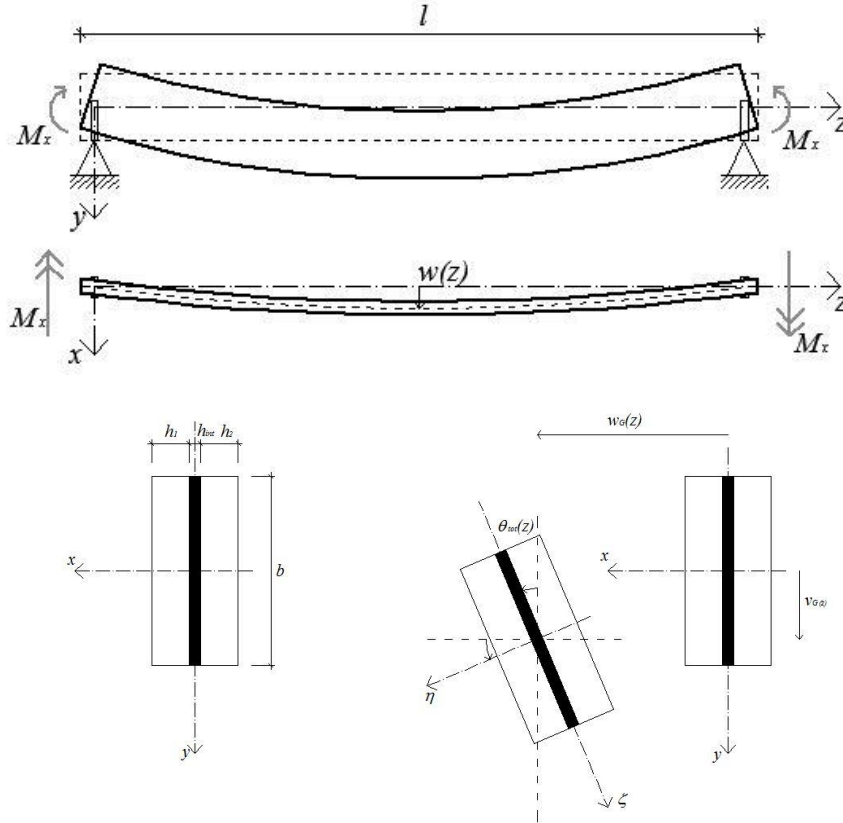


Figure 6.23. Flexural-torsional buckling of a laminated glass beam.

The Euler critical load of the element, in this case, is defined as

$$M_{cr}^{(E)} = C_1 \frac{\pi}{l} \sqrt{EJ_{eq} GJ_{t,tot}} \quad (6.81)$$

where:

$C_1$  correction factor (Table 6.8);

$J_{eq}$  effective moment of inertia with respect to the y axis as defined by Eq. (6.72);

$J_{t,tot} = J_{t,1} + J_{t,2} + J_{t,int}$  torsional moment of inertia of the cross-section;

$J_{t,1} = bh_1^3/3, J_{t,2} = bh_2^3/3$  torsional moment of inertia of each monolithic glass plate;

$J_{t,int} = 4 d^2 A^* \left( 1 - \frac{\tanh \frac{\lambda b}{2}}{\frac{\lambda b}{2}} \right)$  torsional moment of inertia of the interlayer, where

$b$  width of the beam;

$d$  and  $A^*$  defined by Eq. (6.37);

$$\lambda = \sqrt{\frac{G_{int}}{G} \frac{h_1 + h_2}{h_1 h_2 h_{int}}}$$

In this case, in calculating the elastic resisting bending moment  $M_R$  of the laminated beam under bending (Eq. (6.78)) and the normalised slenderness of the element (Eq. (6.79)), the section (elastic)



modulus  $W_x$  is defined as a function of a thickness representing the sum of the thicknesses of the glass plates only, i.e.,  $h = h_1 + h_2$ .

## 6.4.4 Buckling of glass panels

### 6.4.4.1 In-plane compressions

#### 6.4.4.1.1 Monolithic glass

With reference to Figure 6.24, a monolithic glass panel is considered, with thickness  $h$ , perfectly flat, simply supported along the edges and subjected to in-plane compression  $N_y = N_{Ed} = \sigma_y h$ .

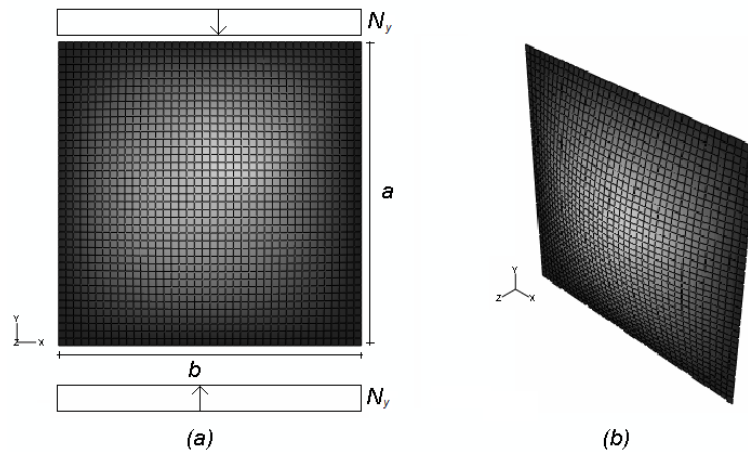


Figure 6.24. Panel simply supported along the edges subjected to in-plane compression.

Under the hypotheses that:

- the undeformed configuration of the panel is flat;
- displacements in the  $x, y$  plane along the edges of the panel are negligible;
- shear deformations in the panel can be neglected;

and by assuming  $N_x = N_{yx} = N_{xy} = 0$ , buckling verification of the compressed element consists in requiring that condition given by Eq. (6.64) is respected, with imperfection factor  $\alpha^* = 0.49$  and  $\alpha_0 = 0.80$ . In this case, the Euler critical load is:

$$N_{cr}^{(E)} = \left( \frac{mb}{a} + \frac{a}{mb} \right)^2 \frac{\pi^2 D}{b^2} = k_\sigma \frac{\pi^2 D}{b^2}, \quad (6.82)$$

where:

$$k_\sigma = \left( \frac{mb}{a} + \frac{a}{mb} \right)^2 \text{ stability coefficient}; \quad (6.83)$$

$$D = \frac{Eh^3}{12(1-\nu^2)} \text{ flexural stiffness of the element, per unit of length}; \quad (6.84)$$

$m$  = number of semi-waves in direction  $y$ , to be assumed in such a way that the buckling load is minimum (usually  $m = 1$ ).

If the monolithic glass panel is not supported along all the edges, the buckling load can be calculated by means of Eq. (6.82), by assuming for the coefficient  $k_\sigma$  the values provided in Figure 6.25.

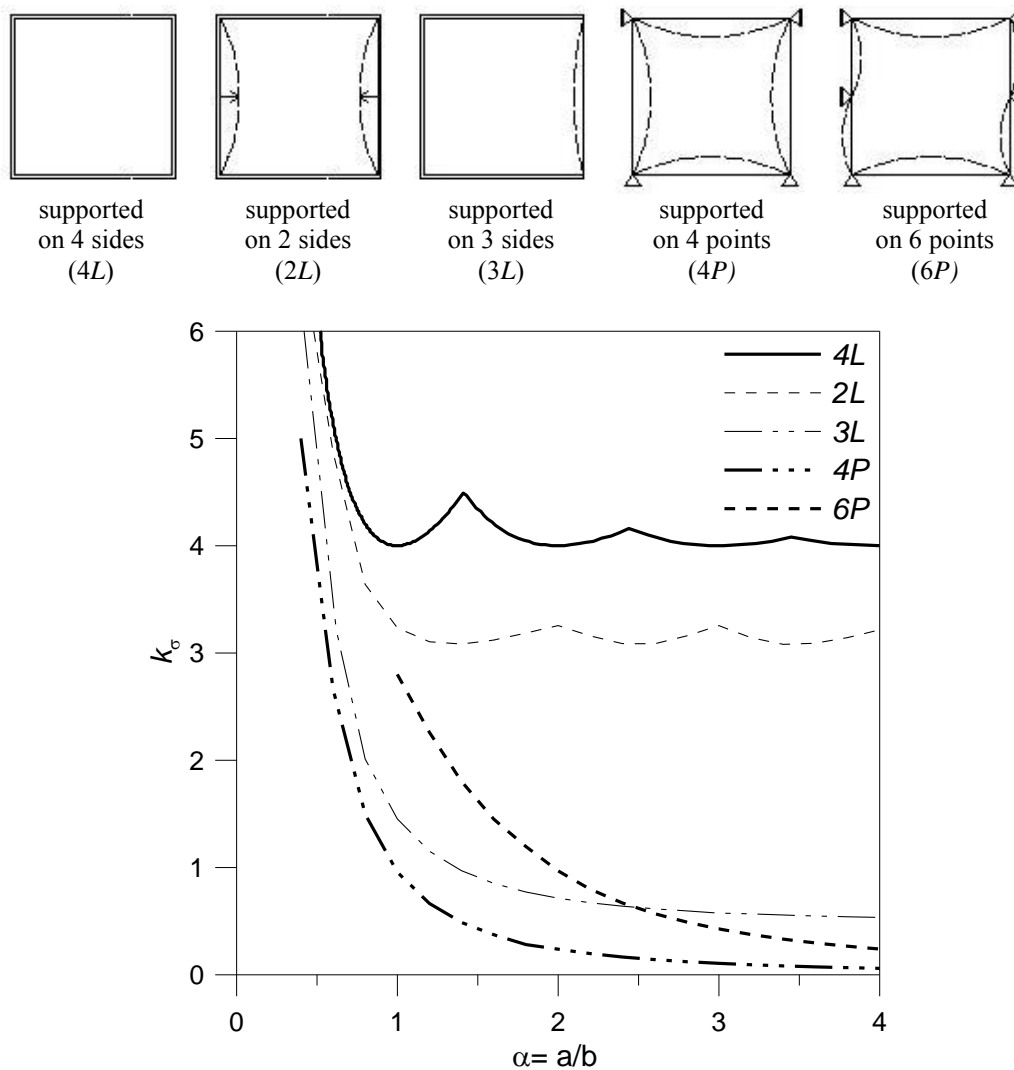


Figure 6.25. Coefficient  $k_\sigma$  for panels compressed in-plane in different support conditions.

The verification is thus considered to be satisfied if the condition given by Eq. (6.64) is respected.

#### 6.4.4.1.2 Laminated glass

Let us now consider a laminated glass panel (of dimensions  $a \times b$ ), consisting of two monolithic glass plates of thicknesses  $h_1$  and  $h_2$  bonded by an interlayer of thickness  $h_{int}$ , simply supported along the edges and subjected to uniform in-plane compression (Figure 6.24).

Buckling verification of the element can be performed again by using Eq. (6.73) for the equivalent thickness, assuming in Eq. (6.74)

$$\beta = \left( \frac{1.06}{\lambda^2} + 1.06 \right), \quad \xi = \min(a, b), \tag{6.85}$$

where  $\lambda = a/b$  is the aspect ratio of the panel ( $\alpha > 1$ ).

The critical load for the panel may thus be calculated by means of Eq. (6.82), by assuming  $h = h_{ef,w}$ .

Buckling verification of the panel consists in requiring that the condition expressed by Eq. (6.64) is satisfied. In this case, the compressed laminated glass buckling resistance  $N_{b,Rd}$ , as defined in Eq. (6.65), must be calculated as a function of the total area  $A = b(h_1 + h_2)$ , representing the sum of the transversal areas of the glass plates only. The same area  $A$  must also be taken into consideration in the calculation of the normalised slenderness of the laminated element, as suggested by Eq. (6.68).

If the glass panel exhibits constraint conditions other than simple support along the edges, the critical load may be calculated by means of Eq. (6.82), by assuming for the coefficient  $k_\sigma$  the values provided in Figure 6.25. The calculation is considered to be satisfied if the limitation represented by Eq. (6.64) is respected.

#### 6.4.4.1.3 Insulating glass

If the panel under in-plane compression consists of insulating glass, to verify its buckling resistance reference may be made, on the safe side, to the instructions set out in Sections 6.4.4.1.1 (monolithic glass) or 6.4.4.1.2 (laminated glass) for the buckling verification of the single plate.

#### 6.4.4.2 In-plane shear stress

##### 6.4.4.2.1 Monolithic glass

With reference to Figure 6.26, let us now consider a monolithic glass flat plane (with thickness  $h$  and elastic modulus  $E$ ), simply supported along its edges and subjected to shear forces  $N_{xy} = \tau_{xy} h = V_{Ed}$ .

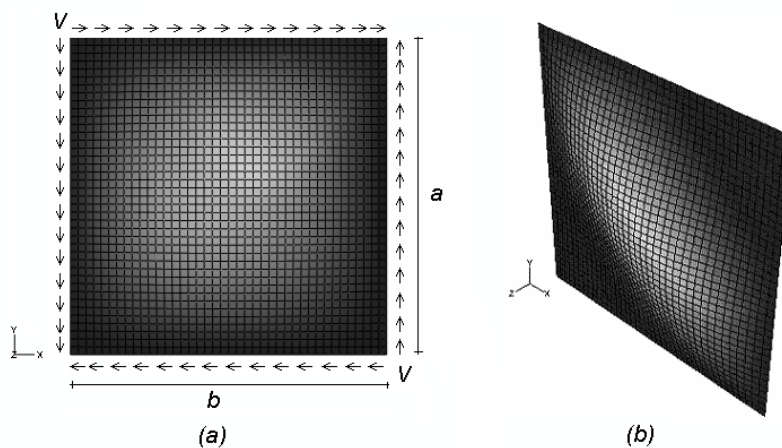


Figure 6.26. Panel supported along its edges and subjected to in-plane shear forces.

The buckling verification of the panel under shear load must be performed by means of the equation

$$V_{Ed} \leq V_{b,Rd}, \tag{6.86}$$

where

$V_{Ed}$ : design shear force per unit length;

$V_{b,Rd}$ : elastic resisting shear force per unit length of the panel, to be calculated by means of the equation

$$V_{b,Rd} = \chi A \tau_{g;d} \quad (6.87)$$

in which

$\chi$  reduction factor as per Eq. (6.66);  
 $\alpha^* = 0.49$  imperfection factor to consider in the calculation of  $\chi$  (Eq. (6.66));  
 $\alpha_0 = 0.50$  coefficient delimiting the curve section in which  $\chi = 1$  as per Eq. (6.66);  
 $A = bh$  resisting area;  
 $\tau_{g;d}$  design shear strength of the material. For buckling verification,  $\tau_{g;d} = f_{g;d}$  can be assumed, as defined in Section 6.4.2.1, or in Eq. (7.5).

In order to perform the buckling assessment of the panel, the value of the reduction factor  $\chi$  must be calculated by assuming in Eq. (6.66) a normalised slenderness of the element equal to

$$\bar{\lambda} = \sqrt{\frac{A \tau_{g;k;st}}{V_{cr}^{(E)}}} \quad (6.88)$$

with

$\tau_{g;k;st}$  characteristic shear strength of the material to consider in buckling calculations. For this purpose we may assume  $\tau_{g;k;st} = f_{g;k;st}$  (Eq. (6.68));

$$V_{cr}^{(E)} = \frac{\pi^2 D}{b^2} k_\tau \quad \text{Euler critical shear stress in the element;} \quad (6.89)$$

$D$  flexural stiffness of the element, defined in Eq. (6.84);

$$k_\tau = \begin{cases} 4.00 + \frac{5.34}{(a/b)^2} & \text{per } a/b < 1, \\ 5.34 + \frac{4.00}{(a/b)^2} & \text{per } a/b \geq 1. \end{cases} \quad \text{stability coefficient.} \quad (6.90)$$

#### 6.4.4.2.2 Laminated glass

Let us now consider a laminated glass panel (of dimensions  $a \times b$ ) consisting of two monolithic glass plates of thicknesses  $h_1$  and  $h_2$  bonded by an interlayer of thickness  $h_{int}$ , simply supported along the edges and subjected to an in-plane shear load (Figure 6.26).

Buckling verification of the element can be performed, again, in accordance with the effective thickness method (Eq. (6.72)), by assuming, for this case, in place of Eq. (6.75), the equations

$$\beta = \left( \frac{5.25}{\lambda^2} + 7.32 \right), \quad \xi = \min(a, b), \quad (6.91)$$

where  $\lambda = a/b$  is the aspect ratio of the panel ( $\alpha > 1$ ).

The critical load for the panel may thus be calculated by means of Eq. (6.82), by assuming  $h = h_{ef,w}$ . Buckling calculation of the panel consists in requiring that the condition expressed in Eq. (6.64) is satisfied. In this case, the buckling resistant shear force per unit length for the laminated panel  $V_{b,Rd}$ , as defined by Eq. (6.87), must be calculated as a function of the total area  $A = b(h_1 + h_2)$ , representing the sum of the transversal areas of the glass plates only. The same area  $A$  must also be taken into consideration in the calculation of the normalised slenderness of the laminated element, as suggested by Eq. (6.88).

#### **6.4.4.2.3 Insulating glass**

If the panel subjected to in-plane shear consists of insulating glass, to verify its stability reference may be made, on the safe side, to the instructions set out in Sections 6.4.4.1.1 (monolithic glass) or 6.4.4.1.2 (laminated glass) for verification of the individual plate.

### **6.5 Post-glass-breakage behaviour**

As extensively discussed in Section 3.1, the fail-safe requirement is predominant in structural glass design. Wherever breakage of the glass may lead to situations which pose a danger to the safety of users (falls from height, injuries due to contact with sharp fragments, etc.), a calculation shall evaluate the behaviour of the element after the total or partial breakage of glass panes. Obviously, prior to this evaluation, a risk analysis of the possible consequences for users of any breakage must be conducted, in order to decide when and under what conditions (i.e. partial or total breakage) it is necessary to conduct a post-glass-breakage calculation.

The matter is certainly of crucial importance from the point of view of the structural safety. Unfortunately, however, existing standards and regulations only marginally deal with this issue.<sup>14</sup> Nevertheless, more recent documents must place post-breakage behaviour at the foundation of any safety verification, in accordance with the modern fail-safe-design approach.

The post-breakage behaviour of glass is an extremely complex issue and continues to be a subject of study. In general, calculation models are not as well established as models that describe the behaviour of sound elements. As a consequence, it is recommended that predictions concerning post-breakage behaviour provided by a model are always corroborated by experimental tests on reduced- or full-scale samples.

#### **6.5.1 General remarks**

The fail-safe approach must consider the partial or total fragmentation of glass components as a result of unexpected actions (chance or exceptional events, acts of vandalism, accidents, etc.). Its goal is therefore to verify that, even in such limit conditions, the element can maintain sufficient load-bearing capacity to withstand self weight and dead loads, as well as the fraction of the live loads to which the element may be subjected upon breakage due to a chance event, thereby preventing danger from falling materials. It is therefore essential, among other things, to verify the capacity of the constraints to absorb the major deformations which are generally caused by the lack of stiffness of glass elements in the post-breakage phase.

---

<sup>14</sup> In mechanical engineering, the fail-safe requirement is a basic concept, acknowledged by a very large number of standards and regulations. In civil engineering, given the structural ductility of materials commonly used in buildings (steel, reinforced concrete, etc.), this requirement is not precisely specified. In the case of glass, however, given the intrinsic brittleness of the material, exceptions exist. For example, the French standard PS92 (seismic design of facades), is based on the risk associated with the potential consequences of breakage, and classifies the expected levels of structural performance on this basis, in certain cases prescribing a specific fail-safe structural requirement.

A structure can be said to be fail-safe if it is able to maintain its structural function, even just at a reduced level, if a part of it is damaged. With specific regard to the scope of this document, when a structure has a “relation” with human users and, moreover, it is made with a material such as glass, which may represent a potential danger for people, a glass structure may be defined as fail-safe when its collapse does not compromise the safety of users.

### **6.5.2 Monolithic glass**

Evaluation of post-breakage behaviour involves the estimation of size and shape of fragments. Generally, when heat-treated glass breaks, it produces smaller fragments than untreated glass. Annealed and heat-strengthened glass are virtually equivalent in this regard, whereas thermally toughened glass breaks almost completely into small parts. Chemically strengthened glass is an exception, as generally the fragments are smaller in size, but of the same order of magnitude as annealed and heat-strengthened glass fragments.

Estimation of the size of fragments formed after the breakage of thermally toughened glass can be made, as an initial approximation, by calculating the energy balance between the release of elastic energy stored as a result of the tempering process and the fracture energy necessary for the separation of the fragments themselves.

### **6.5.3 Laminated glass**

A large number of factors influence performance in the post-critical phase. The most important factors naturally include the type of glass used (toughened, hardened or annealed), the type of polymer interlayer (PVB, EVA, ionoplastic interlayers) and the restraint system.

The stiffness of a laminated panel after breakage of the glass is influenced in particular by [Silvestri, 2009]:

- the stiffness of the polymer interlayer, which obviously depends on type of polymer, characteristic load duration and temperature;
- size and shape of glass fragments, which are a function of type of glass used (annealed, hardened, thermally toughened or chemically strengthened), load type (impulsive, quasi-static, etc.), type of fixing mechanism, loading rate and glass thickness;
- glass-interlayer adhesion, which naturally plays a crucial role in terms of stiffness of the panel after breakage of the glass.

For the sake of convenience, reference may be made to the standard case of two glass plates bonded by an interlayer. In the failure behaviour of laminated glass panels, three stages can generally be observed (see the experiments by Kott and Vogel [Kott & Vogel, 2004(1); Kott & Vogel, 2004(2)]). During stage I, the glass plates forming the laminated package are still intact (Figure 6.27), and the classical Euler-Bernoulli hypotheses hold. Distribution of the tensile and compressive stresses in the glass cross-section is highly dependent on the mechanical properties of the interlayer material and, therefore, on its capacity to transfer shear actions from one plate to the other. The structural behaviour of the plate is accurately represented by sandwich plate theory. Stage I ends when, having reached the ultimate tensile strength of the glass, one of the plates breaks.

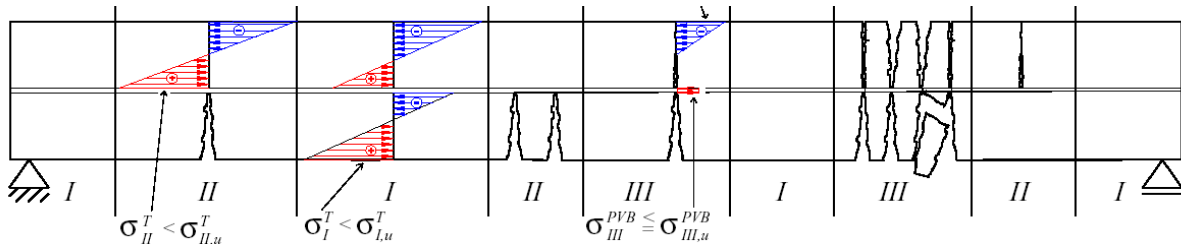
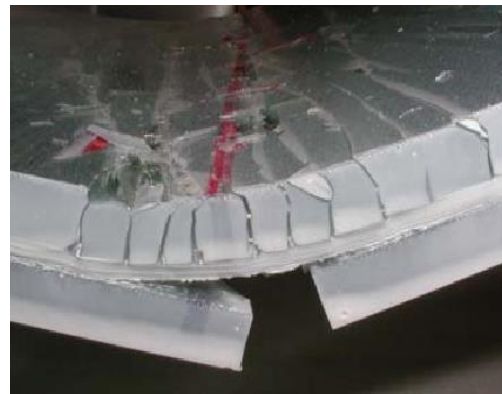
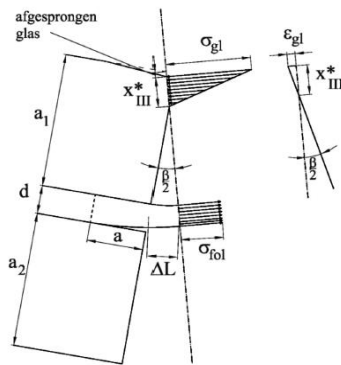


Figure 6.27. Resistant mechanisms in the post-breakage phase as a function of the degree of damage [Kott & Vogel, 2004(2)].

Breakage of the first plate may also occur in sections where internal actions do not exhibit their maximum values. Indeed, stress concentrations caused by defects on the surface of the glass plates as a result of transformation processes (cutting of the plates, etc.), may lead to glass independently of the actions. In the case of displacement-controlled tests, when stresses are compatible with the strength of the material, the whole of the load is carried by the plate remained intact (phase II, Figure 6.27). In this situation, the main role played by the interlayer is to retain the glass fragments. In addition, if the distance between the two cracked sections is sufficiently large, in the zone between the two cracks the polymer continues to transfer of shear forces. Analysis of phase II thus becomes important, especially when the glass breakage is due to accidental causes, such as impacts, explosions, etc. If, on the other hand, a stress-driven test is performed, the plates that have remained intact and are now overloaded break in a chain sequence, leading to the breakage of the whole element (phase III, Figure 6.27). The glass is no longer able to transfer the tensile loads, and thus only the polymer remains in place to guarantee equilibrium. In the compressed zone, the fragments of broken glass balance the internal compression forces, thanks to the contact actions (Figure 6.28). Thus, the residual load-bearing capacity is dependent on the size of the glass fragments that form the broken laminated element (types of glass used), and obviously on the location and type of the fracture path.



(a)

(b)

Figure 6.28. Post-breakage behaviour in proximity to a crack: (a) local model; (b) laminated glass in phase III, detail [Delincé *et al.*, 2008; Belis *et al.*, 2009].

The progressive load-increasing, or its cyclical repetition, leads to the loss of material in the compressed zone and therefore to a flexural stiffness decrease. In the extreme case of fractures extremely close to each other, the broken glass plates are able only to partially balance the compression actions, and the loads are carried almost exclusively by the polymeric interlayer. Depending on the type of glass used, the plates behave either like a tensioned membrane (in the case of thermally toughened glass) or like a system formed by pseudo-hinges positioned in proximity to the fracture lines and connected to each other by the still-intact areas of the laminated package (in the case of annealed, hardened and chemically strengthened glass).

Finally, for large displacements and large deformations of the interlayer, due to a high load or a prolonged uninterrupted load, the glass fragments are so spaced out that only the interlayer carries the

load, by means of a purely membrane-like mechanism. It should be pointed out that the interlayer is still tension-stiffened, if compared with the behaviour of an isolated interlayer material, by the presence of adhering fragments. Nevertheless, during this phase the interlayer deforms extensively, stretching in a viscoplastic manner, until it starts to tear at certain points, generally caused by the contact with the sharp edges of the glass, and, at this point, ultimate failure occurs.

The calculations may be referred to either phase II (with one plate broken) or phase III, with both plates broken (phase III on the left in Figure 6.27). If cyclical actions or exceptional loads are present, the element must in any case be verified in the event of complete shattering of the compressed glass (phase III on the right in Figure 6.27 and Figure 6.28b) and membrane behaviour of the interlayer only.

In the absence of additional analyses or specific experimental tests, as a first order approximation, reference may be made to the simplified model [Bennison, 2009]. After the glass breaks, it is the polymeric interlayer that gives the broken panel its stiffness, and the glass fragments contribute to stiffness *via* two mechanisms:

- they balance compression stresses through direct contact action between the fragments;
- they stiffen the polymer interlayer in the tensioned zone, with a mechanism similar to the tension-stiffening that occurs in reinforced concrete beams.

The stiffness of a fragmented laminated glass panel can therefore be estimated in a conventional manner [Bennison, 2009] by defining an effective elastic modulus  $E_{eff}$  for the damaged plates, which are assumed to be monolithic and of the same thickness as the interlayer only, in the following form

$$E_{eff} = k \frac{l^*}{\lambda^*} E_p \quad (6.92)$$

where

- $k$  constant of proportionality;
- $E_p$  elastic modulus of the interlayer [MPa];
- $l^*$  characteristic dimension of the fragments [mm];
- $\lambda^*$  characteristic length of loss of adhesion between glass and interlayer [mm].

Eq. (6.92) generally provides a lower bound for the stiffness of the panel, but in any case highlights the contribution of the glass fragments. The meaning of the relationship is primarily qualitative; however it defines a relationship of self-similarity which enables the experimental data to be rescaled in accordance with the mechanical performance of the materials used.

In quantitative terms, the model must be calibrated according to experimental results. Based on a large number of tests conducted on full-scale rectangular panels subjected to uniform pressure [Bennison, 2009], the following values (to be considered as examples, but not to be considered in structural calculations) can be given:

- for laminated heat-strengthened glass with PVB or EVA interlayer, at 23°C and with load applied for a characteristic time of 60 seconds,  $E_{eff} = 400$  MPa;
- for laminated heat-strengthened glass with ionoplastic (SG) interlayer, at 23°C and with load applied for a characteristic time of 60 seconds,  $E_{eff} = 12000$  MPa.

With regard to the type of glass used, the following practical rules can be defined. Annealed and strengthened glass have virtually the same stiffness in the event of breakage. Thermally toughened glass has a post-breakage stiffness of around  $\frac{1}{4}$  of the stiffness of annealed or heat-strengthened glass. Chemically strengthened glass has a stiffness that is around 25% lower than that of annealed or heat-strengthened glass.



If temperature and characteristic load duration different from those mentioned above are to be taken into account, the corresponding value can be obtained by appropriately rescaling the effective elastic modulus for (23°C, 60 sec) according to the factor

$$\rho = \frac{G(T, t)}{G(23^{\circ}\text{C}, 60\text{ s})} \quad (6.93)$$

where:

$G(23^{\circ}\text{C}, 60\text{ s})$  = shear elastic modulus of the polymeric interlayer at 23°C, with load applied for a characteristic time of 60 seconds [MPa];

$G(T, t)$  = shear elastic module of the polymeric interlayer for desired conditions of temperature  $T$  and load duration  $t$  [MPa].

In general, the abovementioned reference values must be verified – in the absence of more accurate numerical modelling accounting for the effective shape and dimension of the glass fragments – with reduced-scale and/or, ideally, full-scale tests.

#### **6.5.4 Post-breakage assessments**

- strength assessment.  
In post-breakage conditions, the element must be capable of bearing the loads acting in a critical condition, i.e. self weight and dead loads, as well as an appropriate fraction of accidental loads. Particular attention must be paid, especially in point-fixing systems, to the assessment of the load-bearing capacity of the constraints under critical conditions.
- deformability assessment.  
In the post-failure phase, it must be verified that the deformation of the element is compatible with the design and the configuration of the constraints, preventing, for example, detachment of the elements from their anchorages.
- Verification against risk from falling fragments.  
It must be verified that the dimensions of any fragments which may detach from the interlayer and fall or be projected away from the structure (in the event of impacts or explosions) are not large enough to cause injury to people. Alternatively, suitable protection mechanisms must be put in place to protect people, particularly in the neighborhood of emergency exits and escape routes.
- Assessment of the absence of detachment of glass plates in case of explosions.  
In this regard, practical design rules for the minimum dimensions of the constraints (depth of gripping points) are provided in [The Institution of Structural Engineers, 1999] for the most common cases.
- Assessment of the response under fire conditions, if required.

#### **6.6 Annex – Tables**

The following sections contain a number of ready usable formulas and tables for calculating the maximum tensile stresses and deflection in flat glass plates subjected to uniformly distributed loads, which

---

can be used for monolithic glass elements. The formulas can only be applied only to panels continuously supported along the sides.

The examples examined below provide the maximum stress  $\sigma_{max}$  and maximum displacement  $w_{max}$ , in the following cases:

- a) rectangular plate:
  - simply supported on all sides;
  - simply supported on three sides;
  - simply supported on two sides;
- b) triangular plate simply supported on all sides. In this case, the following cases are considered:
  - right-angled triangle or isosceles triangle;
  - other types of triangle;
- c) circular plate;
- d) special cases:
  - right-angled trapezoidal plate (three orthogonal edges and one inclined edge);
  - plate with four edges: three orthogonal edges and one curved edge;
  - plate with four edges: two parallel edges and two inclined edges (parallel or non-parallel).

The results illustrated have been obtained based on the von Karman theory of thin-plates. Both the linear and non-linear cases are considered.

## 6.6.1 Rectangular plates

### 6.6.1.1 Rectangular plate simply supported on four edges

For rectangular plates simply supported on all edges, subjected to large deformations, the maximum stress  $\sigma_{max}$  and the maximum displacement  $w_{max}$  due to the design action  $F_d$  can be calculated according to the formula provided below. Let  $a$  and  $b$  the dimensions of the plate, with  $a$  denoting the smaller dimension, and with  $h$  the thickness of the plate. The aspect ratio is given by  $\lambda = a/b$ , while the plate is calculated as  $A = ab$ .

The maximum stress  $\sigma_{max}$  due to the design action  $F_d$  can be expressed as

$$\sigma_{max} = k_1 \frac{A}{h^2} F_d . \tag{6.94}$$

The deflection  $w_{max}$  may be determined by means of equation

$$w_{max} = k_4 \frac{A^2}{h^3} \frac{F_d}{E} . \tag{6.95}$$

The values of the non-dimensional coefficients  $k_1$  and  $k_4$  are given in Table 6.9 and Table 6.10, respectively. In the case of rectangular plates supported on all sides,  $k_1$  and  $k_4$  depend on the aspect ratio  $\lambda$  and the normalised load  $p^*$  may be obtained from the equation

$$p^* = \left( \frac{A}{4h^2} \right)^2 \frac{F_d}{E} . \tag{6.96}$$

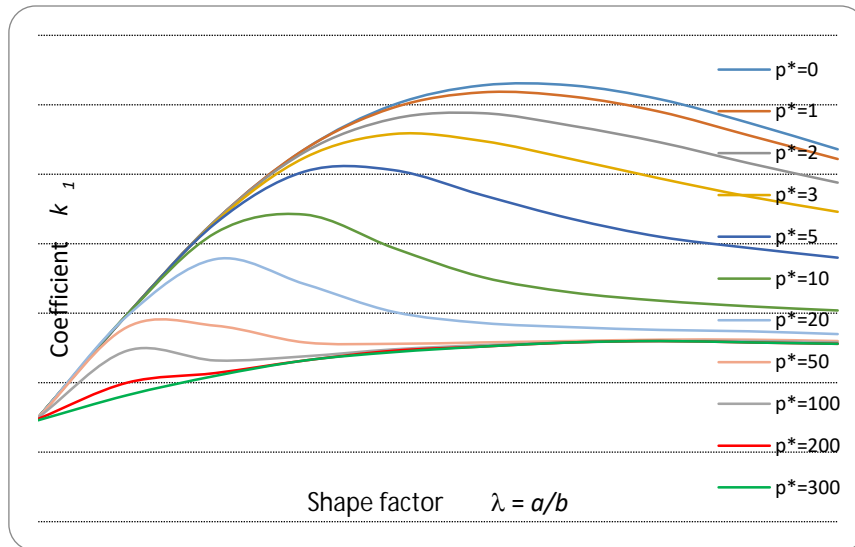


Figure 6.29. Values of non-dimensional coefficient  $k_1$  defined as a function of shape factor  $\lambda$  and load  $p^*$ .

Table 6.9. Values of coefficient  $k_1$  for calculation of maximum stress.

$\lambda=a/b$	$p^*$										
	0	1	2	3	5	10	20	50	100	200	300
1.0	0.268	0.261	0.244	0.223	0.190	0.152	0.135	0.130	0.129	0.128	0.128
0.9	0.287	0.278	0.258	0.234	0.197	0.155	0.137	0.131	0.130	0.129	0.129
0.8	0.304	0.295	0.273	0.247	0.205	0.159	0.138	0.131	0.130	0.130	0.130
0.7	0.314	0.306	0.285	0.261	0.218	0.165	0.140	0.130	0.129	0.129	0.129
0.6	0.314	0.309	0.294	0.274	0.235	0.176	0.143	0.129	0.127	0.126	0.126
0.5	0.300	0.298	0.290	0.279	0.253	0.197	0.151	0.128	0.124	0.123	0.122
0.4	0.268	0.268	0.266	0.262	0.252	0.221	0.171	0.129	0.119	0.116	0.116
0.3	0.217	0.217	0.217	0.216	0.215	0.208	0.189	0.141	0.116	0.107	0.105
0.2	0.149	0.149	0.149	0.149	0.149	0.149	0.148	0.140	0.123	0.100	0.091
0.1	0.075	0.075	0.075	0.075	0.075	0.075	0.075	0.075	0.075	0.074	0.073

$$k_1 = \frac{1}{4 \left[ \frac{1}{z_2^2} + \frac{p^{*2}}{(z_3^2 + (z_4 p^*)^2)} \right]^{0.5}},$$

where

$$z_2 = 24\lambda \left[ 0.0447 + 0.0803 \left( 1 - \exp \left( -1.17 \left( \frac{1}{\lambda} - 1 \right)^{1.073} \right) \right) \right],$$

$$z_3 = 4.5 \left( \frac{1}{\lambda} - 1 \right)^2 + 4.5, \quad z_4 = 0.585 - 0.05 \left( \frac{1}{\lambda} - 1 \right).$$

The values of the coefficient  $k_1$  are considered valid if Poisson’s ratio is between 0.20 and 0.24. If necessary, these values may be interpolated linearly. For small deformations (linear theory), it is assumed that  $p^* = 0$ .

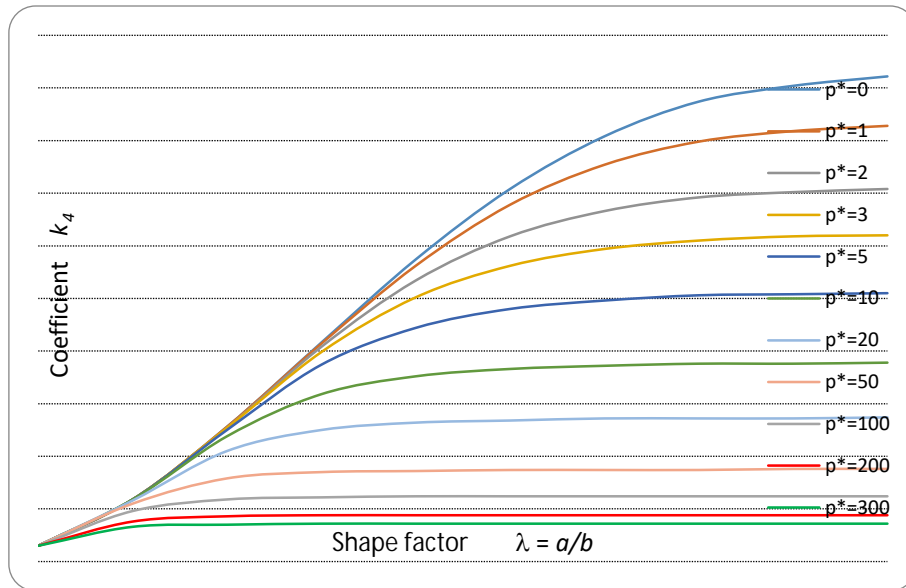


Figure 6.30. Values of non-dimensional coefficient  $k_4$  defined as a function of shape factor  $\lambda$  and load  $p^*$ .

Table 6.10. Values of coefficient  $k_4$  for calculation of maximum displacement.

$\lambda=a/b$	$p^*$										
	0	1	2	3	5	10	20	50	100	200	300
1.0	0.0461	0.0414	0.0354	0.0310	0.0255	0.0189	0.0137	0.0088	0.0062	0.0044	0.0036
0.9	0.0452	0.0409	0.0351	0.0309	0.0254	0.0188	0.0136	0.0088	0.0062	0.0044	0.0036
0.8	0.0437	0.0399	0.0346	0.0305	0.0253	0.0188	0.0136	0.0087	0.0062	0.0044	0.0036
0.7	0.0404	0.0377	0.0333	0.0297	0.0248	0.0186	0.0136	0.0087	0.0062	0.0044	0.0036
0.6	0.0354	0.0339	0.0309	0.0281	0.0240	0.0183	0.0134	0.0087	0.0062	0.0044	0.0036
0.5	0.0287	0.0281	0.0267	0.0251	0.0222	0.0176	0.0132	0.0086	0.0062	0.0044	0.0036
0.4	0.0208	0.0207	0.0204	0.0199	0.0187	0.0159	0.0125	0.0085	0.0061	0.0044	0.0036
0.3	0.0128	0.0128	0.0127	0.0127	0.0125	0.0119	0.0105	0.0079	0.0059	0.0043	0.0035
0.2	0.0059	0.0059	0.0059	0.0059	0.0059	0.0059	0.0058	0.0055	0.0048	0.0038	0.0033
0.1	0.0015	0.0015	0.0015	0.0015	0.0015	0.0015	0.0015	0.0015	0.0015	0.0015	0.0015

$$k_4 = \frac{\left[ \left( \frac{\left( \frac{1}{z_1^4} + 4p^{*2} \right)^{0.5} - \frac{1}{z_1^2}}{2} \right)^{0.5}}{16p^*} \right]}$$

where

$$z_1 = 192(1 - \nu^2)\lambda^2 \left[ 0.00406 + 0.00896 \left( 1 - \exp \left( -1.123 \left( \frac{1}{\lambda} - 1 \right)^{1.097} \right) \right) \right]$$

Note: Per  $p^*=0$ ,  $k_4 = \frac{z_1}{16}$ .

The values of the coefficient  $k_4$  provided in Table 6.10 are considered valid if Poisson's ratio is between 0.20 and 0.24. If necessary, these values may be interpolated linearly. For small deformations (linear theory), it is assumed that  $p^* = 0$ .

### 6.6.1.2 Rectangular plate simply supported on three edges

Let us consider a plate of thickness  $h$  and dimensions  $a$  and  $b$ , with aspect ratio  $\lambda = a/b$ , where  $a$  denotes the shortest edge, simply supported on three edges and subjected to a uniformly distributed load. The maximum stress  $\sigma_{\max}$  and the maximum deflection  $w_{\max}$  are given by formulas analogous to (6.94) and (6.95), with non-dimensional coefficients  $k_1$  and  $k_4$  dependent on the aspect ratio  $\lambda = a/b$ .

#### 6.6.1.1 Rectangular plate simply supported on two edges

If the plate is supported only on two opposite edges of length  $b$  (with  $a$  the dimension of the non-supported edges), and it is subjected to an uniformly distributed load, the maximum stress  $\sigma_{\max}$  is given by

$$\sigma_{\max} = 0.750 \frac{a^2}{h^2} F_d . \quad (6.97)$$

The maximum deflection  $w_{\max}$  can be calculated by means of the following formula:

$$w_{\max} = 0.148 \frac{a^4}{h^3} \frac{F_d}{E} . \quad (6.98)$$

## 6.6.2 Circular plate

Let us consider a circular plate of radius  $a$ , area  $A$  and thickness  $h$ , subjected to a uniformly distributed load  $F_d$ , the maximum stress  $\sigma_{\max}$  and deflection  $w_{\max}$  can be calculated by means of the following formulae:

$$\sigma_{\max} = 0.303 \frac{a^2}{h^2} F_d , \quad (6.99)$$

$$w_{\max} = 0.148 \frac{a^4}{h^3} \frac{F_d}{E} . \quad (6.100)$$

## 6.6.3 Special cases

### 6.6.3.1 Triangular plate simply supported on three edges

The formulae proposed in this Section are applicable only to plates with right-angled triangular or isosceles triangular shape, simply supported on all the edges, subjected to uniformly distributed loads. Given a plate of area  $A$ , with smaller edge of length  $a$  and thickness  $h$ , subjected to an action  $F_d$ , the maximum stress  $\sigma_{\max}$  and maximum deflection  $w_{\max}$  are given by the formulas (6.94) and (6.95). The values of the non-dimensional coefficients  $k_1$  and  $k_4$  depend on the aspect ratio  $\lambda$  and on the normalised load  $p^*$ , as:

- $\lambda = a/b$  for a right-angled triangle (where  $a$  and  $b$  are the length of the minor and major cathetus, respectively);
- $\lambda = a/h$  for an isosceles triangle (where  $a$  is the length of the shortest edge and  $h$  the height);
- $p^*$  normalised load (Eq.(6.96)).

### 6.6.3.2 Right-trapezoidal plate

Let us consider a right-trapezoidal plate with dimensions  $a$ ,  $b$  and  $L$  as illustrated in Figure 6.31, subjected to a uniformly distributed design load  $F_d$ . The maximum stress  $\sigma_{\max}$  and deflection  $w_{\max}$  can be calculated by means of Eqs. (6.94) and (6.95), by considering an *equivalent rectangular* plate with edges  $b$  and  $a^* = a + 2(L - a)/3$ . The aspect ratio of the equivalent rectangular plate is thus

$$\lambda = \frac{\min(a^*, b)}{\max(a^*, b)} \tag{6.101}$$

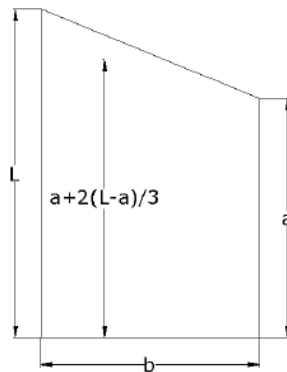


Figure 6.31. Trapezoidal plate (three orthogonal edges and one sloping edge).

The values of the non-dimensional coefficients  $k_1$  and  $k_4$ , which are functions of the aspect ratio  $\lambda$  and the normalised load  $p^*$ , are tabulated in Table 6.9 and Table 6.10, respectively.

### 6.6.3.3 Plate with three orthogonal edges and one curved edge

For a plate with three orthogonal edges and one curved edge, such as the one illustrated in Figure 6.32, subjected to a uniformly distributed load  $F_d$ , the maximum stress  $\sigma$  and deflection  $w_{\max}$  can be calculated by means of Eqs. (6.94) and (6.95), by considering the *equivalent rectangular* plate with edges  $b$  and  $a^* = 0.86L + 0.15a$ . The aspect ratio of the equivalent rectangular plate is given by Eq.(6.101).

The values of the non-dimensional coefficients  $k_1$  and  $k_4$ , which are functions of the aspect ratio  $\lambda$  and the normalised load  $p^*$ , are tabulated in Table 6.9 and Table 6.10 respectively.

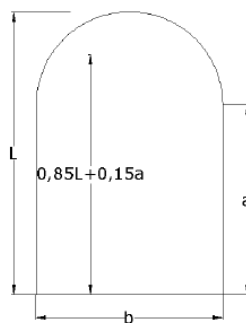


Figure 6.32. Plate with three orthogonal edges and one curved edge.

#### 6.6.3.4 Plate with two parallel and two sloping edges

For a plate with two parallel edges and two sloping edges (which may or may not be parallel) with dimensions  $a$ ,  $b$  and  $d$  as illustrated in Figure 6.33, subjected to a uniformly distributed load  $F_d$ , the maximum stress  $\sigma_{\max}$  and deflection  $w_{\max}$  may be calculated by means of Eqs. (6.94) and (6.95), by considering the *equivalent rectangular* plate with edges  $b$  and  $a^* = (a + L + d) / 3$ .

The aspect ratio of the equivalent rectangular plate is given by Eq. (6.101). The values of the non-dimensional coefficients  $k_1$  and  $k_4$ , dependent on the aspect ratio  $\lambda$  and the normalised load  $p^*$ , are illustrated in Table 6.9 and Table 6.10, respectively.

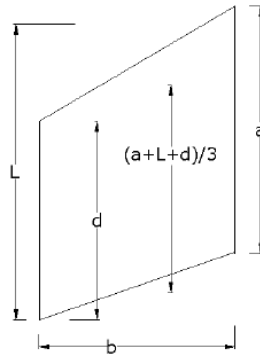


Figure 6.33. Plate with two parallel edges and two sloping edges.

## 7 CALCULATION PRINCIPLES

### 7.1 General remarks

Structural calculations must be carried out in accordance of the basic principles of the Eurocodes. The Limit States for glass structural elements are defined in Section 7.2. They can be obtained by using limitations of the following type:

$$E_d \leq R_d , \tag{7.1}$$

where  $E_d$  and  $R_d$  are, respectively, the design values of action effects and the corresponding response resistance (in terms of resistance or deformation) in a generic limit state.

The main physical and mechanical properties of glass are described in Chapter 2. The general principles to be used in the design of glass element for structural purposes are indicated in Chapter 3. The actions must be determined in accordance with EN 1991, CNR Instructions or current national legislation, but, for what concerns the more specific aspects of glass elements (load duration, temperature effects, seismic force), reference should be made to Chapter 4. Material strength must be evaluated using the methods given in Chapter 5. Modelling, calculation principles and conditions must comply with what is established in Chapter 6.

### 7.2 Limit states

The limit states for glass elements are: Service Limit State (SLS), Ultimate Limit State (ULS) and Collapse Limit State (CLS). A summarised table is given in Table 7.1.

The SLS considers the sound structure subjected to the characteristic design loads. In general, the deformability of the structural element is evaluated, and it must be limited in order to ensuring the functionality of the building (not just the structural functionality).

In normal applications, there are no stress value limits over which the construction functionality is damaged. Therefore, the SLS does not normally include stress verification, at least for the most common structures. Exceptions are verification of Operability Limit State and of Damage Limit State for seismic actions (see para. 4.4.2.2), for which the stress in glass must be lower than the limiting values. The ULSs consider the sound structure, subjected to extreme values of external actions, and are made up of: (1) ULS for glass breakage, (2) ULS for breakage of a material used in composition with glass, (3) ULS for connection interface failure.

The calculation of ULS for glass breakage consist in verifying that the stress at each point is lower than the glass strength. The state of stress to be considered is that consequent to the load combinations described in point 7.3. The maximum principal stress must be compared with the design strength  $f_{g;d}$  of the material, defined in point 7.4, on the basis of what discussed in Chapter 2 regarding the material aspects, and in Chapter 9 for what concerns the procedural control aspects.

The verification of ULS for breakage of the material used in composition with glass mainly involves the interlayers and silicones. A condition for satisfying this verification is that the stress must be lower than the material strength at all points.

The strength to be used in the verification is the design ultimate strength of the material  $f_{m;d}$ , defined starting from the characteristic value of  $f_{m;k}$  through correcting coefficients. The verification also involves a combination of the normal and tangential stress components. The value  $f_{m;k}$  strongly depends on the material: the value of  $f_{m;k}$  must therefore be furnished by the producer, together with adequate proofs of their the statistical consistency, and, in any case, in line with the general theory



presented in chapter 2.2 and according to the acceptance procedures described in Chapter 9. Execution, in accordance with the best practice, can include the request that failure of the materials used in compositions be placed at a hierarchical level above failure of the glass, following the general design principles established in chapter 3.1.

Verifications of ULS for failures at the connection interface involves both glass-interlayer adhesion and the glass surface in direct contact with the fixing systems. The verification only involves the interface and does not include the connecting device, generally made of other materials, to which specific structural regulations are applied. The verification is considered to be satisfied if in all points the tension at the interface is lower than the strength of the interface itself. Even in this case, execution in accordance with the best practice can include the request that interface failure be placed at a higher hierarchical level than failure of glass.

The CLSs consider the glass element as fully or partially fragmented. The CLS is therefore aimed at guaranteeing that a construction with glass structural elements presents an adequate structural behaviour in the post-glass breakage (post-critical) phase at both global and local levels. The need to consider the CLS derives from the intrinsic brittleness of the glass, and also from the possibility – still remote – of spontaneous breakage. Local cracking can, in fact, start off a chain reaction that leads to breakage of the whole element at load levels lower than those defined for the theoretical ULS. The CLS must consider this possibility, verifying that the broken element guarantees the load-bearing capacity for a suitable fraction of the loads at the ULS and/or the SLS, even when the load-bearing capacity of the glass element is decreased by the contribute of the parts subject to local cracking.

Operatively, the CLS considers two possible scenarios: (1) a structural system made of glass elements; (2) a single structural glass element. The CLS must consider the structural situation that emerges after one part of the load-bearing structure has cracked (disregarding the cause), i.e., it has passed the ULS. In general, the structural part to be considered as collapsed must include the parts that are subject to localised actions (e.g. the external plies of a laminate, which are subject to the direct action of applied loads), to which the parts that can crack prematurely should be added, case by case. The CLS verifies that the structure, in this condition, preserves a suitable residual load-bearing capacity and that the cracking mechanism is not too fragile.

(1) In more complex situations, the minimum performance requirements that the damaged structural must guarantee must be established *ad hoc*. The structure must, in any case, guarantee “*fail safe*” behaviour, with specific reference to hierarchy, system redundancy and resilience, as established in chapter 3.1. The residual load-bearing capacity must include, as a minimum, the characteristic values of the self weight of the structure.

(2) In general, the single glass structural element must guarantee section redundancy, never intended as an increase in the sheet thickness, but as an increase in the number of glass layers. In special cases, it is sufficient that the glass structural element – excluding global redundancy as indicated in point (1) – guarantees that its cracking does not represent a risk for the public safety. In the specific case of laminated glass, the performance of a package made up of an interlayer and one or more fragmented glass sheets must be defined according to the criteria established in section 3.1.4.

In the specific case of seismic actions, the general criteria and the different limit states to be considered are given in chapter 4.4. The necessary verification for seismic actions are dealt with separately in Section 7.6.

Table 7.1. Roundup of the various limit states.

	Serviceability Limit State	Ultimate Limit State	Collapse Limit State
Requirement	$E_{SLS;d} \leq C_d$	$E_{ULS;d} \leq R_d$	$E_{CLS;d} \leq R_c$
where the effect of the actions is:	$E_{SLS;d} = E\{F_{SLS;d}\}$	$E_{ULS;d} = E\{F_{ULS;d}\}$	$E_{CLS;d} = E\{F_{CLS;d}\}$
where:	$F_{SLS;d}$ is the design value of a single action or a combination of different actions for the serviceability limit state.	$F_{ULS;d}$ is the design value of a single action or a combination of different actions for the ultimate limit state.	$F_{CLS;d}$ is the design value of a single action or a combination of different actions for the collapse limit state.
$E_{SLS;d}$	is the value of the effect of the action or actions for the serviceability limit state, in terms of stress or deflection.		
$C_d$	is the limit design value for the criterion of the serviceability limit state, in terms of maximum design stress $f_{g;d}$ , or maximum design deflection $w_d$ , for the considered limit state.		
$E_{ULS;d}$	is the value of the effect of the action or actions for the considered ultimate limit state, in general expressed in terms of calculated stress.		
$R_d$	is the design value of the resistance, in general expressed in terms of maximum design stress of the ultimate limit state.		
$E_{CLS;d}$	is the design value of the effect of the action or actions for the collapse limit state.		
$R_c$	is the design value of the resistance to actions for the collapse limit state.		

Satisfaction of the SLS and the ULS is obligatory. The verification of CLS must guarantee that local cracking does not create serious consequences in terms of safety, and that the post-critical behaviour of the structure is adequate (“fail safe” approach with reference to strength, redundancy, hierarchy, as described in Chapter 3.1).

### 7.3 Design actions

The action values must be defined according to UNI EN 1991, the NRC regulations and national standards in force. For what concerns the seismic actions, refer to section 4.4.5. For exceptional forces, refer to Section 4.9.

In the case of other actions (non-seismic and not exceptional), the design loads are defined as follows:

for the Serviceability Limit State

$$F_d = G_1 + G_2 + Q_{k,1} + \sum_i \Psi_{0,i} Q_{k,i} ; \tag{7.2}$$

for the Ultimate Limit State

$$F_d = \gamma_{G1} \cdot G_1 + \gamma_{G2} \cdot G_2 + \gamma_{Q,1} Q_{k,1} + \sum_i \gamma_{Q,i} \Psi_{0,i} Q_{k,i} ; \tag{7.3}$$

for the Collapse Limit State

$$F_d = \gamma_{G1} \cdot G_1 + \gamma_{G2} \cdot G_2 + \gamma_{Q,1} Q_{k,1,\tau} + \sum_i \gamma_{Q,i} \Psi_{0,i} Q_{k,i,\tau} \tag{7.4}$$

where

$F_d$	design action value;
$G_1$	action value caused by the self weight (dead load);
$G_2$	action value caused by the permanent loads;
$Q_{k,1}$	characteristic value of the main variable action (e.g. imposed load on a roof, wind load, snow load), referring to a return period of 50 years;
$Q_{k,i}$	characteristic value associated with variable actions (e.g. wind, snow), referring to a return period of 50 years;
$Q_{k,1,\tau}$	characteristic value of the main variable action (e.g. live load, wind load, snow load), referring to a certain return period ( $\tau = 10$ years);
$Q_{k,i,\tau}$	characteristic value associated with variable actions (e.g. wind, snow), referring to a return period $\tau = 10$ years;
$\psi_{0,i}$	variable load combination coefficient;
$\gamma_{G1}$	partial factor for self weight, including model uncertainties and size tolerances;
$\gamma_{G2}$	partial factor for dead loads, including model uncertainties and size tolerances;
$\gamma_{Q,i}$	partial factor for variable forces, including model uncertainties and size tolerances.

In general, it is opportune to perform the resistance calculation defined by (7.4) at the CLS and, if necessary, buckling verifications on the element under the action of the loads defined by (7.4), according to the criteria defined in Paragraph 6.4.

The post-breakage verification classes are defined in Table 3.9.

The characteristic values of the variable action  $Q_{k,i}$  appearing in the expressions above correspond to the 95% fractile of all the maximum values, in relation to the reference period of the variable action, taken equal to 50 years. These values are established in accordance with UNI EN 1991 and/or current regulations. The values of  $Q_{k,i,\tau}$  represent the characteristic action values referred to the return period  $\tau$ , the values of which can be found by considering the statistical probability distributions given in Chapter 4 for the various actions. For Collapse Limit State verifications,  $\tau = 10$  years is taken conventionally for elements in class 1 and 2.

The characteristic values for the partial load factor,  $\gamma_{Q,i}$ , as well as the combination coefficients  $\psi_{0,i}$ , are indicated in UNI EN 1991 and/or national current regulations. Since in the case of glass elements the size and the dead loads are generally defined with an extremely higher precision than for other material (such as concrete), it is recommended to use the values of  $\gamma_{G1}$  and  $\gamma_{G2}$  that are given in Table 7.2.

Table 7.2. Value of the partial coefficient for self weight and dead loads.

Class	$\gamma_{G1}$		$\gamma_{G2}$	
	If safety decreases	If safety increases	If safety decreases	If safety increases
1	1.3	1	1.5	1
2				

## 7.4 Design value of strength

Structural calculations are generally carried out according to Galileo's criterion (maximum principal stress criterion). The design value of stress to be adopted is that which can guarantee the probability of collapse indicated in Section 3.2.3 as to the design forces, which is different for class 1 or class 2 elements. The design stress is calculated as indicated in chapter 5 (relative to the calculation value), on the basis and within the limits of what is indicated in chapter 2 (regarding the probabilistic distribution of the resistances).

Some aspects to be considered are that the defectiveness of glass is statistically proportional to the surface area of the element and that the resistance also depends upon the duration of the applied action, the temperature and humidity.

The design value of the tensile strength for glass elements under bending  $f_{g;d}$ , to be considered for ULS and CLS verifications, on the basis of the considerations discussed in Chapters 2 and 5, can be summarized as

$$f_{g;d} = \frac{k_{\text{mod}} \cdot k_{ed} \cdot k_{sf} \cdot \lambda_{gA} \cdot \lambda_{gl} \cdot f_{g;k}}{R_M \gamma_M} + \frac{k'_{ed} k_v \cdot (f_{b;k} - f_{g;k})}{R_{M,v} \gamma_{M,v}}, \quad (7.5)$$

where:

$f_{g;k}$ : nominal characteristic value of the tensile strength under bending of annealed glass (before any heat or chemical reinforcing treatment), determined on the basis of the procedures indicated in Chapter 3. In common cases, UNI EN 572-1 is valid, for which  $f_{g;k} = 45 \text{ N/mm}^2$ . Should the nominal value of  $f_{g;k}$  be lower than the value indicated above, the glass does not fall within the materials considered by these instructions.

$k_{\text{mod}}$ : reduction factor that depends on the load duration and the environmental conditions (temperature, humidity), defined in points 2.1.1.2 and 5.4.2, given by (2.16). The values of  $k_{\text{mod}}$  for different load durations (constant actions over time) are indicated in the second column of Table 2.2. For actions that vary in time, chapter 2.1 describes the analytical procedure for calculating  $k_{\text{mod}}$ . In the case of forces that vary significantly over time,  $k_{\text{mod}}$  can be calculated by applying the analytic procedure described in chapter 2.1.

$k_{ed}$  e  $k'_{ed}$ : strength reduction factors defined in Section 5.4.3, respectively for annealed and prestressed glass, depending on the edge finish of the glass element (or of the holes), and on the distance  $d$  from the edge of the point where  $f_{g;d}$  is calculated, to be applied to elements with a stressed edge (e.g. beams, fins, etc.). When  $d > 5s$  ( $s$  = element thickness), or for plates under bending, it is assumed that  $k_{ed} = k'_{ed} = 1$ . When  $d \leq 5s$ , the coefficients should be calculated with a theoretical and/or experimental *ad hoc* study, in agreement with what is established in Section 5.3.3.4. As a reference, Table 7.3 gives some edge coefficient values, estimated in some elementary cases.

$k_{sf}$ : strength reduction factor, depending on the surface conditions of the glass. The value of  $k_{sf}$  must be calculated using an *ad hoc* theoretical and/or experimental study, in accordance with the procedures given in chapter 9. Some reference values are given in Table 7.4.

$\lambda_{gA}$  = scale factor, which considers the area subjected to the maximum stress. This coefficient considers that, for statistical reasons, there is a higher probability of finding defects in larger areas than in smaller ones. If there are no more precise information, as discussed in paragraph 5.4.1 the following expression can be used

$$\lambda_{gA} = \left( \frac{0.24 \text{ m}^2}{k A} \right)^{1/7}, \text{ con } 0.75 \leq \lambda_{gA} \leq 1, \quad (7.6)$$

where  $A$  represents the total area of the plate subjected to tractions, while the coefficient  $k$ , that defines the effective area, is given in Table 7.5 for the most common boundary conditions. Should the resistance verifications be carried out at a distance from the edge of  $d < 5 s$  ( $s$  = plate thickness), it is assumed that  $\lambda_{gA} = 1$ .

$\lambda_{gl}$  = scale factor for the stress near the element edge, to be applied to elements with edge *specifically* under traction (e.g. beams, fins, etc.). This coefficient considers that, from a statistical viewpoint, the length of the edge is penalizing. For tests at a distance of  $d > 5 s$  ( $s$  = element thickness), or in the case of plates under bending (due to out-of-plane load),  $\lambda_{gl} = 1$  is conventionally assumed. Regarding what is shown in Section 5.4.3, if there is no precise information, the following values can be assumed for tests at a distance of  $d < 5 s$  from the edge:

$$\lambda_{gl} = \left( \frac{0.1667 \cdot 0.45 \text{ m}}{k_b l_b} \right)^{1/5} \leq 1 \text{ for polished edges; } \lambda_{gl} = \left( \frac{0.0741 \cdot 0.45 \text{ m}}{k_b l_b} \right)^{1/12.5} \leq 1 \text{ for ground edges.} \quad (7.7)$$

In these expressions,  $l_b$  represents the total length of the edge that is subject to traction. The coefficient  $k_b$  depends on the distribution of the stress along the edge: if there is no more precise information, the values given in Table 7.6 can be used.

$f_{b,k}$  = characteristic value of glass strength after a strengthening treatment. If there is no specific data, the values in Table 7.7 can be used, which must be demonstrated using the procedures discussed in Chapter 9.

$k_v$  = reduction factor of the increase in tensile strength of glass produced using a prestressing treatment (temperature, hardening), to be taken as being null in the case of annealed glass (no treatment). The coefficient  $k_v$  must be calculated by an *ad hoc* theoretical and/or experimental study, in compliance with the general indications given in Chapter 9. Indicative values of  $k_v$  are given in Table 7.8.

$\gamma_M$  = partial factor for tensile strength of annealed glass under bending, including model and geometry uncertainties, with regard to the ULS. For this coefficient, defined in chapter 5.3, the values given in Table 7.9 can be used.

$R_M$  = multiplication factor of the partial coefficient of the float glass that varies for verifications in class 1 or in class 2. For this coefficient, defined in Section 5.2.3 and calibrated with the study cases in Section 5.3.3, the values given in Table 7.10 can be used. The introduction of this coefficient, for the passage from class 2 tests to class 1 tests, shows a variation with respect to the classic Eurocode EN1990 approach, in which the  $\gamma_Q$  coefficients, multiplying the action values, vary with the  $K_{FI}$  multiplication factor (refer to the comments at the end of Section 5.2.3). Here, it is the  $\gamma_M$  coefficient that varies by way of the coefficient  $R_M$ , with  $R_M = 1$  for calculations in the class 2 and  $R_M < 1$  for calculations in the class 1.

$\gamma_{M,v}$  = partial factor relative to the increase of tensile strength (under bending) given by the prestressing treatments, as defined in Chapter 5.5. The values given in Table 7.9 can be used.

$R_{M,v}$  = reduction coefficient that varies for verifications in class 1 and class 2. For this coefficient, defined in Section 5.5.2, the values given in Table 7.10 can be used.

Table 7.3. Indicative values of the  $k_{ed}$  and  $k'_{ed}$  coefficients for verifications near the edge of glass elements and holes, in the case of elements with edge under traction.

Type of glass	Values* of $k_{ed}$ and $k'_{ed}$ at the edge**							
	Cut		Arrissed		Ground		Polished***	
	$k_{ed}$	$k'_{ed}$	$k_{ed}$	$k'_{ed}$	$k_{ed}$	$k'_{ed}$	$k_{ed}$	$k'_{ed}$
Annealed	0.7	0.7	0.7	0.7	0.8	0.8	0.9	0.9
Heat strengthened	to be avoided		to be avoided		0.8	0.8	0.8	0.8
Thermally toughened (tempered)	to be avoided		to be avoided		0.8	0.8	0.8	0.8
Chemically strengthened	to be avoided		to be avoided		0.6	0.7	0.6	0.7
Annealed and patterned	0.7	0.7	0.7	0.7	0.7	0.7	0.7	0.7
(*) Values to be used for verifications at a distance $d < 5s$ from the edge or from holes ( $s$ = element thickness). For $d > 5s$ and for plates under bending it is assumed that $k_{ed} = 1$ .								
(**) Edge finishes are intended as being according to UNI EN ISO 12543-5.								
(***) In the case of glass beams and fins where the maximum tensile stress is at the ribs, it is recommended to use polished edges with a smooth and curved profile.								

Table 7.4. Indicative values of the  $k_{sf}$  coefficient for the various surface profiles.

Glass	$k_{sf}$	
	As produced (2)	Sandblasted
Float glass	1	0.6
Drawn glass	1	0.6
Enamelled glass (float or drawn) (1)	(1)	(0.6)
Patterned glass	0.75	0.45
Enamelled patterned glass (1)	(0.75)	(0.45)
Polished wired glass	0.75	0.45
Patterned wired glass	0.6	0.36
(1) These types of glass are not generally available as annealed glass, but the value of $k_{sf}$ must still be used to calculate the resistance of the prestressed glass.		
(2) Us the “As produced” values of $k_{sf}$ for acid-etched glass.		

Table 7.5. Indicative values of the  $k$  coefficient for defining the effective area in plies under bending due to out-of-plane loads (relative to the Weibull parameter  $m = 7$ ).

Constraining conditions	$k$
Rectangular plate continuously constrained on 4 edges	0.145
Rectangular plate continuously constrained on 2 edges	0.054
Rectangular plate with one edge built in; uniformly distributed load	0.013
Rectangular plate with one edge built in; load distributed on a line parallel to the edge that is built in	0.019
Rectangular plate constrained at 4 points near the corners; uniformly distributed load	0.071

Table 7.6.  $k_b$  coefficient for calculating the scale effect near the edge.

Edge finish	Stress distribution along the edge		
	constant	parabolic	triangular
Raw edge	$k_b = 1$	$k_b = 0.2434$	$k_b = 0.0741$
Polished edge	$k_b = 1$	$k_b = 0.3694$	$k_b = 0.1667$

Table 7.7. Characteristic value of the bending strength of prestressed glass (strengthening treatment must be carried out as indicated in Chapter 9).

Type of glass	Characteristic $f_{b,k}$ bending resistance values for prestressed glass [MPa]		
	Thermally toughened glass (UNI EN 12150), heat soaked thermally toughened (UNI EN 14179)	Heat strengthened glass (UNI EN 1863)	Chemically strengthened glass * (UNI EN 12337)
Float glass or drawn sheet glass	120	70	150
Patterned glass	90	55	100
Enamelled float or drawn sheet glass	75	45	/
Enamelled patterned glass	75	45	/

(\*) Given the difficulty of the chemical strengthening process, it is of particular importance that the material be checked and qualified.

Table 7.8. Indicative values of the reduction factor for tensile strength of the glass following a prestressing treatment.

Prestressing treatment	$k_v$
No treatment	0
Heat treatment with horizontal process	1
Heat treatment with vertical process	0.60
Chemical strengthening *	0.95

(\*) The indicated coefficient can only be used if the chemically strengthened glass is controlled and qualified following the procedures indicated in Section 9.

Table 7.9. Partial factors of annealed glass and prestressed glass.

	Annealed glass*	Prestressed glass*
Partial coefficients	$\gamma_M = 2.50$	$\gamma_{M,v} = 1.35$
(*) Values for ULS verifications. As regards the CLS, the ULS coefficients can be applied to those portions that remain sound.		

Table 7.10.  $R_M$  reduction factors of the partial coefficients for class 1 and 2 verifications.

Class	Annealed glass	Prestressed glass
first	$R_M = 0.7$	$R_{M,v} = 0.9$
second	$R_M = 1$	$R_{M,v} = 1$

The ULS verification should be carried out by comparing the maximum principal tensile stress to the design strength  $f_{g;d}$  given by (7.5).

It is important to notice that, since the  $k_{mod}$  factor depends on the load duration, the design strength varies according to the type of load. In general, to combine the effect of two or more generic actions at the same point, the test can be carried out following a rule similar to the Palmgren-Miner rule for fatigue: it can be assumed that the partial “damage” caused by stress resulting from the  $i$ -th action is directly proportional to the ratio of the stress itself and the design strength for that action. Breakage occurs when the sum of the fractions of “partial damage” reach the unit. The calculation can therefore be carried out by requiring that

$$\sum_{i=1}^N \frac{\sigma^i}{f_{g;d}^i} \leq 1 \tag{7.8}$$

where:

$\sigma^i$  stress caused by the  $i$ -th action at the considered point;

$f_{g;d}^i$  design strength relative to the  $i$ -th action.

The calculation is done for each considered point, where the stresses shall be considered.

In the case of elements subjected to various actions, the Project of European Norm prEN 16612 (2013) prescribes to select, among the various design actions, the dominant action and, then, to calculate the different design actions by way of (7.3), determining in this manner the most onerous load combination. The Project of European Norm prEN 16612 (2013) prescribes to compare the maximum stress corresponding to this condition with the design strength  $f_{g;d}$ ; it is not specified to which load this resistance must refer. This procedure is not justified on theoretical bases, and in certain cases it may not be on the safe side.

### 7.5 Design value of deflection

For what concerns the serviceability limit state, in general the maximum displacement tolerated by glass elements must be evaluated according to their specific application. No uniformity can be found in existing international regulations (e.g. prEN 16612 (2013), DTU 39-P4:2012, Cahier 3488\_V2:2011, Cahier 3574\_V2:2011, BS 6180:2011). The values proposed herein, which are examples and guides, have been therefore selected by comparing the indications of DTU 39-P4:2012, Cahier 3574\_V2:2011, BS 6180:2011. These limits must be critically evaluated by the designer according to each specific case.



In the case of elements that must guarantee resistance to weathering agents, the deformation shall be limited. For rectangular elements, a 50 mm deformation in the centre of the glass (limit recommended by prEN 13612-2013 for example) can sometimes be excessive.

Particular care must be taken with slightly inclined roofing to make sure that the deflection under the effect of combined actions (e.g. dead load + snow) does not annul the slope, creating water stagnation. Usually, respecting the limits proposed in the table below gives an angle greater than or equal to 2%, which can solve the problem, even considering normal installation tolerances.

The deflection must also be controlled not only in the centre of the glass element. Particularly in the case of double glazing, care must be taken not to damage the double glazing seal, therefore the limits indicated by UNI EN 1279-5:2010 (CE marking) along the edge of the glass are  $1/200 d$ , where  $d$  indicates the distance between two consecutive supports or the length of the shortest edge, which in any case must not exceed a value of 12 mm.

In the case of rectangular plates with linear constraints, more specific limitations can be found in Table 7.11. In the case of plates constrained by regular supports, reference can be made to Table 7.12. As far as parapets are concerned, the maximum absolute displacement must not only be compatible with glass integrity, but must also consider the feeling of insecurity felt by the occupants, which could be generated by high levels of deformability.

In a similar manner, the force on glass floors must be limited to prevent the risk of excessive oscillation. Values that are only a reference are given in Table 7.13.

Table 7.11 Values of the design deflection for linear constraints.

Single glass (monolithic or laminated)		Insulating units		No. of con- strained edges
Plate centre	Plate edge	Plate centre	Plate edge	
$1/60^{(1)}$ of $L_{min}$ ; < than 30 mm <sup>(3)</sup>		$1/60^{(1)}$ of $L_{min}$ ; < than 30 mm <sup>(3)</sup>	$1/200^{(2)}$ of $L_{min}$ ; < than 12 mm <sup>(4)</sup>	4
	$1/100^{(2)}$ of $L_{inf}$ ; < than 50 mm <sup>(3)</sup>		$1/150^{(2)}$ of $L_{inf}$ ; < than 50 mm <sup>(3)</sup>	3
	$1/100^{(2)}$ of $L_{inf}$ ; < than 50 mm <sup>(3)</sup>		$1/150^{(2)}$ of $L_{inf}$ ; < than 50 mm <sup>(3)</sup>	2
Notes: (1) at the centre of the plate; (2) unsupported plate edge (3) from DTU 39-P4:2012 (4) from UNI EN 1279-5:2010 $L_{min}$ : shorter edge size $L_{inf}$ : span of the free edge				

Table 7.12 Values of the design deflection for point-fixed elements.

Single glass (monolithic or laminated)	Insulating units	$L_{inf}^{(3)}$
1/100 <sup>(1)</sup> of the distance between the constraining points $L_{inf}$ and < than 50 mm <sup>(2)</sup>	1/150 <sup>(1)</sup> of the distance between the constraining points $L_{inf}$ and < than 50 mm <sup>(2)</sup>	Figure 7.1-a
1/50 of the cantilever length $L_{inf}$ and < than 50 mm <sup>(2)</sup>	1/75 of the cantilever length $L_{inf}$ and < than 50 mm <sup>(2)</sup>	Figure 7.1-b
(1) most deformable edge of the plate; (2) from Cahier 3574_V2:2011; (3) $L_{inf}$ is defined with reference to Figure 7.1.		

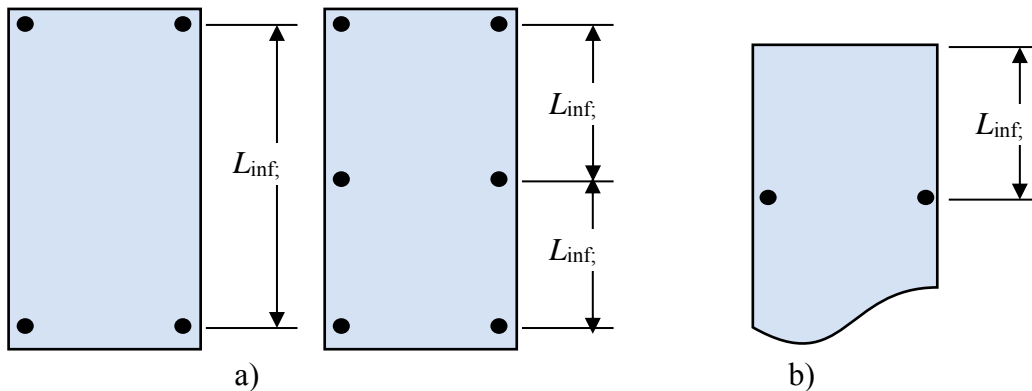


Figure 7.1. Point-fixed plates.

Table 7.13 Indicative values of the maximum permitted displacements – Special cases.

Type of glass	Maximum movement on two consecutive supports at distance $d$	Maximum absolute movement permitted
Single plate – floor	$d / 500$	5 mm
Single plate – built in parapet , with clamped lower edge <sup>(1)</sup>	$d / 50$	25 mm <sup>(2)</sup>
(1) In this case $d$ indicates the parapet height (2) from BS 6180:2011 §8.5.1		

When an element is subjected to two (or more) generic actions, the deflection at one point, referred to the Serviceability Limit State, is evaluated on the basis of the effect superposition principle, such as the sum of the deflections at that same point, caused by different actions:

$$w = \sum_{i=1}^N w_i \leq w_{lim} , \tag{7.9}$$

where

- $w_i$  deflection caused by the  $i$ -th action at the test point;  
 $w_{lim}$  deflection limit value, indicated in the tables.

Superposition of the effects is not valid for non-linear verifications, therefore an analysis that considers the effects of all the loads *contemporaneously* must be carried out. In general, the results of this analysis are lower, in terms of maximum deflection, than those of the linear case. For a first approximation, therefore, Eq. (7.9) can be used even when the single values  $w_i$  are evaluated with non-linear analyses.

The long-term deflection on beams and fins, calculated under the almost permanent load condition, should not exceed 1/250 of the span.

There are no particular regulations for the maximum deflection in the CLS verification, but it is necessary to verify that the displacements are compatible with the constraints, and that they do not compromise the functionality of the structure.

## 7.6 Seismic verifications

The interaction between glass structures and the whole building must always be considered, together with the local behaviour of the glass elements.

The defined performance levels can be reached using design choices and construction measures that involve 1) the use of suitable glass types and sizes; 2) the use of intrinsically ductile systems or connecting systems with a ductile behaviour; 3) the use of connecting systems which guarantee the glass elements a) rigid rotation/translation inside the load-bearing structural system, b) suitable limitation of the stress level.

The SLV (Limit state for the safeguard of human life) must make sure that the system capacity is not lower than the demand. The performance demand is defined in terms of forces and displacements, therefore there are two types of verifications.

- Resistance calculations, where it must be verified that the glass can support accelerations induced by the seismic event.
- Displacement compatibility assessment, where it must be ensured that the interaction between the glass element and the rest of the building is compatible with the presence of glass. In general, this interaction is considered to be satisfactory if, at the SLV, the construction vibration does not lead to contact with the glass element and, therefore, that there are no hammering phenomena. It must also be guaranteed that the glass and/or the connection can compensate the movements of the remaining part of the load-bearing structure during the pre- and/or post-breakage phases.

### 7.6.1 Resistance calculations

In general, these verifications deal with both the in-plane and out-of-plane accelerations.

The former are important only when the glass elements are not secondary elements, namely when a significant part of the overall resistance/rigidity of the structure against the horizontal seismic forces is demanded to them. For these applications, level III or level II reliability methods (Section 5.2.2) should be used to carry out specific studies that can evaluate the effective reliability level of the system.

The verifications against out-of-plane actions are generally not particularly important, because the mass of the glass is limited, and the forces corresponding to the applied accelerations are generally lower than those caused by other actions, such as wind. Maximum acceleration can be estimated approximately using the formulas in Section 4.4.3.

The design strength of the glass frames and fixings is evaluated according to the rules established by current technical regulations on structures of similar material, possibly integrated by the design rules defined in these recommendations.

All the elements of the system must be in line with regulations that are suitable for avoiding early collapse and possible uncontrolled detachment, caused by seismic acceleration correspondent to the considered limit state.

In the case of silicone joints, the stress in glass caused by its contact with the joint shall be suitably verified.

When the dynamic analysis of the whole construction is not available, the acceleration of the glass elements to be used in these tests can be calculated by using local formulas based on (in addition to site seismicity) the height of the glass element in relation to the total height of the building.

### **7.6.2 Deflection verifications**

The verification of the deformation compatibility with movement of the constraining points caused by deformation of the seismic-resistant structure represents the most important verification as far as glass elements are concerned.

The system that connects the glass element to the rear structure must be designed in order to guarantee the performance limits defined by Table 4.7. The seismic activity to be considered for each limit state (defined in section 4.4.2.2) is established in Table 4.8.

The verification procedure is as follows. After defining the use class of the building, the design accelerogram shall be evaluated on the basis of the return period defined by Table 4.6. A structural analysis of the load-bearing frame of the building, carried out using the methods indicated by technical standards (linear or non-linear, static or dynamic analysis), allows to evaluate, for each of the 2 limit states established in paragraph 4.4.2.2, the displacements at the connection point of the glass elements (displacement demand). The action is expressed by, or rather derived from, the relative displacement of the connection points (e.g. in the case of a façade fixed to the building floors, the action is associated with the floor drift produced by the seismic force, relative to the considered limit state). The capacity requested from the system is defined by performance levels given in Table 4.8 for each limit state.

Regarding the ND (No Damage) level, the calculation shall assess that the glass does not break. Only localised breaks can be accepted for the SD (Slight Damage) level. Partial or total glass breakage can be contemplated for HD (Heavy Damage) and F (Failure) levels.

Should the designer consider the possibility of glass breakage, it shall be made sure that the system (glass + connection) is designed to prevent the catastrophic fall of the element when under seismic action. In particular, the performance of the silicon joints must be checked.

## 8 CALCULATION EXAMPLES

The procedures for the structural assessment of glass elements will now be applied to some of the most common cases in design. For the sake of simplicity, an attempt is made to treat every example in the same manner, even if with some repetitions.

According to the general design criteria shown in Chapter 3, structural strength and (section and system) redundancy are fundamental requirements for well-designed structures. Special attention is paid at the post-glass breakage verifications, in accordance with the *fail safe* approach which, due to the intrinsic brittleness of the material, is the design reference criterion.

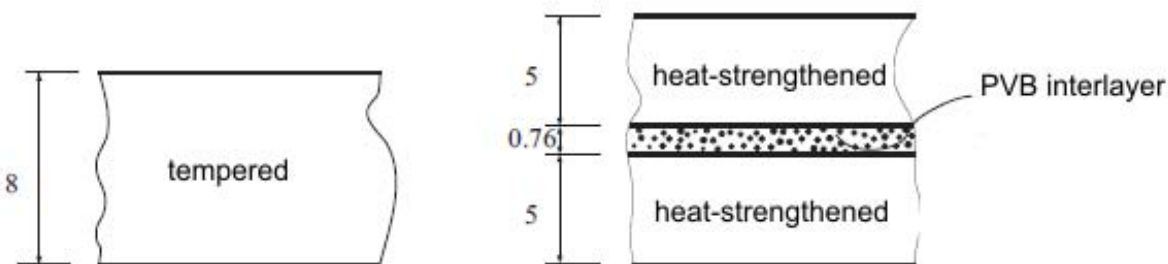
The considered actions on the elements comply with what is indicated by the national technical standard [Italian Building And Construction Standards NTC 2008]. Refer to Chapter 4 for the more specific aspects related to glazing.

The design strength are those indicated in Chapter 7. The corresponding partial coefficients of the material, as well as the various correction factors, were set in Chapter 5 in accordance with the theoretical model and the experimental results given in Chapter 2. Both analytical and numeric schematization and modelling, which make it possible to evaluate the stress and deformation state of the elements, follow the indications given in Chapter 6.

It is evident that in the proposed examples only the mechanical resistance and stability of the glazed element are considered. As reminded in Chapter 1, there are many other aspects, not strictly structural, that influence the design (e.g. sound-proofing) and to which specific technical documents and regulations apply. In addition, the plates must always satisfy the safety requirements in use, and specific product regulations exist for them.

### 8.1 Glass plates simply supported along the edges

The examples proposed here refer to rectangular panels that are simply supported on four edges, under wind action. Rectangular plates (2000 × 1500 mm, with thickness 8 mm) made of monolithic tempered glass are considered here, together with laminated glass made up of two plies of heat strengthened glass, with thickness 5 mm, bonded by a PVB interlayer of thickness 0.76 mm, as shown in Figure 8.1. To evaluate the effect of the geometric shape, a laminated glass square plate (size 1700 × 1700 mm) is also considered.



Calculations are carried out by considering the glass elements in class 1. Analysis of the structural silicon joint that constrains the plates to the underlying frame is also proposed in paragraph 8.1.6.

### 8.1.1 Load analysis

For simplicity, the calculations are carried out by considering only the wind action. As the glass undergoes static fatigue (par. 2.1.1.1), not only the maximum action value, but also its characteristic duration must be defined. This is because actions that are relatively low but with long duration can produce greater damage than peak actions. The verifications are therefore carried out, as described in par. 4.5.1, using wind gusts with peak speeds, and also short gusts (10 minutes averaged wind). A uniformly distributed pressure/depression action equal to  $p_{w,3sec} = \pm 1.2$  kPa was assumed, relative to gusts averaging over 3s, which were applied for a nominal time of 5s (equal to the spectrum integral), in compliance with Table 4.18 of Section 4.10.

The wind pressure averaged over 10 minutes can be obtained using relationship (4.26), which gives

$$\frac{p_{w,10min}}{p_{w,3sec}} = \frac{1}{c_{e,2}},$$

where the coefficient  $c_{e,2}$ , given by the relation (4.27), is

$$c_{e,2}(z) = 1 + \frac{7}{\ln\left(\frac{z}{z_0}\right)} \cdot c_t$$

Usually,  $c_{e,2} > 1$ .

Only the problem of peak wind gusts is developed here. The case of 10 minutes averaged wind load is treated in an identical manner; in the specific case presented here, these conditions may not be the most restrictive for design.

In conclusion, the design actions considered are therefore

- for the deflection evaluation (SLS),  $F_d = p_{w,3sec} = 1.2$  kW/m<sup>2</sup>;
- for the stress evaluation (ULS),  $F_d = \gamma_Q p_{w,3sec} = 1.8$  kW/m<sup>2</sup>.

### 8.1.2 Design strength

The design strengths  $f_{g;d}$  for the case of heat-strengthened glass and tempered glass are calculated with reference to (7.5), according to which

$$f_{g;d} = \frac{k_{mod} k_{ed} k_{sf} \lambda_{gA} \lambda_{gl} f_{g;k}}{R_M \gamma_M} + \frac{k'_{ed} k_v (f_{b;k} - f_{g;k})}{R_{M;v} \gamma_{M;v}},$$

where:

$k_{mod}=0.88$

reduction coefficient for the phenomenon of static fatigue, given in Table 2.2 according to the type of external action and its characteristic duration; for 3 s wind gusts, as suggested in Table 4.18, a characteristic duration (equivalent to the spectrum integral) of 5 s is considered.

$k_{ed} = 1$	strength reduction factors for verifications near the edge of the plate or holes (Table 7.3). In the case under consideration, this coefficient is unitary, because the considered element is a plate under out-of-plane loading;
$k_{sf} = 1$	coefficient for the surface profile of the glass (untreated surface) as <i>per</i> Table 7.4;
$f_{g;k} = 45 \text{ MPa}$	nominal characteristic strength of float glass, as <i>per</i> Table 7.7;
$R_M = 0.7$	reduction factor of the partial coefficient, for tests in class 1 (Table 7.10);
$\gamma_M = 2.50$	partial coefficient of the float glass (Table 7.9);
$f_{b;k}$	characteristic value of the nominal strength for prestressed glass (Table 7.7);
$k'_{ed} = 1$	strength reduction factors for verifications near the edge of the sheet or holes (Table 7.3); in the present case the calculations are carried out away from the edges and this coefficient has no influence;
$k_v = 1$	coefficient for heat treated sheets with horizontal heat treatment (Table 7.8);
$R_{M;v} = 0.9$	reduction factor of the partial coefficient for calculations in class 1 (Table 7.10);
$\gamma_{M;v} = 1.35$	partial coefficient for heat strengthened glass (Table 7.9);
$\lambda_{gl}$	scale factor for stress on the edge, given by (7.7). In the case at hand, with the maximum stress at a distance of $d > 5 s$ from the edge, $\lambda_{gl} = 1$ ;
$\lambda_{gA}$	scale factor that considers the area subjected to the maximum stress, calculated using (7.6), namely

$$\lambda_{gA} = \left( \frac{0.24 \text{ m}^2}{k A} \right)^{1/7}$$

where  $A$  is the total area of the plate under stress; the coefficient that defines the effective area is given in Table 7.5, while for the rectangular plate simply supported on four edges we have  $k=0.145$ . Therefore:

for the square plate:

$$\lambda_{gA} = \left( \frac{0.24 \text{ m}^2}{k A} \right)^{1/7} = \left( \frac{0.24}{0.145 \cdot 1.7 \cdot 1.7} \right)^{1/7} = 0.9235;$$

for the rectangular plate:

$$\lambda_{gA} = \left( \frac{0.24 \text{ m}^2}{k A} \right)^{1/7} = \left( \frac{0.24}{0.145 \cdot 1.5 \cdot 2} \right)^{1/7} = 0.9186.$$

Design strength of the thermally toughened (tempered) glass element:

Table 7.7 gives, for tempered glass,  $f_{b;k} = 120 \text{ MPa}$ , therefore one obtains a design strength equal to:

$f_{g;d} = 82.63 \text{ MPa}$  for the rectangular plate;

$f_{g;d} = 82.51 \text{ MPa}$  for the square plate.

Design strength of the heat strengthened glass element:

Table 7.7 gives, for heat strengthened glass,  $f_{b;k} = 70 \text{ MPa}$ . The design strength is therefore equal to:

$f_{g;d} = 41.47 \text{ MPa}$  for the rectangular plate;

$f_{g;d} = 41.36 \text{ MPa}$  for the square plate.

In the case of single glass (monolithic or laminated), the design deflection in the centre of the plate is given in Table 7.11 and is equal to 1/60 of the minimum plate size. In the considered case:

- for the square plate:  $w_{\max} = 1700/60 = 28.33 \text{ mm}$  ;
- for the rectangular plate:  $w_{\max} = 1500/60 = 25 \text{ mm}$  .

### 8.1.3 Monolithic rectangular plate under wind load

The proposed calculation example includes the analysis of a monolithic plate of tempered glass of size 2000 × 1500 mm (Figure 8.2), thickness 8 mm, considered simply supported on its four edges. The action  $p_{w,3\text{sec}} = \pm 1.2 \text{ kPa}$  is multiplied by the coefficient  $\gamma_Q = 1.5$  in the ULS verifications.

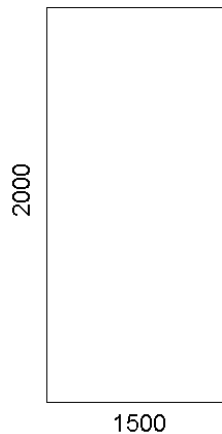


Figure 8.2. Monolithic glass supported on its four edges

Firstly, stress and deflection are calculated analytically, by using the formulas proposed in Paragraph 6.6.1.1; secondly, a finite element analysis is performed. The calculation is made using the hypotheses of both linear and non-linear geometry, and the results obtained with the different methods are compared.

#### 8.1.3.1 Calculation by using formulae and tables

Reference is made to Annex 6.6.1.1 (rectangular plate simply supported on four edges), which supplies formulae and tables for the analytic evaluation of the maximum stress and maximum deflection for flat plates subjected to uniformly distributed loads.

The maximum stress  $\sigma_{\max}$  and the maximum force  $w_{\max}$  resulting from the design action  $F_d$  can be evaluated using formulae (6.94) and (6.95):

$$\sigma_{\max} = k_1 \frac{A}{h^2} F_d, \quad w_{\max} = k_4 \frac{A^2}{h^3} \frac{F_d}{E},$$

where  $a$  is the length of the shorter edge of the plate and  $b$  is the length of the longer edge,

$A = ab$  plate area;

$h$  plate thickness;

$k_1$  dimensionless coefficient, the values of which are given in Table 6.9;



$k_4$  dimensionless coefficient, the values of which are given in Table 6.10.

In the case of rectangular plates simply supported on all edges,  $k_1$  and  $k_4$  depend on the aspect ratio  $\lambda = a/b$  and the normalised load  $p^*$  through the expression (6.96).

In the case being studied:

$$\lambda = a/b = 0.75;$$

$$p^* = \left( \frac{A}{4h^2} \right)^2 \frac{F_d}{E} = \begin{cases} 3.531 & \text{for ULS,} \\ 2.354 & \text{for SLS.} \end{cases}$$

By calculating the ULS stress using the formulas given in Table 6.9, the result is  $k_1 = 0.2427$ , from which it is possible to obtain

$$\sigma_{\max} = k_1 \frac{A}{h^2} F_d = 20.48 \text{ MPa at the SLU};$$

Table 6.10 gives  $k_4 = 0.0325$ , therefore:

$$w_{\max} = k_4 \frac{A^2}{h^3} \frac{F_d}{E} = 9.8 \text{ mm at the SLS.}$$

### 8.1.3.2 Linear FEM calculation

The finite elements analysis is performed for a glass plate subjected to the same constraint and load conditions. The elements are of the “solid” type, with 20 nodes and mixed formulation (of the *in-compatible mode* type). The plate is constrained at the nodes along the edges, with only the out-of-plane translation being rigidly constrained. The distributed load is applied as distributed pressure acting on the faces of the elements. Figure 8.3 and Figure 8.4 give the maximum principal stress at the ULS and the deflection at the SLS, respectively, in the case of linear analysis.

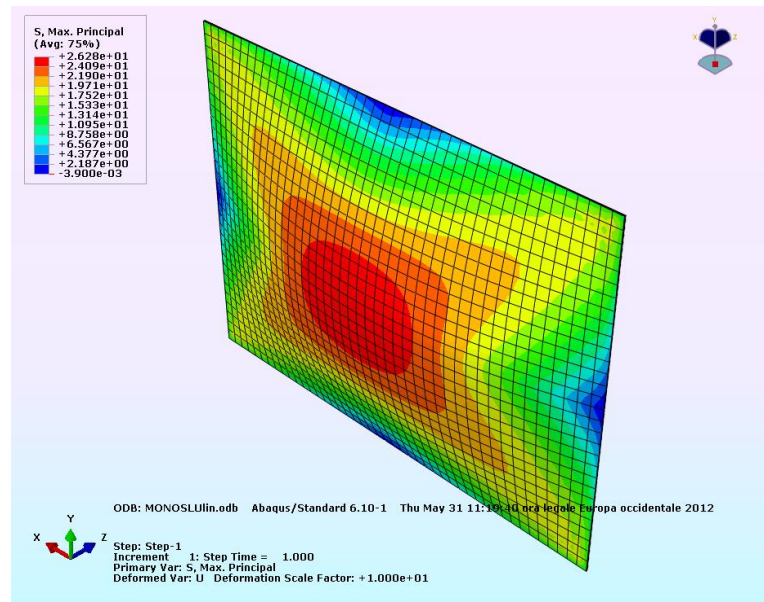


Figure 8.3 Monolithic glass, linear solution: maximum principal stress at the ULS.

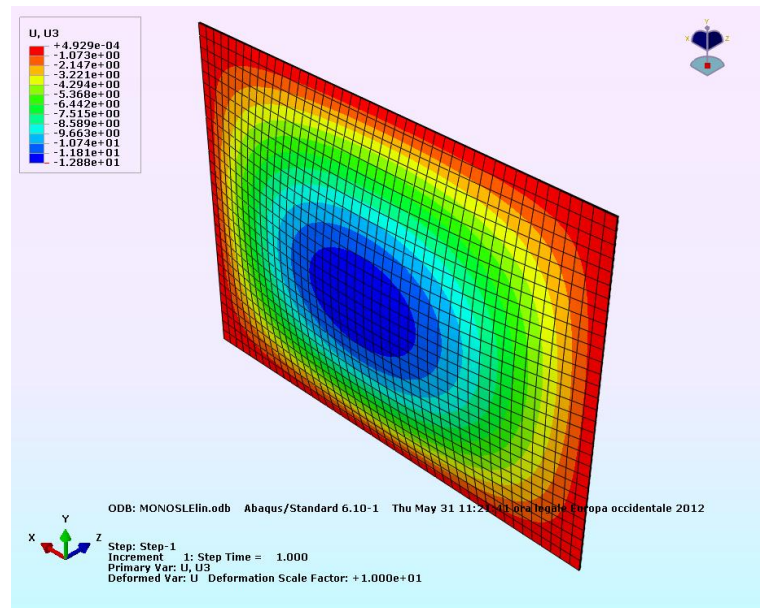


Figure 8.4. Monolithic glass, linear solution: deflection at the SLS.

The following results are obtained by using the linear finite elements model:

$$\sigma_{max} = 26.28 \text{ MPa at the ULS};$$

$$w_{max} = 12.88 \text{ mm at the SLS}.$$

### 8.1.3.3 Non-linear FEM calculation

Analyses for the same plate are repeated using the same finite element model, but in this case the hypotheses are constitutive linear-elastic material response and geometric non-linearity. The geometric stiffness matrix is therefore updated at each integration, following the shape modifications of the plate during load application. Figure 8.5 and Figure 8.6 show the maximum principal stress at the ULS and the deflection at the SLS, respectively.

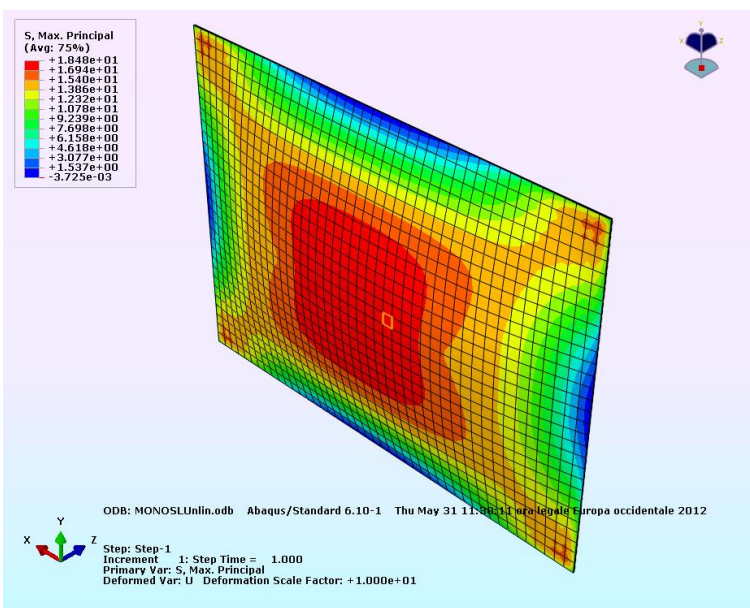


Figure 8.5 Monolithic glass, non-linear solution: maximum principal stress at the ULS.

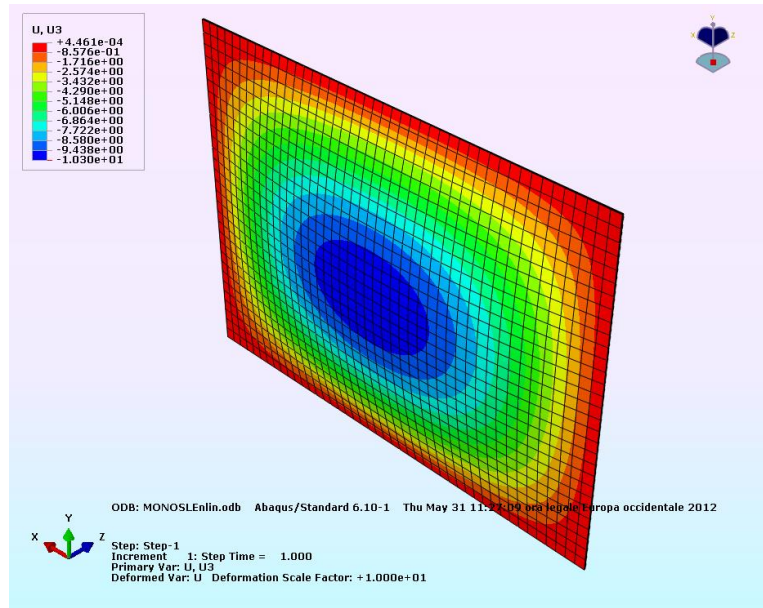


Figure 8.6. Monolithic glass, non-linear solution: deflections at the SLS.

With the geometrically non-linear finite element model, the maximum stress and maximum deflection values of this specific case are lower than those obtained with linear analysis:

$$\sigma_{max} = 18.48 \text{ MPa at the ULS};$$

$$w_{max} = 10.30 \text{ mm at the SLS}.$$

#### 8.1.3.4 Comparison of the results obtained with the various methods

The maximum stress and maximum deflection values obtained with the three solutions above (calculation with formulae, with linear FEM and with non-linear FEM) are given in Table 8.1. When compared, it can be clearly seen how the linear analysis gives rather different results than those of the non-linear theory.

Table 8.1. Comparison of the various solutions for monolithic glass.

METHOD	Maximum force SLS	Maximum stress ULS
Analytic method	9.79 mm	20.48 MPa
Finite Elements (linear)	12.88 mm	26.28 MPa
Finite Elements (non-linear)	10.30 mm	18.48 MPa

Even though it does not give exact results, the analytic calculation can quite accurately evaluate the stress and deflection, making it very useful during the preliminary design phase. The formulas given in Annex 6.6.1 also consider geometric non-linearity: good result agreement can, in fact, be seen with the non-linear finite element solution.

The resistance and deformability verification (see Table 7.11) are satisfied (by considering, on the safe side, the values of maximum stress and deflection obtained with the linear FEM analysis). In fact:

$$\sigma_{\max} = 26.28 < f_{g;d} = 82.63 \text{ MPa};$$

$$w_{\max} = 12.88 < \frac{1}{60} L_{\min} = 25 \text{ mm}.$$

### 8.1.4 Rectangular laminated glass plate under wind load

The case of the rectangular laminated glass plate simply supported on four edges, of size  $2000 \times 1500$  mm (Figure 8.2) and subjected to wind load is proposed here. The considered laminated package is made of two plies of glass, each one 5 mm thick, with two foils of PVB plies as interlayer, each one 0.38 mm thick. The commonly used synthetic indication to identify the thickness of a composite package of this type is “5.5.2” (5 mm of glass + 5 mm of glass + 2 foils for interlayer of standard thickness 0.38 mm).

The properties of the PVB interlayer are generally supplied by the producer. For the case being examined, the properties corresponding to a characteristic load duration of 3 seconds and a temperature of  $50^\circ\text{C}$  (temperature usually reached by a element directly exposed to sunlight) are considered. It is worthwhile highlighting that to evaluate interlayer stiffness, the nominal value of the force duration (3s) has been taken. To calculate glass resistance, as mentioned in Paragraph 8.1.2, a characteristic nominal time of 5 s was taken, conventionally assumed to be equal to the integral of the load spectrum during the life of the building, as described in Section 4.10.

Under these hypotheses, it is assumed that the interlayer-producer has declared, for the temperature and the load duration of the case, a value of the shear modulus of 0.44MPa.

In the example, stress and deflection are calculated using

- the model with effective thickness according to ASTM E1300 (Wölfel-Bennison model), coupled with a finite element analysis (Section 6.3.3.1.4);
- the Enhanced Effective Thickness model (Section 6.3.3.1.5);
- a three-dimensional finite element analysis of the laminate package.

#### 8.1.4.1 Effective thickness model (Wölfel-Bennison)

Referring to paragraph 6.3.3.1, the verification on the overall behaviour of the panel can be carried out, as a first approximation, by considering the laminated element as a monolithic element with thickness equal to the effective thickness, that accounts for the shear transfer produced by the interlayer (level 1 model, as *per* paragraph 6.3.3.1). To do this, we must introduce the shear transfer coefficient, which is a measure of the transfer of shear stress through the interlayer. Referring to the Wölfel-Bennison model, used by the ASTM E1300-09a (Appendix XII), the shear transfer coefficient  $\Gamma$  is defined by formula (6.42), while the deflection- and stress-effective thickness are given respectively by (6.43) and (6.44), namely

$$h_{ef,w} = \sqrt[3]{(h_1^3 + h_2^3 + 12 \Gamma I_s)} \quad , \quad h_{1,ef;\sigma} = \sqrt{\frac{h_{ef,w}^3}{h_1 + 2\Gamma h_{s;2}}}$$

In the case being examined:

$$h_{int} = 0.76 \text{ mm} = \text{interlayer thickness};$$

$$h_1 = h_2 = 5 \text{ mm} = \text{thickness of each glass ply};$$

$$E = 70000 \text{ MPa} = \text{Young's modulus of glass};$$

$a = 1500 \text{ mm} = \text{length of the shorter edge};$

$G_{int} = 0.44 \text{ MPa} = \text{shear modulus of the polymeric interlayer};$

$$d = \frac{h_1 + h_2}{2} + h_{int} = 5.76 \text{ mm};$$

$$I_s = d^2 \frac{h_1 h_2}{h_1 + h_2} = 82.044 \text{ mm}^3 .$$

We therefore obtain, from (6.42):

$$\Gamma = \frac{1}{1 + 9.6 \frac{h_{int} EI_s}{G_{int} l^2 d^2}} = 0.437 \text{ shear transfer coefficient.}$$

The result is therefore:

- Deflection-effective thickness:  $h_{ef,w} = 8.814 \text{ mm};$
- Stress-effective thickness:  $h_{1;ef,\sigma} = h_{2;ef,\sigma} = 9.545 \text{ mm}.$

To calculate stress and deflection, the monolithic plates with efficient thickness, as calculated above, shall be modelled with finite elements.

The following configurations will therefore be analysed:

- for SLS verification, plate of thickness  $h_{ef,w} = 8.814 \text{ mm}$ , subjected to a load  $F_d = p_{w,3sec} = 1.2 \text{ kN/m}^2$ ;
- for ULS verification, plate of thickness  $h_{1;ef,\sigma} = 9.545 \text{ mm}$ , subjected to a load  $F_d = \gamma_Q p_{w,3sec} = 1.8 \text{ kN/m}^2$ .

The elements used are 20-node ‘‘SOLID’’ elements, with mixed formulation; the geometry can be also modelled with SHELL elements. The plate is constrained along its edges, preventing the out-of-plane displacements. The pressure is applied as a distributed load acting on the faces of the elements. Figure 8.7 and Figure 8.8 show the maximum principal stress at the ULS and the deflection at the SLS, respectively.

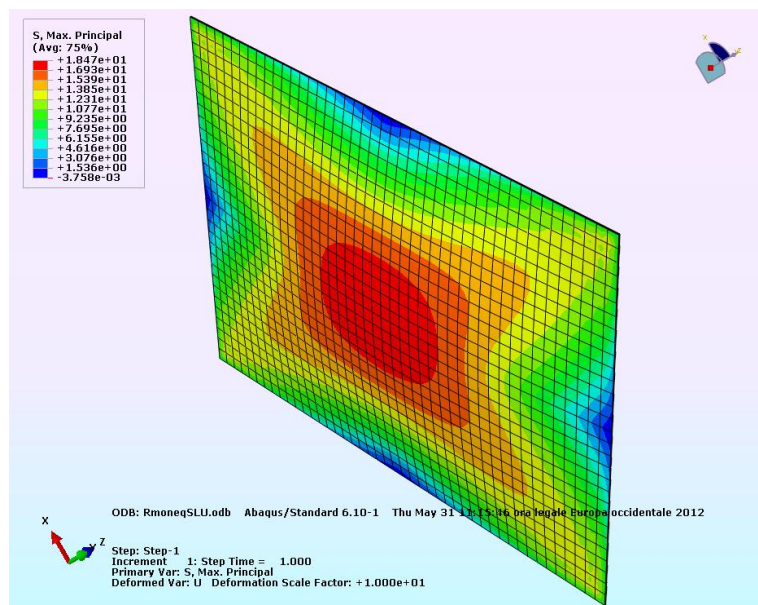


Figure 8.7. Equivalent monolithic plate, thickness  $h_{1;ef,\sigma} = 9.545 \text{ mm}$ : maximum principal stress at the ULS.

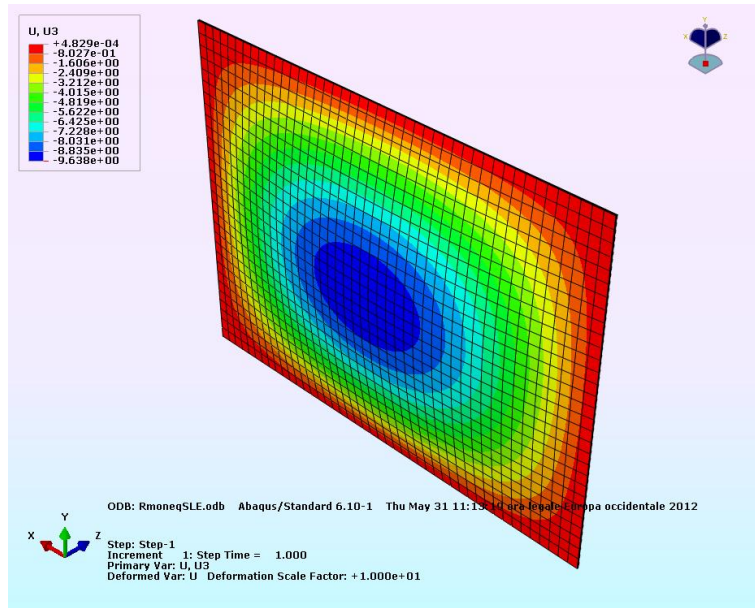


Figure 8.8 Equivalent monolithic plate, thickness  $h_{ef,w} = 8.814$  mm: deflection at the SLS.

The linear elastic calculation is carried out by considering, or not considering, geometric non-linearity.

The following values are obtained with linear analysis:

$$\sigma_{max} = 18.47 \text{ MPa at the ULS};$$

$$w_{max} = 9.638 \text{ mm at the SLS}.$$

By performing a geometrically non-linear analysis, the following values are found:

$$\sigma_{max} = 16.38 \text{ MPa at the ULS};$$

$$w_{max} = 8.437 \text{ mm at the SLS}.$$

#### 8.1.4.2 Model with effective thickness (Enhanced Effective Thickness method)

The problem is now solved by using the “Enhanced Effective Thickness” method described in Section 6.3.3.1. This method suggests to evaluate the deflection-effective thickness as *per* (6.46), i.e.

$$\hat{h}_w = \sqrt[3]{\frac{1}{\frac{\eta}{h_1^3 + h_2^3 + 12I_s} + \frac{1-\eta}{h_1^3 + h_2^3}}};$$

while the stress-effective thickness (for calculating the stress in ply 1 and ply 2) are instead given by (6.48) as

$$\hat{h}_{1,\sigma} = \sqrt{\frac{1}{\frac{2\eta d_1}{h_1^3 + h_2^3 + 12I_s} + \frac{h_1}{\hat{h}_w^3}}}, \quad \hat{h}_{2,\sigma} = \sqrt{\frac{1}{\frac{2\eta d_2}{h_1^3 + h_2^3 + 12I_s} + \frac{h_2}{\hat{h}_w^3}}}.$$

Here  $\eta$  is a non-dimensional coefficient that depends on the geometry, the load and constraint conditions and the mechanical characteristics of glass and interlayer. This coefficient therefore considers the level of coupling offered by the interlayer, and varies between 0 (which corresponds to the layered limit) and 1 (which corresponds to the monolithic limit, with perfectly coupled glass plies). In the case being examined, since  $h_1 = h_2$ , one obtains  $\hat{h}_{1;\sigma} = \hat{h}_{2;\sigma}$ .

The coefficient  $\eta$  is given, according to (6.55), by

$$\eta_{2D} = \frac{1}{1 + \frac{h_{int} E}{G_{int} (1 - \nu^2)} \frac{D_{abs}}{D_{full}} \frac{h_1 h_2}{h_1 + h_2} \Psi},$$

where

$D_{abs} = 1532506$  Nmm : flexural rigidity corresponding to the *layered limit*, defined by (6.52);

$D_{full} = 7633893$  Nmm : flexural rigidity corresponding to the *monolithic limit*, defined by (6.53).

The  $\Psi$  coefficient can be obtained from Table 6.4, according to the load and constraint conditions of the plate, the length of the longest edge ( $a = 2000$  mm) and the aspect ratio  $\lambda = b / a = 0.75$ . For the considered plate, simply supported on four edges and subject to uniform load, the linear interpolation of the tabulated values gives  $\Psi = 6.969 \cdot 10^{-6}$  mm<sup>-2</sup>.

The deflection- and stress-effective thicknesses, evaluated by using equations (6.46) and (6.48), are therefore:

$$\hat{h}_w = 8.241 \text{ mm};$$

$$\hat{h}_{1;\sigma} = \hat{h}_{2;\sigma} = 9.078 \text{ mm}.$$

Using these thicknesses, the linear FEM analysis of the equivalent plate gives these values:

$$\sigma_{max} = 20.42 \text{ MPa at the ULS}$$

$$w_{max} = 11.79 \text{ mm at the SLS}.$$

If a geometrically non-linear analysis is carried out, these values are obtained:

$$\sigma_{max} = 17.19 \text{ MPa at the ULS};$$

$$w_{max} = 9.72 \text{ mm at the SLS}.$$

### 8.1.4.3 Finite element linear analysis of the laminated plate

The specific case deals with a plate composed by two external layers with the mechanical properties of glass, and one interlayer having the mechanical characteristics of PVB. The plate is constrained by the nodes along the edges, with only the out-of-plane displacement being null. The load is distributed over the faces of the elements. Figure 8.10 and Figure 8.11 give the maximum principal stress at the ULS and the deflection at the SLS, respectively, in the hypotheses of material and geometric linearity.

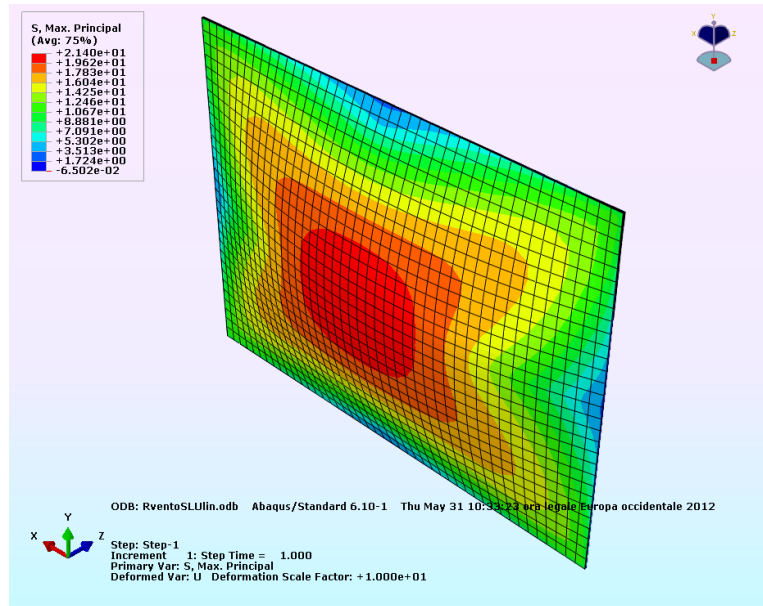


Figure 8.9. Laminated glass, linear solution: maximum principal stress at the ULS.

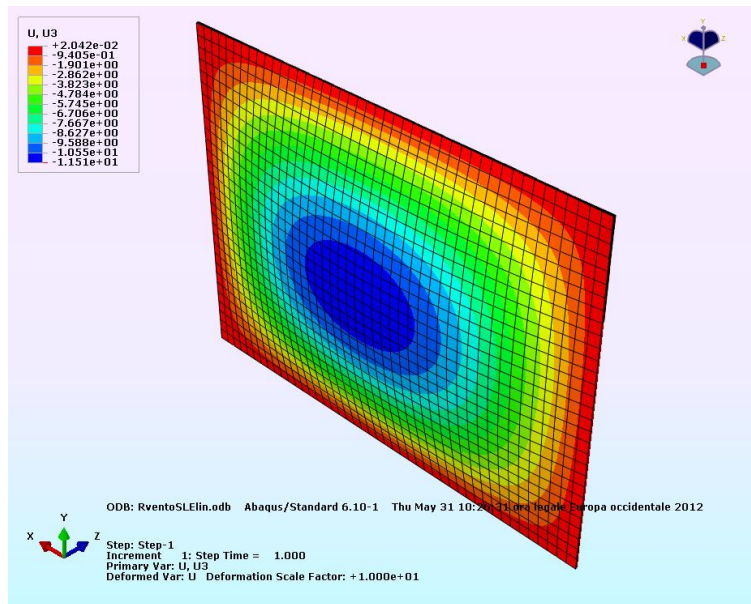


Figure 8.10 Laminated glass, linear solution: deflection at the SLS.

With the linear model, these results are obtained:

$$\sigma_{max} = 21.40 \text{ MPa at the ULS};$$

$$w_{max} = 11.51 \text{ mm at the SLS}.$$

#### 8.1.4.4 Finite element non-linear analysis of the laminated plate

The same finite element analyses are now performed by considering the geometric non-linearity of the problem. Figure 8.11 and Figure 8.12 give the maximum principal stress at the ULS and the deflection at the SLS, respectively.



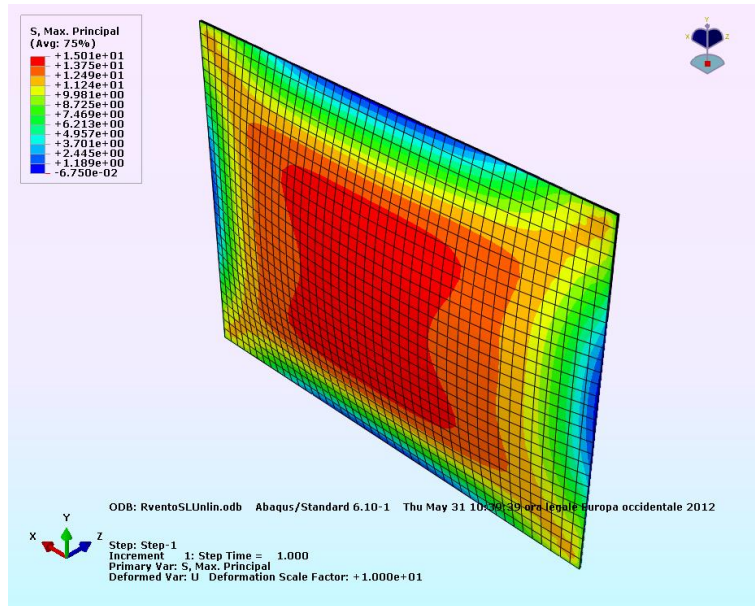


Figure 8.11. Laminated glass, non-linear solution: maximum principal stress at the ULS.

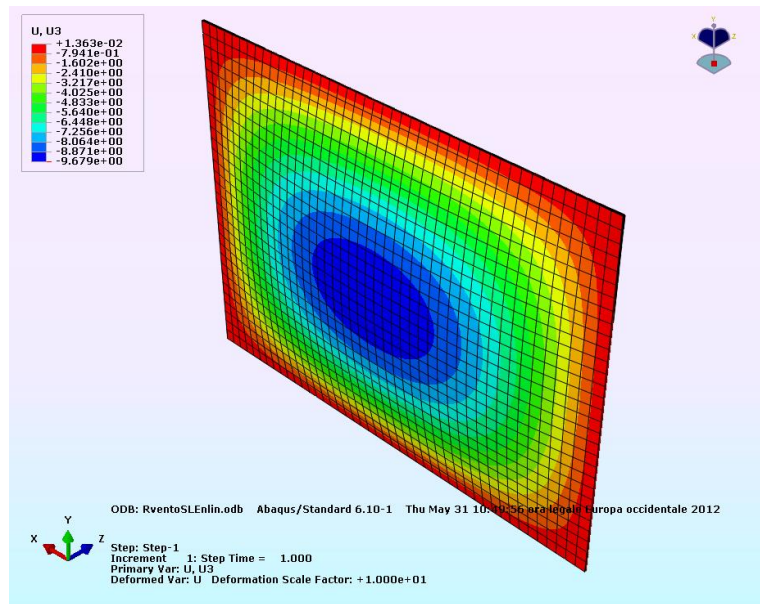


Figure 8.12 Laminated glass, non-linear solution: deflection at the SLS.

The non-linear finite element model gives:

$$\sigma_{max} = 15.01 \text{ MPa at the ULS};$$

$$w_{max} = 9.68 \text{ mm at the SLS.}$$

#### 8.1.4.5 Comparison of the results obtained with the different models and verifications

The obtained solutions are compared in Table 8.2.

Table 8.2. Comparison of the various solutions for rectangular laminated glass.

METHOD		Maximum deflection at the SLS	Maximum stress at the ULS
Wölfel-Bennison	linear	9.648 mm	18.47 MPa
	Non-linear	8.44 mm	16.38 MPa
EET	linear	11.79 mm	20.42 MPa
	Non-linear	9.72 mm	17.19 MPa
FEM	linear	11.51 mm	21.40 MPa
	Non-linear	9.679 mm	15.01 MPa

It is important to observe that, even though the approximated methods (Wölfel-Bennison and E.E.T.) are obtained from the linear elasticity hypothesis, the effective thickness found in this manner is often used in FEM codes that consider geometric non-linearity.

The comparison of the three linear solutions given in Table 8.2 shows that the Wölfel-Bennison effective thickness approach can be used only as a first approximation to qualitatively evaluate the orders of magnitude of stress and deflection, because the obtained precision is strongly influenced by geometric factors, the edge conditions, the mechanical characteristics of the interlayer and the thickness of the glass plies. Its acceptability must therefore always be evaluated carefully by an expert. The E.E.T. method, instead, gives both the stress and the maximum deflection values with better approximation.

The non-linear solution gives lower maximum stress and deflection than those obtained from the linear analysis; in this specific case, therefore, the linear analysis results are on the safe.

The resistance and deformability calculations are satisfied, because even assuming the maximum stress and deflections, obtained from the linear FEM analysis, we have

$$\sigma_{\max} = 21.40 < f_{g,d} = 41.47 \text{ MPa};$$

$$w_{\max} = 11.79 < \frac{1}{60} L_{\min} = 25 \text{ mm}.$$

### 8.1.5 Square laminated glass plate subjected to wind

In general, the Wölfel-Bennison method does not produce accurate results when the glass deformed shape is different from the cylindrical “beam-like” one. To illustrate this aspect, consider the case of a square plate of laminated glass, of size  $1700 \times 1700$  mm, simply supported on four edges. The thickness of each glass plies is, again, 5 mm, and there are two PVB interlayers 0.38 mm thick (in short, the denomination of this plate is 5.5.2).

For what concerns the mechanical characteristics of the PVB, the load duration (3 s) and the plate temperature ( $50^\circ \text{C}$ ) remain unchanged with respect to the previous example; a shear modulus for the interlayer of 0.44 MPa is therefore assumed.

#### 8.1.5.1 Model with effective thickness (Wölfel-Bennison)

Similarly to what has been done in Section 8.1.4.1, by applying the Wölfel-Bennison formula to the case being examined, from (6.42), (6.43) and (6.44), it is possible to calculate

$\Gamma = 0.499$ : shear transfer coefficient;

$h_{ef,w} = 9.072$  mm: deflection-effective thickness;

$h_{ef,\sigma} = 9.738$  mm: stress-effective thickness.

Similarly to Paragraph 8.1.4.1, a finite element model must be used to calculate the stress and deflection of monolithic plates having a thickness equal to the effective thickness calculated above. The elements used here are of the “SOLID” type, with 20 nodes. The plate is constrained along its edges, blocking only the out-of-plane translation. The pressure load is distributed over the planes of the elements.

Figure 8.13 and Figure 8.14 show the maximum principal stress at the ULS and the maximum deflection at the SLS, respectively, calculated by using a linear analysis.

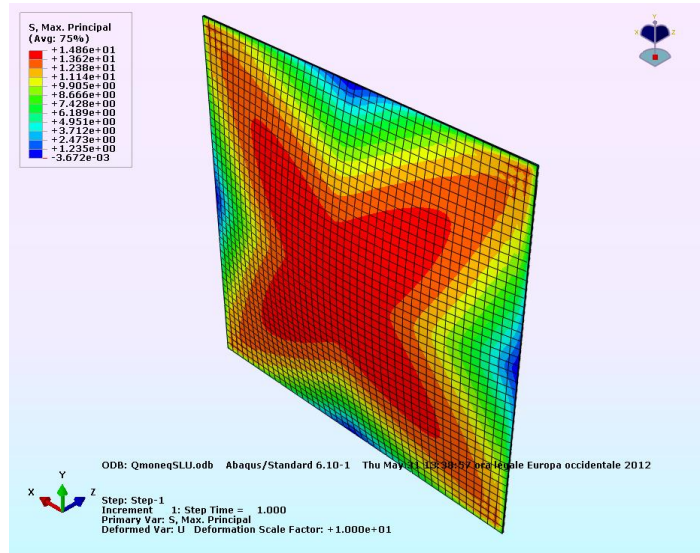


Figure 8.13. Equivalent monolithic plate, thickness  $h_{1,ef,\sigma} = 9.0728$  mm: maximum principal stress at the ULS.

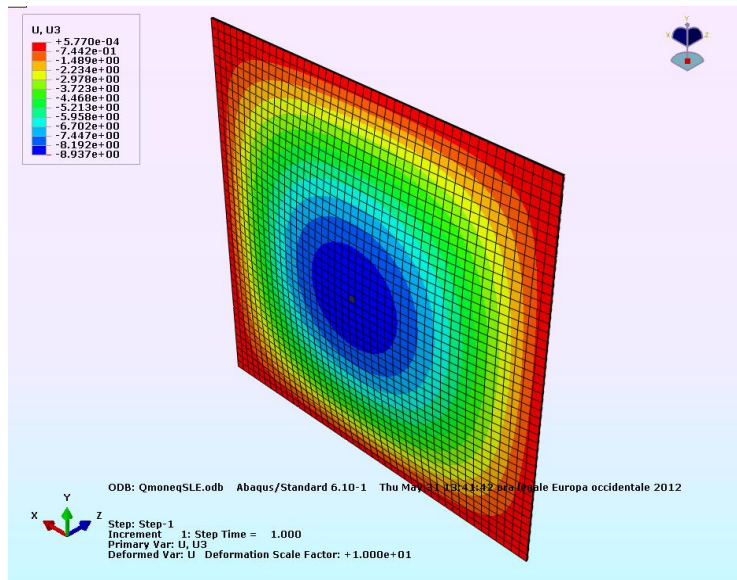


Figure 8.14. Equivalent monolithic plate, thickness  $h_{ef,w} = 9.545$  mm: deflection at the SLS.

The following results are obtained.

In the hypothesis of geometric linearity:

$$\sigma_{max} = 14.86 \text{ MPa at the ULS};$$

$$w_{max} = 8.94 \text{ mm at the SLS}.$$

Geometrically non-linear analyses give:

$\sigma_{max} = 13.74$  MPa at the ULS;

$w_{max} = 7.825$  mm at the SLS.

### 8.1.5.2 Model with effective thickness (Enhanced Effective Thickness model)

The problem is solved firstly using the “Enhanced Effective Thickness” method described in Section 6.3.3.1. In the case being examined, the value  $\Psi = 7.29 \cdot 10^{-6}$  mm<sup>-2</sup> can be obtained from interpolation of Table 6.4; the deflection- and stress-effective thicknesses calculated using the equations (6.46) and (6.48), are therefore:

$$\hat{h}_w = 8.262 \text{ mm};$$

$$\hat{h}_{1,\sigma} = \hat{h}_{2,\sigma} = 9.094 \text{ mm}.$$

The linear FEM model therefore gives:

$\sigma_{max} = 17.25$  MPa at the ULS;

$w_{max} = 12.12$  mm at the SLS.

The non-linear FEM model instead gives:

$\sigma_{max} = 14.79$  MPa at the ULS;

$w_{max} = 9.634$  mm at the SLS.

### 8.1.5.3 Linear FEM calculation

As done before, the finite elements analyses considering linear geometric response are performed. Figure 8.15 and Figure 8.16 show the maximum principal stress at the ULS and the deflection at the SLS, respectively.

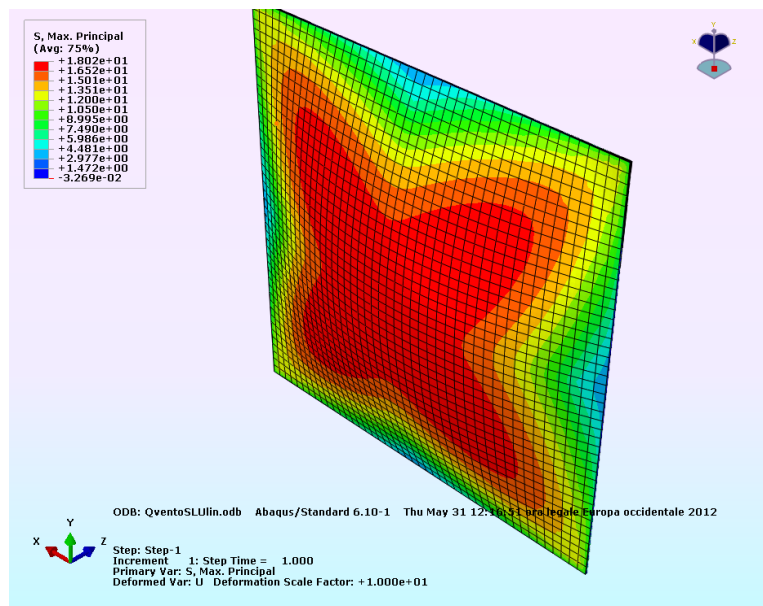


Figure 8.15 Laminated glass, linear solution: maximum principal stress at the ULS.

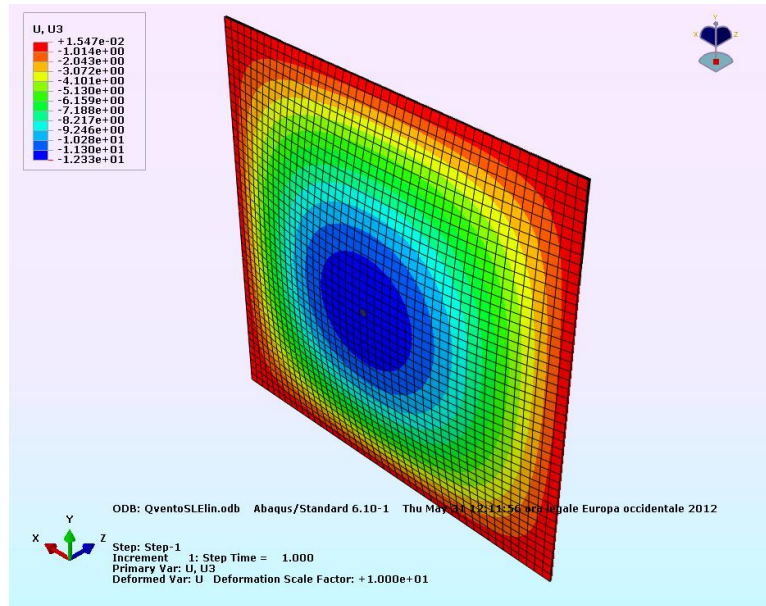


Figure 8.16. Laminated glass, linear solution: deflection at the SLS.

The following results were obtained using this model:

$$\sigma_{max} = 18.02 \text{ MPa at the ULS};$$

$$w_{max} = 12.33 \text{ mm at the SLS.}$$

#### 8.1.5.4 Non-linear FEM calculation

As before, the analysis is now carried out by considering non-linear geometrical behaviour. Figure 8.19 and Figure 8.20 show the maximum principal stress at the ULS and the deflection at the SLS, respectively.

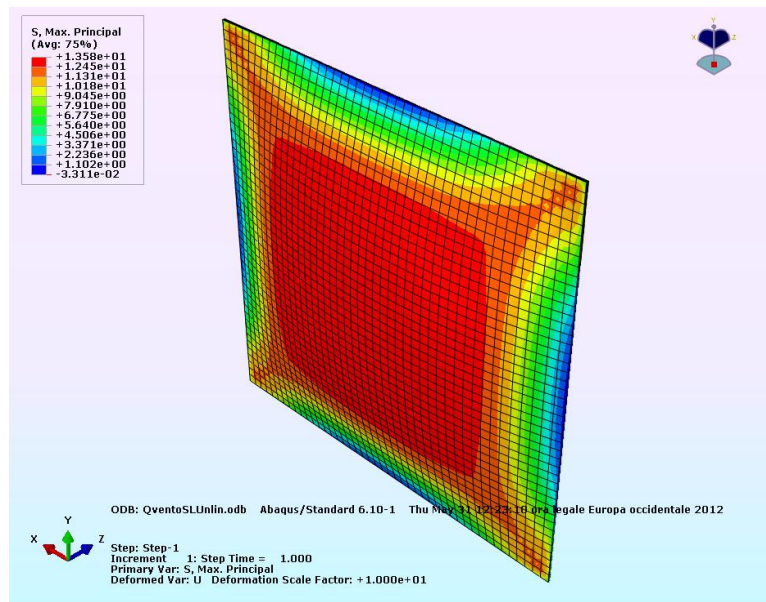


Figure 8.17 Laminated glass, linear solution: maximum principal stress at the ULS.

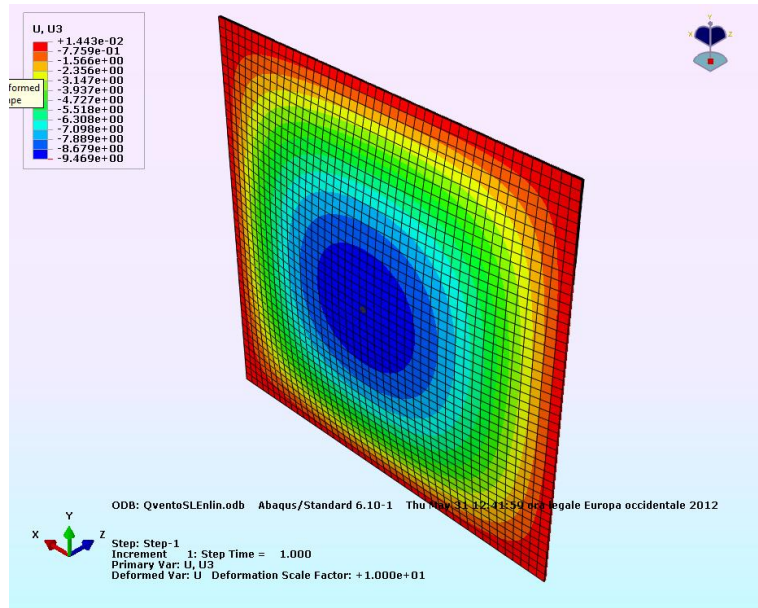


Figure 8.18. Laminated glass, linear solution: deflection at the SLS.

The following results were obtained from this model:

$$\sigma_{max} = 13.58 \text{ MPa at the ULS};$$

$$w_{max} = 9.47 \text{ mm at the SLS}.$$

### 8.1.5.5 Comparison of the results obtained with the various models and verifications

The solutions obtained in the previous paragraphs for the square plate are compared in Table 8.3.

Table 8.3. Comparison of the various solutions for square-shaped laminated glass.

METHOD		Maximum force at the SLS	Maximum stress at the ULS
<b>Wölfel-Bennison</b>	<b>linear</b>	8.937 mm	14.86 MPa
	<b>Non-linear</b>	7.825 mm	13.74 MPa
<b>EET</b>	<b>linear</b>	12.12 mm	17.25 MPa
	<b>Non-linear</b>	9.634 mm	14.79 MPa
<b>FEM</b>	<b>linear</b>	12.33 mm	18.02 MPa
	<b>Non-linear</b>	9.469 mm	13.58 MPa

It can be seen that, also in this case, the E.E.T. method is more accurate than the Wölfel-Bennison method, both for the linear and the non-linear analyses.

In particular, the solution with effective thickness given by the Wölfel-Bennison method evidently underestimates both the maximum force and the maximum stress; the errors are more relevant than those obtained for the rectangular plate (refer to the comparison of the previous solutions, presented in Table 8.2). This phenomenon is due to the fact that the Wölfel-Bennison model is calibrated for simply supported beams; as a result, it becomes much less accurate the further the problem is distant from these conditions.

In addition, it can be observed that the error committed by using the Wölfel-Bennison approach also depends on the characteristics of the interlayer. In fact, if, for this case, further analyses are carried

out, varying the elastic characteristics of the PVB, as can occur as the temperature varies, a comparison of the results offered by the two methods considered here would produce a graph similar to the one shown in Figure 8.19.

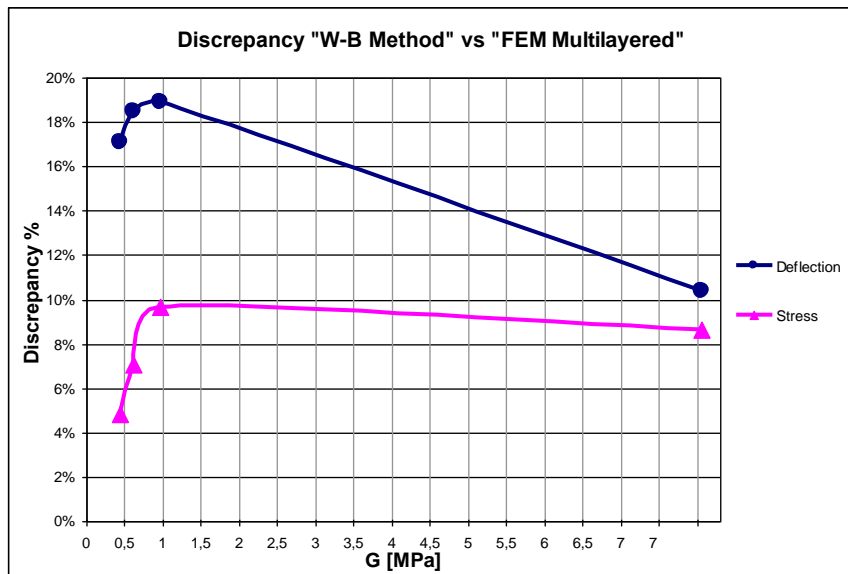


Figure 8.19. Percentage discrepancies between the Wölfel-Bennison solution and the FEM multi-layered solution, as a function of  $G_{int}$ , for the plate 1700x1700 mm, thickness 5.5.2.

On the contrary, the E.E.T. method gives an excellent approximation for both the maximum stress and the maximum deflection.

The non-linear solution gives stress and maximum deflection values that are smaller than those obtained in the linear analysis; the results of the linear analysis therefore add to safety. The resistance and deformability calculations are satisfactory, because taking on stress and maximum deflection that is equal to those obtained using the linear FEM analysis gives:

$$\sigma_{\max} = 18.02 < f_{g;d} = 41.36 \text{ MPa};$$

$$w_{\max} = 12.33 < \frac{1}{60} L_{\min} = 28.33 \text{ mm}.$$

### 8.1.6 Verification of the structural silicone joint

The design of structural silicone joint, bonding the glass to a metallic frame is given below. The considered application is that of a monolithic plate of size 1500 × 2000 × 8 mm subjected to wind (1.2 kPa), already considered in Section 8.1.3.

The calculation is carried out in accordance with the ETAG 002 [ETAG 002-Part 1] standard, supposing that the weight of the glass is not supported mechanically, therefore the silicone joint should also provide for this function. This solution is, generally, not recommended, but the aim of this example is to illustrate the calculation process in the most complex case. The following cases will be considered in particular:

- Short-term load, dynamic type, orthogonal to the lie plane, caused in this specific case by wind;
- Long-term load, permanent type, parallel to the lie plane, in this specific case caused by the weight of the glass element.

The distinction between the two types of load is necessary, because silicone has a strength limit that differs according to these parameters:

- Load duration, related to its viscoelastic behaviour;
- Load direction, because it resists differently to normal or tangential stress.

The strength value can vary from one type of material to another and shall be supplied by the producer. In the case being examined, it is supposed that the data given in Table 8.4 are available; this data are to be considered as indicative for this specific example and cannot be extended to any other case. Note that the data supplied by the producer generally indicate the *allowable stress* in the silicone material, namely the design stress *already* reduced of the partial coefficient of the material, that represents the values to be compared directly with the effects of the action.

Due to the variability of products on today’s market, it is not possible to define a universal statistic that can be used to directly find the partial coefficients of the material, starting from the nominal values of the design resistance. The designer must always make sure that the values indicated by the producer derive from accurate experimental research and, in particular, make sure that these values are effectively permitted for design, including partial coefficients.

Table 8.4. Allowable stress for a particular type of structural silicone (these results cannot be extended to silicone material in general).

Allowable <i>tensile stress</i> $\sigma_{amm}$ for <i>short-term</i> loads	0.140 MPa
Allowable <i>tensile stress</i> $\sigma_{amm}$ for <i>long-term</i> loads	0.014 MPa
Allowable <i>shear stress</i> $\tau_{amm}$ for <i>short-term</i> loads	0.105 MPa
Allowable <i>shear stress</i> $\tau_{amm}$ for <i>long-term</i> loads	0.010 MPa

In addition, the silicone joint must absorb the differential thermal dilations between the glass and the metal support. While the external loads determine the joint width, the thermal force determines its thickness. Regarding the latter, the ETAG 002 standard sets a minimum thickness of 6 mm, even if the calculation leads to a lower value.

### 8.1.6.1 Joint thickness calculation

The thickness of the structural sealing joint is related to the maximum displacement to which it is subjected due to thermal actions.

The following parameters are used in the calculation:

$a = 1500$  mm = short side dimension of the glass plate;

$b = 2000$  mm = long side dimension of the glass plate;

$T_0 = 20$  °C = temperature during silicone application;

$T_c = 55$  °C = maximum temperature of the metallic frame;

$T_v = 80$  °C = maximum glass temperature;

$\alpha_c = 2.4 \times 10^{-5}$  °C<sup>-1</sup> = linear coefficient of thermal expansion of the frame (aluminium in this case);

$\alpha_v = 0.9 \times 10^{-5}$  °C<sup>-1</sup> = linear coefficient of thermal expansion of the glass;

$E_{sil} = 1.5$  MPa = Young’s module of the silicone;

$G_{sil} = 0.5$  MPa = shear module of the silicone;

$\tau_{des} = 0.105$  MPa = design shear stress for short duration loads.



Due to the symmetry of the panel, the maximum movement  $\Delta$  caused by thermal effects, in the case of glass not supported mechanically, and in accordance with [ETAG 002-Part 1], is

$$\Delta = [(T_c - T_0) \times \alpha_c - (T_v - T_0) \times \alpha_v] \times \sqrt{\left(\frac{a}{2}\right)^2 + \left(\frac{b}{2}\right)^2} = 0.375 \text{ mm}.$$

The thickness  $e$  of the joint can therefore be calculated using the formula

$$e = \left| \frac{G \times \Delta}{\tau_{des}} \right|, \quad \text{with } e \geq 6 \text{ mm}.$$

With the problem data we obtain

$$e = \left| \frac{G \times \Delta}{\tau_{des}} \right| = \left| \frac{0.5 \times 0.375}{0.105} \right| = 1.79 \text{ mm} < 6.00 \text{ mm} \quad \Rightarrow \quad e = 6.0 \text{ mm}.$$

### 8.1.6.2 Calculation of the joint under permanent load and wind load

The glazing self-weight is considered as being supported by the structural seals of length  $h_v$  positioned along the two longest edges of the glass, by neglecting the contribution of the horizontal joints. The minimum height  $h_c$  of the joint for permanent loads, according to [ETAG 002-Part 1], is equal to

$$h_{c,dead\_load} = \frac{P}{2 \times \tau_{\infty} \times h_v} = \frac{589}{2 \times 0.0105 \times 2000} = 14.02 \text{ mm},$$

where:

$P = 589 \text{ N}$  = glass plate self-weight;

$h_v = b = 2000 \text{ mm}$  = long side dimension of the glass plate;

$\tau_{\infty} = 0.0105 \text{ MPa}$  = design shear stress for long-term loads (Table 8.4).

The minimum height of the joint  $h_c$  for load caused by wind pressure is equal to

$$h_{c,wind\_load} = \frac{a \times q_w}{2 \times \sigma_{des}} = \frac{1500 \times 1.2 \times 10^{-3}}{2 \times 0.140} = 6.42 \text{ mm},$$

where:

$a = 1500 \text{ mm}$  = shortest edge of the glass plate;

$q_w = 1.2 \text{ kPa}$  = wind pressure;

$\sigma_{des} = 0.140 \text{ MPa}$  = permitted tensile stress for short-term loads.

Once obtained the two minimum heights that are necessary for the two elementary load conditions, the ETAG 002 standard does not supply instructions on how to combine them. According to a consolidated rule, and on the basis of tests carried out by the main producers, the comparison stress for combined stress state tests is the maximum principal stress. The problem of the different effects on resistance caused by loads lasting for different periods of time and acting together in different directions, however, still remains an open problem. A practical rule for testing combined loads is used further on.

In general terms, in addition to the normal stress ( $\sigma_{xx}$ ) caused by the wind, for example, and to the tangential stress ( $\tau_{xy}$ ) caused, for example, by the glazing self-weight, a silicon joint can also be subjected to normal longitudinal stress ( $\sigma_{yy}$ ), for example in double glazing where it is generated by climatic loads.

The principal stress values are

$$\sigma_{1,2} = \frac{\sigma_{xx} + \sigma_{yy}}{2} \pm \sqrt{\left(\frac{\sigma_{xx} - \sigma_{yy}}{2}\right)^2 + \tau_{xy}^2} .$$

When using the practical design rule we must not consider the value of the stress, but the joint widths requested in the elementary load test for each of these stresses. This allows to consider the different effects related to the duration of the different applied loads (e.g. the wind is short-term, the weight is long-term), and their direction (normal or tangential), through the different safety coefficients required by the different conditions.

As such, in general terms, the formula for the joint height under the effect of combined loads working in different directions and for different time periods can be written as

$$h_{tot} = \frac{h_{wind} + h_{climatic}}{2} + \sqrt{\left(\frac{h_{wind} + h_{climatic}}{2}\right)^2 + h_{dead\ load}^2}$$

As the loads of the wind and permanent loads are the only agents in the example being examined, the formula can be reduced to

$$h_c = \frac{1}{2} h_{c,wind\_load} + \sqrt{\left(\frac{1}{2} h_{c,wind}\right)^2 + (h_{c,dead\ load})^2} = \frac{1}{2} \times 6.42 + \sqrt{\left(\frac{1}{2} \times 6.42\right)^2 + (14.02)^2} = 17.6 \text{ mm}.$$

We therefore obtain the size of the joint summarised in Figure 8.20.

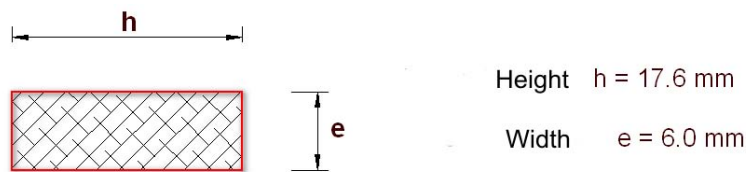


Figure 8.20. Size of the silicone joint in the example being examined.

The application of this approach is subject each time to specific approval by the silicone producer, because it falls outside the [ETAG 002-Part 1] regulations.

Because of this lack of precise indications about regulations, other silicone producers suggest to simply sum the elementary widths, which is on the safe side; this gives a joint of total width

$$h_c = 14.02 + 6.42 = 20.44 \text{ mm} \cong 20 \text{ mm},$$

with an evidently more onerous design.

### 8.1.7 Post-glass-breakage calculations

For the cases examined in Chapter 8.1 it is supposed that there is a safety structure that can protect people should pieces of broken glass fall. It is also supposed that there is no risk of falling from considerable heights in case of breakage, because the element is not a containment structure. In this case, no post-breakage behaviour assessment is necessary.

## 8.2 Point-wise supported plates

### 8.2.1 General remarks

The construction solution of point-wise supported plates developed from the 1970s, following the architectural need to reach the highest level of transparency, eliminating the space requirements of the frame from the construction elements and joining the plates to a structure that was suitably distanced from the transparent façade in order to highlight continuity and structural properties. Obviously, the particular characteristic of this technology is the type of fixing used, which is a small structure in itself because it can be used also with glass elements that are not used as a façade.

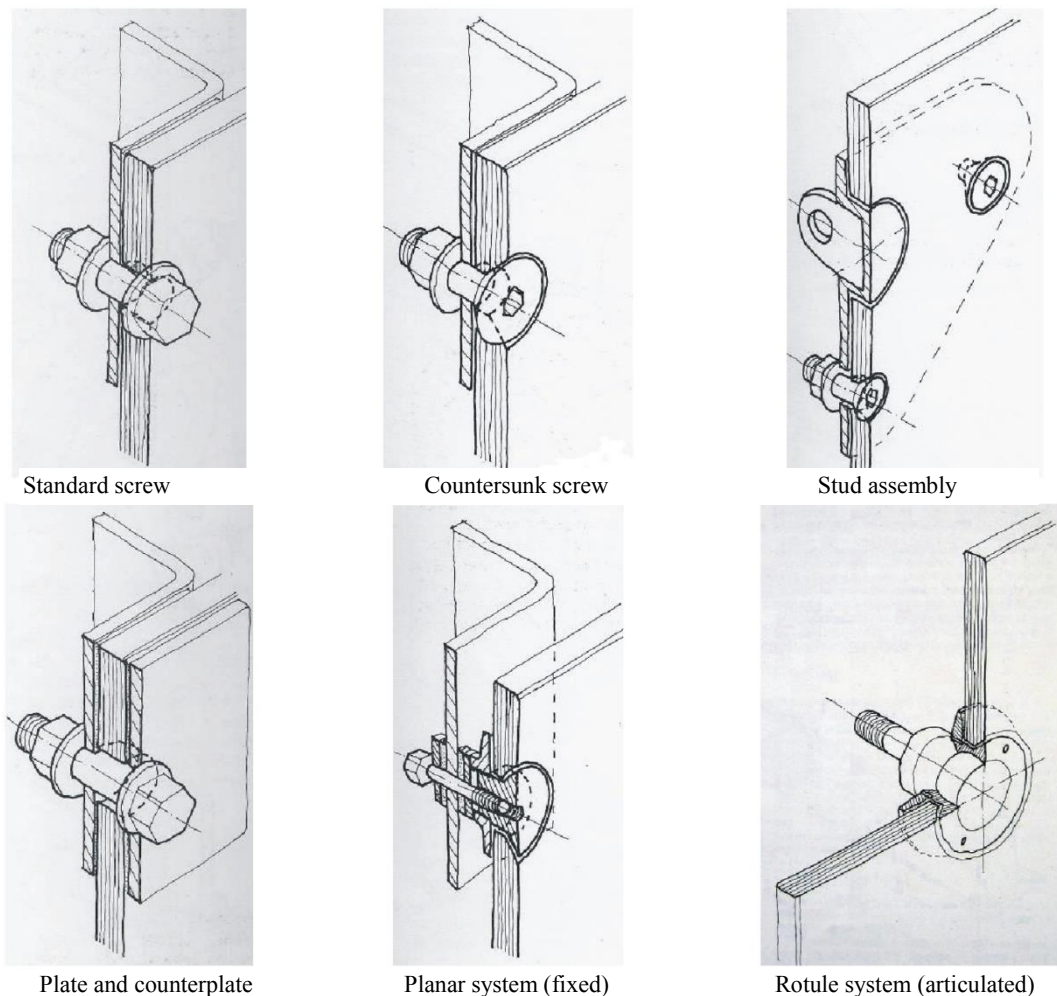


Figure 8.21. Types of point-fixing systems [Rice & Dutton, 1995].

The system uses point-fixings that are sustained by supports, which are connected to the main structure. The characteristic element is the fixing device, which supports the plates and transfers the loads and stresses to the intermediate supports, which in turn transmit them to the rear supporting structure. These point elements are fixed to the plate near the corners through holes that are cut into the glass. These holes can be cylindrical or countersunk, according to the shape of the metal pin they have to hold: in the first case, the flat head of the fixing element remains raised as to the glass plane, while in the second case the conical head of the connection is inserted completely inside the hole. As far as insulating double glass is concerned, the external plate is countersunk in order to host the head of the threaded screw, that is blocked inside the hole by an adjustable sealing bolt positioned on the face of the internal glass.

There are different types of point-fixing systems, which are usually divided into 6 categories [Rice & Dutton, 1995] and are shown in Figure 8.21.

Of these six categories, the ones used most today are the Planar system and the Rotule system. Both these systems transfer the loads out and onto the glass surface, directly through the bolt connection and the panel interface. The substantial difference lies in the transmission of actions, in particular of the bending moment at the base of the support and in the glass (Figure 8.22).

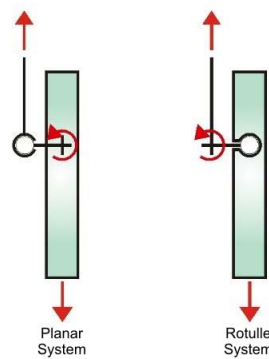


Figure 8.22. Different mechanical behaviour, in the transmission of the bending moment, between the Planar system and the Rotule system

The Planar system was created at the beginning of the Seventies and it consists in a countersunk screw with suitable flexible interlying rings (plastic) that prevent contact between the glass and the other metal components (Figure 8.23).

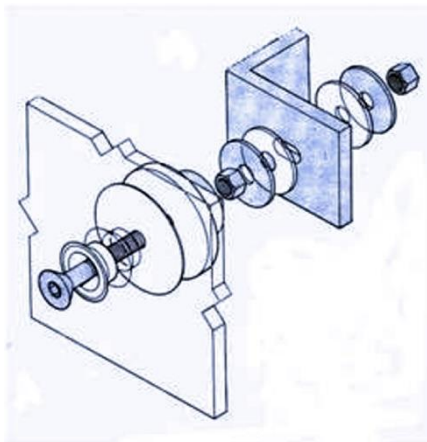


Figure 8.23. Axonometric explosive view of the Planar system

The articulation is outside the panel and it is connected to the plate by a bolt that is rigidly fixed to one edge of the glass by countersunk fixings which give a completely smooth external surface. They

work through the resistance of the panel which, for this reason, must be of tempered glass, both with single and laminated or double glass. This system allows to connect the panel to any type of structure, both vertical and inclined. Furthermore, there are no limits to the glass element height, because each panel can be fixed individually to the structure. An example of Planar type fixing is shown in Figure 8.24.



Figure 8.24. Details of Planar type fixing with “spider” supports.

The rotule system is characterized by the presence of a spherical articulation inside the glass plate. This articulation is free to rotate around the pin that connects it to the intermediate support. In this way, the reciprocal movements of every single element are left free and the bending effects are transferred outside the glass plane, making it possible to create large glass surfaces and a high level of transparency. Differently from the other systems, where the articulated element is outside the glass, the rotule system is more difficult to combine with other components such as the support stay rods. This system was originally developed and studied by Peter Rice (RFR) in 1986 and it was used for the façades of the greenhouse in the *La Villette* Park in Paris

As shown in Figure 8.25, there are three essential components in a rotule system: the central spherical body, which is inserted inside a steel cylinder; the sealing ring, which blocks the articulation against the glass; and the interlying ring of treated aluminium which compensates any geometrical differences that may be present between the steel element and the hole in the glass.

It must be remembered that, for each specific construction system, there is a second difference, namely how the hole is made in the glass plate. There are, in particular, glass elements with through holes or with partial through holes (a hole that passes through only some of the plies in the laminate package). There is a large variety of systems available on the market; therefore an exhaustive list will not be given here. The designer shall, however and in any case, be particularly careful with the stress concentrations that can develop near the hole, above all in the case of systems with partial through holes.

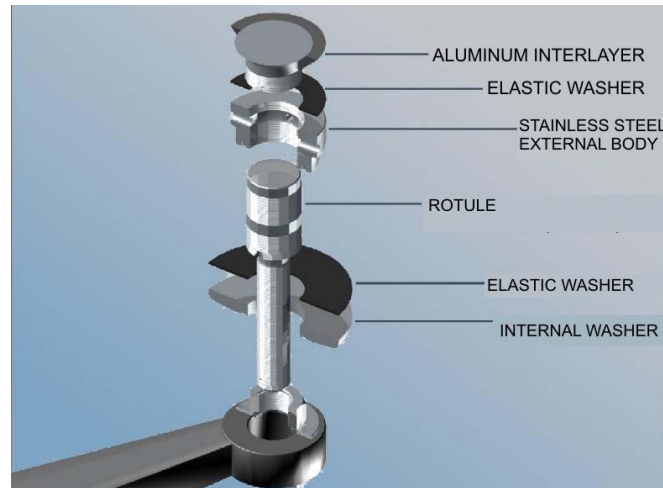


Figure 8.25. Axonometric explosive view of the Rotule system.

### 8.2.2 Static scheme

From a static viewpoint, the system of point-fixed panel includes load transmission that is statically indeterminate in the out-of-plane direction and isostatic for the in-plane loads. A typical example is shown in Figure 8.26. Of the two upper connections, one is fixed and firmly constrained to the structure, while the other allows the glass plate to move in the horizontal direction. Their role is essentially to support the self-weight of the panel and part of the external lateral loads. The lower connections allow both vertical and horizontal displacements, and absorb the differential in-plane displacements caused by thermal dilation and movements in the supporting structure.

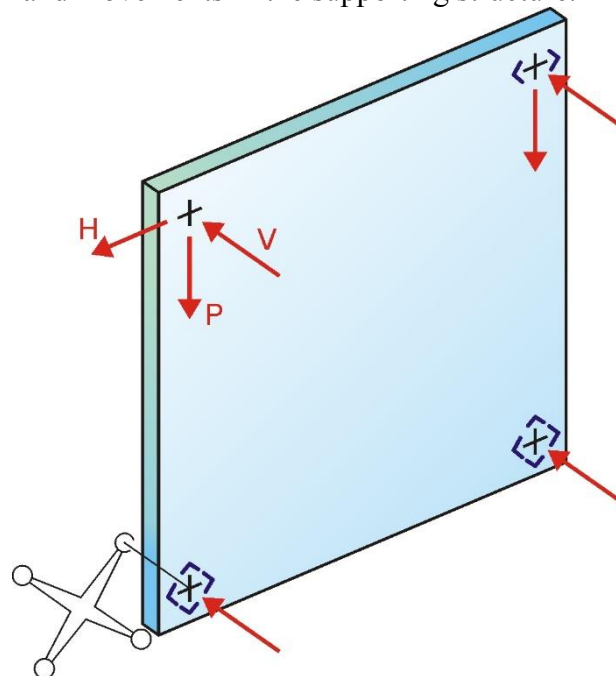


Figure 8.26. Typical layout of point-fixings on a glass plate.

In Figure 8.26 the position of the fixing points on the panel are marked with crosses: the vectors indicate the constraint reactions. In order to allow the movements shown in the figure, the holes in the panel, and in the intermediate supports, are countersunk or slightly larger than the size of the through pin. A typical example is shown in Figure 8.27.



Figure 8.27. An example of an intermediate “spider” type support. Note the different holes at the four ends, which allow the connecting pins to move in specific directions.

These holes, and the correct layout of the intermediate supporting elements between the various plates, are essential for preventing overstress resulting from heat or applied loads.

Great care must be taken when drilling the glass elements: the holes must be aligned with the holes of the surrounding plates. In particular, the countersink holes are extremely delicate points and even a tiny positioning, or drilling error, can cause the stress to distribute in a non-uniform manner, which favours the development and propagation of microcracks that compromise the safety of the whole plate. Irregularly-cut hole-edges shall be avoided completely.

### 8.2.3 Calculation example. Laminated glass plate under wind load

The calculation example involves the analysis of a laminated glass plates of size 2500 × 1500 mm, composed by two sheets of heat strengthened glass, both 10 mm thick, that are connected by a layer of PVB of thickness 0.76 mm (in short 10.10.2), as shown in Figure 8.28.

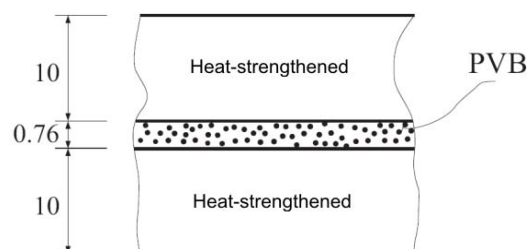


Figure 8.28. Composition of the laminated glass package

The plate is considered to be in class 1, according to Table 3.9 (which must be considered as purely indicative). The plate is constrained at the corners by four point-fixings, positioned as shown in Figure 8.29. The four holes, where the connections will be fixed, have diameter  $\phi = 36.5$  mm.

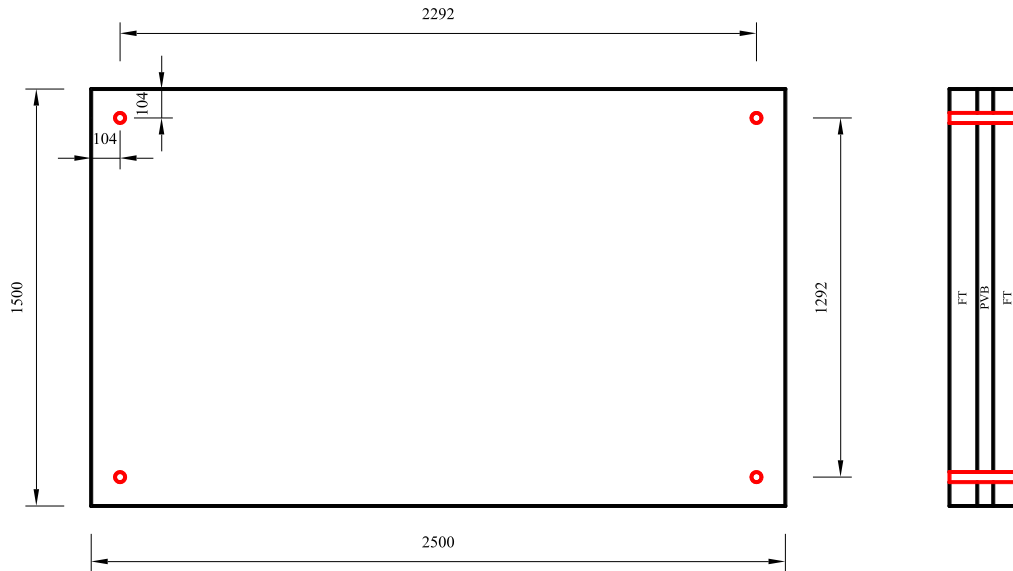


Figure 8.29. Geometric size and layout of the point-fixings.

### 8.2.3.1 Load analysis

For this type of glazing, the self-weight produces important stress caused by contact with the fixing pins. The permanent load analysis must therefore be carried out carefully.

The involved actions are:

#### Self-weight:

Specific self-weight of glass:  $\gamma_v = 25 \text{ kN/m}^3$ ;  
 Specific self-weight of the interlayer:  $\gamma_{PVB} = 10.5 \text{ kN/m}^3$ ;

The self-weight is equivalent to a distributed load of:

$$G = \gamma_v \cdot (h_1 + h_2) + \gamma_{PVB} \cdot h_{int} = 25 \cdot 0.02 + 10.5 \cdot 0.00076 = 0.508 \text{ kN/m}^2.$$

The total weight is therefore 1.90 KN.

The action is considered as applicable to the whole working life of the structure, which is assumed to be 50 years.

#### Wind load:

The wind load for the 3 s gust is assumed to be equivalent to an uniformly distributed load of 0.8 kPa (depression) and of 1 kPa (pressure). The verification should evidently be carried out with relevance to the most onerous condition; therefore

$$p_{w,3\text{sec}} = 1 \text{ kPa.}$$

Since glass is subject to static fatigue (section 2.1.1.1), it is important to define not only the maximum value of the action but also its characteristic duration. The test should therefore be carried out using gusts at peak speed (averaged over 3 s) and short gusts (10 minutes), as indicated in section 4.5.1.

The wind pressure averaged over 10 minutes can be obtained from (4.26), to give



$$\frac{p_{w,10\min}}{p_{w,3\sec}} = \frac{c_{e,1}}{c_e} = \frac{1}{c_{e,2}},$$

where the coefficient  $c_{e,2}$  is given by the ratio (4.27)

$$c_{e,2}(z) = 1 + \frac{7}{\ln\left(\frac{z}{z_0}\right) \cdot c_f},$$

where

$c_f=1$  friction coefficient, the value of which is given by Technical Regulations;

$z$  height from the ground;

$z_0$  reference height, given by Technical Regulations on the basis of the category.

Assuming that exposure to wind is category II, the regulations prescribe  $z_0=0.05$  m; considering that  $z = 50$  m, then  $c_{e,2} = 2.01$ .

The result is therefore  $p_{w,10\min} = 0.498$  kPa.

The different load durations influence the glass strength, through the  $k_{\text{mod}}$  coefficient (inferred from Table 2.2). In addition, when evaluating stress and deformation of a laminated glass element, the shear modulus of the interlayer assumes different values according to the duration of the considered action.

Two different verifications must be carried out in the case of vertical point-fixed glazing. The first considers the global behaviour of the plate by calculating the stress in points that are distant from the constraints and the maximum deflection. The second evaluates the stress concentration near the fixing devices, by using a three-dimensional model.

### 8.2.3.2 Design strength

The design strength of laminated glass elements is calculated separately for the different load conditions; the calculation is performed according to (7.5), i.e.

$$f_{g;d} = \frac{k_{\text{mod}} \cdot k_{ed} \cdot k_{sf} \cdot \lambda_{gA} \cdot \lambda_{gl} \cdot f_{g;k}}{R_M \gamma_M} + \frac{k'_{ed} k_v \cdot (f_{b;k} - f_{g;k})}{R_{M,v} \gamma_{M,v}},$$

where:

$k_{\text{mod}}$  reduction coefficient for static fatigue, given in Table 2.2 according to the type of external action and its characteristic duration;

$k_{ed}$  strength reduction factors for verifications near the edge of the sheet or holes. Since in this case the tests will mainly involve the hole contours, which are considered as having ground edges, a value of  $k_{ed} = 0.8$  is therefore obtained from Table 7.3 for this case. For tests that are distant from the holes, consider  $k_{ed} = 1$ .

$k_{sf}=1$  coefficient for the surface profile of the glass without surface treatment (Table 7.4);

$f_{g;k} = 45$  MPa nominal characteristic resistance of float glass;

$R_M = 0.7$  reduction factor of the partial coefficient, for class 1 assessment (Table 7.10);

$\gamma_M = 2.50$  partial coefficient for float glass (Table 7.9);

$k'_{ed}$  coefficient for tests near the edge of the sheet or holes (Table 7.3); in this case, the tests involve the hole contour, which is considered as having ground edges. A value

of  $k_{ed} = 0.8$  is therefore obtained from Table 7.3. For tests that are distant from the holes, consider  $k_{ed} = 1$ .

$k_v = 1$  coefficient for sheets treated with horizontal heat treatment (Table 7.8);  
 $f_{b;k} = 70$  MPa nominal characteristic strength of thermally toughened glass (Table 7.7);  
 $R_{M;v} = 0.9$  reduction factor of the partial coefficient, for class 1 tests (Table 7.10);  
 $\gamma_{M;v} = 1.35$  partial coefficient for glass that has undergone thermal treatments (Table 7.9);  
 $\lambda_{gA}$  scale factor, calculated using:

$$\lambda_{gA} = \left( \frac{0.24 \text{ m}^2}{k A} \right)^{1/7} = \left( \frac{0.24}{0.071 \cdot 1.5 \cdot 2.5} \right)^{1/7} = 0.985 \leq 1,$$

where  $A$  is the total area of the sheet under stress, while the constraint coefficient is equal to 0.071 in the case of rectangular plate constrained in four points;

$\lambda_{gl}$  scale factor for stress at the edge, calculated using (7.7), where  $l_b$  is the total length of the edge under tensile stress. As the tests involve above all the areas near the holes,  $l_b$  is represented by the total sum of the hole edges length, therefore  $l_b = 4 \times \pi \times 36.5 \text{ mm} = 458.4 \text{ mm}$ . The factor  $k_b$  that appears in Table 7.6 depends on the distribution of the stress at the edge. Uniform distribution is considered in this case, on the side of safeness, therefore  $k_b = 1$ . Regarding the finish, it is assumed that the edge is ground. Eq. (7.7) therefore gives

$$\lambda_{gl} = \left( \frac{0.0741 \cdot 0.45 \text{ m}}{k_b l_b} \right)^{1/12.5} = \left( \frac{0.0741 \cdot 0.45}{1 \cdot 0.458} \right)^{1/12.5} = 0.811 \leq 1.$$

### Design strength for self-weight action

For a conventional load duration equal to 50 years, Table 2.2 gives  $k_{mod} = 0.26$ , with a design strength of:

$$\begin{aligned} f_{g;d}^G &= 20.79 \text{ MPa} && \text{for verifications in proximity of the edges of holes } (d < 5 s); \\ f_{g;d}^G &= 27.16 \text{ MPa} && \text{for verifications at a distance } d > 5 s \text{ from the edge of the holes.} \end{aligned}$$

### Design strength for wind load (t=3 sec)

A conventional duration (equal to the spectrum integral) equal to 5 s is taken for the gust of wind. Table 2.2 gives  $k_{mod} = 0.88$ .

In the case of the global verifications, the maximum stress occurs at a distance from the edges of  $d > 5 s$ , where  $s$  = sheet thickness, and as a result  $k_{ed} = k'_{ed} = 1$ . We therefore obtain a design strength of

$$f_{g;d}^{w,3\text{sec}} = 42.87 \text{ MPa}.$$

The coefficients for local verifications in proximity of holes, with ground edges, are  $k_{ed} = k'_{ed} = 0.8$ . Therefore, we obtain:

$$f_{g;d}^{w,3\text{sec},l} = 31.14 \text{ MPa}.$$

### Design strength for wind load (t=10 min)

Table 2.2 gives,  $k_{mod} = 0.65$  for the load caused by cumulative wind lasting a conventional time of 10 minutes.

In the global test, the maximum stress is obtained at a distance from the edges of  $d > 5s$ , where  $s$  = sheet thickness, therefore, as a consequence,  $k_{ed} = k'_{ed} = 1$ . We therefore obtain a design strength of

$$f_{g;d}^{w,10min} = 37.04 \text{ MPa.}$$

The coefficients for local verifications in proximity of holes with ground glass are  $k_{ed} = k'_{ed} = 0.8$ , which therefore gives:

$$f_{g;d}^{w,10min,l} = 27.30 \text{ MPa.}$$

According to Table 7.12, design limit deflection is  $w_{max} = \frac{L_{inf}}{100} = 22.92 \text{ mm}$ .

### 8.2.3.3 Calculation of stress and deflection due to the self-weight

The design action relative to the Ultimate Limit State is given by

$$F_d = \gamma_G G = 1.3 \cdot 1.90 = 2.47 \text{ kN,}$$

where  $\gamma_G = 1.3$  is the partial factor for permanent actions, including model uncertainty and dimensional tolerance (Table 7.2).

In order to evaluate the deflection at the Serviceability Limit State, the following should be considered:

$$F_d = G = 1.90 \text{ kN,}$$

but, since the plate is positioned vertically, the contribution of the self-weight is negligible.

The properties of the PVB interlayer are considered as being for an infinite load duration and, in favour of safety, at a temperature of 50°C. The shear modulus of the interlayer is supposed to have been supplied by the producer, and as being equal to 0.052 MPa ( $\nu = 0.5$ ).

### 8.2.3.4 Calculation of stress and deflection due to the wind load (3 s)

The design action relative to the Ultimate Limit State is given by

$$F_d = \gamma_Q P_{w,3sec} = 1.5 \text{ kN/m}^2,$$

where  $\gamma_Q = 1.5$  is the partial factor for the variable actions, including model uncertainty and the dimensional tolerances.

In order to evaluate the deflection at the Serviceability Limit State, consider

$$F_d = p_{w,3sec} = 1 \text{ kN/m}^2.$$

The properties of the PVB interlayer are considered for a load duration of 3 s and, on the safe side, at a temperature of 50°C. On the basis of the values supplied by the producer, the shear modulus results as being equal to 0.44 MPa.

#### 8.2.3.4.1 Calculation using the “Enhanced Effective Thickness” method

With reference to paragraph 6.3.3.1.5, the test on the global behaviour of the panel can be carried out considering the laminated glass element as a monolithic glass of thickness equal to the effective thickness, which considers the effects of the shear produced by the polymeric interlayer.

The “Enhanced Effective Thickness” model [Galuppi *et al.*, 2012] is used because it allows to calculate equivalent thicknesses both for “beam” and “plate” geometries. In the case of plates, the equivalent flexural rigidity of the laminated glass plate  $D_{eq}$  is given by the harmonic mean, weighed using the  $\eta_{2D}$  coefficient, of the flexural stiffness of the monolithic plate and that relative to the sliding layers behaviour (layered limit), according to (6.54), i.e.

$$\frac{1}{D_{eq}} = \frac{\eta_{2D}}{D_{full}} + \frac{1 - \eta_{2D}}{D_{abs}} .$$

This coefficient depends on the geometry and the mechanical characteristics of the glass and inter-layer, according to equation (6.55), as

$$\eta_{2D} = \frac{1}{1 + \frac{h_{int} E}{G_{int} (1 - \nu^2)} \frac{D_{abs}}{D_{full}} \frac{h_1 h_2}{h_1 + h_2} \Psi} ,$$

where the  $\Psi$  coefficient can be obtained from Table 6.4, according to the plate size, and the load and constraint conditions. In order to evaluate the behaviour of the plate under consideration, reference can be made, in favour of safety, to a plate of size  $1292 \times 2292$  mm (see Figure 8.29) supported on its four corners, for which  $\Psi = 1.821 \cdot 10^{-6} \text{ mm}^{-2}$  is obtained through linear interpolation. The effective thicknesses, calculated respectively by means of (6.46) and (6.48) are therefore equal to

$$\hat{h}_w = \sqrt[3]{\frac{1}{\frac{\eta}{h_1^3 + h_2^3 + 12I_s} + \frac{1 - \eta}{h_1^3 + h_2^3}}} = 17.348 \text{ mm}; \quad \hat{h}_{1,\sigma} = \hat{h}_{2,\sigma} = \sqrt[3]{\frac{1}{\frac{2\eta d_1}{h_1^3 + h_2^3 + 12I_s} + \frac{h_1}{\hat{h}_w^3}}} = 18.663 \text{ mm}.$$

It is obvious that the values of the stress-effective thicknesses of the two glass plies are equal, because the two sheets of glass are of the same thickness.

Once the effective thicknesses have been calculated, the maximum stress and maximum deflection of the equivalent monolithic plates can be evaluated analytically or by means of FEM analyses. Here it was chosen to use the FEM model.

The linear elastic analyses give:

$$\begin{aligned} \sigma_{max} &= 17.85 \text{ MPa} && \text{maximum stress at the ULS,} \\ w_{max} &= 12.10 \text{ mm} && \text{maximum deflection at the SLS.} \end{aligned}$$

By accounting for the geometric non-linearities, it is obtained instead:

$$\begin{aligned} \sigma_{max} &= 17.97 \text{ MPa} && \text{maximum stress at the ULS;} \\ w_{max} &= 12.10 \text{ mm} && \text{maximum deflection at the SLS.} \end{aligned}$$

### 8.2.3.4.2 3D finite element analysis

To evaluate the maximum stress in the centre of the plate caused by gusts of wind, a three-dimensional laminated glass plate model was made by using ABAQUS software.

To improve the result precision in the subsequent analysis of the concentration of stress at the holes, the mesh, represented in Figure 8.30, was suitably refined. Each part was modelled with 20-node SOLID type elements. The constraints applied are those shown in Figure 8.26, namely the fixed

upper left connection, solidly constrained to the structure, and the upper right connection which permitted horizontal movements of the glass plate. The other two (lower) constraints allow the translation along the vertical and horizontal in-plane directions. Two analyses are then carried out: one for calculating the stress at the ULS ( $F_d=1.5 \text{ kN/m}^2$ ) and one for calculating the deflection at the SLS ( $F_d=1 \text{ kN/m}^2$ ).

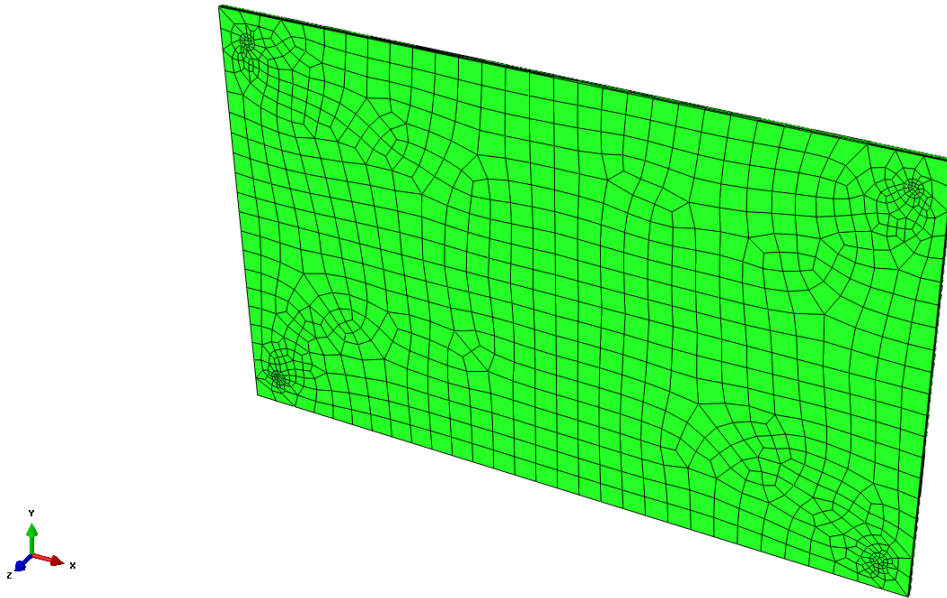


Figure 8.30. Mesh of the 3D model.

The figures below show the distribution of the maximum principal stress for the wind peak test on the external and internal surfaces of the deformed plate (scale of the deformations are opportunely increased).

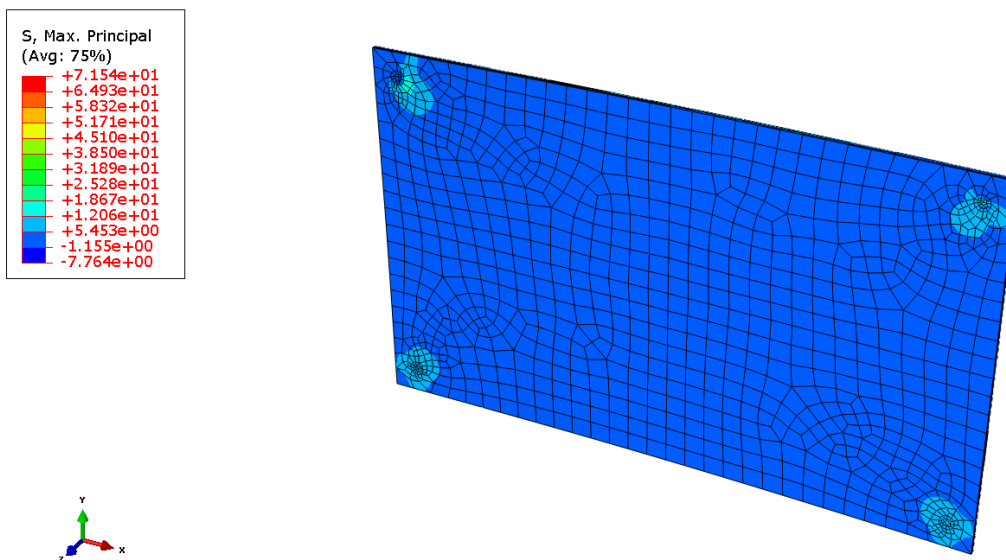


Figure 8.31. Deformation resulting from finite element linear analysis for peak gusts. Maximum principal stress (external surface).

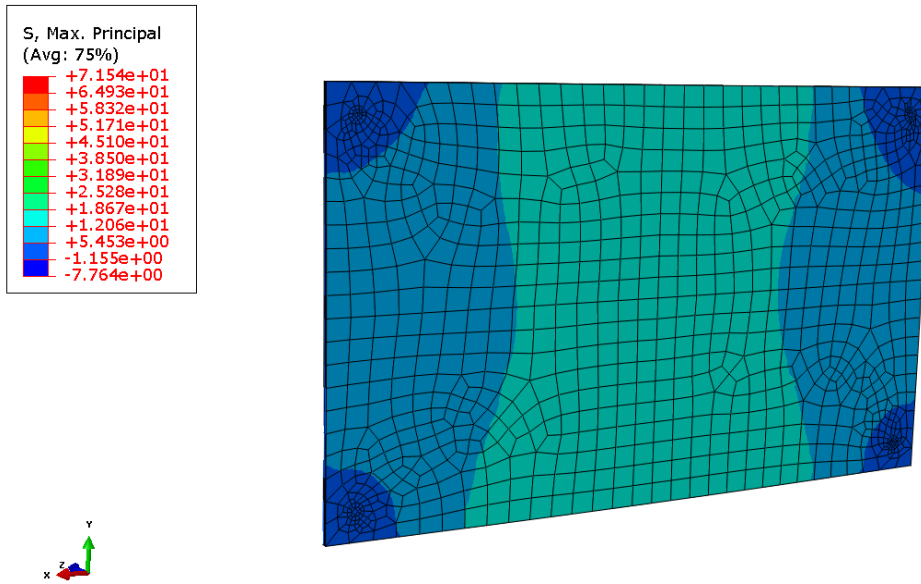


Figure 8.32. Deformation resulting from finite element linear analysis for gusts of 3 s. Maximum principal stress (internal surface).

The linear finite elements analyses allow to evaluate

$$\sigma_{max}^{w,3sec} = 17.28 \text{ MPa} \quad \text{at the ULS;}$$

$$w_{max}^{w,3sec} = 14.60 \text{ mm} \quad \text{at the SLS}$$

By accounting for the geometric non-linearities, it is obtained instead:

$$\sigma_{max}^{w,3sec} = 17.25 \text{ MPa} \quad \text{at the ULS;}$$

$$w_{max}^{w,3sec} = 14.00 \text{ mm} \quad \text{at the SLS.}$$

### 8.2.3.4.3 Comparison of analytical and numerical results

A comparison of the obtained solutions is given in Table 8.5. It shows the values of the maximum deflection and the maximum stress calculated by using the different methods.

Table 8.5. Plate subjected to gusts of wind lasting 3 seconds: comparison of the various solutions.

METHOD		Maximum deflection at the SLS	Maximum stress at the ULS
E.E.T.	linear	12.10 mm	17.85 MPa
	non-linear	12.10 mm	17.97 MPa
FEM 3D	linear	14.6 mm	17.23 MPa
	non-linear	14.00 mm	17.25 MPa

For the plate verifications, the values obtained with the non-linear 3D model are considered, namely

$$\sigma_{max}^{w,3sec} = 17.25 \text{ MPa} \quad \text{at the ULS;}$$

$$w_{max}^{w,3sec} = 14.00 \text{ mm} \quad \text{at the SLS.}$$

### 8.2.3.5 Calculation of stress and deflection due to the wind load (3 s)

The design action for the Ultimate Limit State is given by

$$F_d = \gamma_Q p_{w,10\min} = 0.746 \text{ kN/m}^2$$

where  $\gamma_Q=1.5$  is the partial factor for the variable actions, while the following is considered to calculate the deflection at the Serviceability Limit State:

$$F_d = p_{w,10\min} = 0.498 \text{ kN/m}^2 .$$

The properties of the PVB interlayer are considered for a load duration of 10 minutes and, in favour of safety, at a temperature of 50°C. The shear modulus of the interlayer is assumed to be supplied by the producer, and equal to 0.2 MPa.

#### 8.2.3.5.1 Calculation using the “Enhanced Effective Thickness” method

Similarly to paragraph 8.2.3.4.1, the stress and deflection are preliminary calculated by using the “Enhanced Effective Thickness” model.

The  $\Psi$  coefficient can be obtained from the tables according to the size of the plate, and the load and constraint conditions. Obviously, we obtain  $\Psi = 1.821 \cdot 10^{-6} \text{ mm}^{-2}$  again, as indicated in paragraph 8.2.3.4.1. The deflection- and stress-effective thicknesses are obtained from (6.46) and (6.48):

$$\hat{h}_w = 15.820 \text{ mm};$$

$$\hat{h}_{1,\sigma} = \hat{h}_{2,\sigma} = 17.429 \text{ mm}.$$

Also in this case, these values are used for the FEM calculation of an equivalent monolithic plate. The maximum deflection and maximum stress are equal to

for linear analysis:

$$\sigma_{max} = 10.18 \text{ MPa} \quad \text{at the ULS};$$

$$w_{max} = 7.95 \text{ mm} \quad \text{at the SLS};$$

for non-linear analysis:

$$\sigma_{max} = 10.22 \text{ MPa} \quad \text{at the ULS};$$

$$w_{max} = 7.95 \text{ mm} \quad \text{at the SLS}.$$

Thanks to the analysis, even if approximate, it is evident that the wind action averaged over 10 minutes is much less onerous than the peak action mediated over 3 seconds.

#### 8.2.3.5.2 3D finite element analysis

Two different finite element analyses of the laminated glass plate subjected to 10-minute wind are performed. For simplicity, only the calculation made by accounting for geometric non-linearities is given. Of the two analyses, one is used for calculating the stress at the ULS ( $F_d=0.746 \text{ kN/m}^2$ ) and the other is for calculating the deflection at the SLS ( $F_d=0.498 \text{ kN/m}^2$ ).

The progress of the maximum principal stress on the glass is given in Figure 8.33 and Figure 8.34 for the external and internal surfaces of the plate, respectively.

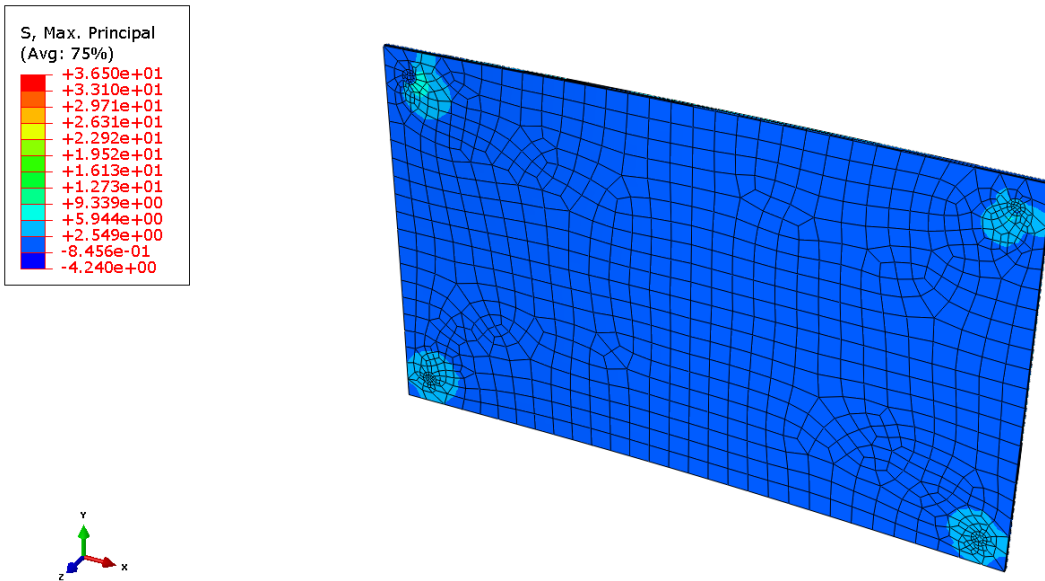


Figure 8.33. Deformation resulting from the finite element linear analysis for gusts of 10 minutes. Maximum principal stress on the glass (external surface).

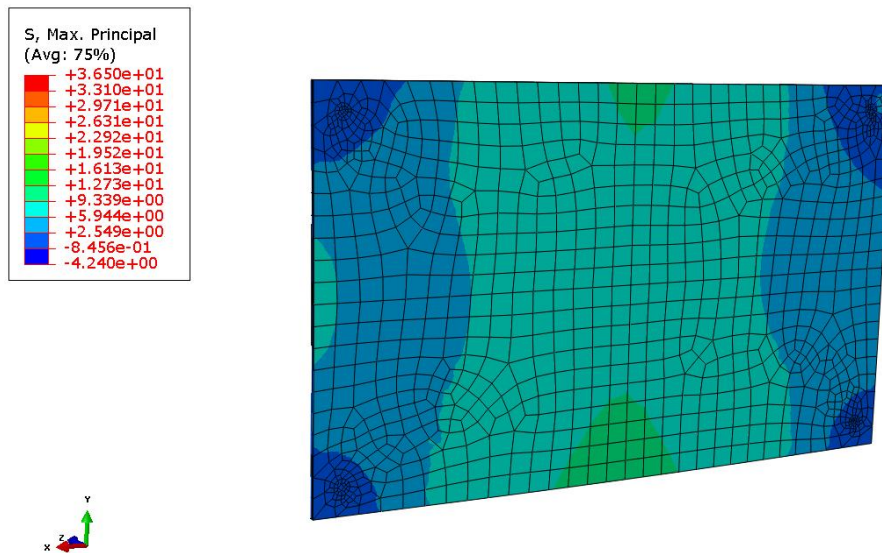


Figure 8.34. Deformation resulting from the finite element linear analysis for gusts of 10 minutes. Maximum principal stress on the glass (internal surface).

The non-linear finite elements analyses allow to evaluate

$$\sigma_{max}^{w,10min} = 9.77 \text{ MPa at the ULS};$$

$$w_{max}^{w,10min} = 8.60 \text{ mm at the SLS}.$$

### 8.2.3.5.1 Comparison of analytical and numerical results

The obtained solutions are compared in Table 8.6: the values of the maximum deflection and the maximum stress calculated using the different methods are given.



Table 8.6. Plate subjected to gusts of wind lasting 10 minutes: comparison of the various solutions.

METHOD		Maximum deflection at the SLS	Maximum stress at the ULS
E.E.T.	linear	7.95 mm	10.18 MPa
	non-linear	7.95 mm	10.22 MPa
FEM 3D (non-linear calculation)		8.60 mm	9.77 MPa

For the verifications, we will considered the maximum stress and the maximum deflection obtained with the FEM 3D non-linear model, namely

$$\sigma_{max}^{w,10min} = 9.77 \text{ MPa at the ULS};$$

$$w_{max}^{w,10min} = 8.60 \text{ mm at the SLS.}$$

### 8.2.3.6 Evaluation of the stress concentration around the holes

The stress concentrations around the holes are caused by: *i*) bending effects caused by the out-of-plane loads; *ii*) direct contact with the support pins along the internal surface of the hole, caused by the in-plane forces. To evaluate the local stress at the holes as a result of *i*), a 3D FEM analysis may be carried out, that considers the effective contact of the element with the fixings. This analysis, which shall consider that the contact is unilateral, is generally very complex from a numerical viewpoint; in addition, the geometry of the effective contact surfaces is generally difficult to determine exactly. It is therefore preferable to propose a simplified method, where the laminated plate is analysed using an FEM 3D model, but *without* considering the presence of the holes. The reactions of the supports are considered as being uniformly distributed along the contact area with the fixings; the maximum bending action in the hole area is therefore evaluated. *A posteriori*, these values are amplified by suitable stress amplification coefficients, using abacuses and tables that can be found in literature.

In the case being examined, a three-dimensional model of the laminated plate is made with ABAQUS software. To improve the precision of the results, the mesh has been refined in the neighborhood of the holes, as it is represented in Figure 8.30. Each part was modelled with solid 20-nodes elements. A uniform wind pressure, dependent on the considered action ( $F_d=1.5 \text{ kN/m}^2$  for testing with wind gusts of 3 seconds and  $F_d=0.746 \text{ kN/m}^2$  for tests with 10-minute gusts) was applied to the plate. The constraint reactions were schematized by considering the result of each reaction as being uniformly distributed along the contact surface, and without considering the presence of the hole.

For what concerns *ii*), calculating the contact forces between the supporting pin and the internal surface of the hole becomes immediate because of the problem is statically determined. Local stress is evaluated, again, by using suitable stress concentration coefficients, which can be found in consolidated technical literature.

Remember that the effective thickness method indicated in chapter 6.3.3.1 must *never* be used to calculate the local stress around the holes, because it only supplies the maximum stress and deflection, usually in the centre of the plate. The FEM three-dimensional analysis is the only possibility for calculating local stress.

**8.2.3.6.1 Wind load**

*Peak wind*

A rotule system, made up of an aluminium interlayer of diameter 59 mm and a cylindrical body of diameter 36 mm, is here considered. The diameter of the holes in the glass is, instead, 36.5 mm (Figure 8.35).

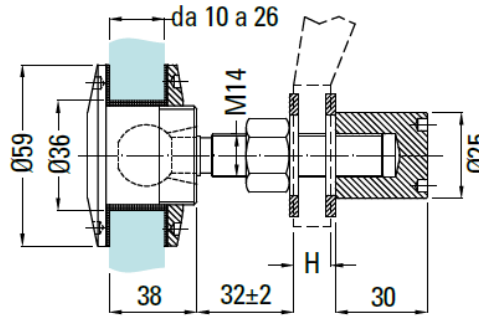


Figure 8.35. Rotule system used in the example.

To evaluate the stress concentration at the hole, the stress was firstly evaluated by assuming that the constraining reaction is uniformly distributed over a circular surface of diameter 59 mm, corresponding to the diameter of the aluminium interlying ring. The laminated element was then modelled with the same mesh used in sections 8.2.3.4.2 and 8.2.3.5.2 (without considering the holes), evaluating the maximum stress  $\sigma$  in correspondence of the circular contact surface. This value was then multiplied by a suitable concentration factor,  $K_t$ , according to the expression

$$\sigma_{\max} = K_t \cdot \sigma .$$

The value of  $K_t$  can be evaluated using the ratio between the hole diameter and the plate thickness, and calculated by using the abacus of Figure 8.36 [Pilkey, 1997]. This value corresponds to a plate with holes, under bending, which well approximates the case being examined. By considering a circular hole of diameter 36.5 mm, our case gives a ratio

$$d / h = 36.5 / 20.76 = 1.76 ,$$

from which

$$K_t \approx 2.05 .$$

The maximum stress on the round surface supplied by the software is equal to:

$$\sigma = 10.34 \text{ MPa} .$$

It follows that

$$\sigma_{\max}^{w,3\text{sec}} = K_t \cdot \sigma = 2.05 \cdot 10.34 = 21.20 \text{ MPa} .$$

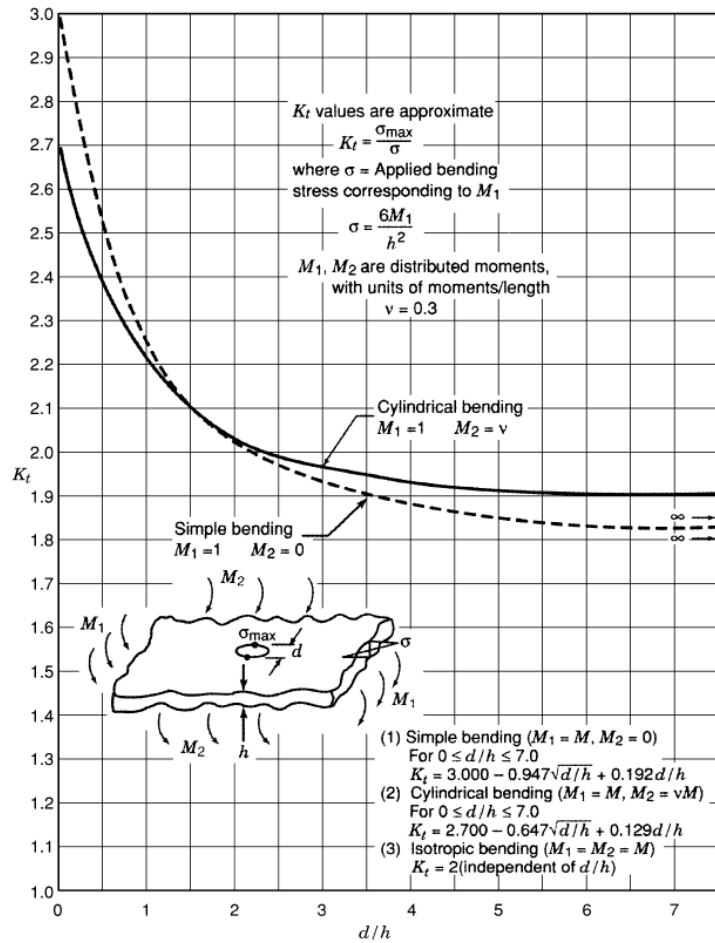


Figure 8.36. Stress concentration factor  $K$ , for an infinite plate under bending, with circular hole [Pilkey, 1997]

Wind averaged over 10 min.

Using the same procedure given in the previous section, the result supplied by the FEM analysis for the stress on the circular surface is equal to:

$$\sigma = 4.13 \text{ MPa};$$

which gives a maximum stress of:

$$\sigma_{max}^{w,10min} = K_t \cdot \sigma = 2.05 \cdot 4.13 = 8.46 \text{ MPa}.$$

### 8.2.3.6.2 Self-weight action

In addition to the stress induced by the wind, the maximum stress on the hole due to the contact between the aluminium gasket and the glass caused by the self-weight of the plate must also be considered. As the plate is hanging from the two upper supports, the force on each support is exactly equal to half the dead load.

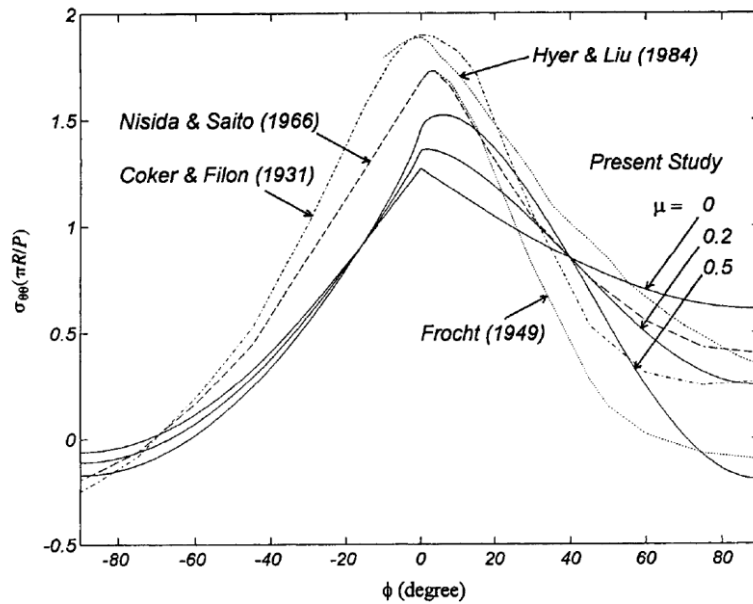


Figure 8.37. Hoop stress normalised as the angle  $\phi$  varies. Maximum tensile stress of the  $\phi = 0^\circ$ . [Ho & Chau, 1997]

Referring to the experimental data given by Ho & Chau [Ho & Chau, 1997] (Figure 8.37), it is evident that the maximum tensile stress (obtained at an angle  $\phi=0^\circ$ ) is about 1.5÷2 greater than the average pressure, evaluated as:

$$p_{ave}^G = \frac{F_d / 2}{2Rs},$$

where:

- $F_d$  force caused by dead load;
- $R$  radius of the hole in the glass plate, equal to 36.5 mm;
- $s$  thickness of the plate, equal to 20.76 mm.

We therefore obtain  $p_{ave}^G = 1.04$  MPa.

On the safe side, a ratio of 2 between the tensile strength and the average pressure is considered. The maximum tensile stress is therefore equal to

$$\sigma_{t,max}^G \approx 2 \cdot p_{media}^G = 3.26 \text{ MPa.}$$

## 8.2.4 Calculation of the plate subjected to different load combinations

To carry out the verifications, it is necessary to combine the effect of the different actions, to which different design strength correspond, as already discussed in paragraph 8.2.3.2.

In this example, the plate subjected to the wind action must be tested globally, together with the local verification near the edges of the holes, both under the wind action and dead load. In the latter case, the criterion (7.8) must be used to combine the effects of the different actions.

### 8.2.4.1 Plate subjected to wind load

The global calculation of the plate subjected to wind action must be performed by considering the midpoint of the longer edge of the plate as a the verification point. As the plate is vertical, the contribution of its self-weight is negligible with respect to that of the wind. One obtains the following:

- Plate subjected to wind action – 3-second gusts:

$$\sigma_{\max}^{w,3\text{sec}} = 17.25 \text{ MPa} \leq f_{g;d}^{w,3\text{sec}} = 42.53 \text{ MPa}$$

- Plate subjected to wind action – gusts averaged over 10 minutes:

$$\sigma_{\max}^{w,10\text{min}} = 9.77 \text{ MPa} \leq f_{g;d}^{w,10\text{min}} = 37.04 \text{ MPa} .$$

The resistance condition has been verified.

Concerning the deflection:

- Plate subjected to wind action – 3-second gusts:

$$w_{\max}^{3\text{sec}} = 14 \text{ mm} < \frac{1}{100} L_{\text{inf}} = 22.92 \text{ mm};$$

- Plate subjected to wind action – gusts averaged over 10 minutes:

$$w_{\max}^{10\text{min}} = 8.6 \text{ mm} < \frac{1}{100} L_{\text{inf}} = 22.92 \text{ mm}.$$

Conditions are satisfied.

### 8.2.4.2 Local testing of the plate subjected to dead load + wind

For what concerns the plate subjected to its self-weight and wind action, a local verification shall be carried out by considering the stress at the holes, as evaluated in paragraph 8.2.3.6. Applying the criterion (7.8), one obtains:

$$\frac{\sigma_{\max}^G}{f_{g;d}^{G,l}} + \frac{\sigma_{\max}^{w,3\text{sec}}}{f_{g;d}^{w,3\text{sec},l}} = \frac{3.26}{20.79} + \frac{21.20}{31.14} = 0.838 \leq 1 ,$$

$$\frac{\sigma_{\max}^G}{f_{g;d}^{G,l}} + \frac{\sigma_{\max}^{w,10\text{min}}}{f_{g;d}^{w,10\text{min},l}} = \frac{3.26}{20.79} + \frac{8.46}{27.30} = 0.467 \leq 1 .$$

The resistance calculations are satisfied.

## 8.2.5 Assessment of the post-breakage behaviour (Collapse Limit State)

According to the *fail safe* approach, it must be considered that an imponderable event can cause some glass components to fragment partially or completely (Chapter 3.1). So, it has to be made sure that even in this limit condition the element can maintain enough load bearing capacity to carry permanent loads, and also a part of the variable loads that is consistent with the working conditions, preventing dangerous falls of material. In the case being examined, the post-breakage behaviour of the plate under the action of the wind must be tested.

As described in Paragraph 6.5.3, three phases can generally be recognised in the behaviour of laminated glass, when broken:

- Phase I, where both the plies of glass are still sound;
- Phase II, which begins after the breakage of the first glass ply, in which the totality of the load is carried by the panel that has remained sound;
- Phase III, in which both the glass plies have broken, and only the polymer can support the tensile strength, while the fragments of broken glass balance the internal compression forces by means of the direct contact actions.

The post-breakage verifications (Collapse Limit State) performed in this specific case refer to phase II, in which one of the two plies has broken. Therefore, there is only one heat strengthened glass ply, with thickness 10 mm, that carries the external actions. Resistance and deformation calculations are carried out on the glass if the external ply is damaged, and the load caused by the wind action is fully supported by the internal ply only. Due to the symmetry of the laminated element, the calculation is similar if it is the internal ply that is damaged.

In accordance with what is indicated in Paragraph 3.2.2, consider a nominal life that is conventionally assumed to be 10 years for the post-breakage tests on class 1 elements. The wind load must therefore be re-scaled to adapt it to the return period. Equations (4.10) and (4.11) can be used to determine the reference wind speed for a return period of 10 years:

$$v_r = v_{b,50} \cdot c_r, \quad c_r = 0.75 \sqrt{1 - 0.2 \ln \left[ -\ln \left( 1 - \frac{1}{T_R} \right) \right]}, \quad \text{for } 5 \text{ years} < T_R \leq 50 \text{ years,}$$

where:

- $c_r$  return period factor;
- $v_{b,50}$  reference speed, defined as the characteristic value of the wind speed at 10 m from the ground, on category II wind exposure, averaged over 10 minutes and referring to a return period of 50 years;
- $T_R$  return period.

Coefficient  $c_r = 0.903$  is therefore obtained for a period  $T_R=10$  years. As the wind pressure is directly proportional to the square of the speed (4.14), the wind pressure at 10 years can be calculated as follows

$$\frac{p_{w,10}}{p_{w,50}} = (0.903)^2 \rightarrow p_{w,10} = (0.903)^2 p_{w,50} = 0.816 \cdot 1 = 0.816 \text{ kN/m}^2$$

As a result of the different load durations, the design strength of the glass assumes different values for the different actions. The design strength values are the same as those calculated in Paragraph 8.2.3.2.

The apex  $p-r$  below indicates stress and deflections related to the post-breakage behaviour.

- **Calculating the stress and deflection of the plate subjected to wind load**

To calculate the deflection, consider the Serviceability Limit State to which a design action equal to the wind load for a period of 10 years is associated:

$$F_d = p_{w,10} = 0.816 \text{ kN/m}^2.$$

The design action for the Ultimate Limit State is given by

$$F_d = \gamma_Q p_{w,10} = 1.22 \text{ kN/m}^2,$$

where:

- $\gamma_Q=1.5$  partial factor for variable actions, including the uncertainties of the model and the dimensional tolerances;
- $p_{w,10}$  wind pressure, referred to a return period of 10 years.

For plate of monolithic glass, thickness 10 mm, and with a peak wind of 3 s,

$$\sigma_{max}^{w,p-r} = 21.66 \leq f_{g;d}^{w,3sec} \quad \text{at the CLS;}$$

The calculation for the 10-minute gusts can be omitted, because the action is less onerous than that of the 3 seconds gust. For the sake of brevity, the calculation of the stress concentrations in relation to the holes and the corresponding verifications is also omitted. This can be performed by following the same procedure given in 8.2.3.6, by considering a single intact monolithic plate in the calculation.

### 8.3 Glass roofs

#### 8.3.1 Glass roof simply supported on two edges, subjected to snow load and anthropic action (maintenance)

The example involves the analysis of a laminated glass roof, made up of one ply of thermally toughened (tempered) glass and one of heat strengthened glass, both 12 mm thick, with ionoplastic interlayers of thickness 1.52 mm, as described in Figure 8.38 (12.12.4, 12 + 12 mm of glass, interlayer thickness  $4 \times 0.38$  mm). The tempered sheet is best positioned externally, because it has a higher resistance to impact than heat strengthened glass. For what concerns the ultimate limit state, the roof is considered to be in class II. For this application, since the plate is simply supported on just two edges, any breakage can easily cause the element to fall, therefore it is considered to be in class 2 even regarding the Collapse Limit State.

The plate has dimensions of  $1400 \times 3000$  mm, and it is simply supported on the long edges; it must therefore be assessed under the action of snow load and live load (maintenance) as prescribed in Italian Regulations [Italian Building And Construction Standards NTC 2008].

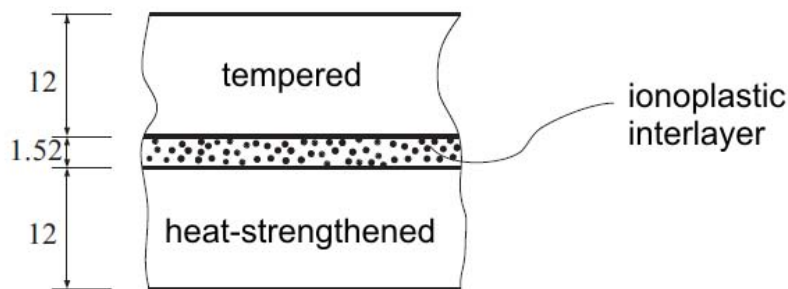


Figure 8.38. Composition of the laminated glass plate

The loads (uniformly distributed) caused by self-weight and snow act on the whole plate, which deforms into an almost cylindrical surface. Approximatively, the stress is uniform at the generators parallel to the longer edges of the plate. As it is well known, for large plates there are an increase of stress at the edges due to the Poisson effect, and as a result the shorter edges (not supported) of the plate become the most stressed. The live (anthropic) load instead acts on a very reduced area,  $50 \times 50$  mm, as *per* [Italian Building And Construction Standards NTC 2008]. The most dangerous position where the load is applied is namely midway along the free edge, causing maximum stress and maximum deflection in this area.

The different load durations (which can be deduced from Table 2.2) influence the resistance of the glass through the  $k_{mod}$  coefficient, calculated in paragraph 8.3.3, which is different according to the considered action. It should also be observed that the snow load is present at low temperatures, while the live (anthropic) load can be present even at high temperatures, for which interlayer stiffness is lower. When evaluating the plate stress and deformation states, different values of the interlayer shear modulus must be used according to the considered action, i.e., its characteristic duration and

the working temperature. It is therefore necessary to calculate the effect of the three actions separately, and then combine them as shown in paragraph 8.3.7.

### 8.3.2 Load analysis

The active loads are made up of:

*Self-weight:*

Specific self-weight of glass:  $\gamma_v = 25 \text{ kN/m}^3$ ;  
 Specific self-weight of the interlayer:  $\gamma_{PVB} = 10.5 \text{ kN/m}^3$ ;

The self-weight is equivalent to a distributed load of

$$G = \gamma_v \cdot (h_1 + h_2) + \gamma_{PVB} \cdot h_{int} = 25 \cdot 0.024 + 10.5 \cdot 0.00152 = 0.62 \text{ kN/m}^2 ;$$

The design load duration is equal to the life of the work, supposed as being 50 years. The reference temperature for calculating the rigidity of the polymeric interlayer is assumed, in favour of safety, to be equal to 50°C.

*Snow load:*

$$q_s = \mu q_{sk} c_e c_T = 1.2 \text{ kN/m}^2 .$$

The design duration of the force is 3 months, while the reference temperature is 10°C. This value is conventional and considers an average between the outdoor and the indoor temperatures. It should be remembered that the stiffness of the interlayer influences the coupling between the glass plies: higher temperatures give lower stiffness. In the particular case of air-conditioned environments, the working temperature of the interlayer should be considered more precisely.

*Live anthropic load (for maintenance):*

Load  $Q_k = 1.20 \text{ kN}$  distributed over an area of  $50 \times 50 \text{ mm}$  (Tab. 3.1.II, [NTC 2008]).

The design action duration is 30 seconds (equal to that of the load caused by temporary transit, see Table 4.18); the reference temperature for calculating the stiffness of the polymeric interlayer is 30°C. This action is used for local verifications, therefore it must not be combined with other action except, obviously, the self weight.

### 8.3.3 Design strength

The design strength of the laminated glass element is calculated separately for the different load conditions; the calculation refers to equation (7.5):

$$f_{g;d} = \frac{k_{mod} k_{ed} k_{sf} \lambda_{gA} \lambda_{gl} f_{g;k}}{R_M \gamma_M} + \frac{k'_{ed} k_v (f_{b;k} - f_{g;k})}{R_{M;v} \gamma_{M;v}}$$

where:

$k_{mod}$  reduction coefficient for static fatigue, given in Table 2.2 according to the type of external load and its characteristic duration;  
 $k_{ed}$  coefficient for tests near the edge of the plate or holes;  $k_{ed} = 1$  is conventionally assumed for plates subjected to bending due to out-of-plane loads;



$k_{sf}=1$	coefficient for the surface profile of the glass without surface treatments (Table 7.4);
$f_{g;k} = 45$ MPa	nominal characteristic resistance of the float glass;
$R_M = 1$	reduction factor of the partial coefficient for class 2 tests (Table 7.10);
$\gamma_M = 2.50$	partial factor for the float glass (Table 7.9);
$k'_{ed} = 0.8$	coefficient for tests near the edge of the plate or holes; $k'_{ed} = 1$ is conventionally assumed for plates subjected to bending due to out-of-plane loads;
$k_v = 1$	coefficient for heat treated plies with horizontal heat treatment (Table 7.8);
$R_{M;v} = 1$	reduction coefficient of the partial factor, for class 2 elements (Table 7.10);
$\gamma_{M;v} = 1.35$	partial factor for glass that has been heat toughened (Table 7.9);
$\lambda_{gA}$	scale factor, which considers the area that undergoes the maximum stress, calculated using:

$$\lambda_{gA} = \left( \frac{0.24 \text{ m}^2}{k A} \right)^{1/7} = \left( \frac{0.24}{0.054 \cdot 1.4 \cdot 3} \right)^{1/7} = 1.008 \Rightarrow \lambda_{gA} = 1$$

where  $A$  is the total area of the plate under traction, while the coefficient  $k = 0.054$  that defines the effective area is given in Table 7.5, for rectangular plates constrained on two edges;

$\lambda_{gl}$	scale factor for edge stress, for verifications at a distance of $d < 5s$ from the edge, given by (7.7). $\lambda_{gl} = 1$ is conventionally assumed in verifications carried out at a distance $d > 5s$ ( $s$ = plate thickness), or in the case of plates subjected to bending due to out-of-plane loads.
----------------	--------------------------------------------------------------------------------------------------------------------------------------------------------------------------------------------------------------------------------------------------------------------------------------------------------------

The  $k_{mod}$  coefficient varies according to the considered action.

### 8.3.3.1 Design strength of the heat strengthened glass ply

For the glass we have

$f_{b;k} = 70$ MPa	nominal characteristic strength of the heat strengthened glass (Table 7.7);
--------------------	-----------------------------------------------------------------------------

#### Design strength for self-weight action

Considering a conventional load duration of 50 years, Table 2.2 gives  $k_{mod} = 0.26$ . The design strength is therefore

$$f_{g;d}^G = 23.20 \text{ MPa.}$$

#### Design strength for snow load:

$k_{mod} = 0.36$ , for a conventional load duration of 3 months (from Table 2.2); which therefore gives a design strength equal to:

$$f_{g;d}^S = 25.00 \text{ MPa.}$$

#### Design strength for live anthropic load (maintenance):

$k_{mod} = 0.78$ , for a conventional load duration of 30 seconds (from Table 2.2), which therefore gives a design strength equal to:

$$f_{g;d}^P = 32.56 \text{ MPa.}$$

### 8.3.3.2 Design strength of the thermally toughened (tempered) glass ply

With laminated glass  $f_{b,k} = 120$  MPa: nominal characteristic strength of tempered glass (Table 7.7);

Design strength for self-weight action:

Considering a conventional load duration of 50 years, Table 2.2 gives  $k_{mod} = 0.26$ , which means a design strength equal to:

$$f_{g;d}^G = 60.24 \text{ MPa.}$$

Design strength for snow load:

$k_{mod} = 0.36$  for a conventional load duration of 3 months (from Table 2.2), which gives a design strength of:

$$f_{g;d}^S = 62.04 \text{ MPa.}$$

Design strength for live anthropic load (maintenance):

$k_{mod} = 0.78$  for a conventional load duration of 30 seconds (from Table 2.2), which gives a design strength of:

$$f_{g;d}^P = 69.60 \text{ MPa.}$$

The design deflection is  $w_{max} = \frac{L_{inf}}{100} = 14$  mm (refer to Table 7.11).

### 8.3.4 Calculation of stress and deflection due to the self-weight

Figure 8.39 shows the element geometry, load and constraint conditions. The design action for the Ultimate Limit State is given by

$$F_d = \gamma_G G = 0.806 \text{ kN/m}^2$$

where  $\gamma_G = 1.3$  is the partial factor for permanent actions, including model uncertainties and dimensional tolerances (Table 7.2).

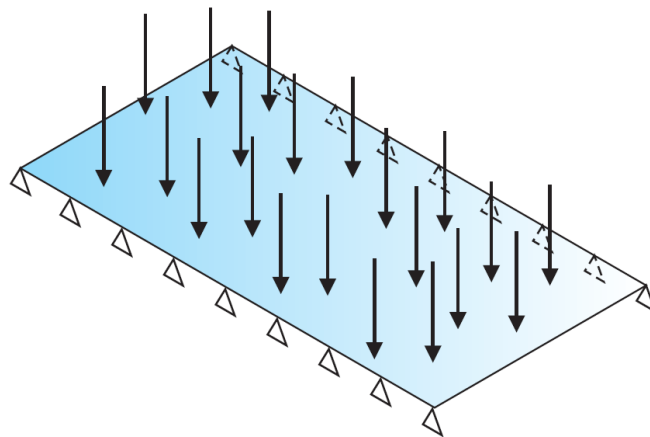


Figure 8.39 Load and constraint conditions for the plate subjected to its self-weight.

To calculate the deflections at the Serviceability Limit State, consider

$$F_d = G = 0.62 \text{ kN/m}^2 .$$

The properties of the ionoplastic polymeric interlayer are considered for infinite time and at 50°C. The interlayer shear modulus is assumed to be 1.5 MPa.

### 8.3.4.1 Calculation using the “Enhanced Effective Thickness” method

The problem is solved firstly using the “Enhanced Effective Thickness” equivalent thickness method described in Section 6.3.3.1, according to which the deflection-effective thickness is a function of a dimensionless coefficient  $\eta$ . As an example, this case will be treated both as a plate and as a simply supported beam.

If we consider the plate with the behaviour of a beam (perfectly cylindrical deformed shape), the expression of  $\eta$  is given by (6.49) as

$$\eta_{1D;2} = \frac{1}{1 + \frac{E h_{int} J_{abs} A^* \Psi}{G_{int} b J_{full}}} ,$$

where the  $\Psi$  coefficient depends on the load and constraint conditions. In particular, for simply supported beams subjected to uniformly distributed load, we have  $\Psi = \frac{168}{17l^2} = 5.042 \cdot 10^{-6} \text{ mm}^{-2}$ , which gives  $\eta_{1D;2} = 0.6914$ . The deflection- and stress- effective thicknesses, calculated using the equations (6.46) and (6.48), are therefore

$$\hat{h}_w = 19.695 \text{ mm};$$

$$\hat{h}_{1,\sigma} = \hat{h}_{2,\sigma} = 21.651 \text{ mm}.$$

If instead we consider 2D plate behaviour, namely accounting for the edge effect regarding plates with large width, the  $\eta$  coefficient is given by (6.55) as

$$\eta_{2D} = \frac{1}{1 + \frac{h_{int} E}{G_{int} (1 - \nu^2)} \frac{D_{abs}}{D_{full}} \frac{h_1 h_2}{h_1 + h_2} \Psi} .$$

The  $\Psi$  coefficient, in this case, can be obtained from Table 6.4, according to the size of the plate and the load and constraint conditions. For the considered plate, which is simply supported on two edges and subjected to uniformly distributed load, interpolation gives  $\Psi = 5.397 \cdot 10^{-6} \text{ mm}^{-2}$  and, as a result,  $\eta_{2D} = 0.6658$ .

The deflection- and stress- effective thicknesses, calculated using equations (6.46) and (6.48), therefore become:

$$\hat{h}_w = 19.409 \text{ mm};$$

$$\hat{h}_{1,\sigma} = \hat{h}_{2,\sigma} = 21.403 \text{ mm}.$$

Note that the values of the effective thicknesses obtained in the hypothesis of beam behaviour and plate behaviour are very similar, because of the approximately cylindrical form of the deformation. Once the equivalent thicknesses have been defined, the maximum stress and maximum deflection are determined analytically, or by using a finite element code with 2D elements of the PLATE or SHELL

type. Table 8.7 gives the maximum stress and maximum deflection values, compared with the results obtained from finite element analysis.

### 8.3.4.2 Calculation using tables (with equivalent thicknesses according to the E.E.T. method)

Once the effective thicknesses have been determined (Chapter 8.3.4.2), the maximum stress and maximum deflection can be found, even using abacuses and tables for analytically calculating the maximum stress and deflections of flat plates subjected to uniformly distributed loads, as proposed in section 6.6. Refer to Annex 6.6.1.3 (rectangular plate simply supported on two edges).

The maximum stress  $\sigma_{\max}$  and the maximum deflection  $w_{\max}$  caused by the design action  $F_d$  can be evaluated using the formulas (6.97) and (6.98):

$$\sigma_{\max} = 0.750 \frac{a^2}{h^2} F_d ;$$

$$w_{\max} = 0.148 \frac{a^4}{h^3} \frac{F_d}{E} ;$$

where

$a = 1400$  mm = length of the unsupported edge of the plate;

$h$  = plate thickness.

When calculating the stress at the ULS and the deflection at the SLS, consider the thicknesses obtained using the “Enhanced Effective Thickness” method (plate). The result is

$$\sigma_{\max} = 0.750 \frac{a^2}{h_{1;\sigma}} F_d = 2.586 \text{ MPa};$$

$$w_{\max} = 0.148 \frac{a^4}{h_w^3} \frac{F_d}{E} = 0.689 \text{ mm} .$$

### 8.3.4.3 3D finite element calculation

In this simulation the laminate package is modelled by using 3D finite element software ABAQUS, modelling the geometry with 20-nodes SOLID elements. Figure 8.40 and Figure 8.41, show the maximum principal stress and maximum sag of the plate, respectively. To highlight the tensile strength at the intrados, the deformed plate is represented upside down.

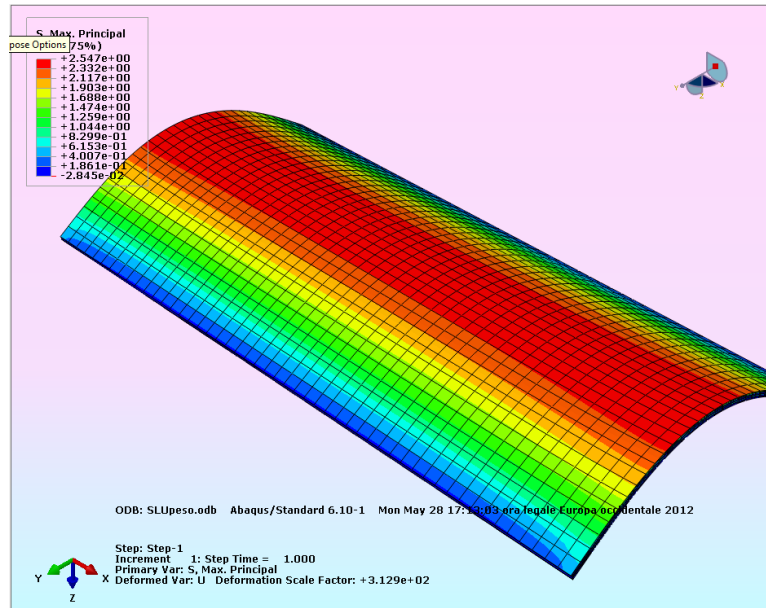


Figure 8.40 Roof subjected to self-weight (represented upside down). Maximum principal stress at the ULS.

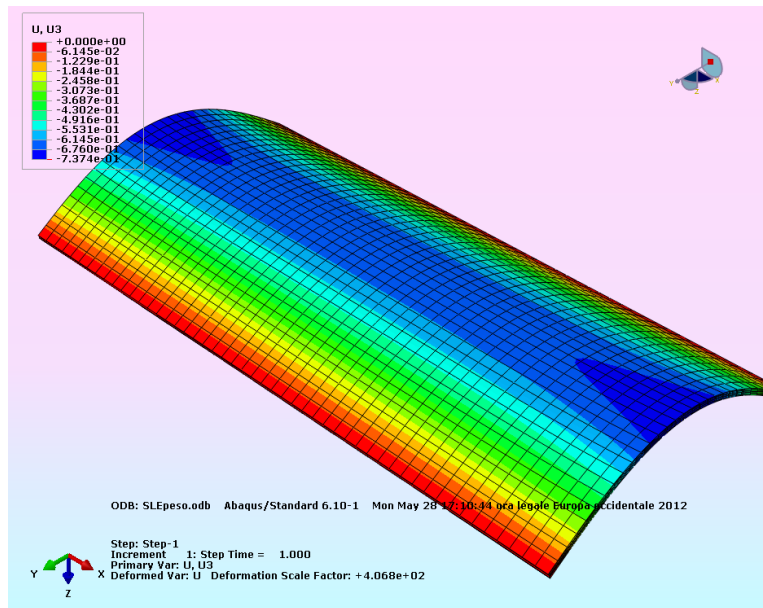


Figure 8.41 Roof subjected to self-weight (represented upside down). Deflection at the SLS.

As can be seen from the figures, the finite element calculation makes it possible to determine:

$$\sigma_{max} = 2.547 \text{ MPa at the ULS};$$

$$w_{max} = 0.737 \text{ mm at the SLS}.$$

### 8.3.4.4 Comparison

The three proposed solutions are now compared in Table 8.7, which gives the values of the maximum deflection and the maximum stress, calculated:

- with an FEM analysis of the equivalent monolithic plate, the effective thicknesses of which were calculated neglecting the effects at the edge and considering the plate as an inflexed beam (E.E.T., beam);

- with an FEM analysis of the equivalent monolithic plate, the effective thicknesses of which were calculated considering the 2D behaviour (E.E.T., plate);
- considering the 3D finite element model.

Table 8.7. Roof subjected to its own dead load: comparison of the various solutions.

METHOD	Maximum deflection at the SLS	Maximum stress at the ULS
E.E.T. beam, FEM analysis	0.730 mm	2.636 MPa
E.E.T. plate, FEM analysis	0.763mm	2.697 MPa
E.E.T. plate, abacuses and tables	0.689 mm	2.586 MPa
3D finite elements	0.737 mm	2.547 MPa

It is evident that the “Enhanced Effective Thickness” approach gives very accurate results. In the case being examined the plate deformed shape is almost cylindrical, therefore even the simple “beam” approach gives excellent results.

The subsequent tests consider the values obtained from the 3D finite element analysis, namely:

$$\sigma_{max}^G = 2.547 \text{ MPa at the ULS};$$

$$w_{max}^G = 0.737 \text{ mm at the SLS.}$$

### 8.3.5 Calculation of stress and deflection due to the snow load

The geometry and the load and constraint conditions of the plate are similar to those of the plate subjected to self-weight, and they are shown in Figure 8.39.

The design action for the Ultimate Limit State is given by

$$F_d = \gamma_Q q_s = 1.8 \text{ kN/m}^2,$$

where

$\gamma_Q=1.5$  partial factor for variable actions, including model uncertainties and dimensional tolerances;  
 $q_s$  snow action.

To calculate the deflections, consider the Serviceability Limit State, with which the associated design action is

$$F_d = q_s = 1.2 \text{ kN/m}^2.$$

The properties of the ionoplastic polymeric interlayer are evaluated for a load duration of 3 months and at 10°C. The shear modulus of the interlayer, inferred from the data of the producer, is assumed to be equal to 170 MPa.

#### 8.3.5.1 Calculation using the “Enhanced Effective Thickness” method

The problem is solved by using the equivalent thicknesses method (Enhanced Effective Thickness) described in Section 6.3.3.1. The deflection- and stress-effective thicknesses can be calculated by using the formulas (6.46) and (6.48) respectively, and they are dependent on the coefficient  $\eta$ , which depends on the geometry (beam or plate), and on the mechanical characteristics of the glass and the

interlayer. The values of the  $\Psi$  coefficient are equal to those calculated for the beam (or plate) that was subjected to its own dead load, namely:

$$\Psi = \frac{168}{17l^2} = 5.042 \cdot 10^{-6} \text{ mm}^{-2} \text{ for beam behaviour;}$$

$$\Psi = 5.397 \cdot 10^{-6} \text{ mm}^{-2} \text{ for plate behaviour (from Table)}$$

The relative values of the equivalent thicknesses are:

$$\hat{h}_w = 25.392 \text{ mm; } \hat{h}_{1,\sigma} = \hat{h}_{2,\sigma} = 25.454 \text{ mm, for beam behaviour;}$$

$$\hat{h}_w = 25.380 \text{ mm; } \hat{h}_{1,\sigma} = \hat{h}_{2,\sigma} = 25.446 \text{ mm, for plate behaviour.}$$

It should be noted that even in this case the effective thicknesses evaluated using the beam and plate model are very similar, because the load and constraint conditions deform the plate in an almost cylindrical manner.

Table 8.8 gives the stress and maximum deflection values, compared with the results obtained from the finite element analysis.

### 8.3.5.2 Calculation using abacuses and tables (with equivalent thicknesses according to the E.E.T. method)

Reference is made to Annex 6.6.1.3 (rectangular plate simply supported on two edges) which supplies formulas and tables that are useful for the analytical calculation of the maximum stress and deflection of flat plates that are subjected to uniformly distributed loads.

The maximum stress  $\sigma_{\max}$  and the maximum deflection  $w_{\max}$  caused by the design action  $F_d$  can be evaluated using formulas (6.97) and (6.98):

$$\sigma_{\max} = 0.750 \frac{a^2}{h^2} F_d ;$$

$$w_{\max} = 0.148 \frac{a^4}{h^3} \frac{F_d}{E} ;$$

where

$a = 1400 \text{ mm} =$  length of the plate edge that is not being supported;

$h =$  plate thickness.

To calculate the stress at the ULS and the deformation at the SLS, consider the effective thicknesses obtained from the “Enhanced Effective Thickness” method (plate) to get

$$\sigma_{\max} = 0.750 \frac{a^2}{h_{1,\sigma}} F_d = 4.087 \text{ MPa;}$$

$$w_{\max} = 0.148 \frac{a^4}{h_w^3} \frac{F_d}{E} = 0.596 \text{ mm}$$

### 8.3.5.3 Finite element calculation

The problem is solved by using Finite Element models, with ABAQUS software, and modelling the geometry with 20-node SOLID elements. Figure 8.40 and Figure 8.41 show the stress and deflection, respectively, undergone by the plate. It should be observed that, to highlight the traction stress at the intrados, the deformed plate is represented upside down.

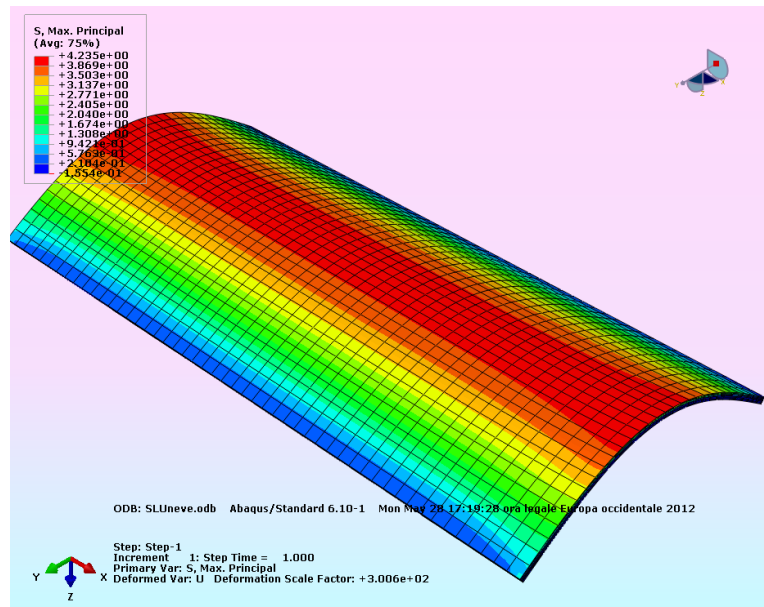


Figura 8.42 Roof subjected to snow load (seen upside down). Maximum principal stress at the ULS.

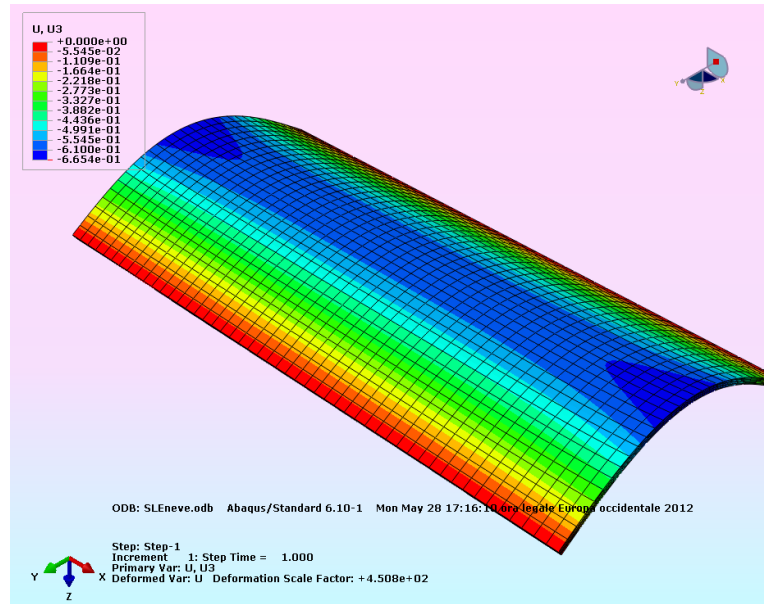


Figure 8.43 Roof subjected to snow load (seen upside down). Deflection at the SLS.

As shown by the figures, the finite element analyses allow to determine:

$\sigma_{max} = 4.235$  MPa at the ULS;

$w_{max} = 0.665$  mm at the SLS.



### 8.3.5.4 Comparison

The three proposed solutions are now compared. Analogously to Table 8.7, Table 8.8 gives the values of maximum deflection and maximum stress calculated using the different methods.

Table 8.8. Roof subjected to snow: comparison of various solutions.

METHOD	Maximum deflection at the SLS	Maximum stress at the ULS
E.E.T. beam, FEM analysis	0.660 mm	4.260 MPa
E.E.T. plate, FEM analysis	0.661 mm	4.261 MPa
E.E.T. plate, abacuses and tables	0.596 mm	4.087 MPa
3D finite element	0.665 mm	4.235 MPa

For the verifications of the glass roof, the maximum stress and maximum deflection obtained from the 3D finite element analysis are considered:

$$\sigma_{max}^S = 4.235 \text{ MPa at the ULS};$$

$$w_{max}^S = 0.665 \text{ mm at the SLS}.$$

### 8.3.6 Calculation of stress and deflection due to the live anthropic load (maintenance)

The design action is given by live anthropic load:

$$F_d = \gamma_Q Q_k = 1.8 \text{ kN},$$

where

$\gamma_Q = 1.5$ : partial factor for the variable actions;

$Q_k$ : live anthropic load (maintenance).

The design load at the Serviceability Limit State to calculate the deflection is given by:

$$F_d = Q_k = 1.2 \text{ kN}.$$

The load is distributed over an area of  $50 \times 50 \text{ mm}$ . The most dangerous condition corresponds to the application of the live anthropic load (maintenance) at the midpoint of the shorter edge (not supported) of the plate, as shown in Figure 8.44.

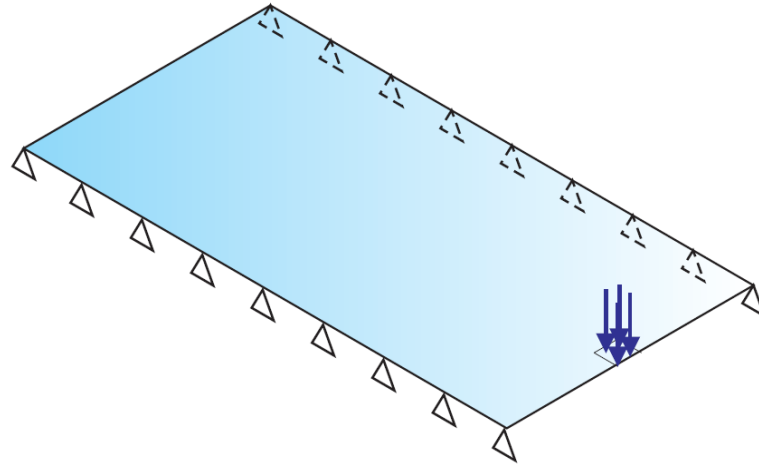


Figure 8.44 Constraint and load conditions for live load (maintenance).

The interlayer properties are considered at a temperature of 30°C, for a load duration of 30 seconds. The shear modulus of the interlayer is therefore equal to 120 MPa, as is presumed from tables supplied by the manufacturer.

It should be remembered that in the case of special conditions, such as a concentrated load, the effective thickness method may lead to inaccurate results. In this study case, therefore, the problem is solved by using a Finite Element model created with ABAQUS software. Figure 8.45 and Figure 8.46 show the plate stress and deflection, respectively.

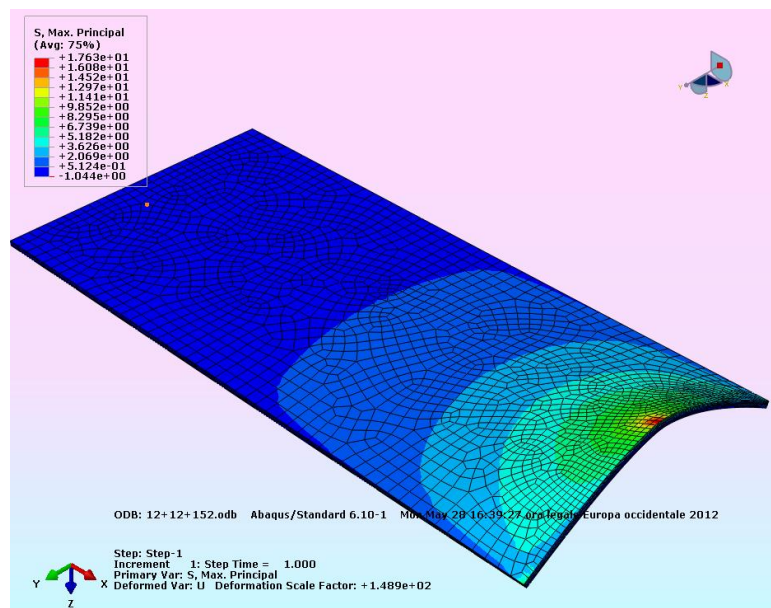


Figure 8.45 Roof subjected to its own dead load and live anthropic load (maintenance) (shown upside down): maximum principal stress at the ULS.

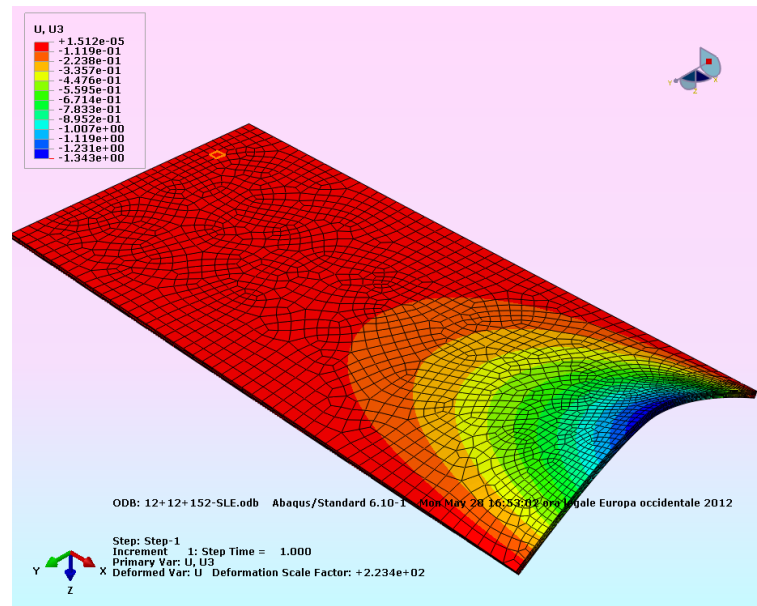


Figure 8.46 Roof subjected to its own dead load and live anthropic load (maintenance) (shown upside down): deflection at the SLS.

The laminated glass plate presents now:

$$\sigma_{max}^P = 17.63 \text{ MPa at the ULS};$$

$$w_{max}^P = 1.343 \text{ mm at the SLS}.$$

### 8.3.7 Calculation of the plate subjected to different load combinations

In order to perform the resistance calculations, the effects of the different actions, that correspond to different design strength, as discussed in 8.3.3, must be combined.

A conventional live anthropic load (maintenance) is used for calculating local effects and should therefore not be combined to the other actions, excluding the self-weight. It is therefore necessary to perform the verifications under the action of:

- self-weight and snow;
- self-weight and live anthropic load (maintenance).

Generally, to combine the effect of two or more generic actions at the same point, expression (7.8) must be used. This verification is at the considered point: therefore stresses acting on the same region must be considered. In the case being examined, all the considered actions cause maximum stress in the midpoint of the shorter edge (not supported); therefore, it is sufficient to apply the criterion (7.8) to the maximum stress evaluated for the different cases (paragraphs 8.3.4, 8.3.5 and 8.3.6).

To calculate the maximum deflection at the Serviceability Limit State, the superposition principle may be used: the deflection at one point is evaluated as the sum of the deflections at that same point, caused by the different actions. The maximum value, calculated using (7.9), must fall within the limits given by Table 7.11.

In our case, the maximum deflection caused by each action appears at the midpoint of the not supported edge; therefore, to calculate the maximum deflection, the only thing that needs to be done is sum the values obtained from paragraphs 8.3.4, 8.3.5 and 8.3.6.

### 8.3.7.1 Calculation of the roof subjected to self-weight and snow

The calculation is carried out with reference to the midpoint of the short edge. Applying the criterion (7.8), one obtains

$$\frac{\sigma_{max}^G}{f_{g;d}^G} + \frac{\sigma_{max}^S}{f_{g;d}^S} = \frac{2.547}{23.20} + \frac{4.235}{25.00} = 0.110 + 0.169 \leq 1.$$

The resistance condition is satisfied.

The maximum sag is given by (7.9):

$$w_{max} = w_{max}^G + w_{max}^S = 0.737 + 0.665 = 1.402 < \frac{1}{100} L_{inf} = 14 \text{ mm.}$$

### 8.3.7.2 Calculation of the roof under self-weight and live load (maintenance)

For the considered case, criterion (7.8) gives

$$\frac{\sigma_{max}^G}{f_{g;d}^G} + \frac{\sigma_{max}^P}{f_{g;d}^P} = \frac{2.547}{23.20} + \frac{17.63}{32.56} = 0.110 + 0.542 \leq 1.$$

The resistance condition is satisfied. It is evident that the most onerous action is the live load for maintenance.

The maximum sag is given by (7.9):

$$w_{max} = w_{max}^G + w_{max}^S = 0.737 + 1.343 = 2.080 < \frac{1}{100} L_{inf} = 14 \text{ mm.}$$

## 8.3.8 Verification of the post-breakage behaviour (Collapse limit state)

As described in Chapter 3.1, the *fail safe* approach forecasts that some glass components can fragment, either partly or completely, as a result of an imponderable event. It is therefore essential to make sure that, even in this collapse limit state, the element maintains a load bearing capacity that is enough to carry permanent loads, both self-weight and dead load, as well as a quota of the variable loads that is estimated as being congruous to the working conditions, and as such which prevent the fall of dangerous material.

The post-breakage of the glass roof must therefore be verified under the action of snow and self-weight, by neglecting the effects of the maintenance live load. It is considered that, if the roof is damaged, maintenance will not be carried out without having first made the roof itself safe, and that during the maintenance operation the operator is supplied with suitable slings as a protection against possible falls.

Regarding the deformability test, in the post-breakage phase the element displacements must be compatible with constraint conception and conformation, for example to prevent detachment from the fixings.

The phase to which the calculation refers in this specific case is phase II (Section 6.5.3), with one of the two glass plies broken, therefore with a single ply of thickness 12 mm.

Should the breakage occur because of overload, the lower ply of heat strengthened glass will be damaged because it is less resistant: the snow load and the dead load of the glass are therefore fully supported by the upper thermally toughened glass ply. Tempered glass may break spontaneously and even a while after it has been installed, for example because of the inclusion of nickel sulphide. It is evident that in this case, only the sheet of heat strengthened glass is intact in phase II and, since this situation is more onerous than the first one, post-breakage calculations will be carried out with reference to a single heat strengthened glass ply.

Following Paragraph 3.2.2, reference is made to a conventional nominal life of 10 years for post-breakage testing of class 2 elements. The snow load must therefore be rescaled to adapt it to the return period. The relation (4.33) can be used to determine the snow load,  $q_{sn}$ , referred to a return period of  $n$  years, by using the expression

$$q_{sn} = q_{sk} \left\{ \frac{1 - V \frac{\sqrt{6}}{\pi} \left[ \ln(-\ln(1 - P_n)) + 0.57722 \right]}{(1 + 2.5923V)} \right\},$$

where:

- $q_{sk}$  characteristic value of the snow load on the ground (with a return period of 50 years);
- $P_n$  yearly probability of exceeding (approximately equivalent to  $1/n$ , where  $n$  is the corresponding return interval expressed in years);
- $V$  variation coefficient of the series of the maximum yearly snow loads.

If there are no more precise indications, a value of 0.6 relative to the most onerous conditions is selected for the coefficient  $V$ , on the safe side.

For a period of  $n = 10$  years, we therefore have

$$q_{sn} / q_{sk} = 0.698.$$

As a result, the design load for a return period of 10 years is equal to

$$q_{s,10} = 0.698 \times 1.2 \text{ kN/m}^2 = 0.837 \text{ kN/m}^2.$$

For the different load durations, the design strength of the glass assumes different values for the different actions. The design strengths are the same as those calculated in Paragraph 8.3.3. To calculate the stress, the relations relative to the plate behaviour of the roof (in other words, the effect at the edge is not neglected) will be used.

The apex  $p-r$  indicates stresses and deflections relative to post-breakage behaviour.

### 8.3.8.1 Calculation for the plate subjected to its own dead load

The design action for the Ultimate Limit State is given by

$$F_d = \gamma_G G = 0.806 \text{ kN/m}^2,$$

where  $\gamma_G = 1.3$  is the partial factor for permanent actions, including model uncertainties and dimensional tolerances (Table 7.2).

To calculate the deflection at the Serviceability Limit State, consider

$$F_d = G = 0.62 \text{ kN/m}^2.$$

For a plate of monolithic glass, thickness 12 mm, subjected to the abovementioned loads, we have:

$$\sigma_{max}^{G,p-r} = 8.938 \text{ MPa at the ULS};$$

$$w_{max}^{G,p-r} = 3.251 \text{ mm at the SLS}.$$

### 8.3.8.2 Calculation of the plate under snow load

For the Collapse Limit State (post-breakage) calculation, the design action is considered as being equal to

$$F_d = \gamma_Q q_{sn} = 1.256 \text{ kN/m}^2,$$

where:

$\gamma_Q=1.5$  partial factor for variable actions, including model uncertainties and dimensional tolerance;  
 $q_{sn}$  snow load.

For a monolithic plate of glass, thickness 12 mm, the FEM analysis can be used to determine the maximum stress, equal to

$$\sigma_{max}^{S,p-r} = 13.37 \text{ MPa.}$$

The verification of the roof subjected to the two combined actions is carried out according to the criterion (7.8), in other words

$$\frac{\sigma_{max}^{G,p-r}}{f_{g;d}^{G,t}} + \frac{\sigma_{max}^{S,p-r}}{f_{g;d}^{S,t}} = \frac{8.938}{23.20} + \frac{13.37}{25} = .385 + .535 = 0.920 \leq 1$$

The resistance condition is satisfied.

## 8.4 Calculation of a built-in parapet

This example regards the calculation of a parapet made of laminated glass, the geometry of which is shown in Figure 8.47. It is assumed that it is part of an ordinary building (category 4 in Table 3.10) with a design life of 50 years. It is hypothesized that the parapet is made up of modules positioned side by side according to the layout indicated by Figure 8.47. For calculation simplicity, the height of the parapet is conventionally assumed to be 1 metre (remember that specific regulations can impose a different height).

As indicated in paragraph 4.3.2, the Collapse Limit State of this structural element also needs to be verified, in order to guarantee that the structural element, even if partially broken, can support the variable live loads given in Table 4.2 and the other variable actions relative to a return period of 10 years.

The loads acting on the structural element are its self-weight, the wind load, seismic actions and crowd loads. Given that the element is vertical, the self-weight only produces slight compression which, even though negligible, is also beneficial because it decreases the maximum traction stress in the glass. The wind action has already been treated in previous cases; this action prevails over the seismic one, given the extent of the masses in play. As an example of the calculation procedure, this case/study consider only the horizontal force caused by the crowd load, which is indeed the most severe action.

Even though the nominal life is considered to be 50 years for the pre-breakage phase and 10 years for the post-breakage phase (see paragraph 3.2.2), in the present case, on the safe side, crowd load for post-breakage assessment shall not be rescaled on the basis of the return period. Consequently, the CLS verification will directly be the most restrictive.

Various alternatives will be examined for the laminate package, in order to illustrate the consequences, at a design level, resulting from these instructions. Considering the minimum thicknesses requested for each situation, it is possible to study the behaviour of the parapet and to evaluate the most convenient solution. Furthermore, the behaviour of the parapet in the case in which a continuous handrail be inserted that connects the adjacent panels at the upper edge, in order to create system redundancy (see par. 3.1.3.2), will be considered.

Different scenarios will be taken into account in order to show the different construction possibilities.

- Parapet in class 1. It is assumed that containing structures acting as fall prevention barriers are present; in this case the parapet can be considered as class 1 for ULS verification and class 0 for

SLS verification. A laminated glass parapet composed by two glass plies will be designed (Chapter 8.4.3)

- Parapet in class 2. It is assumed that there are no other containing structures acting as fall prevention barriers, so the glass must support the horizontal crowd load. The structural element is therefore class 2 (see Table 3.9) as far as the ULS is concerned. If we consider that parapet collapsing does not cause serious consequences, the structure can be considered as class 1 for the CLS. The parapet is designed composed by two glass plies (Chapter 8.4.4), and, successively, two different solutions are proposed: parapet composed by three glass plies (Chapter 8.4.4.1) and parapet with two plies and a distributing handrail (Chapter 8.4.4.2).

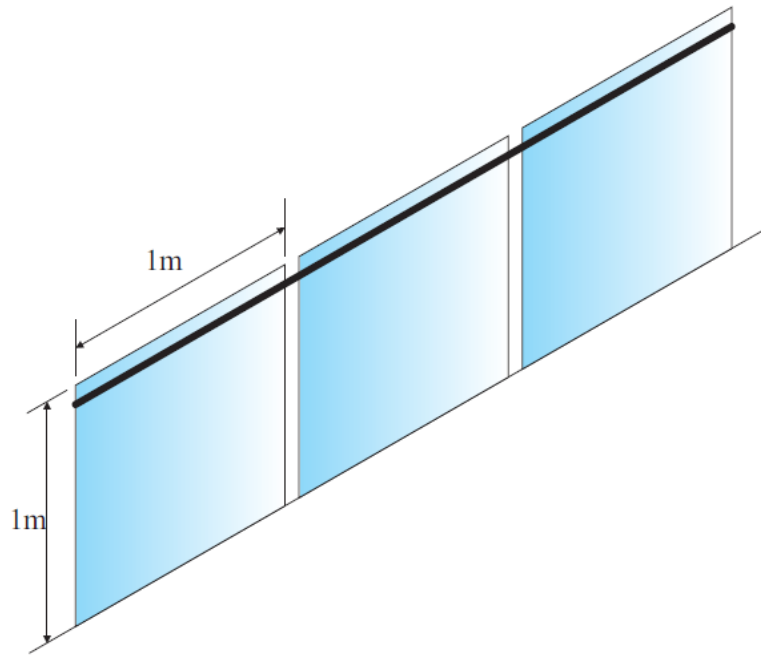


Figure 8.47. Schematic representation of the parapet being analysed.

### 8.4.1 Load analysis

The element is subjected to a load distributed over a horizontal line along the parapet edge, conventionally considered as being

$$H_k = 1 \text{ kN/m.}$$

This chapter will be limited to the verification against this horizontal force; the verifications against other horizontal loads indicated in Table 4.2 (horizontal loads distributed over the whole element and concentrated loads) are carried out in a similar manner. It should be remembered that in compliance with [NTC 2008] the horizontal design actions should not be summed up with the other forces, except for the self-weight and permanent dead loads.

The horizontal forces are considered to be the peak forces, applied for a conventional time interval of 30 s, according to what is indicated in Table 4.18.

For this type of structure, as indicated in Section 4.3.2, the load bearing capacity with respect to the horizontal actions must also be guaranteed if one or more parts of the panel breaks, more specifically if one of the glass layers of the laminated package breaks. Therefore, the CLS verifications are the most restrictive.

The element deformed shape is almost cylindrical; it is therefore possible to consider a beam-like behaviour when calculating the stress.

### 8.4.2 Design strength

As already mentioned, serviceability limit state (SLS) verifications, ultimate limit state (ULS) verifications and collapse limit state (CLS) verifications have to be carried out for the structural element being examined, as indicated in table 7.1. The design limits to be used are given below.

#### Ultimate limit state (ULS) verification

The glass in the laminate package is heat strengthened. The maximum tensile stress induced by the design actions must be lower than the tensile strength due to bending, calculated using (7.5) as follows:

$$f_{g;d} = \frac{k_{mod} k_{ed} k_{sf} \lambda_{gA} f_{g;k}}{R_M \gamma_M} + \frac{k'_{ed} k_v (f_{b;k} - f_{g;k})}{R_{M,v} \gamma_{M,v}}$$

In addition to its dead load, which is of the same duration as the nominal life of the structure, the case being examined has design forces which, for the case at hand, have a nominal duration of 30 s, to which the value of  $k_{mod} = 0.78$  corresponds (Table 2.2).

The other coefficients in (7.5) have the following values:

$k_{ed}$	strength reduction factors for verifications near the edge of the sheet or holes. $k_{ed} = 1$ in the case of plates under out-of-plane loading
$k_{sf} = 1$	coefficient for the surface profile of the glass without surface treatments (Table 7.4)
$f_{g;k} = 45$ MPa	nominal characteristic strength of float glass (Table 7.7);
$\gamma_M = 2.50$	partial factor of the float glass (Table 7.9);
$k'_{ed}$	coefficient for tests near the edge of the plyor holes; $k'_{ed} = 1$ in the case of plies inflexed by orthogonal loads on the median plane;
$k_v = 1$	coefficient for plies that have been heat toughened horizontally (Table 7.8);
$f_{b;k} = 70$ MPa	characteristic value of the nominal strength of the heat strengthened float glass (Table 7.7);
$\gamma_{M,v} = 1.35$	partial coefficient for heat strengthened glass (Table 7.9);
$\lambda_{gA} = 1$	scale factor, calculated using (7.6), which gives:
	$\lambda_{gA} = \left( \frac{0.24 \text{ m}^2}{0.019 \times 1 \text{ m}^2} \right)^{1/7} = 1.437 > 1 \Rightarrow \lambda_{gA} = 1,$
	for a rectangular plate with one edge clamped and the other three edges free; load distributed along a line parallel to the built in edge;
$\lambda_{gl}$	scale factor for the edge stress; $\lambda_{gl} = 1$ in the case of plates under out-of-plane loading.

The reduction factors of the partial coefficients  $R_M$  and  $R_{M,v}$  (Table 7.10) are equal to:

- $R_M = 0.7$ ,  $R_{M,v} = 0.9$  for class 1;
- $R_M = 1$ ,  $R_{M,v} = 1$  for class 2.

Using the previous values gives the design strengths near the built-in edge of the element, which are equal to



$f_{g;d} = 40.63$  MPa for class 1 tests;

$f_{g;d} = 32.56$  MPa for class 2 tests.

It is supposed that the polymer interlayer used in the lamination process is of PVB, and that the producer has guaranteed a shear modulus of  $G = 0.8$  MPa for an assumed design temperature of  $30^\circ\text{C}$  and a characteristic force duration of 30 seconds. The Poisson coefficient for the interlayer is assumed to be  $\nu = 0.50$ .

#### Serviceability limit state (SLS) verification

A calculation must be carried out to ensure that the maximum displacement induced by the design forces is lower than 25 mm and 1/50 of the parapet height (Table 7.13). For the case under consideration, the limit displacement is equal to:

$$w_{\text{lim}} = 1000 \text{ mm}/50 = 20 \text{ mm.}$$

#### **8.4.3 Hypothesis 1. Parapet with fall protection system**

In this case, the behaviour of the parapet (class 1) in the post-breakage phase (CLS) does not need to be tested, as indicated by Table 3.9.

The design therefore refers to the requisites at the SLS and at the ULS.

We considered the possibility of using laminated glass made with two plies of the same thickness, and a PVB interlayer 0.76 mm thick.

By considering the element as a beam, and holding the coefficient  $\gamma_Q$  to be equal to 1.5, the maximum moment at the base is

$M_{\text{max}} = 1$  kNm at the SLS;

$M_{\text{max}} = 1.5$  kNm at the ULS.

By considering the strength value as being equal to 40.63 MPa, we obtain a minimum section (elastic) modulus equal to  $W_{\text{min}} = \frac{M_{\text{max}}}{f_{g;d}} = 36919 \text{ mm}^3$ , which corresponds to a minimum element thickness of

14.88 mm.

We therefore chose to use a laminate package of 8.8.2, in other words made of two glass plies, 8 mm thick, with a PVB interlayer of thickness 0.76 mm. In this case, using the EET method (Chapter 6.3.3.1.5) gives

$\Psi = \frac{5}{2l^2} = 2.5 \cdot 10^{-6} \text{ mm}^{-2}$  (from Table 6.3), which makes it possible to calculate the shear transfer coefficient

$$\eta_{1D;2} = \frac{1}{1 + \frac{Eh_{\text{int}} J_{\text{abs}}}{G_{\text{int}} b J_{\text{full}} A^* \Psi}} = 0.8736,$$

and, as a result,

$$\hat{h}_w = 14.792 \text{ mm;}$$

$$\hat{h}_{1,\sigma} = \hat{h}_{2,\sigma} = 15.622 \text{ mm.}$$

ULS verification

Given  $\hat{h}_{1,\sigma} = \hat{h}_{2,\sigma} = 15.622 \text{ mm}$ , we can calculate the maximum tensile stress (the same for each of the two sheets of glass), which is

$$\sigma_{\max} = \frac{6M_{\max}}{\hat{h}_{1,\sigma}^2 b} = 36.88 \text{ MPa} \leq f_{g;d} = 40.63 \text{ MPa} .$$

SLS verification

The test is carried out considering the force  $H_k$ , not multiplied by the coefficient  $\gamma_Q$ . The corresponding maximum deflection is

$$w_{\max} = \frac{H_k l^3}{3E \frac{\hat{h}_w^3 b}{12}} = 17.65 \text{ mm} \leq w_{\lim} = 20 \text{ mm}$$

**8.4.4 Hypothesis 2. Parapet without fall prevention system**

In this case, as the element is class 2, the design strength is  $f_{g;d} = 32.56 \text{ MPa}$ .

This strength value gives a minimum section (elastic) modulus of  $W_{\min} = \frac{M_{\max}}{f_{g;d}} = 46069 \text{ mm}^3$ , which corresponds to a minimum glass thickness of 16.62 mm.

It is therefore decided to use a laminate package made of two glass plies, 10 mm thick, with a PVB interlayer of thickness 0.76 mm. In this case, the EET method (Chapter 6.3.3.1.5) gives

$$\Psi = \frac{5}{2l^2} = 2.5 \cdot 10^{-6} \text{ mm}^{-2}; \quad \eta_{1D;2} = \frac{1}{1 + \frac{Eh_{\text{int}} J_{\text{abs}} A^* \Psi}{G_{\text{int}} b J_{\text{full}}}} = 0.8736;$$

$$\hat{h}_w = 17.960 \text{ mm};$$

$$\hat{h}_{1,\sigma} = \hat{h}_{2,\sigma} = 19.103 \text{ mm.}$$

Calculation at the ULS

Given  $\hat{h}_{1,\sigma} = \hat{h}_{2,\sigma} = 19.103 \text{ mm}$ , it is possible to calculate the maximum tensile stress (the same for each of the two glass plies) which results as being equal to

$$\sigma_{\max} = \frac{6M_{\max}}{\hat{h}_{1,\sigma}^2 b} = 24.66 \text{ MPa} \leq f_{g;d} = 32.55 \text{ MPa} .$$

SLS calculation

The calculation is carried out considering the force  $H_k$ , not multiplied by the coefficient  $\gamma_Q$ . The corresponding maximum deflection is

$$w_{\max} = \frac{H_k l^3}{3E \frac{\hat{h}_w^3 b}{12}} = 9.86 \text{ mm} \leq w_{\text{lim}} = 20 \text{ mm} .$$

SLC verification

In post-breakage conditions, the calculation is performed by considering only the intact glass ply (thickness 10 mm). The design strength is  $f_{g;d} = 40.63 \text{ MPa}$  . The maximum stress is equal to

$$\sigma_{\max} = \frac{6M_{\max}}{10^2 b} = 90 \text{ MPa} > f_{g;d} = 40.63 \text{ MPa} . \text{ The CLS verification is not satisfied.}$$

Even choosing to increase the ply thicknesses to the *maximum* available for heat strengthened glass, namely 12 mm, would give

$$\sigma_{\max} = \frac{6M_{\max}}{12^2 b} = 62.5 \text{ MPa} > f_{g;d} = 40.63 \text{ MPa} . \text{ The CLS verification is not satisfied.}$$

As a result, a parapet cannot be made with two sheets of toughened glass. Remember that it is not advisable to make parapets with sheets of tempered glass in any case because they fragment completely into tiny pieces when they break, with the obvious catastrophic complete loss of rigidity. Toughened glass, which breaks into larger fragments, is an obligatory choice.

The possible alternatives for solving the impossibility of using laminates with only two sheets of toughened glass are:

- using a laminate package with three sheets of glass (Chapter 8.4.4.1);
- using a handrail that spreads the load between adjacent element (Chapter 8.4.4.2).

In both cases, the most restrictive verification is that related to the Collapse Limit State.

**8.4.4.1 Solution A. Laminated panel with three glass plies**

A laminate package with three glass plies having the same thickness and PVB interlayers of thickness 0.76 mm is considered here.

CLS verification

The calculation is carried on for a laminate made with two glass plies, in the hypothesis that one sheet would break. By considering the maximum bending moment at the base and the minimum section modulus, in the pre-dimensioning phase it is possible to evaluate the minimum section modulus

$$W_{\min} = \frac{M_{\max}}{f_{g;d}} = 36918 \text{ mm}^3 , \text{ which corresponds to a minimum glass thickness (in terms of stress)}$$

equal to 14.88 mm.

A laminate package made with two glass plies, each 8 mm thick, was therefore considered during the post-breakage phase. The effective thickness for calculating the stress is found using the “Enhanced Effective Thickness” method, which gives

$$\hat{h}_{1;\sigma} = \hat{h}_{2;\sigma} = 15.62 \text{ mm} .$$

The maximum tensile stress (the same for each of the two glass plies) is equal to

$$\sigma_{\max} = \frac{6M_{\max}}{\hat{h}_{1;\sigma}^2 b} = 36.88 \text{ MPa} \leq f_{g;d} = 40.63 \text{ MPa} .$$

ULS verification

The verification is carried out by considering the intact laminate package made of three glass plies, each one 8 mm thick. The Enhanced Effective Thickness model can be used to calculate the effective thicknesses of the multilayered elements; the case being examined gives

$$\eta_{1D;2} = 0.921 \text{ from (6.51); for the external sheets, which are subjected to higher level of stress, } \hat{h}_{\sigma} = 22.50 \text{ mm.}$$

The maximum tensile stress is therefore

$$\sigma_{\max} = \frac{6M_{\max}}{\hat{h}_{\sigma}^2 b} = 17.78 \text{ MPa} \leq f_{g;d} = 32.56 \text{ MPa} .$$

SLS verification

The calculation is carried out on the intact laminate package, made of three glass plies, each one of thickness 10 mm, considering the force  $H_k$ , not multiplied by the coefficient  $\gamma_Q$ . According to the Enhanced Effective Thickness method, the deflection-effective thickness is  $\hat{h}_w = 19.88 \text{ mm}$ ; the corresponding maximum deflection results as being

$$w_{\max} = \frac{H_k l^3}{3E \frac{\hat{h}_w^3 b}{12}} = 7.27 \text{ mm} \leq w_{\text{lim}} = 20 \text{ mm} .$$

**8.4.4.2 Solution B. Laminated panel with two glass plies and distributing handrail**

The possibility of using laminated panels made by two glass plies of equal thickness is considered again, but in this case a sufficiently rigid metal handrail is positioned on the upper edge of the glass elements; the purpose of the handrail is to divide the loads among adjacent elements. The continuous hand rail connects the various panels of the parapet to each other; should one of the sheets break, the handrail should be able to transfer a part of the forces acting on the damaged panel to the two adjacent panels. In this manner it is possible to obtain system redundancy, as discussed in paragraph 3.1.3.2.

It is hypothesized to use a laminate package made of two glass plies of thickness 10 mm, bonded by a PVB interlayer of 0.76 mm.

It is also supposed that the load acting on the three element transfers to the various panels proportionally to their rigidity, therefore proportionally to the cube of the thicknesses. The rigidity of integral panels can be calculated on the basis of the deflection-effective thickness which, using the “Enhanced Effective Thickness” in the case of a 10.10.2 package, is equal to  $\hat{h}_w = 17.960 \text{ m}$ .

The effective thickness for calculating the stress is

$$\hat{h}_{1;\sigma} = \hat{h}_{2;\sigma} = 19.103 \text{ mm.}$$

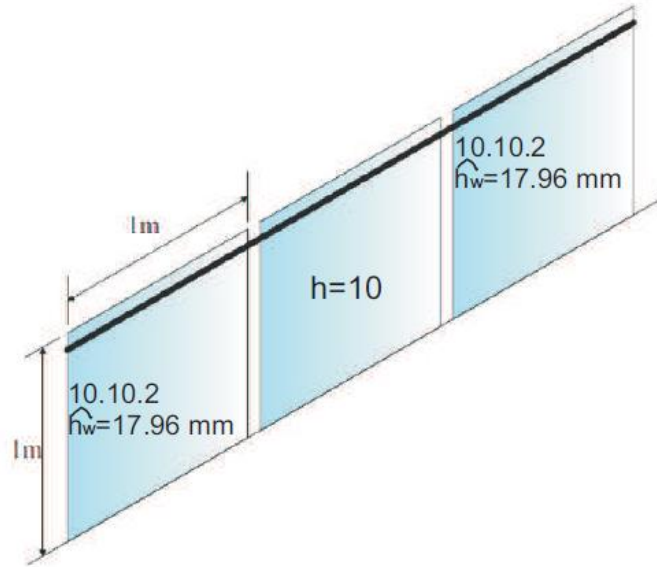


Figure 8.48. Parapet with damaged element, and with handrail that distributes the load to the adjacent elements.

The bending moments acting on the internal and external sheets are therefore, respectively,

$$M_{int} = 3 \cdot \frac{10^3}{10^3 + 2 \cdot 17.960^3} \cdot 1.5 \cdot 10^6 = 0.358 \cdot 10^6 \text{ Nm} ,$$

$$M_{ext} = 3 \cdot \frac{17.960^3}{10^3 + 2 \cdot 17.960^3} \cdot 1.5 \cdot 10^6 = 2.071 \cdot 10^6 \text{ Nm} .$$

#### SLC verification

As a result of the bending moment  $M_{int}$ , the internal element has a maximum stress of

$$\sigma_{max;int} = \frac{6M_{int}}{10^2 b} = 21.45 \text{ MPa} < f_{g;d} = 40.63 \text{ MPa} .$$

Similarly, the maximum stress on the internal sheet is

$$\sigma_{max;ext} = \frac{6M_{ext}}{19.103^2 b} = 34.05 \text{ MPa} < f_{g;d} = 40.63 \text{ MPa} .$$

#### ULS verification

Each element has a maximum stress of

$$\sigma_{max} = \frac{6M}{19.103^2 b} = 24.66 \text{ MPa} < f_{g;d} = 32.56 \text{ MPa} .$$

#### SLS verification

The calculation is carried out on the intact laminate package, made of two glass plies, each one 10 mm thick, considering the force  $H_k$ , not multiplied by the coefficient  $\gamma_Q$ .

The maximum deflection corresponding to the deflection-effective thickness  $\hat{h}_w = 17.960 \text{ mm}$  is

$$w_{max} = \frac{H_k l^3}{3E \frac{\hat{h}_w^3 b}{12}} = 9.86 \text{ mm} \leq w_{lim} = 20 \text{ mm} .$$

### 8.4.5 Final considerations

The importance of the post-breakage phase when dimensioning laminated glass is shown in the example that has just been presented. In general, it is always necessary to assume that a sheet of glass can break prematurely, for example because of an internal defect.

In general, laminated components made with three glass plies are thinner than laminates with just two sheets. Indeed, should one glass break, the load-bearing capacity reduces by about 33% in the case of triple glass, and by about 50% in the case of double glass. The laminate with three glass plies therefore gives good results in terms of “section redundancy”, as explained in section 3.1.3.1.

To avoid excessive glass thickness, it is a good rule to use load distribution devices (the handrail in the example just given) that allow several components to collaborate should one crack. This gives system redundancy, as described in par. 3.1.3.2. It should be remembered that, for simplicity, the handrail in the example above is considered as being rigid. If one considers the deformability of the handrail, the load sharing between the panels changes, especially when the loads are not uniformly distributed. This effect shall be taken into account when the handrail is very slender.

## 8.5 Glass beams and floors

Glass load-bearing beams are generally made so that the bending plane coincides with the midplane of the plate (Figure 8.49). The stress can be calculated using plate theory in generalized plane stress or, if the element is slender, with beam theory. Bending, in any case, causes traction stresses along the edge of the structural element. For this reason, the effective strength under bending is definitely conditioned by the finishing of the glass edge. This is because microdefects are concentrated along the edges due to the cutting process, and here the strength is usually lower than that found on the surfaces. Rounded and polished edge finishes are to be preferred because their strength is higher. In this example, beams with ground edges are considered.

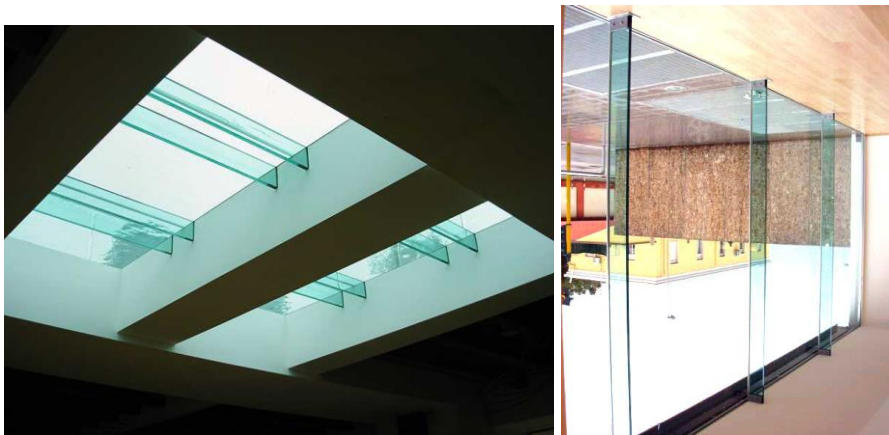


Figure 8.49. Example of glass beams, used in a rooflight or as fins.

Given that glass lacks ductility, and as such does not permit the plastic redistribution of the stress, it is preferable to use isostatic structural schemes. The most common one is obviously that of simply supported beams, which can be obtained by inserting the glass into dedicated metal “shoes”; a soft layer should be applied which, guaranteeing uniform division of the stress and tension on the relative contact surfaces, prevents stress concentrations (Figure 8.50). Similar constraints reduce the risks of beam flexural-torsional buckling phenomena.

To improve the bending behaviour of glass, the edge of the element can be reinforced by connecting it to a material that is more ductile. Compound systems can be made, the behaviour of which depends

on the mechanical characteristics of the materials used and on their effective structural collaboration. Among the various solutions studied today, there are beams with a reinforced intrados, obtained by glueing steel profiles, or carbon- or metal-reinforced fibres.



Figure 8.50. Detail showing the ends of beams inserted into dedicated metallic shoes.

The proposed example (Figure 8.51) is a glass floor, of size 4×5 metres, that is supported by beams, located where crowds do not gather. The beams, made of laminated glass, are 4000 mm long, 350 mm high and are positioned with a centre-to-centre distance (pitch) of 1000 mm. The package is made by using four plies of heat strengthened glass with polished edges, each one 10 mm thick, with a PVB interlayer (Figure 8.52). The presence of the interlayer guarantees better post-breakage behaviour, because it holds fragments, limits the size and spreading of cracks, and gives a residue load bearing capacity. The static scheme is that of a simply supported beam. The floor is made of a laminate package, with each panel having 3 layers of glass (tempered-toughened-tempered), each one 12 mm thick. To guarantee section redundancy, it must be predicted that one of the package elements can be damaged (paragraph 3.1.3.1).

Beams and floor are classified as class 2 elements (Table 3.9). In general, serviceability state (SLS), ultimate limit state (ULS) and collapse limit state (CLS) calculations must be carried out, where the possibility of glass breakage is considered (Table 3.8). As, in the case being examined, the loads are the same as those of the ULS and the CLS, the most restrictive verifications are the CLS, therefore the ULS verification can be omitted because automatically satisfied.

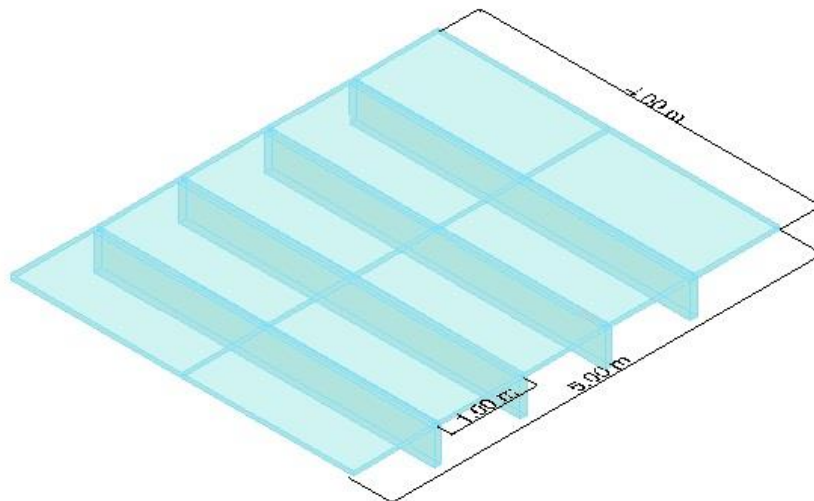


Figure 8.51. Deck with glass beams and floor.

### 8.5.1 Simply supported beam under self-weight, permanent loads and anthropic action

The beam, of length 4000 mm, is made up of 4 glass plies (each one 10 mm thick) of heat toughened glass, coupled vertically by PVB interlayers that are 0.76 mm thick. The geometry of the laminate package is given in Figure 8.52. On the basis of the design configuration, the stress plane is parallel to the element plane. In the bending calculation, therefore, the section can be treated as homogeneous and monolithic with cross section 40×350 mm, by neglecting the presence of the PVB, the contribution of which is certainly negligible.

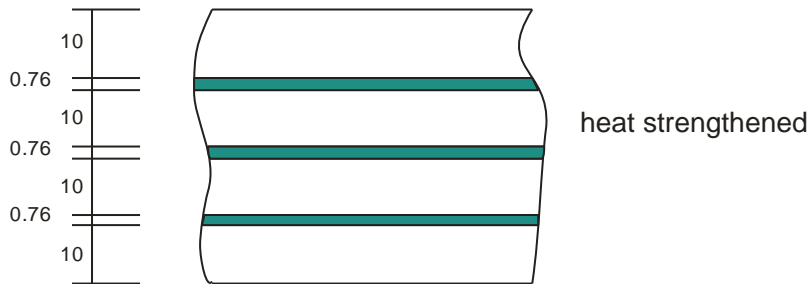


Figure 8.52. Composition of the laminated glass beam.

#### 8.5.1.1 Load analysis

The acting loads include:

*Self-weight:*

Specific self-weight of glass:  $\gamma_v = 25 \text{ kN/m}^3$ ;  
 specific self-weight of the interlayer:  $\gamma_{PVB} = 10.5 \text{ kN/m}^3$ ;

The total weight per unit of length results as being

$$G_1 = (\gamma_v \cdot 4h + \gamma_{PVB} \cdot 3h_{int}) \cdot b = (25 \cdot 4 \cdot 0.01 + 10.5 \cdot 3 \cdot 0.00076) \cdot 0.35 = 0.36 \text{ kN/m} .$$

The design duration is equal to the life of the work, taken to be 50 years. The reference temperature for calculating the stiffness of the polymeric interlayer is assumed, on the safe side, to be 50°C.

*Dead permanent load (weight of the floor):*

The load transmitted to the beam by the floor is

$$G_2 = (25 \cdot 3 \cdot 0.012 + 10.5 \cdot 2 \cdot 0.00076) \cdot 1 = 0.92 \text{ kN/m} ;$$

The design load duration is 50 years.

*Cat. B2 action (transit area for offices open to the public):*

The anthropic action is

$$q_k = 3.0 \text{ kN/m} .$$

The design duration is relative to temporary transit in environments that are not susceptible to crowding (30 seconds). A reference temperature of 50°C was selected for determining the mechanical properties of the polymeric interlayer, on the safe side.



### 8.5.1.2 Design strength

Because of the geometry and loads, the maximum stress is at the edge under traction; the verification will therefore be carried out at a distance of  $d < 5 s$  from the edge. The glass design strength is calculated separately for the different load conditions. In the case of a heat toughened glass beam, the design strength can be calculated by referring to (7.5), by considering reduction coefficients for the edge. The following expression is therefore used

$$f_{g;d} = \frac{k_{mod} k_{ed} k_{sf} \lambda_{gA} \lambda_{gl} f_{g;k}}{R_M \gamma_M} + \frac{k'_{ed} k_v (f_{b;k} - f_{g;k})}{R_{M;v} \gamma_{M;v}},$$

where:

- $k_{mod}$  reduction coefficient for static fatigue, given in Table 2.2 according to the type of external action and its characteristic duration;
- $k_{ed}=0.8$  strength reduction factors for verifications near the edges of the element or holes (Table 7.3) for glass with polished edges;
- $k_{sf}=1$  coefficient for the surface profile of the glass without surface treatments (Table 7.4)
- $f_{g;k} = 45 \text{ MPa}$  nominal characteristic strength of the float glass;
- $R_M=1$  reduction factor of the partial coefficient, for verifications in class 2 (Table 7.10);
- $\gamma_M=2.50$  partial coefficient of the float glass (Table 7.9);
- $k'_{ed} = 0.8$  coefficient for calculations near the edge of the sheet or holes (Table 7.3) for glass with polished edges;
- $k_v = 1$  coefficient for glass plies that have been heat toughened vertically (Table 7.8);
- $f_{b;k} = 70 \text{ MPa}$  nominal characteristic strength of heat strengthened glass (Table 7.7);
- $R_{M;v} = 1$  reduction factor of the partial coefficient, for verifications in class 2 (Table 7.10);
- $\gamma_{M;v} = 1.35$  partial coefficient for pre-stressed glass (Table 7.9);
- $\lambda_{gA}$  scale factor, that considers the area subjected to the maximum tensile stress, calculated using (7.6):

$$\lambda_{gA} = \left( \frac{0.24 \text{ m}^2}{kA} \right)^{1/7} = \left( \frac{0.24 \text{ m}^2}{0.054 \cdot 4 \cdot 0.04} \right)^{1/7} = 1.607 \Rightarrow \lambda_{gA} = 1;$$

where  $A$  is the area subjected to maximum traction, while the coefficient  $k=0.054$  defining the effective area is given in Table 7.5, for a rectangular plate simply supported on two edges;

- $\lambda_{gl}$  scale factor for stress on the edge, for verifications at a distance of  $d < 5 s$  from the edge, given by (7.7); the following should be used for polished edges

$$\lambda_{gl} = \left( \frac{0.0741 \cdot 0.45 \text{ m}}{k_b \cdot l_b} \right)^{1/12.5} = 0.763 \leq 1;$$

- $k_b=0.2434$  coefficient for calculating the scale effect in the neighbourhood of the edge, for parabolic stress distribution (Table 7.6);
- $l_b = 4 \text{ m}$  total length of the edges subjected to traction.

#### Design strength for self-weight and dead loads

Table 2.2 gives  $k_{mod} = 0.26$  for a conventional load duration of 50 years. The design strength therefore becomes:

$$f_{g;d}^G = 17.67 \text{ MPa for verifications near the edges (distance } d < 5 s).$$

Design strength for Cat. B2 forces

For a conventional load duration of 30 seconds,  $k_{mod} = 0.78$  (from Table 2.2), which therefore gives a design strength of:

$$f_{g;d}^0 = 23.39 \text{ MPa for verifications near the edges (distance } d < 5 \text{ s).}$$

The design deflection at the SLS is equal to  $\frac{1}{250} L_{inf} = 16 \text{ mm [ NTC 2008].}$

**8.5.1.3 Calculation of stress and deflection for a beam subjected to self-weight and dead loads at the CLS**

The most restrictive verification is the one regarding the CLS, where it is considered that one of the plies is broken and the load is therefore being carried by the remaining three plies. The considered total thickness of the glass is therefore 30 mm.

The design action for the Collapse Limit State is given by:

$$F_d = \gamma_{G1}G_1 + \gamma_{G2}G_2 = 1.85 \text{ kN/m;}$$

where  $\gamma_{G1}=1.3$  is the partial factor for dead load and  $\gamma_{G2}=1.5$  is the partial factor for permanent dead loads, including model uncertainty and dimensional tolerance (Table 7.2).

The maximum bending moment and the maximum stress are

$$M_d = \frac{1}{8} F_d l^2 = \frac{1}{8} 1.85 \cdot 4^2 = 3.70 \text{ kNm;}$$

$$\sigma_{max}^G = \frac{M_d}{W} = \frac{3.70 \cdot 10^6}{\frac{30 \cdot 350^2}{6}} = 6.04 \text{ MPa.}$$

When calculating the deflections, consider the Serviceability Limit State to which the design action is associated

$$F_d = G_1 + G_2 = 1.28 \text{ kN/m;}$$

to which the maximum deflection

$$w_{max}^G = \frac{5F_d l^4}{384EJ} = \frac{5 \cdot 1.28 \cdot 4000^4}{384 \cdot 70000 \cdot \frac{30 \cdot 350^3}{12}} = 0.57 \text{ mm}$$

corresponds. Therefore, a glass beam subjected to its own dead load and the permanently supported load results as being:

$$\sigma_{max}^G = 6.04 \text{ MPa at the SLC;}$$

$$w_{max}^G = 0.57 \text{ mm at the SLS.}$$

**8.5.1.4 Calculation of stress and deflection for a beam subjected to Cat. B2 action at the CLS**

The design action for the Collapse Limit State at the post-breakage phase is given by:

$$F_d = \gamma_Q q_k = 4.5 \text{ kN/m ,}$$

where

$\gamma_Q=1.5$ : partial factor for variable actions, including model uncertainties and dimensional tolerances;  
 $q_k$ : Cat. B2 action.

The maximum bending moment and the maximum stress are

$$M_d = \frac{1}{8} F_d l^2 = \frac{1}{8} 4.5 \cdot 4^2 = 9.0 \text{ kNm},$$

$$\sigma_{\max}^Q = \frac{M_d}{W} = \frac{9.0 \cdot 10^6}{\frac{30 \cdot 350^2}{6}} = 14.70 \text{ MPa}.$$

When calculating the deflections, consider the Serviceability Limit State to which a design action

$$F_d = q_k = 3.0 \text{ kN/m}$$

is associated; to this, the maximum deflection given below corresponds

$$w_{\max}^Q = \frac{5F_d l^4}{384EJ} = \frac{5 \cdot 3.0 \cdot 4000^4}{384 \cdot 70000 \cdot \frac{30 \cdot 350^3}{12}} = 1.33 \text{ mm}.$$

Briefly, a glass beam subjected to Cat. B2 action results to have

$$\sigma_{\max}^Q = 14.70 \text{ MPa at the CLS};$$

$$w_{\max}^Q = 1.33 \text{ mm at the SLS}.$$

### 8.5.1.5 Verification of the beam under different load combinations

In resistance verifications, the effects of the different actions, which have different design resistances, should be combined. To be more thorough, remember that the [NTC 2008] indicate that even conventional loads, excluding all other actions except permanent loads, that are concentrated on a reduced area must be considered. For exposure brevity, this test is not developed here. In the case being examined, only the verification against the action of self-weight, permanent dead load and distributed live load will be carried out.

#### CLS verification

The verification is performed at a punctual level according to the expression (7.8). In the case being examined, all the considered actions cause maximum stress at the midpoint of the beam, therefore the criterion (7.8) is applied directly to the values evaluated previously for the different cases.

The self-weight, permanent dead load and accidental load give

$$\frac{\sigma_{\max}^G}{f_{g;d}^G} + \frac{\sigma_{\max}^Q}{f_{g;d}^Q} = \frac{6.04}{17.67} + \frac{14.70}{23.39} = 0.970 \leq 1.$$

The verification is satisfied

#### SLS verification

As indicated in paragraph 7.5, the effects only need to be overlapped when calculating the maximum deflection at the Serviceability Limit State: the deflection at one point is evaluated as the sum of the deflections, caused by the different actions, at that same point. The maximum deflection caused by each action occurs at the midpoint of the beam; therefore, one has to just sum up the values found previously for each load condition. In the case being examined we have

$$w_{\max} = w_{\max}^G + w_{\max}^Q = 0.57 + 1.33 = 1.90 \text{ mm} < \frac{1}{250} L_{inf} = 16 \text{ mm}.$$

The deformability verification is therefore satisfied.

## 8.5.2 Rectangular floor simply supported on two edges, subjected to self-weight and anthropic action

In accordance with Table 3.8, the floor is made of laminated glass composed by three glass plies (tempered-heat strengthened-tempered) of thickness 12 mm, connected by PVB interlayers of thickness 0.76 mm (Figure 8.53).

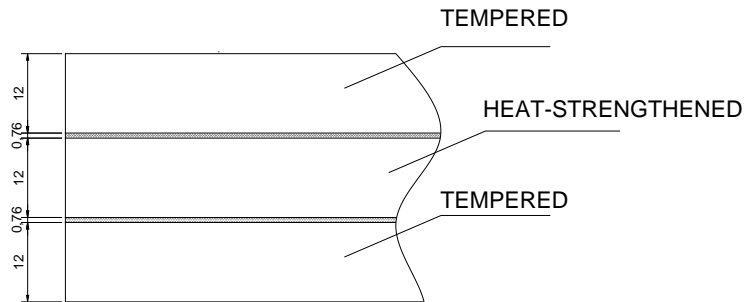


Figure 8.53. Composition of the laminated glass sheet.

The panels are of size 1000×2000 mm and are supported by the beam on their longer edges. They are subjected to the action of self-weight and anthropic live load, consisting in an uniformly distributed load and a conventional pseudo-concentrated load for calculating local effects, concentrated on a small area. The uniformly distributed loads (self-weight and uniformly distributed live load) act on the whole of the plate surface, which deforms into an almost cylindrical shape. Approximately, the stress is therefore uniform on the generators parallel to the long edges of the plate but, given the width, there is an edge effect, so the shorter edges (not supported) are subjected to higher stresses. The floor is also subjected to a concentrated load which, as indicated in the [NTC 2008], act on an area of size 50x50 mm. Maximum stress and maximum deflection are located halfway along the non-supported edge, where the load is applied. This load is essentially for the maintenance phase and it is not applied if one of the glass plies is damaged.

Floor behaviour is analysed with reference to the following phases:

phase I – pre-breakage behaviour in which the three glass plies of the package are intact;

phase II – behaviour after the breakage of the upper glass ply, subjected to the direct action of the loads, therefore the supporting package is made of two plies, one toughened and one tempered.

For verification against the live concentrated load, in addition to the permanent loads, reference is made to phase I. For verification against the distributed live loads, reference is made to phase II, considering the possibility of breakage of one ply, in agreement with Paragraph 3.1.4.

### 8.5.2.1 Load analysis

The acting loads are:

*Self-weight:*

specific self-weight of the glass:  $\gamma_v = 25 \text{ kN/m}^3$ ;  
 specific self-weight of the interlayer:  $\gamma_{PVB} = 10.5 \text{ kN/m}^3$ ;

The total self-weight is  $G = (25 \cdot 3 \cdot 0.012 + 10.5 \cdot 2 \cdot 0.00076) = 0.92 \text{ kN/m}^2$ .

The design duration relative to the dead load is 50 years.

Cat. B2 action (transit area of offices open to the public)

$$q_k = 3.0 \text{ kN/m}^2 \quad (\text{Tab. 3.1.II of [NTC 2008]}).$$

Design duration is relative to temporary transit in environments that are not susceptible to crowding (30 seconds). In favour of safety, a temperature of 50°C is assumed, which corresponds to an inter-layer shear modulus of 0.44 MPa.

Cat. B2 action for local effects (transit area of offices open to the public)

$$Q_k = 2.0 \text{ kN} \quad \text{distributed over an area of } 50 \times 50 \text{ mm (Tab. 3.1.II of [NTC 2008]}).$$

The design duration of the action is 30 seconds (the same as that of the action caused by temporary transit, as *per* Table 2.2). On the safe side, a temperature of 50°C is assumed, which corresponds to an interlayer shear modulus of 0.44 MPa.

The action is to be used for independent local tests, and therefore it must only be combined with the dead load; other actions are excluded.

**8.5.2.2 Design strength**

The design strength of laminated glass is calculated separately for the different load conditions. In the case of a floor made of three glass plies (tempered-heat strengthened-tempered), the design strength for both types of glass must be calculated. Referring to (7.5),

$$f_{g;d} = \frac{k_{mod} k_{ed} k_{sf} \lambda_{gA} \lambda_{gl} f_{g;k}}{R_M \gamma_M} + \frac{k'_{ed} k_v (f_{b;k} - f_{g;k})}{R_{M;v} \gamma_{M;v}}$$

where:

- $k_{mod}$  reduction coefficient for static fatigue, given in Table 2.2 according to the type of external action and its characteristic duration;
- $k_{ed}=1$  strength reduction factors for verifications near the sheet edge or holes for a plate under out-of-plane loading;
- $k_{sf} = 1$  coefficient for the surface profile of the glass without surface treatment (Table 7.4)
- $f_{g;k} = 45 \text{ MPa}$  nominal characteristic strength of the float glass;
- $R_M = 1$  reduction factor of the partial coefficient, for class 2 tests (Table 7.10);
- $\gamma_M = 2.50$  partial factor of the float glass (Table 7.9);
- $k'_{ed} = 1$  strength reduction factors for verifications near the edge of the sheet or holes with plate under out-of-plane loading;
- $k_v = 1$  coefficient for heat treated sheets with horizontal heat treatment (Table 7.8);
- $R_{M;v} = 1$  reduction factor of the partial coefficient, for class 2 tests (Table 7.10);
- $\gamma_{M;v} = 1.35$  partial factor for pre-stressed glass (Table 7.9);
- $\lambda_{gA}$  reduction factor of the resisting stress, calculated with (7.6):

$$\lambda_{gA} = \left( \frac{0.24}{k \cdot A} \right)^{1/7} = 1.12 \Rightarrow \lambda_{gA} = 1;$$

$k=0.054$ , for a rectangular plate simply supported on two edges (Table 7.5);  
 $A=2 \text{ m}^2$ ;

$\lambda_{gl}$  scale factor for edge stress; for a plate under out-of-plane loading  $\lambda_{gl} = 1$ ;

The nominal characteristic strength of thermally toughened (tempered) glass is  $f_{b;k} = 120 \text{ MPa}$  for tempered glass, and  $f_{b;k} = 70 \text{ MPa}$  for heat strengthened glass (Table 7.7); the coefficient  $k_{mod}$  varies according to the considered action.

Design strength for self-weight

Table 2.2 gives  $k_{\text{mod}} = 0.26$  for a conventional load duration of 50 years. The design strength therefore becomes

$$f_{g;d}^G = 60.24 \text{ MPa for tempered glass;}$$

$$f_{g;d}^G = 23.20 \text{ MPa for heat strengthened glass.}$$

Design strength for Cat. B2 action:

In this case  $k_{\text{mod}} = 0.78$ , for a conventional load duration of 30 seconds (from Table 2.2); the design strength is therefore

$$f_{g;d}^Q = 69.60 \text{ MPa, for tempered glass;}$$

$$f_{g;d}^Q = 32.56 \text{ MPa, for heat strengthened glass.}$$

The design deflection, given by Table 7.13, is equal to  $\frac{1}{500} L_{\text{inf}} = 2 \text{ mm}$ .

**8.5.2.3 Phase I – pre-breakage behaviour**

Tests are carried out at the ULS and the SLS during this phase, considering all three plies as being sound and for the following load combinations:

1. dead load + category B2 action (distributed load)
2. dead load + category B2 action (concentrated load).

All tests are given for completeness. It should be noted that only load condition 2 is necessary with the ULS verification, because the most determinant calculation relative to the first load condition is that of the CLS (phase II).

**8.5.2.3.1 Calculation of stress and deflection for the plate under self-weight**

The design action for the Ultimate Limit State is given by

$$F_d = \gamma_G G = 1.20 \text{ kN/m}^2,$$

where  $\gamma_G = 1.3$ , the partial factor for permanent actions, including model uncertainties and dimensional tolerances (Table 7.2).

When calculating the deflections consider the Serviceability Limit State, to which a design action is associated:

$$F_d = G = 0.92 \text{ kN/m}^2.$$

The properties of the PVB interlayer are considered for a period of 50 years and at a temperature of 50°C. On the basis of values communicated by the manufacturer, the interlayer shear modulus is assumed equal to 0.052 MPa.

**8.5.2.3.1.1 Calculation of the plate under self-weight (Enhanced Effective Thickness method)**

The verification of the global behaviour of the panel can be carried out in an approximate manner, holding the laminate to be a monolithic glass of thickness equal to an effective thickness, which considers the effects on the shear transfer produced by the interlayer. The Enhanced Effective Thickness model, which is recorded in Chapter 6.3.3.1.5, gives the relations that can be used to determine the

effective thicknesses, even for multi-layered elements (see [Galuppi & Royer-Carfagni, 2013b]). As the deformation is almost cylindrical, beam behaviour can be considered. In the case being examined, the laminate package is made of three glass plies, all of the same thickness  $h$ , connected by interlayers of the same thickness  $h_{int}$ , the shear transfer coefficient is given by (6.51), and results as being

$$\eta_{1D,N} = \frac{1}{1 + \frac{Eh_{int}}{12 G_{int}} \frac{Nh^3(N+1)}{h^2 + (h+h_{int})^2(N^2-1)} \Psi},$$

in which

$N=3$ : number of glass plies;

$h = 12$  mm: thickness of each sheet of glass;

$h_{int}=0.76$  mm: thickness of each interlayer;

$\Psi$  = coefficient that depends on the load and constraint conditions, and which can be obtained from Table 6.3; in the case being examined  $\Psi = \frac{168}{17l^2} = 9.8824 \cdot 10^{-6} \text{ mm}^{-2}$ .

The shear transfer coefficient is  $\eta_{1D,N} = 0.0765$ .

The deflection- and stress-effective thickness are evaluated using (6.46) and (6.48), resulting in

$\hat{h}_w = 17.724$  mm ;

$\hat{h}_{1,\sigma} = \hat{h}_{3,\sigma} = 21.355$  mm for the external plies (tempered glass);

$\hat{h}_{2,\sigma} = 21.539$  mm for the internal ply (toughened glass).

Since the different plies composing the floor have different strengths, it is necessary to evaluate the stress-effective thicknesses of the external and internal plies. Indeed, both types of glass need to be evaluated in order to calculate the maximum tensile stress acting on each one, because the coupling is not perfect.

The finite element analysis of the equivalent monolithic plate allows to calculate:

$\sigma_{max}^G = 2.05$  MPa at the ULS, external sheets;

$\sigma_{max}^G = 2.01$  MPa at the ULS, internal sheet;

$w_{max}^G = 0.387$  mm at the SLS.

#### 8.5.2.3.1.2 Calculation of the plate under self-weight (finite element method)

In this simulation, the laminate package is modelled by using 3D finite element analysis with 20-nodes SOLID elements. Figure 8.54 and Figure 8.55 show, respectively, the stress at the ULS and the deflection at the SLS of the plate.

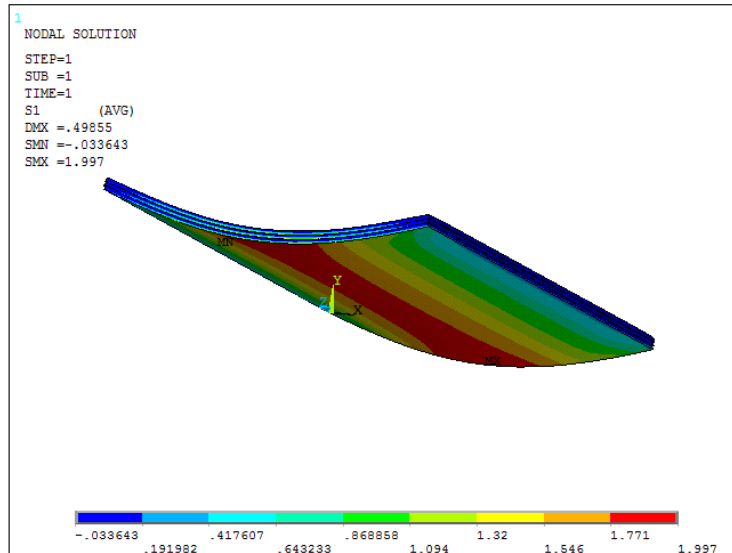


Figure 8.54. Floor subjected to self-weight: maximum principal stress at the ULS.

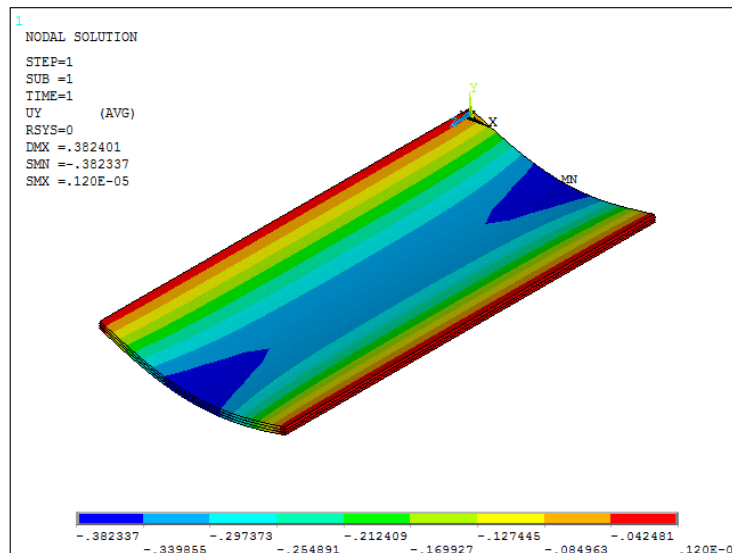


Figure 8.55. Floor subjected to self-weight: deflection at the SLS.

Briefly, for the panel subjected to self-weight, the results are:

$$\sigma_{\max}^G = 2.00 \text{ MPa} \quad \text{at the ULS, external layers;}$$

$$\sigma_{\max}^G = 1.94 \text{ MPa} \quad \text{at the ULS, internal layer;}$$

$$w_{\max}^G = 0.38 \text{ mm} \quad \text{at the SLS.}$$

### 8.5.2.3.1.3 Comparison of the analytical and numerical results

The comparison of the results obtained using the different methods to calculate the maximum deflection and maximum stress values is indicated in Table 8.9. From here it is evident that the E.E.T. model allows to evaluate stress and deflection of the multilayered glass element with excellent approximation.



Table 8.9. Plate subjected to its own weight: comparison of various solutions.

METHOD	Maximum deflection (SLS)	Maximum stress (ULS), external layers	Maximum stress (ULS), internal layer
E.E.T.	0.39 mm	2.05 MPa	2.01 MPa
F.E.M.	0.38 mm	2.00 MPa	1.94 MPa

In order to perform the verifications of the glass plate, the following values obtained using the 3D non-linear model were considered:

$$\sigma_{\max}^G = 2.00 \text{ MPa at the ULS, external plies;}$$

$$\sigma_{\max}^G = 1.94 \text{ MPa at the ULS, internal ply;}$$

$$w_{\max}^G = 0.38 \text{ mm at the SLS.}$$

#### 8.5.2.3.2 Calculation of stress and deflection for the plate subjected to Cat. B2 force

The design action for the Ultimate Limit State is given by the uniformly distributed load

$$F_d = \gamma_Q q_k = 4.5 \text{ kN/m,}$$

where  $\gamma_Q=1.5$ : partial factor for variable actions, including model uncertainties and dimensional tolerances;

$q_k$ : Cat. B2 action.

To calculate the deflections, consider the Serviceability Limit State with a design action of

$$F_d = q_k = 3.0 \text{ kN/m.}$$

#### 8.5.2.3.2.4 Calculation of the plate subjected to Cat. B2 action (Enhanced Effective Thickness method)

Similarly to paragraph 8.5.2.3.1.1, even here the test on the global behaviour of the panel can be carried out, as a first approximation, by using the E.E.T. model. For the case being examined,

$$\Psi = \frac{168}{17l^2} = 9.8824 \cdot 10^{-6} \text{ mm}^{-2}, \text{ therefore}$$

$$\eta_{1D,N} = \frac{1}{1 + \frac{Eh_{\text{int}}}{G_{\text{int}}} \frac{Nh^3(N+1)}{h^2 + (h+h_{\text{int}})^2(N^2-1)} \Psi} = 0.412.$$

The deflection- and stress-effective thickness are evaluated using (6.46) and (6.48), with the following result:

$$\hat{h}_w = 20.199 \text{ mm ;}$$

$$\hat{h}_{1;\sigma} = \hat{h}_{3;\sigma} = 24.559 \text{ mm for the external layers (tempered glass);}$$

$$\hat{h}_{2;\sigma} = 26.206 \text{ mm for the internal layer (heat strengthened glass).}$$

Using a finite element analysis of the equivalent monolithic sheet, it is possible to calculate  
 $\sigma_{\max}^G = 5.82 \text{ MPa}$  at the ULS, on the external layers;  
 $\sigma_{\max}^G = 5.11 \text{ MPa}$  at the ULS, internal layer;  
 $w_{\max}^G = 0.854 \text{ mm}$  at the SLS.

**8.5.2.3.2.5 Calculation of the plate subjected to Cat. B2 action (finite element method)**

In this case, the problem is solved by using the Finite Element method, modelling the laminate package using SOLID elements with 20 nodes. Figure 8.56 and Figure 8.57 give the values of the maximum principal stress and the plate deflection, respectively.

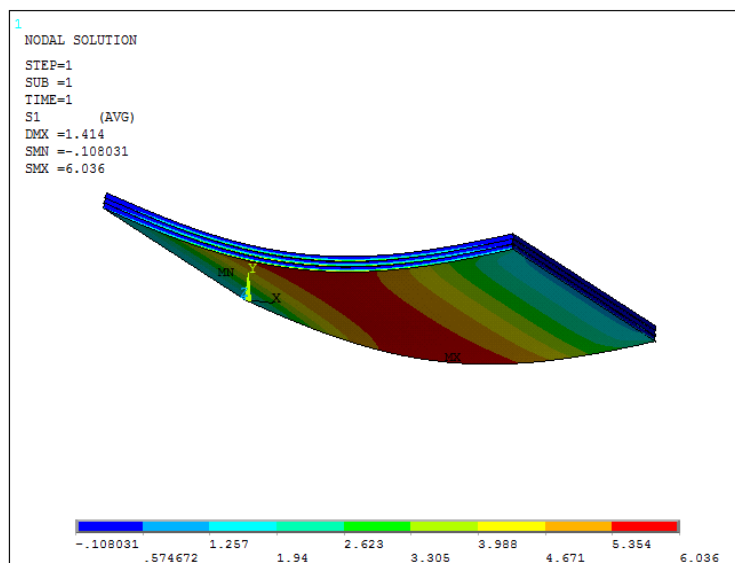


Figure 8.56. Floor subjected to a category B2 live load: maximum principal stress at the ULS.

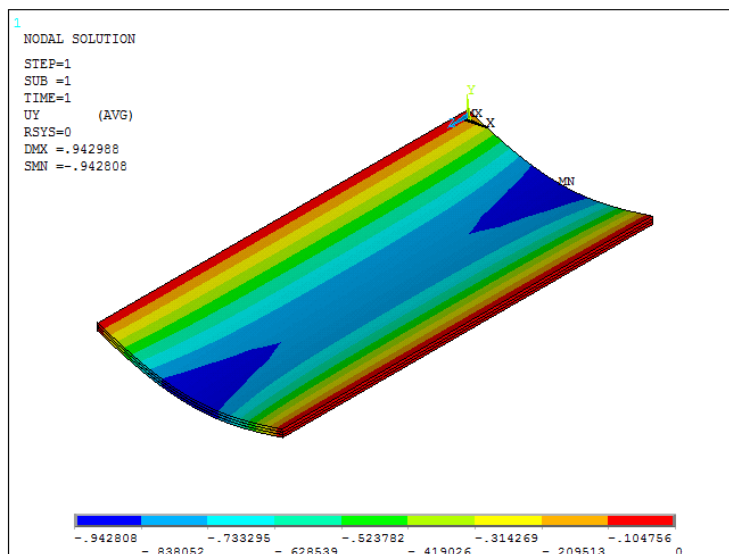


Figure 8.57. Floor subjected to a category B2 live load: deflection at the SLS.

The finite element analysis of the sheet gave the following results:  
 $\sigma_{\max}^q = 6.04 \text{ MPa}$  at the ULS, external plies;

$\sigma_{\max}^q = 5.50$  MPa at the ULS, internal ply;  
 $w_{\max}^q = 0.94$  mm at the SLS.

**8.5.2.3.2.6 Comparison of the analytical and numerical results**

The values of the maximum deflection and the maximum stress obtained by using the various methods are given in Table 8.10. It should be noted that, once again, the E.E.T. model gives an excellent approximation of the stress and deflection values of the multi-layered laminated of glass.

Table 8.10. Plate subject to category B2. comparison of various solutions.

METHOD	Maximum deflection (SLS)	Maximum stress (ULS), external layers	Maximum stress (ULS), internal layer
E.E.T.	0.854 mm	5.82 MPa	5.11 MPa
F.E.M.	0.94 mm	6.04 MPa	5.50 MPa

In order to perform the verifications of the glass plate, the values obtained using the 3D FEM model are considered, namely

$\sigma_{\max}^G = 6.04$  MPa at the ULS, external plies;  
 $\sigma_{\max}^G = 5.50$  MPa at the ULS, internal ply;  
 $w_{\max}^G = 0.94$  mm at the SLS.

**8.5.2.3.3 Calculation of stress and deflection for the plate subjected to a Cat. B2 concentrated load**

The design action for the Ultimate Limit State is given by

$$F_d = \gamma_Q Q_k = 3.0 \text{ kN,}$$

where

$\gamma_Q=1.5$ : partial factor for variable actions, including model uncertainties and dimensional tolerances;  
 $Q_k$ : Cat. B2 action.

To calculate the deflection consider the Serviceability Limit State, to which a design action is associated

$$F_d = Q_k = 2.0 \text{ kN.}$$

The load is distributed over an area of 50×50 mm. The most severe condition corresponds to the application of the load at the midpoint of the shorter edge (not supported) of the sheet.

The problem is solved using a 3D Finite Element analysis. Figure 8.58 and Figure 8.59 show the plate stress and deflection, respectively.

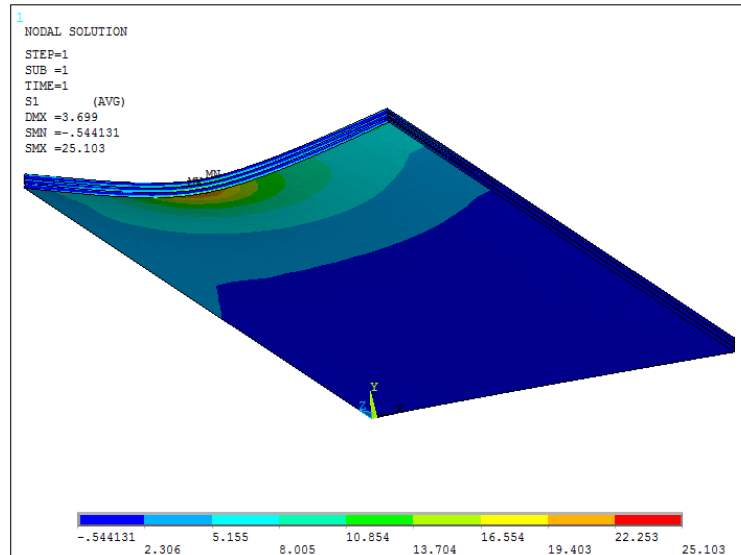


Figure 8.58. Floor subjected to a concentrated load: maximum principal stress at the ULS.

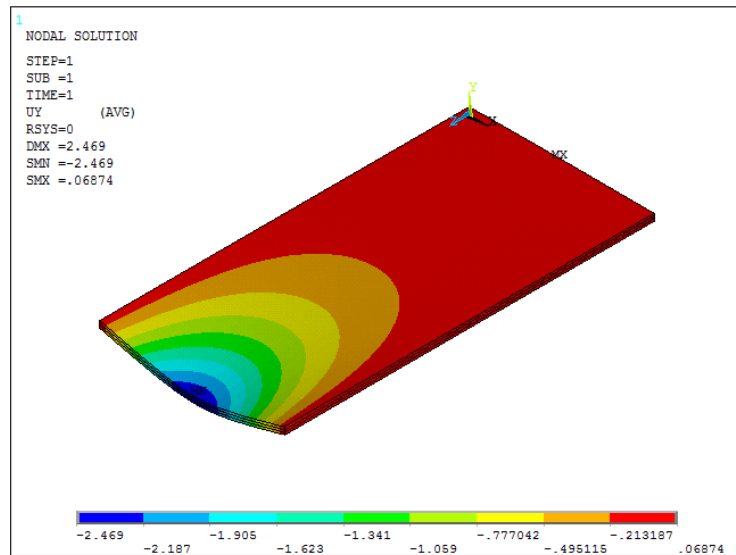


Figure 8.59. Floor subjected to a concentrated load: deflection at the SLS.

The analysis gives

$$\sigma_{\max}^Q = 25.10 \text{ MPa} \quad \text{at the ULS, external layers;}$$

$$\sigma_{\max}^Q = 18.75 \text{ MPa} \quad \text{at the ULS, internal layer;}$$

$$w_{\max}^Q = 2.50 \text{ mm} \quad \text{at the SLS.}$$

#### 8.5.2.3.4 Verification of the floor subjected to different load combinations

In order to perform the verifications, the effect of the different actions, that correspond to different design strength, must be combined, as done in the previous examples. As we are dealing with a pointwise stress verification, the stress acting in the same test area must be considered. In the case being examined, all the considered actions cause maximum stress at the midpoint of the shorter edge (not supported): as a result, it is sufficient to apply the criterion (7.8) at the maximum stress evaluated for the different cases.

To calculate the maximum sag, all that has to be done is to superimpose the effects. In this case the maximum deflection caused by each load can be found at the midpoint of the side that is not supported, therefore to calculate the maximum deflection all that needs to be done is to sum the already-calculated values. The maximum value must be within the limits given in Table 7.13.

#### 8.5.2.3.4.7 Verification of the floor subjected to self-weight and distributed live load

##### ULS verification

The calculations are carried out using (7.9), at the intrados of the ply of tempered glass and at that of the heat strengthened glass.

The following results from the stress verification on the tempered glass ply

$$\frac{\sigma_{\max}^G}{f_{g;d}^G} + \frac{\sigma_{\max}^q}{f_{g;d}^q} = \frac{2.00}{60.24} + \frac{6.04}{69.60} = 0.120 \leq 1$$

The following results from the stress verification on the heat strengthened glass ply

$$\frac{\sigma_{\max}^G}{f_{g;d}^G} + \frac{\sigma_{\max}^q}{f_{g;d}^q} = \frac{1.94}{23.20} + \frac{5.50}{32.56} = 0.253 \leq 1$$

The resistance verification is satisfied.

##### SLS verification

The maximum deflection, according to (7.9), is

$$w_{\max} = w_{\max}^G + w_{\max}^q = 0.38 + 0.94 = 1.32 \text{ mm} < \frac{1}{500} L_{inf} = 2 \text{ mm} .$$

The deformability verification is satisfied.

#### 8.5.2.3.4.8 Verification of the floor under self-weight and concentrated live load

##### ULS verification

The tests are carried out, using (7.8), at the midpoint of the short edge, at the intrados of the sheet of tempered glass and of the heat strengthened glass ply.

The stress verification on the tempered glass ply is:

$$\frac{\sigma_{\max}^G}{f_{g;d}^G} + \frac{\sigma_{\max}^Q}{f_{g;d}^Q} = \frac{2.00}{60.24} + \frac{25.10}{69.60} = 0.394 \leq 1$$

The stress verification on the heat strengthened glass ply is:

$$\frac{\sigma_{\max}^G}{f_{g;d}^G} + \frac{\sigma_{\max}^q}{f_{g;d}^q} = \frac{1.94}{23.20} + \frac{18.75}{32.56} = 0.660 \leq 1 .$$

The resistance condition is satisfied. It should be noted, however, that the most onerous condition is found in the internal glass layer.

### SLS verification

The maximum deflection is given by (7.9):

$$w_{\max} = w_{\max}^G + w_{\max}^Q = 0.38 + 2.50 = 2.88 \text{ mm} .$$

This value is slightly higher than that considered as being admissible ( $L_{inf}/500$ ), but as this is a conventional test for calculating local effects, this excess can be tolerated.

### **8.5.2.4 Phase II – Verification of the post-breakage behaviour**

The post-breakage behaviour of the glass floor under the action of the anthropic load and self-weight is evaluated in this phase. Regarding the deformability, the sag shall be checked to be compatible with the capacity of the constraints during the post-breakage phase. In this specific case, reference is made to phase II, in which the breakage of a ply of tempered glass is hypothesised. The remaining laminate package is therefore composed by a tempered glass ply and a heat strengthened ply. The action of the concentrated load, which represents a conventional action, is not considered here because it has to be accounted for only in phase I, pre-breakage. In favour of safety, the anthropic actions were not rescaled to consider a reduced return period of 10 years.

Regarding the dead load, the following design action is considered for the Collapse Limit State:

$F_d = \gamma_G G = 1.20 \text{ kN/m}^2$ , where  $\gamma_G=1.3$  is the partial factor for permanent actions, including model uncertainties and dimensional tolerances (Table 7.2).

For the imposed distributed load, a design action at the CLS equal to  $F_d = \gamma_Q q_k = 4.5 \text{ kN/m}^2$ , is considered, where:

$\gamma_Q=1.5$ : partial factor for variable actions, including model uncertainties and dimensional tolerance;  
 $q_k$ : Cat. 2 action.

For completeness, the deflection calculation is also given, evaluated by considering a design action

$$F_d = q_k = 3.0 \text{ kN/m}^2.$$

#### **8.5.2.4.1 Calculation of stress and deflection for the plate under self-weight**

This calculation is made using the “Enhanced Effective Thickness” method described in Section 6.3.3.1.5. As the structure deformation is almost cylindrical, the effective thicknesses are calculated by modelling the element as a simply supported beam. The properties of the PVB interlayer are considered for a period of 10 years and at a temperature of 50°C. On the basis of values obtained from a supplier, the shear modulus of the interlayer is equal to 0.052 MPa.

The values obtained from the simple calculation with beam (1D) model are subsequently compared to those obtained using a 3D FEM analysis of the equivalent monolithic element. In this way the edge effect can be considered, which is neglected when doing a beam-like analysis.

For the case of a simply supported beam subjected to a uniform load, we have  $\Psi = 168/17l^2 = 9.8824 \cdot 10^{-6} \text{ mm}^{-2}$ . The dimensionless coefficient  $\eta$ , which considers the coupling offered by the interlayer, is calculated using (6.49) and is equal to

$$\eta = \frac{1}{1 + \frac{Eh_{int}}{G_{int}b} \frac{J_1 + J_2}{J_{tot}} \frac{A_1 A_2}{A_1 + A_2} \Psi} = 0.0675.$$

The deflection-effective thickness is evaluated using (6.46) and is equal to

$$h_w = 15.39 \text{ mm.}$$

The stress-effective thicknesses of plies 1 and 2 are, instead, given by (6.48):

$$h_{1;\sigma} = h_{2;\sigma} = 17.28 \text{ mm.}$$

In the considered case, the floor plies have different strengths, therefore the verification regarding the maximum tensile stress acting on each ply must be carried out on both of them. The interface stress on the toughened glass sheet, which is important given that the coupling between sheets is not perfect, shall be calculated (Figure 6.16).

The effective thickness used to carry out the calculation of the sheet of heat strengthened glass, as resulting from (6.57), is

$$\hat{h}_{INT1;\sigma} = \sqrt{\frac{1}{\left| \frac{2\eta d_1}{h_1^3 + h_2^3 + 12I_s} - \frac{h_1}{h_w^3} \right|}} = 17.58 \text{ mm.}$$

The design action for the Collapse Limit State is given by

$$F_d = \gamma_G G = 1.20 \text{ kN/m}^2,$$

where  $\gamma_G = 1.3$  is the partial factor for the permanent actions, including model uncertainty and dimensional tolerance (Table 7.2).

The maximum bending moment and the maximum stress are

$$M_d = \frac{1}{8} F_d l^2 = \frac{1}{8} (1.20 \cdot 2) \cdot l^2 = 0.30 \text{ kNm};$$

$$\sigma_{\max}^G = \frac{M_d}{W_{eq}} = \frac{0.30 \cdot 10^6}{\frac{2000 \cdot 17.28^2}{6}} = 3.01 \text{ MPa.}$$

The maximum tensile stress on the sheet of heat strengthened glass is

$$\sigma_{\max;ind}^G = \frac{M_d}{W_{eq}} = \frac{0.30 \cdot 10^6}{\frac{2000 \cdot 17.58^2}{6}} = 2.91 \text{ MPa.}$$

To calculate the deflections, the Serviceability Limit State associated with a design action

$$F_d = G = 0.92 \text{ kN/m}^2$$

shall be considered, to which the following maximum deflection corresponds

$$w_{\max}^G = \frac{5F_d l^4}{384EJ} = \frac{5 \cdot (0.92 \cdot 2) \cdot 1000^4}{384 \cdot 70000 \cdot \frac{2000 \cdot 15.39^3}{12}} = 0.56 \text{ mm.}$$

After this simplified beam calculation, as a comparison the laminate package is now calculated using the 3D Finite Element model of the equivalent monolithic element, with the thicknesses evaluated by using the EET method. Figure 8.60, Figure 8.61 and Figure 8.62 show the maximum stress for tempered glass and toughened glass, and plate deformation, respectively.

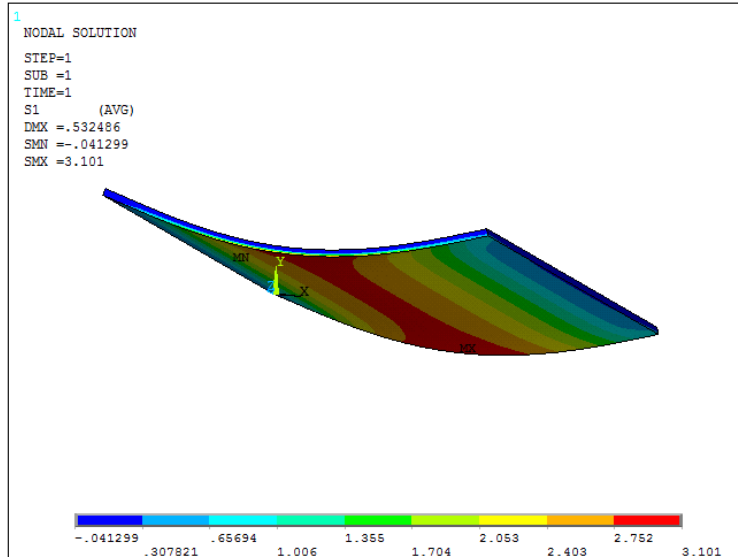


Figure 8.60. Floor subjected to self-weight: maximum principal stress at CLS

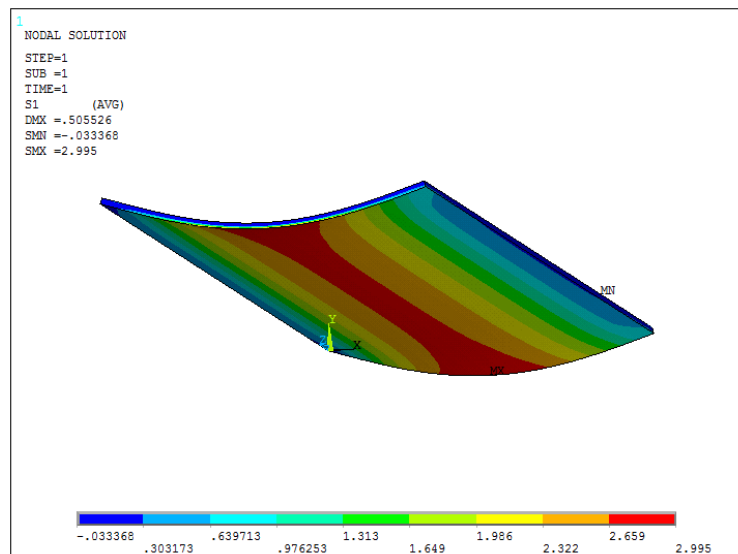


Figure 8.61. Floor subjected to self-weight: maximum principal stress at CLS (heat strengthened glass ply).



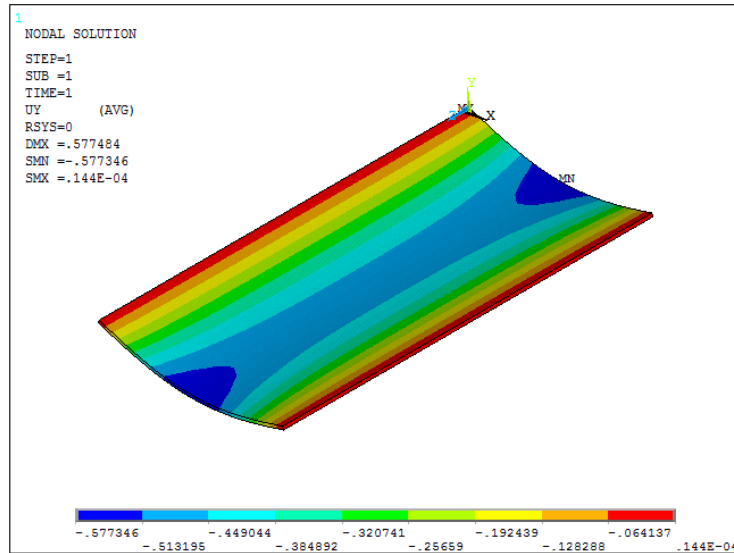


Figure 8.62. Floor subjected to self-weight: deflection at.SLS.

Therefore, the glass plate has:

$$\sigma_{\max}^G = 3.10 \text{ MPa at the CLS (3D model);}$$

$$w_{\max}^G = 0.58 \text{ mm at the SLS (3D model).}$$

The maximum tensile stress on the heat strengthened glass ply is

$$\sigma_{\max;\text{ind}}^G = 2.99 \text{ MPa at the CLS (3D model).}$$

Note that the stress values are slightly higher than those calculated using the beam model. This difference is caused by the edge effect, where the stress increases if the elements are thin and considerably large.

#### 8.5.2.4.2 Calculation of the stress and deflection for the plate subjected to a Cat. B2 action (distributed)

The maximum stress and maximum deflection are calculated, again, by using the equivalent thickness method E.E.T. shown in Section 6.3.3.1. The properties of the PVB interlayer are considered for a load duration of 30 seconds and at a temperature of 50°C. The shear modulus of the interlayer, according to the values supplied by a producer, is equal to 0.3 MPa.

After the simplified (beam) calculation, the stress and maximum deflection are calculated using a 3D FEM analysis of the equivalent monolithic sheet, but only for result comparison.

The simply supported beam is subjected to a uniformly distributed load, leading to  $\Psi = \frac{168}{17l^2} = 9.8824 \cdot 10^{-6} \text{ mm}^{-2}$ ; the coefficient  $\eta$  becomes

$$\eta = \frac{1}{1 + \frac{Eh_{\text{int}}}{G_{\text{int}}b} \frac{J_1 + J_2}{J_{\text{tot}}} \frac{A_1 A_2}{A_1 + A_2} \Psi} = 0.2946.$$

The geometric parameters necessary for calculating the effective thicknesses are the same as those calculated in paragraph 8.5.2.4.1. The deflection-effective thickness according to (6.46) is

$$h_w = 16.48 \text{ mm.}$$

The stress-effective thicknesses of plies 1 and 2 are, instead, given by (6.48):

$$h_{1,\sigma} = h_{2,\sigma} = 18.47 \text{ mm.}$$

As the plies have different strength, the internal heat strengthened glass ply must also be verified. Its effective thickness is

$$\hat{h}_{INT1;\sigma} = \sqrt{\frac{1}{\left| \frac{2\eta d_1}{h_1^3 + h_2^3 + 12I_s} - \frac{h_1}{h_w^3} \right|}} = 20.27 \text{ mm.}$$

The design action for the Ultimate Limit State is given by the distributed load:

$$F_d = \gamma_Q q_k = 4.5 \text{ kN/m}$$

where

$\gamma_Q=1.5$ : partial factor for variable actions, including model uncertainty and dimensional tolerances;  
 $q_k$ : Cat. B2 action.

$$M_d = \frac{1}{8} F_d l = \frac{1}{8} (4.5 \cdot 2) \cdot 1 = 1.125 \text{ kNm};$$

$$\sigma_{\max}^q = \frac{M_d}{W_{eq}} = \frac{1.125 \cdot 10^6}{\frac{2000 \cdot 18.47^2}{6}} = 9.90 \text{ MPa.}$$

The maximum tensile stress on the ply is

$$\sigma_{\max;\text{ind}}^G = \frac{M_d}{W_{eq}} = \frac{1.125 \cdot 10^6}{\frac{2000 \cdot 20.27^2}{6}} = 8.21 \text{ MPa.}$$

In order to calculate the deflection, the Serviceability Limit State, to which a design action

$$F_d = q_k = 3.0 \text{ kN/m,}$$

is associated, is considered. The correspondent maximum deflection is

$$w_{\max}^q = \frac{5F_d l^4}{384EJ} = \frac{5 \cdot (3.0 \cdot 2) \cdot 1000^4}{384 \cdot 70000 \cdot \frac{2000 \cdot 16.48^3}{12}} = 1.50 \text{ mm.}$$

The maximum stress and the deflection can now be calculated using a 3D Finite Element model of the equivalent monolithic plate. Figure 8.63 and Figure 8.64 show the maximum stress on the layer of tempered glass and on the heat strengthened glass layer, respectively; Figure 8.65, instead, shows the plate deflection.

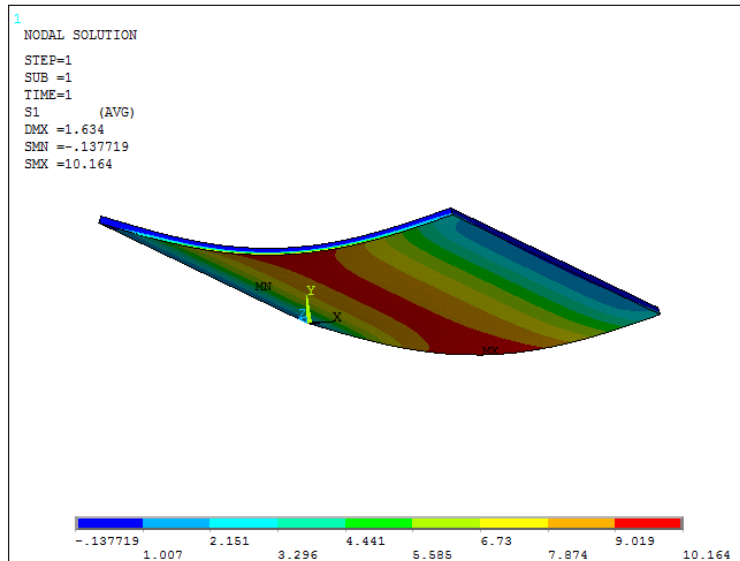


Figure 8.63. Floor subjected to Cat.B2 action (distributed): maximum principal stress at CLS

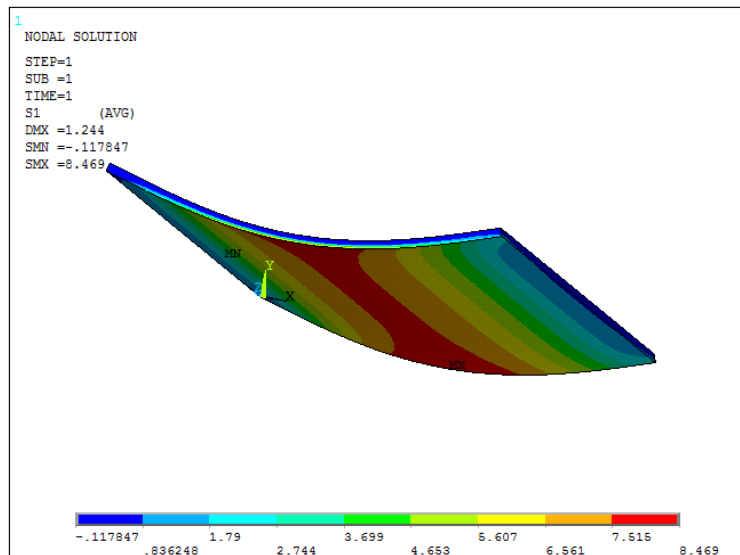


Figure 8.64. Floor subjected to Cat.B2 action: maximum principal stress at CLS (heat strengthened glass ply).

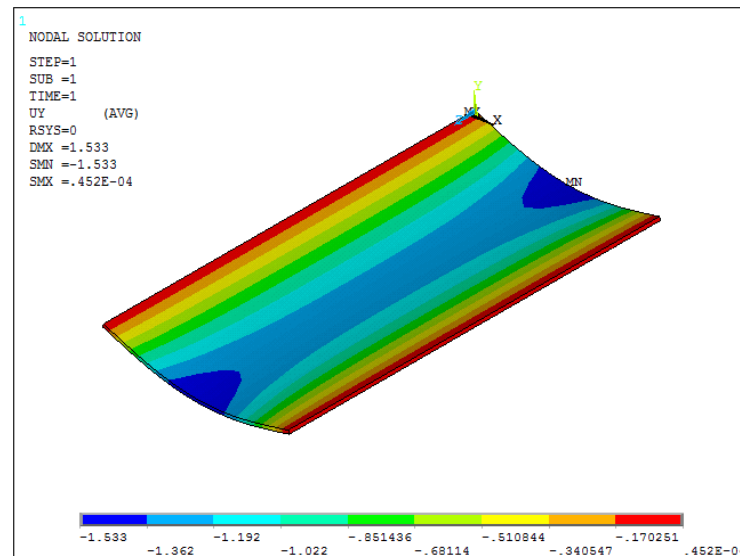


Figure 8.65. Floor subjected to Cat.B2 action (distributed): deflection at SLS.

The analyses of the plate give:

$$\sigma_{\max}^q = 10.16 \text{ MPa at the CLS};$$

$$w_{\max}^q = 1.53 \text{ mm at the SLS}.$$

The maximum tensile stress on the heat strengthened glass ply is:

$$\sigma_{\max;\text{ind}}^q = 8.47 \text{ MPa at the CLS}.$$

Again, the value of the maximum stresses obtained from the FEM analysis are slightly higher than those calculated with the beam model because of the edge effect, already mentioned previously.

#### 8.5.2.4.3 Verification of the floor under self-weight and distributed live load

To carry out the CLS verification, the values of the maximum stress calculated previously with the analytic method and with the finite element calculation must be combined according to (7.8). A local verification should be carried out, considering the results of the finite element method, at the midpoint of the shorter edge of both the tempered and heat strengthened glass plies.

Considering the results of the F.E.M. analysis, the stress verification on the tempered glass ply gives

$$\frac{\sigma_{\max}^G}{f_{g;d}^G} + \frac{\sigma_{\max}^q}{f_{g;d}^q} = \frac{3.10}{60.24} + \frac{10.16}{69.60} = 0.197 \leq 1.$$

The stress verification on the heat strengthened glass ply gives

$$\frac{\sigma_{\max}^G}{f_{g;d}^G} + \frac{\sigma_{\max;\text{ind}}^q}{f_{g;d}^q} = \frac{2.99}{23.20} + \frac{8.47}{32.56} = 0.389 \leq 1.$$

The resistance condition are satisfied.

## 8.6 Glass fin that supports a façade

The proposed example involves fins of depth 0.45 m, positioned with 2.0 m pitch, and which support the glass façade of height 4.0 m shown in Figure 8.66.

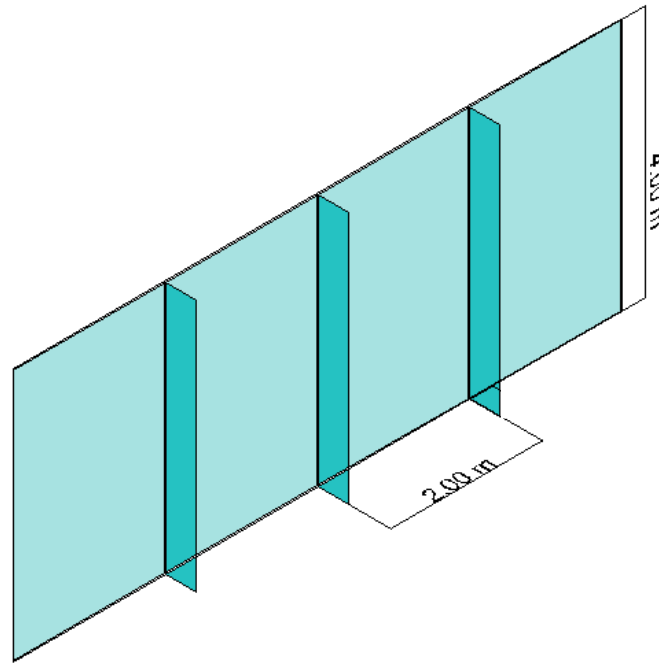


Figure 8.66 Glass façade made of sheets and fins.

Each fin is made by coupling two sheets of heat strengthened glass, each one of thickness 12 mm, with a PVB interlayer of thickness 1.52 mm, as shown in Figure 8.67.

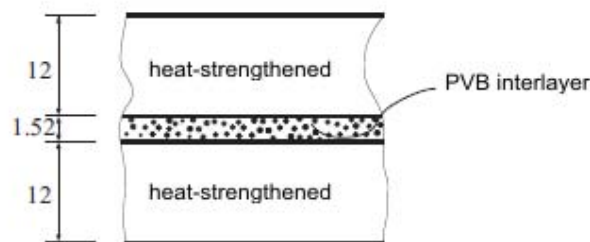


Figure 8.67. Composition of the laminated package.

The calculation example deals specifically with the fin. For the façade plates one can refer to the previous examples.

The fin “hangs”, in other words it is hinged at the upper extremity and it is free to move in an axial direction at the lower extremity. It is assumed that the dead load of the façade is carried by another supporting system (e.g. a suspension cable, or that the plates have been stacked, in contact one above the other): under these hypotheses, the fin comes into play with the action of the wind only.

The glass façade is made by joining the glass sheets to the fin using point supports. Under these conditions, the fin behaves in the same manner as an indirect loaded beam and, supposing it has a support at its midpoint, the maximum bending moment of the fin coincides with that which would result if the façade was linearly constrained to the fin along its whole length, namely

$$M_d = \frac{1}{8} F_d l^2,$$

where  $F_d$  is due to the wind action. In general, if the fixing of the façade to the fin is almost continuous, one can consider the action transmitted by the façade as being distributed along the whole length of the fin, even when calculating the inflections.

The fins are classified as class 2 elements (Table 3.7).

Fin behaviour is analysed referring to the following phases:

phase I – pre-breakage behaviour, where both the glass plies are still sound (SLE and SLU tests);

phase II – post-breakage behaviour, after one glass ply has broken, where the load totality is carried by the intact ply (SLC test).

### 8.6.1 Load analysis

The acting loads are:

*Self-weight:*

specific self-weight of the glass:  $\gamma_v = 25 \text{ kN/m}^3$ ;

specific self-weight of the interlayer:  $\gamma_{PVB} = 10.5 \text{ kN/m}^3$ ;

The dead load is  $G = (25 \cdot 2 \cdot 0.012 + 10.5 \cdot 0.00152) \cdot 0.45 = 0.277 \text{ kN/m}^2$  (which corresponds to a total weight of 1.11 kN).

The design load duration is 50 years.

*Wind action:*

To consider the possible effects of static fatigue (Paragraph 2.2.1.1), the verifications are carried out as described in Paragraph 4.5.1, both for wind at a peak speed (averaged over 3 s), and for 10 minutes averaged wind.

The gust of wind (3 seconds) has a pressure equal to  $p_w = 1.2 \text{ kN/m}^2$ .

The wind pressure averaged over 10 minutes can be found using the relation (4.26)

$$\frac{p_{w,10\text{min}}}{p_{w,3\text{sec}}} = \frac{1}{c_{e,2}},$$

where according to (4.27),  $c_{e,2}$  is given by

$$c_{e,2}(z) = 1 + \frac{7}{\ln\left(\frac{z}{z_0}\right)c_t},$$

where:

$c_t=1$ : friction coefficient, the value of which is obtained from the Technical Standards;

$z$ : height from the ground;

$z_0$ : reference height, supplied by the Technical Standards on the basis of the category.

Assuming that exposure to the wind is category II, we have  $z_0=0.05 \text{ m}$ ; considering  $z=50 \text{ m}$  gives  $c_{e,2} = 2.01$  and it is therefore possible to calculate the wind pressure for a 10 minutes duration as

$$p_{w,10\text{min}} = 1,2 / 2,01 = 0,597 \text{ MPa}.$$

### 8.6.2 Design strength

The design strength of the glass is calculated separately for the different actions. Referring to (7.5) and considering that, in the case being examined, the verifications will be performed in the neighborhood of the fin borders

$$f_{g;d} = \frac{k_{mod} k_{ed} k_{sf} \lambda_{gl} \lambda_{gA} f_{g;k}}{R_M \gamma_M} + \frac{k_{ed}' k_v (f_{b;k} - f_{g;k})}{R_{M;v} \gamma_{M;v}},$$

where:

- $k_{mod}$  reduction coefficient for static fatigue, given in Table 2.2 according to the type of external action and its characteristic duration;
- $k_{ed}=0.8$  strength reduction factors for verifications near the edge of the sheet or holes (Table 7.3), for glass with polished edges;
- $k_{sf}=1$  coefficient for the surface profile of the glass without surface treatments (Table 7.4)
- $f_{g;k} = 45$  MPa nominal characteristic strength of the float glass;
- $R_M=1$  multiplicative factor of the partial coefficient, for class 2 tests (Table 7.10);
- $\gamma_M=2.50$  partial factor of the float glass (Table 7.9);
- $k_{ed}' = 0.8$  strength reduction factors for verifications near the edge of the sheet or holes (Table 7.3), for glass with polished edges;
- $k_v = 1$  coefficient for heat treated sheets with horizontal heat treatment (Table 7.8);
- $f_{b;k} = 70$  MPa nominal characteristic strength of the thermally toughened glass (Table 7.7);
- $R_{M;v} = 1$  multiplicative factor of the partial coefficient, for class 2 tests (Table 7.10);
- $\gamma_{M;v} = 1.35$  partial factor for pre-stressed glass (Table 7.9);
- $\lambda_{gA}$  scale factor for verification distant from the edges; in the case being examined  $\lambda_{gA}=1$ ;
- $\lambda_{gl}$  scale factor for stress near the edges, calculated for the considered beam using (7.7); for ground edges,

$$\lambda_{gl} = \left( \frac{0.0741 \cdot 0.45}{k_b \cdot l_b} \right)^{1/12.5} = 0.763 \leq 1,$$

where:

- $k_b = 0.2434$  coefficient for calculating the size effect near the edge (Table 7.6);
  - $l_b = 4$  m total length of the edge subjected to traction.
- The  $k_{mod}$  coefficient varies according to the considered action.

Design strength for self-weight :

As  $k_{mod} = 0.26$ , for a conventional load duration of 50 years, (Table 2.2), the following is obtained:

$$f_{g;d}^G = 17.67 \text{ MPa.}$$

Design strength for wind load (3 seconds):

The reduction coefficient for static fatigue in the case of gust of wind and its characteristic duration (equivalent to the spectrum integral), equal to 5 seconds, as suggested in Table 4.18, is  $k_{mod} = 0.88$  (Table 2.2); the correspondent design strength, is therefore

$$f_{g;d}^{w,3sec} = 24.49 \text{ MPa.}$$

Design strength for wind load (10 minutes):

As  $k_{mod} = 0.65$ , for a conventional load duration equal to 10 minutes (Table 2.2), we obtain a design strength of

$$f_{g;d}^{w,10min} = 21.96 \text{ MPa.}$$

For what concerns the design deformation, the fin can be compared to a column (EN13830). The lower of the two values  $L/200=20$  mm and 15 mm is therefore used, so that  $w_{lim}=15$  mm.

### 8.6.3 Phase I – Pre-breakage behaviour

#### 8.6.3.1 Calculation of stress for the fin subjected to self-weight

As a result of self-weight, the fin is subjected to traction by the load that is distributed vertically; the tensile stress can therefore be simply calculated as  $\sigma_{\max}^G = \frac{F_d}{A}$ , where  $A$  is the area of the transversal section of the fin, of size  $450 \times (12+12)$  mm, and the design action for the Ultimate Limit State is given by

$$F_d = \gamma_{G1} G_1 = 1.44 \text{ kN},$$

where  $\gamma_{G1}=1.3$  is the partial factor for dead load including model uncertainties and dimensional tolerance (Table 7.2).

The uniform tensile stress is therefore

$$\sigma_{\max}^G = \frac{F_d}{A} = \frac{1.44 \cdot 10^3}{24 \cdot 450} = 0.13 \text{ MPa}.$$

The contribution of the polymer can be neglected in this analysis.

#### 8.6.3.2 Calculation of stress and deflection for the fin subjected to the wind load

On the basis of the design configuration, the stress plane is parallel to those of the plies composing the fin. Therefore, when calculating its bending response, the section, of size  $24 \times 450$  mm, can be treated as homogeneous and monolithic.

As the glass is subjected to static fatigue (Paragraph 2.2.1.1), verifications should be carried out, as described in Paragraph 4.5.1, both in the case of wind with a peak speed (averaged over 3 seconds), and 10 minutes averaged wind. In the case being examined, it is evident that as the action of the gust of 10 minutes is undoubtedly lower than that of the gusts of 3 s and the strength are of the same order, the most onerous condition is that relative to the force of 3 s. This calculation will, however, be carried out for completeness.

##### 8.6.3.2.1 Calculation of stress and deflection for the fin under wind gust (3 s)

The design action for the Ultimate Limit State is supplied by

$$F_d = \gamma_Q p_w i = 3.60 \text{ kN/m},$$

where

$\gamma_Q=1.5$ : partial factor for the variable action, including model uncertainties and dimensional tolerances;

$p_w=1.2 \text{ kN/m}^2$ : action of the peak wind;

$i=2 \text{ m}$ : pitch of the fins.

The maximum bending moment is given by



$$M_d = \frac{1}{8} F_d l^2 = \frac{1}{8} 3.60 \cdot 4^2 = 7.20 \text{ kNm};$$

the maximum stress is therefore

$$\sigma_{\max}^{w,3\text{sec}} = \frac{M_d}{W} = \frac{7.20 \cdot 10^6}{\frac{24 \cdot 450^2}{6}} = 8.89 \text{ MPa.}$$

The Serviceability Limit State to which a design action

$$F_d = p_w i = 2.4 \text{ kN/m}$$

is associated should be considered when calculating the deflections. The correspondent maximum deflection is

$$w_{\max}^{w,3\text{sec}} = \frac{5F_d l^4}{384EJ} = \frac{5 \cdot 2.4 \cdot 4000^4}{384 \cdot 70000 \cdot \frac{24 \cdot 450^3}{12}} = 0.627 \text{ mm.}$$

### 8.6.3.2.2 Calculation of stress and deflection for the fin subjected to 10 minutes averaged wind load

The design action for the Ultimate Limit State is given by

$$F_d = \gamma_Q p_{w,10\text{min}} i = 1.79 \text{ kN/m},$$

where

$\gamma_Q=1.5$  partial factor for variable actions, including model uncertainties and dimensional tolerances;

$p_{w,10\text{min}}$  wind action (10 minutes)

$i$  pitch of the fins.

The maximum bending moment is given by

$$M_d = \frac{1}{8} F_d l^2 = \frac{1}{8} 1.79 \cdot 4.0^2 = 3.58 \text{ kNm};$$

The maximum stress is therefore

$$\sigma_{\max}^{w,10\text{min}} = \frac{M_d}{W} = \frac{3.58 \cdot 10^6}{\frac{24 \cdot 450^2}{6}} = 4.42 \text{ MPa.}$$

The Serviceability Limit State to which a design action

$$F_d = p_w i = 1.19 \text{ kN/m}$$

is associated, should be considered when calculating the deflections. The correspondent maximum deflection is

$$w_{\max}^{w,10\text{min}} = \frac{5F_d l^4}{384EJ} = \frac{5 \cdot 1.19 \cdot 4000^4}{384 \cdot 70000 \cdot \frac{24 \cdot 450^3}{12}} = 0.311 \text{ mm.}$$

It is evident that actions and stresses caused by the force of the 10 minutes averaged wind are lower than those caused by the wind gusts (3 seconds).

### 8.6.3.3 Test on the fin subjected to different load combinations

In order to perform the verifications, the effect of the different actions, which correspond to different design strengths, have to be combined. The beam subjected to the action of dead load, permanent load and wind load (both the 3-second and 10-minute) must be verified. The verifications should be carried out according to the expression (7.8). To calculate the maximum deflection  $w$  at the Serviceability Limit State, the expression (7.9) can be used, and the result is positive if

$$w \leq w_{lim},$$

where  $w_{lim} = 15$  mm. In the case being examined, the maximum deflection caused by each action is in the midpoint of the fin. The dead load does not cause any deflection due to bending in the fin.

#### 8.6.3.3.1 Verification of the fin subjected to self-weight and wind load (3 s)

Following the criterion (7.8) gives

$$\frac{\sigma^G}{f_{g;d}^G} + \frac{\sigma_{max}^{w,3sec}}{f_{g;d}^{w,3sec}} = \frac{0.13}{17.67} + \frac{8.89}{24.49} = 0.370 \leq 1.$$

The ULS verification is satisfied.

The maximum deflection is:

$$w_{max} = w_{max}^{w,3sec} = 0.2627 \text{ mm} < 15 \text{ mm}.$$

The SLS verification is satisfied.

#### 8.6.3.3.2 Verification of the fin under self-weight and wind load (10 minutes)

In accordance with the criterion (7.8)

$$\frac{\sigma^G}{f_{g;d}^G} + \frac{\sigma_{max}^{w,10min}}{f_{g;d}^{w,10min}} = \frac{0.13}{17.67} + \frac{4.42}{21.96} = 0.209 \leq 1.$$

The ULS verification is satisfied.

The maximum deflection at the SLS is:

$$w_{max} = w_{max}^{w,10min} = 0.311 \text{ mm} < 15 \text{ mm}.$$

The SLS verification is satisfied.

### 8.6.3.4 Lateral-torsional buckling verification

The flexural-torsional buckling verification of the fin is carried out in both cases of wind, namely 3 seconds and 10 minutes, by hypothesising, in favour of safety, a temperature of 50°C.

### 8.6.3.4.1 Lateral-torsional buckling verification for gusts of wind (3 s)

The action produces a maximum design bending moment  $M_{ed} = 7.20$  kNm.

The critical Euler bending moment  $M_{cr}^{(E)}$  of the element can be evaluated using the equation (6.81), or

$$M_{cr}^{(E)} = C_1 \frac{\pi}{L_0} \sqrt{EJ_{eq} GJ_{t,tot}},$$

where:

$E = 70000$  N/mm<sup>2</sup> the Young's modulus of glass;

$G = 28455$  N/mm<sup>2</sup> (shear modulus of glass, calculated by considering  $\nu=0.23$ );

$C_1 = 1.13$  (coefficient given by Table 6.8 for parabolic distribution of the bending moment).

To calculate the equivalent moment of inertia  $J_{eq}$ , in accordance with the equation (6.72), the equivalent thickness  $h_{ef;w}$  must be found (6.73). For the case under consideration:

$$d = 0.5(h_1 + h_2) + h_{int} = 13.52 \text{ mm};$$

$$I_s = \frac{h_1 + h_2}{h_1 h_2} d^2 = 1096.74 \text{ mm}^3;$$

$$\Gamma_b = \frac{1}{1 + \pi^2 \frac{h_{int} E I_s}{G_{int} I^2 d^2}} = 0.5277;$$

with  $G_{int} = 0.44$  MPa (for a load duration of 3 seconds, under the hypothesis of  $T=50^\circ\text{C}$ ).

We therefore obtain:

$$h_{ef;w} = \sqrt[3]{h_1^3 + h_2^3 + 12\Gamma_b I_s} = 21.82 \text{ mm}; \quad J_{eq} = \frac{b h_{ef;w}^3}{12} = 3.898 \cdot 10^5 \text{ mm}^4.$$

The torsional moment of inertia of the laminated glass section is given by

$$J_{t,tot} = J_{t,1} + J_{t,2} + J_{t,int};$$

where

$$J_{t,1} = \frac{b h_1^3}{3} = J_{t,2} = \frac{b h_2^3}{3} = 259200 \text{ mm}^4; \quad J_{t,int} = J_s \left( 1 - \frac{\tanh \frac{\lambda b}{2}}{\frac{\lambda b}{2}} \right) = 5.444 \cdot 10^4 \text{ mm}^4;$$

with

$$\lambda = \sqrt{\frac{G_{int}}{G} \frac{h_1 + h_2}{h_1 h_2 h_{int}}} = 0.0013; \quad J_s = 4 \left( \frac{h_1 + h_2}{2} + h_{int} \right) \frac{h_1 h_2}{h_1 + h_2} b = 1.974 \cdot 10^6 \text{ mm}^4.$$

We therefore have

$$J_{t,tot} = J_{t,1} + J_{t,2} + J_{t,int} = 5.728 \cdot 10^6 \text{ mm}^4;$$

which can be used to determine:

$$M_{cr}^{(E)} = C_1 \frac{\pi}{L_0} \sqrt{EJ_{eq} GJ_{t,tot}} = 1.872 \cdot 10^7 \text{ Nmm}.$$

The beam buckling strength (resisting bending moment) of the fin is given by the relation (6.78) in the form

$$M_{b,Rd} = \chi_{LT} M_R = \chi_{LT} W_x f_{g;d} ,$$

where the reduction factor is given by (6.66) according to the normalised slenderness of the laminated element, calculated by using (6.79) as

$$\bar{\lambda} = \bar{\lambda}_{LT} = \sqrt{\frac{W_x f_{gk;st}}{M_{cr}^{(E)}}} = 1.426;$$

with:

$f_{gk;st} = k_{mod} k_{ed} k_{sf} \lambda_{gl} \lambda_{gA} f_{g;k} + k'_{ed} k_v (f_{b;k} - f_{g;k}) = 44.19 \text{ N/mm}^2$  (design tensile strength to be considered in buckling verifications, as defined in paragraph 6.4.2.1);

$$W_x = \frac{b^2 h_{ef;w}}{6} = 861300 \text{ mm}^3 \text{ (section modulus);}$$

$$\Phi = 0.5 \left[ 1 + \alpha^* (\bar{\lambda} - \alpha_0) + \bar{\lambda}^2 \right] = 1.676,$$

given by (6.67) with  $\alpha^*=0.26$ ;  $\alpha_0=0.20$ ; (paragraph 6.4.3);

$f_{g;d} = 24.49 \text{ N/mm}^2$  (design strength of glass against a 3-minute wind action).

We therefore have:

$$\chi_{LT} = \frac{1}{\Phi + \sqrt{\Phi^2 - \bar{\lambda}^2}} = 0.3911;$$

$$M_{b,Rd} = \chi_{LT} M_R = \chi_{LT} W_x f_{g;d} = 8.25 \cdot 10^6 \text{ Nmm} .$$

The following results from the buckling verification:

$$\frac{M_{Ed}}{M_{b,Rd}} = \frac{7.20 \cdot 10^6}{8.25 \cdot 10^6} = 0.87 < 1;$$

#### 8.6.3.4.2 Lateral-torsional buckling verification for the 10 minutes averaged wind load

The force produces a maximum design bending moment  $M_{ed} = 3.58 \cdot 10^6 \text{ kNm}$ .

The beam buckling resistance (resisting bending moment) of the fin is given by the relation (6.78), i.e.,

$$M_{b,Rd} = \chi_{LT} M_R = \chi_{LT} W_x f_{g;d} ,$$

where the reduction factor is given by (6.66) according to the normalised slenderness of the laminated element, calculated using (6.79); namely

$$\bar{\lambda} = \bar{\lambda}_{LT} = \sqrt{\frac{W_x f_{gk;st}}{M_{cr}^{(E)}}} = 1.320 ,$$

with:

$f_{gk;st} = k_{mod} k_{ed} k_{sf} \lambda_{gl} \lambda_{gA} f_{g;k} + k'_{ed} k_v (f_{b;k} - f_{g;k}) = 37.86 \text{ N/mm}^2$  (design tensile strength to be considered in buckling verifications, as defined in paragraph 6.4.2.1);

$$W_x = \frac{b^2 h_{ef;w}}{6} = 861300 \text{ mm}^3 \text{ (section modulus);}$$

$$\Phi = 0.5 \left[ 1 + \alpha^* (\bar{\lambda} - \alpha_0) + \bar{\lambda}^2 \right] = 1.517 , \text{ given by (6.67) with } \alpha^*=0.26; \quad \alpha_0=0.20;$$

$f_{g;d} = 21.82 \text{ N/mm}^2$  (design strength of the glass for a 10-minute wind force).

We therefore have

$$\chi_{LT} = \frac{1}{\Phi + \sqrt{\Phi^2 - \bar{\lambda}^2}} = 0.4417 ;$$

$$M_{b,Rd} = \chi_{LT} M_R = \chi_{LT} W_x f_{g;d} = 8.35 \cdot 10^6 \text{ Nmm} .$$

From the buckling verification it results that:

$$\frac{M_{Ed}}{M_{b,Rd}} = \frac{3.58 \cdot 10^6}{8.35 \cdot 10^6} = 0.43 < 1 .$$

### 8.6.4 Phase II – Post-breakage behaviour

The post-breakage behaviour of the glass fin subjected to self-weight and the wind action is now considered. These verifications are carried out by considering one damaged glass ply, and that the load is entirely carried by the only remaining ply. During the post-breakage phase, it must be made sure that element deformation is compatible with the concept and design of the constraints.

In accordance with what has been presented in Section 3.2.2, in the post-breakage verifications reference is made to a conventional nominal life of 10 years. To rescale the wind action, the relations (4.10) and (4.11) are used, which allow to determine the reference speed for a return period of 10 years according to the expression

$$v_r = v_{b50} \cdot c_r, \quad c_r = 0.75 \sqrt{1 - 0.2 \ln \left[ -\ln \left( 1 - \frac{1}{T_R} \right) \right]}, \text{ per } 5 \text{ anni} < T_R \leq 50 \text{ anni},$$

where:

$c_r$  return coefficient;

$v_{b50}$  reference speed, defined as the characteristic value of the wind speed at 10 m from ground level on a level II category of soil, averaged over 10 minutes and referring to a return period of 50 years.

$T_R$  return period.

A period of  $T_R=10$  years therefore gives  $c_r = 0.903$ . As the pressure of the wind is directly proportional to the square of the speed, for (4.14), the pressure of the wind for 10 years can be calculated as follows:

$$\frac{p_{w,10}}{p_{w,50}} = c_r^2 \rightarrow p_{w,10} = (0.903)^2 p_{w,50} = 0.816 \cdot 1.2 = 0.979 \text{ kN/m}^2$$

The design strength are the same as those calculated in paragraph 8.6.2. In the following, the apex  $p$ - $r$  indicates stress and deflections relative to post-rupture behaviour.

#### 8.6.4.1 Calculation of stress for the fin subjected to self-weight

The design action for the Collapse Limit State is given by

$$F_d = \gamma_{G1} G_1 = 1.44 \text{ kN}$$

where  $\gamma_{G1}=1.3$  is the partial factor for the dead loads including model uncertainties and dimensional tolerance (Table 7.2), to which the maximum tensile stress corresponds

$$\sigma_{\max}^{G;p-r} = \frac{F_d}{A} = \frac{1.44 \cdot 10^3}{12 \cdot 450} = 0.27 \text{ MPa.}$$

#### 8.6.4.2 Calculation of stress and deflection for the fin under gusts of wind (3 s)

The design action for the CLS is given by

$$F_d = \gamma_Q p_{w,10,3sec} i = 2.94 \text{ kN/m ,}$$

where

$\gamma_Q=1.5$  partial factor for variable action s, including model uncertainties and dimensional tolerance;

$p_{w,10,3 sec}$  wind load for a  $T_R=10$  years,

$i$  pitch of the fins.

The maximum stress is

$$M_d = \frac{1}{8} F_d l^2 = \frac{1}{8} 2.94 \cdot 4^2 = 5.87 \text{ kNm ;}$$

$$\sigma_{\max}^p = \frac{M_d}{W} = \frac{5.87 \cdot 10^6}{\frac{12 \cdot 450^2}{6}} = 14.50 \text{ MPa.}$$

#### 8.6.4.3 Calculation of stress and deflection for the fin subjected to the 10 minutes averaged wind action

The pressure of the wind lasting 10 minutes, for a return period of 10 years, results, according to paragraph 8.6.1, as

$$p_{w,10,10min} = 0.979/2.01 = 0.487 \text{ MPa.}$$

The design action for the CLS is given by

$$F_d = \gamma_Q p_{w,10,10min} i = 1.46 \text{ kN/m ,}$$

where

$\gamma_Q=1.5$  partial factor for variable actions, including model uncertainties and dimensional tolerances;

$p_{w,10,10min}$  wind load (10 minutes);

$i$  pitch of the fins.

The maximum stress is

$$M_d = \frac{1}{8} F_d l^2 = \frac{1}{8} 1.46 \cdot 42.92^2 = 2.92 \text{ kNm;}$$

$$\sigma_{\max}^{p,10min,p-r} = \frac{M_d}{W} = \frac{2.92 \cdot 10^6}{\frac{12 \cdot 450^2}{6}} = 7.22 \text{ MPa.}$$

### 8.6.4.4 CLS verification of the fin subjected to different load combinations

Combining the forces according to (7.8) gives the following

#### Verification of the fin subjected to self-weight and wind load (3 s)

The CLS verification is carried out at the midpoint of the fin. We have

$$\frac{\sigma_{f_{g;d}}^{G,p-r}}{f_{g;d}^G} + \frac{\sigma_{\max}^{w,3sec,p-r}}{f_{g;d}^{w,3sec}} = \frac{0.27}{17.67} + \frac{14.50}{24.49} = 0.607 \leq 1.$$

The resistance condition is satisfied.

#### Test on the fin subjected to self-weight and wind load (10 minutes)

The CLS verification is carried out at the midpoint of the fin.

$$\frac{\sigma_{f_{g;d}}^{G,p-r}}{f_{g;d}^G} + \frac{\sigma_{\max}^{w,10min,p-r}}{f_{g;d}^{w,10min}} = \frac{0.27}{17.67} + \frac{7.22}{21.96} = 0.344 \leq 1.$$

The resistance condition is satisfied.

The flexural-torsional buckling test, omitted here for brevity, is carried out in the same manner as indicated in section 8.6.3.4.

## 8.7 Buckling calculations in special cases

In this paragraph, making specific reference to Paragraph 6.4, buckling calculations for some special cases of laminated glass elements are carried out.

For the case of a beam, of size  $b = 200$  mm and  $l = 1000$  mm, the verifications are carried out in the cases of axial compression (Paragraph 8.7.2) and bending (Paragraph 8.7.3).

Subsequently (par. 8.7.4) a panel of laminated glass, of size  $a = 1000$ mm  $\times$   $b = 1000$ mm under in-plane compression is considered.

In both cases, the laminated package (Figure 8.68) is made of two plies of annealed float glass ( $h_1 = h_2 = 10$  mm) bonded by a PVB interlayer ( $h_{int} = 1.52$  mm).



Figure 8.68. Composition of the laminated glass elements for buckling verifications.

### 8.7.1 Design strength

The design strength according to (7.5) is given by

$$f_{g;d} = \frac{k_{mod} \cdot k_{ed} \cdot k_{sf} \cdot \lambda_{gA} \cdot \lambda_{gl} \cdot f_{g;k}}{R_M \gamma_M} + \frac{k'_{ed} k_v \cdot (f_{b;k} - f_{g;k})}{R_{M,v} \gamma_{M,v}},$$

where:

$k_{mod} = 0.88$  reduction coefficient for the static fatigue, for load duration of 3 seconds as per Table 2.2;

$k_{sf}=1$	coefficient for the surface profile of the glass (no treatment) (Table 7.4);
$f_{g;k} = 45 \text{ MPa}$	nominal characteristic strength of the float glass (Table 7.7);
$R_M = 1$	multiplicative factor of the partial coefficient, for class 2 calculations (Table 7.10);
$\gamma_M = 2.50$	partial factor of the float glass (Table 7.9);

Since

$f_{b;k} = 45 \text{ MPa}$	the nominal characteristic strength of the annealed float glass without treatment (Table 7.7),
----------------------------	------------------------------------------------------------------------------------------------

when calculating  $f_{g;d}$  the expression (7.5) is reduced to

$$f_{g;d} = \frac{k_{\text{mod}} \cdot k_{ed} \cdot k_{sf} \cdot \lambda_{gA} \cdot \lambda_{gl} \cdot f_{g;k}}{R_M \cdot \gamma_M},$$

where  $\lambda_{gA}$ ,  $\lambda_{gl}$  e  $k_{ed}$  are defined according to the constraint and load condition, indicated as follows. We have:

$k_{ed}=0.9$	strength reduction factors for verifications near the edges of the element or holes (Table 7.3) for glass with polished edges; for tests at a distance of $d > 5s$ from the edge, we have $k_{ed}=1$ ;
$\lambda_{gA}$	scale factor for verification distant from the edges, calculated using (7.6);
$\lambda_{gl}$	scale factor for stress verification at the edge, calculated using (7.7).

These coefficients are different for the three considered cases.

#### Design strength for compressed beam

The strength reduction factor  $\lambda_{gA}$ , calculated using (7.6), is

$$\lambda_{gA} = \left( \frac{0.24 \text{m}^2}{kA} \right)^{1/7} = 1.557 \Rightarrow \lambda_{gA} = 1$$

where:

$$k = 0.054 \text{ (Table 7.3, rectangular plate simply supported on two edges)}$$

$$A = b \cdot l = 0.2 \text{ m}^2.$$

The scale factor for stress at the edge, since that the maximum tensile stresses are in the centre of the plate (as in the case of a plate under out-of-plane loading) is  $\lambda_{gl}=1$ . It is also assumed that  $k_{ed} = 1$ . The design strength for the beam subjected to axial compression is therefore:

$$f_{g;d} = \frac{k_{\text{mod}} \cdot k_{ed} \cdot k_{sf} \cdot \lambda_{gA} \cdot \lambda_{gl} \cdot f_{g;k}}{R_M \cdot \gamma_M} = 15.84 \text{ MPa}.$$

#### Design strength for beam under bending

Given that the maximum tensile stresses is reached near the edge of the element ( $d < 5s$ ),  $\lambda_{gA} = 1$  is assumed. The scale factor for stress at the edge  $\lambda_{gl}$ , calculated by (7.7), is instead (for polished edges)

$$\lambda_{gl} = \left( \frac{0.1667 \cdot 0.45 \text{m}}{k_b \cdot l_b} \right)^{1/5} = \left( \frac{0.1667 \cdot 0.45}{0.3694 \cdot 1} \right)^{1/5} = 0.727,$$



where:

$k_b = 0.3694$  (Table 7.6, polished edge, parabolic distribution of tension);

$l_b = 1\text{m}$ : edge length.

Finally, the coefficient  $k_{ed}$  for verifications near the edges is  $k_{ed} = 0.9$  (Table 7.3,  $d < 5s$ ).

The design strength for the beam subjected to *bending* is therefore:

$$f_{g;d} = \frac{k_{\text{mod}} \cdot k_{ed} \cdot k_{sf} \cdot \lambda_{gA} \cdot \lambda_{gl} \cdot f_{g;k}}{R_M \cdot \gamma_M} = 10.36 \text{ MPa} .$$

Design strength for panel subjected to in-plane compression

The strength reduction factor  $\lambda_{gA}$ , calculated using (7.6), is

$$\lambda_{gA} = \left( \frac{0.24\text{m}^2}{kA} \right)^{1/7} = \left( \frac{0.24}{0.145 \cdot 1 \cdot 1} \right)^{1/7} = 1.075 \quad ,$$

where:

$k = 0.145$  (Table 7.3, rectangular plate simply supported on four edges);

$A = 1 \times 1 = 1\text{m}^2$ .

As the value is higher than the unit, we assume  $\lambda_{gA} = 1$

As the maximum tensile stress is reached at the centre of the panel ( $d > 5s$ ),  $\lambda_{gl} = 1$ ,  $k_{ed} = 1$  is assumed.

The design strength for the panel subjected to compression is therefore

$$f_{g;d} = \frac{k_{\text{mod}} \cdot k_{ed} \cdot k_{sf} \cdot \lambda_{gA} \cdot \lambda_{gl} \cdot f_{g;k}}{R_M \cdot \gamma_M} = 15.84 \text{ MPa}.$$

## 8.7.2 Compressed beam

The buckling verification carried out on a beam of laminated glass subjected to axial compression (design load  $N_{Ed} = 5000\text{N}$ ) is described below.

The considered beam, obtained by assembling two plies of annealed float glass ( $h_1 = h_2 = 10 \text{ mm}$ ) and a PVB interlayer ( $h_{int} = 1.52 \text{ mm}$ ), has dimensions  $b = 200 \text{ mm}$ ,  $l = 1000 \text{ mm}$ . It is assumed that the design load is a permanent load (design life = 50 years); the reference temperature is the environmental temperature ( $20 \text{ }^\circ\text{C}$ ). The shear modulus of the interlayer, according to the data furnished by a producer, is  $G_{int} = 0.052\text{N/mm}^2$ .

The buckling verification of the laminated beam is carried out on the basis of (6.64). To that end, the Eulerian critical load  $N_{cr}^{(E)}$  of the element must be evaluated using (6.71), i.e.,

$$N_{cr}^{(E)} = \frac{\pi^2 E J_{eq}}{l^2} ,$$

where  $E = 70000\text{N/mm}^2$  is the elastic modulus of glass and the equivalent moment of inertia  $J_{eq}$  is calculated according to (6.72). The effective thickness  $h_{ef;w}$ , given by (6.73), must therefore be evaluated. The case being examined gives:

$$d = 0.5(h_1 + h_2) + h_{\text{int}} = 11.52 \text{ mm} ;$$

$$I_s = d^2 \frac{h_1 h_2}{h_1 + h_2} = 6.64 \cdot 10^2 \text{ mm}^3 .$$

The shear transfer coefficient is given by (6.74):

$$\Gamma_b = \frac{1}{1 + \pi^2 \frac{h_{\text{int}} EI_s}{G_{\text{int}} l^2 d^2}} = 0.0098 .$$

We therefore obtain:

$$h_{ef;w} = \sqrt[3]{h_1^3 + h_2^3 + 12\Gamma I_s} = 12.76 \text{ mm} ; J_{eq} = \frac{bh_{ef;w}^3}{12} = 3.46 \cdot 10^4 \text{ mm}^4 .$$

The Eulerian critical load is therefore:

$$N_{cr}^{(E)} = \frac{\pi^2 EJ_{eq}}{l^2} = 23921 \text{ N} .$$

The following values are defined:

$$A = b(h_1 + h_2) = 4000 \text{ mm}^2 : \text{transversal area of the glass plies only;}$$

$f_{gk,st}$  : design tensile strength to be considered in buckling verifications (annealed float glass, to be calculated as shown in (6.70)):

$$f_{gk,st} = k_{\text{mod}} \cdot k_{ed} \cdot k_{sf} \cdot \lambda_{gA} \cdot \lambda_{gl} \cdot f_{g;k} = 39.60 \text{ MPa} ;$$

$$\bar{\lambda} = \sqrt{\frac{Af_{gk,st}}{N_{cr}^{(E)}}} = 2.57 : \text{normalised slenderness of the laminated element, given by (6.68);}$$

$$\chi = \frac{1}{\Phi + \sqrt{\Phi^2 - \bar{\lambda}^{-2}}} = 0.122 : \text{reduction factor given by (6.66), with } \alpha^* = 0.71 \text{ and } \alpha_0 = 0.60 .$$

The compressed beam buckling resistance is therefore equal to:

$$N_{b,Rd} = \chi Af_{g;d} = 7730 \text{ N} .$$

The buckling verification has been satisfied, being in (6.64)

$$N_{Ed} = 5000 \text{ N} \leq N_{b,Rd} = 7730 \text{ N} .$$

### 8.7.3 Beam under bending

The same beam considered in section 8.7.2, is here considered for flexural-torsional buckling (with design load  $M_{Ed} = 1 \cdot 10^6 \text{ Nmm}$ ). Also in this circumstance, it is assumed that the element is at environmental temperature of 20°C and that the design load has a duration of 50 years.

The buckling verification of the laminated beam is carried out on the basis of (6.77). The Euler critical bending moment  $M_{cr}^{(E)}$  of the element must be evaluated using the expression (6.81), i.e.

$$M_{cr}^{(E)} = C_1 \frac{\pi}{l} \sqrt{EJ_{eq} GJ_{t,tot}} = 8.63 \cdot 10^6 \text{ Nmm},$$

with:

$$E = 70000 \text{ N/mm}^2;$$

$$G = 28455 \text{ N/mm}^2, \text{ shear modulus of glass, calculated considering } \nu = 0.23;$$

$$G_{int} = 0.052 \text{ N/mm}^2, \text{ shear modulus of interlayer (value supplied by the producer for } T = 20^\circ \text{ and permanent load);}$$

$$C_I = 1, \text{ for constant bending moment distribution (Table 6.8);}$$

$$J_{eq} = \frac{bh_{ef,w}^3}{12} = 1.66 \cdot 10^5 \text{ mm}^4;$$

$$J_{t,1} = \frac{bh_1^3}{3} = 6.67 \cdot 10^4 \text{ mm}^4;$$

$$\lambda = \sqrt{\frac{G_{int}}{G} \frac{h_1 + h_2}{h_1 h_2 h_{int}}} = 0.001;$$

$$J_s = 4d^2 \frac{h_1 h_2}{h_1 + h_2} b = 5.31 \cdot 10^5 \text{ mm}^4;$$

$$J_{t,int} = J_s \left( 1 - \frac{\tanh \frac{\lambda b}{2}}{\frac{\lambda b}{2}} \right) = 2.97 \cdot 10^3 \text{ mm}^4;$$

$$J_{t,tot} = J_{t,1} + J_{t,2} + J_{t,int} = 1.36 \cdot 10^5 \text{ mm}^4.$$

The characteristic tensile strength to be considered in buckling verifications (annealed float glass, to be calculated as indicated by (6.70)) is

$$f_{gk,st} = k_{mod} \cdot k_{ed} \cdot k_{sf} \cdot \lambda_{gA} \cdot \lambda_{gl} \cdot f_{g;k} = 25.91 \text{ MPa}.$$

The normalised slenderness of the laminated element is from Eq. (6.79):

$$\bar{\lambda} = \bar{\lambda}_{LT} = \sqrt{\frac{W_x f_{gk,st}}{M_{cr}^{(E)}}} = 0.632,$$

where  $W_x = b^2(h_1 + h_2)/6 = 1.33 \cdot 10^5 \text{ mm}^3$  is the section modulus of the glass beam.

The resisting bending moment of the beam is therefore, according to (6.78), equal to

$$M_{b,Rd} = \chi_{LT} M_R = \chi_{LT} W_x f_{g;d},$$

where

$$\Phi = 0.5 \left[ 1 + \alpha^* (\bar{\lambda} - \alpha_0) + \bar{\lambda}^2 \right] = 0.756,$$

with  $\alpha^* = 0.26$ : imperfection factor,  $\alpha_0 = 0.20$ : coefficient that defines the branch of curve in which  $\chi = 1$ , and the reduction factor (Eq. (6.66)) is

$$\chi_{LT} = \frac{1}{\Phi + \sqrt{\Phi^2 - \bar{\lambda}_{LT}^2}} = 0.854.$$

The lateral-torsional buckling verification can be considered as satisfied, being (Eq. (6.77))

$$M_{Ed} = 1 \cdot 10^6 \text{ Nmm} \leq M_{b,Rd} = 1.18 \cdot 10^6 \text{ Nmm}.$$

### 8.7.4 Compressed panel

The buckling calculation carried out on a panel of laminated glass subjected to in-plane compression (with design load  $N_{Ed} = 10^5 \text{ N}$ ) is described below.

The considered panel, obtained by assembling two plies of annealed float glass ( $h_1 = h_2 = 10 \text{ mm}$ ) and a PVB interlayer ( $h_{int} = 1.52 \text{ mm}$ ), is of size  $a = 1000 \text{ mm} \times b = 1000 \text{ mm}$  ( $\lambda = a/b = 1$ ). It is hypothesized that the element, simply supported along all its edges, is at an environmental temperature of  $20^\circ\text{C}$  and that the design load duration is 50 years; the shear modulus of the interlayer is  $0.052 \text{ MPa}$ , according to the data supplied by the producer.

The compressed panel buckling verification is carried out on the basis of (6.64). To this extent, the Euler critical load  $N_{cr}^{(E)}$  of the element must be evaluated by using (6.82), as

$$N_{cr}^{(E)} = \left( \frac{mb}{a} + \frac{a}{mb} \right) \frac{\pi^2 D_{ef}}{b^2} = k_\sigma \frac{\pi^2 D_{ef}}{b^2},$$

with  $m = 1$  and  $k_\sigma = 4$ .

The equivalent flexural rigidity per unit length  $D_{ef}$  is calculated, in accordance with (6.84), considering the equivalent thickness  $h_{ef;w}$ . Therefore

$$d = 0.5(h_1 + h_2) + h_{int} = 11.52 \text{ mm};$$

$$I_s = d^2 \frac{h_1 h_2}{h_1 + h_2} = 6.64 \cdot 10^2 \text{ mm}^3.$$

The shear transfer coefficient is defined by (6.74) in the form

$$\Gamma_b = \frac{1}{1 + \pi^2 \beta \frac{EI_s h_{int}}{G_{int} \xi^2 d^2}} = 0.0046,$$

where  $\beta = \frac{1.06}{\lambda^2} + 1.06 = 2.12$  e  $\xi = \min(a, b) = 1000 \text{ mm}$  are given by (6.85).

We therefore have:

$$h_{ef;w} = \sqrt[3]{h_1^3 + h_2^3 + 12\Gamma I_s} = 12.68 \text{ mm};$$

$$D_{ef} = \frac{E h_{ef;w}^3}{12(1 - \nu^2)} = 1.27 \cdot 10^7 \text{ Nmm};$$

$$N_{cr}^{(E)} = k_\sigma \frac{\pi^2 D_{ef}}{b^2} = 4.95 \cdot 10^5 \text{ N}.$$

The normalised slenderness of the laminated element is given by (6.68) and for this case is equal to

$$\bar{\lambda} = \sqrt{\frac{A f_{gk,st}}{N_{cr}^{(E)}}} = 1.265,$$

where  $A = b(h_1 + h_2) = 20000 \text{ mm}^2$  is the total area of the transversal section (sum of the transversal areas of the glass plies), and  $f_{gk,st} = 39.60 \text{ N/mm}^2$  is the tensile strength to be considered in buckling verifications (annealed float glass, Table 7.7 to be calculated as shown in paragraph 8.7.2).

We therefore have

$$\Phi = 0.5 \left[ 1 + \alpha^* (\bar{\lambda} - \alpha_0) + \bar{\lambda}^2 \right] = 1.414 \text{ for (6.67), with } \alpha^* = 0.49 \text{ and } \alpha_0 = 0.80;$$

$$\chi = \frac{1}{\Phi + \sqrt{\Phi^2 - \bar{\lambda}^2}} = 0.489 \text{ for (6.66).}$$

The buckling resistance of the compressed panel is therefore, from Eq. (6.65), equal to

$$N_{b,Rd} = \chi A f_{g;d} = 1.549 \cdot 10^5 \text{ N}.$$

The buckling verification is satisfied, because (Eq. (6.64)):

$$N_{Ed} = 10^5 \text{ N} \leq N_{b,Rd} = 1.549 \cdot 10^5 \text{ N}.$$

## 9 MATERIAL IDENTIFICATION, QUALIFICATION AND ACCEPTANCE PROCEDURES

This chapter provides indications and concepts about material control in relation to their design and construction requirements. These instructions are not legally compulsory regulations at the present stage, but they aim at helping to fully understand the critical points in the construction process. What is presented hereafter complies with national and international regulations in force at the time of the present writing. New proposals, clearly indicated as such, are in any case presented with a double purpose: on the one hand, they can be used in accordance among the parties (clients and others) in a contract or tender contract and, on the other hand, they can urge producers and national organisms to prepare other regulatory documents.

The glass to be used in structural applications is produced industrially. The mechanical properties of the glass that are required for use in a structural environment are the same as those indicated in the corresponding product standards.

The calculation and verification procedures defined in the previous chapters are held as being valid for material having the aforementioned mechanical characteristics. In accordance with technical structural codes that are currently in force in Italy ([NTC2008] - Italian Building and Construction Standards 2008), to verify and certify that the mechanical characteristics comply with these requirements, the materials and products for structural use must be:

- Identified univocally by the producer according to applicable procedures.
- Qualified under the responsibility of the producer according to applicable procedures.
- Accepted by the construction manager by acquisition and verification of the qualifying documents, as well as with possible experimental procedures for acceptance.

Controlling glass performance, when used structurally, means that a suitable level of confidence has to be reached, and it can be obtained using suitable identification, qualification and acceptance procedures. The material that is commonly used in glass composition, such as the polymer interlayers used in laminated glass, are also subjected to controls. The definition of the identification, qualification and acceptance procedures for material for structural use is transferred to the technical regulations on constructions that are currently adopted at a national or European level.

### 9.1 An overview of national (Italian) regulations

The Italian Building and Construction Standards [NTC 2008] that are currently in force indicate the possibility of using glass as a material for creating elements with structural functions in chapter 4.6, which reads:

#### **4.6 CONSTRUCTIONS MADE OF OTHER MATERIALS**

*Materials that are not traditional or not treated in these technical standards can be used to create structural elements or construction works, subject to authorisation from the Central Technical Service (CTS) on the advice of the High Council of Public Works, authorisation that involves the use of the material in specific structural typologies proposed on the basis of procedures defined by the Central Technical Service.*

*The materials defined here include concrete with a resistance class of above C70/85, fibre-reinforced concrete, construction steel works not included in § 4.2, aluminium alloys, copper alloys, steel lattice beams merged in casting concrete, fibre-reinforced polymer materials, panels with composite polyurethane or polystyrene, non-traditional brickwork materials, structural glass, materials other than steel acting as a reinforcement for reinforced concrete.*

It can be inferred from this article that glass can be used to produce structural elements only following authorisation from the CTS for a specific application, on the basis of procedures that control the material as defined by the CTS.

Furthermore, Chapter 11 of the NTC2008, regarding the certification of materials and products for construction, clearly indicates that the material and products for structural use must be:

- *identified* univocally by the producer, according to the applicable procedures;
- *qualified* under the responsibility of the producer, according to the applicable procedures;
- *accepted* by the construction manager with acquisition and checking of the qualifying documentation, as well as with possible experimental proof for acceptance.

Material and product certification, and in particular its identification and qualification, must fall into one of the three cases given below

*A) materials and products for structural use for which a harmonised European standard is available, the reference of which is published in the Official Journal of the European Union. At the end of the transitional period, their use in works is only possible if they are CE marked, pursuant to Directive 89/106/EEC “Construction products” (CPD), acknowledged in Italy by the Presidential Decree no. 246 of 21/04/1993, as amended by Italian Presidential Decree no. 499 of 10/12/1997;*

*B) materials and products for structural use that are not part of a harmonised standard, or for which the reference standard falls into the transitional period, and for which qualification with the methods and procedures indicated in these standards is instead forecasted. The case in which the producer has voluntarily opted for CE marking, during the transitional period of the specific harmonised standard, is excluded;*

*C) materials and products for structural use that is innovative or not mentioned in this chapter and which does not fall into types A) or B). In such cases the producer can apply CE Marking in compliance with European Technical Approval (ETA), or, alternatively, same producer shall be in possession of a “Technical Suitability for Use” Certificate released by the Central Technical Service on the basis of Guidelines approved by the High Council of Public Works.*

It will be only possible to place glass material certification for structural use in case A) above, when specific harmonised standards are available.

## **9.2 An overview of European legislations**

### **9.2.1 Specific regulations relative to glass for structural use**

There are no harmonised standards specifically for glass used in structural elements. In 2013 the CEN TC250 WG3 technical committee began working on the new Eurocode specifically for glass structural applications but, as this document is being written, it is not even available in a preliminary form.

### 9.2.2 Standards for glass used in construction works

Harmonised European standards currently exist that refer to glass used in constructions, but not specifically for structural use. Some of these standards contain some indications on the minimum mechanical properties that the glass should have.

The three most common types of glass used in constructions are:

- a) laminated glass, according to UNI EN 14449:2005;
- b) toughened glass, considered in the UNI EN 12150-2:2005;
- c) insulating glass, referred to by UNI-EN 1279-5:2005.

All these standards are for glass used as *Glass in building* and their aim is to evaluate compliance of different products with the objective of CE marking.

It should be highlighted that these standards have already been in force for several years; in Italy, CE marking for tempered glass has been obligatory since 01/09/2006, and since 01/03/2007 for laminated windows and insulating walls.

Each standard indicates the requirements that the glass should have. For example, the requirements for laminated glass are given in chapter 4.3.2 of UNI EN 14449:2005.

It should be highlighted that the required properties refer to basic requirements for construction products established in Annex I of CPR 305/2011 (which abrogates and replaces the Directive 89/106/EEC). In particular, the product standards mentioned above deal with these requirements:

- basic requirement 2: Safety in case of fire;
- basic requirement 4: Safety and accessibility in use;
- basic requirement 6: Energy economy and heat retention.

It should be noted that basic requirement 1 - mechanical resistance and stability, to which reference must in any case be made for structural applications, is not considered explicitly. In spite of this, the product standards indicate minimum values of the mechanical properties, established to guarantee resistance to wind, snow, permanent and/or service loads. These properties must be satisfied for basic requirement 4 – safety and accessibility in use.

Tempered, laminated and insulating glass are therefore covered by harmonised standards that also indicate the procedures for obtaining CE marking. Even if this marking does not cover the basic requirements of point 1, it represents obligatory qualification certification. It should be remembered that the NTC2008 explicitly indicate that:

*Concerning materials and products with CE marking, the Construction manager must, during the acceptance phase, make sure that the marking appears and request from each supplier, for each different product, the Certificate or Declaration of Compliance to the harmonised part of the specific European standard or the specific European Technical Approval, as is applicable.*

*The Construction manager must also ensure that those same products are part of the typologies, classes and/or families indicated in said documentation.*

*In the case of products without CE marking, the Construction manager must make sure of the ownership and validity regime of the Qualification Certificate (case B) or the Technical Suitability for Use Certificate (case C) released by the Central Technical Service of the High Council of Public Works.*

Regarding the compliance certificate systems, system 1, system 3 or system 4 are available according to use.



The performance constancy of the glass products mentioned above is evaluated and verified through Factory Production Control (FPC) and with Type Testing (TT). TT tests must be carried out according to what is indicated in the harmonised standards. As an example, in Chapter 5.2.2 of UNI EN 14449:2005 (laminated glass), the standards specify all the characteristics that have to be controlled with an FPC. Internal surveillance must be continual and there may possibly be an inspection by a third party institute every six months. The annexes to the mentioned standard give a brief outline of the tests to carry out for determining the mechanical characteristics. As an example for laminated glass they mention

C.2 Ball Drop test

C.3 Pendulum impact tests

C.4 Mechanical tests on the polymer interlayer.

A test method for defining the resistance of the glass-polymer interface has still not been univocally defined, but some possible alternative procedures are mentioned. These tests can be integrated, when necessary and/or specifically indicated by the designer, with the tests given below.

Annex ZA of UNI EN 14449:2005 gives all the aspects that must be checked for each basic requirement. The following are mentioned, as an example:

Table ZA.1 – Relevant clauses for laminated glass and/or laminated safety glass and intended use in buildings and construction works

- Safety in the case of fire –
- Resistance to fire (for glass for use in a glazed assembly intended specifically for fire resistance)
- Reforce to fire
- External fire performance
- Safety in Use –
  - Bullet resistance: Shatter properties and resistance to attack
  - Explosion resistance: Impact behaviour and resistance to attack
  - Burglar resistance: Shatter properties and resistance to attack
  - Pendulum body impact resistance : Shatter properties(safe breakability) and resistance to impact
  - Mechanical resistance: Resistance against sudden temperature changes and temperature differentials
  - Mechanical resistance: Resistance against wind, snow, permanent and imposed load and/or imposed loads
- **Protection against noise:**-Direct airborne sound reduction
- **Energy conservation and heat retention:**
  - Thermal properties
  - Radiation properties:
    - light transmittance and reflectance
    - solar energy characteristics

For use in systems that are resistant to fire, the evaluation and testing system 1 for the constancy of performance should be applied. This forecasts TTs and FPCs being carried out by a third party institute.

Regarding the material used, the performance declaration of the producer must include the mechanical resistance characteristic. The producer must therefore demonstrate that the mechanical characteristics of the product have undergone systematic controls and that they have exceeded an established limit. In other words, the mechanical resistance cannot be excluded or indicated as NPD (*No performance determined*). Annex ZA.4m in fact, states: *The “No performance determined” (NPD) option may not be used where the characteristic is subject to a threshold level. Otherwise, the NPD option may be used when and where the characteristic, for a given intended use, is not subject to regulatory requirements in the Member State of destination.*

Finally, the prEN 16612 “*Glass in building – determination of the load resistance of glass sheets by calculation and testing*” elaborated by the CEN-TC 129 WG8, and currently on its way to being approved, should also be recalled. This document proposes, for elements without a structural function

used as cladding, calculation and design methods and also gives representative values of the material strengths.

### **9.3 Mechanical properties of glass**

The calculation and verification procedures in these instructions were determined and perfected assuming materials and products with specific mechanical characteristics. The values assumed for these characteristics are the same as those established in the product standards that are currently in force. These values were proposed also by the prEN 16612 project standard, recently elaborated by the CEN-TC 129 WG8.

In particular, for soda-lime float glass, the producer must ascertain, using the qualification procedures, a characteristic tensile resistance under bending that is no lower than 45 MPa, intended as being a characteristic value that corresponds to the 5% fractile of the resistance distribution.

The executors of the secondary tempering and toughening processes, through the qualification procedure, must ascertain the mechanical performances indicated in Table 7.7, where the values of the tensile resistance indicated are still intended as characteristic corresponding to the 5% fractile of the resistance distribution.

The executors of surface treatments (acid etching, enamelling, moulding) must together ascertain, using the qualification procedure, the characteristic values (5% fractile) indicated in Table 7.4.

### **9.4 Additional controls on glass**

We suggest interpreting the test values of the material resistance using distributions that are compatible with those introduced in these instructions, in accordance with what is shown in Chapter 2.1.3.

The procedures for qualification, product sampling, test methods, definition of the accredited organisms for carrying out the tests, the controls to be carried out by relative third parties, the product quality management systems and the resulting certifications must be defined in the standards that are being elaborated by the CEN TC 250, or by competent national organisms.

These standards also indicate how the material should be identified by the producer by way of documents and/or brands that can be consulted immediately. Those who carry out the second processes and surface treatments must, in the same manner, identify the transformed product with documents and/or brands to permit recognition. The branch from which each material or each product originates must be identifiable and traceable, from its origin to the last transformer.

#### **9.4.1 Mechanical tests**

The following are normalized tests to measure the characteristic tensile resistance for glass bending, as shown in Chapter 2.1.2.3.

- Test with double concentric rings on flat specimens, on large stressed surfaces, as defined by the UNI EN 1288-2.
- Test with specimens supported at two points (bending at four points), as defined by the UNI EN 1288-3.

- Test with double concentric rings on flat specimens, on small stressed surfaces, as defined by the UNI EN 1288-5.
- Test on profiled glass, as defined by the UNI EN 1288-4.

Tests other than those mentioned above can be used as long as supported scientifically and in any case in line with the aforementioned UNI EN 1288-1 or other pertinent standards.

In particular, we propose, as a validly proven alternative to the previous mechanical tests, the bending test with double concentric rings, carried out on geometries that are identical to those indicated in the UNI EN 1288-2 but without overpressure, as long as the analytic calculation of the effective area is made, as established in Section 2.1.3.

Point load tests can be carried out according to ISO 614.

The measured values should be elaborated with Weibull type statistics, as indicated in Chapter 2.1.3 of these Instructions and in compliance with the following regulatory indications:

UNI EN 12603: 2004 Glass in building. Procedures for goodness of fit and confidence intervals for Weibull distributed glass strength data

ASTM 1239-06a Standard Practice for Reporting Uniaxial Strength Data and Estimating Weibull Distribution Parameters for Advanced Ceramics.

ISO 20501: 2003 Fine ceramics (advanced ceramics, advanced technical ceramics) - Weibull statistics for strength data.

Referring to the ASTM C 1368 can be useful for calculating the coefficient  $k_{\text{mod}}$  that defines the decrease of resistance according to load application duration (static fatigue as described in Section 2.1.2.2.2).

#### **9.4.2 Additional tests for thermally or chemically pre-stressed glass**

The following experimental tests are suggested, not as alternatives but as complementary to each other.

- Mechanical resistance at bending test, to be carried out as indicated in Section 9.4.1.
- Test for measuring surface compression using diffractometry techniques, demonstrated by calibration, according to UNI-EN 12150 part 2 (point B.1.2).

In the case of glass treated with HST, the mechanical tests must be carried out *after* the HST cycle. The kiln for HST must be calibrated periodically.

The tests must comply with UNI EN 12150 , UNI EN 1863 and UNI EN 14179.

### **9.5 Mechanical characterisation of the materials used in composition with glass**

The materials commonly used in composition with glass are polymer interlayers, adhesives and silicones.

#### **9.5.1 Polymer interlayers**

The interlayer must guarantee a suitable adhesion capacity to the glass sheet and maintain the fragments after the glass has broken. The interlayer also allows the shear coupling, even if partial, of the

---

component sheets, guaranteeing bending as a composite package. To determine the load-bearing capacity of the laminated glass during the pre-breakage phase, determining the rigidity of the interlayer, as described in section 6.3.3, is therefore of primary importance.

#### **9.5.1.1 Proposal for a mechanical characterisation of the interlayer**

At a European level, the CEN TC 129-WG 8 recently introduced the project of standard prEN 16613 *Glass in building - Laminated glass and laminated safety glass - Determination of inter-layer mechanical properties*, proposing a classification of the interlayers in families of rigidity on the basis of experimental tests. This classification and the calculation method based on it, proposed in the prEN 16612, should be considered carefully for the reasons indicated in paragraph 6.3.3.1.3.

To correctly evaluate the mechanical performance of laminated glass, a specific characterisation of the mechanical properties of the interlayer appears to be necessary.

Regarding characterisation of the long term properties of the plastic material, we suggest referring to dynamic tests, in particular those under cyclic driving forces, considered at an international level by ISO 6721 (sections 1-11). At the current moment, sections 1, 2 and 3 are UNI EN ISO, while the other 4-10, even though already defined, are still in the approval state; part 11, instead, is currently classified as DC (*draft comitate*), and therefore not effectively accessible. American standards such as the ASTM D4065-06 are also available.

It is also important to consider the possible effects of environmental degradation. For this purpose, the samples can be previously subjected to simulated environmental degradation as described in Paragraph 2.2.1.5. The methods and duration of the treatments that simulate environmental degradation must be defined in order to reproduce the effects of the environmental conditions effectively produced during the lifetime of the structure.

When preparing samples, the plastic material elements that are to be tested should be conditioned beforehand, namely treated in an autoclave at the working temperatures of laminated glass. This condition is usually produced by placing the polymer specimen between two glass elements, to which adhesion is not permitted. In spite of this, wherever possible, the samples to be subjected to mechanical testing should be tested when they are adhering to the glass. It is advisable to subject plastic material samples (adhering or not to the glass) to tangential stress states.

It is better if two sets of test are carried out: the first to assess the value of the glass transition temperature  $T_g$ ; the second set is necessary for determining the elastic constants according to temperature and stress frequency, and therefore the “master curve”, as for example the  $G(T_{ref}, f)$  curve reported in Figure 2.19, as well as the parameters of the equation by Williams, Landel and Ferry.

Of particular interest are the values of the secant elastic moduli of the interlayer according to the duration of the stress force, the temperature and the level of degradation and, preferably, the values of the parameters necessary for defining viscoelasticity models. These data are necessary for evaluating the effects of the shear coupling between the various component plies, as described in Section 6.3.3. Should these data be lacking, the laminate cannot be schematised in the calculations as a package of glass sheets that are totally free to move relatively, without coupling (layered behaviour, defined in Section 6.3.3.1).

The material used as the interlayer must be made identifiable and qualified by the producer with certification of its physical and mechanical properties.

The procedures for product sampling, the test methods, the definition of the accredited institutions for carrying out the tests, the controls to be done by appointed third parties, the product quality management systems and the resulting certifications must be regulated by relative standards or technical recommendations.

#### **9.5.1.2 Proposal for mechanical characterisation of the laminate**

Laminated glass must be made with glass and interlayers that have already been qualified by the producers. The glass-interlayer adhesion properties, however, and the shear force transfer capacity between the sheets through the interlayer in the finished product, depend very much on the lamination process.

It is therefore preferred that laminate qualification be cared for by the final transformer, who collects the conformity certificates of the constituents, but controls, using another characterisation process, the correspondence between the resistance and the bending rigidity of the sheets effectively produced with the respective expected values, obtained from the mechanical properties of the components. This test can be obtained from:

- Bending strength tests (as indicated in Section 9.4.1) at high temperature. If there are no specific considerations, this can in general be taken as being +50°C, but in any case it must correspond to the effective maximum working temperature of the glass.
- Bending strength tests (as indicated in Section 9.4.1) at low temperature. If there are no specific considerations, this can in general be assumed as being equal to -10°C, but in any case it must correspond to the effective minimum working temperature of the sheets.
- Humidity resistance tests.
- “Toughness” test as per Annex C of UNI EN 14449.

The bending resistance tests at high and low temperatures can be carried out at room temperature, extracting the forecasted data at high and low temperatures on the basis of a theoretical model calibrated on the basis of specific tests.

The tests should be carried out on samples that represent all the compositions/typologies indicated in the design, in compliance with the methods indicated by UNI EN 14449. It is important for the test samples to be subjected to lamination in the same conditions of current production as the sheets produced for structural use.

The procedures for product sampling, the test methods, the definition of the accredited institutions for carrying out the tests, the controls to be made by appointed third parties, the product quality management systems, and also the resulting certifications, must comply with what is indicated in the relative technical standards in force.

### **9.5.2 Adhesives and sealants**

Adhesives and sealants differ because of materials and applications, so much so that a distinction has to be made.

#### **9.5.2.1 Adhesives for structural use**

When failing of the adhesive reduces the structural safety conditions (e.g. if the breakage of one or more connections made with the adhesive can cause structure overstress and/or determine the fall of a part of the structure), an adhesive for structural use shall be used specifically.

Structural adhesives shall be subjected to specific controls, typical for materials for structural use. Data of interest are:

- (1) The results of internal controls carried out on the product.
- (2) The characteristic value of the adhesion capacity, obtained with mechanical tests on the product.
- (3) The results of tests carried out according to alternative documents of proven validity (among which ASTM C1184-05 can also be considered).
- (4) The characteristic value of the tensile and shear strength, the average value of the Young's elastic modulus and the shear modulus, including the dependence of these parameters on the temperature and load duration.

The procedures for product sampling, the test methods, the definition of the institutes qualified to perform the tests, the controls to be carried out by the assigned third party subjects, the product quality management system, and also the resulting certification, must comply with what is indicated in specific standards or technical recommendations.

The calculations must always verify the structural strength of connections made with an adhesive.

### **9.5.2.2 Structural sealants**

Those sealants that mechanically connect elements are usually, somehow improperly, called “structural sealants”. A typical example is structural silicone, used to connect the glass panes to the metal frames behind them.

The individual materials and products, just like the process used to join the glass to the metal frame elements, must be tested according to the production control procedures indicated in pertinent technical standards, when applicable. Of interest are UNI EN 15434 regarding sealants, UNI EN 13022 regarding the glass and ETAG 002 regarding the adhesion process of the glass to the frame elements. If the structural sealant is used as an adhesive to create a structure, the qualification procedures established by technical standards that refer to materials and products for structural use must be applied.

### **9.5.3 Gasket elements**

For the purposes of structural behaviour, elements used as gaskets should only be considered when their stiffness can interfere with the static/dynamic behaviour of the structural object they are to be used with. In this case, for the material used, the average value of the elastic modulus and the shear modulus, including the dependence of these parameters on the temperature and load duration, must be determined.

## **9.6 Proposal for additional controls in the construction site**

In relation to the importance of the work, the client can request, at his discretion, special control procedures, inserting the desiderata in the contract and the tender specifications.

Materials and components must be accepted by the Construction manager, who acquires and verifies the accompanying documents which confirm their properties, and/or with experimental tests, in respect of current standards and possible additional indications established by the client.

The Client, the Builder, the Construction manager, the Tester, the Producers and subsequent intermediaries must archive the accompanying documentation, guaranteeing availability for a number of years determined by the relative laws in force.

Material and components must be contemplated in the “Maintenance Plan”.

The Construction manager accepts the material and products on the basis of the mechanical property controls carried out with experimental tests. The procedures for product sampling, the test methods, the definition of the institutes qualified to carry out the tests, must comply with what is indicated in the relative technical standards in force, and possible additional regulations indicated by the client.

We suggest the following indications, which represent general good practice.

Special attention must be given to controlling tempered or thermally toughened glass, because at times these processes are carried out by micro-companies that do not have suitable production controls. Frequently, unfortunately, glass with mechanical characteristics lower than those given in Table 7.7 are supplied. In particular, the systematic measurement (non destructive) of the surface compression according to UNI-EN 12150 part 2 (point B.1.2) is recommended on a sample that represents the batch being produced. Regarding glass that has been *chemically toughened*, this measure is not representative because of the limited thickness of the compressed layer. For this type of glass, the control and test procedure must be agreed upon between the client, the Construction manager and the producer, basing themselves on destructive tests in general.

As regards laminated glass, it is advisable for the Construction manager to carry out controls for verifying the mechanical resistance of the composite package. In this case, the mechanical tests carried out according to the methods given in Section 9.4.1 must include the extraction of at least one sample from each autoclave cycle.

At the moment of the order, the supplier will be requested to produce samples of transformed glass (e.g. tempered and/or laminated glass) using the same material (glass and polymer) used for the second working process (tempering/lamination). The number of samples must be commensurate to the importance of the work but, if there are no evaluations of a more precise nature, it is held as appropriate to prepare three specimens for every supply of 300 m<sup>2</sup> of glass used or lower. The size of the specimens must comply with the test methods given at point 9.4.1.

The Construction manager shall have the experimental tests carried out by an official laboratory, or another laboratory that is qualified for carrying out mechanical tests on construction materials.

## **9.7 “Standard” material identification document**

It is envisaged that the producers provide a *material identification document*, which shall always be attached to the product, with a list of the main mechanical properties.

The document should supply a detailed description, in terms of commercial name, type of glass, type of interlayer, production technology, post-production treatment typology, marking, and any other general information considered useful, as well as a geometric and physical characterisation. Each product data sheet shall indicate the dimensional tolerances or the declaration of conformity, in compliance with product standards.

The document should also have indications on the storage conditions and on the usage and safety precautions.

## **9.8 Acceptance procedures**

In the points that follow, some general notes regarding the responsibilities and actions that the various operators should carry out to guarantee the quality of the materials used in the structural applications of glass are proposed.

### **9.8.1 Material choice and tests: duties and responsibilities of the operators**

Client

---

- Prepares the contract and the tender specification, including, where desired, special indications for material controls.

#### Producers and/or suppliers

- Production of the basic materials (glass, polymers for the interlayer, material for structural adhesion) must be the constant objective of quality control programs. The latter shall cover, in addition to the production techniques, all the elements that make up the system (glass, polymer for the interlayer, material for structural adhesion). All the procedures and instructions used by the producer must be documented systematically, and be available to the relative subjects.
- The qualification procedures, which are established by standards that regulate the use of materials and products of structural use, shall be cared for by the producer.
- Strengthening, toughening, tempering, Heat Soak Test (HST), lamination operations, and in general all the second processes of glass, shall be equipped with quality control procedures for the determination, on a statistical basis, of the mechanical characteristics of the end product.
- The basic glass producers and transformers, according to what is indicated by the obligations of law, must supply evidence of the tests and controls carried out on the products and the process, to guarantee that each production batch complies with the declared specifications.
- When possible, the products must carry a mark that permits total traceability. In the contrary case, the products must be accompanied by labels or cards that contain all the information for their traceability.
- The producers and/or suppliers that can propose complete systems (glass + connecting systems) shall supply, in addition to the mechanical and physical characteristics of the individual components, also the mechanical characteristics of the complete system. These values must be supported by experimental evaluations carried out in a laboratory or *in situ* (tests on full-scale structure) and documented by detailed test reports.

#### Designer

- Shall clearly indicate in the design the quality and characteristics (geometric, mechanical and physical) of the components of the glass structure specifying, where necessary, the minimum acceptance requirements.
- Shall specify what the material acceptance and application criteria are. In the first case, the designer shall indicate to the Construction manager which sampling and tests are to be carried out. As an example, on the basis of the importance and entity of the application, he can suggest carrying out tests for verifying some or all the mechanical and physical characteristics declared by the producer in the supplied technical documents. The designer can indicate possible tests to be carried out *in situ* to verify the quality of the installation.
- The designer who designs complete systems (glass + connecting systems) shall give, in addition to the mechanical and physical characteristics of the individual components, even the mechanical characteristics of the complete system.

#### Tender companies and installers

- Shall supply the material indicated by the designer, using producers and/or suppliers who guarantee product quality.
- Shall make sure that the products comply with the regulations indicated by the designer and, if material with the indicated requirements is not available, they shall agree on possible alternatives with the designer and/or the Construction manager.



- Shall make sure that the products are accompanied by suitable technical documents, that give the values of the mechanical and physical characteristics and, if necessary, the certificates regarding the tests that were carried out.

#### Construction manager

- Carries out a decisional role on product acceptance.
- Shall make sure, both during the contract phase with the supplier and when delivered, that the supplied material is the same as the indications of the designer.
- Shall check the origin of the supplied material. The glass and other materials used in composition with it shall carry the producer's mark and the indications for product identification; in the contrary case, the material shall have labels giving the information necessary for traceability. The other materials shall be supplied with labels giving the information necessary for traceability.
- Shall verify the mechanical and physical characteristics of the products using the documents that accompany the supply.
- On the basis of the importance and entity of the application, request the carrying out of dedicated experimental tests for evaluating the quality of the materials and verify result-correspondence with the values supplied by the producer. These tests are to be carried out in laboratories with proved experience and with equipment that is suitable for characterising the material. The acceptance criteria shall be based on the maximum deviation permitted of the obtained results, as to the values obtained during the production controls. In this case, it shall be made sure that the test procedures are the same and that the samples are obtained with the same material and the same production techniques. Tests to determine the mechanical and physical characteristics should be requested, to be carried out on both virgin and pre-conditioned samples to verify, for example, the permanence of the performance as the load application time, the temperature, or the humidity, vary.

#### Certifying and inspection institutions, test laboratories

- Shall have proven skills in the characterisation of glass , polymer and silicon based materials.
- Shall have suitable measuring and testing equipment.
- Shall carry out the experimental tests following the procedures indicated in the specific regulations for the pertinent material.
- Shall issue detailed test and audit reports, giving all the information requested and the results of the tests and controls.

#### Tester

Should it be requested to test the glass structure, in compliance with the habitual controls described in current laws, the tester shall:

- Verify the quality of the materials used through the certificates that accompany the supply;
- Verify material acceptance by the Construction manager;
- Verify the results of possible experimental acceptance tests requested by the Construction manager;
- Request additional tests if held as being necessary.

### **9.8.2 Transport, storage and movement**

The transport, storage, use and preservation methods of the basic materials and the end product are important for guaranteeing that the properties of the individual components do not alter, and also for guaranteeing respect of the safety standards.

- Transport. The components of the glass system shall be packed and transported in a suitable manner, in respect of possible applicable standards.
- Storage. To preserve the properties of the glass element and guarantee respect of the safety standards, the components shall be preserved observing the recommendations of the supplier and/or producer. To preserve the properties of the polymers used for the interlayers and the adhesive material, it is important that they be preserved at suitable temperature and humidity levels, meticulously following the specifications of the producer. The producer shall indicate the time and methods of storage within which the properties of the materials remain unaltered. Any element that has exceeded the intermediate storage time, or which has deteriorated or been contaminated, must not be used. All the components held as being unusable shall be eliminated as specified by the producer, and also as indicated by possible regulations in force regarding environmental protection.
- Movement. The producer shall supply, for all the components of the glass system, the technical data sheets giving the information on movement, above all in terms of safety (MSDS – Material Safety Data Sheet).

## 10 REFERENCES

### 10.1 Monographies and scientific articles

- AA. VV., *Engineered materials handbook – Adhesives and sealants*, Vol. 3, ASM International, USA, 1990.
- Aben, H. and Guillemet, C., *Photoelasticity of Glass*. Springer-Verlag, Berlin, (pp.18-20), 1993.
- Adams, R.D. and Peppiatt, N.A., Effect of Poisson's ratio strains in adherends on stresses of an idealized lap joint, *J. Strain Analysis*, **8**(2):134-139, 1973.
- Adams, R.D. and Wake, W.C., *Structural adhesive joints in engineering*, Elsevier Applied Science Publisher, USA, 1984.
- Arruda, E.M. and Boyce, M.C., A three-dimensional constitutive model for the large stretch behaviour of rubber elastic materials, *Journal of Mechanics and Physics of Solids*, **41**(2): 389-412, 1993.
- Batdorf S.B. and Heinisch, H. L., Weakest link theory reformulated for arbitrary fracture criterion, *Journal of the American Ceramic Society*, **61**(7-8):355-358, 1978.
- Beason, W.L., *A failure prediction model for window glass*. NTIS Accession no. PB81-148421, Texas Tech University, Institute for Disaster Research, 1980.
- Beason, W.L., and Morgan, J.R., Glass failure prediction model, *Journal of Structural Engineering*, **110**(2):197-212, 1984.
- Behling, S. and Behling, S., *Glass: Structure and Technology*, New York, Prestel, 1999.
- Belis, J., Depauw, J., Callewaert, D., Delincé, D., Van Impe, R., Failure mechanisms and residual capacity of annealed glass/SGP laminated beams at room temperature, *Engineering Failure Analysis*, **16**:1866–1875, 2009.
- Bennison, S., Structural Properties of Laminated Glass, Short Course, *Glass Processing Days*, Tampere (Fi), 2009.
- Bertoldi, M. and Sglavo, V.M., Influence of composition on Fatigue Behavior and Threshold Stress Intensity Factor of Borosilicate Glasses, *J.Am.Ceram.Soc.*, **85**: 2499-2506, 2002.
- Bertolini, L., Bolzoni, F., Cabrini, M., Pedferri, P., *Tecnologia dei materiali. Ceramici, polimeri e compositi*, Città Studi Edizioni, Torino 2001.
- Bigwood, D.A. and Crocombe, A.D., Elastic analysis and engineering design formulae for bonded joints, *International Journal of Adhesion and Adhesives*, **9** (4): 229–242, 1989.
- Borsellino, C., Calabrese, L., Di Bella, G., Valenza, A., Comparisons of processing and strength properties of two adhesive systems for composite joints, *International Journal of Adhesion and Adhesives*, **27**(6): 446-457, 2007.
- Brode H.L., Numerical solution of spherical blast waves, *J. App. Phys.*, 1955.
- Brown, W.G., A Load Duration Theory for Glass Design, *Publication NRCC 12354*, 1972.
- Brückner-Foit, A., Fett, F., Schirmer, K.S. and Munz, D., Discrimination of multiaxiality criteria using brittle fracture loci, *J. Eur. Ceram. Soc.*, **16**:1201-1207, 1996.
- Button, D. and Pye, B., *Glass in building: a guide to modern architectural glass performance*: Pilkington, Oxford (UK), Boston: Butterworth Architecture, 1993.
- CEN/TC129/WG8, “N230E - An overview of prEN 13474 and the work of CEN/TC129/WG8 from which it was developed”, Feb. 2006.
- Chao, L.Y. and Shetty, D.K., Equivalence of Physically based Statistical Fracture Theories for Reliable Analysis of Ceramics in Multi-axial Loading, *J. Am. Ceram. Soc.*, **73** (7): 1917-1921, 1990.

- Ciarlet, P.G., *Mathematical Elasticity: Three-dimensional elasticity*, in Studies in Mathematics and Its Applications. North-Holland, 1988.
- Cottone, A., Giambanco, G. and Spada, A., Valutazione della resistenza di adesione e della lunghezza efficace di incollaggio nei giunti adesivi tramite le leggi dell'effetto scala, *XVIII GIMC Conference*, 2010.
- Dall'Igna, R., D'Este, A. and Silvestri, M., Comments on test methods for determination of structural glass strength, *XXV ATIV Conference Proceedings*, 5-13, 2010.
- De Bortoli L., Valutazione della risposta dinamica di una parete vetro-acciaio soggetta a carico esplosivo, *Tesi di Laurea*, Università di Trieste, AA 2002-2003.
- Delincé, D., Callewaert, D., Belis, J. and Van Impe, R., Post-breakage behaviour of laminated glass in structural applications, *Challenging Glass, Conference on Architectural and Structural Applications of Glass*, pp. 459-469, 2008.
- D'Haene, P., and Savineau, G., Mechanical properties of laminated safety glass - FEM Study, *Glass Performance Days*, Tampere, Finlandia, pag. 594, 2007.
- Dodd, G., Essential elements of bolted structural glass systems, In: Ledbetter, S., Harris, R., editors, *Proceedings of International Conference in Building Envelope Systems and Technology*, Bath (UK), Centre for Window & Cladding Technology, 1997.
- Dowdle, B.M. and Cole, R.N., The shape of fixings, In: Ledbetter, S., Harris, R., editors, *Proceedings of Glass in Buildings*, Bath (UK): Centre for Window & Cladding Technology, 1999.
- Durchholtz, M., Goer, B. and Helmich, G., Method of reproducibility predamaging float glass as a basis to determinate the bending strength, *Glotech. Ber. Glass Sci. Technol.*, **68**(8): 251-258, 1995.
- Dutton, H., Structural glass architecture, *Proceedings of Glass Processing Days*, Tampere, Finland, 1999.
- Evans, A. G., A method for evaluating the time-dependent failure characteristics of brittle materials and its application to polycrystalline alumina, *Journal of Materials Science*, **7**:1137-1146, 1972.
- Evans, A. G., Slow crack growth in brittle materials under dynamic loading conditions. *Int. J. Fracture*, **10**(2): 251-259, 1974.
- Evans A.G., A General Approach for the Statistical Analysis of Multiaxial Fracture. *Journal of the American Ceramic Society*, **61**(7-8):302-308, 1978.
- Ferry, J. D., *Viscoelastic properties of polymers*, John Wiley & Sons, New York, 1980.
- Fischer-Cripps, A.C. and Collins, R.E., Architectural Glazings: Design Standards and Failure Models, *Building and Environment*, **30**(1):29-40, 1995.
- Fischer-Cripps, A.C., *Introduction to contact mechanics*, In: Mechanical Engineering Series, Springer, 2007.
- Galuppi, L. and Royer-Carfagni, G., The effective thickness of laminated glass plates, *Journal of Mechanics of Materials and Structures*, **7**: 375-400, 2012.
- Galuppi, L. and Royer-Carfagni, G., Effective thickness of laminated glass beams: New expression via a variational approach, *Engineering Structures*, **38**:53-67, 2012.
- Galuppi, L., Manara, G. and Royer-Carfagni, G., Practical Expression for the design of laminated glass, *Composites, part B: engineering*, **45**: 1677-1688, 2013.
- Galuppi, L., Royer-Carfagni, G., On the inconsistency of a formulation for the effective thickness of laminated glass, recently implemented by standards, *Composites, part B: engineering*, in press, 2013.
- Galuppi, L., Royer Carfagni, G., The enhanced Effective thickness method for laminated glass, *Proceedings Glass Performance Days (GPD) 2013*, Tampere Finland, June 13-15, 2013.
-

- Goland, M. and Reissner, E. The stresses in cemented joints, *ASME Journal of Applied Mechanics*, **7**:A17-A27, 1944.
- Green, D. J. Compressive Surface Strengthening of Brittle Materials, *J. Mater. Sci.*, **19**:2165-2171, 1984.
- Haldimann, M., Fracture strength of structural glass elements – analytical and numerical modelling, testing and Design, *Thesis n. 3671*, EPFL Lausanne, CH, 2006.
- Heffernan P., *Fundamentals of Blast Waves*, Royal Military College of Canada, Kingston, ON, 2006.
- Ho, K. C. and Chau, K. T., An Infinite Plane loaded by a Rivet of a Different Material. *Int. J. Solids Structures*, **34**(19): 2477-2496, 1997.
- Hugoniot, H., Propagation des Mouvements dans les Corps et spécialement dans les Gaz Parfaits, *Journal de l'Ecole Polytechnique*, **57**: 3, 1887.
- Jousset, P., Hyperelastic material modelling - Sikasil SG-500, *SIKA Internal Report*, 2007.
- Jousset, P., and Rachik, M., Development of an Inverse Identification Procedure to Evaluate Material Constitutive Parameters for the Finite Element Simulation of Structural Adhesives, *2nd European Hyperworks Technology Conference*, 2008.
- Kausch, H.H., Heymans, N., Plummer, C.J. and Decroly, P., *Matériaux polymères: propriétés mécaniques et physiques*, Presses Polytechniques et Universitaires Romandes, Lausanne, 2001.
- Kinney, G.F., *Explosive Shocks in Air*, Macmillan, New York, 1962.
- Kinney, G. F., *Engineering properties and application of plastics*, John Wiley & Sons, New York, 1967.
- Kott, A. and Vogel, T., Safety of laminated glass structures after initial failure, *Structural Engineering International*, **14**: 134-138, 2004 (1).
- Kott, A. and Vogel, T., Controlling the post-breakage behavior of laminated safety glass, *Proceedings International Symposium on the Application of Architectural Glass*, Monaco, 2004 (2).
- Krohn, M.H., Hellmann, J.R., Shelleman, D.L., Pantano, C.G. and Sakoske, G.E., Strength and Fatigue of float glass before and after enameling, *The Glass Researcher*, **11**(2): 24-28, 2002.
- Lawn, B.R. and Wilshaw, T.R., *Fracture of Brittle Solids*, Cambridge University Press, 1975.
- Le Bourhis E., *Glass: Mechanics and Technology*, John Wiley & Sons, 2008.
- Madsen, H.O. , Krenk, S. , Lind, N.C., *Methods of structural safety*, Prentice-Hall, 1985.
- Mays, G.C. , Smith, P.D., *Blast effects on buildings*, Thomas Telford, Londra, 1995.
- Moffatt, G., Pearsall, W., Wulff, J., The structure and properties of materials, vol. I: "Structure", Wiley, 1965.
- Mooney, M., A Theory of Large Elastic Deformation, *Journal of Applied Physics*, **11**(9): 582-592, 1940.
- Munz, D. and Fett, T., *Ceramics. Mechanical Properties, Failure Behaviour, Materials Selection*, Springer-Verlag, Heidelberg, (pp.181-189), 1999.
- Newmark, N.M., Siess, C.P. and Viest, I.M., Test and analysis of composite beams with incomplete interforce, *Proceedings of the Society for Experimental Stress Analysis*, **9**:75-92, 1951.
- Ogden, R.W., Large deformation isotropic elasticity on the correlation of theory and experiment for incompressible rubberlike solids. *Proceedings of the Royal Society of London*, A326: 565-584, 1972.
- Pilkey, W. D. *Peterson's Stress Concentration Factors*. John Wiley & Sons, Inc., 2<sup>nd</sup> Edition, 1997.

- Porter, M.I. and Houlsby, G.T., Development Crack Size and Limit State Design methods for edge abraded glass members, *Report N. OUEL 2111/99*, University of Oxford, 1999.
- Rankine W.J.H., On the Thermodynamic Theory of Waves of Finite Longitudinal Disturbance, *Phil. Trans. Roy. Soc.*, **160**:277-288, 1870.
- Rice, P. and Dutton, H., *Structural glass*, UK: E & FN Spon, 2<sup>nd</sup> edition, 1995.
- Rivlin, R.S., Large elastic deformation of isotropic materials. IV. Further developments of the general theory. *Philosophical Transfoces of the Royal Society of London A*, **241**(835): 379-397, 1948.
- Royer-Carfagni and G., Silvestri, M., A proposal for an arch footbridge in Venice made of structural glass masonry. *Engineering Structures*, **29**(11): 3015-3025, 2007.
- Ryan, P., Otlet, M., Ogden, R.G., *Steel supported glazing systems*, UK: Steel Construction Institute, SCI Publication 193, 1997.
- Schittich, C., Staib, G., Balkow, D., Schuler, M. and Sobek, W., *Glass construction manual*, Munich (Germany): Institut fur internationale Architektur-Dokumentation, 1999.
- Schittich, C., Glass architecture in the second half of the 20<sup>th</sup> century, In: *Glass Construction Manual*, Basel, Birkhäuser, 2001.
- Sedlacek, G., Blank, K., Laufs, W., and GÜsgen, J., *Glas im Konstruktiven Ingenieurbau*, Ernst & Sohn, Berlin, 1999.
- Sglavo, V. M. and Green, D. J., in *Proc. 104<sup>th</sup> Ann. Ntg American Ceramic Society*, St. Louis, 2002a.
- Sglavo, V. M. and Green, D. J., Measurement of fatigue limit in silicate glasses in R. Bradt (a cura di), *Fracture Mechanics of Ceramics*, Dordrecht ; Boston ; New York, N.Y.: Kluwer academic, p. 305-312, 2002b.
- Shand, E.B., Fracture velocity and fracture energy of glass in the fatigue range, *J. Am. Ceram. Soc.* **44**(1): 21-26, 1961.
- Silvestri, M., Sul Comportamento Post-Critico di Pannelli in Vestro Stratificato, *Tesi di Dottorato*, Dottorato di ricerca in Ingegneria Civile, Università degli Studi di Parma, 2009.
- Stamm, K. and Witte, H. *Sandwichkonstruktionen – Berechnung, Fertigung, Ausführung*. Springer Verlag, 1974.
- Treloar, L.R.G., Stresses and Birefringence in Rubber subjected to General Homogeneous Strain, *Proc Phys Soc*, **60**: 135-144, 1948.
- Treloar, L.R.G., *The Physics of Rubber Elasticity*, Clarendon Press, Oxford, 3<sup>rd</sup> Edition, 1975.
- The Institution of Structural Engineers, *Structural use of glass in buildings*, The Institution of Structural Engineers press, London, 1999.
- Van Duser, A., Jagota, A., and Bennison, S. J., Analysis of glass/polyvinyl butyral laminates subjected to uniform pressure, *Journal of Engineering Mechanics*, **124** (4): 435-442, 1999.
- Volkersen, O., Recherches sur la théorie des assemblages collés, *Construction Métallique*, **4**:3-13, 1965.
- Vyzantiadou, M.A. and Avdelas, A.V., Point fixed glazing systems: technological and morphological aspects, *Journal of Constructional Steel Research*, **60**: 1227-1240, 2004.
- Wan, K.T., Lathabai, S. and Lawn, B.R., Crack velocity functions and thresholds in brittle solids, *J. Am. Ceram. Soc.*, **44**: 21-26, 1961.
- Wereszczak, A. A., Kirkland, T. P., Ragan, M. E. Strong, K. T. Lin, H.-T. and Patel, P. Size scaling of tensile failure stress in a float soda-lime-silicate glass. *Int. J. Appl. Glass Sci.*, **1** (2):143–50, 2010.
- Wiederhorn, S.M., Influence of Water Vapor on Crack Propagation in Soda-Lime Glass, *J. Am. Ceram. Soc.*, **50**: 407-410, 1967.
-

Wiederhorn, S.M., Fracture Surface Energy of Glass, *J. Am. Ceram. Soc.*, **52**: 99-105, 1969.

Wiederhorn, S. M. and Bolz, L. H. Stress corrosion and static fatigue of glass. *Journal of the American Ceramic Society*, **53**(10):543-548, 1970.

Wölfel E., Elastic Composite: An Approximation Solution and its Application Possibilities, *Stahlbau*, **6**: 173–180, 1987.

## 10.2 Technical Regulations and Standards

AS 1288-2006. *Glass in buildings – Selection and Installation*. Australia Standard, 2006.

ASTM C1184-05, *Standard Specification for Structural Silicone Sealants*, American Society for Testing Material (ASTM), 2005.

ASTM C1239-06a, *Standard Practice for Reporting Uniaxial Strength Data and Estimating Weibull Distribution Parameters for Advanced Ceramics*, American Society for Testing Material (ASTM), 2006.

ASTM C1368, *Standard test method for determination of slow crack growth parameters of advanced ceramics by constant stress-rate flexural testing at ambient temperature*, American Society Testing of Materials (ASTM), 2001.

ASTM C1422-99, *Standard Specification for Chemically Strengthened Flat Glass*, American Society for Testing Material (ASTM), 1999.

ASTM D4065-06, *Standard Practice for Plastics: Dynamic Mechanical Properties: Determination and Report of Procedures*, American Society for Testing Material (ASTM), 2006.

ASTM E1300-09a, *Standard Practice for Determining Load Resistance of Glass in Buildings*, American Society for Testing Material (ASTM), 2009.

BS 6399-1:1996, *Loading for Buildings. Part 1- Code of practice for dead and imposed loads*, British Standard Institute BSI, September 1996.

CNR-DT 207/2008, *Istruzioni per la valutazione delle azioni e degli effetti del vento sulle costruzioni*, Consiglio Nazionale delle Ricerche (CNR), 2008.

CPR 305/2011, *Marcatatura CE*, Construction Products Regulation (CPR), 2011.

CSTB 3488-V2. *Vitrages extérieurs collés – Cahier des prescriptions techniques*, Cahier du CSTB, Livraison 444, Cahier 3488, Mars 2011.

DTU 39 P3:2006, *Travaux de bâtiment - Travaux de vitrerie-miroiterie - Partie 3 : Mémento calculs des contraintes thermiques*, Française de Normalisation(NF), 2006.

EN ISO 17025:2000, *General requirements for the competence of testing and calibration laboratories*, European Standards (EN), 2000.

EN ISO 45011:1998, *General requirements for bodies operating product certification systems (ISO IEC Guide 65 1996)*, European Standards (EN), 1998.

ETAG 002, *Guideline for European Technical Approval for Structural Sealant Glazing Systems (SSGS)*, October 2001.

FEMA 273, *Seismic Rehabilitation Guidelines*, Federal Emergency Management Agency.

ISO 614:2012, *Ships and marine technology - Toughened safety glass panes for rectangular windows and side scuttles - Punch method of non-destructive strength testing*, International Organization for Standardization (ISO), 2012.

ISO 6721-1:2011, *Plastics - Determination of dynamic mechanical properties -- Part 1: General principles*, International Organization for Standardization (ISO), 2011.

ISO 6721-4:2008, *Plastics - Determination of dynamic mechanical properties -- Part 4: Tensile vibration - Non-resonance method*, International Organization for Standardization (ISO), 2008.

ISO 6721-11:2011, *Plastics - Determination of dynamic mechanical properties - Part 11: Glass transition temperature*, International Organization for Standardization (ISO), 2011.

ISO 20501: 2003, *Fine ceramics (advanced ceramics, advanced technical ceramics) - Weibull statistics for strength data*, International Organization for Standardization (ISO), 2003.

ISO/DIS 16933:2007, *Glass in building – Explosion resistant security glazing - Test and classification for arena air blast loading*, International Organization for Standardization (ISO), 2007.

L. 1086/71, *Norme per la disciplina delle opere in conglomerato cementizio, normale e precompresso ed a struttura metallica*, 1971.

NTC 2008, *Nuove Norme Tecniche per le Costruzioni*, DM Infrastrutture 14/01/2008.

NTC 2009, *Nuova Circolare delle Norme Tecniche per le Costruzioni*, Circolare Consiglio Superiore Lavori Pubblici 02/02/2009, n. 617.

PMC Part 2: *Load Models. Probabilistic Model Code*, Joint Committee on Structural Safety, 2001.

prEN 13474/3 (edizione 2005), *Glass in building - Determination of the strength of glass panes - Part 3: General method of calculation and determination of strength of glass by testing*, CEN TC 129.

prEN 13474/3 (edizione 2009), *Glass in building - Determination of the strength of glass panes - Part 3: General method of calculation and determination of strength of glass by testing*, CEN TC 129.

prEN 13474 (edizione 2012), *Glass in building – determination of the load resistance of glass panes by calculation and testing*, CEN TC 129.

prEN16612 (edizione 2013), *Glass in building – determination of the load resistance of glass panes by calculation and testing*, CEN/TC 129.

prEN16613 (edizione 2013), *Glass in building - Laminated glass and laminated safety glass - Determination of interlayer mechanical properties*, CEN/TC 129.

prEN THSTR - 2004, *Glass in building - Thermal Stress Calculation Method*, Progetto di Norma Europea, 2004.

prEN THSTR - 2007, *Glass in building - Thermal Stress Calculation Method*, Progetto di Norma Europea, 2004.

TM 5-1300, *Structures to resist the effects of accidental explosions*, US Department of the Army Technical Manual, Nov. 1990.

TRLV, *Technische Regeln für die Verwendung von Linienförmig gelagerten Verglasungen*, (ora DIN 18008).

UNI 5364 :1976, *Impianti di riscaldamento ad acqua calda. Regole per la presentazione dell'offerta e per il collaudo*, Ente Nazionale Italiano di Unificazione (UNI), 1976.

UNI 7697 :2007, *Criteri di sicurezza nelle applicazioni vetrarie*, Ente Nazionale Italiano di Unificazione (UNI), 2007.

UNI 10349 :1994, *Riscaldamento e raffrescamento degli edifici. Dati climatici*, Ente Nazionale Italiano di Unificazione (UNI), 1994.

UNI 10805:1999, *Ringhiere, balaustre o parapetti prefabbricati - Determinazione della resistenza meccanica a carico statico di colonne e colonne-piantone*, Ente Nazionale Italiano di Unificazione (UNI), 1999.

UNI 10806:1999, *Ringhiere, balaustre o parapetti prefabbricati - Determinazione della resistenza meccanica ai carichi statici distribuiti*, Ente Nazionale Italiano di Unificazione (UNI), 1999.



UNI 10809:1999, *Ringhiere, balaustre o parapetti prefabbricati - Dimensioni, prestazioni meccaniche e sequenza delle prove*, 1999.

UNI EN 572-1:2004, *Vetro per edilizia - Prodotti di base di vetro di silicato sodocalcico - Parte 1: Definizioni e proprietà generali fisiche e meccaniche*, Ente Nazionale Italiano di Unificazione (UNI), 2004.

UNI EN 572-2:2004, *Vetro per edilizia - Prodotti di base di vetro di silicato sodocalcico - Parte 2: Vetro float*, Ente Nazionale Italiano di Unificazione (UNI), 2004.

UNI EN 572-3:2004, *Vetro per edilizia - Prodotti di base di vetro di silicati sodocalcico - Parte 3: Vetro lustro armato*, Ente Nazionale Italiano di Unificazione (UNI), 2004.

UNI EN 572-4:2004, *Vetro per edilizia - Prodotti di base di vetro di silicato sodocalcico - Parte 4: Vetro tirato*, Ente Nazionale Italiano di Unificazione (UNI), 2004.

UNI EN 572-5:2004, *Vetro per edilizia - Prodotti di base di vetro di silicato sodocalcico - Parte 5: Vetro stampato*, Ente Nazionale Italiano di Unificazione (UNI), 2004.

UNI EN 572-6:2004, *Vetro per edilizia - Prodotti di base di vetro di silicato sodocalcico - Parte 6: Vetro stampato armato*, Ente Nazionale Italiano di Unificazione (UNI), 2004.

UNI EN 572-7:2004, *Vetro per edilizia - Prodotti di base di vetro di silicato sodocalcico - Parte 7: Vetro profilato armato e non armato*, Ente Nazionale Italiano di Unificazione (UNI), 2004.

UNI EN 572-8:2004, *Vetro per edilizia - Prodotti di base di vetro di silicato sodocalcico - Parte 8: Forniture in dimensioni fisse*, Ente Nazionale Italiano di Unificazione (UNI), 2004.

UNI EN 572-9:2005, *Vetro per edilizia - Prodotti di base di vetro di silicato sodocalcico - Parte 9: Valutazione della conformità/ Norma di prodotto*, Ente Nazionale Italiano di Unificazione (UNI), 2005.

UNI EN 673:2011, *Vetro per edilizia. Determinazione della trasmittanza termica (valore U) - Metodo di calcolo*, Ente Nazionale Italiano di Unificazione (UNI), 2011.

UNI EN 1096-1:2012, *Vetro per edilizia - Vetro rivestito - Parte 1: Definizioni e classificazione*, Ente Nazionale Italiano di Unificazione (UNI), 2012.

UNI EN 1279-1:2004, *Vetro per edilizia - Vetrate isolanti - Parte 1: Generalità, tolleranze dimensionali e regole per la descrizione del sistema*, Ente Nazionale Italiano di Unificazione (UNI), 2004.

UNI EN 1279-5:2010, *Vetro per edilizia - Vetrate isolanti - Parte 5: Valutazione della conformità*, Ente Nazionale Italiano di Unificazione (UNI), 2010.

UNI EN 1279-6:2004, *Vetro per edilizia - Vetrate isolanti - Parte 6: Controllo della produzione in fabbrica e prove periodiche*, Ente Nazionale Italiano di Unificazione (UNI), 2004.

UNI EN 1288-1:2001, *Vetro per edilizia - Determinazione della resistenza a flessione del vetro - Principi fondamentali delle prove sul vetro*, Ente Nazionale Italiano di Unificazione (UNI), 2001.

UNI EN 1288-2:2001, *Vetro per edilizia - Determinazione della resistenza a flessione del vetro - Prova con doppi anelli concentrici su provini piani, su grandi superfici sollecitate*, Ente Nazionale Italiano di Unificazione (UNI), 2001.

UNI EN 1288-3:2001, *Vetro per edilizia - Determinazione della resistenza a flessione del vetro - Prova con provino supportato in due punti (flessione in quattro punti)*, Ente Nazionale Italiano di Unificazione (UNI), 2001.

UNI EN 1288-5:2001, *Vetro per edilizia - Determinazione della resistenza a flessione del vetro - Prova con doppi anelli concentrici su provini piani, su piccole superfici sollecitate*, Ente Nazionale Italiano di Unificazione (UNI), 2001.

UNI EN 1748-1-1:2005, *Vetro per edilizia - Prodotti di base speciali - Vetri borosilicati - Parte 1- 1: Definizioni e proprietà generali fisiche e meccaniche*, Ente Nazionale Italiano di Unificazione (UNI), 2005.

UNI EN 1748-2-1:2005, *Vetro per edilizia - Prodotti di base speciali - Vetro ceramica - Parte 2-1: Definizioni e proprietà generali fisiche e meccaniche*, Ente Nazionale Italiano di Unificazione (UNI), 2005.

UNI EN 1863-1:2012, *Vetro per edilizia - Vetro di silicato sodocalcico indurito termicamente - Parte 1: Definizione e descrizione*, Ente Nazionale Italiano di Unificazione (UNI).

UNI EN 1990:2006 (EC0), Eurocodice - Criteri generali di progettazione strutturale, 2006.

UNI EN 1991 (EC1), Eurocodice 1 - Azioni sulle strutture.

UNI EN 12150-1:2001, *Vetro per edilizia - Vetro di silicato sodocalcico di sicurezza temprato termicamente - Definizione e descrizione*, Ente Nazionale Italiano di Unificazione (UNI), 2001.

UNI EN 12150-2:2005, *Vetro per edilizia - Vetro di silicato sodocalcico di sicurezza temprato termicamente - Parte 2: Valutazione di conformità/Norma di prodotto*, Ente Nazionale Italiano di Unificazione (UNI), 2005.

UNI EN 12337-1:2001, *Vetro per edilizia - Vetro di silicato sodocalcico indurito chimicamente - Definizione e descrizione*, Ente Nazionale Italiano di Unificazione (UNI), 2001.

UNI EN 12543-1:2002, *Prove non distruttive - Caratteristiche delle macchie focali di tubi radiogeni industriali per utilizzo in prove non distruttive - Parte 1: Metodo a scansione*, Ente Nazionale Italiano di Unificazione (UNI), 2002.

UNI EN 12543-2:2008, *Prove non distruttive - Caratteristiche delle macchie focali di tubi radiogeni industriali per utilizzo in prove non distruttive - Parte 2: Metodo radiografico per camera con foro a spillo*, Ente Nazionale Italiano di Unificazione (UNI), 2002.

UNI EN 12600:2004, *Vetro per edilizia - Prova del pendolo - Metodo della prova di impatto e classificazione per il vetro piano*, Ente Nazionale Italiano di Unificazione (UNI), 2004.

UNI EN 12603: 2004, *Vetro per edilizia - Procedure di validità dell'aggiustamento e intervalli di confidenza dei dati di resistenza del vetro per mezzo della legge di Weibull*, Ente Nazionale Italiano di Unificazione (UNI), 2004.

UNI EN 13022-1: 2010, *Vetro per edilizia - Vetrate strutturali sigillate - Parte 1: Prodotti vetrari per sistemi di vetrate strutturali sigillate per vetrate monolitiche supportate e non, e vetrate multiple*, Ente Nazionale Italiano di Unificazione (UNI), 2010.

UNI EN 13022-2: 2010, *Vetro per edilizia - Vetrate strutturali sigillate - Parte 2: Regole di posa*, Ente Nazionale Italiano di Unificazione (UNI), 2010.

UNI EN 13024-1: 2012, *Vetro per edilizia - Vetro di borosilicato di sicurezza temprato termicamente - Parte 1: Definizione e descrizione*, Ente Nazionale Italiano di Unificazione (UNI), 2012.

UNI EN 13830: 2005, *Facciate continue - Norma di prodotto*, Ente Nazionale Italiano di Unificazione (UNI), 2005.

UNI EN 14019:2004, *Facciate continue - Resistenza all'urto - Requisiti prestazionali*, Ente Nazionale Italiano di Unificazione (UNI), 2004.

UNI EN 14178-1:2005, *Vetro per edilizia - Prodotti di base di vetro a matrice alcalina - Parte 1: Vetro float*, Ente Nazionale Italiano di Unificazione (UNI), 2005.

UNI EN 14179-1:2005, *Vetro per edilizia - Vetro di sicurezza di silicato sodocalcico temprato termicamente e sottoposto a "heat soak test" - Parte 1: Definizione e descrizione*, Ente Nazionale Italiano di Unificazione (UNI), 2005.

UNI EN 14321-1:2005, *Vetro per edilizia - Vetro di sicurezza a matrice alcalina temprato termicamente - Parte 1: Definizione e descrizione*, Ente Nazionale Italiano di Unificazione (UNI), 2005.

UNI EN 14449:2005, *Vetro per edilizia - Vetro stratificato e vetro stratificato di sicurezza - Valutazione della conformità/Norma di prodotto*, Ente Nazionale Italiano di Unificazione (UNI), 2005.

UNI EN 15434:2010, *Vetro per edilizia - Norma di prodotto per sigillante strutturale e/o resistente ai raggi UV* (per impiego in vetrate strutturali sigillate e/o in vetrate isolanti con sigillante esposto), Ente Nazionale Italiano di Unificazione (UNI), 2010.

UNI EN ISO 527, *Materie plastiche - Determinazione delle proprietà a trazione*, Ente Nazionale Italiano di Unificazione (UNI).

UNI EN ISO 604:2008, *Materie plastiche - Determinazione delle proprietà a compressione*, Ente Nazionale Italiano di Unificazione (UNI), 2008.

UNI EN ISO 6721-1:2011, *Materie plastiche - Determinazione delle proprietà dinamico-meccaniche - Parte 1: Principi generali*, Ente Nazionale Italiano di Unificazione (UNI), 2011.

UNI EN ISO 8339, *Costruzioni edili - Sigillanti - Determinazione delle proprietà a trazione (Estensione a rottura)*, Ente Nazionale Italiano di Unificazione (UNI).

UNI EN ISO 9000:2005, *Sistemi di gestione per la qualità - Fondamenti e vocabolario*, Ente Nazionale Italiano di Unificazione (UNI), 2005.

UNI EN ISO 12543-2:2011, *Vetro per edilizia - Vetro stratificato e vetro stratificato di sicurezza - Parte 2: Vetro stratificato di sicurezza*, Ente Nazionale Italiano di Unificazione (UNI), 2011.

UNI EN ISO 12543-4:2011, *Vetro per edilizia - Vetro stratificato e vetro stratificato di sicurezza - Metodi di prova per la durabilità*, Ente Nazionale Italiano di Unificazione (UNI), 2011.

UNI EN ISO 12543-5:2011, *Vetro per edilizia - Vetro stratificato e vetro stratificato di sicurezza - Parte 5: Dimensioni e finitura dei bordi*, Ente Nazionale Italiano di Unificazione (UNI), 2011.

VORSCHLAG ÖNORM B 3716-1:2006 , *Glas im Bauwesen – Konstruktiver Glasbau Teil 1: Grundlagen*, 2006.

This Technical Document has been prepared by a Task Group whose members are:

Amadio Prof. Ing. Claudio	- University of Trieste
Badalassi Dr. Ing. Massimo	- University of Pisa
Bedon Dr. Ing. Chiara	- University of Trieste
Biolzi Prof. Ing. Luigi	- Polytechnical Institute of Milano
Briccoli Bati Prof. Arch. Silvia	- University of Firenze
Cagnacci Dr. Ing. Emanuele	- University of Firenze
Consolini Dr. Arch. Laura	- Polytechnical University of Marche
Cuomo Prof. Ing. Massimo	- University of Catania
Dall'Igna Ing. Roberto	- Glass Experimental Station, Venezia
D'este Ing. Alberto	- Glass Experimental Station, Venezia
Faggiano Dr. Ing. Beatrice	- University "Federico II", Napoli
Fagone Dr. Ing. Mario	- University of Firenze
Foraboschi Prof. Ing. Paolo	- University IUAV, Venezia
Franco Ing. Annalisa	- University of Pisa
Galuppi Dr. Ing. Laura	- University of Parma
Lani Dr. Ing. Leonardo	- University of Pisa
Maceri Prof. Ing. Franco	- University "Tor Vergata", Roma
Manara Ing. Giampiero	- Permasteelisa Group, Vittorio Veneto
Mognato p.i. Ennio	- Glass Experimental Station, Venezia
Nisticò Prof. Ing. Nicola	- University "La Sapienza", Roma
Orlando Prof. Ing. Maurizio	- University of Firenze
Poggi Prof. Ing. Carlo	- Technical University of Milano
Ranocchiali Dr. Arch. Giovanna	- University of Firenze
Rigone Prof. Ing. Paolo	- Polytechnical Institute of Milano
Royer Carfagni Prof. Ing. Gianni	- University of Parma
Salvatore Prof. Ing. Walter	- University of Pisa
Silvestri Dr. Ing. Mirko	- Glass Experimental Station, Venezia
Speranzini Prof. Ing. Emanuela	- University of Perugia
Spinelli Prof. Ing. Paolo	- University of Firenze

Coordinator:

Royer Carfagni Prof. Ing. Gianni

Secretary:

Galuppi Dr. Ing. Laura

In particular, the various chapters were written by:

CHAPTER 1: S. Briccoli Bati, B. Faggiano, G. Royer-Carfagni, E. Speranzini.

CHAPTER 2: R. Dall'Igna, A. D'Este, M. Fagone, P. Foraboschi, G. Ranocchiali, G. Royer-Carfagni, M. Silvestri.

CHAPTER 3: L. Biolzi, E. Cagnacci, B. Faggiano, P. Foraboschi, L. Lani, M. Orlando, P. Rigone, G. Royer-Carfagni, E. Speranzini, P. Spinelli.

CHAPTER 4: E. Cagnacci, L. Lani, G. Manara, N. Nisticò, M. Orlando, P. Rigone, G. Royer-Carfagni, P. Spinelli.

CHAPTER 5: M. Badalassi, L. Biolzi, G. Royer-Carfagni, W. Salvatore.

CHAPTER 6: C. Amadio, C. Bedon, L. Consolini, M. Cuomo, L. Galuppi, G. Manara, G. Ranocchiali, G. Royer-Carfagni, M. Silvestri.

CHAPTER 7: L. Biolzi, P. Foraboschi, G. Royer-Carfagni, W. Salvatore.

CHAPTER 8: A. Franco, L. Galuppi, G. Manara, G. Royer-Carfagni, E. Speranzini.

CHAPTER 9: "Advisory Committee on Technical Recommendations for Construction" of the National Research Council of Italy.

The Italian version of this Technical Document has been approved in a preliminary version on July 5<sup>th</sup> 2012 and in the final version on December 5<sup>th</sup> 2013, at the conclusion of the public inquiry, with the changes made to it, by the "Advisory Committee on Technical Recommendations for Construction" of the National Research Council of Italy, whose members are:

ANGOTTI Prof. Franco	- University of Firenze
ASCIONE Prof. Luigi	- University of Salerno
AURICCHIO Prof. Ferdinando	- University of Pavia
BARATTA Prof. Alessandro	- University "Federico II" - Napoli
COSENZA Prof. Edoardo	- University "Federico II" - Napoli
MACERI Prof. Franco, <i>Chairman</i>	- University "Tor Vergata" - Roma
MANCINI Prof. Giuseppe	- Polytechnical Institute of Torino
MAZZOLANI Prof. Federico Massimo	- University "Federico II" - Napoli
PINTO Prof. Paolo Emilio	- University "La Sapienza" - Roma
POGGI Prof. Carlo	- Polytechnical Institute of Milano
ROYER-CARFAGNI Prof. Gianni	- University of Parma
SAVOIA Prof. Marco	- University of Bologna
SCARPELLI Prof. Giuseppe	- Polytechnical University of Marche
SOLARI Prof. Giovanni	- University of Genova
URBANO Prof. Carlo	- Polytechnical Institute of Milano
VINCI Arch. Roberto	- National Research Council
ZANON Prof. Paolo	- University of Trento

The present English translation has been approved on December 12<sup>th</sup> 2016, by the "Advisory Committee on Technical Recommendations for Constructions" of the National Research Council of Italy, in its new composition:

ANGOTTI Prof. Franco	- University of Firenze
ASCIONE Prof. Luigi	- University of Salerno
AURICCHIO Prof. Ferdinando	- University of Pavia
BARATTA Prof. Alessandro	- University "Federico II" - Napoli
COSENZA Prof. Edoardo	- University "Federico II" - Napoli
DI PRISCO Prof. Marco	- Polytechnical Institute of Milano
LAGOMARSINO Prof. Sergio	- University of Genova
MACERI Prof. Franco <i>Chairman</i>	- University "Tor Vergata" - Roma
MANCINI Prof. Giuseppe	- Polytechnical Institute of Torino
MAZZOLANI Prof. Federico Massimo	- "Federico II" University - Napoli
OCCHIUZZI Prof. Antonio	- National Research Council
PINTO Prof. Paolo Emilio	- University "La Sapienza" - Roma
POGGI Prof. Carlo	- Polytechnical Institute of Milano
PROTA Prof. Andrea	- University "Federico II" - Napoli
ROYER CARFAGNI Prof. Gianni	- University of Parma

SAVOIA Prof. Marco

SCARPELLI Prof. Giuseppe

SOLARI Prof. Giovanni

URBANO Prof. Carlo

ZANON Prof. Paolo

- University of Bologna

- Polytechnical University of Marche

- University of Genova

- Polytechnical Institute of Milano

- University of Trento